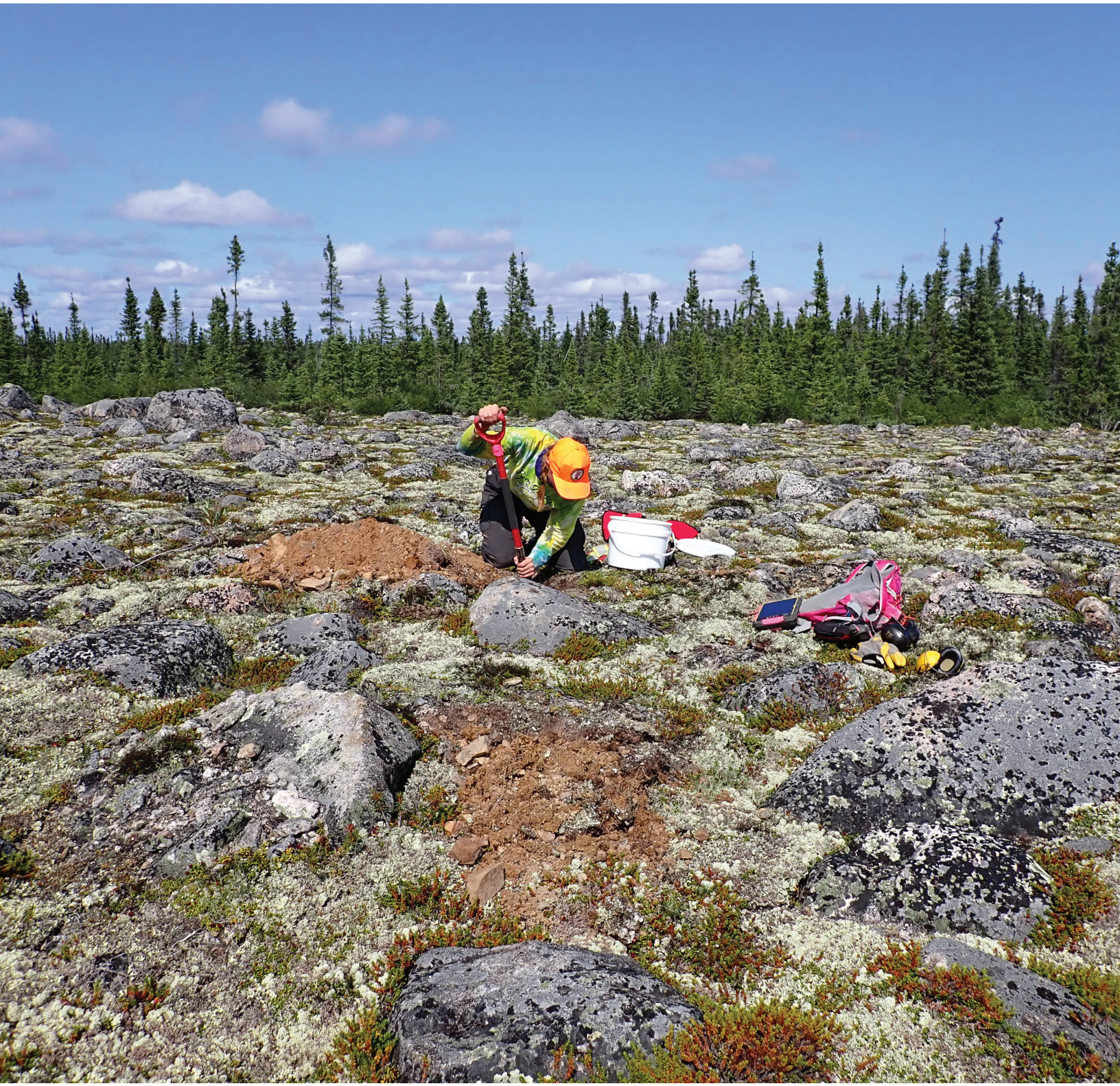
Report of Activities 2024



Manitoba



REPORT OF ACTIVITIES
2024

Manitoba Economic Development, Investment, Trade and Natural Resources
Manitoba Geological Survey

Manitoba

© King's Printer for Manitoba, 2024

Every possible effort is made to ensure the accuracy of the information contained in this report, but Manitoba Economic Development, Investment, Trade and Natural Resources does not assume any liability for errors that may occur. Source references are included in the report and users should verify critical information.

Any third party digital data and software accompanying this publication are supplied on the understanding that they are for the sole use of the licensee, and will not be redistributed in any form, in whole or in part. Any references to proprietary software in the documentation and/or any use of proprietary data formats in this release do not constitute endorsement by Manitoba Economic Development, Investment, Trade and Natural Resources of any manufacturer's product.

When using information from this publication in other publications or presentations, due acknowledgment should be given to the Manitoba Geological Survey. The following reference format is recommended:

Manitoba Geological Survey 2024: Report of Activities 2024; Manitoba Economic Development, Investment, Trade and Natural Resources, Manitoba Geological Survey, 241 p.

Published by:
Manitoba Economic Development, Investment, Trade and Natural Resources
Manitoba Geological Survey
360–1395 Ellice Avenue
Winnipeg, Manitoba
R3G 3P2 Canada
Telephone: 1-800-223-5215 (General Enquiry)
204-945-6569 (Publication Sales)
Fax: 204-945-8427
Email: minesinfo@gov.mb.ca
Website: manitoba.ca/minerals

ISBN: 978-0-7711-1651-3

This publication is available to download free of charge at manitoba.ca/minerals

Front cover photo:
Manitoba Geological Survey summer student Sara Bergen in northern Manitoba digging between boulders to find undisturbed till to sample for till processing.

REPORT OF ACTIVITIES 2024



Minister's Message

I am pleased to present the *Report of Activities 2024* for the Manitoba Geological Survey (MGS). This annual report highlights key geoscientific research and activities conducted over the past year, including 27 reports, six data repositories and one preliminary map. This comprehensive document, built on a scientific commitment to excellence, drives exploration, investment and development of our province's rich and diverse mineral resources sector.

The research and data collection conducted by the MGS are essential for supporting responsible mineral development, attracting investment and creating jobs. By providing accurate and accessible geological information, we are helping to position Manitoba as a leading destination for mining and exploration. I encourage readers of this year's volume to connect with the MGS to aid in your geological exploration of the province.

MGS geologists present at global conferences, support academic and industry partnerships, and stay at the forefront of research to deliver top tier geoscience studies and reports, advancing the provincial knowledge base.

In 2024, the MGS continued its vital role in exploring and understanding Manitoba's mineral resources. Our focus on critical minerals intensified as we recognize the importance of these minerals in supporting emerging technologies and a sustainable future. Through advanced geoscience techniques and strategic partnerships, we made substantial progress in identifying and assessing potential deposits of valuable commodities.

Manitoba's new Critical Minerals Strategy will focus on opportunities to support the transition to a clean, green economy in ways that create long-term economic growth, resilient communities, and positive socio-economic outcomes for all, including stronger focus on Indigenous inclusion and partnership in the spirit of Truth and Reconciliation.

The MGS is committed to fostering strong and collaborative relationships, including those with Indigenous communities. We recognize the importance of Indigenous knowledge and perspectives to our work and are dedicated to ensuring that our activities respect and benefit Indigenous rights and interests. Through meaningful engagements and partnerships, we are working together to develop sustainable and responsible resource management plans that address the needs of all Manitobans.

I commend the MGS team for their efforts, dedication and expertise. Their work is vital to ensuring that mineral resources are managed sustainably, supporting our province's economic growth and environmental stewardship.

Original signed by

Honourable Jamie Moses

Manitoba Economic Development, Investment, Trade and Natural Resources

Rapport d'activités 2024



Message du ministre

J'ai le plaisir de présenter le *Rapport d'activités 2024* de la Direction des services géologiques. Ce rapport annuel souligne les principales recherches et activités géoscientifiques menées au cours de la dernière année, dont 27 rapports, six dépôts de données et une carte préliminaire. Ce document complet, fondé sur un engagement scientifique envers l'excellence, stimule l'investissement, l'exploration et le développement dans le secteur, riche et diversifié, des ressources minérales de notre province.

Les recherches et la collecte de données menées par les Services géologiques sont essentielles pour soutenir le développement responsable des minéraux, attirer des investissements et créer des emplois. En fournissant des renseignements géologiques précis et accessibles, nous contribuons à faire du Manitoba une destination de choix pour l'exploitation et l'exploration minières. J'encourage les lecteurs du volume de cette année à communiquer avec les Services géologiques pour faciliter leur exploration de la province.

Leurs géologues participent à des conférences mondiales, appuient des partenariats sectoriels et universitaires et demeurent à l'avant-garde de la recherche afin de produire des études et des rapports géoscientifiques de premier ordre qui élargissent les connaissances de la province.

En 2024, les Services géologiques ont continué de jouer un rôle essentiel dans l'exploration et la compréhension des ressources minérales du Manitoba. Nous avons accentué nos efforts concernant les minéraux critiques, car nous reconnaissons leur importance pour les nouvelles technologies et un avenir durable. Grâce à des techniques géoscientifiques avancées et à des partenariats stratégiques, nous avons réalisé d'importants progrès dans le repérage et l'évaluation de gisements potentiels de précieuses matières premières.

La nouvelle Stratégie manitobaine sur les minéraux critiques mettra l'accent sur les occasions de soutenir la transition vers une économie propre et verte de façon à créer une croissance économique à long terme, des collectivités résilientes et des résultats socioéconomiques positifs pour tous, en accordant une plus grande importance à l'inclusion des Autochtones et aux partenariats dans un esprit de vérité et de réconciliation.

Les Services géologiques se sont engagés à favoriser des relations solides et collaboratives, y compris avec les collectivités autochtones. Nous reconnaissons l'importance du savoir et des perspectives autochtones dans notre travail et nous nous engageons à faire en sorte que nos activités respectent les droits et intérêts autochtones et leur soient bénéfiques. Grâce à d'importants engagements et partenariats, nous collaborons pour élaborer des plans durables et responsables de gestion des ressources qui répondent aux besoins de tous les Manitobains.

Je félicite les Services géologiques pour leurs efforts, leur dévouement et leur expertise. Leur travail est essentiel pour garantir que les ressources minérales sont gérées de façon durable afin de soutenir la croissance économique et la gérance environnementale de notre province.

Original signé par

Monsieur Jamie Moses

Ministre du Développement économique, de l'Investissement, du Commerce et des Ressources naturelles

Foreword

On behalf of the Manitoba Geological Survey (MGS), I am privileged to present the *Report of Activities 2024*—the annual peer-reviewed volume of geoscience project results by the MGS and its partners.

The MGS comprises five sections within the Minerals, Petroleum and Geoscience Division: (1) Precambrian Geoscience (Tania Martins, Chief Geologist); (2) Sedimentary Geoscience (Michelle Nicolas, Chief Geologist); (3) Geoscience Data Management (Greg Keller, Manager); (4) the Resource Centre (Peggy Syljuberget, Manager); and (5) Core Library Facilities (Colin Epp, Manager).

Our participation in national and international events was strong this year, including oral and poster presentations. A highlight includes the MGS geologists attending the Geological Association of Canada–Mineralogical Association of Canada–International Symposium on Granitic Pegmatites (GAC-MAC-PEG) in Brandon, exhibiting, organizing sessions, giving presentations and workshops, and guiding field trips. It was an excellent opportunity to highlight our expertise and contribution to the continuously growing body of knowledge on Manitoba's geology. The MGS presented and exhibited at GeoConvention 2024 in Calgary, where Michelle Nicolas presented on the collaborative work she has been doing on the helium prospectivity in Manitoba; this study used a new innovative technique to analyze pore space commodities in underexplored horizons. Peggy Syljuberget attended the ARMA Canada Information Conference in Calgary, presenting a case study of collaborative research on the potential for artificial intelligence to benefit managing records and information governance. As the MGS in-house pegmatites expert, Tania Martins' extensive knowledge of lithium-bearing pegmatites has attracted global attention. She was invited to present at various international workshops and conferences to talk about Manitoba's pegmatites. Events she has attended include the United Nations Economic Commission for Europe as part of her work with the Minerals Working Group. Additionally, Tania presented on Manitoba's lithium potential at the 37th International Geological Congress (IGC) in South Korea as part of the Canadian delegation. This delegation successfully bid for Canada to host the IGC in 2028.

To support the new Captured Carbon Storage Act, MGS hydrogeologist Efe Enaworu attended the national Carbon Capture, Utilization, and Storage convention, participating in workshops and sessions to broaden his knowledge of deep saline aquifers for carbon storage. Quaternary geologists Michelle Gauthier and Tyler Hodder represented the MGS at the Canadian Quaternary Association Biennial Meeting (CANQUA) in Regina where Tyler provided a keynote presentation, Michelle gave an oral presentation, and both co-authored several posters. This involvement in the conference resulted in new collaborations to advance research and project initiatives in Manitoba.

This year's 27 articles and Preliminary Map cover a diverse thematic and geographic range, including field observations, bedrock mapping, core work, office compilations, updates to our datasets, geochronology and mineral occurrences, and pore space resource potential. Benefitting from three years of increased internal resources, the MGS has produced the highest number of reports in almost 20 years. This has allowed the MGS to participate in multi-jurisdictional partnerships and collaborations with the universities of Manitoba, Toronto, Alberta, New Brunswick, British Columbia, Copenhagen, Western and Laurentian University, as well as with industry stakeholders and independent consultants. We look forward to ongoing collaborations with all the stakeholders to complement our capacity to produce world-class geoscience investigations.

This year's Report of Activities continues to highlight the critical mineral potential of Manitoba, including updates on the Mineral Deposits Database, application of Quaternary sediment stratigraphy and mapping to locate lithium-bearing pegmatites, and new evidence for sulphide mineralization coincident with hydrocarbon-bearing units in southwestern Manitoba. Continued work on assessing helium and now hydrogen sources and the economic potential of these critical elements in subsurface sediment pore spaces is expanding the exploration areas of the province. A multidisciplinary study on pegmatites in the Archean Bird River domain looks at characterizing the area around known pegmatite deposits. Results from this study will help to better understand how these deposits form and will provide additional exploration tools. Also reported herein is ongoing work in Thompson, Lynn Lake, and Snow Lake areas, from preserving our archival Precambrian drillcore collection to bedrock mapping and geochronological dating. Other works discuss land-use planning and economic development for the north, including Quaternary mapping in the far north and pore space resource assessment of the Hudson Bay Lowland. New and renewed projects resulting in reports on high-purity silica sand, deep saline aquifer water chemistry compilation from oil and gas wells, continued updated mapping of aggregate deposits, and application of geophysical methods to map buried aggregate resources are a reflection of the geologists who have recently joined our team.

The six Data Repository Items result from progressive work on pore space commodities, drillcore salvaged from our Thompson core library, and field-based ice-flow indicators from the multidisciplinary study in southeastern Manitoba. The geochemical data from samples collected in 2022 and 2023 are an added resource for the Lynn Lake greenstone belt. Additionally, historical geochemistry datasets and maps from the Cross Lake area provide new information to further our understanding of the Superior province's critical mineral potential.

We continued to build capacity by hiring for the Sedimentary Geoscience Section: Victoria Markstrom as the Industrial Minerals and Sedimentary Geologist, Patricia Fraino as the Stratigrapher and Sedimentary Geologist, Efe Enaworu as the Hydrogeologist, and Jason Marks as the Geophysicist. We welcomed Jessica Janssens as the Geologist Assistant to the Precambrian Geoscience Section. The Geoscience Data Management Section added a GIS Specialist, Ben Wheadon, and a 3-D Geological Modeller, Cole Derksen. We welcomed Delaney O'Hara as our new Communications and Publications Specialist and Elizabeth

Locken as our Confidential Records Keeper in the Resource Centre. The increase in support staff and filling all the positions in the Sedimentary Geoscience Section will significantly impact our overall capacity to succeed in our operational mandate.

The production of the Report of Activities and other MGS publications is a collective achievement made possible by the dedicated efforts of our entire team. I want to extend a special mention to Colin Epp and Paul Belanger for their field and expediting support and the meticulous maintenance of our equipment this year. Their efforts formed the backbone of our field program and provided client access to our core library facilities. I want to acknowledge Greg Keller and his team of GIS specialists and geologists for their support with our GIS products and services. I also want to acknowledge Bob Davie and his team from RnD Technical for their outstanding professional technical editing services, and Craig Steffano for managing report production and publication layout with assistance from Delaney O'Hara. I sincerely thank every member of the MGS team for their contributions to this year's milestone achievement.

Tafa Kennedy, Ph.D., P.Geo.

Director, Manitoba Geological Survey

Avant-propos

J'ai le privilège de présenter, au nom de Services géologiques Manitoba (SGM), le *rapport d'activités 2024*, qui est le recueil annuel examiné par les pairs indiquant les résultats de projets géoscientifiques exécutés par SGM et ses partenaires.

SGM comprend cinq sections au sein de la Division des minéraux, du pétrole et des géosciences : (1) Section du Précambrien (Tania Martins, géologue en chef); (2) Section de la géologie sédimentaire (Michelle Nicolas, géologue en chef); (3) Section de la gestion des données géoscientifiques (Greg Keller, gestionnaire); (4) Section du centre de ressources (Peggy Syljuberget, gestionnaire); et (5) Section des installations de stockage de carottes de forage (Colin Epp, gestionnaire).

Notre participation aux événements nationaux et internationaux a été forte cette année, et a pris la forme de présentations données de vive voix et au moyen d'affiches. Parmi les faits saillants, mentionnons la présence de géologues de SGM au Symposium international sur les pegmatites granitiques de l'Association géologique du Canada-Association minéralogique du Canada (AGC-AMC-PEG) à Brandon. Les géologues ont présenté des expositions, organisé des séances, donné des présentations et des ateliers, et guidé des sorties éducatives. Ce symposium a constitué une excellente occasion de souligner notre expertise et notre contribution à l'ensemble croissant de connaissances sur la géologie du Manitoba. SGM a présenté et exposé à la GeoConvention 2024 à Calgary, où Michelle Nicolas a présenté le travail en collaboration qu'elle a exécuté sur la prospectivité de l'hélium au Manitoba; cette étude repose sur une nouvelle technique novatrice d'analyse des produits de l'espace interstitiel dans des horizons sous-explorés. Peggy Syljuberget a assisté à la conférence d'information d'ARMA Canada à Calgary, où elle a présenté une étude de cas sur la recherche en collaboration sur le potentiel de l'intelligence artificielle d'améliorer la gestion des dossiers et la gouvernance de l'information. En tant qu'experte interne des pegmatites de SGM, Tania Martins, grâce à ses vastes connaissances, a attiré l'attention du monde entier en abordant les pegmatites contenant du lithium. Elle a été invitée à faire une présentation à diverses conférences et à divers ateliers internationaux pour discuter des pegmatites du Manitoba. Parmi les événements auxquels elle a participé, mentionnons la conférence de la Commission économique des Nations Unies pour l'Europe, dans le cadre de ses travaux au sein du groupe de travail sur les minéraux. De plus, Tania a présenté un exposé sur le potentiel du lithium du Manitoba au cours du 37^{e} Congrès international de géologie (CIG) tenu en Corée du Sud, en tant que membre de la délégation canadienne. Cette délégation a réussi à faire accepter la candidature du Canada à titre d'hôte du CIG en 2028.

Pour appuyer la nouvelle Loi sur le stockage de carbone capté, Efe Enaworu, hydrogéologue à SGM, a assisté à la convention nationale sur le captage, l'utilisation et le stockage du carbone, participant à des ateliers et des séances visant à approfondir ses connaissances sur les aquifères salins profonds pour le stockage du carbone. Les géologues du Quaternaire Michelle Gauthier et Tyler Hodder ont représenté SGM à la réunion biennale de l'Association canadienne pour l'étude du Quaternaire (CANQUA) tenue à Regina, au cours de laquelle Tyler a présenté un exposé principal, Michelle a fait une présentation et les deux ont coécrit le contenu de plusieurs affiches. Cette participation à la conférence a donné lieu à de nouvelles collaborations visant à faire progresser les initiatives de recherche et de réalisation de projets au Manitoba.

Les 27 articles et la carte préliminaire de cette année traitent une gamme thématique et géographique diversifiée, y compris les observations sur le terrain, la cartographie du substrat rocheux, les travaux de base, les compilations de bureau, les mises à jour de nos ensembles de données, la géochronologie et les occurrences minérales, et le potentiel des ressources de l'espace interstitiel. Bénéficiant de trois années de ressources internes accrues, SGM a produit le plus grand nombre de rapports en près de 20 ans. Cela a permis à SGM de prendre part à des partenariats et à des collaborations multijuridictionnelles avec les universités du Manitoba, de Toronto, de l'Alberta, du Nouveau-Brunswick, de la Colombie-Britannique et de Copenhague, avec l'Université Western et l'Université Laurentienne, ainsi qu'avec des intervenants de l'industrie et des experts-conseils indépendants. Nous nous réjouissons à l'idée de collaborer de façon continue avec tous les intervenants pour renforcer notre capacité de produire des études géoscientifiques de calibre mondial.

Le rapport d'activités de cette année continue de mettre en lumière le potentiel du minéral critique du Manitoba, y compris des mises à jour de la base de données sur les gisements minéraux, l'application de la stratigraphie et de la cartographie du Quaternaire pour localiser les pegmatites contenant du lithium, et les nouvelles données probantes sur la minéralisation des sulfures coïncidant avec les unités contenant des hydrocarbures dans le sud-ouest du Manitoba. La poursuite des travaux d'évaluation des sources d'hélium et maintenant d'hydrogène et le potentiel économique de ces éléments essentiels dans les espaces souterrains de pores de sédiments agrandissent les zones d'exploration de la province. Une étude multidisciplinaire sur les pegmatites dans le domaine de la Bird River de l'Archéen porte sur la caractérisation de la zone entourant des gisements de pegmatite connus. Les résultats de cette étude nous permettront de mieux comprendre comment ces gisements se forment et permettront de concevoir d'autres outils d'exploration. Les travaux en cours dans les régions de Thompson, de Lynn Lake et de Snow Lake, qui concernent autant la préservation de notre collection archivistique de carottes de forage précambriennes à la cartographie du substrat rocheux et à la datation géochronologique, sont également indiqués dans le présent document. D'autres travaux traitent de la planification de l'aménagement du territoire et du développement économique pour le Nord, y compris la cartographie du Quaternaire dans le Grand Nord et l'évaluation des ressources de l'espace interstitiel des basses-terres de la baie d'Hudson. Des projets nouveaux et renouvelés qui ont permis de préparer des rapports sur le sable de silice de grande pureté, la compilation de la chimie des eaux aquifères salines profondes à partir de puits de pétrole et de gaz, la mise à jour constante de la cartographie des gisements d'agrégats et l'application de méthodes géophysiques pour cartographier les ressources d'agrégats enfouies sont les réalisations des géologues qui se sont récemment joints à notre équipe.

Les six éléments du dépôt de données découlent de travaux progressifs sur les produits de base de l'espace interstitiel, les carottes de forage récupérées dans notre installation de stockage de carottes de forage de Thompson et les indicateurs d'écoulement de glace sur le terrain tirés de l'étude multidisciplinaire menée dans le sud-est du Manitoba. Les données géochimiques des échantillons recueillis en 2022 et en 2023 constituent une ressource supplémentaire pour la ceinture de roche verte du lac Lynn. De plus, les ensembles de données géochimiques historiques et les cartes de la région de Cross Lake donnent de nouveaux renseignements qui nous permettront de mieux comprendre le potentiel du minéral critique de la province du lac Supérieur.

Nous avons continué de renforcer nos capacités en embauchant du personnel à la Section de la géologie sédimentaire : Il s'agit de Victoria Markstrom, en qualité de géologue des minéraux industriels et des sédiments, de Patricia Fraino, en qualité de stratigraphe et géologue des sédiments, d'Efe Enaworu, en qualité d'hydrogéologue, et de Jason Marks, en qualité de géophysicien. Nous avons accueilli Jessica Janssens en qualité d'adjointe géologue à la Section du Précambrien. La Section de la gestion des données géoscientifiques compte désormais un spécialiste des SIG, Ben Wheadon, et un modélisateur géologique en 3D, Cole Derksen. Nous avons accueilli Delaney O'Hara à titre de nouvelle spécialiste des communications et des publications, et Elizabeth Locken à titre de responsable de la gestion des documents confidentiels au Centre de ressources. L'augmentation du nombre de membres du personnel de soutien et la dotation de tous les postes à la Section de la géologie sédimentaire auront une incidence considérable sur notre capacité générale de bien exécuter notre mandat opérationnel.

La production du rapport d'activités et d'autres publications de SCM est une réalisation collective rendue possible grâce aux efforts dévoués de toute notre équipe. Je tiens à remercier tout particulièrement Colin Epp et Paul Belanger de leur soutien sur le terrain, de leur soutien expéditif et de l'entretien méticuleux de notre équipement cette année. Leurs efforts ont constitué l'épine dorsale de notre programme sur le terrain et ont permis aux clients d'avoir accès à nos installations de stockage de carottes de forage. Je souhaite remercier Greg Keller et son équipe de spécialistes et de géologues des SIG de leur soutien à l'égard de nos produits et services des SIG. Je tiens également à remercier Bob Davie et son équipe de RnD Technical de leurs services professionnels exceptionnels de révision technique, ainsi que Craig Steffano, pour la gestion de la production de rapports et de la mise en page des publications, avec l'aide de Delaney O'Hara. Je remercie sincèrement chacun des membres de l'équipe du SCM de leur contribution à l'atteinte du jalon de cette année.

La directrice des services géologiques du Manitoba,

Tafa Kennedy, Ph.D., P.Geo.

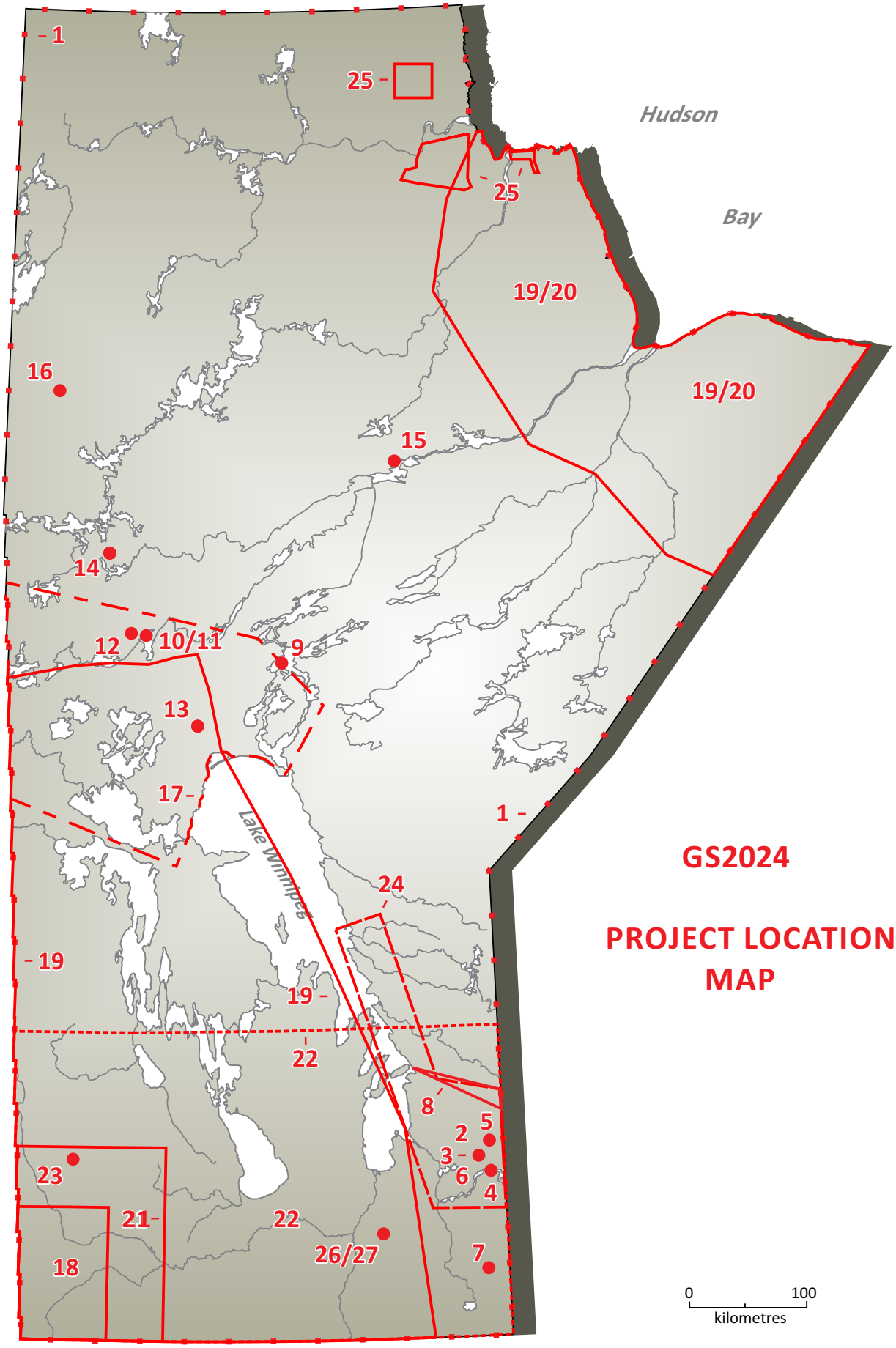

1
25
Hudson
Bay
25
19/20
19/20
16
15
14
12
10/11
9
13
17
1
Lake Winnipeg
24
19
19
22
8
5
2
3
6
4
23
21
22
18
26/27
7
GS2024
PROJECT LOCATION MAP
0
100
kilometres

Table of Contents

Minister's Message iii

Message du ministre iv

Foreword
by T. Kennedy v

Avant-propos
par T. Kennedy vi

GS2024 Project Location Map viii

PRECAMBRIAN

GS2024-1
Progress report on the Manitoba Mineral Deposits Database
by M.L. Rinne 1

GS2024-2
Updated structural interpretations in the Bird River domain, southeastern Manitoba (parts of NTS 52L5, 6, 11, 12)
by M.L. Rinne and T. Martins 4

GS2024-3
Preliminary results from field investigations in the Cat Lake–Winnipeg River pegmatite field, southeastern Manitoba (parts of NTS 52L5, 6, 11, 12)
by C. Nambaje, T. Martins, C.R.M. McFarlane, M. Kaczmer, M.L. Rinne and L. Groat 10

GS2024-4
Paragenetic relationships between zones 80 and 90 at the Tanco pegmatite, southeastern Manitoba (part of NTS 52L6)
by C.M. Breasley, T. Martins, R.L. Linnen and L.A. Groat 27

GS2024-5
Cat Tail pegmatite: zonation and mineralogy, Cat Lake area, southeastern Manitoba (part of NTS 52L11)
by T. Martins and J. Janssens 33

GS2024-6
Preliminary observations from the Cat Lake–Winnipeg River pegmatite field, southeastern Manitoba (parts of NTS 52L5, 6, 11): evidence for the effect of structural setting and emplacement mechanism on the size and morphology of lithium-bearing pegmatites
by T.K. Cawood, S.R. Beyer, N. Mohammadi, C.J.M. Lawley, T. Martins and M.L. Rinne 38

GS2024-7
Precise U-Pb zircon age and geochemical constraints on the geodynamic settings of the Falcon Lake intrusive complex and S-type Caddy Lake granite intrusion in the western Superior province, southeastern Manitoba (parts of NTS 52E11, 14)
by X.M. Yang 49

GS2024-8
Preliminary field observations of Mesoarchean metamorphosed sedimentary and intrusive rocks in the Rice Lake greenstone belt, eastern Manitoba (parts of NTS 52L14, 52M3, 62P1)
by E. Tonboe, P. Waterton, R. Haugaard, S.D. Anderson and C.G. Couëslan 66

GS2024-9
Spodumene-bearing pegmatites from the Cross Lake pegmatite field, east-central Manitoba: mineralogy and petrography descriptions (parts of NTS 63I12, 63J9)
by T. Martins, J. Janssens and P. Lenton 77

GS2024-10
Geological investigation of the Roberts Lake fault at Roberts Lake, north-central Manitoba (part of NTS 63J13)
by K.D. Reid 85

GS2024-11
Geochronological update of sedimentary, volcanic and plutonic rocks in the Snow Lake area, north-central Manitoba (parts of NTS 63J13, 63K16)
by K.D Reid 92

GS2024-12
Research activities at the Lalor mine, Snow Lake, west-central Manitoba (part of NTS 63K16)
by S.M. Ballantyne, M. Stewart, K.D. Reid, M.O. Anderson, C. Venturi and N. Richardson 98

GS2024-13
Investigation of volcanic rocks along the eastern margin of the sub-Phanerozoic Thompson nickel belt, central Manitoba (part of NTS 63J3)
by C.G. Couëslan 104

GS2024-14
Bedrock mapping in the northwestern Burntwood Lake area, Kisseynew domain, west-central Manitoba (part of NTS 63N7)
by C.G. Couëslan and M.A. Friesen 116

GS2024-15
Thompson Facility and Compound core recovery project, east-central Manitoba (parts of NTS 64A1, 8): year two
by C.G. Couëslan 127

GS2024-16
New uranium-lead zircon dates from the Lynn Lake greenstone belt, northwestern Manitoba (part of NTS 64C14): implications for diverse granitoid magmatism and gold mineralization
by X.M. Yang 129

GS2024-17
Initial results from a long-period magnetotelluric survey in the Flin Flon, Snow Lake and The Pas area, west-central Manitoba (NTS 63F, G, J, K, parts of 63B, I, N)
by B.F.W. Chase, J. Marks, A. Williamson, A. Maki, K. Moshtaghian and M.J. Unsworth 145

PHANEROZOIC

GS2024-18
Rock volatiles analysis of drill cuttings to evaluate the helium and hydrocarbon prospectivity of southwestern Manitoba (parts of NTS 62F2, K3)
by M.P.B. Nicolas, C.M. Smith and M.P. Smith 153

GS2024-19
Geologic hydrogen in the Williston and Hudson Bay basins, southwestern and northeastern Manitoba (parts of NTS 53, 54, 62, 63)
by M.P.B. Nicolas 164

GS2024-20
Pore space resource potential of the Paleozoic sequence in the Hudson Bay Basin, northeastern Manitoba (parts of NTS 53N, O, 54A–F, K, L)
by M.P.B. Nicolas 172

GS2024-21
Compilation of saline water analysis data from oil and gas wells, southwestern Manitoba (NTS 62F, G, J, K, N)
by E. Enaworu and M.P.B. Nicolas 181

GS2024-22
Distribution of the lithological units of the Winnipeg Formation, southern Manitoba (NTS 62F–K, N–P)
by V.L. Markstrom 185

GS2024-23
Preliminary observations from the Manson Field's Reston-Amaranth-Lodgepole oil reservoir, southwestern Manitoba (part of NTS 62K)
by P.J. Fulton-Regula 192

QUATERNARY

GS2024-24
Reconnaissance-scale Quaternary geology investigations to support lithium exploration in southeastern Manitoba (parts of NTS 52L, M, 62P, 63A)
by T.J. Hodder and O.B. Lian 200

GS2024-25
Quaternary site data, till composition and ice-flow indicators between the North Knife River and the Seal River, and in the Gross Lake area, far northeastern Manitoba (parts of NTS 54L10–15, 54M5, 6, 12)
by M.S. Gauthier and S. Bergen 209

GS2024-26
Geophysical imaging of a buried gravel deposit in the Rural Municipality of Taché, southeastern Manitoba (part of NTS 62H15)
by J.W. Rentz, J. Marks, A. Frederiksen and R. Guerard 219

GS2024-27
Preliminary results of a multi-electrode resistivity survey of a buried gravel deposit in the Rural Municipality of Taché, southeastern Manitoba (part of NTS 62H15)
by J. Marks and J.W. Rentz 226

PUBLICATIONS

Manitoba Geological Survey Publications Released December 2023 to November 2024 234

External Publications 238

GS2024-1

Progress report on the Manitoba Mineral Deposits Database

by M.L. Rinne

Summary

The Manitoba Geological Survey began work to update the provincial Mineral Deposits Database (MDD) in 2020. This report summarizes changes to the MDD during the past year, including the consolidation of existing occurrence data and the addition of several thousand new (i.e., historical but previously unrecognized) mineral occurrences, representing a wide range of commodities including critical minerals. The updated mineral occurrence data are published as GeoFile 5, with annual updates.

In Brief:

- The Mineral Deposits Database contains data regarding mineral occurrences in Manitoba
- In 2024, thousands of new mineral occurrence records were added to the database, and work is ongoing
- New mineral occurrence data are shared annually in GeoFile 5

Citation:
Rinne, M.L. 2024: Progress report on the Manitoba Mineral Deposits Database; *in* Report of Activities 2024, Manitoba Economic Development, Investment, Trade and Natural Resources, Manitoba Geological Survey, p. 1–3.

Introduction

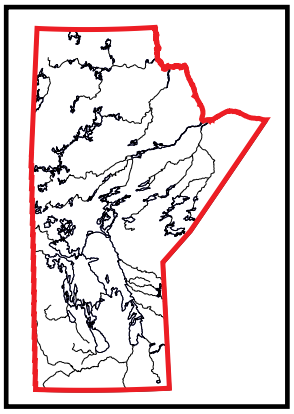
The MDD is Manitoba's primary repository of mineral occurrence data, with locations, selected geochemical data and other information compiled for mines, major prospects and other mineral occurrences. Up-to-date mineral occurrence data are necessary to inform mineral potential assessments, exploration targeting and related aspects of land-use planning.

Since updates to the MDD began in 2020, the Manitoba Geological Survey (MGS) has identified and partially catalogued thousands of mineral occurrences in the province (Figure GS2024-1-1). The criteria used to identify each mineral occurrence, as well as the methods used to collect new mineral occurrence data, are described in Rinne (2021). After sample co-ordinates and other necessary information are captured (an ongoing process), these new occurrence data are shared annually in GeoFile 5. Many of the new occurrence records in GeoFile 5-2024 (Rinne, 2024) are preliminary and lack detailed information aside from the occurrence location, data source(s) and relevant geochemical values. This is a deliberate choice to prioritize timely public releases in favour of completeness, as other information (such as detailed geological descriptions) is time consuming to find and enter for minor occurrences, or in many cases it is simply not available in the source reports. In future updates, some fields may be filled in the existing records as new information is received.

Summary of 2024 updates

Updates to the MDD during the past year involved

- Addition of several thousand new mineral occurrence records collected primarily from nonconfidential industry assessment reports, with 2024 updates focusing mostly on the Superior province. Across the southern parts of the province, new occurrence data relating to potash, helium and silica sand were also gathered from industry websites and recent MGS publications (e.g., Nicolas, 2018).
- Inclusion of all minesite points across the province, taken from Manitoba Economic Development, Investment, Trade and Natural Resources (2024). These sites are classified as separate minesites in the MGS GIS Map Gallery (Manitoba Economic Development, Investment, Trade and Natural Resources, 2024). In the MDD, however, some sites are classified as mine-related infrastructure instead of mines; this prevents counting single deposits as multiple mines, in cases where the deposit is mined from several shafts or access points.
- Deletion or consolidation of approximately 1200 existing records from the 2023 database, mostly to prevent duplication or overlap with other records, and to remove irrelevant/unimportant results. For example, many findings of trace disseminated pyrite without assay data were classified as occurrences in previous versions of the database (Conley et al., 2009) but have been deleted from the 2024 database.
- Hundreds of minor corrections (mostly typos or optical character recognition errors, and some location revisions), some in response to helpful feedback from database users. As in past releases, GeoFile 5-2024 is certain to contain errors—many inherited from the original sources—and users are advised to consult the accompanying ReadMe document that explains some of the limitations of the database.



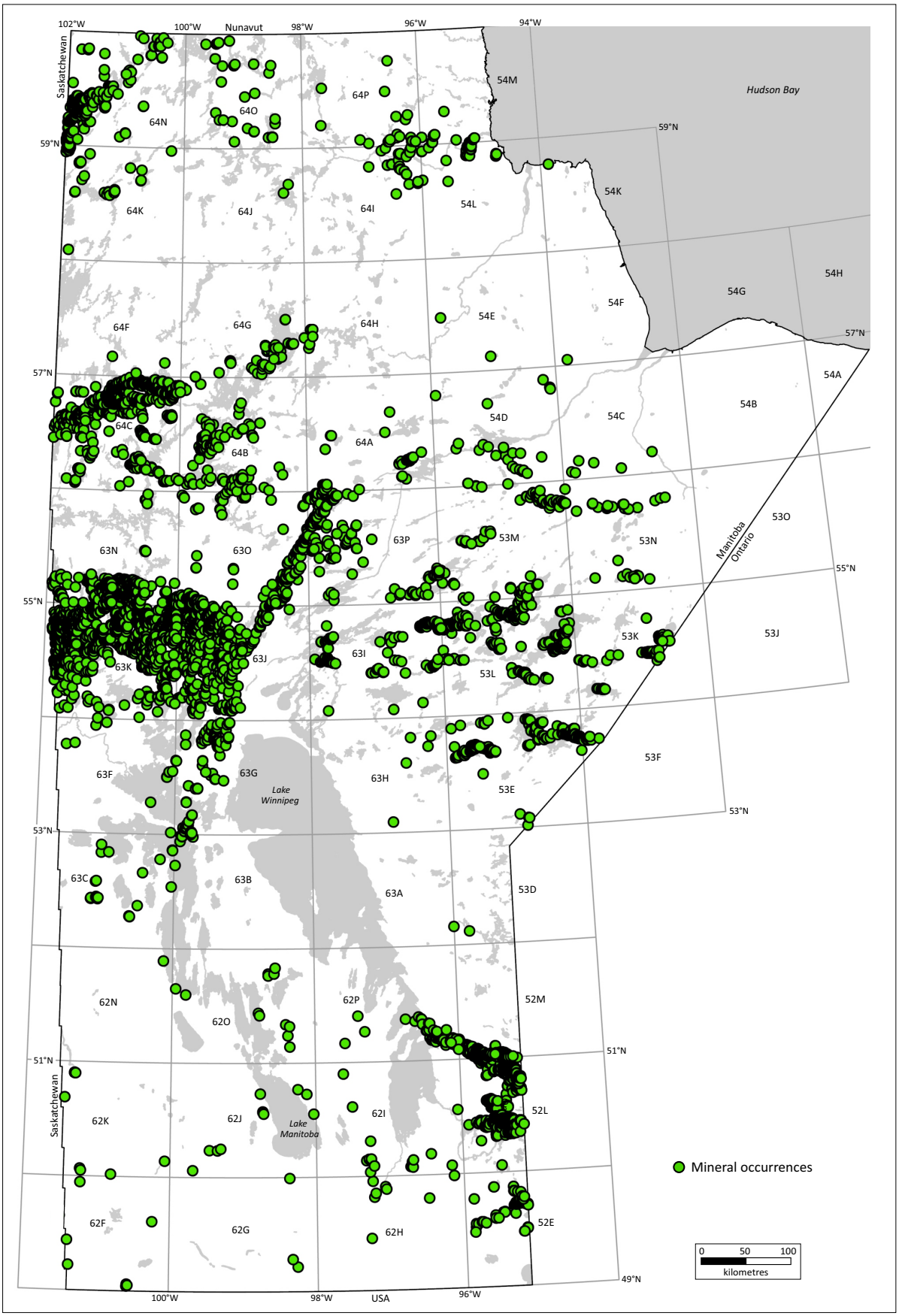


Figure GS2024-1-1: *Map of Manitoba showing the locations of mineral occurrences in the 2024 version of the Mineral Deposits Database (Rinne, 2024). These occurrence data can be subdivided by commodity type, selected geochemical values or other fields in GeoFile 5-2024.*

- Addition of more categories to the "Occurrence classification" and "Sample medium" fields, in order to better capture specific cases such as ore mineral separates or concentrates sampled from operating mines.
- Addition of a "Mineral deposit model" field, essentially following the classification scheme of Hofstra et al. (2021), with some modifications including the addition of general deposit types for coal, brine and silica sand deposits. This classification was selected to be compatible with the Critical Minerals Mapping Initiative[1]. In GeoFile 5-2024, a tentative deposit model—or depending on the available data, a less precise "deposit group" of Hofstra et al. (2021)—has been assigned to the three operating mines in Manitoba (Tanco, Thompson and Lalor), and to about half of the 264 historical mine records. As updates proceed, many occurrences are likely to remain unclassified as they lack sufficient data or context needed to infer a deposit model.

Future work

Since 2020, MDD updates were primarily targeted at remote regions of Manitoba that were underrepresented in the existing database. The updates have been carried out mostly region-by-region, with areas of focus occasionally adjusted in response to community requests for mineral occurrence maps. Updates are now mostly complete in NTS 53, 54 and 64, though these regions are likely to see a few minor changes (e.g., additional occurrences, corrections) in future releases.

Further work is planned to involve processing of text and assay tables in remaining assessment reports, which are mostly covering parts of NTS 63; continued georeferencing of mineral occurrences that have been tentatively identified but not yet spatially located; gathering more comprehensive data concerning quarries and industrial minerals; and continued population of blank fields in existing records as new information is gathered. It is also anticipated that additional fields or other changes may be necessary to accommodate future use cases.

Economic considerations

Since 2020, Manitoba's Mineral Deposits Database has expanded from 2760 occurrences to approximately 19 600, along with thousands of tentative occurrences awaiting georeferencing for inclusion in future releases. Compared to the previous MDD, the current version of the database provides a much more comprehensive picture of the spatial distribution of various mineral commodities in Manitoba. This new dataset supports better decision-making regarding land use and mineral potential, and enables more thorough evaluations of Manitoba's critical-mineral systems.

Acknowledgments

Reviews of this report were provided by V. Markstrom and M. Gauthier. Assistance with data entry and georeferencing was provided by M. Friesen (University of Manitoba), J. Kristof (University of Manitoba) and K. Peters (University of Winnipeg). Some revisions to the Mineral Deposits Database during the past year were made thanks to helpful feedback by database users, especially G. Salo and R. Turmel.

References

Conley, G.G., Heine, T.H., Prouse, D.E. and Leskiw, P.D. 2009: Mineral Deposits Database; Manitoba Science, Technology, Energy and Mines, Manitoba Geological Survey.

Hofstra, A., Lisitsin, V., Corriveau, L., Paradis, S., Peter, J., Lauzière, K., Lawley, C., Gadd, M., Pilote, J., Honsberger, I., Bastrakov, E., Champion, D., Czarnota, K., Doublier, M., Huston, D., Raymond, O., VanDerWielen, S., Emsbo, P., Granitto, M. and Kreiner, D. 2021: Deposit classification scheme for the Critical Minerals Mapping Initiative Global Geochemical Database; U.S. Geological Survey, Open File Report 2021–1049, 60 p.

Manitoba Economic Development, Investment, Trade and Natural Resources 2024: Geoscience service; *in* GIS Map Gallery, Manitoba Economic Development, Investment, Trade and Natural Resources, Manitoba Geological Survey, URL <https://rdmaps.gov.mb.ca/Html5Viewer/index.html?viewer=MapGallery_Geology.MapGallery> [September 2024].

Nicolas, M.P.B. 2018: Summary of helium occurrences in southwestern Manitoba; *in* Report of Activities 2018, Manitoba Growth, Enterprise and Trade, Manitoba Geological Survey, p. 110–118.

Rinne, M.L. 2021: Updates to the Manitoba Mineral Deposits Database, east-central and northwestern Manitoba (NTS 53E, F, 64J, K, N, O); *in* Report of Activities 2021, Manitoba Agriculture and Resource Development, Manitoba Geological Survey, p. 1–7.

Rinne, M.L. 2024: Updates to the Manitoba Mineral Deposits Database; Manitoba Economic Development, Investment, Trade and Natural Resources, Manitoba Geological Survey, GeoFile 5-2024, Microsoft® Excel® file.

[1] The Critical Minerals Mapping Initiative is a joint effort by the geological surveys of Canada, Australia and the United States. This initiative aims to build a global database for critical mineral geochemistry, and ultimately to support a more robust critical mineral supply chain. More information is available at https://www.usgs.gov/centers/gggsc/science/critical-minerals-mapping-initiative-cmmi.

GS2024-2

Updated structural interpretations in the Bird River domain, southeastern Manitoba (parts of NTS 52L5, 6, 11, 12)

by M.L. Rinne and T. Martins

Summary

In 2023, the Manitoba Geological Survey began a project to revisit the Bird River domain, an area rich in critical minerals ranging from pegmatite-hosted commodities such as lithium, cesium, and tantalum, to ultramafic-associated commodities including nickel, chromium, and platinum-group elements. Recent findings relating to structural controls on the emplacement of rare-element-bearing pegmatites are described in this report. Combined with findings from past studies, results from this study suggest that the mineralized pegmatite dikes intruded in two dominant orientations during the start of brittle deformation in the Bird River domain: the first generally belt-parallel (following an overall eastward trend along reactivated shears, many following major lithological boundaries such as greenstone belt margins) and the second dominantly north-northeast-trending along late sinistral brittle-ductile shears.

In Brief:

- The Bird River domain contains a wide range of commodities and styles of mineralization
- Bedrock mapping in 2024 involved structural studies of rare-element–bearing pegmatites
- Findings suggest that mineralized pegmatite dikes intruded during the start of brittle deformation in the Bird River domain, in two dominant orientations

Citation:
Rinne, M.L. and Martins, T. 2024: Updated structural interpretations in the Bird River domain, southeastern Manitoba (parts of NTS 52L5, 6, 11, 12); *in* Report of Activities 2024, Manitoba Economic Development, Investment, Trade and Natural Resources, Manitoba Geological Survey, p. 4–9.

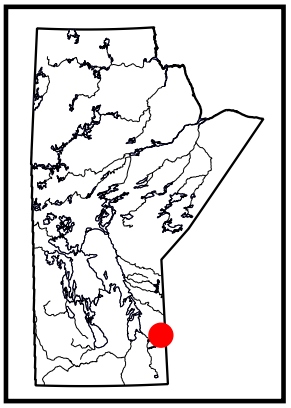
Introduction

During the summer of 2024, Manitoba Geological Survey (MGS) geologists and field assistants spent approximately five weeks documenting the bedrock geology of the Bird River domain, which included structural studies on pegmatite occurrences. This work was undertaken as part of a mapping and data compilation project in collaboration with the Geological Survey of Canada, University of New Brunswick, and MGS (Cawood et al., 2024; Hodder and Lian, 2024; Nambaje et al., 2024) to

- compile and digitize existing geoscience data—including regional and local geophysical survey data, recent mapping, and new mineral occurrence data—to produce a new geological map of the eastern part of the Bird River domain in southeastern Manitoba;
- evaluate the application of till exploration techniques in the region, particularly for pegmatite-associated commodities, including lithium (see Hodder and Lian, 2024 for more information);
- investigate structural controls on pegmatite emplacement in the region; and
- improve spatial coverage of known mineral occurrences and commodity types, ultimately allowing for more comprehensive evaluations of the timing, geodynamic setting, and structural controls on the various mineral systems in the Bird River domain.

Fieldwork in 2023 and 2024 was partly intended to document the structural geology of known pegmatite occurrences. While mapping and compilation are ongoing, recent structural findings provide an update to the preliminary structural model for pegmatite emplacement in the Bird River domain presented in this report. The updated model builds on past models (especially Kremer, 2010), with new details that highlight the role of both early (ductile) and later (brittle-ductile) structures in pegmatite emplacement and geometry.

Structural geology of the Bird River domain



The Bird River domain refers to all rocks north of the Winnipeg River domain (bounded by the poorly defined Winnipeg River fault) and south of the English River domain (bounded by the Cat Lake–Euclid Lake fault zone; Figure GS2024-2-1). Within the Bird River domain, supracrustal rocks south of the Maskwa Lake batholith make up the southern limb of the Bird River greenstone belt (see Gilbert, 2006; Gilbert et al., 2008) and pegmatites in that region are assigned to the Winnipeg River pegmatite district (Černý et al., 1981). Supracrustal rocks north of the Maskwa batholith (near the Cat Lake–Euclid Lake fault zone in Figure GS2024-2-1) are contiguous and likely cogenetic with the main part of the Bird River belt (Yang and Houlé, 2020). Pegmatites along that northern limb of the Bird River belt are assigned to the Cat Lake–Maskwa Lake pegmatite district (Černý et al., 1981).

The structural geology of the Bird River domain has been described by several workers, including Duguet et al. (2005), Duguet et al. (2009), Gilbert et al. (2008), Kremer and Lin (2006), and Kremer (2010). As summarized in Table GS2024-2-1, the study area records a relatively early episode of orog-

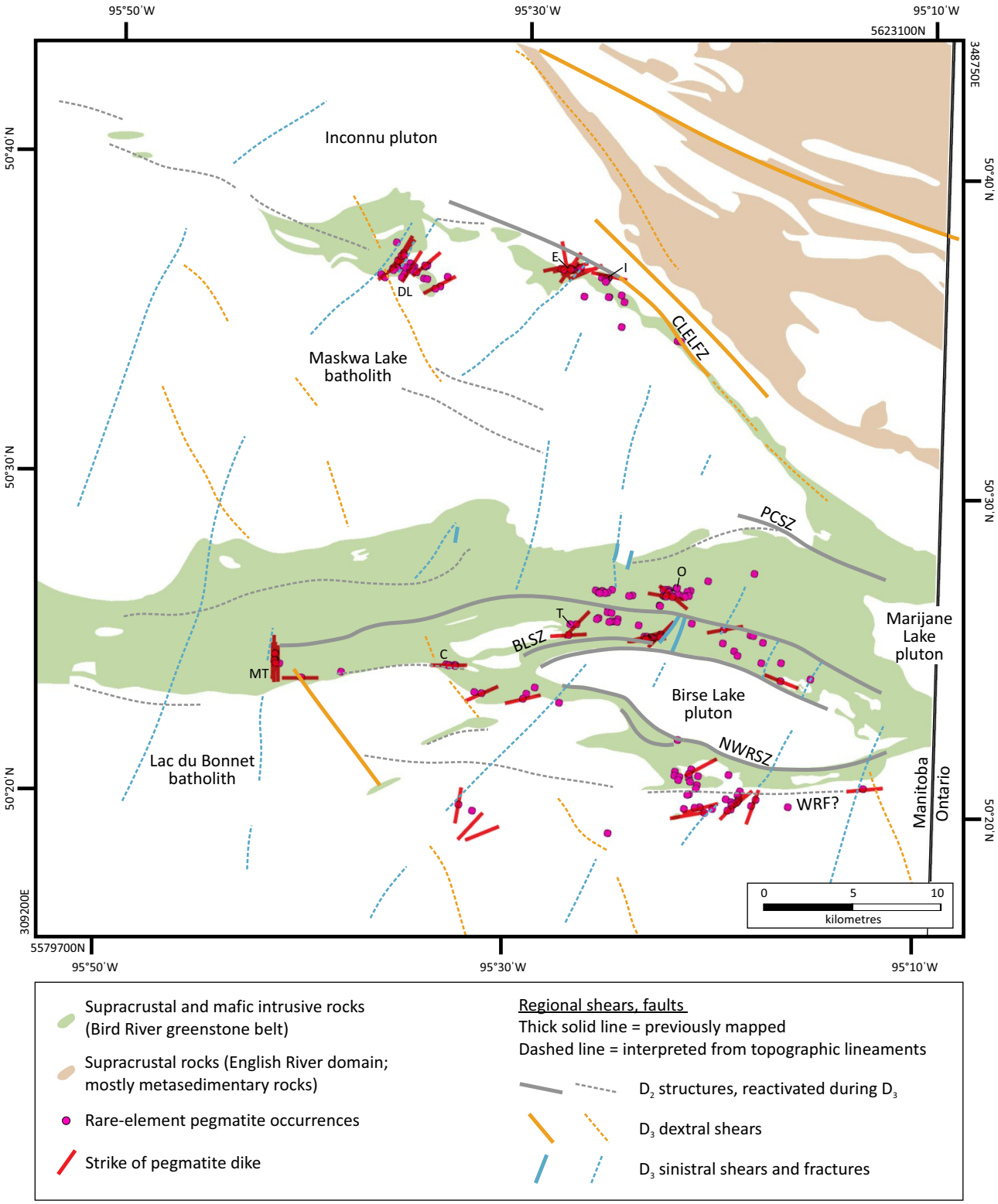


Figure GS2024-2-1: *Simplified map of the Bird River domain, with major structural elements labeled (modified from Martins et al., 2023). For clarity, lakes, rivers, and road networks are omitted, and background geology has been simplified to show only supracrustal-dominant and mafic intrusive units (i.e., approximate greenstone belt outlines). Rare-element–bearing pegmatite occurrences indicated with red dots are from Rinne (2024) and exclude barren (unmineralized or simple granitic) pegmatites, subsurface findings and questionable occurrences such as the Ben Group pegmatites. Red lines indicate the approximate strike of steeply dipping pegmatite dikes, compiled from a series of industry reports cited in Rinne (2024). Abbreviations for labeled structures: BLSZ, Bernic Lake shear zone; CLELFZ, Cat Lake–Euclid Lake fault zone; NWRSZ, North Winnipeg River shear zone; PCSZ, Peterson Creek shear zone; WRF, Winnipeg River fault. Abbreviations for selected pegmatite occurrences: C, Crocodile; DL, Donner Lake area (including West and Main dikes); E, Eagle; I, Irgon; MT, Matty and Tappy; O, Odd; T, Tanco. Corner co-ordinates are in UTM Zone 15, NAD83.*

Table GS2024-2-1: Summary of deformation events in the Bird River domain (after Kremer, 2010).

Deformation event	Related structures	Association with rare-element–bearing pegmatites
D_1	Rare, locally preserved isoclinal folds	Predates intrusion of pegmatites
D_2	Pervasive planar fabric in supracrustal rocks Upright isoclinal folds Formation-bounding shear zones with mostly vertical offset	Predates pegmatite intrusion, but D_2 structures are strong pre-existing fabric and commonly follow major rheological contrasts like greenstone belt margins; D_2 shears (reactivated during D_3) are sites of later pegmatite emplacement
D_3	Repeated reactivation of D_2 shear zones Conjugate near-vertical[1] brittle-ductile shears±fractures (NNE-trending sinistral±south-side-up; SE-trending dextral shears)	Initial pegmatite emplacement along D_2 shears (possibly ductile during intrusion; e.g., Oompa Loompa pegmatite), then into D_3 brittle-ductile shears (more brittle) Continued D_3 deformation results in pegmatites (all orientations) locally overprinted and crosscut by D_3 shears
D_4	Late brittle fractures (dominantly north-trending, subvertical; and northeast-southwest-trending, moderately dipping)	Postdates pegmatite intrusion

[1] In Tanco gabbro, late D_3 expressed as conjugate near-horizontal fractures (local vertical dilation?)

eny resulting in a strong pervasive planar fabric in most supracrustal rocks (D_2), with significant vertical displacement along D_2 structures. Most major units or crustal blocks in Figure GS2024-2-1, including the Birse Lake pluton and Maskwa Lake batholith, were in place prior to D_2 deformation; one younger exception is the Marijane Lake pluton (2645.6 ±1.3 Ma; Gilbert et al., 2008).

Regional deformation progressed to increasingly brittle failure during D_3, when south- or south-southeast-directed stresses were accommodated by a combination of reactivated D_2 shears and a set of conjugate, near-vertical, brittle-ductile D_3 shears. Deformation phases D_1–D_4, and the D_2–D_3 transition in particular, may represent stages of one prolonged orogenic episode; for example, Duguet et al. (2006) described the entire Bird River domain as a "pop-up structure assumed to have developed during a progressive single transpressive event."

The D_3 phase of deformation also records the first appearance of brittle deformation, manifest as brittle-ductile shears with small fracture planes, and minor fractures. Lithium-bearing pegmatites appear to have been emplaced specifically during (or at) the D_3 brittle-ductile transition, a finding emphasized by Kremer (2010) and further supported by recent bedrock observations described in this report.

A preliminary compilation of dike orientations (indicated by red lines in Figure GS2024-2-1) suggests that most of the pegmatite dikes in the Bird River domain are steeply or vertically dipping, and trend either parallel to the Bird River greenstone belt (approximately east-west; along reactivated D_2 shears) or approximately north to northeast (along D_3 structures; Figure GS2024-2-2). In general, pegmatites emplaced into reactivated D_2 shears show

1) overall high strain, some possibly developed during pegmatite cooling and/or during emplacement of repeated pegmatite injections (see Cawood et al., 2024);
2) some features consistent with emplacement into a hot ductile shear, such as bulbous lobate contacts, lack of well-developed chill margins or, in the case of the Oompa Loompa pegmatite, "incipient boudinage that is interpreted to record increments of [D_3] strain" (Kremer, 2010); and
3) a surface trend following the general trend of the Bird River greenstone belt and D_2 structures, generally east to southeast (Figure GS2024-2-1).

whereas pegmatites emplaced into brittle-ductile D_3 shears and fractures generally show

1) relatively low strain (though commonly overprinted by discrete brittle-ductile D_3 shears; e.g., Figure GS2024-20-2f);
2) features consistent with emplacement into brittle or brittle-ductile structures, such as near-planar margins parallel to the associated structures;
3) an overall north-northeast or northeast surface trend; and
4) slightly later emplacement than the D_2-parallel dikes.

Most of the D_3-parallel features documented in the field are clearly dikes (i.e., magmatic in origin and showing characteristics such as chill margins or complex zoning). However, a few of the thinner examples (such as the crosscutting spodumene- or quartz and spodumene-filled features in Figures GS2024-2-2b, d) have characteristics perhaps more consistent with a magmatic-hydrothermal transition. Further investigation could explore the possible role of late hydrothermal fluids in lithium mineralization or remobilization during late D_3 deformation.

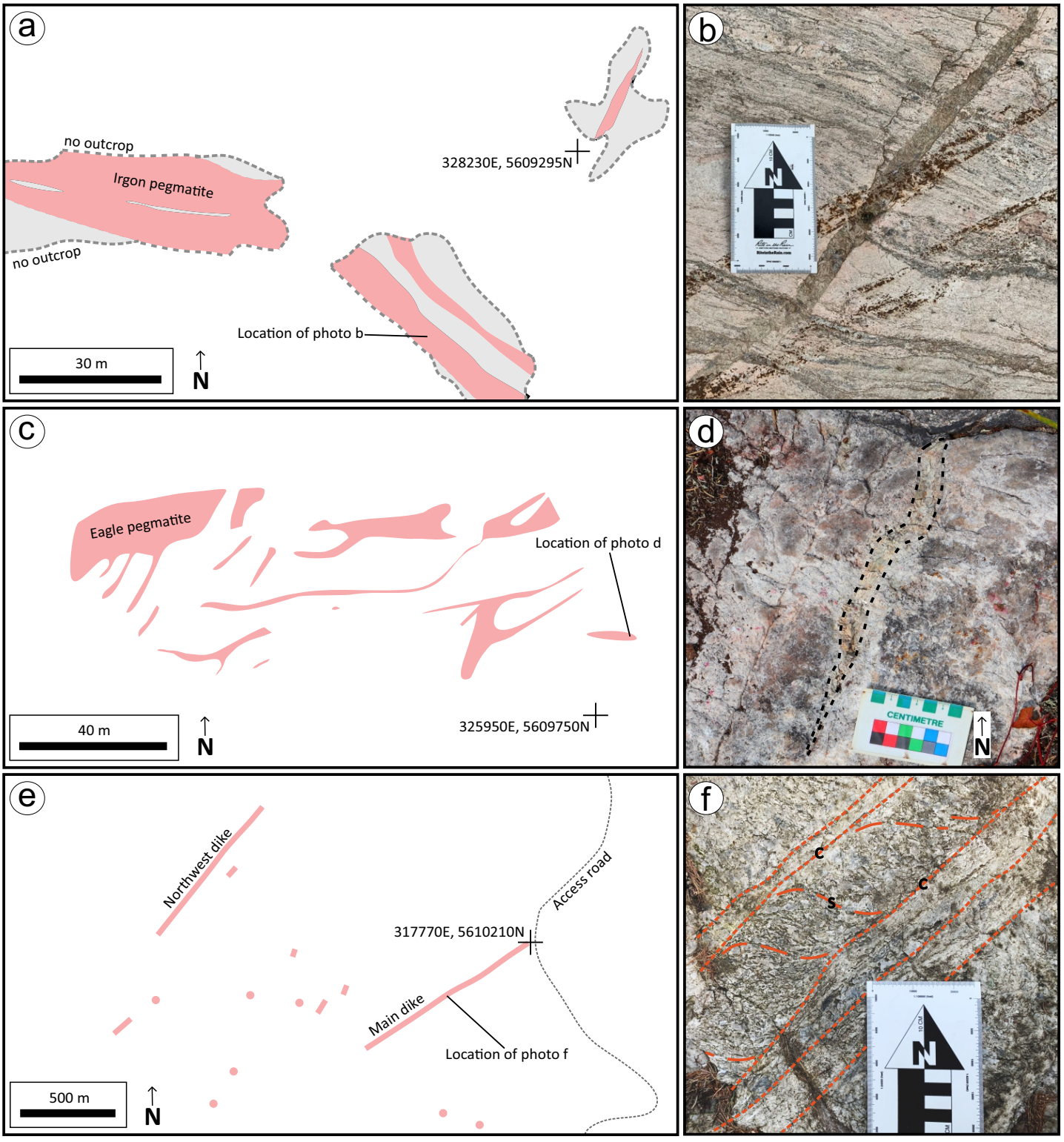


Figure GS2024-2-2: *Simplified pegmatite traces and outcrop photographs of selected occurrences in the Cat Lake–Maskwa Lake pegmatite district, showing* ***a)*** *a map of the eastern exposed portion of the Irgon pegmatite, with the main part of the dike locally bifurcated and striking parallel to the regional D_2 fabric, along with a north-northeast-striking and less-deformed spodumene-bearing dike to the northeast;* ***b)*** *sheared (by D_3) spodumene-bearing Irgon dike crosscut by north-northeast-striking brittle D_3 structures infilled with quartz and spodumene;* ***c)*** *outcrop map of the eastern part of the Eagle pegmatite, with the main or thickest portions following the regional D_2 fabric, and a series of apophyses striking north-northeast along D_3 structures;* ***d)*** *part of the Eagle pegmatite crosscut by brittle-ductile D_3 shears and associated late spodumene (outlined);* ***e)*** *map of pegmatite exposures near Donner Lake, with surface traces of the steeply-dipping Main and Northwest dikes labeled, along with pink dots and short line segments indicating the locations and trend of other pegmatite dikes;* ***f)*** *part of the northeast-striking Main dike, crosscut by northeast-striking D_3 shears with a sinistral C-S fabric (labeled). Eagle pegmatite outlines in panel c are simplified from detailed bedrock mapping (unpublished data from New Age Metals Inc., 2024). All co-ordinates are in UTM Zone 15, NAD83.*

The Eagle and Irgon pegmatites display higher D_3 strain along the D_2-parallel dikes and lower strain generally along north-northeast-striking (D_3 sinistral shear-hosted) dikes or apophyses. This is interpreted to reflect local partitioning of D_3 strain mostly along reactivated D_2 structures (and/or D_3 strain partitioned strongly along major lithological boundaries), as opposed to a generation of much earlier and more deformed lithium-bearing pegmatite.

In the Donner Lake area, pegmatite dikes are mostly steeply dipping and follow a north-northeast or northeast trend (Figure GS2024-2-2e). This includes the largest two dikes in the area, the Main and Northwest dikes, which have a combined inferred resource estimate of 6.81 Mt of ore grading 1.39% Li_2O (Millar et al., 2023). These dikes are interpreted to have been emplaced along D_3 sinistral brittle-ductile shears and were found to have been crosscut by the same set of structures (Figure GS2024-2-2f).

South of the Maskwa batholith (Winnipeg River pegmatite district), there are several north-northeast-trending pegmatite dikes, along with a series of likely related north-northeast-trending structures evident in previous mapping (thick blue lines in Figure GS2024-2-1) and prominent topographic lineaments. Both the Odd dike and the Crocodile pegmatite were found to have minor north- or north-northeast-trending apophyses from a D_2-parallel main dike, perhaps similar to the Eagle pegmatite dikes depicted in Figure GS2024-2-2c. It is also possible that the Matty and Tappy dikes are controlled by sinistral D_3 shears that trend northward in that part of the belt (Figure GS2024-2-1). In general, however, the relationship between rare-element-bearing pegmatites and late D_3 structures is currently not as clear in the Winnipeg River pegmatite district as it is in the Cat Lake–Maskwa Lake district.

Emplacement model for Li-bearing pegmatites

Based on a combination of past and recent field observations, and previous models (especially Kremer, 2010), the emplacement of rare-element-bearing pegmatite intrusions in the Bird River domain appears to have involved

1) During early D_3: ascent of highly fractionated magmas specifically along major reactivated D_2 shears such as the Bernic Lake shear zone. In some locations, injections along these reactivated structures may have occurred repeatedly to produce banded and variably strained pegmatite dikes (Cawood et al., 2024).

2) Late D_3: continued uplift, exhumation and/or cooling promote increasingly brittle rock failure. Continued south- or south-southeast-directed stress is partly accommodated along the reactivated D_2 shears, but they are at this point nearly perpendicular to the regional stress field; consequently, more shortening is being accommodated by a developing network of vertical, brittle conjugate structures that trend mostly north-northeast (with sinistral offset) and southeast (dextral offset).

3) Late D_3: continued proliferation of dilatant sites in D_3 structures, allowing for larger volumes of magma emplacement; at this time, rare-element-bearing magmas ascending along reactivated D_2 shears are also injected into the newly opened D_3 structures, particularly into the set of sinistral brittle-ductile shears and fractures trending north-northeast. Along with dikes, some late spodumene may precipitate in D_3-parallel veins, possibly from fluids derived from pressure-controlled exsolution and local accumulation of magmatic volatiles.

This sequence of events closely follows the genetic model proposed by Kremer (2010) for the Tanco pegmatite. One important exception is that in the Tanco area, while the conjugate D_3 brittle-ductile structures continued to form in a north-northwest-directed stress field, the least principal stress (or the direction of likely dilation for magma emplacement) apparently rotated from an east-west to a near-vertical axis (Kremer, 2010). This could reflect a transition from a wrench to a thrust regime in progressively shallowing crust during D_3. Alternatively, Kremer (2010) suggested that this simply reflects differing strain responses by different hostrock units, with the Tanco gabbro representing an unusually competent, large, and vertically oriented unit that was perhaps more prone to vertical dilation during the end of D_3.

Economic considerations

The Bird River domain is a geologically diverse and well-mineralized area, and study and compilation work is ongoing. With respect to rare element-bearing pegmatites specifically, recent findings and structural interpretations suggest targeting major D_2 shear zones, dilatant sites within those zones (e.g., jogs or releasing bends, especially viewed in a north–south section), D_3 shear zones, and zones where D_3 shears intersect D_2 structures or major lithological boundaries such as batholith margins.

Acknowledgments

Reviews of this report were provided by X.M. Yang and C. Couëslan. Fieldwork was possible thanks to site visits and logistical advice from geologists K. Roberts and L. Le Léannec (Grid Metals Corp.), and M. Kaczmer (Axiom Exploration Group Ltd.), along with the expert logistical support of C. Epp and P. Belanger, and field assistants J. Kristof (University of Manitoba) and K. Peters (University of Winnipeg).

References

Cawood, T.K., Beyer, S.R., Mohammadi, N., Lawley, C.J.M., Martins, T. and Rinne, M.L. 2024: Preliminary observations from the Cat Lake–Winnipeg River pegmatite field, southeastern Manitoba (parts of NTS 52L5, 6, 11): evidence for the effect of structural setting and emplacement mechanism on the size and morphology of lithium-bearing pegmatites; *in* Report of Activities 2024, Manitoba Economic Development, Investment, Trade and Natural Resources, Manitoba Geological Survey, p. 38–48.

Černý, P., Trueman, D.L., Ziehlke, D.V., Goad, B.E. and Paul, J. 1981: The Cat Lake–Winnipeg River and the Wekusko Lake pegmatite fields, Manitoba; Manitoba Energy and Mines, Mineral Resources Division, Economic Geology Report ER80-1, 215 p.

Duguet, M., Lin, S., Gilbert, H.P. and Corkery, M.T. 2005: Preliminary results of geological mapping and structural analysis of the Bird River greenstone belt, southeastern Manitoba (NTS 52L5 and 6); *in* Report of Activities 2005, Manitoba Industry, Economic Development and Mines, Manitoba Geological Survey, p. 117–124.

Duguet, M., Gilbert, H.P., Corkery, M.T. and Lin, S. 2006: Geology and structure of the Bird River Belt, southeastern Manitoba (NTS 52L5 and 6); *in* Report of Activities 2006, Manitoba Science, Technology, Energy and Mines, Manitoba Geological Survey, p. 170–183.

Duguet, M., Lin, S., Davis, D.W., Corkery, T.M. and McDonald, J. 2009: Long-lived transpression in the Archean Bird River greenstone belt, western Superior Province, Southeastern Manitoba; Precambrian Research, v. 174, no. 3–4, p. 381–407, URL <https://doi.org/10.1016/j.precamres.2009.09.001>.

Gilbert, H.P. 2006: Geological investigations in the Bird River area, southeastern Manitoba (parts of NTS 52L5N and 6); *in* Report of Activities 2006, Manitoba Science, Technology, Energy and Mines, Manitoba Geological Survey, p. 184–205.

Gilbert, H.P., Davis, W.D., Duguet, M., Kremer, P.D., Mealin, C.A. and MacDonald J. 2008: Geology of the Bird River Belt, southeastern Manitoba (parts of NTS 52L5, 6); Manitoba Science, Technology, Energy and Mines, Manitoba Geological Survey, Geoscientific Map MAP2008-1, scale 1:50 000.

Hodder, T.J. and Lian, O.B. 2024: Reconnaissance-scale Quaternary geology investigations to support lithium exploration in southeastern Manitoba (parts of NTS 52L, M, 62P, 63A); *in* Report of Activities 2024, Manitoba Economic Development, Investment, Trade and Natural Resources, Manitoba Geological Survey, p. 200–208.

Kremer, P.D. 2010: Structural geology and geochronology of the Bernic Lake area in the Bird River greenstone belt, Manitoba: evidence for syn-deformational emplacement of the Bernic Lake pegmatite group; M.Sc. thesis, University of Waterloo, Waterloo, Ontario, 91 p.

Kremer, P.D. and Lin, S. 2006: Structural geology of the Bernic Lake area, Bird River greenstone belt, southeastern Manitoba (NTS 52L6): implications for rare element pegmatite emplacement; *in* Report of Activities 2006, Manitoba Science, Technology, Energy and Mines, Manitoba Geological Survey, p. 206–213.

Martins, T., Rinne, M.L., Breasley, C. and Adediran, H. 2023: Preliminary results from field investigations in the Bird River domain of the Archean Superior province, Manitoba (parts of NTS 52L5, 6, 11, 12); *in* Report of Activities 2023, Manitoba Economic Development, Investment, Trade and Natural Resources, Manitoba Geological Survey, p. 4–13.

Millar, R., Saheed, F. and Ward, I. 2023: Mineral resource estimate for the Donner Lake lithium property southeastern Manitoba, Canada; NI 43-101 report prepared for Grid Metals Corp., 2 p., URL <https://gridmetalscorp.com/site/assets/files/5356/september6.pdf> [September 2024].

Nambaje, C., Martins, T., McFarlane, C.R.M., Kaczmer, M., Rinne, M.L. and Groat, L. 2024: Preliminary results from field investigations in the Cat Lake–Winnipeg River pegmatite field, southeastern Manitoba (parts of NTS 52L5, 6, 11, 12); *in* Report of Activities 2024, Manitoba Economic Development, Investment, Trade and Natural Resources, Manitoba Geological Survey, p. 10–26.

Rinne, M.L. 2024: Updates to the Manitoba Mineral Deposits Database; Manitoba Economic Development, Investment, Trade and Natural Resources, Manitoba Geological Survey, GeoFile 5-2024, Microsoft® Excel® file.

Yang, X.M. and Houlé, M.G. 2020: Geology of the Cat Creek–Euclid Lake area, Bird River greenstone belt, southeastern Manitoba (parts of NTS 52L11, 12); Manitoba Agriculture and Resource Development, Manitoba Geological Survey, Geoscientific Report GR2020-1, 105 p., map at 1:20 000 scale.

Note:

On November 7, 2024, GS2024-3 was updated with corrections to Figure GS2024-3-6 on page 16.

GS2024-3

Preliminary results from field investigations in the Cat Lake–Winnipeg River pegmatite field, southeastern Manitoba (parts of NTS 52L5, 6, 11, 12)

by C. Nambaje[1], T. Martins, C.R.M. McFarlane[1], M. Kaczmer[2,3], M.L. Rinne and L. Groat[4]

In Brief:

- The Cat Lake-Winnipeg River pegmatite field is highly prospective for elements considered critical
- Lithological and structural controls of rare-element mineralized pegmatites were noted regionally

Citation:
Nambaje, C., Martins, T., McFarlane, C.R.M., Kaczmer, M., Rinne, M.L. and Groat, L. 2024: Preliminary results from field investigations in the Cat Lake–Winnipeg River pegmatite field, southeastern Manitoba (parts of NTS 52L5, 6, 11, 12); *in* Report of Activities 2024, Manitoba Economic Development, Investment, Trade and Natural Resources, Manitoba Geological Survey, p. 10–26

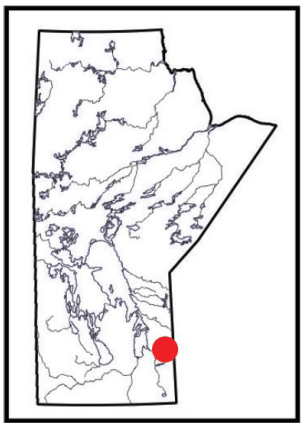
Summary

This report highlights preliminary results from detailed fieldwork that was conducted in the Cat Lake–Winnipeg River pegmatite field of southeastern Manitoba for the field season extending from May to July 2024. This work is a collaboration between the Manitoba Geological Survey (MGS), the University of New Brunswick (UNB), The University of British Columbia (UBC) and the exploration company New Age Metals. During fieldwork, numerous pegmatite groups and their hostrocks were examined and approximately 200 samples collected for further studies. Preliminary field investigations indicate that there are different generations of pegmatites. Some of them are simple and barren at their present surface (e.g., Eaglenest Lake pegmatite group, Axial pegmatite group and Birse Lake pegmatite group). Others are highly evolved and enriched in potential critical metals, including deposits of lithium, tantalum, tin, beryllium and cesium (e.g., Bernic Lake pegmatite group, Maskwa Lake pegmatite series, Eagle-Irgon pegmatite group, Lac du Bonnet pegmatite group, Shatford Lake pegmatite group, Greer Lake pegmatite group, Cat Lake pegmatite group and Rush Lake group). It has generally been noted that pegmatites emplaced in more mafic country rocks and/or intermediate country rocks are those that tend to be highly evolved and enriched in rare elements compared to those emplaced in more felsic country rocks, which are barren. The underlying cause of this observation will be addressed in future studies.

Introduction

Critical minerals have been identified as a priority for Canada. The Government of Canada updated a list of 34 minerals and metals considered critical for the sustainable economic success of the country and its allies, and to position Canada as the leading mining nation (Government of Canada, 2024). Several elements and minerals considered critical for economic success are found in rare-element pegmatites, including cesium, lithium, niobium, tantalum, tin and rare-earth elements (Linnen et al., 2012). Lithium is not only a critical element but also a key component in batteries for electric vehicles and consequently vital to Canada's commitment to climate action, environmental protection and economic growth.

The Cat Lake–Winnipeg River pegmatite field is well known for its multiple lithium-bearing pegmatites, particularly the world-class Tanco rare-metals pegmatite deposit. This pegmatite field is also known for its prospectivity for lithium and other critical elements (e.g., niobium, tantalum, cesium, tin, beryllium) hosted in granitic pegmatites (Černý et al., 1981). Most of the previous studies in this area focused on locally selected pegmatites (e.g., Camacho et al., 2012, 2014; Breasley et al., 2021, 2022, 2024; Martins et al., 2023; Roush et al., 2023; London, 2024), but the Cat Lake–Winnipeg River pegmatite field as a whole has not been studied on a regional scale or in detail since the late 1970s (Černý et al., 1981). Therefore, the present fieldwork focused on the regional geology of the entire Cat Lake–Winnipeg River pegmatite field.



Fieldwork for the 2024 season included detailed mineralogy and textural and structural observations, as well as sampling of different pegmatite types, hostrocks and pegmatite-related granite intrusions from the study area. Recent drillcores were also examined and sampled. Overall, the current project aims to infer the source of pegmatites, age, mode of emplacement, structural controls and how country-rock type influences the style of mineralization in rare-element pegmatites

[1] Department of Earth Sciences, University of New Brunswick, Fredericton, New Brunswick, claude.nambaje@unb.ca
[2] New Age Metals Inc., Richmond, British Columbia
[3] Axiom Exploration Group, Saskatoon, Saskatchewan
[4] Department of Earth, Ocean and Atmospheric Sciences, The University of British Columbia, Vancouver, British Columbia

of the Cat Lake–Winnipeg River pegmatite field. This information will contribute to a better understanding of the geological context of the pegmatite field, which will lead to better exploration for critical minerals and metals in the region.

Geological setting

This project focuses on the Cat Lake–Winnipeg River pegmatite field, located within the Neoarchean Bird River greenstone belt (BRGB) of the western Superior Province in southeastern Manitoba (Figure GS2024-3-1). The BRGB is part of an east-trending supracrustal belt that extends 150 km from Lac du Bonnet in the west to Separation Lake (Ontario) in the east (Figure GS2024-3-1; Percival et al., 2006a, b; Gilbert et al., 2008). The BRGB is in fault contact with the English River basin to the north and the Winnipeg River terrane to the south (Figure GS2024-3-1). It is divided into northern and southern arms that are separated by the Maskwa Lake batholith, which contains intrusive phases ranging in age from 2.85 to 2.73 Ga (Gilbert et al., 2008).

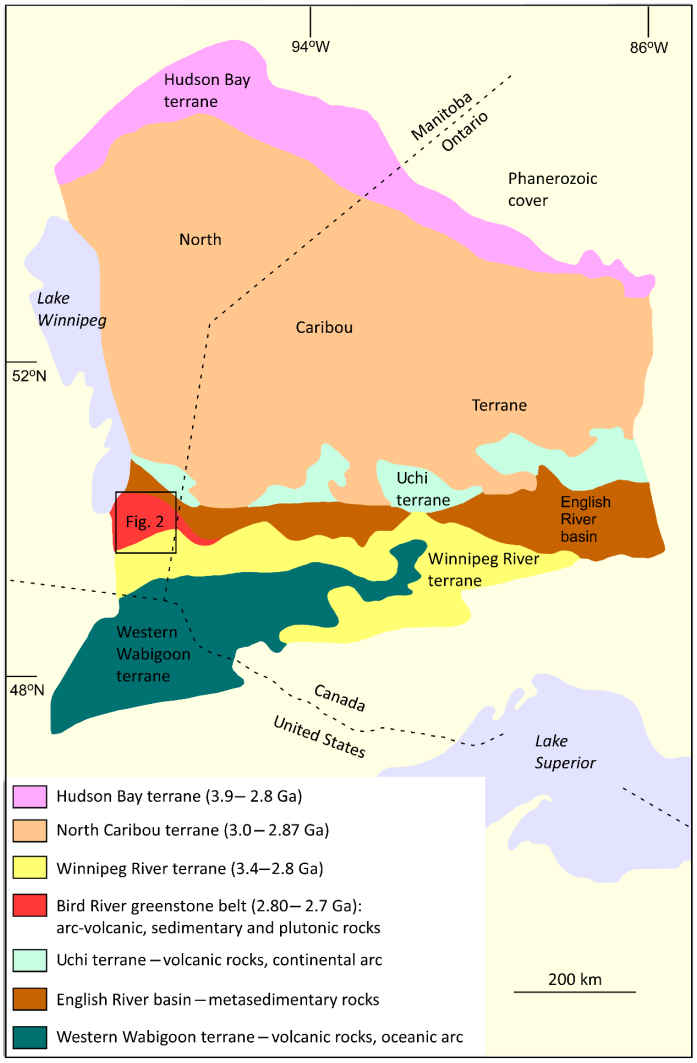


Figure GS2024-3-1: *Simplified geology of the northwestern Superior province, showing the regional geological setting of the Bird River greenstone belt (map after Gilbert et al., 2008; Yang and Houlé, 2020). Black box shows the location of Figure GS2024-3-2.*

The southern part of the BRGB has been subdivided into two sequences (northern and southern panels) that are geochemically distinct (Gilbert et al., 2008). Both are composed of ca. 2.75–2.72 Ga juvenile arc-type metavolcanic and associated metasedimentary rocks. These two panels are separated by the Booster Lake formation (< ca. 2.71 Ga; Gilbert, 2006; Gilbert et al., 2008), a turbiditic sequence with clastic sedimentary rocks from the fluvial-alluvial deposits of the Flanders Lake formation to the east (Gilbert, 2006; Gilbert et al., 2008; Mealin, 2008; Duguet et al., 2009; Kremer, 2010; Figure GS2024-3-2).

The northern part of the BRGB includes the Cat Creek–Euclid Lake area, underlain by a suite of greenstone assemblages formed in a continental-margin setting adjacent to the Mesoarchean Maskwa Lake batholith (Yang 2012, 2013, 2014; Yang and Houlé, 2020). The greenstone assemblages consist mainly of mafic–felsic volcanic and related intrusive rocks; epiclastic and minor volcaniclastic rocks; and mafic–ultramafic layered intrusions. These were intruded by younger phases of tonalite-trondhjemite rocks from a granodiorite suite (i.e., Maskwa Lake batholith II of Yang and Houlé, 2020), late peraluminous granitoid rocks and pegmatites (e.g., Yang et al., 2019; Yang and Houlé, 2020).

In terms of mineral occurrences and resources, the BRGB is endowed with a unique combination of Li-Ta-Cs rare-metal–bearing pegmatites (e.g., Tanco pegmatite; Martins et al., 2023; Rinne, 2023), shear-hosted gold mineralization and Ni-Cu-PGE-Cr minerals associated with mafic–ultramafic intrusions that may have been formed during an extensive Neoarchean Bird River magmatic event proposed by Houlé et al. (2013, 2015).

Results and discussion

Fieldwork was conducted on different pegmatite groups of the Cat Lake–Winnipeg River pegmatite field and their hostrocks. This pegmatite field was subdivided into two pegmatite districts, the Cat Lake–Maskwa Lake district in the north and the Winnipeg River district in the south. The pegmatites were separated into groups of spatially, mineralogically and geochemically related bodies (Černý et al., 1981). The Cat Lake–Maskwa Lake district includes the Maskwa Lake series (MWL), Eagle-Irgon group (EAI), Beryl-Tourmaline group (BET), Cat Lake group (CAT) and Central Claim group (CC). The Winnipeg River district includes the Shatford Lake group (SHL), Lac du Bonnet group (LdB), Greer Lake group (GL), Eaglenest Lake group (ENL), Axial group (AX), Birse Lake group (BIS), Rush Lake group (RL) and Bernic Lake group (BL; Figure GS2024-3-2).

Maskwa Lake pegmatite series (MWL)

In the MWL, the visited pegmatite is locally known as the 'Main dike' (Figure GS2024-3-2, sites CNM-88 and -89)[5]. It is a

[5] All site locations refer to Figure GS2024-3-2.

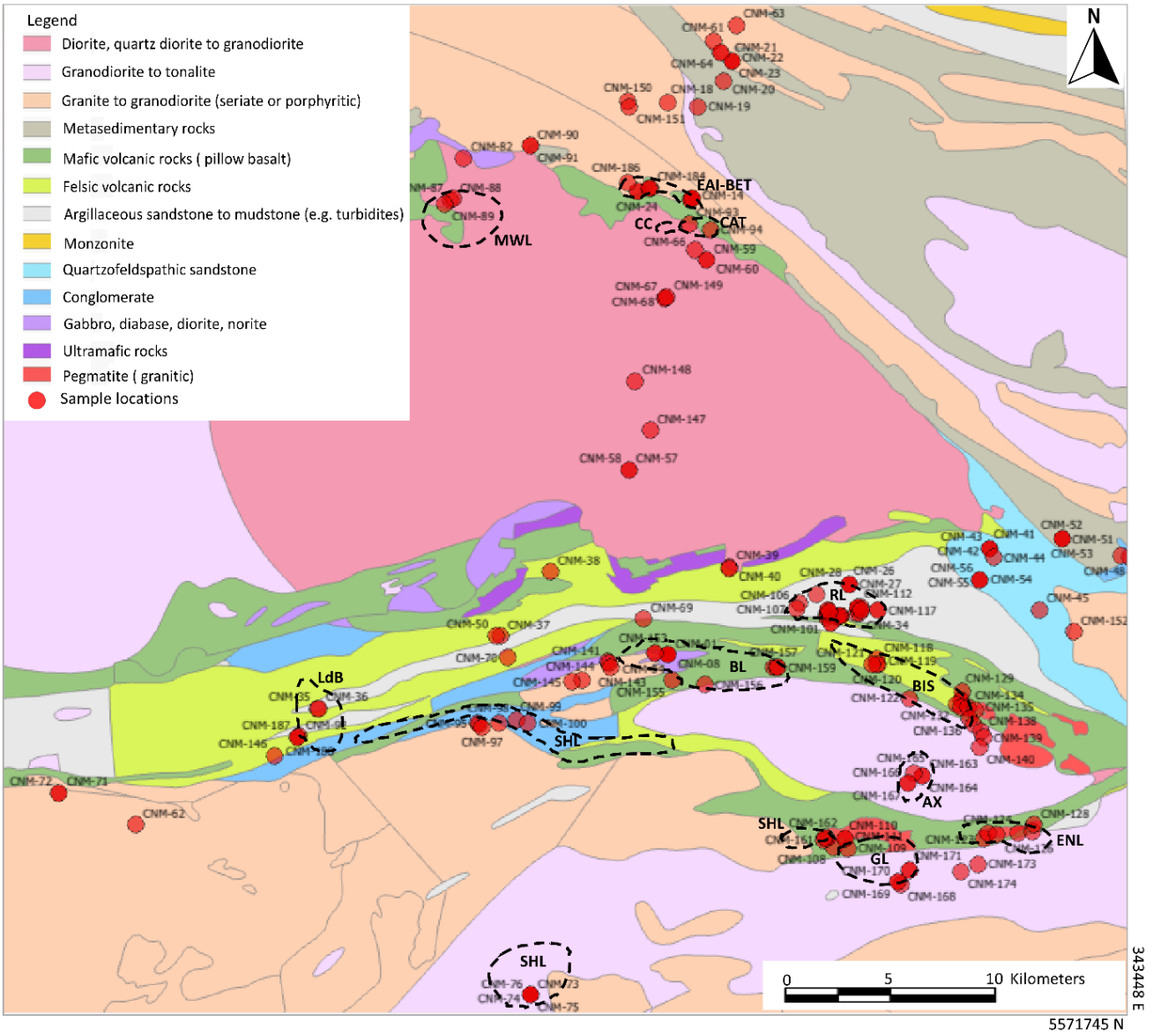


Figure GS2024-3-2: *Simplified geology of the Bird River Greenstone Belt (BRGB), modified from the 250 000 compilation map of the Manitoba Geological Survey (Černý et al., 1981, Gilbert et al., 2008; Yang, 2013), with locations investigated in this project from the Cat Lake–Winnipeg River pegmatite field and the English River basin. The dotted black outline indicates the different pegmatite groups (after Černý et al., 1981). Abbreviations: AX, Axial group; BET, Beryl-Tourmaline group; BIS, Birse Lake group; BL, Bernic Lake group; CAT, Cat Lake group; CC, Central Claim group; EAI, Eagle-Irgon group; ENL, Eaglenest Lake group; GL, Greer Lake group; LdB: Lac du Bonnet group; MWL, Maskwa Lake series; RL, Rush Lake group; SHL, Shatford Lake group.*

Li-rich spodumene-bearing pegmatite dike that is about 1.5 km long and 5 m wide, and more than 650 m deep (as per historical drilling). This pegmatite dike strikes N42°E and dips 74°NW, and is hosted by porphyritic anorthosite to metagabbro. The main foliation of the anorthosite gabbro is oriented N70°E, and the contacts of the pegmatite with the hostrock are sharp and marked by local patches of holmquistite in the metagabbro (Figure GS2024-3-3a). The observed mineralogy of this pegmatite includes plagioclase, quartz, muscovite, spodumene, K-feldspar, plagioclase and apatite. The spodumene is white, with a crystal size that can vary between 1 and 5 cm long (Figure GS2024-3-3b). This pegmatite dike is locally deformed and stretched in sinistral deflection. The main foliation strikes N46°E and the aplitic texture predominates the deformed portion.

Another pegmatite outcrop, locally named the 'Sand pegmatite', was observed northeast of the MWL (CNM-90). The Sand pegmatite is exposed for more than 15 m and is hosted in granodiorite with an irregular contact (Figure GS2024-3-3c). The mineralogy of this pegmatite includes biotite, plagioclase (±K-feldspar), quartz, garnet and accessory greenish beryl and black tourmaline (Figure GS2024-3-3d). No spodumene was observed in the outcrop and no drilling has been done on this pegmatite to check the subsurface mineralogical variations.

Eagle-Irgon pegmatite group (EAI)

In the Eagle-Irgon pegmatite group, the F.D. No. 5 pegmatite (CNM-17, 184 and 186), Eagle pegmatite (CNM-24) and Irgon

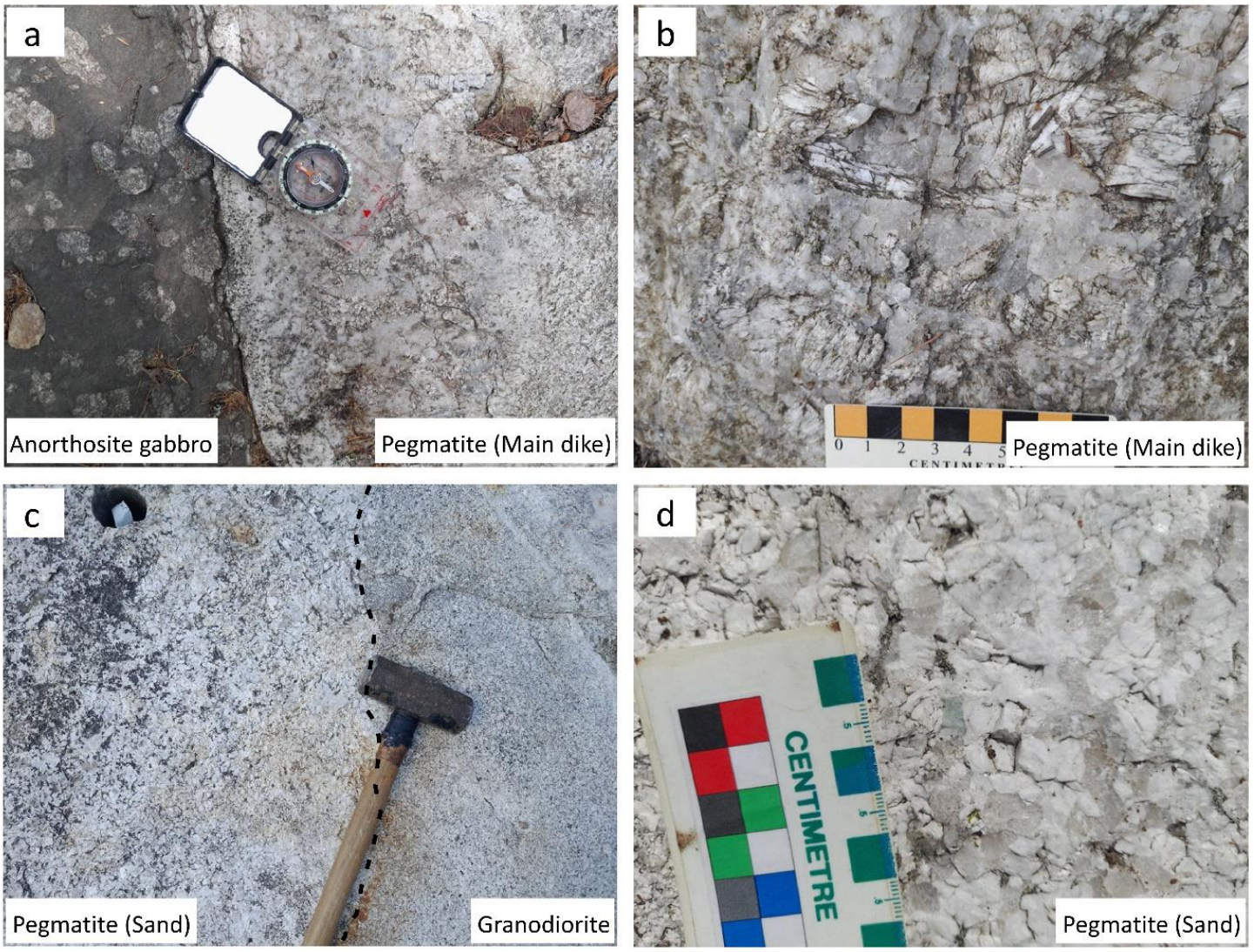


Figure GS2024-3-3: *Field photos of pegmatite in the Maskwa Lake Series (MWL):* ***a)*** *Li-rich spodumene-bearing pegmatite hosted by the porphyritic anorthosite metagabbro;* ***b)*** *pegmatite with white spodumene crystals that vary between 1 and 5 cm in length;* ***c–d)*** *pegmatite hosted in granodiorite with irregular contact and greenish beryl.*

pegmatite (CNM-14, 83, 85) were investigated in this study. The F.D. No .5 pegmatite is composed of green spodumene, K-feldspar, plagioclase, quartz, biotite, muscovite, black tourmaline, beryl and apatite. It is hosted in granodiorite, but part of the pegmatite narrows between the granodiorite and amphibolite (Figure GS2024-3-4a). The core zone of this pegmatite is enriched in hematized plagioclase and green spodumene (Figure GS2024-3-4b), while the wall-contact zone is enriched in K-feldspar, hematized plagioclase, quartz and beryl (Figure GS2024-3-4c). See Roush et al. (2023) for a more detailed mineralogical description of the F.D. No. 5 pegmatite.

The Eagle pegmatite is a Li-mineralized pegmatite hosted in a granodiorite, with holmquistite formation in the contact zone. The main Eagle pegmatite has an exposed thickness varying between 3 and 4 m, and strikes east and dips 80°S. The main minerals in this pegmatite are hematized plagioclase (±K-feldspar), quartz, muscovite and green spodumene. In the studied outcrops, the pegmatite has been subjected to sinistral shearing that is most evident in a narrow pegmatite vein from the same area (Figure GS2024-3-4d). Sinistral-sense movement/deformation is also related to north-northeast–trending fractures reflected in the main pegmatite dike (Figure GS2024-3-4e). Two generations of Li mineralization are observed in the field: the first occurs as disseminated spodumene within the easterly oriented pegmatite (Figure GS2024-3-4e and f), while the second occurs as north-northeast-trending fracture-filling spodumene (Figure GS2024-3-4f). See Roush et al. (2023) for a more detailed mineralogical description of the Eagle pegmatite.

Two different pegmatite dikes were observed at Irgon: the highly deformed Irgon pegmatite (Figure GS2024-3-5a–c) and the undeformed Irgon pegmatite (Figure GS2024-3-5d–g). The undeformed pegmatite (CNM-14 and 85) is found to the northeast, 60 m from the deformed pegmatite (CNM-83). Both dikes are Li mineralized and beryl occurs in the undeformed pegmatite as

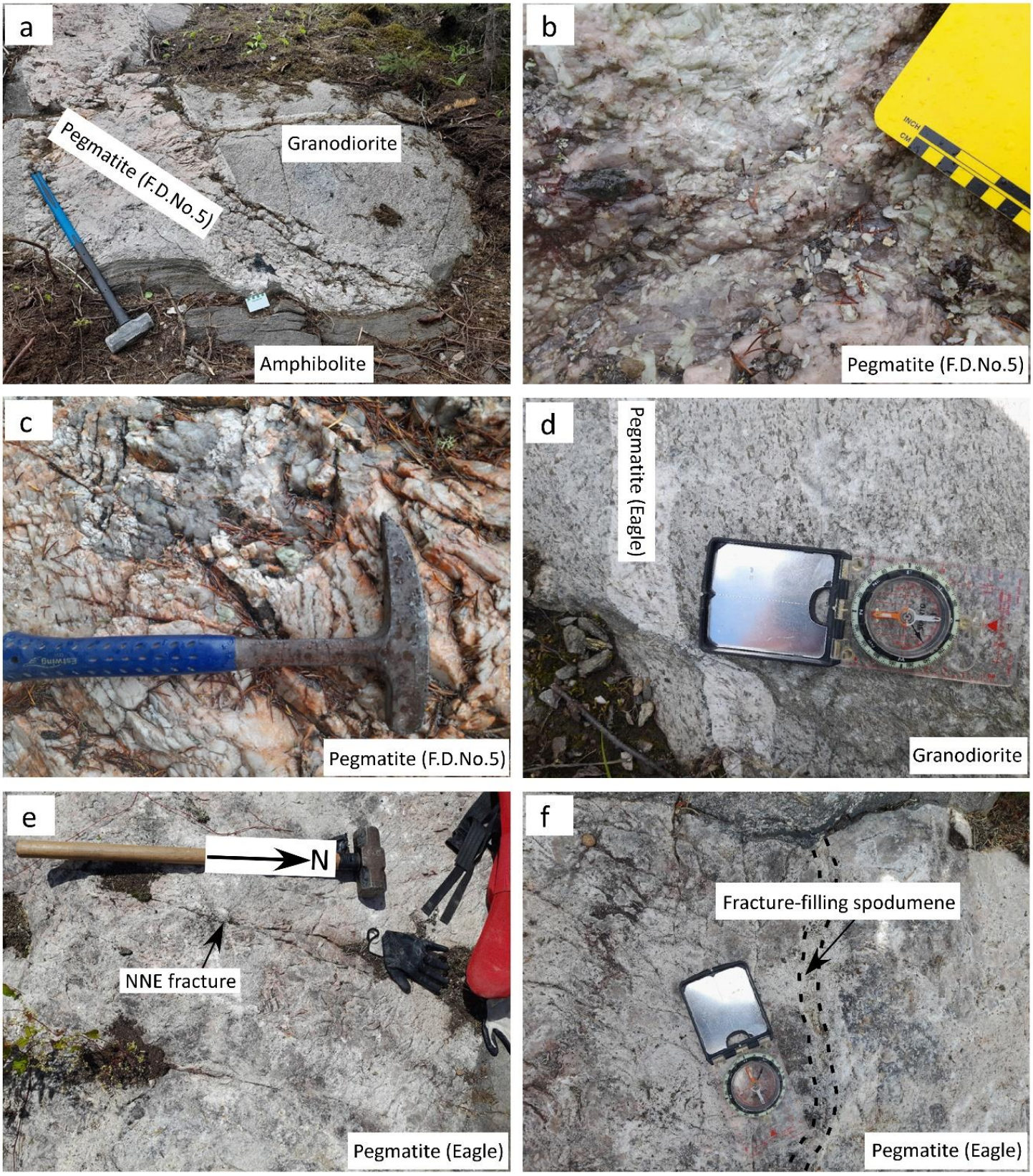


Figure GS2024-3-4: *Field photos of F.D. No. 5 and Eagle pegmatites:* ***a)*** *spodumene-bearing F.D. No. 5 pegmatite emplaced between granodiorite and amphibolite;* ***b)*** *F.D. No. 5 pegmatite core zone rich in hematized plagioclase and green spodumene;* ***c)*** *wall-contact zone rich in K-feldspar–hematized plagioclase, quartz and beryl;* ***d)*** *Eagle pegmatite subjected to sinistral sense of shear;* ***e)*** *related NNE fractures reflected in the wide pegmatite with primary spodumene;* ***f)*** *secondary Li-mineralization in the form of NNE-trending fracture-filling spodumene.*

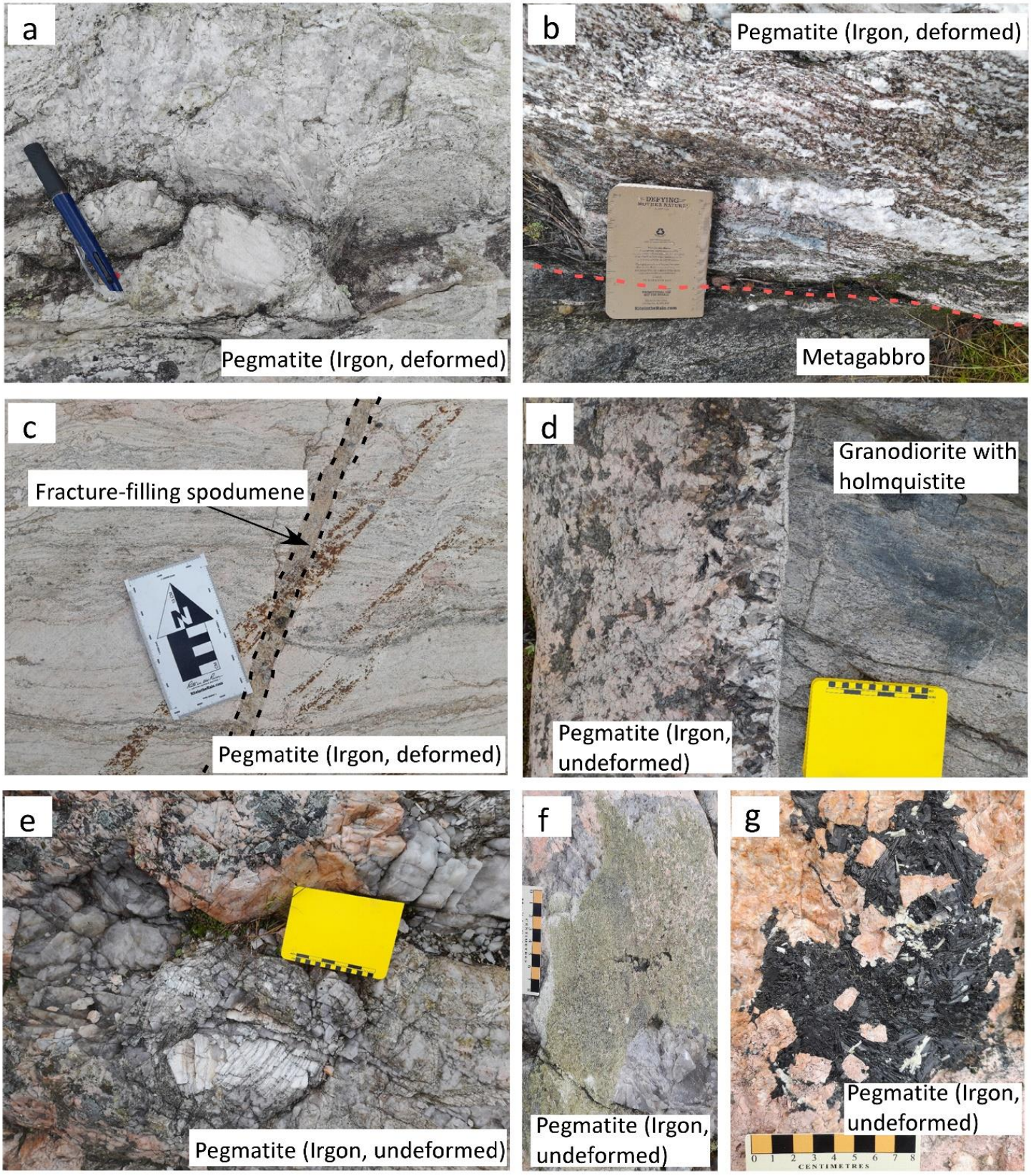


Figure GS2024-3-5: *Field photos of deformed and undeformed Irgon pegmatite:* ***a, b)*** *highly deformed pegmatite composed of spodumene (whitish, primary), plagioclase, greenish to whitish muscovite, garnet, bluish apatite and quartz;* ***c)*** *secondary Li mineralization appearing as fracture-filling spodumene that trends NNE (N40°E);* ***d)*** *undeformed pegmatite emplaced across the deformation fabric of the granodiorite;* ***e)*** *undeformed pegmatite with coarse spodumene (whitish) and hematized plagioclase (pinkish gradational colour); and* ***f)*** *undeformed pegmatite with greisen (agglomeration of greenish mica); and* ***g)*** *black tourmaline and beryl associated with pink K-feldspar.*

well. The highly deformed pegmatite is composed of spodumene (whitish, primary), plagioclase, K-feldspar, greenish to whitish muscovite, garnet, bluish apatite and quartz (Figure GS2024-3-5a and b). It is a very highly deformed pegmatite, highly foliated and sheared, with the foliation planes striking east to N50°W (Figure GS2024-3-5a–c). The pegmatite is emplaced parallel to the deformation fabric of the host metagabbro that contains holmquistite towards the contact. The thickness of this deformed pegmatite is 10–15 m; it is cut by a quartz vein striking N42°E and dipping 70°E. Late Li mineralization is present as a fracture-filling spodumene vein that trends N40°E (Figure GS2024-3-5c). This indicates that there are at least two stages of Li mineralization in this area, consistent with what was observed at the Eagle pegmatite. There are also minor north-trending fractures in the same deformed pegmatite that cut across the NNE-trending fractures.

The undeformed Irgon pegmatite is composed of spodumene (whitish), hematized plagioclase (pinkish gradational colour) with or without K-feldspar, muscovite (often greenish), quartz, greisen, black tourmaline and beryl (GS2024-3-5d–g). Its thickness ranges from 3 to 5 m and its strike is between N30°E and N40°E, with dip 70°E. It is hosted in a granodiorite and cross-cuts the general fabric of the hostrock (GS2024-3-5d). The granodiorite is enriched in holmquistite towards the contact with the pegmatite. This granodiorite is foliated N50°W, the same as in the nearby deformed Irgon pegmatite and its hostrock. The highly deformed pegmatite is endowed with later fractures that are oriented NNE (mainly N40°E), consistent with the trend of the undeformed pegmatite and later fracture-filling spodumene vein.

Cat Lake pegmatite group (CAT)

Two different pegmatite outcrops were studied this summer (CNM-93 and CNM-94), one near Cat Lake and another near Euclid Lake. Both are hosted in a fine- to medium-grained metamorphosed basalt (Figure GS2024-3-6a).

The pegmatite near Cat Lake is composed of plagioclase (hematized), greenish muscovite, quartz, K-feldspar, garnet (in the aplitic zone) and a few grains of spodumene (Figure GS2024-3-6b). This pegmatite is oriented N80°W to E-W, measures 20 m in width and is slightly deformed, with an E-W foliation defined by muscovite flakes GS2024-3-6a). The pegmatite outcrop near

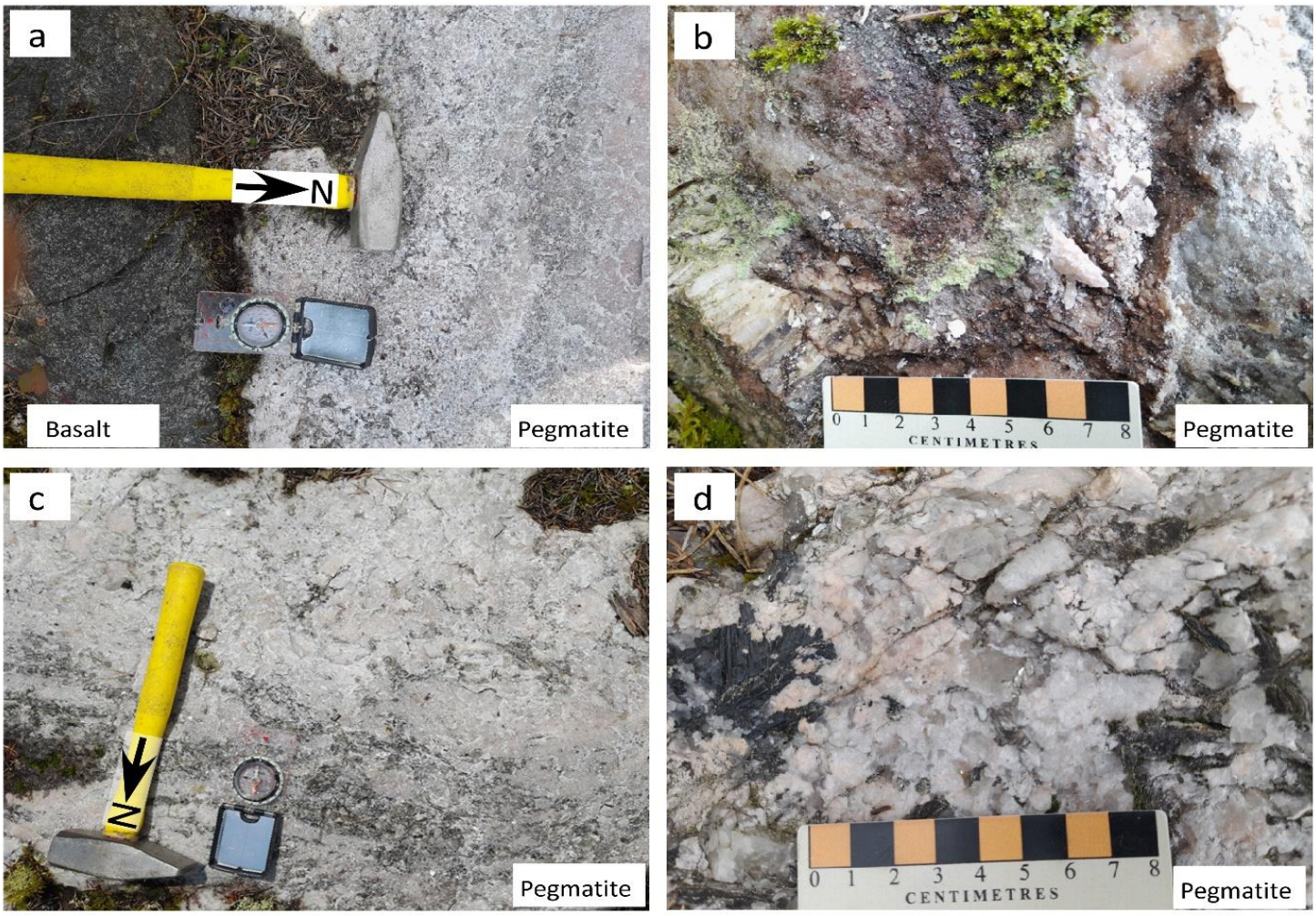


Figure GS2024-3-6: *Field photos of Cat Lake pegmatite group (CAT):* ***a)*** *E-W deformed pegmatite hosted in metabasalt near Cat Lake;* ***b)*** *pegmatite composed of plagioclase (hematized), greenish muscovite, quartz, K-feldspar, garnet (in the aplitic zone) and a few grains of spodumene, near Cat Lake;* ***c)*** *slightly deformed with an E-W foliation, near Euclid Lake;* ***d)*** *pegmatite composed of plagioclase, blocky K-feldspar or/and hematized plagioclase, quartz, greenish muscovite, garnet (in the aplitic zone), apatite and black tourmaline, near Euclid Lake.*

Euclid Lake 150 m long and up to 5 m wide. This dike strikes N60°E to E-W, with a dip of 70°NNW. It exhibits an E-W deformation pattern indicated by the alignment of muscovite flakes (Figure GS2024-3-6c). It is composed of plagioclase, blocky K-feldspar and/or hematized plagioclase, quartz, greenish muscovite, garnet (in the aplitic zone), apatite and black tourmaline (Figure GS2024-3-6c–d).

Shatford Lake pegmatite group (SHL)

The pegmatites investigated in this project area are the Crocodile pegmatite (CNM-99) Success pegmatite (CNM-100; northern side of the Lac du Bonnet batholith), Silverleaf pegmatite (CNM-108), Huron pegmatite (CNM-109), Annie pegmatite (CNM-110), two pegmatites (CNM-161, 162) located west of the Annie pegmatite (east side of the Lac du Bonnet batholith) and pegmatites at Point du Bois (CNM-74, 76; southeast side of the Lac du Bonnet batholith; *see* Figure GS2024-3-2).

The pegmatites on the north side of the Lac du Bonnet batholith intruded and cut the east-west deformation fabric of the host intermediate volcanic rock (andesite; Figure GS2024-3-7a). The Success pegmatite is 1 m thick, oriented N42°E and dips at 40°S. It is composed of plagioclase, muscovite, K-feldspar, quartz and garnet (which is predominant in the aplite portion of the pegmatite; Figure GS2024-3-7a). The Crocodile pegmatite is 1.5 m thick, oriented between N42°W and N60°W, and dips at 70°SSW. It is composed of coarse grains of plagioclase, smoky quartz, muscovite and an aplitic zone (often hematized) containing garnet, blue-green apatite, and accessory grains of cassiterite and tantalite (Figure GS2024-3-7b).

The Silverleaf pegmatite is a lithium-bearing pegmatite with a surface exposure of approximately 80 m by 45 m and is partially excavated. Previous studies indicate that the Silverleaf pegmatite was emplaced in metabasalt as a subvertical dike with a voluminous outer zone of garnetiferous aplite, and a complex stack of pegmatitic zones in the interior (Bannatyne, 1985; Camacho et al., 2012). It is composed of spodumene, quartz, feldspar, muscovite, lepidolite, garnet and apatite. The pegmatitic zone contains large spodumene (Figure GS2024-3-7c). Late lepidolite masses were observed filling a fracture within the outer zone of garnetiferous aplite (Figure GS2024-3-7d).

The Huron pegmatite is a niobium-yttrium-fluorine (NYF) pegmatite located amidst the dominant lithium-cesium-tantalum (LCT)–family pegmatites of the field (Černý, 1991). The Huron pegmatite is hosted in amphibolite and much of the outcrop has been mined out, hindering detailed field investigations. Previous studies indicate that the Huron pegmatite formed a subhorizontal, slightly saddle-shaped body at least 100 m by 30 m by 4 m in size (Camacho et al., 2014; Figure GS2024-3-7e). It consists of five concentric zones that are affected by three late assemblages of metasomatic veining: 1) aplitic border zone; 2) graphic pegmatite zone that is thin and intermittent, with quartz, oligoclase, K-feldspar, biotite and rare garnet; 3) medium- to coarse-grained (1–8 cm) albitic wall zone containing subordinate quartz, biotite and muscovite; 4) blocky intermediate to core-margin zone of K-feldspar with locally abundant quartz; and 5) quartz core, apparently segmented into several isolated pods. This concentric zonal pattern is only insignificantly disturbed by a fine- to medium-grained albitic replacement unit, which is locally developed in the blocky zone and cut by late anastomosing albite veinlets (Camacho et al., 2014).

A late hydrothermal assemblage of Ca>Mg, Fe-bearing minerals (such as epidote, chlorite, bavenite, titanite and probably fersmite) fills miarolitic cavities and fissures, or replaces primary minerals (such as albite and beryl; Camacho et al., 2014). The albitic wall zone (zone 3) is by far the main carrier of the rare-element mineral assemblage of beryl, zircon, thorite, uraninite, niobian rutile, columbite-group minerals, gadolinite-(Y), microlite, and monazite-(Ce; Camacho et al., 2014). Stringers of columbite-(Fe)-tantalite, uraninite, and monazite-(Ce) commonly follow fractures, occasionally accompanied by quartz veinlets, and they locally branch from the fractures into the feldspar matrix (Figure GS2024-3-7f). However, all of these minerals are members of a single, paragenetically coherent suite generated within the pegmatite body. No evidence is available for either different relative ages of individual minerals or of their associations, or their introduction from outside the pegmatite body as genetically unrelated material. Additional information on the Huron pegmatite is available in Paul (1984) and Camacho et al. (2014).

The Annie pegmatite and two pegmatites located to the west of it (east side of the Lac du Bonnet batholith) are exposed as coarse-grained pegmatite, often with a voluminous zone of garnetiferous aplite, hosted in a green mica–rich granite (Figure GS2024-3-7g). The contact between pegmatite and granite appears to be gradual and not obvious from field observation. However, recent geophysical data (New Age Metals, unpublished data) indicate that these pegmatites occur along the demagnetized E-W corridor in a granite, where this corridor is characterised by a strong K-Th-U radiometric anomaly. This granite is composed of plagioclase, K-feldspar, green muscovite, quartz and garnet. It is similar to Neoarchean S-type granites characterized by very low magnetic susceptibility values and emplaced along or proximal to tectonic boundary zones in the region (Yang et al., 2019). The pegmatites are composed of K-feldspar, muscovite, plagioclase and quartz, and garnet in the aplite zone. The garnet-bearing aplitic bands trend E-W within the pegmatite and are consistent with E-W deformation fabrics observed in the region (Figure GS2024-3-7g).

The pegmatite at Point du Bois (southeast side of the Lac du Bonnet batholith) appears as pink pegmatite that intrudes granodiorite (Figure GS2024-3-7h). The pegmatite dike varies in strike between N-S and N30°E, and dips at 70°W. Its thickness ranges between 1 and 2 m in the outcrop and appears not to have any zoning. It is composed of K-feldspar, biotite, muscovite and quartz.

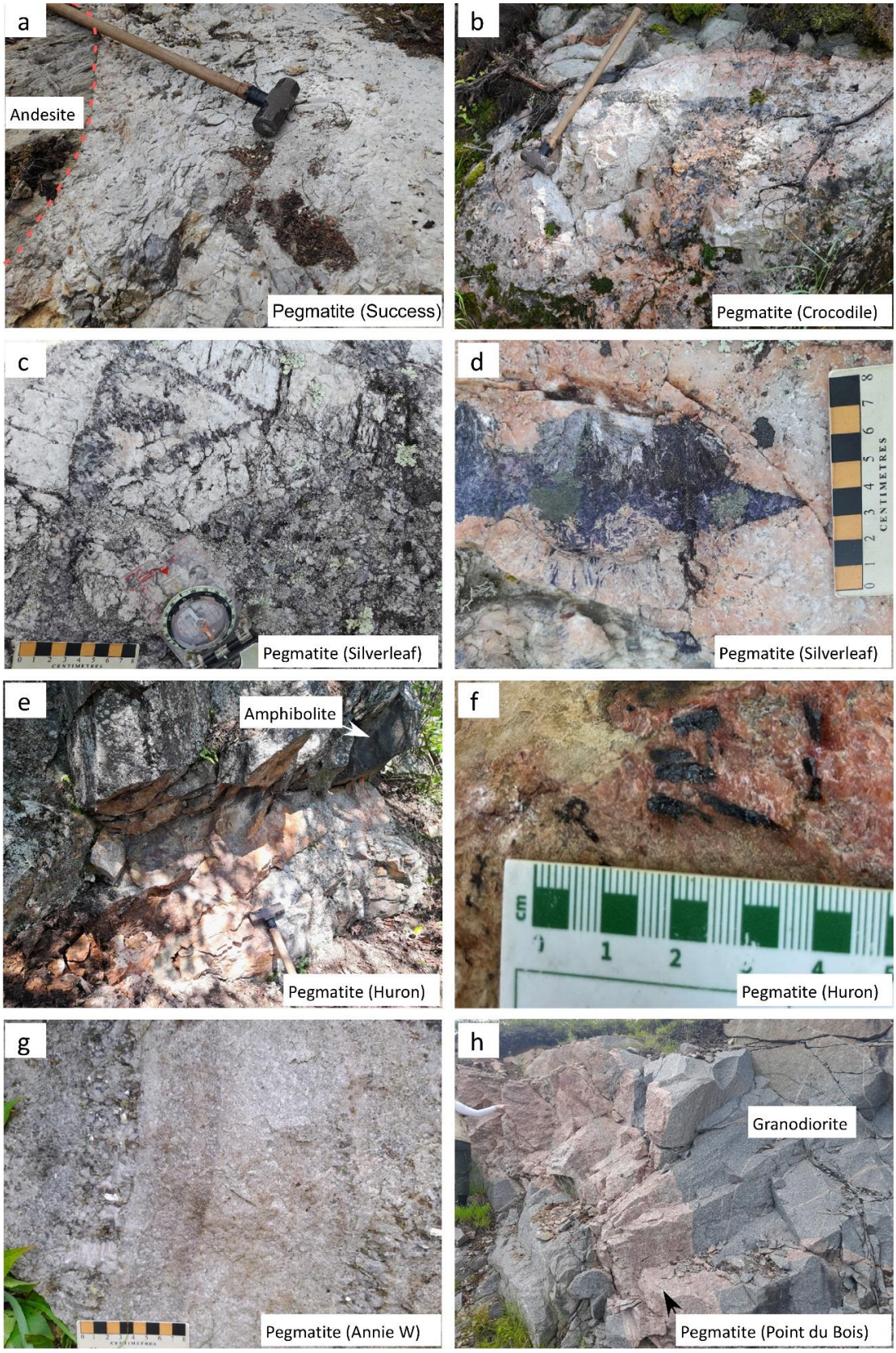


Figure GS2024-3-7: *Field photos of Shatford Lake pegmatite group (SHL):* ***a)*** *pegmatite intruding and cutting the deformation fabric of the hostrock andesite;* ***b)*** *pegmatite with coarse grains of plagioclase, smoky quartz, muscovite and an aplitic zone that is often hematized;* ***c)*** *pegmatite with large spodumene (white in colour);* ***d)*** *late lepidolite aggregate as fracture filling in the pegmatite;* ***e, f)*** *tantalite-mineralized, K-feldspar–rich pegmatite hosted in amphibolite;* ***g)*** *coarse-grained pegmatite (hosted in a green mica–rich granite) with E-W garnet-bearing aplitic bands within the pegmatite;* ***h)*** *pink (K-feldspar–rich) pegmatite intrusion in the granodiorite.*

Lac du Bonnet pegmatite group (LdB)

The Lac du Bonnet pegmatite group belongs to the widespread class of well-differentiated, blocky lithium pegmatites with primary zonal spodumene (Černý et al., 1981). This pegmatite group includes the Tappy and Matty Li-rich spodumene-bearing pegmatites that were studied in this project (CNM-92, -187, -188; Figure GS2024-3-2). The Tappy pegmatite, studied in detail by Roush et al. (2023), consists of feldspar, muscovite, quartz, spodumene and tantalite. It is exposed for more than 50 m with a N-S orientation and its width ranges between 1.5 and 4 m (Bannatyne, 1985; Roush et al., 2023). It is hosted in a metamorphosed pillow basalt and has a main foliation striking N63°E. See Roush et al. (2023) for a more detailed description of the Tappy pegmatite. The Matty pegmatite is hosted in a silicified meta-andesite and its emplacement cuts across the main fabric of the hostrock (Figure GS2024-3-8a). It strikes between N-S and N10°E, and dips 70°W based on surface measurements, but it appears that the body actually dips eastward, based on drilling intercepts (New Age Metals, unpublished drilling data), while the main foliation of the hostrock strikes N60°E. The Matty pegmatite consists of plagioclase, muscovite (greenish), quartz, spodumene (slightly greenish), hematized plagioclase (or K-feldspar) and tiny black minerals with metallic lustre that could be tantalite (Figure GS2024-3-8b).

Greer Lake pegmatite group (GL)

The Greer Lake pegmatites are dominantly concordant bodies that pinch and swell within the foliation of the host tonalitic gneiss/granodiorite, both along strike and downdip (Černý et al., 1981). The Jewel pegmatite (CNM-169) and Grace One pegmatite (CNM-171) were visited (Figure GS2024-3-2). The major outcrop of the Jewel pegmatite has been mined out (for beryl), thus limiting detailed field investigations; however, its emplacement is parallel to the foliation of the hostrock (granodiorite; Figure GS2024-3-9a). The jewel pegmatite contains coarse grains of K-feldspar, biotite, quartz, beryl and garnet (Figure GS2024-3-9b-c). The Grace One pegmatite, which was also historically mined for beryl, is oriented N44°E, parallel to the foliation of the hostrock. It is approximately 10 m wide and appears to have emplaced along a contact between granodiorite and granite. This pegmatite is composed of very coarse grains of muscovite, quartz, plagioclase and occasional beryl and K-feldspar (Figure GS2024-3-9d). Garnet appears in some portions of the pegmatite that are hematized.

Eaglenest Lake pegmatite group (ENL)

The Eaglenest Lake pegmatites visited during this project were CNM-123, -124, -125, -127 and -128 (Figure GS2024-3-2). The Eaglenest Lake pegmatites are hosted in granite and their contact with the hostrock appears gradational. These dikes seem to be pegmatitic phases transitioning from leucogranite with the same mineralogy (Figure GS2024-3-10a). Internally, the dikes are homogeneous or slightly concentrically zoned, with medium-grained albite+quartz+K-feldspar along the margins, passing gradually into a coarse blocky K-feldspar+quartz core with green mica (muscovite; Figure GS2024-3-10b–d). Garnet is usually found close to the margins. The Eaglenest lake pegmatites are barren at their present erosional surface.

Axial pegmatite group (AX)

The Axial pegmatite group is located in the Birse Lake granodiorite (e.g., CNM-165, -166; Figure GS2024-3-2). These pegmatites are generally concordant with the E-W foliation of this granodiorite body (Figure GS2024-3-11a). They pinch and swell, with attendant warping of the foliation. These pegmatites are composed of K-feldspar, plagioclase, green muscovite

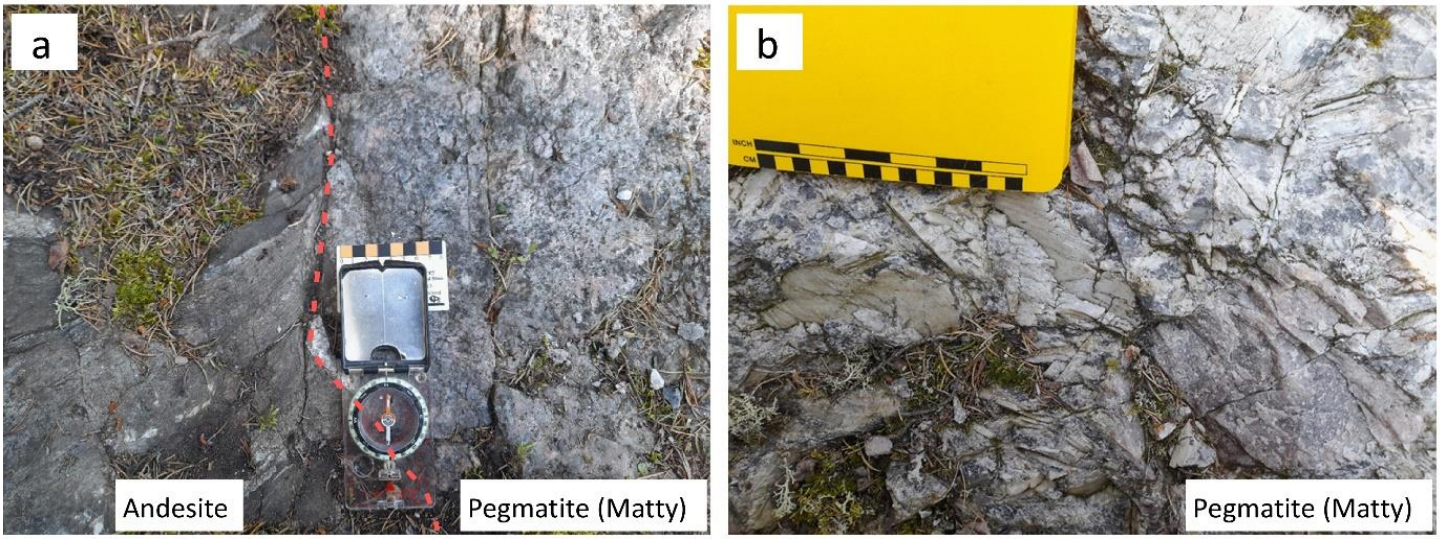


Figure GS2024-3-8*: Field photos of the Lac du Bonnet pegmatite group (LdB):* ***a)*** *pegmatite emplaced in silicified-metamorphosed andesite and cutting across the main fabric of the hostrock;* ***b)*** *Li-mineralized pegmatite with coarse primary spodumene (slightly greenish).*

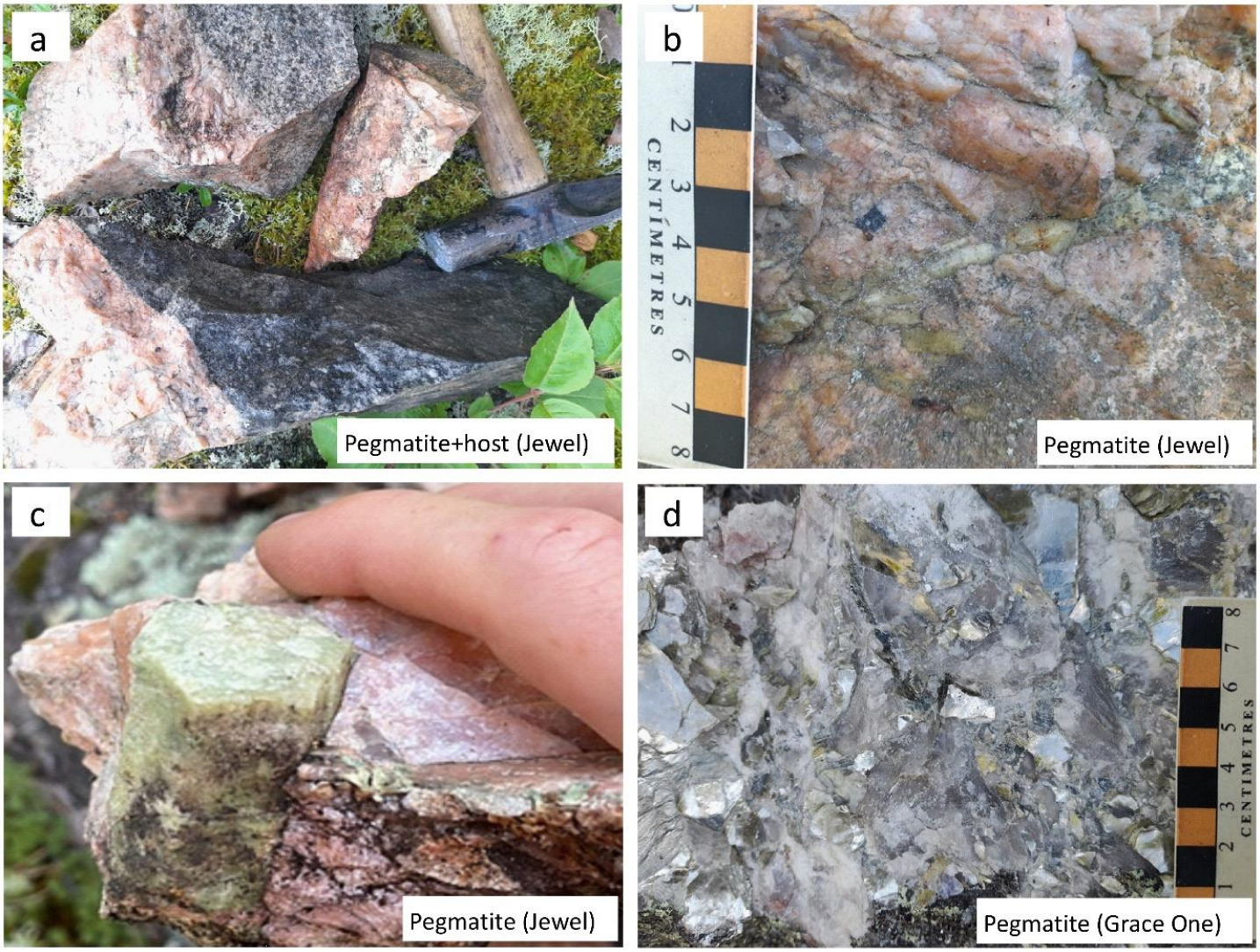


Figure GS2024-3-9: *Field photos of the Greer Lake pegmatite group (GL):* ***a)*** *beryl-mineralized pegmatite hosted by granodiorite;* ***b)*** *pink (K-feldspar–rich) pegmatite with beryl mineralization;* ***c)*** *euhedral Beryl (greenish) from the Jewel pegmatite;* ***d)*** *book of muscovite–rich pegmatite at the Grace One pegmatite.*

and quartz, often with dotted brown and black garnet (Figure GS2024-3-11b). In the Birse Lake pluton, there are some other pegmatite dikes that cut across the foliation of this body (Figure GS2024-3-11c). The observed crosscut pegmatite has biotite in addition to the main minerals of the other pegmatites indicated above (Figure GS2024-3-11d). Contacts of the Axial pegmatite group with the host are sharp (Figure GS2024-3-11a, c), implying a late emplacement of the pegmatite into the granodiorite. No rare-element minerals have been observed in Axial pegmatite group. These pegmatites are barren at their present surface, which corroborates the observations made by Černý et al. (1981).

Birse Lake pegmatite group (BIS)

This pegmatite group extends from Tin Lake to northwest of the north end of Birse Lake and the southeastern part of Osis Lake (Černý et al., 1981). In this group, the visited pegmatite locations are CNM-119, -121, -129, -130 and -132 (Figure GS2024-3-2). In the northwestern part, a huge outcrop of ONW pegmatite (CNM-119 and -121) investigated for this project appears in the zone with a high radiometric anomaly (New Age Metals, unpublished geophysical data). This pegmatite is composed of abundant coarse K-feldspar, black tourmaline, biotite, quartz, muscovite and accessory garnet (Figure GS2024-3-12a). It strikes almost E-W, parallel to the deformation fabric of the hostrock, and dips 70°S. The hostrock is an intermediate metavolcanic unit, possibly a deformed andesite. In the southeastern part (Tin Lake pegmatites), some of the visited pegmatites appear as dikes oriented N-S and dipping subvertically to 80°W These are around 20 m wide and cut across the deformed intermediate volcanic rock (andesite) with a foliation striking N44°W and dipping 72°NE. However, some others appear as massive bodies of pegmatite to pegmatitic granite with the same mineralogical composition as the elongated dikes and are often evolved, with high contents of muscovite and dotted black tourmaline (Figure GS2024-3-12b).

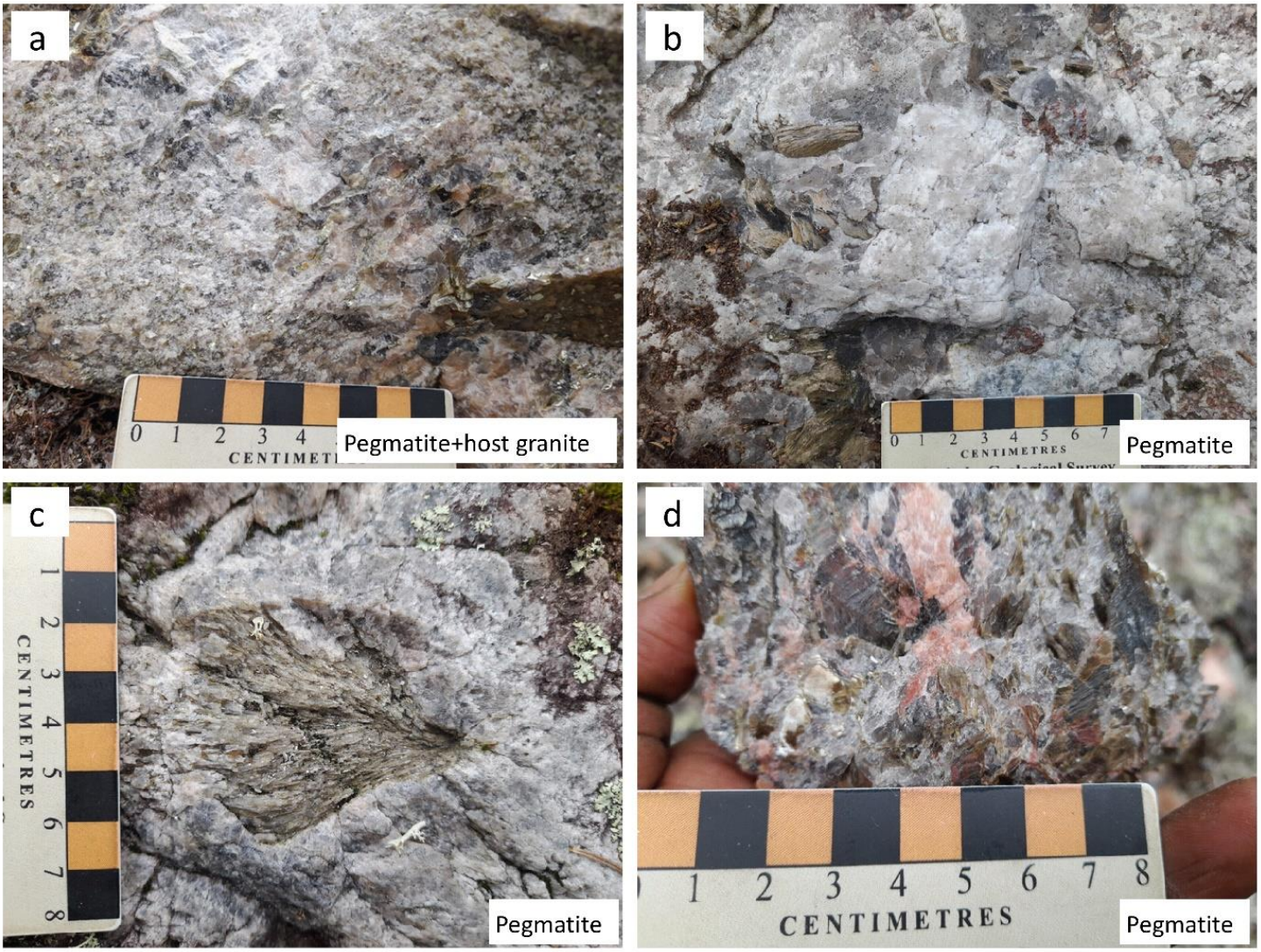


Figure GS2024-3-10: *Field photos of the Eaglenest Lake pegmatite group (ENL):* ***a)*** *pegmatitic phases transitioning from leucogranite with the same mineralogy;* ***b–d)*** *pegmatite composed of coarse, blocky K-feldspar+quartz core with green mica (muscovite).*

Previous studies classified the Birse Lake pegmatite group as not very differentiated, weakly albitized, beryl-bearing, blocky, muscovite-microcline pegmatites with incipient tendency to more diversified mineralization only in the most fractionated bodies (Černý et al., 1981). However, no rare-metal mineralization was observed in the exposed pegmatites during the current fieldwork.

Rush Lake pegmatite group (RL)

This pegmatite group is located north and west of Rush Lake, and west of the westernmost extent of the Osis Lake pegmatitic granite (Černý et al., 1981). In this group, the visited pegmatite locations are CNM-26, -27, -29, -31, -32, -34, -101, -104 (Blue Bird pegmatite), -105 (Odd pegmatite), -106 (Odd-west pegmatite) and -107 (Cubo/Stannite pegmatite), along with related drillcores CNM-114, -115, -175, -176, -180, -183, -189 and -190 (Figure GS2024-3-2). The Rush Lake pegmatites are generally concordant with the layering and E-W foliation of their hostrocks (e.g., CNM-26, -27, -31, -32, -105, -106 and -107), with only minor local discordances at very low angles (e.g., CNM-29, -34, -101 and -104). The contact reaction is commonly characterized by formation of black tourmaline between the pegmatite and metasedimentary hostrock (Figure GS2024-3-13a). Some of the E-W–oriented pegmatites were subjected to N-S fracturing in both the pegmatite and the hostrock (Figure GS2024-3-13a). However, the emplacement of pegmatite often filled both the E-W and N-S openings (Figure GS2024-3-13b).

Rush Lake pegmatites are generally composed of plagioclase, green muscovite, K-feldspar, quartz, black tourmaline and garnet (Figure GS2024-3-13c, d). A difference in mineralogy is the blue tourmaline observed at the Blue Bird pegmatite (Figure GS2024-3-13d). The Blue Bird pegmatite outcrops over more than 50 m^2 and trends N60°E. Rare-element mineralization, such as Ta and Nb-oxide minerals, occurs mostly as small irregular grains and is

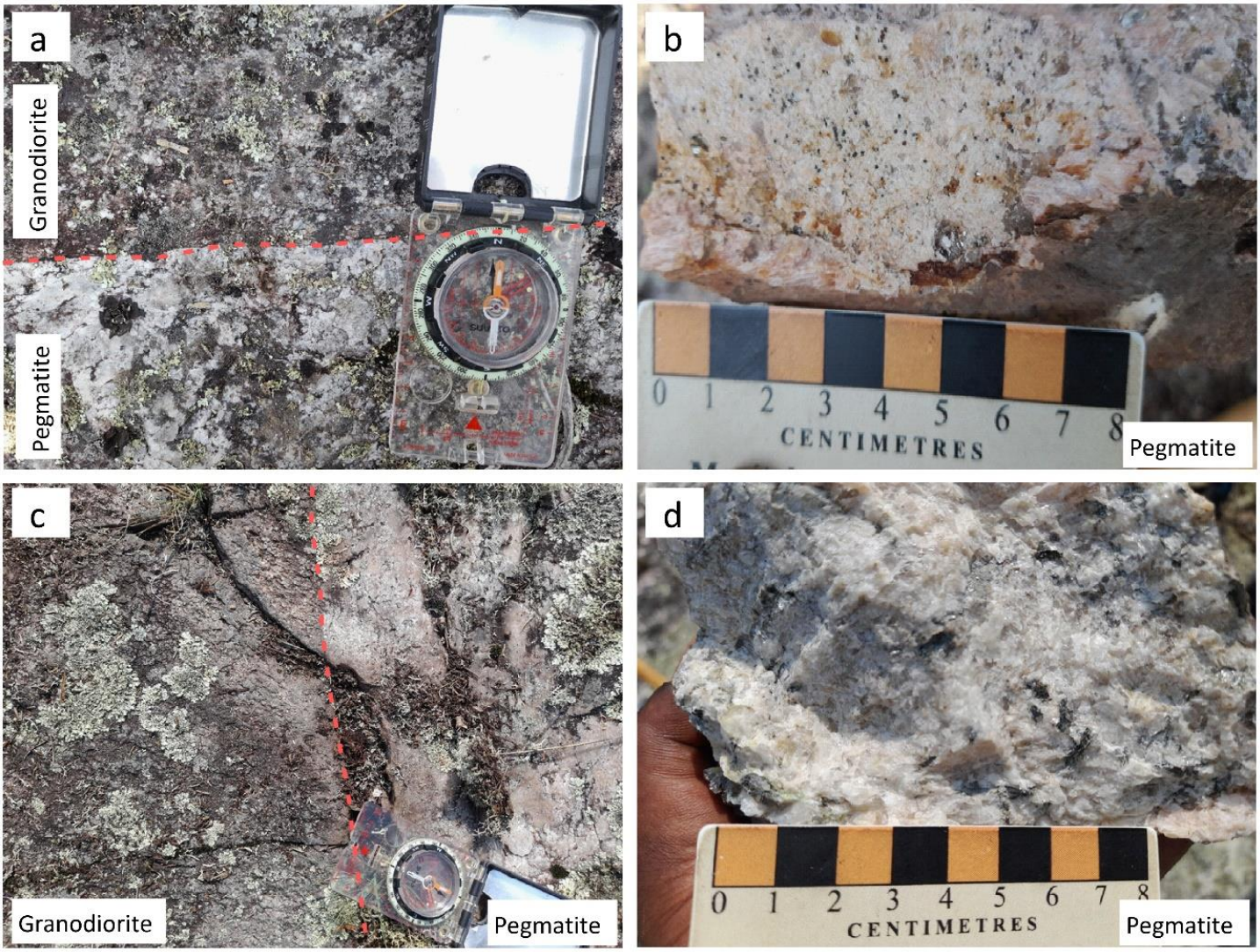


Figure GS2024-3-11: *Field photos of Axial pegmatite group (AX):* ***a)*** *pegmatite in the Birse Lake granodiorite, with sharp contact but generally concordant with the foliation of the hostrock;* ***b)*** *pegmatite with dotted brown and black garnet;* ***c)*** *pegmatite dikes in the Birse Lake pluton that cut across the foliation of the hostrock;* ***d)*** *crosscut pegmatite with biotite, in addition to the main minerals observed in other pegmatites, from the Birse Lake pluton.*

indistinguishable from cassiterite in some pegmatites. Previous studies indicate that the pegmatites of the Rush Lake group can be classified as fully differentiated, partly to extensively replaced spodumene, albite-microcline and petalite-albite-microcline pegmatites, with or without lepidolite, and have remarkable Cs enrichment (Černý et al., 1981). However, no Li-bearing minerals were observed in the pegmatite at surface during the current fieldwork.

Bernic Lake pegmatite group (BL)

Exposures of this group are concentrated at the eastern end of Bernic Lake, the only exception being the Tanco pegmatite at its northwestern extremity. In this group, the visited pegmatite locations are CNM 01-13 (Tanco pegmatite), CNM 153 (west of Tanco, around Bernic Lake), CNM 155 (Jack nut pegmatite) and CNM 157-159 (Pegmatite 7 (Coe) –9 (Buck), eastern end of Bernic Lake; Figure GS2024-3-2). The Tanco pegmatite is zoned with mineral content that possibly indicates progressive differentiation of the pegmatite and an increasing extent of metasomatic reactions. The Tanco pegmatite zones have been described extensively in previous work (e.g., Černý et al., 1998; Černý, 2005; Stilling et al., 2006; Breasley et al., 2022). Near the eastern end of Bernic Lake, pegmatite dikes trend mainly E-W, parallel to the structural fabric of the gabbro hostrock, and dip 40°N (Figure GS2024-3-14a). The pegmatite evidently filled conjugate directions of fractures/joints in the hostrock (Figure GS2024-3-14b).

The contact zone is mainly characterized by K-feldspar that developed in the pegmatite toward the contact with the hostrock, while black tourmaline developed in both the pegmatite and the hostrock (Figure GS2024-3-14a, b). The most obvious rare-element mineralization observed from the outcrop is white beryl (Figure GS2024-3-14c), white spodumene (Figure GS2024-3-14d) and tantalite in the aplitic zone. The shapes and orientations of the Bernic Lake pegmatites are controlled in part by the rheology

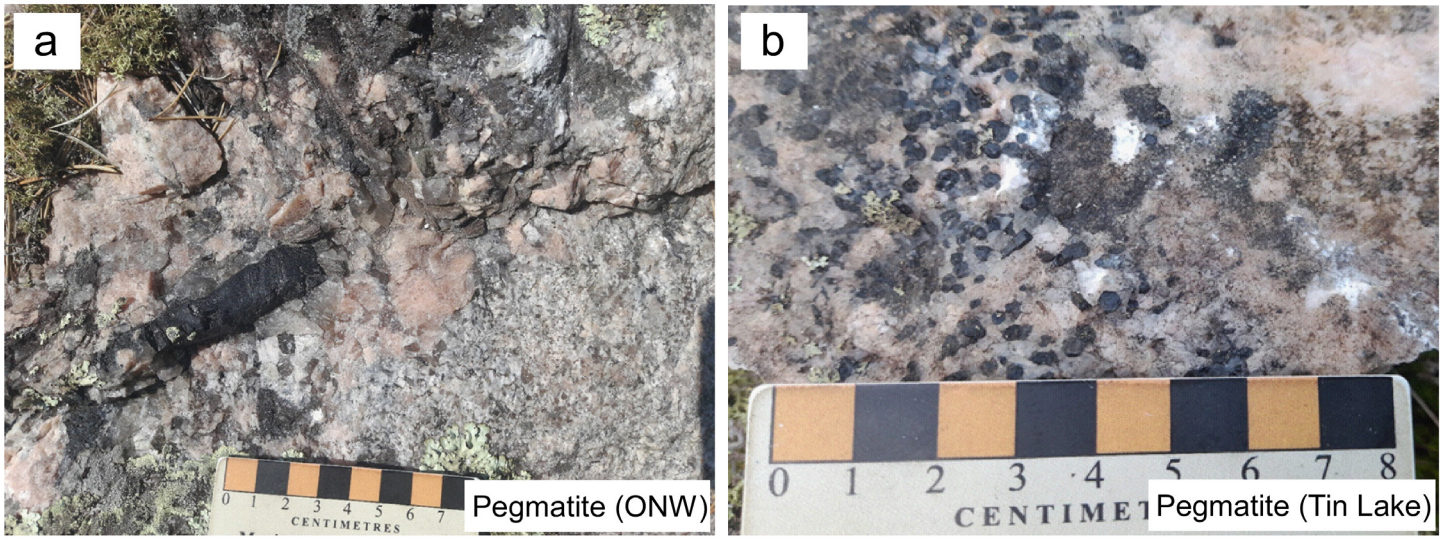


Figure GS2024-3-12*: Field photos of Birse Lake pegmatite group (BIS):* ***a)*** *pegmatite with abundant coarse-grained K-feldspar, black tourmaline, biotite, quartz, occasional muscovite and accessory garnet;* ***b****) evolved pegmatite, with high contents of green muscovite and dotted black tourmaline.*

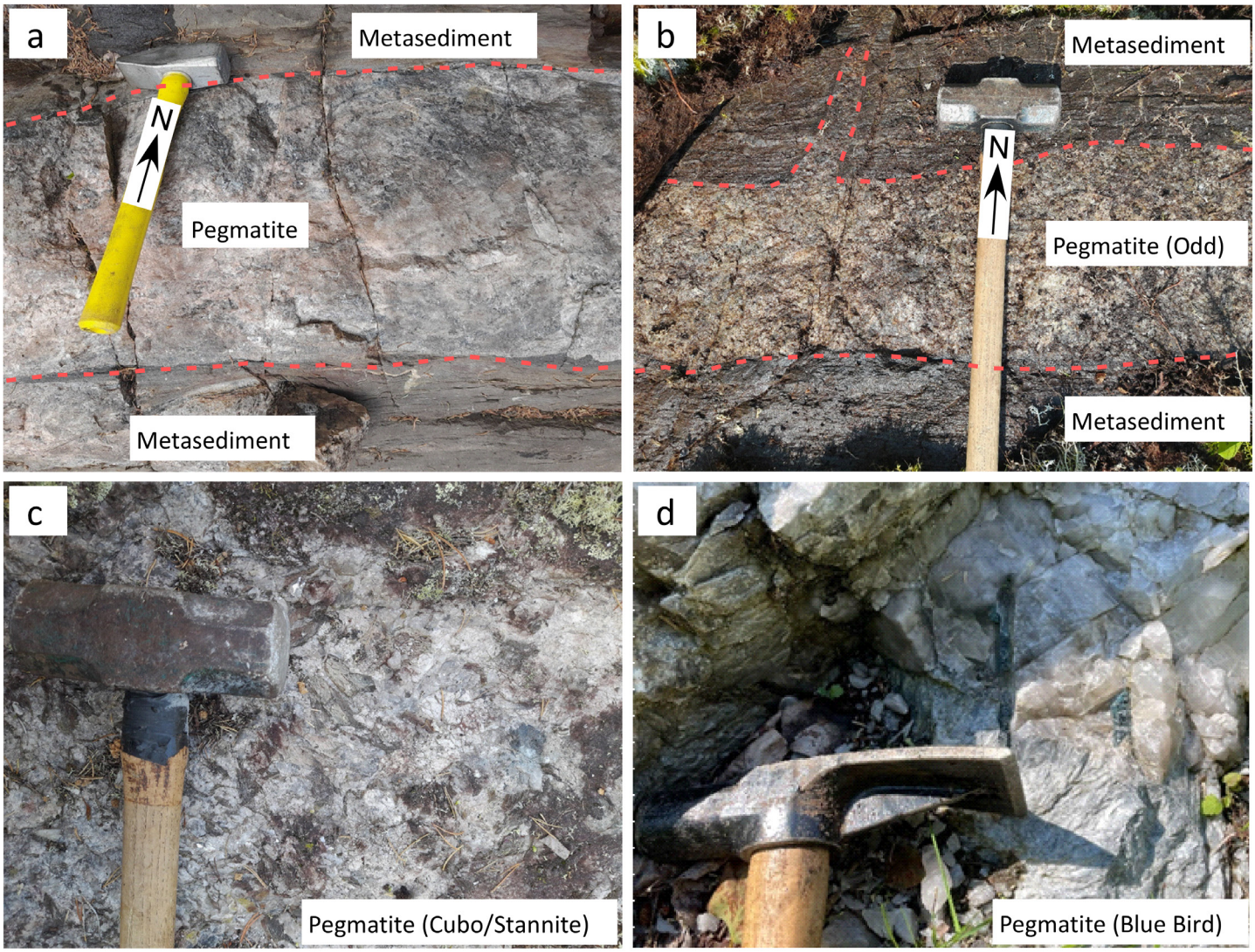


Figure GS2024-3-13: *Field photos of Rush Lake pegmatite group (RL):* ***a)*** *pegmatite emplaced parallel to E-W foliation of the metasedimentary hostrock, with formation of black tourmaline in the contact;* ***b)*** *emplacement of the pegmatite that filled both the E-W and N-S openings;* ***c)*** *main minerals forming the RL pegmatite (plagioclase, green muscovite, K-feldspar, quartz, black tourmaline and garnet);* ***d)*** *pegmatite with blue tourmaline in the outcrop*

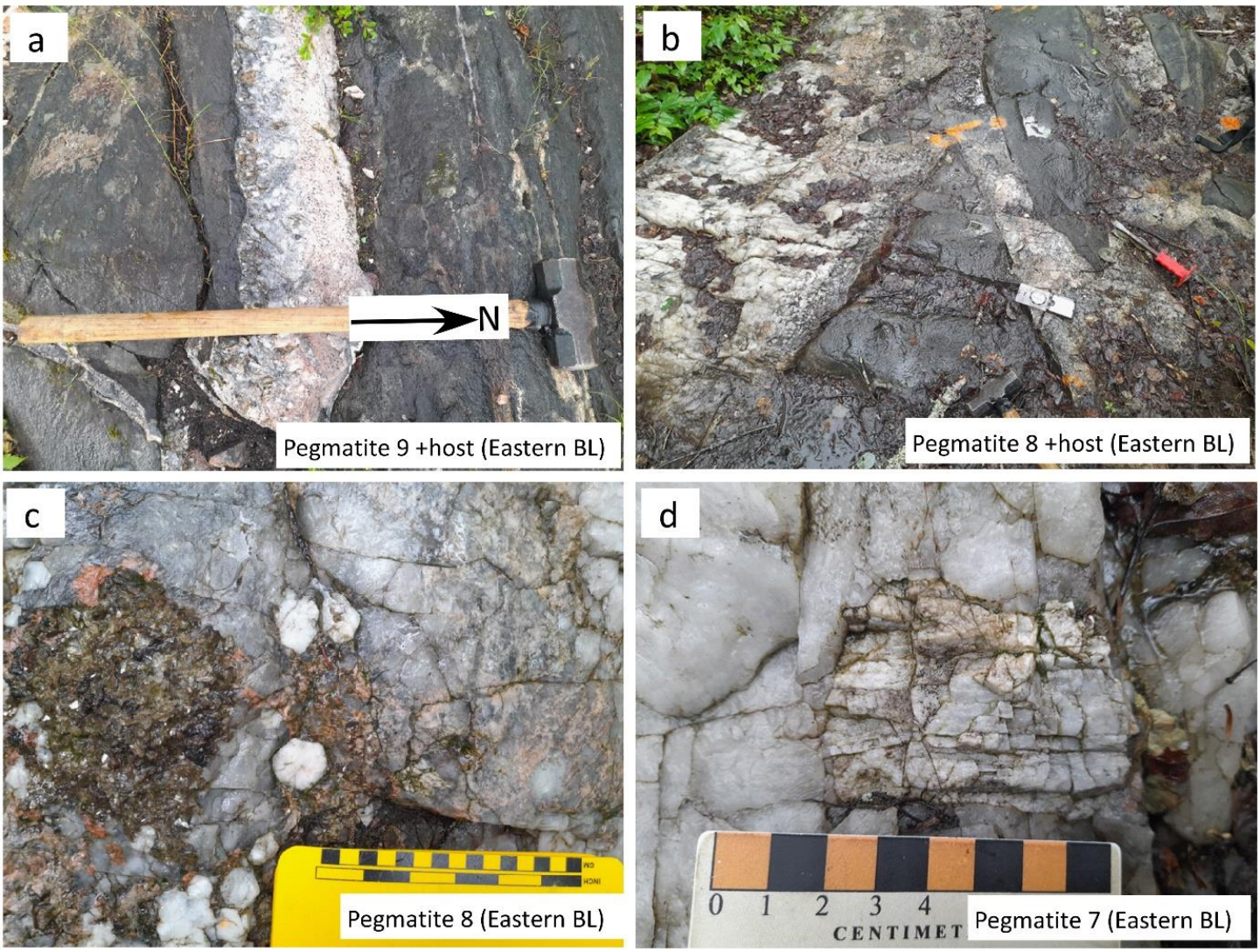


Figure GS2024-3-14*: Field photos of Bernic Lake group (BL):* ***a)*** *pegmatite trending E-W, parallel to the structural fabric of the hostrock (gabbro) with shallow dip;* ***b)*** *E-W pegmatite that bisected and filled fractures/joints in the hostrock;* ***c)*** *euhedral beryl (white) mineralization in the pegmatite;* ***d)*** *Li-mineralized pegmatite with coarse white spodumene****.***

of the hostrocks into which they were emplaced. Rheologically competent lithologies responded to strain by brittle fracture and the pegmatites occurring therein are flat and tabular; rheologically incompetent lithologies responded to strain by ductile-brittle deformation and the pegmatites therein are irregular, folded and/or boudinaged (Kremer, 2010).

Economic considerations

The Cat Lake–Winnipeg River pegmatite field contains lithium and other critical elements (e.g., tantalum, tin, niobium, cesium, beryllium), and mining is currently underway for lithium in Tanco's world-class pegmatite deposit. Preliminary field investigations in the Cat Lake–Winnipeg River pegmatite field indicate that the pegmatites emplaced in mafic hostrocks and/or intermediate hostrocks are highly evolved and enriched in potential critical minerals, including lithium, tantalum, tin, beryllium and cesium deposits. Those emplaced in more felsic hostrocks are barren at their present surfaces. Based on these field investigations, combined with knowledge of the type of hostrock and mineralogy of the pegmatites, the economic potential of various groups of pegmatite in the Cat Lake-Winnipeg River pegmatite field is ranked and shown in Figure GS2024-3-15.

Acknowledgments

Logistical and field support from the Manitoba Geological Survey and Axiom Group Consulting is very much appreciated. Thanks also go to K. Peters (University of Winnipeg) for assistance during the fieldwork. New Age Metals Inc. is thanked for providing financial support through a Mitacs grant to C.R.M. McFarlane (University of New Brunswick) and L. Groat (University of British Columbia).

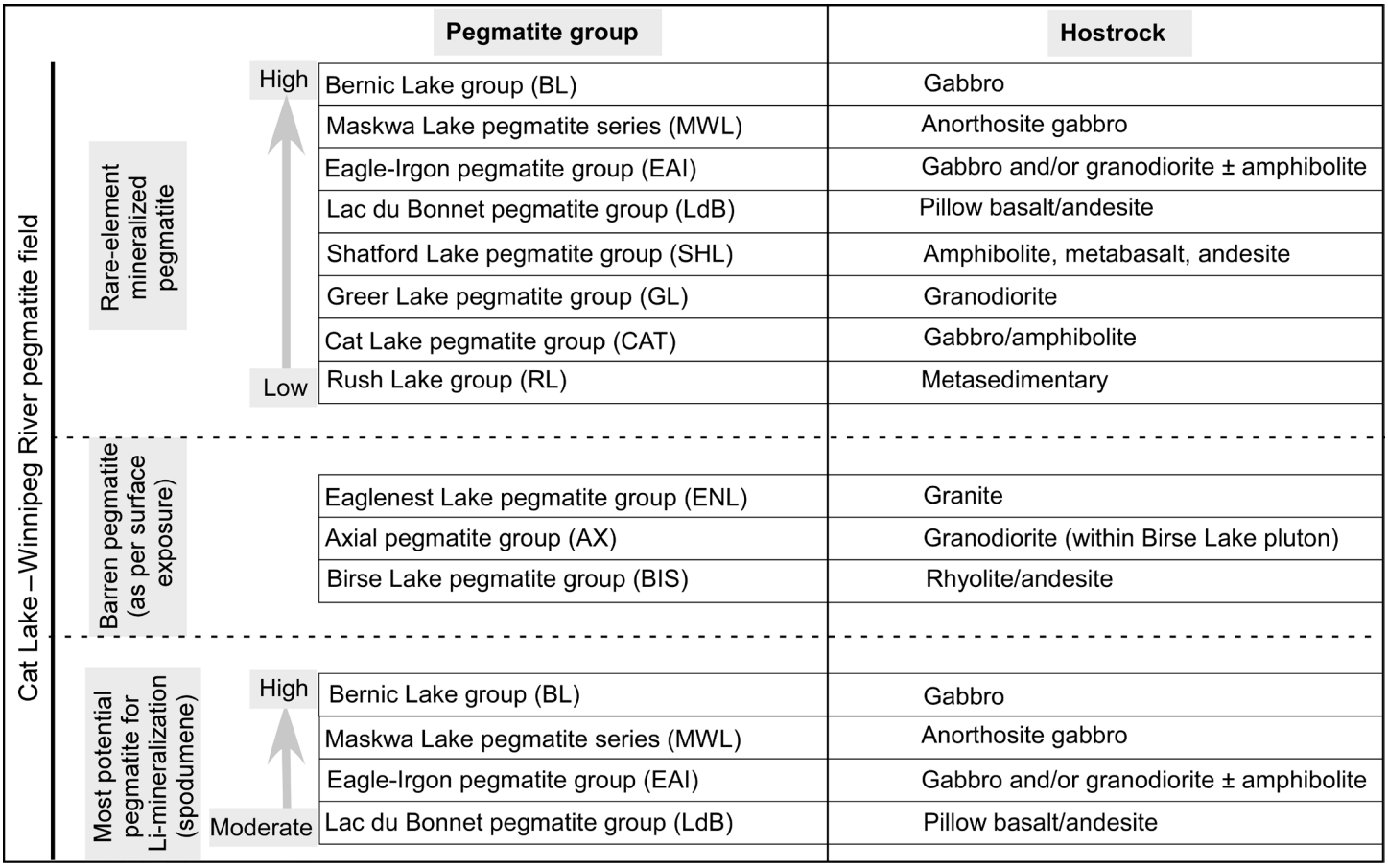


Figure GS2024-3-15: *Summary of Cat Lake–Winnipeg River pegmatite groups with consideration of their economic potential.*

References

Bannatyne, B.B. 1985: Industrial minerals in rare-element pegmatites of Manitoba; Manitoba Department of Energy and Mines, Mineral Resources Division, Economic Geology Report ER84-1, 96 p.

Breasley, C.M., Barker, I.R., Linnen, R.L., Martins, T. and Groat, L.A., 2024: The use of X-ray micro-computed tomography to visualize and quantify lithium-bearing silicate minerals in pegmatites: examples from the Tanco pegmatite, Manitoba, Canada; American Mineralogist, URL <https://doi.org/10.2138/am-2024-9439>.

Breasley, C.M., Martins, T., Groat, L.A. and Linnen, R.L. 2021: Results of a preliminary investigation into the lithium mineralization, distribution trends and remobilization in the Tanco pegmatite, southeastern Manitoba (part of NTS 52L6); *in* Report of Activities 2021, Manitoba Agriculture and Resource Development, Manitoba Geological Survey, p. 8–17.

Breasley, C.M., Martins, T., Linnen, R.L. and Groat, L.A. 2022: Investigating textural and geochemical relations of lithium mineralization in the Tanco pegmatite, southeastern Manitoba (part of NTS 52L6); *in* Report of Activities 2022, Manitoba Natural Resources and Northern Development, Manitoba Geological Survey, p. 25–35.

Camacho, A., Baadsgaard, H., Davis, D.W. and Černý, P., 2012: Radiogenic isotope systematics of the Tanco and Silverleaf granitic pegmatites, Winnipeg River pegmatite district, Manitoba; The Canadian Mineralogist, v. 50, p. 1775–1792.

Camacho, A., Baadsgaard, H., Paul, B.J. and Černý, P. 2014: Radiogenic isotope systematics of the Huron claim pegmatite and the Shatford Lake pegmatite group, Winnipeg River pegmatite district, Manitoba; The Canadian Mineralogist, v. 52, p. 857–872.

Černý, P. 1991: Fertile granites in Precambrian rare-element pegmatite fields: is geochemistry controlled by tectonic setting or source lithologies? Precambrian Research, v. 51, p. 429–468.

Černý, P. 2005: The Tanco rare-element pegmatite deposit, Manitoba: regional context, internal anatomy, and global comparisons; *in* Rare-Element Geochemistry and Mineral Deposits, R.L. Linnen and I.M. Samson (ed.), Geological Association of Canada, Short Course Notes, v. 17, p. 127–158.

Černý, P., Ercit, T. and Vanstone, P. 1998: Mineralogy and petrology of the Tanco rare-element pegmatite deposit, southeastern Manitoba; International Mineralogical Association, 17th General Meeting, Toronto, Ontario, Field Trip Guidebook B6, 74 p.

Černý, P., Trueman, D.L., Ziehlke, D.V., Goad, B.E. and Paul, J. 1981: The Cat Lake–Winnipeg River and the Wekusko Lake pegmatite fields, Manitoba; Manitoba Energy and Mines, Mineral Resources Division, Economic Geology Report ER80-1, 215 p.

Duguet, M., Lin, S., Davis, D.W., Corkery, M.T. and McDonald, J. 2009: Long-lived transpression in the Archean Bird River greenstone belt, Western Superior Province, southeastern Manitoba; Precambrian Research, v. 174, p. 381–407.

Gilbert, H.P. 2006: Geological investigations in the Bird River area, southeastern Manitoba (parts of NTS 52L5N and 6); *in* Report of Activities 2006, Manitoba Science, Technology, Energy and Mines, Manitoba Geological Survey, p. 184—205.

Gilbert, H.P., Davis, D.W., Duguet, M., Kremer, P.D., Mealin, C.A. and MacDonald, J. 2008: Geology of the Bird River Belt, southeastern Manitoba (parts of NTS 52L5, 6); Manitoba Science, Technology, Energy and Mines, Manitoba Geological Survey, Geoscientific Map MAP2008-1, scale 1:50 000.

Government of Canada 2024: Canada's Critical minerals; Government of Canada, URL <https://www.canada.ca/en/campaign/critical-minerals-in-canada/critical-minerals-an-opportunity-for-canada.html> [August 2024].

Houlé, M.G., Lesher, C.M., McNicoll, V.J., Metsaranta, R.T., Sappin, A.-A., Goutier, J., Bécu, V., Gilbert, H.P. and Yang, X.M. 2015: Temporal and spatial distribution of magmatic Cr-(PGE), Ni-Cu-(PGE), and Fe-Ti-(V) deposits in the Bird River–Uchi–Oxford-Stull–La Grande Rivière–Eastmain domains: a new metallogenic province within the Superior Craton; *in* Targeted Geoscience Initiative 4: Canadian Nickel–Copper–Platinum Group Elements–Chromium Ore Systems — Fertility, Pathfinders, New and Revised Models, D.E. Ames and M.G. Houlé, (ed.); Geological Survey of Canada, Open File 7856, p. 35–48.

Houlé, M.G., McNicoll, V.J., Bécu, V., Yang, X.M. and Gilbert, H.P. 2013: New age for the Mayville Intrusion: implication for a large mafic-ultramafic event in the Bird River Greenstone Belt, southeastern Manitoba; Geological Association of Canada–Mineralogical Association of Canada, Joint Annual Meeting, Winnipeg, Manitoba, May 22–24, 2013, Abstract with Programs.

Kremer, P. 2010: Structural geology and geochronology of the Bernic Lake area in the Bird River greenstone belt, Manitoba: evidence for syn-deformational emplacement of the Bernic Lake pegmatite group; M.Sc. thesis, University of Waterloo, Waterloo, Ontario, 100 p.

Linnen, R.L., Van Lichtervelde, M. and Černý, P. 2012: Granitic pegmatites as sources of strategic metals; Elements, v. 8, p. 275–280.

London, D. 2024: The Tanco pegmatite at Bernic Lake Manitoba, Canada; Rocks and Minerals, v. 99, no. 1, p. 60–77.

Martins, T., Rinne, M.L., Breasley, C. and Adediran, H. 2023: Preliminary results from field investigations in the Bird River domain of the Archean Superior province, Manitoba (parts of NTS 52L5, 6, 11, 12); *in* Report of Activities 2023, Manitoba Economic Development, Investment, Trade and Natural Resources, Manitoba Geological Survey, p. 4–13.

Mealin, C.A. 2008: Geology, geochemistry and Cr-Ni-Cu-PGE mineralization of the Bird River sill: evidence for a multiple intrusion model; M.Sc. thesis, University of Waterloo, Waterloo, Ontario, 155 p.

Paul, B.J. 1984: Mineralogy and petrology of the Huron Claim pegmatite, southeastern Manitoba; M.Sc. thesis, University Manitoba, Winnipeg, Manitoba.

Percival, J.A., McNicoll, V. and Bailes, A.H. 2006a. Strike-slip juxtaposition of ca. 2.72 Ga juvenile arc and >2.98 Ga continent margin sequences, and its implications for Archean terrane accretion, western Superior Province, Canada; Canadian Journal of Earth Sciences, v. 43, p. 895–927.

Percival, J.A., Sanborn-Barrie, M., Skulski, T., Stott, G.M., Helmstaedt, H., and White, D.J. 2006b. Tectonic evolution of the western Superior Province from NATMAP and LITHOPROBE studies; Canadian Journal of Earth Sciences, v. 43, p. 1085–1117.

Rinne, M.L. 2023: Progress report on the Manitoba Mineral Deposits Database; *in* Report of Activities 2023, Manitoba Economic Development, Investment, Trade and Natural Resources, Manitoba Geological Survey, p. 1–3.

Roush, J., Martins, T., McFarlane, C.R.M., Rinne, M.L. and Groat, L. 2023: Preliminary examination of the Tappy, Eagle and F.D. No. 5 pegmatites in the Cat Lake–Winnipeg River pegmatite field, southeastern Manitoba (parts of NTS 52L5, 11); *in* Report of Activities 2023, Manitoba Economic Development, Investment, Trade and Natural Resources, Manitoba Geological Survey, p. 20–26.

Stilling, A., Černỳ, P. and Vandstone, P.J., 2006: The Tanco pegmatite at Bernic Lake, Manitoba, XVI-Zonal and bulk compositions and their petrogenetic significance; The Canadian Mineralogist, v. 44, no. 3, p. 599–623.

Yang, X.M. 2012: Bedrock geology of the Cat Creek area, Bird River greenstone belt, southeastern Manitoba (part of NTS 52L12); Manitoba Innovation, Energy and Mines, Manitoba Geological Survey, Preliminary Map PMAP2012-3, scale 1:12 500.

Yang, X.M. 2013: Bedrock geology of the Cat Lake–Euclid Lake area, Bird River greenstone belt, southeastern Manitoba (parts of NTS 52L11, 12); Manitoba Mineral Resources, Manitoba Geological Survey, Preliminary Map PMAP2013-7, scale 1:10 000.

Yang, X.M. 2014: Bedrock geology of the Cat Creek area, Bird River greenstone belt, southeastern Manitoba (part of NTS 52L12); Manitoba Mineral Resources, Manitoba Geological Survey, Preliminary Map PMAP2014-3, scale 1:10 000.

Yang, X.M. and Houlé, M.G. 2020: Geology of the Cat Creek–Euclid Lake area, Bird River greenstone belt, southeastern Manitoba (parts of NTS 52L11, 12); Manitoba Agriculture and Resource Development, Manitoba Geological Survey, Geoscientific Report GR2020-1, 105 p., 1 map at 1:20 000 scale.

Yang, X.M., Drayson, D. and Polat, A. 2019: S-type granites in the western Superior Province: a marker of Archean collision zones; Canadian Journal of Earth Sciences, v. 56, p. 1409–1436.

GS2024-4

Paragenetic relationships between zones 80 and 90 at the Tanco pegmatite, southeastern Manitoba (part of NTS 52L6)

by C.M. Breasley[1], T. Martins, R.L. Linnen[2] and L.A. Groat[3]

Summary

In May 2024, a map was produced of the underground face of the H-pillar in the Tanco pegmatite mine in southeastern Manitoba to investigate the relationships between the Cs-rich pollucite zone (zone 80) and Li-rich lepidolite zone (zone 90). Observations revealed a complex crystallization history recorded by multiple crosscutting relationships. The paragenetic sequence is interpreted to have initially involved the crystallization of primary blocky K-feldspar in zone 40 and pollucite in zone 80. During subsequent metasomatism, K-feldspar was nearly completely replaced with Li-rich micas. A meshlike veining pattern of lepidolite within the pollucite is found close to the contact between the two zones. A later-stage albitization event acted to form secondary aplite veins within a late-stage viscous siliceous residual liquid. A rapid depressurization of the system, potentially due to incompatible and volatile element crystallization, could have led to the flash quartz zone crystallization, which fractured the aplite bands and portions of the massive lepidolite zone. A final alteration stage of spodumene, recorded in green clays such as kaolinite and montmorillonite, occurred as a final paragenetic event.

In Brief:

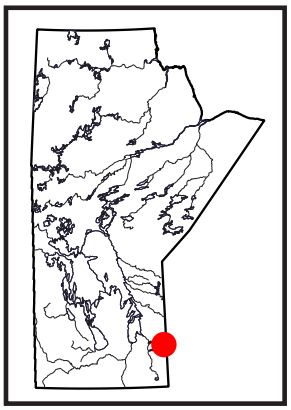
- A face map was created of the H-pillar at the Tanco pegmatite showing the complex crystallization history between the Cs-rich pollucite zone (zone 80) and Li-rich lepidolite zone (zone 90)
- Future work will involve creating thin sections of all aplite veins and representative mineralogical assemblages sampled to obtain micro-scale mineralogical information

Citation:
Breasley, C.M., Martins, T., Linnen, R.L. and Groat, L.A. 2024: Paragenetic relationships between zones 80 and 90 at the Tanco pegmatite, southeastern Manitoba (part of NTS 52L6); *in* Report of Activities 2024, Manitoba Economic Development, Investment, Trade and Natural Resources, Manitoba Geological Survey, p. 27–32.

Introduction

The economically important mineralization and complex crystallization styles of pegmatites make them a topical and fascinating field of study in economic geology. The Tanco pegmatite is a Li-Cs-Ta (LCT)–bearing deposit located in southeastern Manitoba, Canada. It is known to be one of the most evolved and economically important pegmatites in the world and has historically been mined for Cs from pollucite {$(Cs,Na)_2Al_2Si_4O_{12}•(H_2O)$} and Ta from tantalite ({$(Fe, Mn)Ta_2O_6$}; Černý, 2005). It is currently the site of the largest Li mine in Canada, targeting spodumene {$LiAlSi_2O_6$}, dominantly in the form of spodumene and quartz intergrowths (SQUI). The Tanco pegmatite has been the basis of multiple pertinent studies that provide crucial insights into pegmatite geochemical evolution and mineralization (e.g., Černý et al., 1981, 1996; Bannatyne, 1985; van Lichtervelde et al., 2006; Brown et al., 2017; Breasley et al., 2022).

The current work is part of an ongoing Ph.D. project that began in August 2021, focusing on the lithium mineralization patterns in zones 45 and 50 of the Tanco pegmatite (Breasley et al., 2021, 2022, 2023). During sample collection in May 2024, an underground mine face of pollucite mineralization in contact with massive lepidolite was mapped in detail (the H-pillar) and paragenetic information was recorded. This project aims to add more information to the paragenetic sequence documented in literature for the Tanco pegmatite deposit, specifically with respect to the genetic relationship between the lepidolite and pollucite mineralized zones. This report includes a detailed map of the underground face of the H-pillar and interpretations regarding paragenetic relationships.



Geological setting

The Tanco pegmatite is located in southeastern Manitoba, Canada, where it forms part of the Bernic Lake group of pegmatites in the Cat Lake–Winnipeg River pegmatite district within the Bird River greenstone belt (Figure GS2024-4-1; Černý et al., 1981). The Bernic Lake formation is composed predominantly of mafic volcanic rocks, including the gabbro intrusion that hosts the Tanco pegmatite. The interpreted age of crystallization of the Tanco gabbro is 2723.1 ±0.8 Ma (U-Pb zircon dating; Černý, 2005; Gilbert, 2008; Kremer, 2010). The U-Pb tantalite dating of the Tanco pegmatite showed an intrusive age of 2641 ±3 Ma (Camacho et al., 2012) and U-Pb zircon dating revealed an age of 2647.4 ±1 Ma

[1] Department of Earth, Ocean and Atmospheric Sciences, The University of British Columbia, Vancouver, British Columbia, cbreasley@eoas.ubc.ca
[2] Department of Earth Sciences, Western University, London, Ontario
[3] Department of Earth, Ocean and Atmospheric Sciences, The University of British Columbia, Vancouver, British Columbia

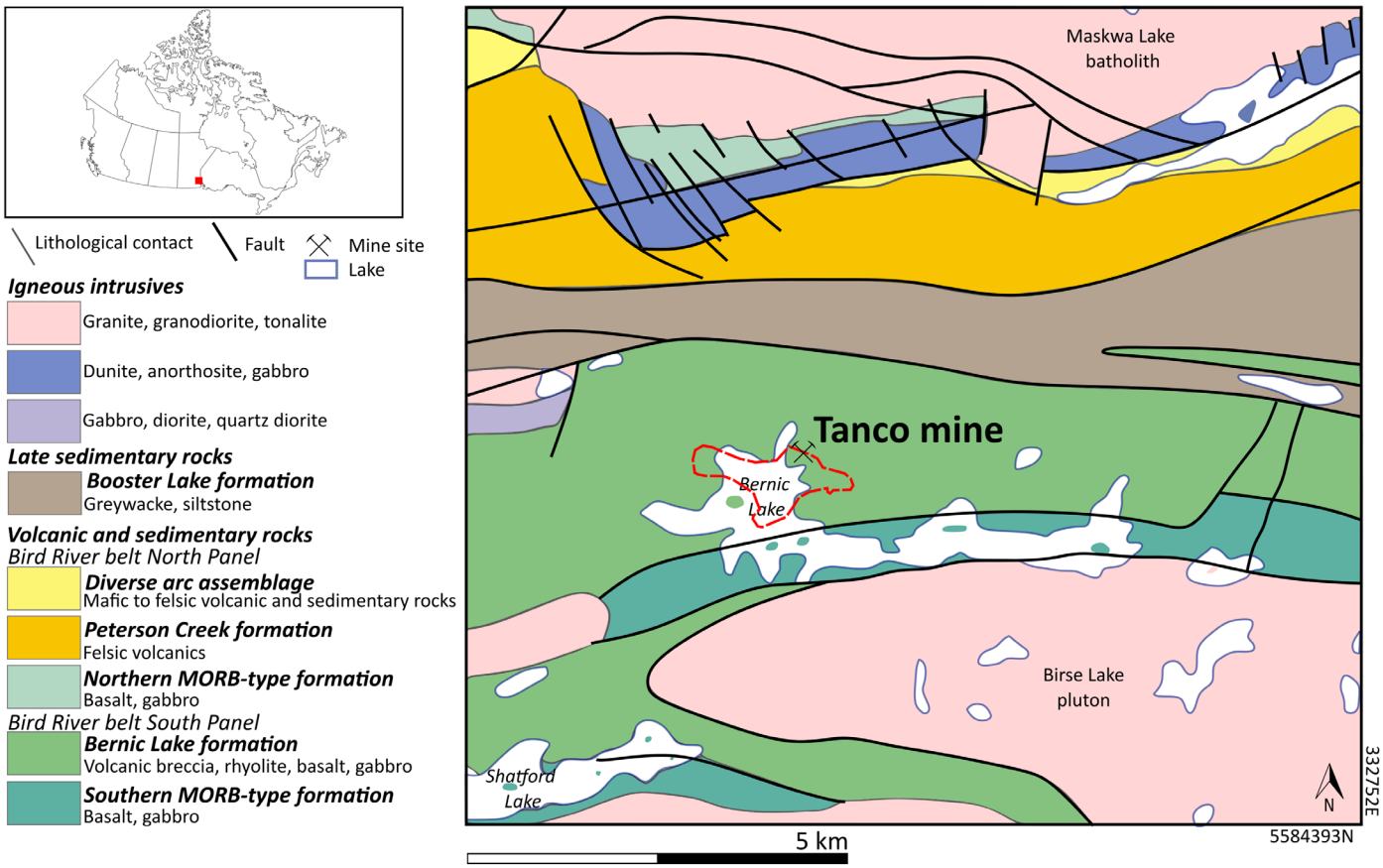


Figure GS2024-4-1: *Local geology surrounding the Tanco pegmatite (dashed red outline; Stilling et al., 2006) in southeastern Manitoba. All co-ordinates are in UTM Zone 15N, NAD83. From Breasley et al. (2021, 2022) and Gilbert (2008). Abbreviation: MORB, mid-ocean–ridge basalt.*

(Kremer, 2010). Multiple other pegmatites exist within the Bernic Lake group of pegmatites (Černý et al., 1981), however, the Tanco pegmatite is the largest, most fractionated and most enriched in Li, Cs and Ta.

The Tanco pegmatite

The Tanco pegmatite is a 1520 by 1060 by 100 m bilobate intrusion (Černý, 2005). It is classified as a petalite subtype, complex, LCT (Černý and Ercit, 2005) or Group 1 pegmatite (Wise et al., 2022). The pegmatite has been historically divided into nine major zones (10–90) based on varying geochemistry, textures and mineralogy (Černý et al., 1998; Černý, 2005; Stilling et al., 2006). A detailed review of the zonation of the Tanco pegmatite can be found in Breasley et al. (2022). A brief overview of the zones investigated in this study are reported below.

Zone 40 (lower intermediate zone) is dominantly composed of blocky microcline-perthite crystals with SQUI, quartz, albite, mica and amblygonite as minor phases (Černý et al., 1996).

Zone 50 (upper intermediate zone) is often found with a gradational contact to zone 40 and is the most lithium enriched, containing abundant SQUI, amblygonite and pollucite (Černý et al., 1996).

Zone 80 (pollucite zone) is genetically part of zone 50, however, due to the massive nature of pollucite mineralization, it is better described as a discrete ore zone. Zone 80 is commonly crosscut by veins containing micas, feldspars and quartz (Černý et al., 1996). Pollucite at the Tanco pegmatite is typically grey to white in appearance and internally heterogenous. It is commonly found braided with sericite, spodumene and adularia. The microscopic internal structure reveals that analcime is intruded by multiple generations of increasingly Cs- and Al-enriched veins until almost Na-free end-member pollucite occurs (Černý and Simpson, 1978; Černý et al., 1998). The zone's 'tapioca'-like texture is attributed to Cs-analcime aggregates and late-stage adularia (Černý, 2005).

Zone 90 (lepidolite zone) is thought to be metasomatic in origin, having replaced blocky feldspar crystals. The mineralogy is mostly massive purple lithian muscovite with minor amounts of albite, quartz and microlite (Černý et al., 1996). Lithian muscovite and lepidolite form the bulk of zone 90 (Figure GS2024-4-2a). The typical interlocking massive micas in this zone are pale to dark purple in appearance (Rinaldi et al., 1972).

Summary of fieldwork

During field work in May 2024, a map of the underground face of the H-pillar was produced and a representative sample

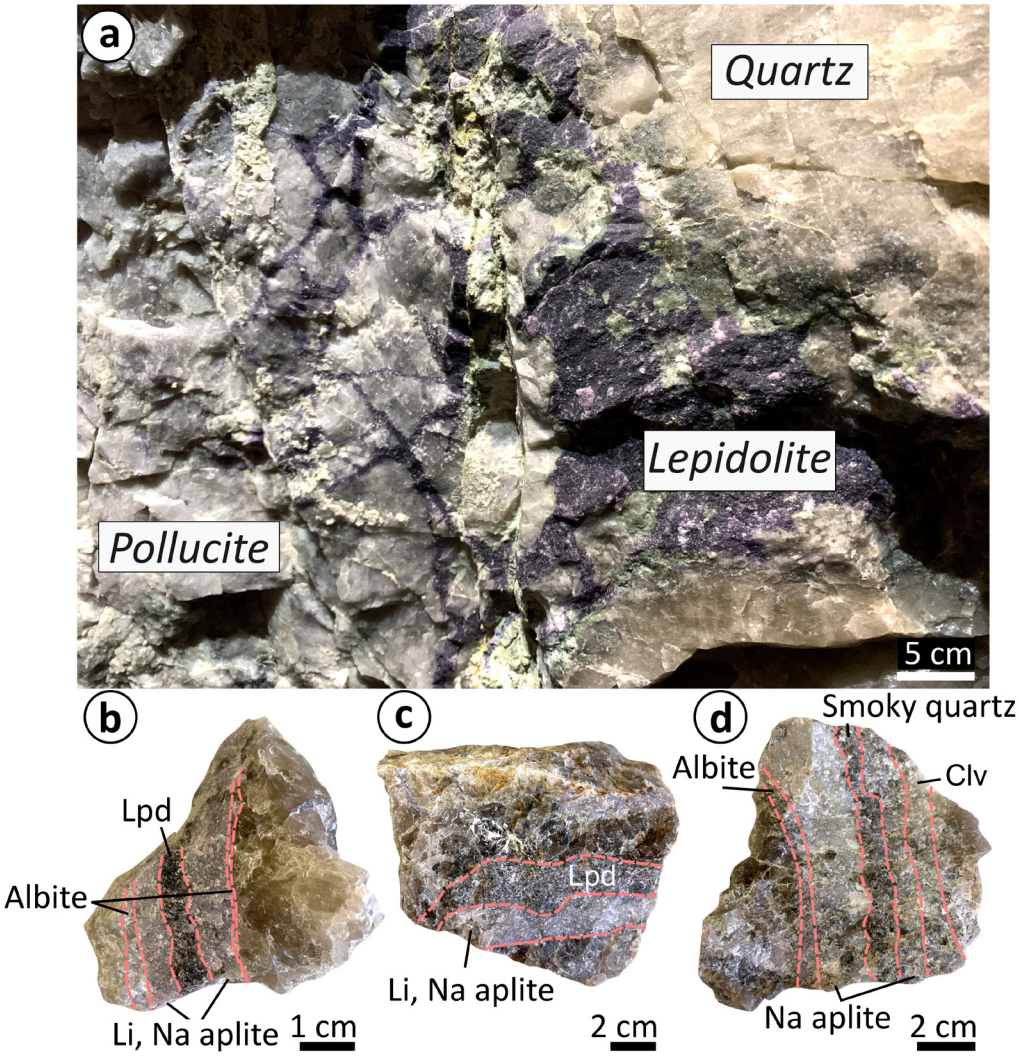


Figure GS2024-4-2: a) *The pollucite and lepidolite zone contact evident on the H-pillar face, Tanco mine. Rock samples from the H-pillar show* ***b)*** *type I purple aplite vein with concentric zonation,* ***c)*** *type II purple aplite vein and* ***d)*** *type III blue aplite vein. See Figure GS2024-4-3 for rock sample locations. Abbreviations: Lpd, lepidolite; Clv, cleavelandite.*

set was collected. This pillar was selected due to the interesting textural features it shows in relation to the Cs and Li mineralization and to the pristine exposures. This section was deemed to be promising in revealing information regarding the paragenetic crystallization sequence of the multiple zones in the Tanco pegmatite.

Observations

Several mineralogical and zonation relationships were seen at the H-pillar (Figures GS2024-4-2, -3a). The pollucite is crosscut by multiple meshlike veins of lepidolite (Figure GS2024-4-3a). Aplites and lepidolites are fragmented and interstitially infilled with massive quartz. The various aplites seen in the H-pillar show variable layering with three major aplite veins. The first aplite vein type (I; Figures GS2024-4-2b, -3b) has concentric layering with a central portion of monomineralic lepidolite, surrounded by a pale lavender aplite and finally coated by a thin rim of white albite, which locally shows cleavelandite textures. The second (II) and third (III) major aplite vein types are also present in the H-pillar (Figures GS2024-4-2c, d, -3c). The second aplite type (II) shows an upper portion of monomineralic lepidolite with a lower zone of pale purple aplite similar to the mineralogy in the type I aplite (Figures GS2024-4-2c, -3c). Finally, the third aplite type (III) hosts multiple layers. Looking at Figures GS2024-4-2d and -3c, curved blue aplite bands have a pure white albite rim on the left and it coats pale purple aplite to the right. This purple aplite has a gradational contact with the light blue aplite to its right and then a central portion of smoky quartz is found. The blue aplite to the right of the quartz hosts radial cleavelandite textures. It can be noted that the aplites are generally more purple in appearance toward the left and bluer toward the right.

Paragenetic interpretation

The following paragenetic sequence of events was interpreted from underground pillar face and hand sample observations:

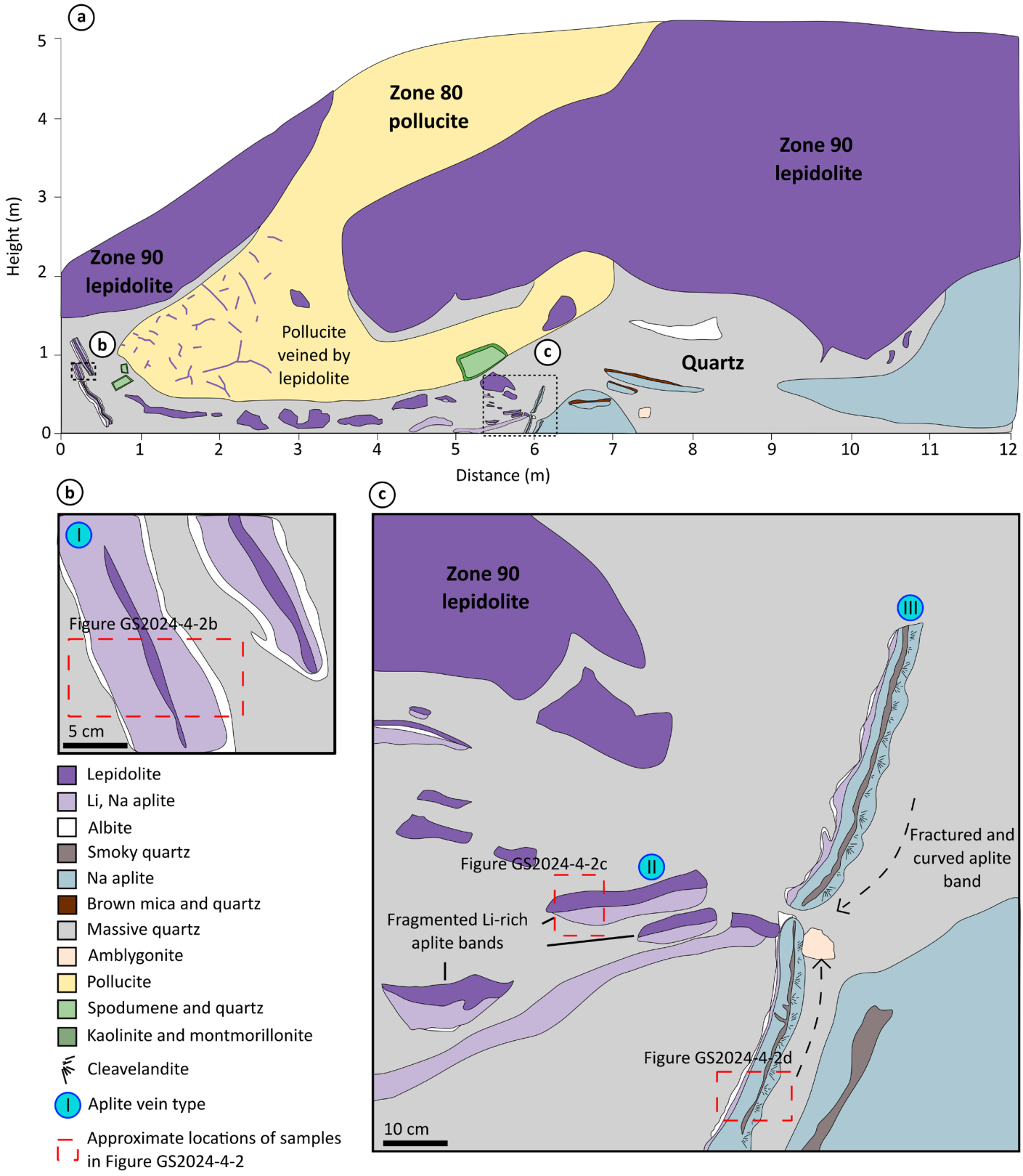


Figure GS2024-4-3: a) *Mineralogical relationships between the pollucite zone (80) and the lepidolite zone (90) evident on the H-pillar face, Tanco mine;* ***b, c)*** *details of the textural and mineralogical features shown in a), including the crosscutting relationships.*

1) The first crystals that formed in the H-pillar were blocky K-feldspars, which are attributed to zone 40 with a gradational contact to zone 50 and paragenetically linked to the primary pollucite, minor SQUI and amblygonite in zone 80. This acted to deplete the melt in Cs, Na and K.
2) Subsequently, the massive zone 90 lepidolite (Figure GS2024-4-3) formed via the pervasive alteration of blocky K-feldspars, removing K from the system and crystallizing Li and F into lithian muscovite and lepidolite.
3) An albitization phase followed this event, which formed the blue aplitic albite (Na aplite) and complex veins of aplites. These veins cut through a massive quartz unit and are fragmented and locally curved (Figure GS2024-4-3). They are associated with increased amounts of Na and local Li when purple in appearance due to the assumed presence of lithian muscovite. It is interpreted that the aplite veins originally formed in a late-stage hyperviscous siliceous residual liquid, which was subsequently crystallized rapidly.
4) A final massive quartz unit is interpreted to be the last to crystallize. Due to the fragmented nature of the aplite veins, it is interpreted that a localized depressurization of the system fragmented the veins (London, 2008; Roda-Robles et al., 2015). This could have been triggered by the precipitation of incompatible elements from the liquid, such as Li, in the albitization phase, which triggered the siliceous residual liquid to crystallize rapidly. This hypothesis could explain the fragmented nature of the lepidolite zone and the aplites, which are crosscut with late-stage quartz (Figure GS2024-4-3c).
5) At a later stage, a sericitization event altered the pollucite and a final late-stage clay alteration of SQUI produced vivid green kaolinite and montmorillonite rims.

Future work

Future work will involve creating thin sections of all sampled aplite veins and representative mineralogical assemblages to obtain microscale mineralogical information. Electron probe microanalyses will also be performed to gain geochemical insights into the various phases of aplite formation at the H-pillar. These results will help constrain the geochemistry of the different paragenetic stages.

Economic considerations

Pegmatites contain multiple minerals that can be extracted for economic purposes (Linnen et al., 2012). Studying the paragenesis through textural relationships of various minerals can enhance the understanding of pegmatite systems, improving the ability to target economically mineral-rich areas effectively. Cesium and lithium, both of which can be found in pegmatites, were identified as critical minerals by the Government of Canada (Natural Resources Canada, 2021). Cesium is an essential element with diverse applications. A primary use of Cs is the production of cesium formate, a very dense liquid that is used to stabilize drills, which is particularly useful in environmentally sensitive areas (Martins et al., 2024).

As the world transitions to a decarbonized economy, the demand for Li for batteries has been increasing making the study of pegmatite mineralization sequences that host Li topical and important (Zubi et al., 2018). Future work will help understand the textural and geochemical relationships between the lepidolite and pollucite zones at the Tanco pegmatite, which will aid in understanding pegmatite crystallization dynamics and zone geochemical interactions.

Acknowledgments

The authors sincerely thank the Tantalum Mining Corporation of Canada Ltd. (TANCO)–Sinomine Resource Group Co., Ltd. team for their enthusiasm and support for this project, notably M. Johnson, S. Rankmore and J. Champagne. Special gratitude is extended to C. Deveau (Sinomine Resource Group Co., Ltd.) for continued support of this project. A debt of gratitude is extended to all employees at the Tanco mine, without whom this project could have never taken place. Thanks are extended to the Manitoba Geological Survey for their continuing logistical and field support. The authors also extend their thanks toward L. Koopmans and C. Nambaje for valuable field assistance. Edits provided by E. Yang and K. Reid assisted in improving drafts of this manuscript. RnD Technical editing services are acknowledged for assistance in editorial work, and C. Steffano is thanked for layout and final edits.

References

Bannatyne, B.B. 1985: Industrial minerals in rare-element pegmatites of Manitoba; Manitoba Energy and Mines, Geological Services, Economic Geology Report ER84-1, 96 p.

Breasley, C., Martins, T., Deveau, C., Hutchins, A., Linnen, R., Groat, L., Landry, E. and Moser, D. 2023: Mining and processing of micro spodumene-quartz intergrowths at the Tanco pegmatite, Manitoba; Prospectors & Developers Association of Canada, Annual Convention, March 5–8, 2023, Toronto, Ontario, poster presentation, URL <https://www.researchgate.net/profile/Catriona-Breasley/publication/369143305_Mining_and_processing_of_micro_spodumene-quartz_intergrowths_at_the_Tanco_pegmatite_Manitoba/links/640baae866f8522c389616c5/Mining-and-processing-of-micro-spodumene-quartz-intergrowths-at-the-Tanco-pegmatite-Manitoba.pdf?_tp=eyJjb250ZXh0Ijp7ImZpcnN0UGFnZSI6InB1YmxpY2F0aW9uIiwicGFnZSI6InB1YmxpY2F0aW9uIn19> [September 2024].

Breasley, C.M., Martins, T., Groat, L.A. and Linnen, R.L. 2021: Results of a preliminary investigation into the lithium mineralization, distribution trends and remobilization in the Tanco pegmatite, southeastern Manitoba (part of NTS 52L6); *in* Report of Activities 2021, Manitoba Agriculture and Resource Development, Manitoba Geological Survey, p. 8–17.

Breasley, C.M., Martins, T., Linnen, R.L. and Groat, L.A. 2022: Investigating textural and geochemical relations of lithium mineralization in the Tanco pegmatite, southeastern Manitoba (part of NTS 52L6); *in* Report of Activities 2022, Manitoba Natural Resources and Northern Development, Manitoba Geological Survey, p. 25–35.

Brown, J.A., Martins, T. and Černý, P. 2017: The Tanco pegmatite at Bernic Lake, Manitoba, XVII, mineralogy and geochemistry of alkali feldspars; The Canadian Mineralogist, v. 55, no. 3, p. 483–500.

Camacho, A., Baadsgaard, H., Davis, D.W. and Černý, P. 2012: Radiogenic isotope systematics of the Tanco and Silverleaf granitic pegmatites, Winnipeg River pegmatite district, Manitoba; The Canadian Mineralogist, v. 50, no. 6, p. 1775–1792.

Černý, P. 2005: The Tanco rare-element pegmatite deposit, Manitoba: regional context, internal anatomy, and global comparisons; *in* Rare-Element Geochemistry and Mineral Deposits, R.L. Linnen and I.M. Samson (ed.), Geological Association of Canada, Short Course Notes 17, p. 127–158.

Černý, P. and Ercit, T.S. 2005: The classification of granitic pegmatites revisited; The Canadian Mineralogist, v. 43, no. 6, p. 2005–2026.

Černý, P. and Simpson, F.M. 1978: The Tanco pegmatite at Bernic Lake, Manitoba, X, pollucite; The Canadian Mineralogist, v. 11, p. 325–333.

Černý, P., Ercit, T. and Vanstone, P. 1996: Petrology and mineralization of the Tanco rare-element pegmatite, southeastern Manitoba (Field Trip A3); Geological Association of Canada–Mineralogical Association of Canada, Joint Annual Meeting, May 27–29, 1996, Winnipeg, Manitoba, 63 p.

Černý, P., Ercit, T. and Vanstone, P. 1998: Mineralogy and petrology of the Tanco rare-element pegmatite deposit, southeastern Manitoba; International Mineralogical Association, 17th General Meeting, August 9–14, 1998, Toronto, Ontario, Field Trip Guidebook B6, 74 p.

Černý, P., Trueman, D.L., Ziehlke, D.V., Goad, B.E. and Paul, B.J. 1981: The Cat Lake-Winnipeg River and the Wekusko Lake pegmatite fields, Manitoba; Manitoba Energy and Mines, Manitoba Resources Division, Economic Geology Report ER80-1, 215 p.

Gilbert, H.P. 2008: Stratigraphic investigations in the Bird River greenstone belt, Manitoba (part of NTS 52L5, 6); *in* Report of Activities 2008, Manitoba Science, Technology, Energy and Mines, Manitoba Geological Survey, p. 121–138.

Kremer, P.D. 2010: Structural geology and geochronology of the Bernic Lake area in the Bird River greenstone belt, Manitoba: evidence for syn-deformational emplacement of the Bernic Lake pegmatite group; M.Sc. thesis, University of Waterloo, Waterloo, Ontario, 91 p.

Linnen, R.L., van Lichtervelde, M. and Černý, P. 2012: Granitic pegmatites as sources of strategic metals; Elements, v. 8, no. 4, p. 275–280.

London, D. 2008: Pegmatites; The Canadian Mineralogist, Special Publication no. 10, 347 p.

Martins, T., Breasley, C.M., Groat, L.A., Linnen, R.L., Deveau, C. and Rankmore, S. 2024: The Tanco mine: geological setting, internal zonation, mineralogy and mining of a world-class rare element pegmatite deposit; Geological Association of Canada–Mineralogical Association of Canada, Joint Annual Meeting, May 19–22, 2024, Brandon, Manitoba, Field Trip Guidebook FT-7, 30 p.

Natural Resources Canada 2021: Canada's list of critical minerals; Government of Canada, URL <https://www.nrcan.gc.ca/criticalminerals> [March 2021].

Rinaldi, R., Černý, P. and Ferguson, R.B. 1972: The Tanco pegmatite at Bernic Lake, Manitoba, VI, lithium-rubidium-cesium micas; The Canadian Mineralogist, v. 11, p. 690–707.

Roda-Robles, E., Simmons, W., Pesquera, A., Gil-Crespo, P.P., Nizamoff, J. and Torres-Ruiz, J. 2015: Tourmaline as a petrogenetic monitor of the origin and evolution of the Berry-Havey pegmatite (Maine, USA); American Mineralogist, v. 100, no. 1, p. 95–109.

Stilling, A., Černý, P. and Vanstone, P.J. 2006: The Tanco pegmatite at Bernic Lake, Manitoba, XVI, zonal and bulk compositions and their petrogenetic significance; The Canadian Mineralogist, v. 44, no. 3, p. 599–623.

van Lichtervelde, M., Linnen, R.L., Salvi, S. and Didier, B. 2006: Evaluating the role of metagabbro rafts on tantalum mineralization in the Tanco pegmatite, Manitoba; The Canadian Mineralogist, v. 44, p. 625–644.

Wise, M.A., Müller, A. and Simmons, W.B. 2022: A proposed new mineralogical classification system for granitic pegmatites; The Canadian Mineralogist, v. 60, no. 2, p. 229–248.

Zubi, G., Dufo-López, R., Carvalho, M. and Pasaoglu, G. 2018: The lithium-ion battery: state of the art and future perspectives; Renewable and Sustainable Energy Reviews, v. 89, p. 292–308.

GS2024-5

Cat Tail pegmatite: zonation and mineralogy, Cat Lake area, southeastern Manitoba (part of NTS 52L11)

by T. Martins and J. Janssens

Summary

The Cat Tail pegmatite is located east of Cat Lake in a part of the Cat Lake–Winnipeg River pegmatite field in southeastern Manitoba. The pegmatite does not outcrop and is only known from diamond drillholes. This report presents a hand-sample description of the mineralogy and pegmatite zonation of the Cat Tail dike. The pegmatite can be divided into five zones of primary crystallization based on texture and mineralogy: border, wall, intermediate, central and quartz core. Late fracture filling and fracture-controlled replacement veinlets of spodumene that crosscut the primary zones are also visible. Interest in hard-rock lithium related to pegmatites has risen dramatically, and Manitoba is well endowed with these pegmatites and is seen as a prime location to study and explore for these types of mineral deposits.

In Brief:

- The zonation of the spodumene-bearing Cat Tail pegmatite is described
- Future work includes petrography and detailed mineral chemistry characterization

Citation:
Martins, T. and Janssens, J. 2024: Cat Tail pegmatite: zonation and mineralogy, Cat Lake area, southeastern Manitoba (part of NTS 52L11); *in* Report of Activities 2024, Manitoba Economic Development, Investment, Trade and Natural Resources, Manitoba Geological Survey, p. 33–37.

Introduction

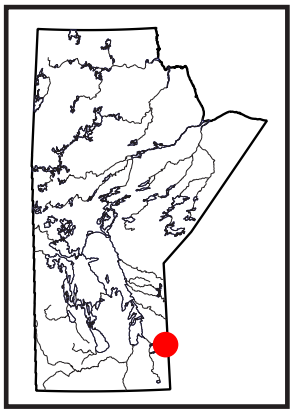
The Bird River domain in southeastern Manitoba has seen considerable exploration work in the last few years, particularly for spodumene-bearing pegmatites, the primary source of hard-rock lithium (Li) in the region. Global demand for battery metals, including Li, continues to be high due to the incentive to transition to a low-carbon economy. Furthermore, Canada has recognized Li to be a critical element (Government of Canada, 2024) to support economic growth, competitiveness and job creation, the advancement of reconciliation with Indigenous peoples and fostering of diverse, inclusive workplaces and communities, and to enhance global security and partnerships with allies to avoid global supply-chain disruptions (Government of Canada, 2022).

Granitic pegmatites are well known to be one of the best sources for many elements considered critical (e.g., Ta, Cs, Rb) but are particularly known for their Li enrichment (Linnen et al., 2012). Manitoba is well positioned in the supply of Li, amongst other critical elements, as demonstrated by a long history of exploration in the Bird River domain and production of spodumene concentrate from the Li-Cs-Ta (LCT)–bearing pegmatite at the Tanco mine.

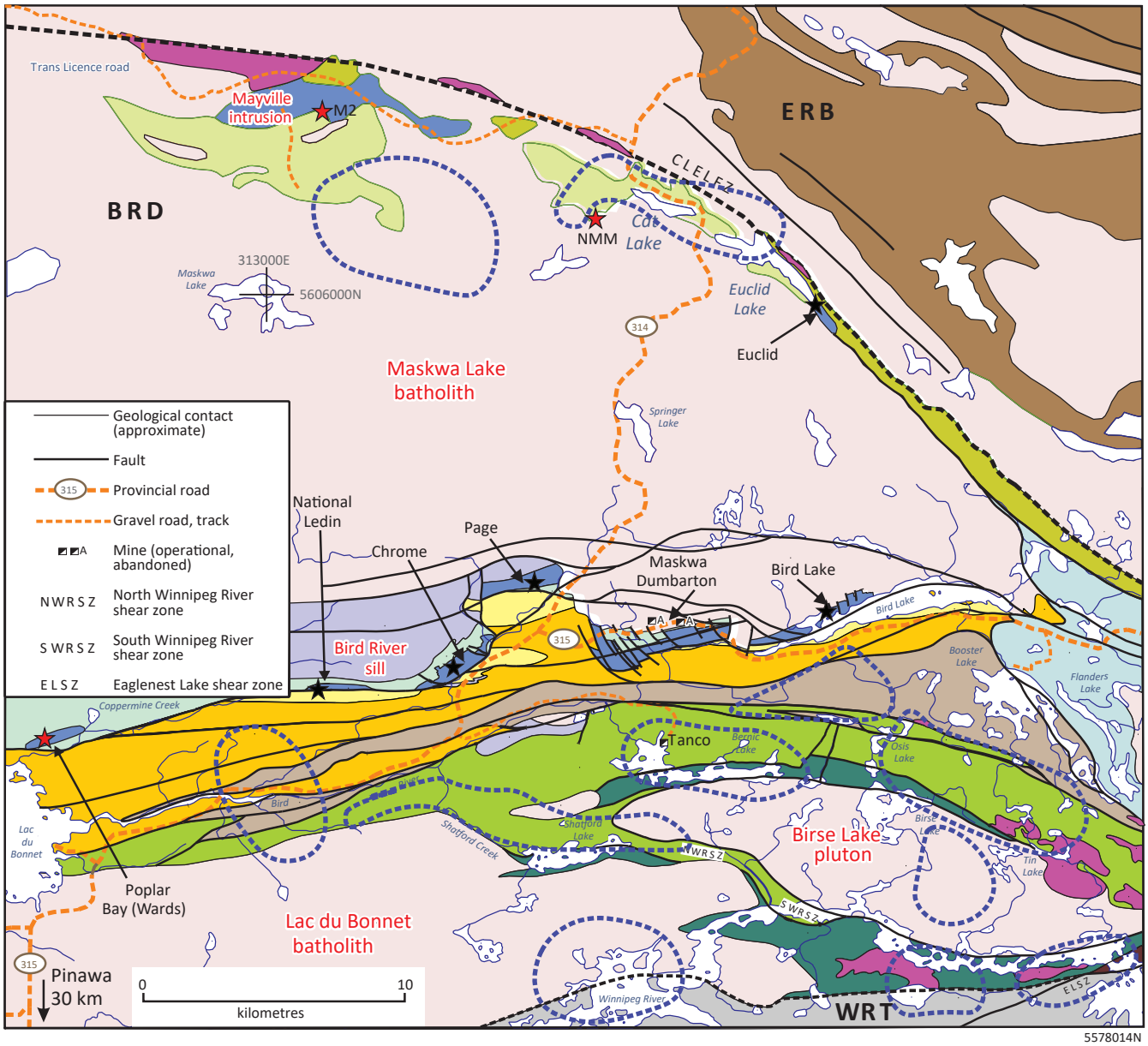
The Cat Tail pegmatite is a good example of a spodumene-bearing pegmatite that was recently discovered by diamond-drilling east of Cat Lake, approximately 180 km northeast of Winnipeg, Manitoba. This report focuses on describing the zonation of the Cat Tail pegmatite from drillcore donated by W.S. Ferreira to Manitoba's drillcore libraries in Winnipeg.

Geological setting

The Cat Tail pegmatite is considered part of the Eagle-Irgon pegmatite group of the Cat Lake–Winnipeg River pegmatite field, as defined by Černý et al. (1981). The Cat Lake–Winnipeg River pegmatite field is part of the Bird River domain of the Superior province (Figure GS2024-5-1). The Bird River domain is separated from the English River domain to the north by the Cat Lake–Euclid Lake fault and from the Winnipeg River domain to the south by the Winnipeg River fault.



An integral part of the Bird River domain is the Bird River greenstone belt, located along the southern side of the domain (Figure GS2024-5-1). The Bird River greenstone belt (BRGB) is an east-trending supracrustal belt that extends for 150 km from Lac du Bonnet in the west to Separation Lake (Ontario) in the east. The BRGB has been subdivided into two geochemically distinct sequences (northern and southern panels), both of which are composed of ca. 2.75–2.72 Ga juvenile, arc-type metavolcanic and associated metasedimentary rocks. These two panels are separated by the Booster Lake Formation (<2712 ±17 Ma; Gilbert, 2006), a turbiditic sequence with classic Bouma-type features that is considered penecontemporaneous with clastic fluvial-alluvial deposits of the Flanders Lake Formation immediately to the east (Figure GS2024-5-1; Gilbert, 2006). For a detailed geological description of the BRGB, the reader is referred to work by Gilbert and co-authors (e.g., Gilbert, 2006; Gilbert et al., 2008).



Bird River domain

Intrusive rocks

- S-type granite
- Granite, granodiorite, tonalite
- Gabbro, diorite, quartz diorite
- Pyroxenite, anorthosite, gabbro

Late sedimentary rocks

Flanders Lake formation

- Arenite, polymictic conglomerate

Volcanic and sedimentary rocks

Bird River belt South Panel

Bernic Lake formation

- Heterolithic volcanic breccia, rhyolite, basalt, andesite

Eaglenest Lake formation

- Greywacke, siltstone

Southern MORB-type formation

- Basalt, aphyric; gabbro

Bird River belt North Panel

- Massive to fragmental, mafic to felsic volcanic and sedimentary rocks

Peterson Creek formation

- Massive to fragmental felsic volcanic rocks

Northern MORB-type formation

- Basalt, aphyric; gabbro

Cat Lake area

- Sedimentary and volcanic rocks, related gneiss
- Tholeiitic basalt

English River basin

- Paragneiss, granitoid intrusive rocks, migmatite, pegmatite

Winnipeg River terrane

- Tonalite, granodiorite, granitoid gneiss

- Ni-Cu-PGE deposit/occurrence
- Cr-PGE deposit/occurrence
- Domain or terrane boundary

***Figure GS2024-5-1**: Tectonic assemblages of the Bird River domain, southeastern Manitoba (modified from Gilbert et al., 2008, 2013; Yang et al., 2013). Abbreviations: BRD, Bird River domain; CLELFZ, Cat Lake–Euclid Lake fault zone, indicated by the bold dashed line; ERB, English River basin; M2, Mayville deposit; NMM, New Manitoba mine; WRT, Winnipeg River terrane. Blue dashed lines represent location of the pegmatite groups from the Cat Lake–Winnipeg River pegmatite field (after Černý et al., 1981).*

North of the BRGB, the Bird River domain consists of a granitoid terrane (Maskwa Lake batholith) that contains intrusive phases ranging from 2.85 to 2.73 Ga (Gilbert et al., 2008; Figure GS2024-5-1). This north side of the Bird River domain was ascribed to the northern limb of the BRGB by Yang and Houlé (2020). These authors described the Cat Creek–Euclid Lake area as underlain by a suite of greenstone assemblages formed in a continental-margin setting adjacent to the Mesoarchean Maskwa Lake batholith. The greenstone assemblages consist mainly of mafic–felsic volcanic and related intrusive rocks, epiclastic and minor volcaniclastic rocks, and mafic–ultramafic layered intrusions. These were intruded by younger phases of tonalite-trondhjemite-granodiorite rocks (i.e., Maskwa Lake batholith II of Yang and Houlé, 2020), late peraluminous granite and pegmatite intrusions.

Cat Tail pegmatite

The Cat Tail pegmatite was discovered in 2018 by diamond-drilling when an attempt was made to intersect a possible extension of the Irgon pegmatite. The exploration program consisted of seven NQ-size drillholes (Figure GS2024-5-2a) totalling 1256 m, with six of the holes (CT-18-01 to CT-18-06) located to target the pegmatite. The true width of the pegmatite has not been determined and it remains open at depth and along strike (Figure GS2024-5-2b; Assessment File 52L19666, Manitoba Economic Development, Investment, Trade and Natural Resources, Winnipeg). A detailed description of the discovery and detailed logs of the diamond-drill holes can be found in this assessment file. A spodumene occurrence near the pegmatite discovered by drilling was previously reported by M.G. Smerchanski in 1948 (Assessment File 98073).

The hostrocks for the Cat Tail pegmatite are a mafic volcanic unit, which locally contains holmquistite (Li-bearing amphibole) as the contact with the pegmatite is approached. The Cat Tail pegmatite can be classified as LCT complex type, rare-element class, spodumene-bearing pegmatite according to the classification of Černý and Ercit (2005). Observations for the present report were based on available sections of drillholes CT18-01 to CT-18-06 kept in Manitoba's drillcore libraries. The drillcore was selectively sampled for thin sections for future petrographic work.

Pegmatite zonation

The Cat Tail pegmatite can be divided into five zones of primary crystallization: border, wall, intermediate, central and quartz core. Later fracture filling and fracture-controlled replacement veinlets of spodumene that crosscut the primary zones are also visible.

The border zone is pink and fine to medium grained. The primary minerals present are quartz, albite, Fe-oxides and possible columbite group minerals (CGM). Albite of the cleavelandite habit is visible throughout this zone. Small stringers of biotite measuring 1–5 cm (locally up to 30 cm) are present as xenoliths of country rock (Figure GS2024-5-3a). Pegmatite contains a local foliation, and the pink colour is most likely due to hematization occurring locally as red veinlets that crosscut the foliation (Figure GS2024-5-3a). Hematization is not pervasive throughout the entire border zone.

The wall zone is pink and medium grained. The pink colour is due to both the presence of K-feldspar and localized hematite staining. The main minerals are quartz, K-feldspar, albite, muscovite and occasional clumps of biotite (possibly partially assimilated from the country rock). In places, a fabric is observed in the orientation of the quartz. Minor modal components include tourmaline, Fe-oxides (possibly ilmenite) and CGM.

The intermediate zone is up to 2.4 m wide (apparent width); it is medium to coarse grained with localized hematite in late fractures. Clots of the country rock are present but fewer than what is observed in the wall zone. Main mineral phases are quartz, albite, spodumene, K-feldspar and muscovite, with minor components including tourmaline, Fe-oxides (possibly ilmenite), apatite, Li-Mn-Fe phosphates and CGM. Typical primary spodumene content varies between 3 and 10% but is locally up to 25% modal content. Late veinlets of spodumene crosscut quartz and feldspars, and spodumene is also observed replacing feldspars.

The central zone is white and medium to very coarse grained, with local layers of aplite, and is variably strained, ranging from nonfoliated to intensely foliated locally (Figure GS2024-5-3b). Additionally, some areas with the coarse-grained quartz and spodumene association do not present any foliation. Bands of the aplitic texture interchange with the very coarse grained texture of the pegmatite. The aplite bands are mostly composed of albite, whereas the coarser grained bands contain mainly albite, spodumene, quartz and K-feldspar, with minor apatite and garnet. In the coarser grained layers, late spodumene veinlets surround and overprint larger crystals of quartz and feldspar (Figure GS2024-5-3b). Spodumene in the central zone is mostly white, but a light green colour variety is also present.

The quartz core zone is composed mainly of quartz with minor feldspar and a platy purple mineral tentatively identified as lepidolite. This zone is cut by spodumene and Fe-oxide veinlets.

Economic considerations

A better understanding and characterization of Li-bearing pegmatites from the Cat Lake–Winnipeg River pegmatite field further enhances the role and potential of Manitoba as a Li producer, particularly in the vicinity of the Tanco mine. Lithium is amongst the 34 elements that Canada considers critical (Government of Canada, 2024) for its potential to support Canada's economic growth and its direct role in the green revolution (Government of Canada, 2022). Rare-element pegmatites such as the Cat Tail dike are a source of hard-rock Li that is expected to continue to grow in the future (U.S. Geological Survey, 2024). Manitoba plays an increasingly important role in the production

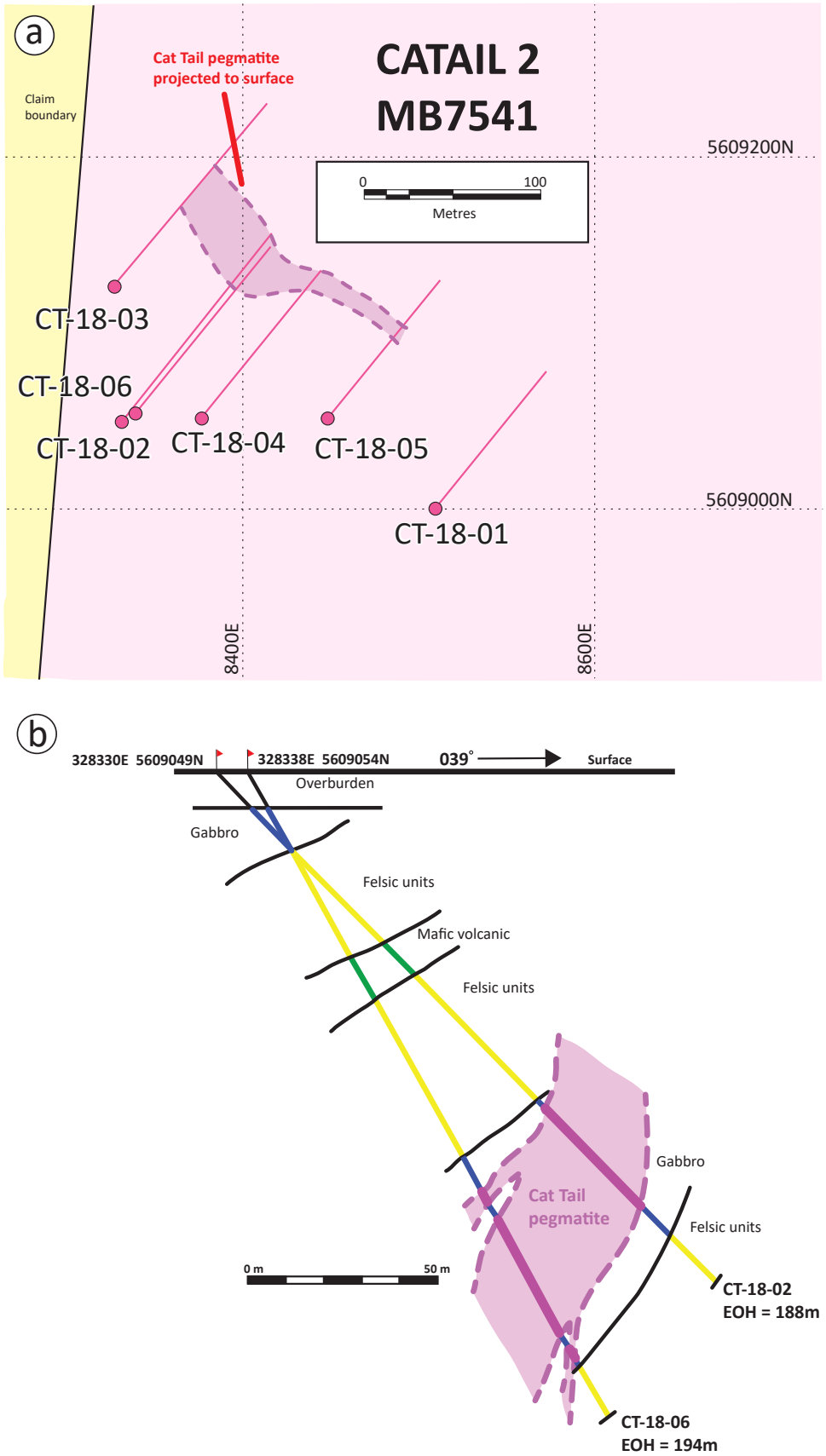


***Figure GS2024-5-2**: Maps showing **a)** location of drillholes within the Cat Tail pegmatite claim area, with the pegmatite projected to surface; and **b)** idealized cross-section of drillholes CT-18-02 and CT-18-06. Modified from Assessment File 52L19666 (Manitoba Economic Development, Investment, Trade and Natural Resources, Winnipeg). Abbreviation: EOH, end of hole.*

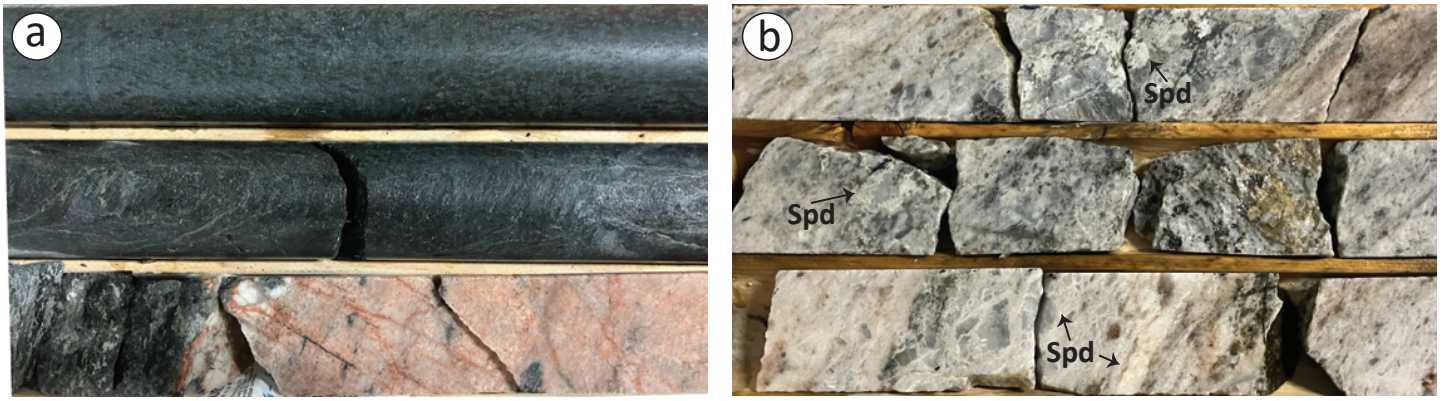


Figure GS2024-5-3*: Drillcore photos of the Cat Tail pegmatite:* ***a)*** *hostrock (volcanic unit) of the Cat Tail pegmatite and pegmatite border zone with late hematite veinlets and biotite clots;* ***b)*** *central zone of the pegmatite exhibiting foliation and late spodumene replacing feldspars and in stringers surrounding larger feldspar and quartz crystals. Abbreviations: Spd, spodumene. Drillcore is approximately 47.6 mm in diameter.*

of hard-rock Li with the extraction of spodumene at the Tanco mine. Future work on the Cat Tail pegmatite will include petrographic descriptions, mineralogical studies and geochronology. These data will help provide a better understating of the level of fractionation of the pegmatite and timing of emplacement, which can have implications for exploration for pegmatite-hosted Li in this part of Manitoba.

Acknowledgments

Acknowledgment is due to W. Ferreira for introducing the authors to the Cat Tail pegmatite and his enthusiasm and interest in discussing the drillcore. Appreciation is also due to the staff at the Manitoba Geological Survey's Midland Sample and Core Library (C. Epp and P. Belanger) for retrieving the drillcore and facilitating the work. Thanks go to E. Yang and K. Reid for critical reviews of a previous version of the manuscript. C. Steffano did the layout of the report. RnD Technical provided technical editing services.

References

Černý, P. and Ercit, T.S. 2005: The classification of granitic pegmatites revisited; The Canadian Mineralogist, v. 43, no. 6, p. 2005–2026.

Černý, P., Trueman, D.L., Zeihlke, D.V., Goad, B.E. and Paul, B.J. 1981: The Cat Lake–Winnipeg River and the Wekusko Lake pegmatite fields, Manitoba; Manitoba Department of Energy and Mines, Mineral Resources Division, Economic Geology Report ER80-1, 216 p.

Gilbert, H.P. 2006: Geological investigations in the Bird River area, southeastern Manitoba (parts of NTS 52L5N and 6); *in* Report of Activities 2006, Manitoba Science, Technology, Energy and Mines, Manitoba Geological Survey, p. 184–205.

Gilbert, H.P., Davis, W.D., Duguet, M., Kremer, P.D., Mealin, C.A. and MacDonald, J. 2008: Geology of the Bird River Belt, southeastern Manitoba (parts of NTS 52L5, 6); Manitoba Science, Technology, Energy and Mines, Manitoba Geological Survey, Geoscientific Map MAP2008-1, scale 1:50 000.

Gilbert, H.P., Houlé, M.G., Yang, X.M., Scoates, J.S., Scoates, R.F.J., Mealin, C.A., Bécu, V., McNicoll, V. and Galeschuk, C.R. 2013: Mafic and ultramafic intrusive rocks and associated Ni-Cu-(PGE) and Cr-(PGE) mineralization in the Bird River greenstone belt, southeast Manitoba; Geological Association of Canada–Mineralogical Association of Canada, Joint Annual Meeting, Field Trip Guidebook FT-C2; Manitoba Innovation, Energy and Mines, Manitoba Geological Survey, Open File OF2013-7, 51 p.

Government of Canada 2022: Introducing Canada's Critical Minerals Strategy; Government of Canada, URL <https://www.canada.ca/en/campaign/critical-minerals-in-canada/canadas-critical-minerals-strategy.html> [June 2024].

Government of Canada 2024: Canada's critical minerals; Government of Canada, URL <https://www.canada.ca/en/campaign/critical-minerals-in-canada/critical-minerals-an-opportunity-for-canada.html> [September 2024].

Linnen, R.L., van Lichtervelde, M. and Černý, P. 2012: Granitic pegmatites as sources of strategic metals; Elements, v. 8, no. 4, p. 275–280.

U.S. Geological Survey 2024: Lithium; United States Geological Survey, Mineral Commodity Summaries, January 2024, p. 110–111, URL <https://pubs.usgs.gov/periodicals/mcs2024/mcs2024-lithium.pdf> [June 2024].

Yang, X.M. and Houlé, M.G. 2020: Geology of the Cat Creek–Euclid Lake area, Bird River greenstone belt, southeastern Manitoba (parts of NTS 52L11, 12); Manitoba Agriculture and Resource Development, Manitoba Geological Survey, Geoscientific Report GR2020-1, 105 p., 1 map at 1:20 000 scale.

Yang, X.M., Gilbert, H.P. and Houlé, M.G. 2013: Cat Lake–Euclid Lake area in the Neoarchean Bird River greenstone belt, southeastern Manitoba (parts of NTS 52L11, 12): preliminary results of bedrock geological mapping and their implications for geodynamic evolution and metallogeny; *in* Report of Activities 2013, Manitoba Mineral Resources, Manitoba Geological Survey, p. 70–84.

GS2024-6

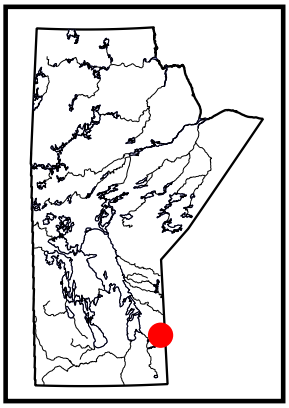
Preliminary observations from the Cat Lake–Winnipeg River pegmatite field, southeastern Manitoba (parts of NTS 52L5, 6, 11): evidence for the effect of structural setting and emplacement mechanism on the size and morphology of lithium-bearing pegmatites

by T.K. Cawood[1], S.R. Beyer[1], N. Mohammadi[1], C.J.M. Lawley[1], T. Martins and M.L. Rinne

In Brief:

- Field observations were made at several lithium-bearing pegmatites and their hostrocks in southeastern Manitoba to investigate how the structural setting and emplacement mechanisms may influence their size and shape
- The shape of the pegmatite-host rock contacts vary significantly among the pegmatites visited, reflecting the rheology of the host rock at the time of emplacement
- The pegmatites display a variety of internal fabrics, ranging from randomly oriented crystals formed by static crystallization from a melt with no subsequent deformation, to well-developed planar fabric that likely accommodated deformation during emplacement

Citation:
Cawood, T.K., Beyer, S.R., Mohammadi, N., Lawley, C.J.M, Martins, T. and Rinne, M.L. 2024: Preliminary observations from the Cat Lake–Winnipeg River pegmatite field, southeastern Manitoba (parts of NTS 52L5, 6, 11: evidence for the effect of structural setting and emplacement mechanism on the size and morphology of lithium-bearing pegmatites); *in* Report of Activities 2024, Manitoba Economic Development, Investment, Trade and Natural Resources, Manitoba Geological Survey, p. 38–48.



Summary

In August 2024, field observations were made at several lithium-bearing pegmatites in southeastern Manitoba to investigate how their structural setting and emplacement mechanisms may influence their size and shape. The observed pegmatites intrude a variety of hostrock types (including metamorphosed basalt, intermediate volcanics, gabbro and granodiorite). These pegmatite intrusions display a range of sizes (with dike widths ranging from less than 1 m up to 100 m) and morphologies (ranging from planar dikes to subequidimensional bodies). Contacts between pegmatite and hostrocks are typically sharp but vary from planar to bulbous and irregular in form. Whereas most of the observed pegmatites display internal fabrics indicative of static crystallization, one has well-developed compositional banding that is likely magmatic in origin, and another displays high-strain zones due to solid-state ductile deformation. Future work will include thin-section microstructural observations and analysis by electron backscatter diffraction to distinguish between fabrics resulting from magmatic flow and those resulting from solid-state ductile shearing.

Introduction

Rare-metal–bearing granitic pegmatites are an important source of lithium, cesium and tantalum (e.g., Tanco, Manitoba; Bikita, Zimbabwe; Greenbushes, Australia). They are also potentially significant sources of various other metals and minerals that are considered 'critical' (Natural Resources Canada, 2024), including bismuth, fluorspar, niobium, the rare-earth elements, tin, titanium and uranium.

Granitic pegmatites typically occur in groups, which may be dominated by a single large pegmatite (such as the Tanco pegmatite, which is up to 1520 m long, 1060 m wide, and ~100 m thick [Stilling et al., 2006], and is significantly larger than other known pegmatites in its immediate vicinity), or may comprise a sheeted swarm of numerous parallel, narrow (metre-scale) pegmatite dikes separated by barren hostrock (like the Little Nahanni pegmatite group, Northwest Territories; Groat et al., 2003). This has major implications for whether a pegmatite or pegmatite group can be mined economically. The shape of the pegmatite group, and the morphology of the individual pegmatite dikes within it, is likely a result of the mechanism of emplacement and the presence or absence of subsequent deformation. However, few studies have directly addressed the emplacement mechanisms of pegmatites and how different structural controls can result in different morphologies (e.g., Brisbin, 1986; Kremer, 2010; Silva et al., 2023).

Factors that may influence the emplacement mechanism (and resulting morphology) of pegmatites and pegmatite groups include the volume and addition rate of melt; melt pressure versus confining pressure; the stress state of the crust (compressional, extensional or transform); the rheology of the hostrock (which is a function of lithology, grain size, temperature and fluid content, among others); the degree of strain localization (with more localized deformation possibly channeling melts into fewer, larger pegmatite bodies); the presence and nature of structural-trap sites; and the possible superposition of multiple melt pulses (Brisbin, 1986; Passchier and Trouw, 2005; Hall and Kisters, 2012; Plunder et al., 2022; see also summary in Ching, 2024). Empirically, it is noted by industry geologists that pegmatites emplaced into coarse-grained granitic or gabbroic rocks tend to be planar dikes with sharp contacts, whereas those emplaced into fine-grained metasedimentary or mafic metavolcanic rocks tend to be highly irregular in shape.

[1] Natural Resources Canada, Geological Survey of Canada–Central, Ottawa, Ontario

This report details field observations made on pegmatites in the Cat Lake–Winnipeg River pegmatite field of Manitoba, as part of a larger field campaign investigating the structural setting and emplacement mechanisms of more than 30 pegmatites across the western Superior province. The size and morphology of the pegmatites and the characteristics of the hostrock are documented for each. Results will be compiled with similar data (e.g., Černý et al., 1981; Martins et al., 2013, Table 1) from Canada and globally to investigate potential relationships between the mechanisms of pegmatite emplacement and the resultant size and morphology of the pegmatites and pegmatite groups.

Geological setting

The Cat Lake–Winnipeg River pegmatite field is hosted largely by the Bird River domain, located in the western portion of the Archean Superior province (Figure GS2024-6-1). The Bird River domain includes the northern Cat Creek–Euclid Lake area (Yang and Houlé, 2020) and a southern area that is subdivided into north and south panels separated by the metasedimentary Booster Lake and Flanders Lake formations (Gilbert, 2006).

Pegmatites of the Cat Lake–Winnipeg River field are divided into the Cat Lake–Maskwa Lake and Winnipeg River pegmatite districts, each of which comprises a number of distinct groups of pegmatites that are spatially, mineralogically and geochemically related (Černý et al., 1981). The term pegmatite 'series' is used when the relationships between the pegmatites is less clear.

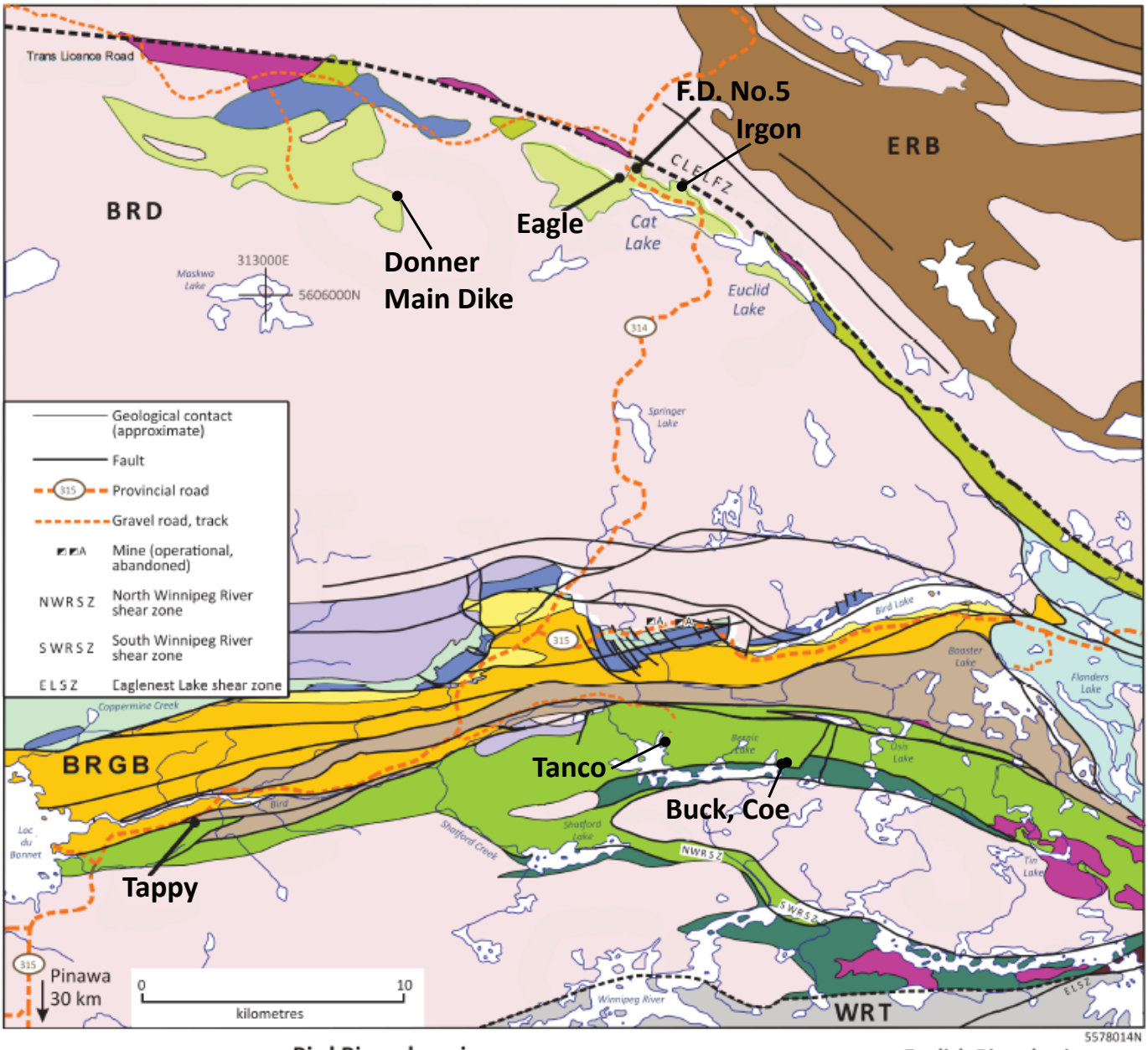
Rare-metal pegmatites of the Cat Lake–Maskwa Lake pegmatite district intruded largely metabasalt of the Lamprey Falls Formation, north of the Maskwa Lake batholith (Černý et al., 1981). The Donner Main Dike (Figure GS2024-6-1) forms part of the Maskwa Lake pegmatite series. Most of the pegmatites in this series are subvertical, northeast-striking dikes, parallel to nearby shear and fault zones (Černý et al., 1981). The spodumene-bearing Main Dike comprises three closely spaced parallel pegmatites, all of which are ~3–5 m thick with some pinch-and-swell variation, up to 550 m in length and display sharp contacts (Černý et al., 1981; Bannatyne, 1985). The Donner NW Dike contains petalite and is similarly narrow (~5 m), with an exposed length of ~250 m, and has sharp contacts (Černý et al., 1981). The Eagle, F.D. No. 5 and Irgon pegmatites form part of the Eagle-Irgon pegmatite group. Most of these pegmatites form lenticular, subvertical bodies that strike westerly, are concordant with the hostrock foliation and have common pinch-and-swell variations in thickness (Černý et al., 1981), although F.D. No. 5 forms part of a plug-shaped granitic intrusion (Bannatyne, 1985). Irgon displays a banded gneissic fabric parallel to the dike contacts (Bannatyne, 1985), suggesting subsolidus deformation (Černý et al., 1981). If continuous, the Eagle pegmatite may be 1100 m long and 6–12 m thick (Černý et al., 1981).

Rare-metal pegmatites of the Winnipeg River pegmatite district intrude the south panel of the Bird River greenstone belt (Figure GS2024-6-1). The Tanco, Buck and Coe pegmatites form part of the Bernic Lake pegmatite group, which intrudes mafic metavolcanics and associated subvolcanic gabbroic intrusions along the sheared contacts between and within the Southern MORB-type and Bernic Lake formations (Černý et al., 1981; Martins and Kremer, 2012). Pegmatite/hostrock contacts are sharp and straight or bulbous, and attitudes vary from east to northeast striking and subhorizontal to subvertical (Martins et al., 2013). All the larger pegmatites of this group form flat subhorizontal sheets with sharp straight contacts that occupy late fractures, such as the Tanco pegmatite (~1520 m long, 1060 m wide and up to ~100 m thick; Stilling et al., 2006) and the thinner Pegli pegmatite (at least 2.5 km long, but a maximum of 10 m thick), whereas the more steeply dipping dikes in the group are much smaller and have strongly brecciated wallrocks (Černý et al., 1981). The Tappy pegmatite likely forms part of the Lac du Bonnet pegmatite group. Pegmatites in this group strike north-northwest (parallel to a nearby dextral strike-slip fault), dip steeply to vertically, crosscut the layering and foliation of the hostrocks with sharp contacts, and have exposed lengths up to 40 m and widths up to 3 m (Černý et al., 1981; Roush et al., 2023). Some of the smaller pegmatites display brecciated textures and appear deformed (Černý et al., 1981).

Previous work on pegmatite emplacement in Manitoba

The mechanism by which pegmatite-forming melts are emplaced into the crust is directly linked to the shape and size of the resulting pegmatites. Several important studies that have looked at the emplacement of such melts were focused on localities in Manitoba. One study, by Brisbin (1986), used examples of pegmatites in the Winnipeg River field (along with other examples from around the world) to demonstrate how pegmatites emplaced in the brittle upper crust are typically tabular sheets, oriented perpendicular to the direction of minimum resistance to intrusion (which is determined by lithostatic and deviatoric stresses, as well as local factors such as strength anisotropies in the hostrock). In contrast, pegmatites emplaced into ductile hostrock deep in the crust are typically lensoid to irregular in morphology.

A second study, reported in Kremer and Lin (2006) and Kremer (2010), investigated the Bernic Lake pegmatite group and suggested that the exceptionally large, generally flat-lying, tabular Tanco pegmatite formed during the late stages of deformation. They suggest that melt was emplaced into a subhorizontal, brittle, conjugate fracture set in a unit of competent, coarse-grained gabbro surrounded by less competent, finer grained, foliated metavolcanic and volcaniclastic rocks in a brittle-ductile shear zone. In contrast, nearby pegmatites of the same age as Tanco (like the Oompa Loompa pegmatite) were emplaced into the surrounding metavolcanic rocks, which were undergoing ductile deformation at the same time as the stronger, coarse-grained metagabbro was experiencing brittle fracture. As a result, these pegmatites are smaller and highly irregular in shape, and were



Bird River domain

Intrusive rocks

- S-type granite
- Granite, granodiorite, tonalite
- Gabbro, diorite, quartz diorite
- Pyroxenite, anorthosite, gabbro

Late sedimentary rocks

Flanders Lake formation

- Arenite, polymictic conglomerate

Booster Lake formation

- Greywacke, siltstone

Volcanic and sedimentary rocks

Bird River belt south panel

Bernic Lake formation

- Heterolithic volcanic breccia, rhyolite, basalt, andesite

Eaglenest Lake formation

- Greywacke, siltstone

Southern MORB-type formation

- Basalt, aphyric; gabbro

Bird River belt north panel

- Massive to fragmental, mafic to felsic volcanic and sedimentary rocks

Peterson Creek formation

- Massive to fragmental felsic volcanic rocks

Northern MORB-type formation

- Basalt, aphyric; gabbro

Cat Lake area

- Sedimentary and volcanic rocks, related gneiss
- Tholeiitic basalt

English River basin

- Paragneiss, granitoid intrusive rocks, migmatite, pegmatite

Winnipeg River terrane

- Tonalite, granodiorite, granitoid gneiss

------ Domain or terrane boundary

Figure GS2024-6-1: *Tectonic assemblages of the Bird River greenstone belt (from Yang and Houlé, 2020), labelled with the locations of pegmatites visited. Abbreviations: BRD, Bird River domain; BRGB, Bird River greenstone belt; CLELFZ, Cat Lake–Euclid Lake fault zone; ERB, English River basin; MORB, mid-ocean–ridge basalt; WRT, Winnipeg River terrane.*

deformed during ongoing shear. The difference in emplacement styles and resulting pegmatite morphologies is thus attributed to the difference in the rheologies of the hostrocks (Kremer and Lin, 2006; Kremer, 2010).

A third study found that the orientation of spodumene-bearing pegmatites in the Wekusko Lake pegmatite field can be attributed to their spatial relationship to regional-scale fault zones (Silva et al., 2023). One group of pegmatites was emplaced into tension gashes (extensional fractures), another into extensional shear fractures and a third into en échelon fractures between strike-slip structures.

Summary of fieldwork

Between August 12 and 15, 2024, various pegmatites in the Cat Lake–Winnipeg River pegmatite field were visited, including Tanco, Coe pegmatites 7 and 8, Buck pegmatite 9, Irgon, Eagle, F.D. No. 5, Tappy and the Donner Main Dike (Figure GS2024-6-1). At each site where there was sufficient outcrop, observations were made on

- the quality of the outcrop;
- the morphology of individual pegmatites (whether they are planar dikes, pipe-like bodies or irregular in shape);
- the nature of the pegmatite group (a single isolated pegmatite, a dominant large pegmatite in a swarm of smaller pegmatites or a sheeted swarm of similar-size pegmatites);
- the approximate size of the dominant pegmatites (as the cross-sectional width);
- the nature and form of the pegmatite/hostrock contacts (sharp or gradational; planar, gently curved, bulbous or highly irregular);
- the pegmatite orientation relative to hostrock fabrics;
- the characteristics of the hostrock (lithology, grain size, tectonic fabrics and interpreted rheology during pegmatite emplacement);
- and whether the pegmatites display internal fabrics indicative of magmatic flow or solid-state deformation.

These observations are summarized in Table GS2024-6-1. Where feasible, observations were documented with photographs, aerial photographs (using a drone) and field sketches. The hostrock at selected localities was also sampled for future petrographic studies, to better constrain the metamorphic grade and conditions of deformation.

In addition to the key characteristics listed in Table 1, several pegmatites display other notable features. Coe pegmatites 7 and 8 both host abundant angular xenoliths of metabasalt, with lesser metagabbro (Figure GS2024-6-2a).

Most of the pegmatites observed display no internal deformation fabrics (Table GS2024-6-1) and comprise crystals with random orientations, or locally crystals oriented perpendicular to contacts with hostrock or xenoliths. In contrast, the main dike at Irgon displays well-developed decimetre-scale compositional banding parallel to the overall orientation of the dike (subvertical, easterly trend) and the main foliation in the hostrock (Figure GS2024-6-3a, d). The banding is defined by variations in texture, mineralogy and grain size. Bands include fine-grained aplite and coarse K-feldspar-spodumene-quartz-muscovite pegmatite, and are parallel to a variably developed foliation defined by the preferred orientation of micas and mica-rich lenses or schlieren. Abundant meso-scale structures are also observed, such as boudinage of coarse pegmatitic bands, symmetrical 'eyes' to asymmetrical sigma clasts of feldspar, and S-C fabrics (Figure GS2024-6-3b, c).

Like many of the other pegmatites, parts of the steeply dipping, northeast-trending Donner Main Dike comprise randomly oriented crystals with no internal fabrics. Along strike, however, other parts display strongly developed anastomosing to planar fabrics parallel to the dike walls (Figure GS2024-6-4). These fabrics include ~10–20 cm wide zones in which the pegmatite-forming minerals have undergone major grain-size reduction. The asymmetry of foliation curved into these high-strain zones indicates sinistral shear. Other shear sense indicators, including S-C bands and centimetre-scale quartz sigma porphyroclasts, consistently indicate a sinistral shear sense, although no lineations were observed; thus, the true direction of motion remains unknown. The hostrock (a fine-grained metavolcanic rock with abundant decimetre-scale feldspar glomerocrysts) appears unstrained, as does the curvilinear to bulbous pegmatite/hostrock contact, with local 5–20 cm irregular pegmatite apophyses.

At the northwestern corner of the F.D. No. 5 outcrop, a narrow (0.5 m wide) shear zone is developed in the relatively undeformed host granitoid (Figure GS2024-6-5). The shear zone contains highly foliated, fine-grained mylonite or ultramylonite having sharp contacts with the coarse-grained undeformed granitoid on either side. It trends approximately east-northeast with a steep dip to the north-northwest before disappearing to the east, where it is obscured by a narrow apophysis extending out from the main body of the pegmatite. This apophysis appears to grade gradually into the mylonite of the shear zone.

Preliminary interpretations

The shapes of the pegmatite/hostrock contacts vary significantly among the pegmatites visited, reflecting the rheology of the hostrock at the time of emplacement (Table GS2024-6-1). Pegmatites with planar contacts that sharply crosscut the hostrock fabrics (e.g., the subhorizontal Buck pegmatite 9), along with pegmatites with planar contacts that host angular xenoliths of wallrock (e.g., the subvertical, xenolith-rich Coe pegmatites 7 and 8) are interpreted to reflect melt emplaced into brittle fractures. Similarly, the Tanco pegmatite is thought to have been emplaced into subhorizontal brittle fractures (Kremer, 2010). Rock may fail in a brittle manner at relatively shallow crustal levels and low temperatures. Alternatively, brittle failure may be induced in deeper, hotter conditions by hydrofracturing if

Table GS2024-6-1: Summary of field observations made on pegmatites and their hostrocks in the Cat Lake–Winnipeg River pegmatite field. Abbreviations: bt, biotite; fsp, feldspar; ms, muscovite; peg, pegmatite; PT, pressure-temperature; qz, quartz; spod, spodumene; SQUI, spodumene-quartz intergrowth

Pegmatite	Location (Decimal degrees)		Location (UTM, Zone 15)		Outcrop	Pegmatite morphology	Nature of pegmatite group	Dike width	Contact		Orientation	
	N	E	E	N					Nature	Form	Relative to host foliation	Dip
Tanco	50.429	-95.453	325813.616	5589149.478	None: underground mine	Sheet/saddle-like sill	Single dominant	Up to 100 m[1] total	Sharp[2]	Planar to curvilinear[2]	Cross cuts[2]	Subhorizontal
Coe, pegmatite 7*	50.422	-95.391	330174.009	5588278.376	Poor: small exposure in forest	-	-	1 m exposed	Sharp	Planar	-	-
Coe, pegmatite 8*	50.422	-95.389	330284.131	5588253.688	Good: clear outcrop in forest	Broad sheet-like dike	Part of a loose group	5 m total	Sharp	Planar	Subparallel	Subvertical
Buck, pegmatite 9*	50.422	-95.388	330344.964	5588243.942	Good: clear outcrop in small cliff on edge of swamp	Sheet-like sill	Part of a loose group	4 m exposed	Sharp	Planar	Cross cuts	Subhorizontal
Irgon - NE apophysis	50.610	-95.428	328245.553	5609307.480	Excellent: large clear exposure	Two subparallel sheet-like dikes	Two ~2-4 m wide branches	Two 2-4 m branches total	Sharp	Bulbous to curvilinear	Cross cuts	Likely subvertical
Irgon - main dike	50.610	-95.428	328194.991	5609255.715	Excellent: large clear exposure	One dominant s heet-like dike	Single dominant dike, with several narrower parallel dikes	Up to 20 m total	Sharp	Mostly planar (small area on N side has irregular, bulbous contact)	Parallel	Subvertical
Eagle	50.614	-95.460	325960.174	5609776.857	Moderate: scattered small exposures on hills	Sheet-like dikes	Multiple parallel dikes[3]	Parallel dikes cm to several m total[3]	Sharp	Bulbous, curvilinear to irregular	Cross cuts	-
F.D. No. 5	50.615	-95.454	326390.664	5609881.669	Good: large outcrop in forest, cleaned	Sub-equidimensional body (pipe?)	Single pegmatite visible	Blob/pipe shape, up to 15 m across	Sharp to diffuse over mm	Planar to curvilinear	Cross cuts	-
Tappy	50.403	-95.693	308661.022	5586926.294	Moderate: discontinuous, small exposures	Sheet-like dikes	At least two parallel dikes	1.5-4 m[3] total	Sharp	Planar to curvilinear	Cross cuts	Steep
Donner - main dike	50.614	-95.579	317521.646	5610034.923	Good: ~200 m-long clear ridge plus other smaller outcrops	Sheet-like dike	Single pegmatite visible	1.5-5 m total	Sharp	Gently undulating to irregular; locally planar	Cross cuts	Steep

*Names according to Bannatyne (1985)

References:

[1] Stilling et al. (2006); [2] Kremer (2010); [3] Roush et al. (2023)

Table GS2024-6-1 (continued): Summary of field observations made on pegmatites and their hostrocks in the Cat Lake–Winnipeg River pegmatite field. Abbreviations: bt, biotite; fsp, feldspar; ms, muscovite; peg, pegmatite; PT, pressure-temperature; qz, quartz; spod, spodumene; SQUI, spodumene-quartz intergrowth

Pegmatite	Host lithology (meta-…)	Grain size	Fabric	Interpreted rheology during emplacement	Li-minerals	Concentric zoning	Banding/ compositional layering	Magmatic fabric	Solid state fabric	Notes
Tanco	Gabbro	Medium to coarse	Massive to moderately foliated	Brittle[2]	SQUI	Yes	-	-	No	
Coe, pegmatite 7*	Basalt	Fine	-	Brittle	Petalite, SQUI	-	-	-	No	
Coe, pegmatite 8*	Basalt, local gabbro	Fine to medium (<mm)	Massive to weakly foliated	Brittle	-	Yes: contact - aplite - coarse qz-ms - qz core	No	No	No	Abundant angular xenoliths of host rock
Buck, pegmatite 9*	Basalt	Fine	Moderately foliated	Brittle	SQUI, spodumene	No: irregular variations	No	No	No	
Irgon - NE apophysis	Intermediate volcanics, variable	Fine to medium (~mm), locally porphyritic	Weak to moderately foliated	Ductile	SQUI	No	No	No	No	
Irgon - main dike	Gabbro & basalt	Coarse to fine	Gabbro highly sheared, with anastomosing high-strain zones; basalt strongly foliated	Ductile	SQUI	No	Yes	Possibly	Possibly	Peg emplacement at PT conditions of bt stability; into major dextral shear zone
Eagle	Granodiorite	Coarse	Most weakly foliated, with rare cm-scale localized shear zones	Ductile	Spodumene	No	No	No	No	
F.D. No. 5	Granodiorite (& lesser basalt)	Coarse (& fine)	Weakly foliated (& strongly foliated)	Semi-brittle to ductile	Spodumene	Yes: weak, diffuse qz-spod core	No	Weak: aligned xenoliths	No	At W edge, peg extends into a 0.5m localized shear zone in granodiorite: replacive?
Tappy	Basalt	Fine	Weak to moderately foliated	Semi-brittle to ductile	Spodumene[3]	-	No	No	No	
Donner - main dike	Glomerocrystic volcanic	Fine with dm-scale fsp glomerocrysts	Massive	Ductile	Spodumene	No	-	Possibly	Yes: high-strain zones with grainsize decrease	Peg accommodated sinistral shear, host undeformed.

Abbreviations: bt, biotite; fsp, feldspar; ms, muscovite; peg, pegmatite; PT, pressure-temperature; qz, quartz; spod, spodumene; SQUI, spodumene-quartz intergrowth.

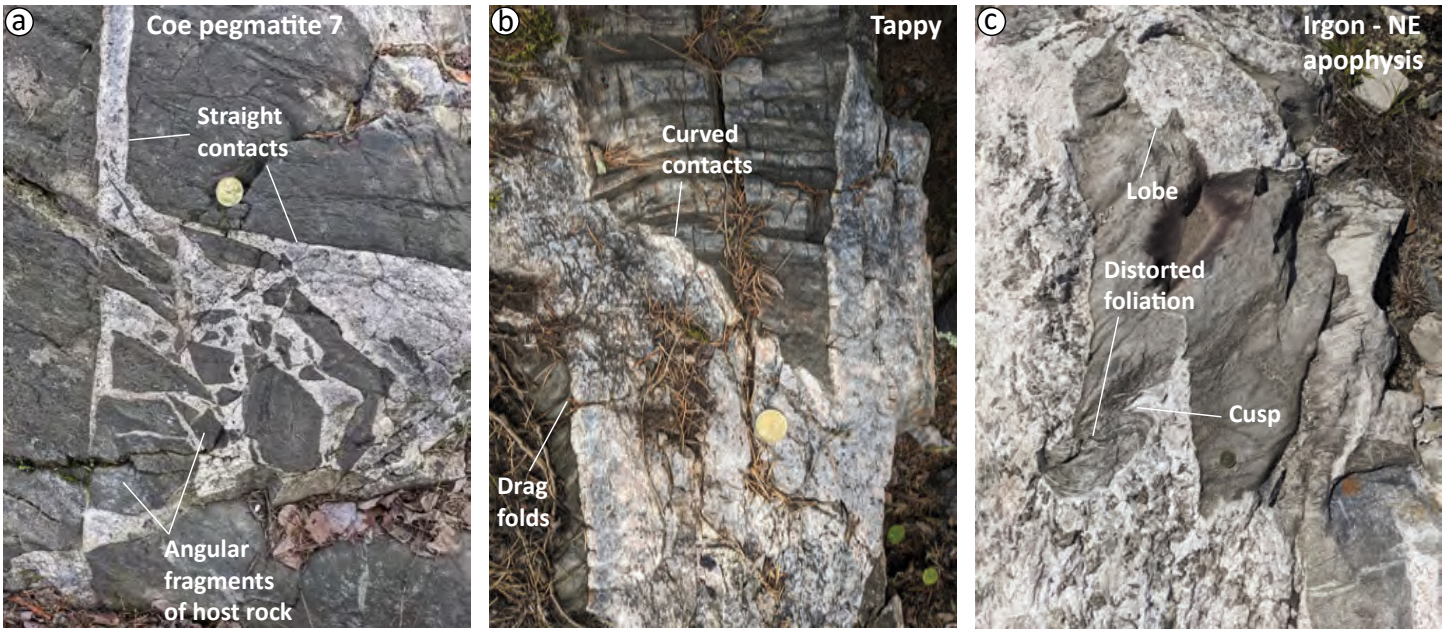


Figure GS2024-6-2: *Different styles of pegmatite/hostrock contacts:* ***a)*** *planar contacts at Coe pegmatite 7, where the host foliation is sharply truncated and the abundant hostrock xenoliths are angular;* ***b)*** *curved to gently bulbous contacts at Tappy; note the gentle curvature of the host foliation against the pegmatite, defining a weak drag fold;* ***c)*** *an irregular contact, characterized by abundant cusps and lobes, at the Irgon–NE apophysis; the hostrock foliation is locally highly distorted.*

the fluid pressure of the pegmatite-forming melt is high enough to overcome the compressive-stress conditions plus the tensile strength of the hostrock (Brisbin, 1986).

Other pegmatites, with curvilinear to bulbous and locally highly irregular contacts that crosscut the hostrock fabric, are interpreted as being emplaced when the hostrock was ductile. These include the Irgon NE apophysis, Eagle and Donner Main Dike pegmatites, which were emplaced into a variety of host lithologies, including mafic and intermediate metavolcanics, metagabbro and metagranodiorite. This indicates that melt emplacement occurred at a deep enough crustal level that ambient temperatures were high enough for all these different lithologies to be ductile. Several pegmatites in the Separation Lake greenstone belt in Ontario display similar irregular pegmatite/hostrock contacts, and Ching (2024) suggested that the pegmatite-forming melts acted as viscous indenters into the weakened, ductile hostrock.

At the roughly east-trending Irgon main dike, a small area on the north side preserves an irregular, bulbous pegmatite/host contact, whereas most of the main dike has strongly planar contacts that are parallel to the ductile foliation in the adjacent hostrocks. This suggests that the Irgon main dike was emplaced into ductile hostrock but that most of the pegmatite was controlled by the pre-existing anisotropy of the sheared host, or that the contacts were smoothed during subsequent ductile shearing.

The pegmatites also display a variety of internal fabrics that reflect different emplacement and subsequent deformation histories. Most of them comprise randomly oriented crystals or crystals that grew perpendicularly from hostrock or xenolith contacts. These pegmatites are interpreted to have crystallized from a melt under static conditions and do not record any subsequent solid-state deformation.

In contrast, Irgon and parts of the Donner Main Dike display strong internal fabrics. The compositional banding in the Irgon main dike resembles banding/layering described from within the Separation Rapids pluton in Ontario and from the nearby Glitter, Big Mack and Big Whopper pegmatites (Ching, 2024), and banding in pegmatites in the Red Cross Lake pegmatite field in Manitoba (Brisbin et al., 2012) that has been interpreted as primary magmatic layering developed during emplacement or subsequent flow of the melt. The authors support these interpretations and further suggest that each individual compositional band could represent a distinct pulse of melt. This is supported by unpublished observations made by some of the authors in Ontario where the wide (tens of metres) Big Whopper and Bolt pegmatites transition from banded pegmatite with banding-parallel rafts of hostrock into hostrock with abundant narrow (metres to centimetres), parallel, sheeted dikes of pegmatite. These narrow dikes typically each display a single composition, mineral assemblage and grain size (e.g., a single dike may comprise only aplite or only coarse K-feldspar–rich pegmatite). One possible interpretation is that these narrow dikes each formed from a single pulse of melt and, where numerous such pulses were emplaced in the same location, they built up a wide composite pegmatite dike over time.

The various meso-scale structures observed within the Irgon pegmatite, such as boudinage, asymmetrical porphyroclasts and S-C fabrics, could reflect three processes: 1) magmatic flow dur-

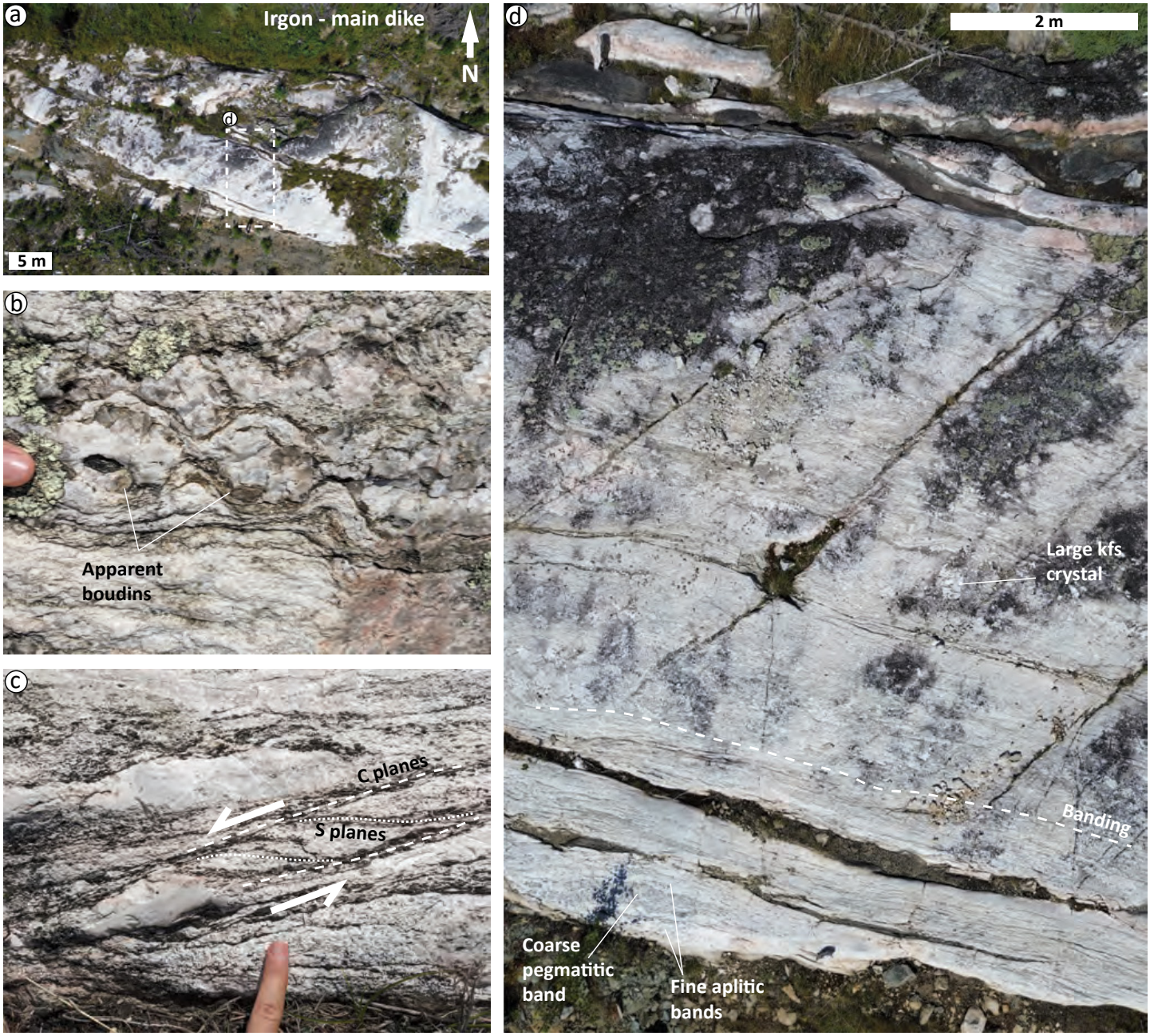


Figure GS2024-6-3: *Key characteristics of the Irgon pegmatite:* ***a)*** *aerial drone photograph of the western portion of the main Irgon dike;* ***b)*** *apparent boudins of coarse pegmatitic material within the main dike;* ***c)*** *S-C structures developed within the pegmatite;* ***d)*** *higher resolution image of aerial drone photograph in (a), showing compositional banding parallel to the pegmatite walls. Abbreviation: kfs, K-feldspar.*

ing melt emplacement; 2) magmatic flow during deformation that occurred before the pegmatite had fully crystallized; or 3) solid-state deformation that occurred under ductile conditions after complete crystallization. Microstructural observations are required to distinguish these possible origins.

Those parts of the Donner Main Dike composed of randomly oriented crystals may have formed by static crystallization from a melt with no subsequent deformation. The parts with a well-developed fabric, however, likely accommodated deformation. The apparent reduction in grain size in some internal high-strain zones suggests that minerals experienced dynamic recrystallization, indicating that at least some of the deformation occurred during solid-state ductile deformation. In contrast, the hostrock and the pegmatite/hostrock contact appear unstrained, suggesting that all deformation was accommodated within the pegmatite itself (or within a narrow shear zone/fault that was intruded and obscured by the pegmatite).

At F.D. No. 5, the occurrence of a narrow pegmatite apophysis extending into and along a discrete shear zone in the hostrock suggests that the pegmatite-forming melts may have locally

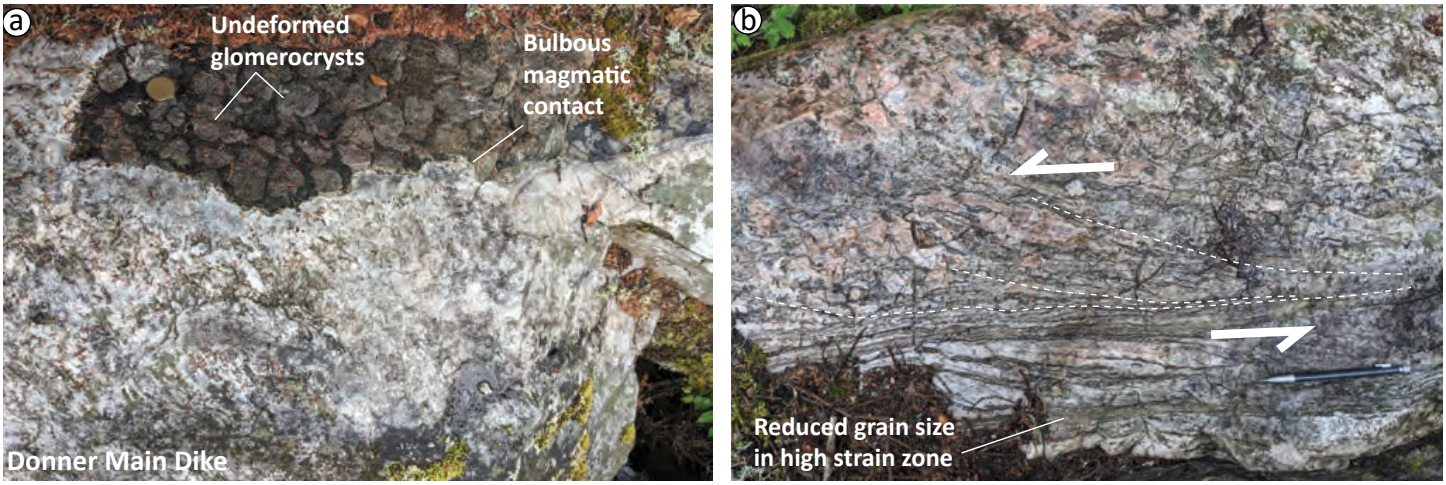


Figure GS2024-6-4: *Outcrop photographs of the Donner Main Dike:* ***a)*** *undeformed part of the dike, with a curved, bulbous magmatic contact; the hostrock is everywhere undeformed;* ***b)*** *highly sheared part of the dike, with asymmetric foliation development indicating sinistral shear, and grain-size reduction in high-strain zones.*

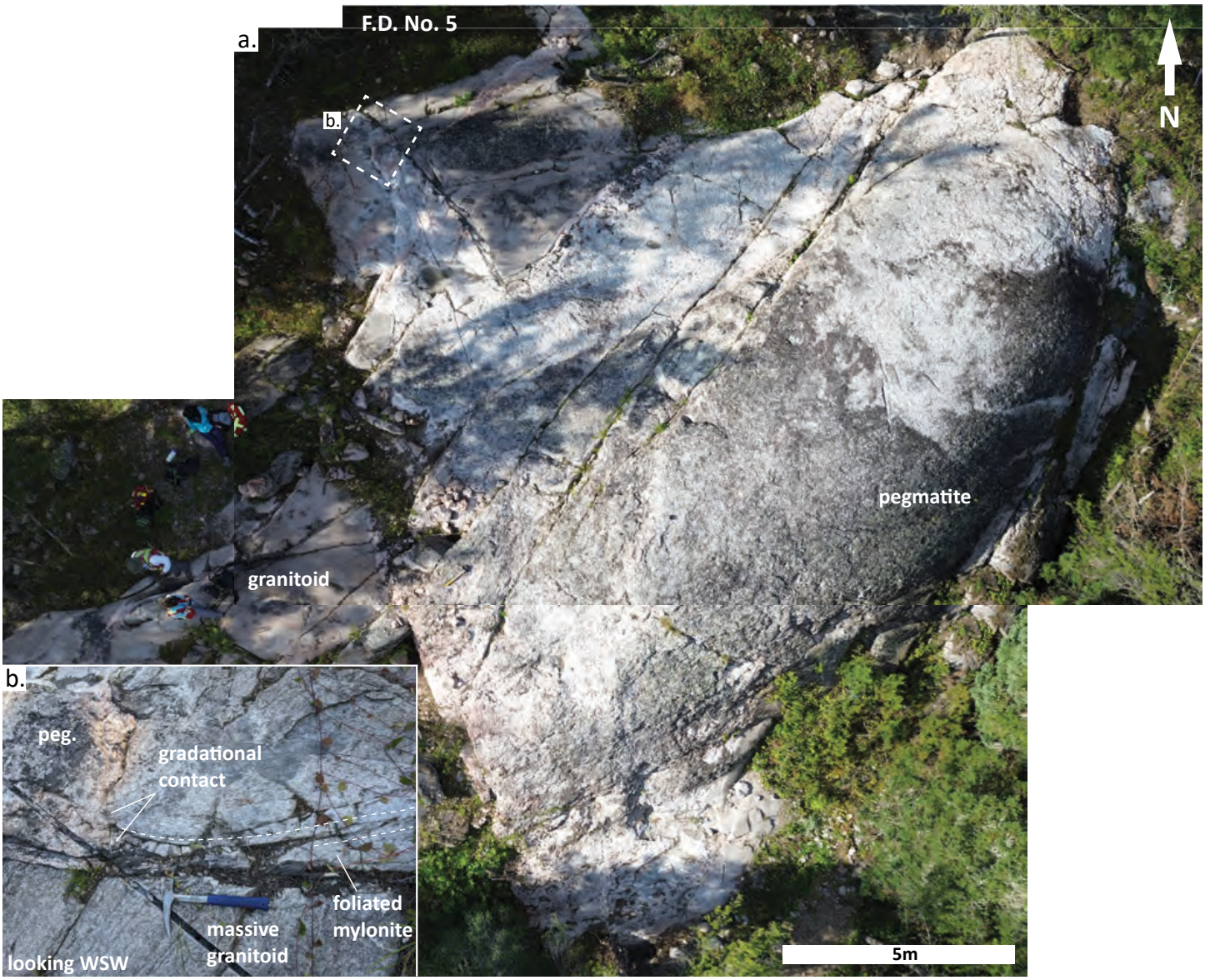


Figure GS2024-6-5: *The F.D. No. 5 pegmatite:* ***a)*** *aerial drone photograph;* ***b)*** *close-up photograph of a small shear zone in the host metagranitoid, partially invaded by an apophysis of the pegmatite.*

intruded pre-existing ductile shear zones. Similarly, the Irgon and Donner Main Dikes may have also intruded pre-existing shear zones, with ongoing deformation along the shear zones being accommodated by magmatic flow (while the dikes were still molten) and subsequent solid-state ductile deformation (as they cooled and crystallized). The gradational contact at F.D. No. 5 further suggests that the melt may have partially replaced material within the shear zone.

Economic considerations

Rare-metal pegmatites host a wide variety of metals and minerals that are considered critical by Canada and other countries (Bauer et al., 2023; Natural Resources Canada, 2024), because of their importance in the modern global economy and the 'green transition' (e.g., Linnen et al., 2012). In particular, Li is a crucial component of Li-ion batteries, which are widely used in applications from electric vehicles to cellphones. Manitoba, and Canada as a whole, host numerous occurrences of Li-bearing rare-metal pegmatites. However, only the largest (and most evolved) pegmatites, such as Tanco in Manitoba and the North American Lithium complex in Quebec, are currently being exploited. This highlights the importance of the size and shape of rare-metal pegmatites in making them attractive for mining.

Understanding what controls the morphology of pegmatites is therefore important for exploration targeting (e.g., Silva et al., 2023). The preliminary observations presented here tentatively suggest that large pegmatites may develop in long-lasting structural trap sites that were reactivated numerous times or continuously over a period of time. If correct, this suggests that exploration for large pegmatites should target structural trap sites along or within major shear zones or faults (similar to those targeted for orogenic gold mineralization; e.g., Groves et al., 2018).

Acknowledgments

The authors thank the First Nations of Treaty 3 for kindly sharing access to their traditional territories, and Sinomine, New Age Metals and Grid Metals Corp. for their support of this fieldwork. The logistical support and guidance provided by the Manitoba Geological Survey, along with K. Roberts and L. Lé Leannec of Grid Metals Corp., and M. Kaczmer of Axiom Group, is greatly appreciated. This study is supported by the Critical Minerals Geoscience and Data (CMGD) initiative of the Geological Survey of Canada (GSC).

References

Bannatyne, B.B. 1985: Industrial minerals in rare-element pegmatites of Manitoba; Manitoba Energy and Mines, Geological Services, Economic Geology Report ER84-1, 96 p., URL <https://manitoba.ca/iem/info/libmin/ER84-1.pdf> [October 2024].

Bauer, D., Khazdozian, H., Mehta, J., Nguyen, R.T., Severson, M.H., Vaagensmith, B.C., Toba, L., Zhang, B., Hossain, T., Sibal, A.P., Smith, B.J., Riddle, M.E., Graziano, D.J., Mathew, T., Cuscaden, P., Dai, Q., Iloeje, C., Edgemon, L., Sarna, C. and Quaresima, J. 2023: 2023 Critical materials strategy; United States Department of Department of Energy, 270 p., URL <https://doi.org/10.2172/1998242>.

Brisbin, W.C. 1986, Mechanics of pegmatite intrusion; American Mineralogist, v. 71, p. 644–651.

Brisbin, W.C., Eby, R.K., Corkery, M.T., Cerny, P., Chackowsky, L.E., Ferreira, K., Halden, N.M., Meintzer, R.E. and Trueman, D.L. 2012: Extreme fractionation and deformation of the leucogranite-pegmatite suite at Red Cross Lake, Manitoba, Canada, III. Description of shearing and mylonitization textures in the lepidolite pegmatites; The Canadian Mineralogist, v. 50, p. 1823–1838, URL <https://doi.org/10.3749/canmin.50.6.1823>.

Černý, P., Trueman, D.L., Zeihlke, D.V., Goad, B.E. and Paul, B.J. 1981: The Cat Lake–Winnipeg River and the Wekusko Lake pegmatite fields, Manitoba; Manitoba Department of Energy and Mines, Mineral Resources Division, Economic Geology Report ER80-1, 216 p.

Ching, J.G.W. 2024: Field, textural, and geochronological investigations into the intrusion dynamics and crystallization histories of the Separation Rapids rare-metal pegmatites, northwestern Ontario; M.Sc. thesis, University of Manitoba, 173 p.

Gilbert, H.P. 2006: Geological investigations in the Bird River area, southeastern Manitoba (parts of NTS 52L5N and 6); *in* Report of Activities 2006, Manitoba Science, Technology, Energy and Mines, Manitoba Geological Survey, p. 184–205.

Groat, L.A., Mulja, T., Mauthner, M.H.F., Ercit, T.S., Raudsepp, M., Gault, R.A. and Rollo, H.A. 2003: Geology and mineralogy of the Little Nahanni rare-element granitic pegmatites, Northwest Territories; The Canadian Mineralogist, v. 41, p. 139–160.

Groves, D.I., Santosh, M., Goldfarb, R.J. and Zhang, L. 2018: Structural geometry of orogenic gold deposits: implications for exploration of world-class and giant deposits; Geoscience Frontiers, v. 9, p. 1163–1177, URL <https://doi.org/10.1016/j.gsf.2018.01.006>.

Hall, D. and Kisters, A. 2012: The stabilization of self-organized leucogranite networks — implications for melt segregation and far-field melt transfer in the continental crust; Earth and Planetary Science Letters, v. 355–356, p. 1–12, URL <http://doi.org/10.1016/j.epsl.2012.08.033> [October 2024].

Kremer, P.D. 2010: Structural geology and geochronology of the Bernic Lake area in the Bird River greenstone belt, Manitoba: evidence for syn-deformational emplacement of the Bernic Lake pegmatite group; M.Sc. thesis, University of Waterloo, 91 p.

Kremer, P.D. and Lin, S. 2006: Structural geology of the Bernic Lake area, Bird River greenstone belt, southeastern Manitoba (NTS 52L6): implications for rare element pegmatite emplacement; *in* Report of Activities 2006, Manitoba Science, Technology, Energy and Mines, Manitoba Geological Survey, p. 206–213.

Linnen, R.L., Van Lichtervelde, M. and Černý, P. 2012: Granitic pegmatites as sources of strategic metals: Elements, v. 8, p. 275–280, URL <https://doi.org/10.2113/gselements.8.4.275>.

Martins, T. and Kremer, P.D. 2012: Rare metals in southeastern Manitoba: pegmatites from Bernic Lake and Rush Lake (parts of NTS 52L6); *in* Report of Activities 2012, Manitoba Innovation, Energy and Mines, Manitoba Geological Survey, p. 54–58.

Martins, T., Kremer, P. and Vanstone, P. 2013: The Tanco mine: geological setting, internal zonation and mineralogy of a world-class rare element pegmatite deposit; Geological Association of Canada–Mineralogical Association of Canada, Joint Annual Meeting, Field Trip Guidebook FT-C1; Manitoba Innovation, Energy and Mines, Manitoba Geological Survey, Open File OF2013-8, 17 p.

Natural Resources Canada 2024: Canada's critical minerals; Natural Resources Canada, URL <https://canada.ca/en/campaign/critical-minerals-in-canada/critical-minerals-an-opportunity-for-canada.html> [September 2024].

Passchier, C.W. and Trouw, R.A.J. 2005: Microtectonics, 2nd edition; Springer Science and Business Media, Würzburg, 366 p.

Plunder, A., Le Pourhiet, L., Räss, L., Gloaguen, E., Pichavant, M. and Gumiaux, C. 2022: Pegmatites as geological expressions of spontaneous crustal flow localization: Lithos, v. 416–417, URL <https://doi.org/10.1016/j.lithos.2022.106652>.

Roush, J., Martins, T., McFarlane, C.R.M., Rinne, M.L. and Groat, L. 2023: Preliminary examination of the Tappy, Eagle and F.D. No. 5 pegmatites in the Cat Lake–Winnipeg River pegmatite field, southeastern Manitoba (parts of NTS 52L5, 11); *in* Report of Activities 2023, Manitoba Economic Development, Investment, Trade and Natural Resources, Manitoba Geological Survey, p. 20–26.

Silva, D., Groat, L., Martins, T. and Linnen, R. 2023. Structural controls on the origin and emplacement of lithium-bearing pegmatites; The Canadian Journal of Mineralogy and Petrology, v. 61, p. 1–10, <https://doi.org/10.3749/2300045>.

Stilling, A., Černý, P. and Vanstone, P.J. 2006: The Tanco pegmatite at Bernic Lake, Manitoba, XVI. Zonal and bulk compositions and their petrogenetic significance; The Canadian Mineralogist, v. 44, p. 599–623.

Yang, X.M. and Houlé, M.G. 2020: Geology of the Cat Creek–Euclid Lake area, Bird River greenstone belt, southeastern Manitoba (parts of NTS 52L11, 12); Manitoba Agriculture and Resource Development, Manitoba Geological Survey, Geoscientific Report GR2020-1, 105 p., 1 map at 1:20 000 scale.

GS2024-7

Precise U-Pb zircon age and geochemical constraints on the geodynamic settings of the Falcon Lake intrusive complex and S-type Caddy Lake granite intrusion in the western Superior province, southeastern Manitoba (parts of NTS 52E11, 14)

by X.M. Yang

In Brief:

- The 2695.7 ±1.0 Ma Falcon Lake igneous complex consists of calcalkaline and alkaline rocks
- The calcalkaline quartz monzonite was emplaced post-amalgamation of the Wabigoon and Winnipeg River domains, while the alkaline diorite was likely emplaced in an extensional regime
- The Caddy Lake S-type granite is genetically linked to rare-metal pegmatites, emplaced in a terrane boundary zone

Citation:
Yang, X.M. 2024: Precise U-Pb zircon age and geochemical constraints on the geodynamic settings of the Falcon Lake intrusive complex and S-type Caddy Lake granite intrusion in the western Superior province, southeastern Manitoba (parts of NTS 52E11, 14); *in* Report of Activities 2024, Manitoba Economic Development, Investment, Trade and Natural Resources, Manitoba Geological Survey, p. 49–65.

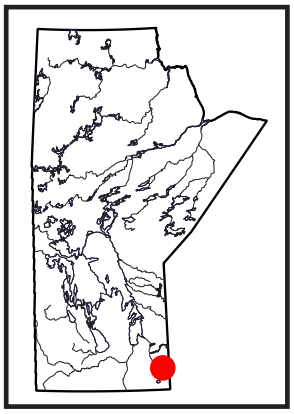
Summary

Precise timing and geochemical characterization of granitoid intrusions are key to exploring intrusion-related mineral deposits, including gold and rare metals, and/or critical minerals (e.g., lithium, tantalum, cesium, rare-earth elements, zirconium). Previous investigations revealed that these types of mineralization are either hosted in, or related to, a variety of intrusions in the Wabigoon domain and its boundary zone with the Winnipeg River domain of the western Superior province in southeastern Manitoba. However, little is known about their timing and the specific geodynamic processes that led to the diverse intrusion-related mineralization in the region. The new precise U-Pb zircon age of 2695.7 ±1.0 Ma provided here for the Falcon Lake intrusive complex is accompanied by geochemical data allowing a better understanding of the geodynamic settings and associated mineral potential that developed during the assembly of the western Superior province in southeastern Manitoba. The Falcon Lake intrusive complex is a unique, compositionally zoned and layered composite intrusion formed by two distinct magma series: calcalkaline and alkaline. These magmas likely originated within different geodynamic environments and exhibit distinct mineral potential. The calcalkaline magma, which displays Neoarchean sanukitoid characteristics, is hypothesized to have formed from partial melting of a depleted mantle previously metasomatized by slab-related melts and/or fluids. This process was likely triggered by the upwelling of hot asthenospheric mantle caused by slab break-off. The calcalkaline rocks dominate the Falcon Lake intrusive complex and are associated with significant gold mineralization. In contrast, the alkaline magma is thought to have been generated through the partial melting of residues left by the earlier extraction of tonalite-trondhjemite-granodiorite suites during intra-arc extension due to slab rollback. This magma, characterized by high zirconium (330 ppm) and elevated total rare-earth-element concentrations (>462 ppm), together with the calcalkaline magma, contributed to continental crust growth in the western Superior province (craton).

Approximately 4.5 km north of the Falcon Lake complex lies the ca. 2687 ±7 Ma Caddy Lake muscovite-biotite (two-mica) granite, which is an S-type intrusion emplaced in response to crustal thickening from the collision of the Wabigoon and Winnipeg River domains of the western Superior province. Given the established genetic linkage between S-type granites and critical-metal–bearing pegmatites—such as those containing lithium, tantalum and cesium—exploration of the Caddy Lake granite could reveal significant potential for critical-mineral mineralization in the region.

Introduction

The Manitoba Geological Survey's ongoing multiyear program 'Granitoids in Manitoba: petrogenesis and metallogeny' focused in 2024 on the timing and geodynamic evolution of granitoid rocks in the Falcon Lake intrusive complex (FLIC) and the Caddy Lake granite intrusion in the western Superior province, southeastern Manitoba. The FLIC, which is one of few well-preserved Archean layered intrusions in Manitoba characterized by intact primary magmatic fabrics (e.g., compositional layering, magma-flow foliation and lineation), hosts, and/or is associated with, significant gold mineralization (Fingler, 1991; Tirschmann, 1992). It provides an excellent opportunity for investigating the timing, petrogenesis, metallogeny and geodynamic settings of such layered igneous complexes of Archean age. The FLIC was dated previously by Halden et al. (2007) using laser-ablation microprobe, inductively coupled plasma–mass spectrometry (LAM-ICP-MS) techniques, yielding U-Pb zircon ages ranging from 2733 ±33 Ma to 2723 ±9 Ma, with large uncertainties. The dates suggest that a more precise timing of the phases and processes that influenced the FLIC is required when studying its petrogenesis and geodynamic setting(s) because: 1) magmatism lasting for >10 m.y. seems to conflict with the view that the FLIC formed by fractionation of a mantle-derived magma (e.g., Mandziuk et al., 1989a, b;



Tirschmann, 1992); and 2) the dates themselves are inconsistent with temporal and spatial associations of various magmatic rocks produced during the central Superior orogeny (or locally termed Kenoran orogeny; see Percival et al., 2006, 2012), including collision-related granitic rocks such as S-type granites that are the source for rare-metal (e.g., lithium, tantalum, cesium) pegmatites in the region and elsewhere (e.g., Černý et al., 1981; Černý and Ercit, 2005; Yang, 2014, 2023; Yang et al., 2019; Macdonald, 2024).

The ca. 2687 ±7 Ma Caddy Lake two-mica granite intrusion is an S-type granite located approximately 4.5 km north of the FLIC (Figure GS2024-7-1). This granite can be termed leucogranite as it contains less than 5% ferromagnesian minerals (Yang, 2014, 2023; Yang et al., 2019). Based on Halden et al. (2007), the intrusion is 36 m.y. younger than the youngest phase quartz monzonite (2723 ±9 Ma) of the FLIC, which raises the aforementioned problem of inconsistent dates. However, the fundamental question of 'what geodynamic processes link the origin of the FLIC to the Caddy Lake S-type granite intrusion?' remains to be answered.

Examination of the new, precise U-Pb zircon date for the FLIC presented in this study, when considered along with the geochemistry of the complex and the occurrence of the Caddy Lake S-type granite in terms of their distinct geodynamic settings and mineral potential, assists in better understanding geodynamic evolution and related mineralization during the assembly of the Wabigoon and Winnipeg River domains, which constitute part of the western Superior province. In addition to addressing the aforementioned problems, the major findings from this study provide insights into the tectonic evolution of the western Superior Province in southeastern Manitoba, as well as the mineral potential of the region during various stages of geodynamic processes, as recorded by the FLIC and the Caddy Lake granite intrusion.

Geological setting

The FLIC is situated in southeastern Manitoba, near the Ontario border, approximately 112 km east of Winnipeg along Trans-Canada Highway 1 (Figure GS2024-7-1). It occurs as a stock with an exposed area of approximately 10 km^2. It is emplaced into the northwestern portion of the Wabigoon domain that consists of Archean supracrustal sequences of basaltic–andesitic metavolcanic to metavolcaniclastic rocks uncomformably overlain by subordinate metasedimentary rocks including conglomerate, greywacke, arkosic sandstone and mudstone (Blackburn et al., 1991; Tirschmann, 1992; Ayer, 1998a). The emplacement of the FLIC appears to have been controlled by deep transcrustal faults. The generally east-northeast regional structural trend of the greenstone belt, manifested by subvertical folding, is characterized by major foliation dipping steeply to the north and metamorphic mineral assemblages of upper-greenschist to middle-amphibolite facies (Tirschmann, 1992; Ayer, 1998a).

The FLIC is a concentric, compositionally zoned and layered composite intrusion of sigmoidal shape displaying outer, lens-shaped bodies of gabbro units and dioritic gabbro tails (units A to D; see Figure GS2024-7-2; Mandziuk et al., 1989a, b). The main part of the complex consists of an old outer zone of diorite to granodiorite (unit E) and a younger inner zone of quartz monzonite (unit F), according to earlier detailed bedrock geology mapping at 1:5000 scale (Mandziuk, 1989; Figure GS2024-7-2). Primary rhythmic layering and fabrics of mineral lineation and foliation are well preserved in the FLIC, suggestive of its post-kinematic features formed during magma emplacement rather than tectonic deformation (Mandziuk et al., 1989a, b). Xenoliths of country rocks and cognate inclusions are common, particularly in the central part (units E and F) of the complex. Detailed petrographic descriptions of each lithological unit of the FLIC, presented in Tirschmann (1992), indicate that myrmekitic textures are evident in all units of the FLIC, together with perthitic textures in units E and F. This strongly suggests that their parental magmas are water saturated (cf. Candela, 1997; Yang and Lentz, 2005; Winter, 2014).

The presence in the core of the FLIC of two major breccia pipes (Figure GS2024-7-2) hosted by the quartz monzonite to minor monzogranite intrusive phases of unit F is worth noting (Figure GS2024-7-3a). The breccia pipes appear to comprise in situ quartz monzonite fragments in very fine grained silicified and sericitized monzonitic matrix. The fragments are angular to irregular in shape and range from block to lapilli in size. These breccias likely formed via implosion of an internal boiling process during late-stage magmatic hydrothermal evolution of the FLIC (Gibbins, 1971; Halwas, 1984), resulting in disseminated sulphide (quartz-carbonate) mineralization and/or veinlets consisting of pyrite, pyrrhotite, sphalerite, galena, and chalcopyrite and locally gold (Mandziuk et al., 1989a; Fingler, 1991; Tirschmann, 1992).

The Caddy Lake two-mica leucogranite intrusion, which displays an arcuate shape, is situated about 4.5 km north of the FLIC (Figure GS2024-7-1). It has a U-Pb zircon age of 2687 ±7 Ma dated by Halden et al. (2007) using LAM-ICP-MS techniques. This granite contains accessory garnet, epidote, zircon, apatite and allanite (Duncan, 1989), and is an S-type granite that is part of the Rennie River plutonic suite (Yang, 2014, 2023; Yang et al., 2019). The Caddy Lake intrusion was emplaced across the terrane boundary between the Winnipeg River and Wabigoon domains of the western Superior province. It cut the gneissic tonalite-trondhjemite-granodiorite (TTG) suites of the Winnipeg River domain and intruded into metasedimentary rocks that unconformably overlie metavolcanic to metavolcaniclastic rocks of the Wabigoon domain (Figure GS2024-7-1). More importantly, critical metals (e.g., Li, Ta, Cs) hosted in pegmatites (e.g., Lucy and Artdon pegmatite dikes; see Davies et al., 1962; Bannatyne, 1985) are thought to be associated genetically with S-type granites in the region and elsewhere (Černý and Meintzer, 1988; Černý and Ercit, 2005; Yang, 2014, 2023; Yang et al., 2019).

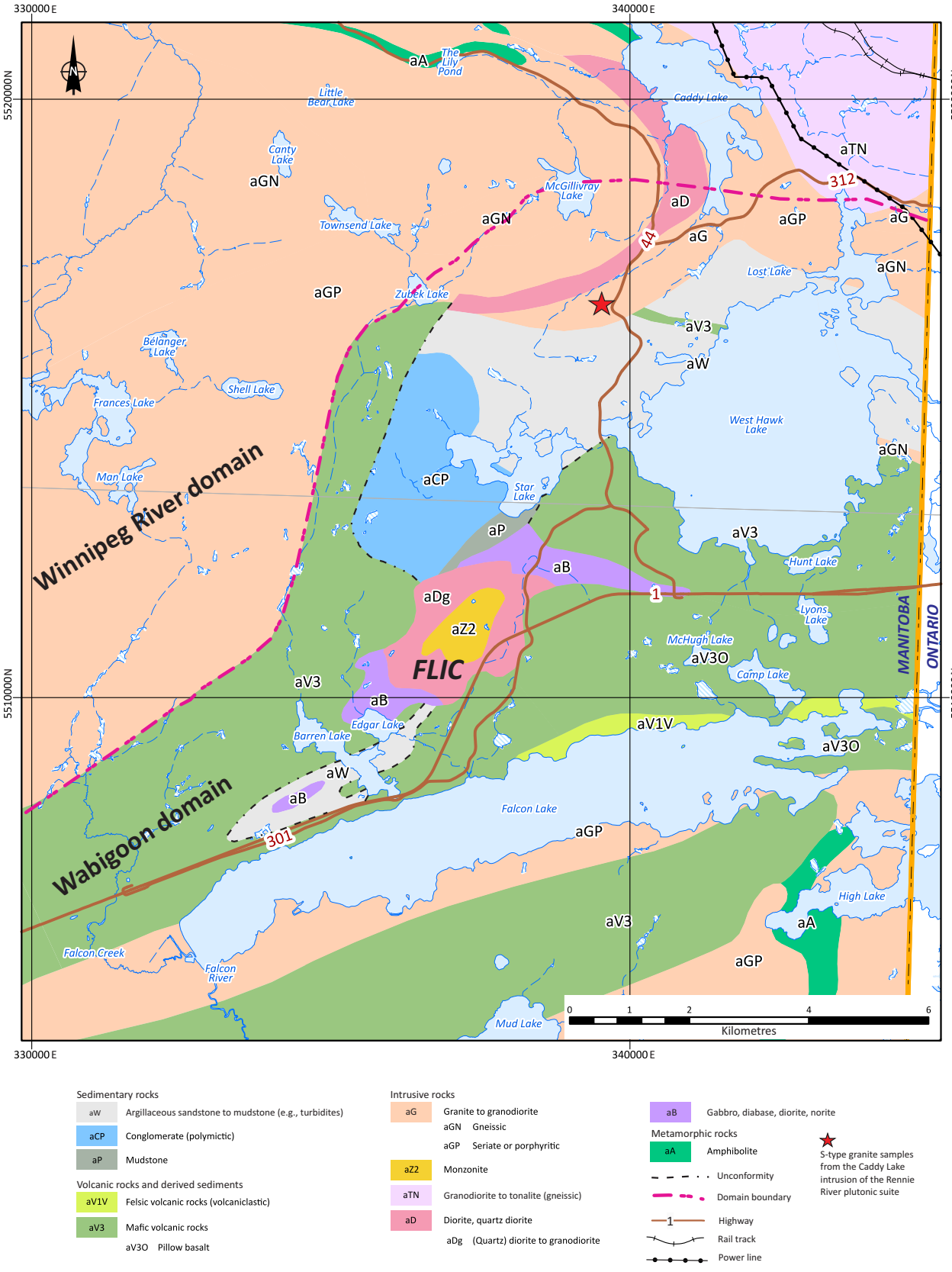


Figure GS2024-7-1: *Regional geology of the Falcon Lake area, showing that the Falcon Lake intrusive complex (FLIC) occurs in metavolcanic to metavolcaniclastic and metasedimentary rock units of the Archean Wabigoon domain that is flanked by gneissic granitoids of tonalite-trondhjemite-granodiorite suites within the southern margin of the Winnipeg River domain (modified from Manitoba Energy and Mines, 1987). Pink dashed line represents the terrane boundary between the Wabigoon and Winnipeg River domains. Location of samples from the S-type Caddy Lake leucogranite intrusion of the Rennie River plutonic suite (Yang, 2014; Yang et al., 2019) is indicated by the red star. All co-ordinates are in UTM Zone 15, NAD83.*

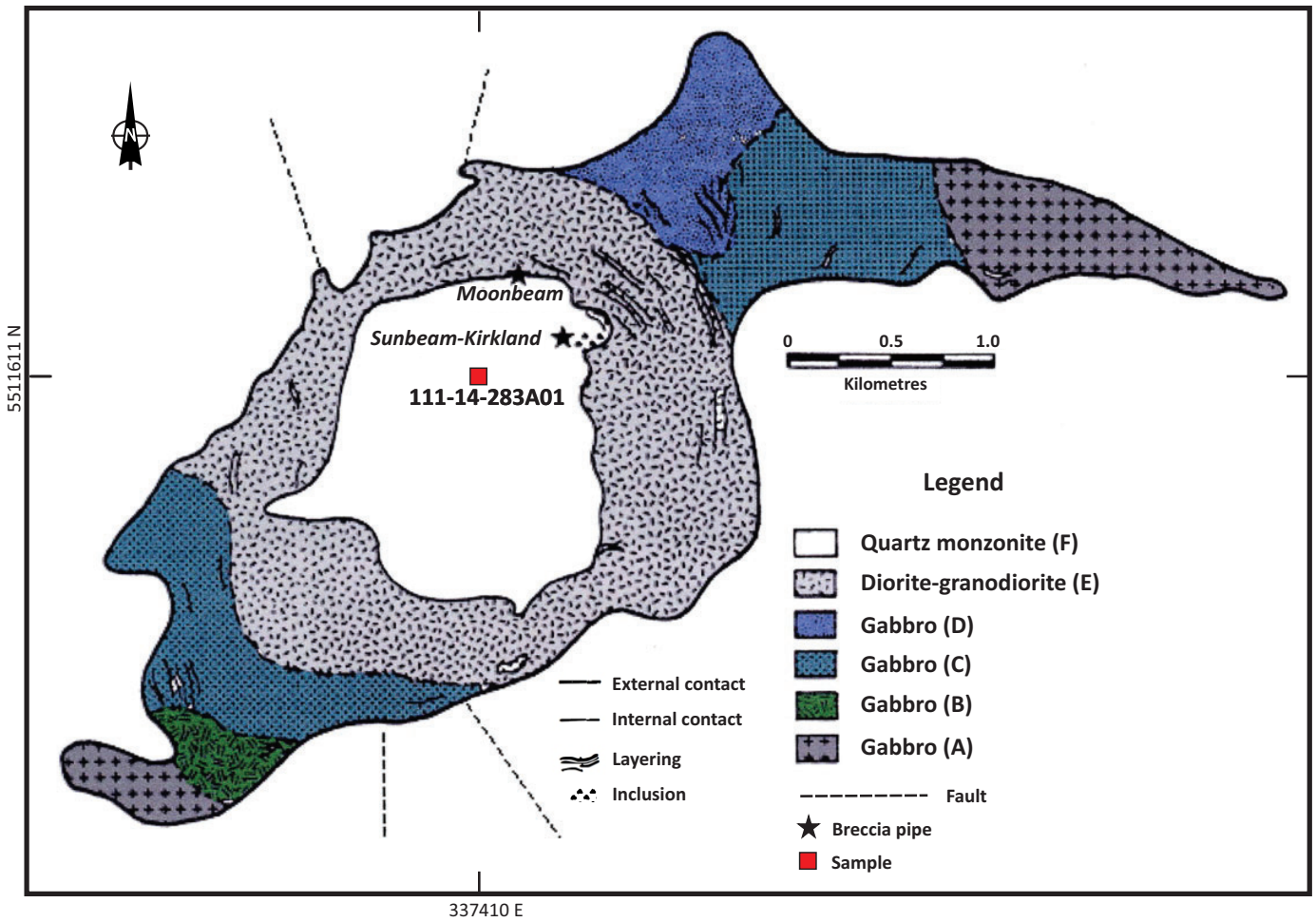


Figure GS2024-7-2: *Simplified geology map of the Falcon Lake intrusive complex (FLIC) that consists of four older gabbroic units (A to D) in the outer zones, and two younger, main internal units (E and F) of quartz diorite to granodiorite and quartz monzonite (modified after Mandziuk et al., 1989a, b). Also shown are the locations of two breccia pipes and the geochronological sample collected for this study. All co-ordinates are in UTM Zone 15, NAD83.*

Sample descriptions

To update the age and geochemistry of the FLIC, a whole-rock sample (111-14-283A01) was collected from unit F quartz monzonite in the core of the FLIC for precise U-Pb zircon dating and geochemical analysis (Figure GS2024-7-2). This quartz monzonite is massive, medium grained and equigranular to seriate, but locally contains a few euhedral K-feldspar phenocrysts (up to 2.2 cm in length). It consists of 30–40% plagioclase, 30–35% hornblende, 20–25% K-feldspar, 5–10% quartz and minor biotite (Figure GS2024-7-3b, c). As determined by electron probe micro-analyzer (Tirschmann, 1992), plagioclase comprises 24.9–30.3% anorthite belonging to oligoclase. Thus, in the petrological sense, this rock should be termed 'granitic rock' (s.l.), as constrained by the anorthite content of the plagioclase and bulk-rock composition (this study). Myrmekitic texture in some parts of the plagioclase margin and the perthitic microcline are evident, suggestive of the water-saturated magma from which these minerals crystallized (Candela, 1997; Yang and Lentz, 2005; Winter, 2014). Accessory minerals are magnetite, zircon, titanite, apatite and allanite. Tirschmann (1992) pointed out the presence of ilmenite rims on some magnetite crystals, indicative of a reaction with late-magmatic hydrothermal fluids. The quartz monzonite has a moderately high magnetic susceptibility (MS) value of 11.7×10^{-3} SI, indicative of its oxidized state and consistent with the presence of magnetite and titanite. These features are typical of normal I-type and magnetite-series granites (Yang 2014, 2023), as outlined in Chappell and White (1974, 2001), and Ishihara (1977, 1981, 2004).

The Caddy Lake leucogranite is massive, equigranular and medium-grained, and undeformed. It consists of 40–45% K-feldspar, 30–35% quartz, 20–25% plagioclase, up to 5% biotite, minor muscovite, and up to 1% garnet (Figure GS2024-7-3d). This granite has a very low MS value of 0.045×10^{-3} SI, similar to that of reduced S-type and ilmenite-series granites (Yang 2014, 2023) according to Chappell and White (1974, 2001), and Ishihara (1977, 1981, 2004).

Geochemical characteristics

Elemental-analysis results for the FLIC rocks, including partial rare-earth elements (REEs), were reported by Tirschmann

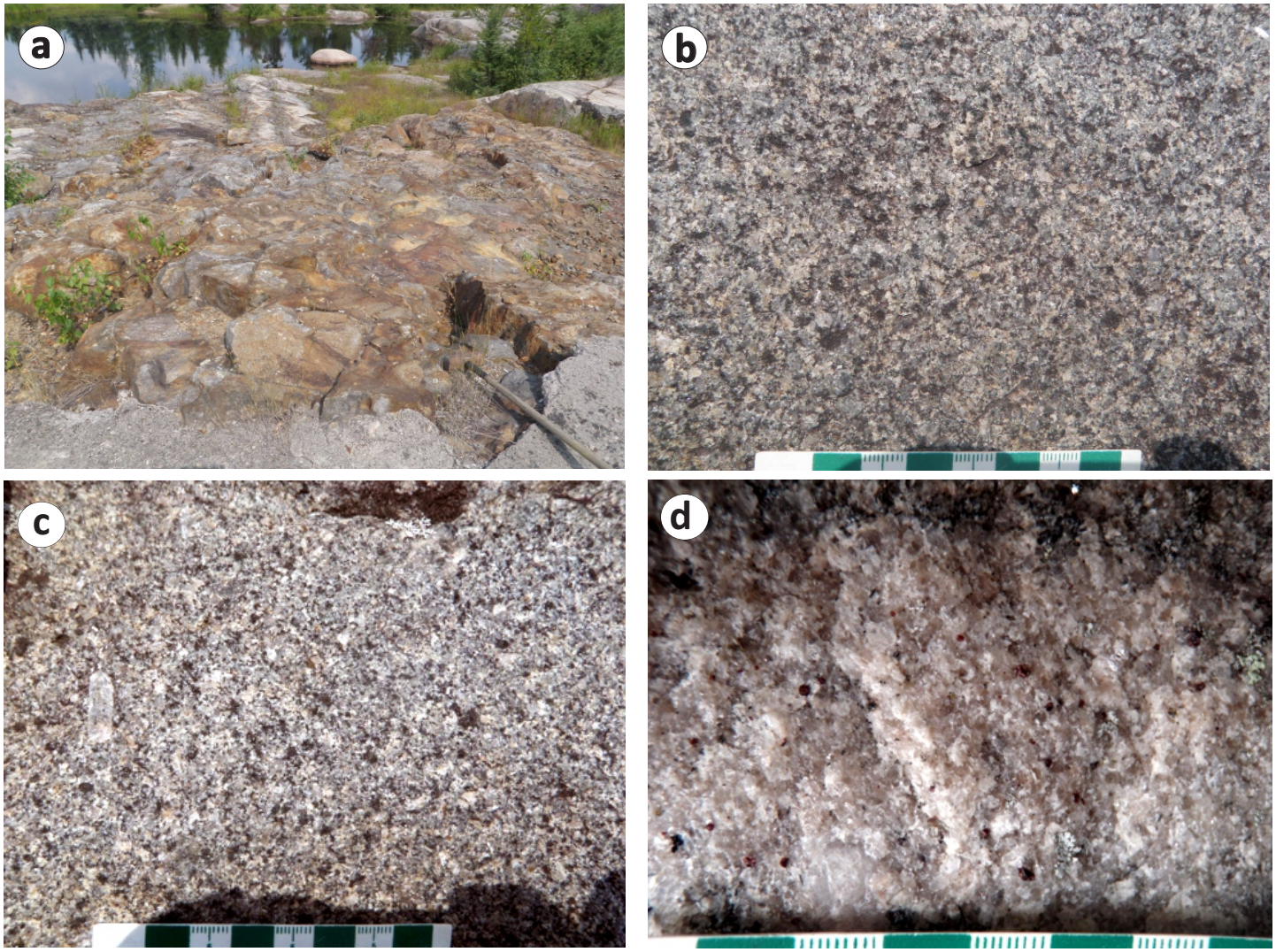


Figure GS2024-7-3: *Field photographs of outcrops of the Falcon Lake intrusive complex (FLIC):* ***a)*** *sulphide-bearing breccia pipe (337473E, 5511650N) in the core of the FLIC (sledgehammer handle at right for scale);* ***b)*** *medium-grained quartz monzonite (337410E, 5511611N);* ***c)*** *quartz monzonite from the same outcrop as in (b), showing a few euhedral to subhedral K-feldspar phenocrysts;* ***d)*** *massive, medium-grained, undeformed, garnet-bearing two-mica leucogranite from the Caddy Lake intrusion (339676E, 5516634N). All co-ordinates are in UTM Zone 15, NAD83.*

(1992). The analytical data are summarized and tabulated in Table GS2024-7-1, alongside the complete elemental-analysis results (including full REE data) from three bulk-rock samples acquired during this study. As a first step, the main geochemical characteristics of the FLIC and Caddy Lake granite are presented in a set of geochemical diagrams showing sample alkalinity, alumina and silica saturation state, as well as Fe*{=FeO^{total}/(FeO^{total}+MgO)} ratios. Then, Nd-Sr-O isotopic data published in the relevant literature are briefly reviewed to investigate the nature of the source rocks.

Major and trace elements

Heterogeneity in geochemical compositions is apparent, as shown in the mineralogical classification diagrams of CIPW (Cross, Iddings, Pirsson and Washington) normative Q' versus ANOR, as well as of K_2O versus SiO_2, for the whole-rock samples from the FLIC compared with those from the Caddy Lake leucogranite intrusion (Table GS2024-7-1; Figure GS2024-7-4a, b). The FLIC bulk-rock samples range in lithology from quartz monzonite, quartz monzodiorite, monzonite, monzogabbro to gabbro. Only one sample of unit F falls in the field of monzogranite. Most of the samples plot along the alkalic-calcic trend defined by Frost et al. (2001; see Whalen and Frost, 2013), although some from units A, B and E deviate from this pattern. According to the classification of Peccerillo and Taylor (1976), most of the samples from unit E are shoshonitic and samples from unit F are high-K calcalkaline, indicative of their enrichment in K_2O (Figure GS2024-7-4b), in contrast to sodic TTGs. Results from samples of units A to D are more scattered, displaying various magmatic affinities ranging from arc tholeiitic, calcalkaline, to high-K calcalkaline and shoshonitic series. Such a large variation in K_2O and SiO_2 contents is hardly generated by common magmatic fractionation, as thought previously, but can be readily explained by hydrothermal

Table GS2024-7-1: Major (wt. %) and trace (ppm) elements data of whole-rock samples from the Falcon Lake intrusive complex (FLIC) and Caddy Lake intrusion (CLI).

Intrusion	CLI		FLIC										
Lithology	Granite	Granite	Quartz monzonite	Gabbro		Gabbro	Gabbro	Gabbro		Diorite		Quartz monzonite	
Unit			F	A		B	C	D		E		F	
Sample	14-258A01	14-259A01*	14-283A01	AVE	STDV	AVE	AVE	AVE	STDV	AVE	STDV	AVE	STDV
	n = 1	n = 1	n = 1	n = 4		n = 2	n = 2	n = 4		n = 12		n = 5	
Data source	Yang, 2023		Tirschmann, 1992										
SiO_2	76.03	74.74	66.1	52.85	2.84	47.44	55.90	52.83	2.33	57.13	3.36	67.23	1.08
TiO2	0.049	0.009	0.323	1.00	0.18	0.30	0.90	1.08	0.18	0.80	0.20	0.27	0.06
Al_2O_3	13.51	14.01	15.22	17.15	0.57	16.79	20.20	18.64	1.38	16.91	0.87	16.17	0.23
$Fe_2O_3^{T1}$	1.27	0.77	3.61										
Fe_2O_3				3.02	0.33	3.21	2.55	3.30	0.99	3.49	1.31	1.72	0.30
FeO				7.18	0.94	6.92	3.89	5.06	0.70	3.98	1.71	1.46	0.27
MnO	0.035	0.008	0.058	0.14	0.01	0.17	0.10	0.11	0.02	0.10	0.03	0.05	0.02
MgO	0.1	0.02	1.27	4.92	1.42	10.02	1.86	3.15	0.69	3.10	0.96	0.98	0.21
CaO	1.1	0.89	2.99	7.92	1.77	12.93	6.79	7.52	1.13	5.37	1.15	2.77	0.15
Na_2O	3.42	3.39	4.28	3.28	0.29	1.84	4.21	3.48	0.18	3.72	0.34	3.99	0.27
K_2O	4.95	5.28	4.05	1.81	1.34	0.24	3.13	2.95	0.51	3.94	0.72	4.47	0.14
P_2O_5	<0.01	0.04	0.19	0.44	0.39	0.21	0.40	0.89	0.30	0.43	0.19	0.03	0.02
LOI	0.31	0.19	1.24	0.59	0.19	1.10	0.55	0.53	0.16	0.66	0.27	0.52	0.18
Total	100.8	99.35	99.33	100.30		101.15	100.77	99.54		99.63		99.65	
σ^2	2.1	2.4	3.0	2.7	0.9	1.0	4.2	4.3	0.8	4.3	1.0	3.0	0.2
τ^3	205.9	1180.0	33.9	14.3	3.4	51.4	18.3	14.4	3.2	17.1	3.5	45.8	7.9
Sc	1	<1	5										
V	<5	<5	41										
Cr	30	<20	50										
Co	2	<1	8										
Ni	<20	<20	<20										
Cu	<10	<10	20										
Zn	60	<30	50										
Ga	18	20	19										
As	<5	<5	77										
Rb	232	238	146	65	54	8	95	101	3	150	36	160	21
Sr	74	52	668	666	116	756	1170	1159	161	857	109	703	50
Y	13.9	25.6	9.7	22	8	13	20	20	6	19	5	4	5
Zr	61	24	172	168	128	42	221	271	146	330	63	171	33
Nb	5.1	1.9	11.6	7	9	1	12	10	6	18	4	9	3
Sn	2	3	2										
Cs	3.4	5.3	6.1										
Ba	308	121	1022										
				N = 2		N = 2	N = 1	N = 2		N = 3		N = 2	
La	15.6	4.37	67.4	65.8		11.18	123	113.3		117.7		58.2	
Ce	28.3	7.32	121	128.5		22.45	243	223.5		234.3		103.5	

[1] $Fe_2O_3^T$ denotes total Fe_2O_3.

[2] The Rittmann Serial Index $\sigma = (Na_2O+K_2O)^2/(SiO_2-43)$, units in wt. % (Rittmann, 1962).

[3] The Gottini index $\tau = (Al_2O_3-Na_2O)/TiO_2$, units in wt. % (Grasso, 1968).

Abbreviations: AVE, average; CLI, Caddy Lake intrusion; FLIC, Falcon Lake intrusive complex; LOI, loss-on-ignition; STDV, standard deviation; n, number of samples analyzed; N, number of samples analyzed for rare-earth elements using instrumental neutron activation analysis (Tirschmann, 1992).

Table GS2024-7-1 (continued): Major (wt. %) and trace (ppm) elements data of whole-rock samples from the Falcon Lake intrusive complex (FLIC) and Caddy Lake intrusion (CLI).

Intrusion	CLI		FLIC											
Lithology	Granite	Granite	Quartz monzonite	Gabbro		Gabbro	Gabbro	Gabbro		Diorite		Quartz monzonite	
Unit			F	A		B	C	D		E		F	
Sample	14-258A01	14-259A01*	14-283A01	AVE	STDV	AVE	AVE	AVE	STDV	AVE	STDV	AVE	STDV
	n = 1	n = 1	n = 1	n = 4		n = 2	n = 2	n = 4		n = 12		n = 5	
Data source	Yang, 2023		Tirschmann, 1992										
Pr	3.21	0.75	13										
Nd	11.4	2.85	42.6	53.45		16.2	92.4	93.75		91.4		32.9	
Sm	2.42	0.83	5.73	7.765		2.845	12.9	13.15		13.3		4.8	
Eu	0.342	0.214	1.32	1.49		1.025	2.49	2.92		2.7		1.1	
Gd	2.21	1.87	3.47										
Tb	0.37	0.45	0.42	0.93		0.59	0.84	0.75		0.8		0.4	
Dy	2.22	3.33	2.01										
Ho	0.46	0.73	0.37										
Er	1.44	2.13	1.11										
Tm	0.231	0.325	0.158										
Yb	1.56	2.13	0.95	1.765		0.69	1.79	1.615		1.9		1.0	
Lu	0.249	0.312	0.141	0.24		0.085	0.25	0.195		0.3		0.2	
Hf	1.8	1.1	4.1										
Ta	0.63	0.55	1.13										
W	1.5	<0.5	2.3										
Tl	1.19	1.33	0.71										
Pb	53	34	23										
Th	27.8	5.85	25.6										
U	9.03	8.86	8.39										
ΣREE	70	28	260	260		55	477	449		462		202	
Sr/Y	5.3	2.0	68.9	35.5	19.0	58.1	64.0	63.0	23.8	48.8	18.5	294.7	137.8
La/Yb	10.0	2.1	70.9	37.3		18.6	68.7	68.9		60.6	4.0	56.9	
Nb/Y	0.4	0.1	1.2	0.2	0.3	0.0	0.6	0.5	0.3	1.1	0.5	3.4	1.7

[1] $Fe_2O_3^T$ denotes total Fe_2O_3.

[2] The Rittmann Serial Index $\sigma = (Na_2O+K_2O)^2/(SiO_2-43)$, units in wt. % (Rittmann, 1962).

[3] The Gottini index $\tau = (Al_2O_3-Na_2O)/TiO_2$, units in wt. % (Grasso, 1968).

Abbreviations: AVE, average; CLI, Caddy Lake intrusion; FLIC, Falcon Lake intrusive complex; LOI, loss-on-ignition; STDV, standard deviation; n, number of samples analyzed; N, number of samples analyzed for rare-earth elements using instrumental neutron activation analysis (Tirschmann, 1992).

alteration or crustal contamination in open systems (cf. Winter, 2014; Rollinson and Pease, 2021). More recently, source potash enrichment induced by recycling of sediments has been used to explain high-K calcalkaline to shoshonitic magmatism (Wang et al., 2024), but this mechanism is not likely to have produced such a chaotic relationship as that shown in Figure GS2024-7-4b. Collectively, the FLIC samples are much less evolved than the leucogranite samples from the Caddy Lake intrusion, which plot in the syenogranite field and are attributed to the calcalkaline series, in terms of their Rittmann Serial Index ($\sigma = \{(Na_2O + K_2O)^2/(SiO_2 – 43)\}$, units in wt. %; Rittmann, 1962) values of 2.1 to 2.4 (Table GS2024-7-1), based on Yang (2007), and to the high-K calcalkaline series, based on their magmatic affinity (Figure GS2024-7-4b).

Based on the Shand's index diagram (Figure GS2024-7-5a; Maniar and Piccoli, 1989), the FLIC samples are exclusively metaluminous (except for one quartz monzonite sample from unit F that is peraluminous), whereas leucogranite samples from the Caddy Lake intrusion are moderately peraluminous. It should be noted that the FLIC samples are characterized by the presence of a CIPW normative association of quartz+hypersthene+diopside, suggestive of a dominantly calcalkaline affinity (Yoder and Tilley, 1962; Yang, 2007). The Caddy Lake leucogranite samples contain 0.58–1.33 wt. % normative corundum, consistent with their peraluminous signature. On the Fe* ratios versus SiO_2 plot (not shown), based on Frost et al. (2001), the FLIC rocks are exclusively magnesian, which suggests that they were formed by relatively oxidized magmas, whereas the ferroan nature of the Caddy

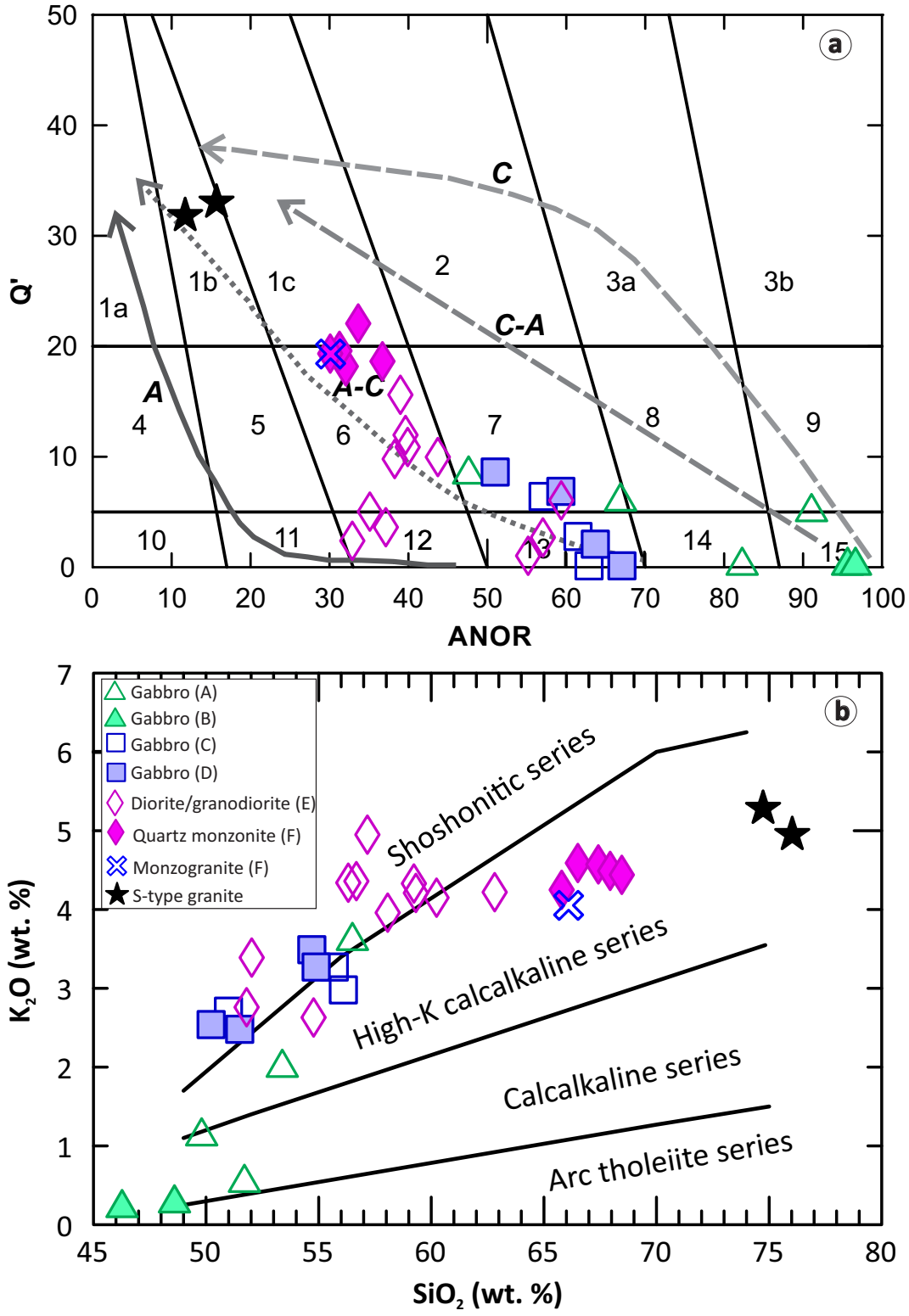


Figure GS2024-7-4: *Geochemical classification of whole-rock samples from the Falcon Lake intrusive complex and the Caddy Lake S-type granite intrusion of the Rennie River plutonic suite:* ***a)*** *the CIPW (Cross, Iddings, Pirsson and Washington) normative Q' versus ANOR diagram (after Streckeisen and Le Maitre, 1979); where Q' = 100 x Qz/(Qz + Or + Ab + An) and ANOR = 100 x An/(An + Or), identifies the rock types as alkali-feldspar granite (1a), syenogranite (1b), monzogranite (1c), granodiorite (2), tonalite (3a), calcic tonalite (3b), alkali-feldspar quartz syenite (4), quartz syenite (5), quartz monzonite (6), quartz monzodiorite (7), quartz diorite (8), quartz gabbro (9), alkali-feldspar syenite (10), syenite (11), monzonite (12), monzogabbro (13), diorite (14), gabbro (15), and the coarse dashed and solid lines with arrows indicate differentiation trends of different magmatic suites (after Whalen and Frost, 2013), including calcic (C), calcalkalic (C-A), alkali-calcic (A-C), alkalic (A), based on the modified alkali-lime index (Frost et al., 2001). Abbreviations: Ab, albite; An, anorthite; Or, orthoclase; Qz, quartz;* ***b)*** *K_2O (wt. %) versus SiO_2 (wt. %) magmatic-series discrimination diagram (after Peccerillo and Taylor, 1976). Data from Tirschmann (1992) and Yang (2023).*

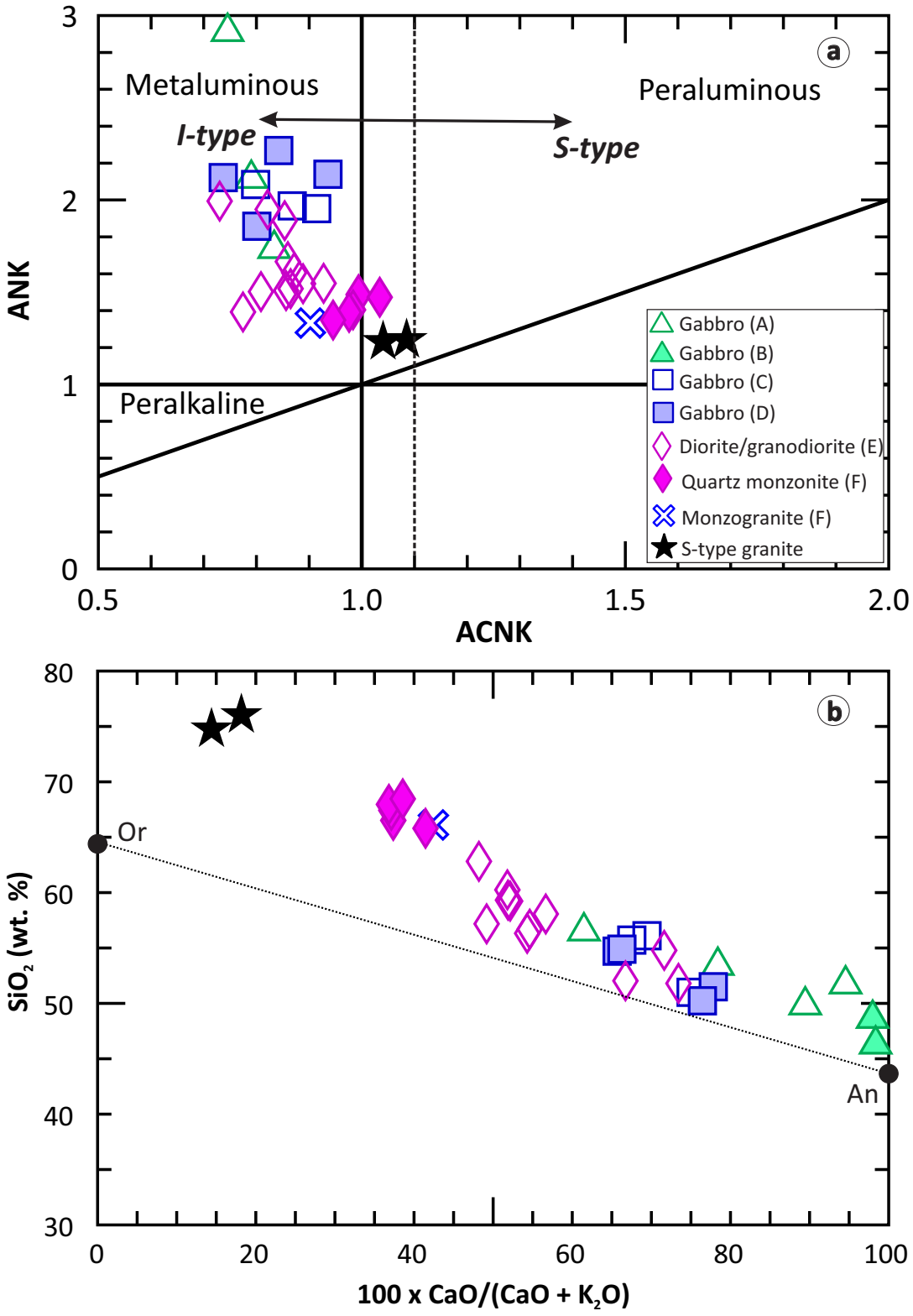


Figure GS2024-7-5: *Discrimination diagrams of the alumina- and silica-saturation state of whole-rock samples from the Falcon Lake intrusive complex and the Caddy Lake S-type granite intrusion of the Rennie River plutonic suite:* ***a)*** *Shand's index plot (A/CNK = {Al_2O_3 /(CaO + Na_2O + K_2O)}, A/NK = {Al_2O_3/(Na_2O + K_2O)}), in which the vertical dashed line (A/CNK = 1.1) separates strongly peraluminous S- from I-type granites (after Chappell and White, 1974, 2001; fields from Maniar and Piccoli, 1989);* ***b)*** *SiO_2 (wt. %) versus CaO/(CaO + K_2O) diagram identifying the silica-saturation state of the samples, where the dashed line (silica-saturation line) expressed by the equation: SiO_2 = –21.6 × {CaO/(CaO + K_2O)} + 64.8, units in wt. %) intercepting the y-axis at SiO_2 contents of 64.8 wt. % and 43.2 wt. % as defined by orthoclase (Or) and anorthite (An), respectively (modified from Enrique and Esteve, 2019), separates the rocks that are silica undersaturated (below the line) from those that are silica oversaturated (above the line). Data from Tirschmann (1992) and Yang (2023).*

Lake leucogranites indicates that they formed through reduced magmatic differentiation.

The FLIC samples all plot above the silica-saturation line (Figure GS2024-7-5b) as defined by Enrique and Esteve (2019), which suggests that their parental magmas are exclusively silica oversaturated. This is consistent with petrographic observations that the rocks in units A to F of the FLIC contain quartz, despite the fact that they show an enormous difference in modal quartz contents (Tirschmann, 1992). Although there appears to be a high correlation between the SiO_2 contents of the FLIC rocks and their CaO/(CaO+K_2O) ratios, compositional gaps are evident between units F and E, between units E and D, as well as between units D and A, and B. Such gaps were noted by Gibbins (1971), whose observations were dismissed by Tirschmann (1992) as simply a function of sampling bias transposed onto the Harker diagrams. As previously mentioned, the compositional variation (Figure GS2024-7-4b) cannot be explained by fractional crystallization along the liquid line of descent of the same parental melt in a closed system. Compared with the FLIC, the Caddy Lake leucogranites are much more evolved in composition as indicated by their very low CaO/(CaO + K_2O) ratios (<20), high τ[1] (Gottini index; see Grasso, 1968) values of 206–1180 and high silica contents of 74.74–76.03 wt. % (Table GS2024-7-1; Figure GS2024-7-5b).

Since alkalis and silica are readily affected by hydrothermal alteration (Figure GS2024-7-4a, b), it is necessary to adopt an immobile geochemical proxy, such as the Nb/Y ratio of high-field-strength elements (Pearce, 1996; Lentz, 1998; Rollinson and Pease, 2021), to assess the alkalinity of igneous rocks. This can be done by calculating the predicted σ* value with the analyzed Nb/Y ratio of a sample in question (Yang and Lawley, 2024). A comparison of the σ* with the measured σ value of the sample would then provide information about both alkali and silica mobility as well as alkalinity of the sample. Gabbro samples in units A to D have low Nb/Y ratios of 0.0–0.71 (Figure GS2024-7-6a), returning σ* values of 0.8–3.3 that suggest they must be calcic to calcalkaline. The σ* values are mostly comparable to measured σ values, although some are a little lower than the measured values (3.8–5.4) that exhibit a large range (Figure GS2024-7-6a), indicating addition of alkalis, particularly of K_2O, due to hydrothermal alteration (Yang and Lawley, 2024). Quartz monzonite samples from unit F have Nb/Y ratios >0.8 but σ values between 1.2 and 3.5, which suggests they contain notable Fe-Ti oxide-mineral (e.g., magnetite, ilmenite) cumulates that crystallized from a calcalkaline parental magma. Unit E diorite samples show varied Nb/Y and σ values, and mostly fall in the alkaline-series field (Figure GS2024-7-6a); they contain remarkably high Zr (average 330 $\pm$63 ppm; Table GS2024-7-1) and ΣREE values (>462 ppm; Table GS2024-7-1), although some plot outside of the field. These outliers may have been caused either by hydrothermal alteration, or by cumulous Fe-Ti–oxide minerals, which hypothesis is supported by petrographic investigations (Mandziuk, 1989; Mandziuk et al., 1989b; Tirschmann, 1992).

All samples from the FLIC have (Nb/Y) concentrations less than 60 ppm (Table GS2024-7-1) and thus cannot be postkinematic A-type granites (Whalen et al., 1987; Eby, 1990, 1992; Whalen and Hildebrand, 2019). Except for unit B gabbro, the FLIC rocks mostly display high La/Yb (>20) and Sr/Y (>40) ratios (Figure GS2024-7-6b) as well as very high Sr contents (Table GS2024-7-1), suggesting that their source region may have lacked plagioclase but contained a significant amount of garnet because of high pressure (Rapp and Watson, 1995; Rapp et al., 2003). These rocks exhibit enriched light-REE patterns without notable Eu anomalies (not shown), indicative of rocks formed from a parental magma characterized by high oxygen fugacity. Geochemically, the FLIC rocks are indistinguishable from Neoarchean sanukitoids and/or adakitic granitoids elsewhere (Shirey and Hanson, 1984; Stern and Hanson, 1991; Martin et al., 2005, 2009; Richards and Kerrich, 2007; Sun et al., 2010; Yang and Lawley, 2024; Yousefi and Lentz, 2024). They more closely resemble post-arc slab-failure granitoids given the degree of differentiation manifested by their silica contents (Hildebrand et al., 2018; Whalen and Hildebrand, 2019; Hildebrand and Whalen, 2021; Zwanzig, 2024). Hence, the occurrence of the FLIC sanukitoids could be used as a geological marker for geodynamic processes including slab failure and/or slab break-off caused by terrane collision.

Nd-Sr-O isotopes

Trace Nd-isotope analysis reveals that the quartz monzonite sample (111-14-283A01) from unit F of the FLIC has an initial ε_{Nd}^{t} (where ε is the degree on neodymium [Nd] enrichment relative to depleted mantle and *t* the time of formation of the rock) value of +1.1, a depleted-mantle Nd-model–age T_{DM} (where T is the age in Ga and $_{DM}$ means 'depleted mantle') of 2.89 Ga and a two-stage depleted-mantle Nd-model age of 2.79 Ga (Yang, 2023). This suggests that its parental magma may have been derived from a depleted-mantle source that had separated from primitive mantle at ca. 2.89 Ga and likely resided in the source region for about 100 m.y. During this period, the depleted mantle may have been metasomatized by melts and/or fluids derived from subduction as evidenced by a moderately low initial $(^{87}Sr/^{86}Sr)_i$ of 0.7027 (Halden et al., 2007) and a geochemical signature characterized by elevated light-REE concentrations (Table GS2024-7-1). In contrast, the Caddy Lake granite intrusion may have been derived from partial melting of immature crustal materials, as suggested by its $\delta^{18}O$ values of +8 to +9‰ (Duncan, 1989) and initial $(^{87}Sr/^{86}Sr)_i$ of 0.7087 (n = 7; see Farquharson and Clark, 1971) as well as geochemical fingerprinting in terms of high-field-strength elements (e.g., of high Zr and Nb contents; Figure GS2024-6).

[1] $\tau = (Al_2O_3 - Na_2O)/TiO_2$, units in wt. %; τ was proposed by Grasso (1968) and is referred to as the 'Gottini index' that can readily be used to describe the degree of magmatic differentiation (Yang, 2007), where a higher τ value signifies a greater level of differentiation.

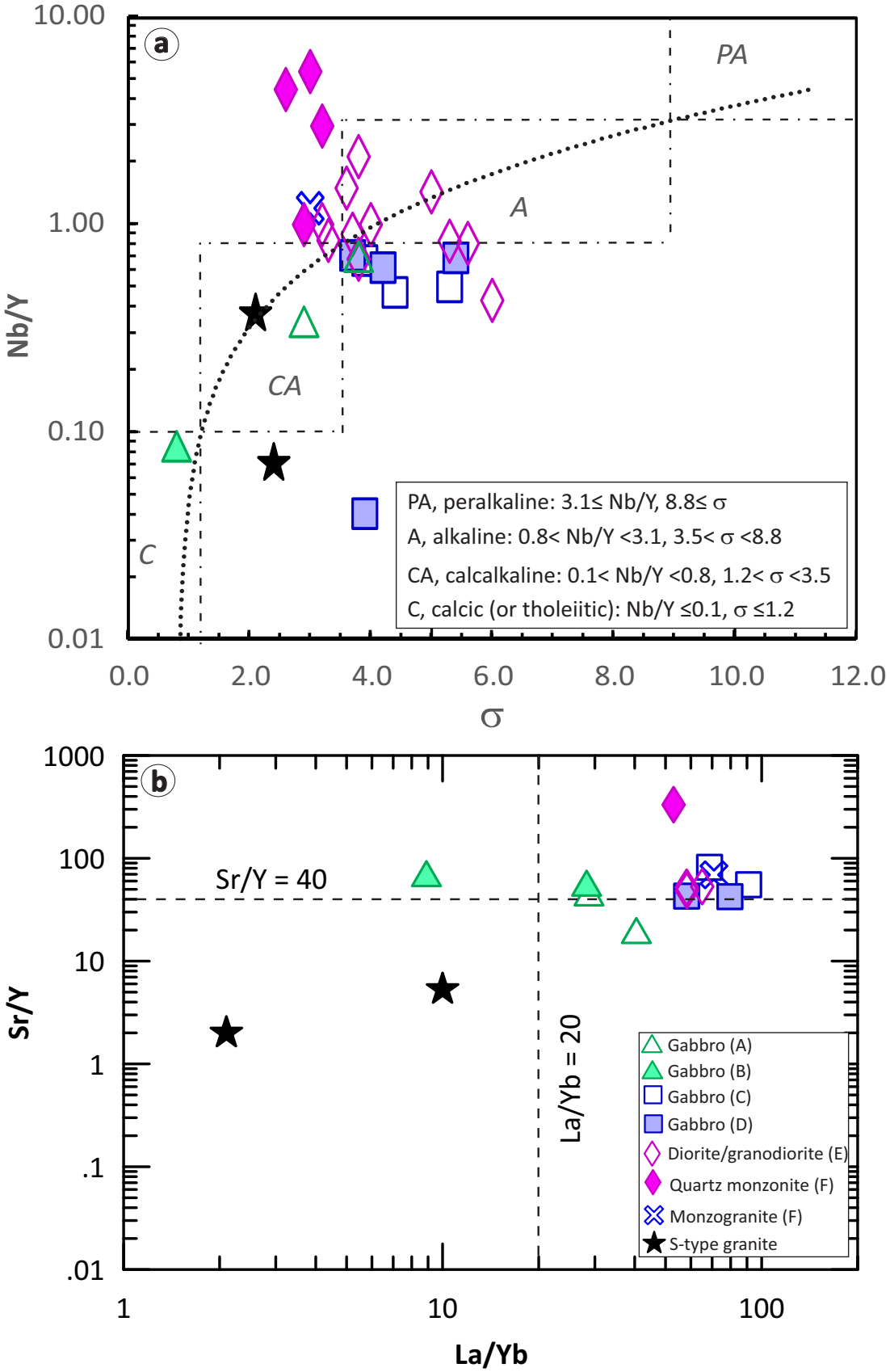


Figure GS2024-7-6: *Geochemical discrimination diagrams for whole-rock samples from the Falcon Lake intrusive complex and the Caddy Lake S-type granite intrusion of the Rennie River plutonic suite:* ***a)*** *Nb/Y versus σ plot (after Yang and Lawley, 2024), where σ = $(Na_2O + K_2O)^2/(SiO_2 – 43)$, units in wt. % (Rittmann Serial Index; Rittmann, 1962);* ***b)*** *Sr/Y versus La/Yb plot (after Richards and Kerrich, 2007). Data from Tirschmann (1992) and Yang (2023).*

U-Pb zircon dating

A new U-Pb zircon date for the FLIC is presented and compared with previously published geochronological data, including the age of the Caddy Lake granite, since determining precise timing is essential to a better understanding of the geodynamic evolution of the complex within the context of accretionary tectonics in the western Superior craton.

Methods

Uranium-lead zircon geochronological analysis was performed at the Jack Satterly Geochronology Laboratory at the University of Toronto (Toronto, Ontario) using high-precision chemical abrasion-isotope dilution-thermal ionization mass spectrometry (CA-ID-TIMS) dating techniques (Hamilton, 2022). A detailed methodology can be found in Yang (2024).

Results

The zircon population from the dated quartz monzonite sample (111-14-283A01) comprises a range of grain sizes and a mixture of relatively pristine to variably turbid or cloudy grains locally charged with inclusions and cracks. These features are commonly observed in magmatic zircons (Corfu et al., 2003). In the case of some of the zircon crystals (inset a, Figure GS2024-7-7), even chemical abrasion did not much improve the precision of the analyses. Three best-quality prismatic zircon grains (Z1, Z2 and Z3 in inset b, Figure GS2024-7-7) were annealed, etched, and analyzed for U-Pb chemical and isotope compositions. These grains have Th/U ratios of 0.76–0.85, typical of magmatic zircons (Rubatto, 2017). The U-Pb isotopic data (Table GS2024-7-2) are variably discordant but are quite colinear, with an anchored (0 Ma) regression yielding an upper intercept age of 2695.7 ±1.0 Ma (mean square of weighted deviates or MSWD = 0.99, probability or *P* = 0.37), as shown in Figure GS2024-7-7. This age agrees well with the $^{207}Pb/^{206}Pb$ age of the concordant analytical result for Z3 at 2695.6 ±1.8 Ma (see Table GS2024-7-2). This age of 2695.7 ±1.0 Ma is interpreted as the emplacement and/or crystallization age of the quartz monzonite phase in unit F of the FLIC.

Discussion

The precise age of 2695.7 ±1.0 Ma reported here correlates well with late- or post-tectonic granitoids, including components of the Neoarchean sanukitoid suites found elsewhere in the Wabigoon domain of the western Superior province (e.g., ca. 2698–2690 Ma; Stern and Hanson, 1991; Ayer, 1998b; Stevenson et al., 1999; Lin and Beakhouse, 2013). However, this new date differs from three U-Pb zircon ages reported previously by Halden et al. (2007) using LAM-ICP-MS techniques: 2723 ±9 Ma on unit F quartz monzonite, 2724 ±10 Ma on unit E diorite and 2733 ±15 Ma on unit C gabbro in the FLIC. Although the Halden et al. (2007) ages are indistinguishable within uncertainties, they do not match the $^{206}Pb/^{238}U$ age of 2695.7 ±1.0 Ma obtained in this study. The discrepancy between the dating results of Halden et al. (2007) and this study may be due to an inaccurate correction for common Pb. However, the limited data provided in the table of Halden et al. (2007) do not allow for a thorough assessment of such a possibility. Alternatively, combining the precise date of this study with the dates from Halden et al. (2007) suggests that the FLIC may have a protracted history of 37 m.y. That explanation does not seem to be very probably for such a small composite stock as the FLIC. Given the techniques used in Halden et al. (2007) and in this current study, the CA-ID-TIMS U-Pb zircon age of 2695.7 ±1.0 Ma reported herein should be adopted as crystallization (and/or emplacement) age for the FLIC.

The Caddy Lake S-type granite was dated at 2687.2 ±6.7 Ma by Halden et al. (2007) also using LAM-ICP-MS U-Pb zircon techniques, which age is generally consistent with its emplacement into a thickened crust setting due to terrane collision between the Wabigoon and Winnipeg River domains. If that assumption is correct, the Caddy Lake granite must have occurred just after the emplacement of the FLIC at 2695.7 ±1.0 Ma. Thus, the FLIC and Caddy Lake intrusions must have been postorogenic or postcollisional granitoid intrusions that stitched and welded the merged domains (see Percival et al., 2006, 2012; Yang et al., 2019). In addition to the previously described undeformed fabrics evident in the FLIC (Mandziuk et al., 1989a, 1989b; Tirschmann,1992) and Caddy Lake granite, this conclusion is based largely on the interpretations outlined below:

- The FLIC is geochemically comparable to Archean sanukitoids, which likely formed by partial melting of a depleted mantle metasomatized previously by slab-related melts and/or fluids. Such melting took place only after terrane collision, triggered by upwelling of hot asthenospheric mantle because of slab break-off or failure (Martin et al., 2005; Hildebrand et al., 2018; Whalen and Hildebrand, 2019; Hildebrand and Whalen, 2021).
- The precise timing of FLIC crystallization (or emplacement) at 2695.7 ±1.0 Ma indicates that it was emplaced during a postorogenic stage after the Wabigoon domain was docked at the southern margin of the Winnipeg River domain ca. 2700 Ma (see Percival et al., 2006, 2012), but before emplacement of the ca. 2687±7 Ma Caddy Lake S-type granite intrusion into thickened crust resulting from terrane collision (Yang et al., 2019).

The main findings

Listed below are several major findings from this report, which has addressed the problems thus far identified with, and advanced the understanding of, geodynamic evolution and related mineralization associated with the formation of the western Superior province.

- Geodynamic evolution of the western Superior province was recorded in the FLIC, which was emplaced after docking of the Wabigoon domain on the southern margin (present

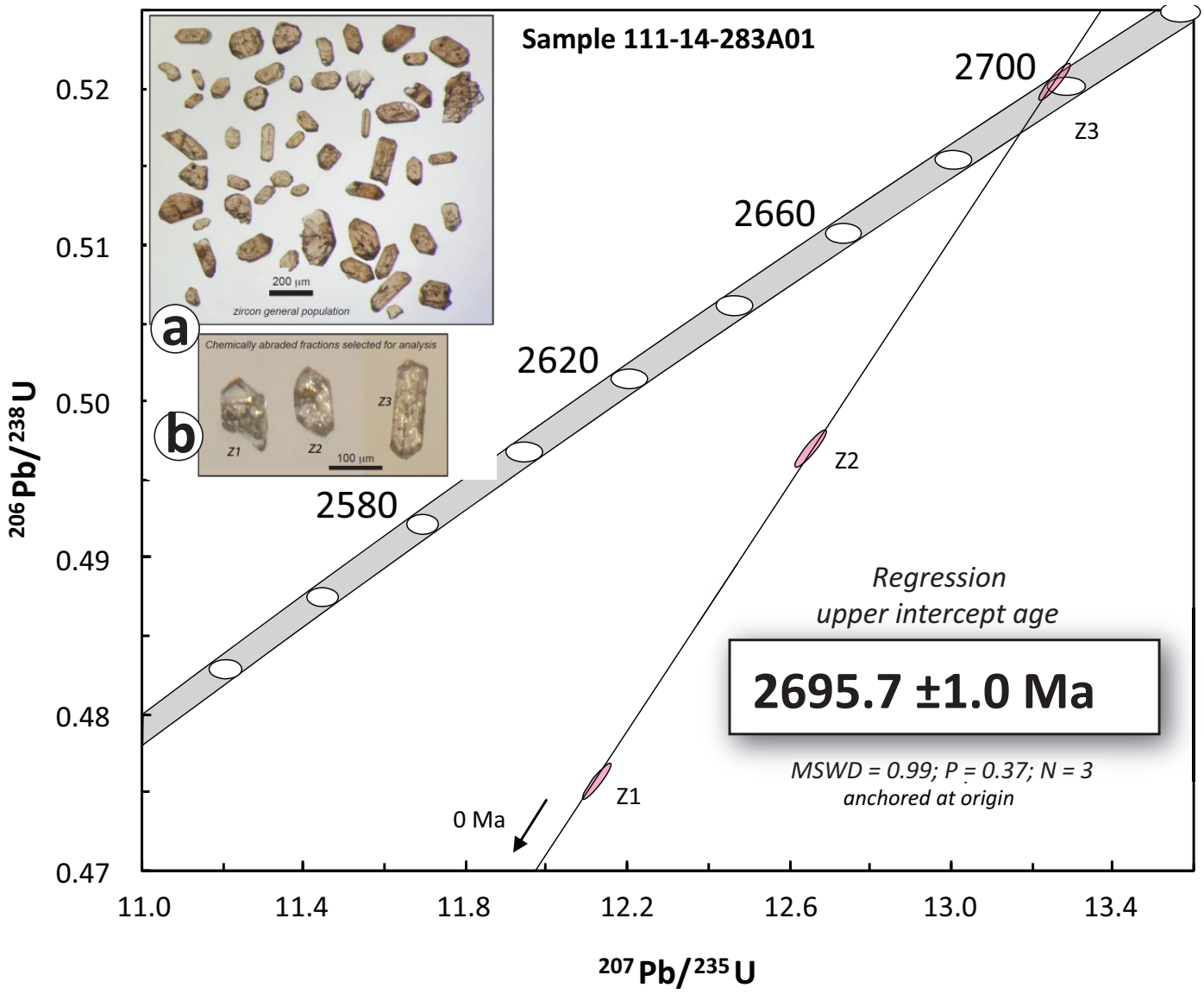


Figure GS2024-7-7: *Concordia diagram of chemical abrasion-isotope dilution-thermal ionization mass spectrometry U-Pb zircon age data for the quartz monzonite sample from the Falcon Lake intrusive complex in the Wabigoon domain of the western Superior craton, where Z1, Z2 and Z3 represent the three best-quality prismatic zircon grains analyzed. Abbreviations: MSWD, mean square of weighted deviates; N, number of analyses; P, probability.*

coordinates) of the Winnipeg River domain dominated by gneissic TTGs.

- The FLIC displays the geochemical signature of sanukitoids that may have been derived from partial melting of depleted mantle metasomatized by prior slab melts and/or fluids, indicating the termination of net growth of continental crust in the western Superior craton.
- The slightly younger Caddy Lake S-type leucogranite was emplaced across the terrane boundary zone between the Wabigoon and Winnipeg River domains, which may have host-rock potential for critical-element mineralization within pegmatites that are genetically related to the S-type granites. However, the crust-derived S-type granites did not contribute to net growth of continental crust in the western Superior province.
- The FLIC and Caddy Lake S-type granite formed during distinct tectonic stages of the geodynamic evolution involved in the assembly of the western Superior province. Firstly, terrane collision led to slab break-off (or failure), which triggered partial melting of the metasomatized, depleted mantle due to upwelling of hot asthenospheric mantle, resulting in the formation of the FLIC. Subsequently, heat from this mantle process induced partial melting of the thickened crust, which led to the formation of the S-type granite.

Economic considerations

The 2695.7 ±1.0 Ma Falcon Lake intrusive complex is a concentric, layered, composite intrusion, comprising two distinct parental magmas: the units A to D and F are calcalkaline, and unit E belongs to the alkaline series. The calcalkaline magmas

Table GS2024-7-2: Uranium-lead isotopic data for zircon in the quartz monzonite sample from the Falcon Lake intrusive complex in the Wabigoon domain of the western Superior craton obtained using chemical abrasion-isotope dilution-thermal ionization mass spectrometry.

Sample/ fraction	Description	U (ppm)	Th/U	Pb^T (pg)	Pb_c (pg)	$^{206}Pb/^{204}Pb$	$^{207}Pb/^{235}U$	± 2σ	$^{206}Pb/^{238}U$	± 2σ	Corr. Coeff. (rho)	$^{207}Pb/^{206}Pb$	± 2σ	$^{207}Pb/^{235}U$	± 2σ	$^{206}Pb/^{238}U$	± 2σ	$^{207}Pb/^{206}Pb$	± 2σ	Disc. (%)
Quartz monzonite sample from the Falcon Lake intrusive complex: 111-14-283A01 (location: UTM Zone 15 NAD83: 337410E, 5511611N)																				
Z1	1 brkn, cls, shrp tip	340	0.853	314	2.38	6953	12.12315	0.02906	0.475757	0.000931	0.9273	0.184812	0.000173	2614.0	2.2	2508.8	4.1	2696.5	1.5	8.4
Z2	1 cls, dt, shrt pr	257	0.763	226	2.73	4444	12.65210	0.03150	0.496996	0.000979	0.9168	0.184633	0.000192	2654.1	2.3	2600.9	4.2	2694.9	1.7	4.2
Z3	1 cls-grey, c-e, dt, flat 3:1 pr	204	0.806	191	2.48	4114	13.25546	0.03232	0.520500	0.000974	0.9118	0.184703	0.000196	2698.0	2.3	2701.3	4.1	2695.6	1.8	-0.3

All analyzed zircon fractions represent best optical quality (crack-, inclusion-, core-free), freshest (least altered) available grains. All zircons were chemically abraded.

Pb^T is total amount (in picograms) of Pb.

Pb_c is total measured common Pb (in picograms) assuming the isotopic composition of laboratory blank: 206/204 - 18.49 ±0.4%; 207/204 - 15.59 ±0.4%; 208/204 - 39.36 ±0.4%.

Pb/U atomic ratios are corrected for spike, fractionation, blank, and, where necessary, initial common Pb; $^{206}Pb/^{204}Pb$ is corrected for spike and fractionation.

Th/U is model value calculated from radiogenic $^{208}Pb/^{206}Pb$ ratio and $^{207}Pb/^{206}Pb$ age, assuming concordance.

Disc. (%) indicates percent discordance for the given $^{207}Pb/^{206}Pb$ age.

Uranium decay constants are from Jaffey et al. (1971).

Abbreviations: brkn, broken; c-e, cloudy-etched; Coeff., coefficient; cls, colourless; dt, doubly-terminated; pr, prismatic; shrp, sharp; shrt, short; Z, zircon.

with sanukitoid signature may have formed as a result of partial melting of a depleted mantle previously metasomatized by slab-related melts and/or fluid; upwelling of hot asthenospheric mantle likely triggered the partial melting of the depleted lithospheric mantle due to slab break-off. Large to giant Au and/or porphyry Cu-Au ore deposits are notably thought to be closely linked to sanukitoid (and/or adakitic) intrusions (Richards and Kerrich, 2007; Sun et al., 2010; Lin and Beakhouse; 2013; Whalen and Hildebrand, 2019; Yang and Lawley, 2024; Yousefi and Lentz, 2024). The alkaline magma was generated by the partial melting of residues left behind by earlier extraction of voluminous I-type granitoids (i.e., TTGs), due to intra-arc extension caused by slab rollback. This process, together with formation of the FLIC, contributed to the net growth of the continental crust in the western Superior craton and produced high Zr (330 ppm) and total REE contents (>462 ppm) in the magma/rock (i.e., unit E diorite; Table GS2024-7-1).

Additionally, sulphide minerals (e.g., pyrite, pyrrhotite, chalcopyrite, arsenopyrite, sphalerite and molybdenite) and gold mineralization are present in the breccia pipes interpreted to have formed by implosion from a late volatile-rich magma (water saturated) within the core of the FLIC (i.e., unit F; Mandziuk et al., 1989a, b). Up to 6.5 g/t gold was reported in grab samples from the Moonbeam breccia pipe as well as in the contact zones between the country rocks to the northwest of the FLIC (Fingler, 1991). This type of mineralization resembles porphyry Cu-Au systems to some extent, as reported by Fingler (1991), consistent with quartz-biotite-sericite-pyrite (±carbonate) alteration present in fractured breccia, likely at the exposed root of the porphyry system.

Furthermore, spodumene, lepidolite and beryl are present in some granitic pegmatite dikes (e.g., Lucy and Artdon pegmatites) that occur in the Falcon Lake area (Davies et al., 1962; Bannatyne, 1985), and they may have been sourced from the Caddy Lake S-type granite intrusion that is part of the Rennie River plutonic suite. This is consistent with the fact that S-type granites are closely linked to critical-metal mineralization (Li, Ta, Cs, Be) hosted in granitic pegmatites. More recently, Grid Metals Corp. has reported drilling intercepts of high-grade rare-metal pegmatites (e.g., 12.2 m grading 2.2% Li_2O and 3.3 m grading 10.3% Cs_2O) at its Falcon West lithium property (Grid Metals Corp., 2024). The promising mineral exploration results confirm high prospectivity for rare metals hosted in pegmatite dikes that are associated genetically with S-type granite intrusions emplaced into the terrane boundary (or collision) zone between the Wabigoon and Winnipeg River domains of the western Superior province, southwestern Manitoba.

Acknowledgments

The author thanks D. Drayson for enthusiastic field assistance, H. Adediran for technical support, and C. Epp and P. Belanger for cataloguing and processing of the samples. Special thanks go to M. Hamilton at the University of Toronto for providing high-quality CA-ID-TIMS U-Pb zircon data via an analytical contract with the Manitoba Geological Survey. The manuscript has benefited greatly from constructive reviews by M.S. Gauthier and T. Martins, technical editing by M.F. Dufour, and report layout by C. Steffano.

References

Ayer, J.A. 1998a: Petrogenesis and tectonic evolution of the Lake of the Woods greenstone belt, western Wabigoon Subprovince, Ontario, Canada; Ph.D. thesis, University of Ottawa, Ottawa, Ontario, 207 p.

Ayer, J.A. 1998b: The mafic minerals of the Falcon Island ultrapotassic pluton, Lake of the Woods, Ontario: progressive reduction during fractionation; Canadian Mineralogist, v. 36, p. 49–66.

Bannatyne, B.B. 1985: Industrial minerals in rare-element pegmatites of Manitoba; Manitoba Energy and Mines, Geological Services, Economic Geology Report ER84-1, 96 p., URL <https://manitoba.ca/iem/info/libmin/ER84-1.pdf> [September 2023].

Blackburn, C.E., John, G.W., Ayer, J. and Davis, D.W. 1991: Wabigoon Subprovince; *in* Geology of Ontario, P.C. Thurston, H.R. Williams, R.H. Sutcliffe and G.M. Stott (ed.), Ontario Geological Survey, Special Volume 4, Part 1, p. 303–381.

Candela, P.A. 1997: A review of shallow, ore-related granites: textures, volatiles, and ore metals; Journal of Petrology, v. 38, p. 1619–1633.

Černý, P. and Ercit, T.S. 2005: The classification of granitic pegmatites revisited; The Canadian Mineralogist, v. 43, p. 2005–2026, URL <http://doi.org/10.2113/gscanmin.43.6.2005>.

Černý, P. and Meintzer, R.E. 1988: Fertile granites in the Archean and Proterozoic fields of rare-element pegmatites: crustal environment, geochemistry and petrogenetic relationships; *in* Recent Advances in the Geology of Granite-Related Mineral Deposits, R.P. Taylor and D.F. Strong (ed.), Canadian Institute of Mining, Metallurgy and Petroleum, Special Publication, v. 39, p. 170–207.

Černý, P., Trueman, D.L., Ziehlke, D.V., Goad, B.E. and Paul, B.J. 1981: The Cat Lake–Winnipeg River and the Wekusko Lake pegmatite fields, Manitoba; Manitoba Energy and Mines, Mineral Resources Division, Economic Geology Report ER80-1, 215 p., URL <https://manitoba.ca/iem/info/libmin/ER80-1.zip> [October 2018].

Chappell, B.W. and White, A.J.R. 1974: Two contrasting granite types; Pacific Geology, v. 8, p. 173–174.

Chappell, B.W. and White, A.J.R. 2001: Two contrasting granite types: 25 years later; Australian Journal of Earth Sciences, v. 48, p. 489–499.

Corfu, F., Hahnchar, J.M., Hoskin, P.W.O. and Kinny, P. 2003: Atlas of zircon textures; Reviews in Mineralogy and Geochemistry, v. 53, p. 469–500.

Davies, J.F., Bannatyne, B.B., Barry, G.S. and McCabe, H.R. 1962: Geology and mineral resources of Manitoba; Manitoba Department of Mines and Natural Resources, Mines Branch, Miscellaneous Report, 190 p., URL <https://manitoba.ca/iem/info/libmin/MISC1.pdf> [August 2024].

Duncan, C. 1989: Constraints on petrogenetic models of the Caddy Lake granite in southeastern Manitoba; B.Sc. thesis, University of Manitoba, Winnipeg, Manitoba, 186 p.

Eby, G.N. 1990: The A-type granitoids: a review of their occurrence and chemical characteristics and speculations on their petrogenesis; Lithos, v. 26, p. 115–134, URL <https://doi.org/10.1016/0024-4937(90)90043-Z>.

Eby, G.N. 1992: Chemical subdivision of the A-type granitoids: petrogenetic and tectonic implications; Geology, v. 20, p. 641–644.

Enrique, P. and Esteve, S. 2019: A chemical approximation to the modal QAPF and normative Q' (F')-ANOR classification of the igneous rocks based on their SiO_2-CaO-K_2O content; Geogaceta, v. 66, p. 91–94.

Farquharson, R.B. and Clark, G.S. 1971: Rb-Sr geochronology of some granitic rocks in southeastern Manitoba; *in* Geoscience Studies in Manitoba, A.C. Turnock (ed.), Geological Association of Canada, Special Paper 9, p. 111–117.

Fingler, J. 1991: Precious metal mineralization related to the Falcon Lake Intrusive Complex, southeastern Manitoba; M.Sc. thesis, University of Manitoba, Winnipeg, Manitoba, 145 p.

Frost, B.R., Barnes, C.G., Collins, W.J., Arculus, R.J., Ellis, D.J. and Frost, C.D. 2001: A geochemical classification for granitic rocks; Journal of Petrology, v. 42, p. 2033–2048.

Gibbins, W.A. 1971: Geology of the Falcon lake stock, southeastern Manitoba; *in* Geoscience Studies in Manitoba, A.C. Turnock (ed.), Geological Association of Canada, Special Paper 9, p. 129–135.

Grasso, V.G. 1968: The TiO_2 frequency in volcanic rocks; Geologische Rundschau, v. 57, p. 930–935.

Grid Metals Corp. 2024: Falcon West Lithium Project; Grid Metals Corp., URL <https://gridmetalscorp.com/properties/lithium-donner-falcon-west/> [August, 2024].

Halden, N.M., Mandziuk, W.S., Young, J., Clark, G.S. and Yang, P. 2007: LAM-ICP-MS zircon dating of the Falcon Lake Intrusive Complex and Caddy Lake granite, southeastern Manitoba, Canada; Proceedings of the Geologists' Association, v. 118, p. 25–35, URL <https://doi.org/10.1016/S0016-7878(07)80044-7>.

Halwas, D. 1984: The Sunbeam-Kirkland breccia pipe, Southeastern Manitoba; B.Sc. thesis, University of Manitoba, Winnipeg, Manitoba, 56 p.

Hamilton, M.A. 2022: Report on U-Pb CA-ID-TIMS geochronology of Archean and Proterozoic rock units in support of Manitoba Geological Survey bedrock mapping programs, 2018–2022; Jack Satterly Geochronology Laboratory, Department of Earth Sciences, University of Toronto, Toronto, Ontario, 51 p.

Hildebrand, R.S. and Whalen, J.B. 2021: Arc and slab-failure magmatism of the Taconic Orogeny, western New England, USA; *in* Pannotia to Pangaea: Neoproterozoic and Paleozoic Orogenic Cycles in the Circum-Atlantic Region, J.B. Murphy, R.A. Strachan and C. Quesada (ed.), Geological Society of London, Special Publications, v. 503, p. 409–422, URL <https://doi.org/10.1144/SP503-2019-247>.

Hildebrand, R.S., Whalen, J.B. and Bowring, S.A. 2018: Resolving the crustal composition paradox by 3.8 billion years of slab failure magmatism and collisional recycling of continental crust; Tectonophysics, v. 734–735, p. 69–88.

Ishihara, S. 1977: The magnetite-series and ilmenite-series granitic rocks; Mining Geology, v. 27, p. 293–305.

Ishihara, S. 1981: The granitoid series and mineralization; Economic Geology, Seventy-fifth Anniversary Volume (1905–1980), p. 458–484, URL <https://doi.org/10.5382/AV75>.

Ishihara S. 2004: The redox state of granitoids relative to tectonic setting and Earth history: the magnetite-ilmenite series 30 years later; Earth and Environmental Science, Transactions of the Royal Society of Edinburgh, v. 95, p. 23–33, URL <https://doi.org/10.1017/S0263593300000894>.

Jaffey, A.H., Flynn, K.F., Glendenin, L.E., Bentley, W.C. and Essling, A.M. 1971: Precision measurement of half-lives and specific activities of ^{235}U and ^{238}U; Physical Review, v. 4, p. 1889–1906.

Lentz, D.R. 1998: Petrogenetic evolution of felsic volcanic sequences associated with Phanerozoic volcanic-hosted massive sulphide systems: the role of extensional geodynamics; Ore Geology Review, v. 12, p. 289–327.

Lin, S. and Beakhouse, G.P. 2013: Synchronous vertical and horizontal tectonism at late stages of Archean cratonization and genesis of Hemlo gold deposit, Superior craton, Ontario, Canada; Geology, v. 41, p. 359–362.

Macdonald, J. 2024: Emplacement mechanisms of rare-element pegmatites, Separation Lake greenstone belt, northwest Superior Province; M.Sc. thesis, University of Manitoba, Winnipeg, Manitoba, 193 p.

Mandziuk, W.S. 1989: Primary structures of the Falcon Lake Intrusive Complex, Southeastern Manitoba; M.Sc. thesis, University of Manitoba, Winnipeg, Manitoba, 103 p.

Mandziuk, W.S., Brisbin, W.C. and Scoates, R.F.J. 1989b: Igneous structure in the Falcon Lake igneous complex, southeastern Manitoba; The Canadian Mineralogist, v. 27, p. 81–92.

Mandziuk, W.S., Tirschmann, P.A., Fingler, J., Halden, N., Brisben, W.C. and Scoates, R.F.J. 1989a: The Falcon Lake igneous complex; *in* Investigations by Geological Survey of Canada in Manitoba and Saskatchewan during 1984–1989 Mineral Development Agreements, A.G. Galley (ed.), Geological Survey of Canada, Open File 2133, p. 83–95, URL <https://doi.org/10.4095/127284>.

Maniar, P.D. and Piccoli, P.M. 1989: Tectonic discrimination of granitoids; Geological Society of America Bulletin, v. 101, p. 635–643.

Manitoba Energy and Mines 1987: Kenora, NTS 52; Manitoba Energy and Mines, Bedrock Geology Compilation Map 52F, preliminary edition, scale 1:250 000.

Martin, H., Moyen, J.-F. and Rapp, R. 2009: The sanukitoid series: magmatism at the Archaean-Proterozoic transition; Earth and Environmental Science, Transactions of the Royal Society of Edinburgh, v. 100, Special Issue 1–2, p. 15–33.

Martin, H., Smithies, R.H., Rapp, R., Moyen, J.-F. and Champion, D. 2005: An overview of adakite, tonalite–trondhjemite–granodiorite (TTG), and sanukitoid: relationships and some implications for crustal evolution; Lithos, v. 79, p. 1–24.

Pearce, J.A. 1996: A user's guide to basalt discrimination diagrams; *in* Trace Element Geochemistry of Volcanic Rocks: Applications for Massive Sulphide Exploration, D.A. Wyman (ed.), Geological Association of Canada, Short Course Notes 12, p. 79–113.

Peccerillo, A. and Taylor, S.R. 1976: Geochemistry of Eocene calc-alkaline volcanic rocks from the Kastamonu area, Northern Turkey; Contributions to Mineralogy and Petrology, v. 58, p. 63–81.

Percival, J.A., Sanborn-Barrie, M., Skulski, T., Stott, G.M., Helmstaedt, H. and White, D.J. 2006: Tectonic evolution of the western Superior Province from NATMAP and LITHOPROBE studies; Canadian Journal of Earth Sciences, v. 43, p. 1085–1117.

Percival, J.A., Skulski, T., Sanborn-Barrie, M., Stott, G.M., Leclair, A.D., Corkery, M.T. and Boily, M. 2012: Geology and tectonic evolution of the Superior Province, Canada, Chapter 6; *in* Tectonic Styles in Canada: The LITHOPROBE perspective, J.A. Percival, F.A. Cook and R.M. Clowes (ed.), Geological Association of Canada, Special Paper 49, p. 321–378.

Rapp, R.P. and Watson, E.B. 1995: Dehydration melting of metabasalt at 8–32 kbar: implications for continental growth and crust-mantle recycling; Journal of Petrology, v. 36, p. 891–931.

Rapp, R.P., Shimizu, N. and Norman, M.D. 2003: Growth of early continental crust by partial melting of eclogite; Nature, v. 425, p. 605–609.

Richards, J.P. and Kerrich, R. 2007: Special paper: Adakite-like rocks: their diverse origins and questionable role in metallogenesis; Economic Geology, v. 102, p. 537–576.

Rittmann, A. 1962: Volcanoes and Their Activity; Wiley, New York, New York, 305 p.

Rollinson, H. and Pease, V. 2021: Using Geochemical Data to Understand Geological Processes (2nd edition); Cambridge University Press, Cambridge, United Kingdom, 346 p., URL <https://doi.org/10.4324/9781315845548>.

Rubatto, D. 2017: Zircon: the metamorphic mineral; Reviews in Mineralogy and Geochemistry, v. 83, p. 297–328.

Shirey, S.B. and Hanson, G.N. 1984: Mantle derived Archaean monzodiorites and trachyandesites; Nature, v. 310, p. 222–224.

Stern, R.A. and Hanson, G.N. 1991: Archean high-Mg granodiorite: a derivative of light rare earth element-enriched monzodiorite of mantle origin; Journal of Petrology, v. 32, p. 201–238.

Stevenson, R., Henry, P. and Gariépy, C. 1999: Assimilation fractional crystallization origin of Archean sanukitoid suites: Western Superior Province, Canada; Precambrian Research, v. 96, p. 83–99.

Streckeisen, A.L. and Le Maitre, R.W. 1979: A chemical approximation to modal QAPF classification of the igneous rocks; Neues Jahrbuch für Mineralogie, v. 136, p. 169–206.

Sun, W.D., Ling, M.X., Yang, X.Y., Fan, W.M., Ding, X. and Liang, H.Y. 2010: Ridge subduction and porphyry copper-gold mineralization: an overview; Science China Earth Sciences, v. 53, p. 475–484.

Tirschmann, P.A. 1992: Geochemistry and fractional crystallization history of the Falcon Lake Intrusive Complex; M.Sc. thesis, University of Manitoba, Winnipeg, Manitoba, 191 p.

Wang, W., Lu, Y., Gao, L., Sun, G., Zhou, X., Yao, J., Yang, W. and Liang, X. 2024: Late Archean K-rich intermediate magmatism driven by deep supracrustal recycling; Chemical Geology, v. 662, art. 122215, URL <https://doi.org/10.1016/j.chemgeo.2024.122215>.

Whalen, J.B. and Frost, C.D. 2013: The Q-ANOR diagram: a tool for the petrogenetic and tectonomagmatic characterization of granitic suites; Geological Society of America, South-Central Section, 47th Annual Meeting, April4–5, 2013, Abstracts with Programs, v. 45, no. 3, p. 24, URL–<https://www.researchgate.net/publication/290161821_The_Q-ANOR_diagram_A_tool_for_the_petro-genetic_and_tectonomagmatic_characterization_of_granitic_suites_abstract> [September 2018].

Whalen, J.B. and Hildebrand, R.S. 2019: Trace element discrimination of arc, slab failure, and A-type granitic rocks; Lithos, v. 348–349, art. 105179, URL <https://doi.org/10.1016/j.lithos.2019.105179>.

Whalen, J.B., Currie, K.L. and Chappell, B.W. 1987: A-type granites: geochemical characteristics, discrimination and petrogenesis; Contributions to Mineralogy and Petrology, v. 95, p. 407–419.

Winter, J.D. 2014: Principles of Igneous and Metamorphic Petrology (second edition); Pearson Education Limited, Essex, England, 738 p.

Yang, X.M. 2007: Using the Rittmann Serial Index to define the alkalinity of igneous rocks; Neues Jahrbuch für Mineralogie, v. 184, p. 95–103.

Yang, X.M. 2014: Granitoid rocks in southeastern Manitoba: preliminary results of reconnaissance mapping and sampling; *in* Report of Activities 2014, Manitoba Mineral Resources, Manitoba Geological Survey, p. 49–63, URL <https://manitoba.ca/iem/geo/field/roa14pdfs/GS-4.pdf> [December 2015].

Yang, X.M. 2023: Progress report on the study of granitoids in Manitoba: petrogenesis and metallogeny; Manitoba Economic Development, Investment and Trade, Manitoba Geological Survey, Open File OF2022-3, 119 p., URL <https://manitoba.ca/iem/info/libmin/OF2022-3.zip> [March 2023].

Yang, X.M. 2024: New uranium-lead zircon dates from the Lynn Lake greenstone belt, northwestern Manitoba (part of NTS 64C14): implications for diverse granitoid magmatism and gold mineralization; *in* Report of Activities 2024, Manitoba Economic Development, Investment, Trade and Natural Resources, Manitoba Geological Survey, p. 129–144.

Yang, X.M. and Lawley, C.J.M. 2024: Rapid switch in geodynamic setting revealed by episodic granitoid magmatism in the Lynn Lake greenstone belt of Paleoproterozoic Trans-Hudson Orogen, Manitoba, Canada; Lithos, v. 470–471, art. 107534, URL <https://doi.org/10.1016/j.lithos.2024.107534>.

Yang, X.M. and Lentz, D.R. 2005: Chemical composition of rock-forming minerals in gold-related granitoid intrusions, southwestern New Brunswick, Canada: implications for crystallization conditions, volatile exsolution and fluorine-chlorine activity; Contributions to Mineralogy and Petrology, v. 150, p. 287–305.

Yang, X.M., Drayson, D. and Polat, A. 2019: S-type granites in the western Superior Province: a marker of Archean collision zones; Canadian Journal of Earth Sciences, v. 56, p. 1409–1436, URL <https://doi.org/10.1139/cjes-2018-0056>.

Yoder, H.S., Jr. and Tilley, C.E. 1962: Origin of basalt magmas: an experimental study of natural and synthetic rock systems; Journal of Petrology, v. 3, p.342–532.

Yousefi, F. and Lentz D.R. 2024: Formation of high-silica adakites and their relationship with slab break-off: implications for generating fertile Cu-Au-Mo porphyry systems; Geoscience Frontiers, v. 15, art. 101927, URL <https://doi.org/10.1016/j.gsf.2024.101927>.

Zwanzig, H. 2024: Tectonic model of the Paleoproterozoic western Trans-Hudson Orogen; *in* GAC–MAC–PEG 2024 Brandon Meeting: Abstracts, Volume 47, Geoscience Canada, v. 51, no. 2, p. 128, URL <https://doi.org/10.12789/geocanj.2024.51.211>.

GS2024-8

Preliminary field observations of Mesoarchean metamorphosed sedimentary and intrusive rocks in the Rice Lake greenstone belt, eastern Manitoba (parts of NTS 52L14, 52M3, 62P1)

by E. Tonboe[1], P. Waterton[1], R. Haugaard[2], S.D. Anderson[3] and C.G. Couëslan

In Brief:

- Field observations and samples of Mesoarchean metamorphosed sedimentary and intrusive rocks were collected with the goal of understanding the early western Superior province crust
- 3.0 Ga tonalitic gneisses of the North Caribou terrane contain several serpentinized ultramafic pods and are overlain by mature Mesoarchean metasediments.

Citation:
Tonboe, E., Waterton, P., Haugaard, R., Anderson, S.D. and Couëslan, C.G. 2024: Preliminary field observations of Mesoarchean metamorphosed sedimentary and intrusive rocks in the Rice Lake greenstone belt, eastern Manitoba (parts of NTS 52L14, 52M3, 62P1); *in* Report of Activities 2024, Manitoba Economic Development, Investment, Trade and Natural Resources, Manitoba Geological Survey, p. 66–76.

Summary

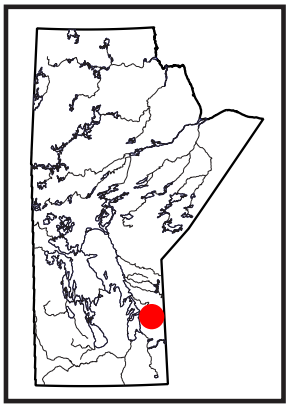
This report provides field observations from the eastern shore of Lake Winnipeg (Lewis-Storey assemblage), and from Wallace (Wallace assemblage) and Garner (Garner Lake intrusive complex) lakes. Fieldwork was carried out in August 2024 to collect samples for a Ph.D. project involving the nature, composition and growth of early crust of the western Superior province. Highlights of the fieldwork include findings of fuchsite-bearing quartzite in the Lewis-Storey assemblage as well as ultramafic pods within the tonalitic gneiss of the North Caribou terrane.

Introduction

The Rice Lake greenstone belt in eastern Manitoba is well studied and mapped due to its significant lode-gold deposits, good exposure and easy access, providing a good framework for geological fieldwork. In August 2024, fieldwork was carried out along the eastern shore of Lake Winnipeg, and at Wallace and Garner lakes with a focus on Mesoarchean metamorphosed sedimentary and intrusive rocks. The purpose of the fieldwork was to collect data via observations of type exposures and samples (n = 91) for a Ph.D. project that will investigate the nature, composition and formation of the early crust of the western Superior province, primarily through the study of clastic sedimentary rocks.

The eastern shore of Lake Winnipeg (Black Island–Seymourville area) was mapped at 1:20 000 scale by Bailes and Percival (2005) and has been the subject of several studies (e.g., Percival and Whalen, 2000; Percival et al., 2006). The Wallace Lake area has not been mapped recently but is relatively well described and studied (e.g., Sasseville and Tomlinson, 2000; Sasseville et al., 2006; Fralick et al., 2008), whereas the Garner Lake area was mapped in 1:20 000 by Anderson (2013a). These well characterized areas allowed for targeted and detailed fieldwork.

Mature, clastic sediments contain the concentrated detritus of exposed landmasses over a large region. They can therefore provide insights into the composition and history of their source area, and many inferences on the nature and evolution of the Archean crust come from such sediments and resulting sedimentary rocks (e.g., O'Neil et al., 2024). However, interpreting the nature of this crust is not straightforward and may depend on the geochemical proxies used. For example, estimates of the relative proportions of mafic and felsic rocks in the Archean crust range from mafic-dominated, when determined using trace element ratios involving Ni and Cr (e.g., Tang et al., 2016), to felsic-dominated, when using Sm/Nd ratios (Garçon, 2021) or major element contents (Lipp et al., 2021). Existing methods for reconstructing the timing of the growth of Earth's continental crust are also significantly biased toward detecting felsic crust formation. This is due to their reliance on isotopes, such as Sm-Nd, which are present in much higher concentrations in felsic rocks, or on zircon, which predominantly crystallizes in felsic magmas (e.g., Dhiume et al., 2017).



Haugaard et al. (2021) demonstrated a new method for detecting mafic and ultramafic crust using detrital chromite in terrigenous clastic sedimentary rocks. Chromite crystallizes exclusively in mafic and ultramafic magmas, contains information about the magma from which it crystalized (e.g., Barnes and Roeder, 2001; Barnes et al., 2022) and can be dated using the rhenium-osmium (Re-Os) method (Haugaard et al., 2021). Detrital chromite can thus be used to reconstruct the growth of mafic and ultramafic crust in a manner similar to that which uses Hf isotopes in zircon to trace felsic crust evolution. Chromite is resistant to transport and weathering and is often found as heavy-mineral laminations or within fuchsite-rich horizons (Cr-rich mica) in quartz arenites. Quartz arenites are chemi-

[1] Department of Geosciences and Natural Resource Management, University of Copenhagen, Copenhagen, Denmark
[2] Harquail School of Earth Sciences, Laurentian University, Sudbury, Ontario
[3] Department of Earth Sciences, University of Manitoba, Winnipeg, Manitoba

cally mature sedimentary rocks that likely sampled large source areas, potentially making them representative of the regional crust that was exposed during their deposition.

The oldest rocks in the Rice Lake greenstone belt area are 3.0 Ga tonalitic gneisses of the North Caribou terrane, which are overlain by mature quartzites of the Lewis-Storey and Wallace assemblages. The maximum depositional age for the Lewis-Storey quartzite is constrained by detrital zircons to be 2991 Ma, with a minimum age of 2978 Ma defined by a crosscutting rhyolite sill (Percival et al., 2006). Little is known of the crustal precursors to the tonalitic gneisses, as well as whether or not mafic and ultramafic rocks were a common component of the early North Caribou terrane crust. Detrital chromite and zircon of the Lewis-Storey and Wallace assemblages might contain this information.

During fieldwork, samples of quartzites and associated metasedimentary rocks were collected at Wallace Lake and along the eastern shore of Lake Winnipeg to recover detrital chromite and zircon. Additionally, samples of the basement gneisses and associated ultramafic pods were collected as potential sources of detrital zircon and chromite. Finally, a layered intrusion, the Garner Lake intrusive complex, was investigated to understand the magmatic processes associated with such an intrusion. Although too young to be a source of detrital chromite in the metasedimentary rocks sampled at Lake Winnipeg and Wallace Lake, the intrusion might be an analogue to the heavily serpentinized ultramafic pods of unknown age within the 3.0 Ga tonalitic gneiss at the eastern shore of Lake Winnipeg.

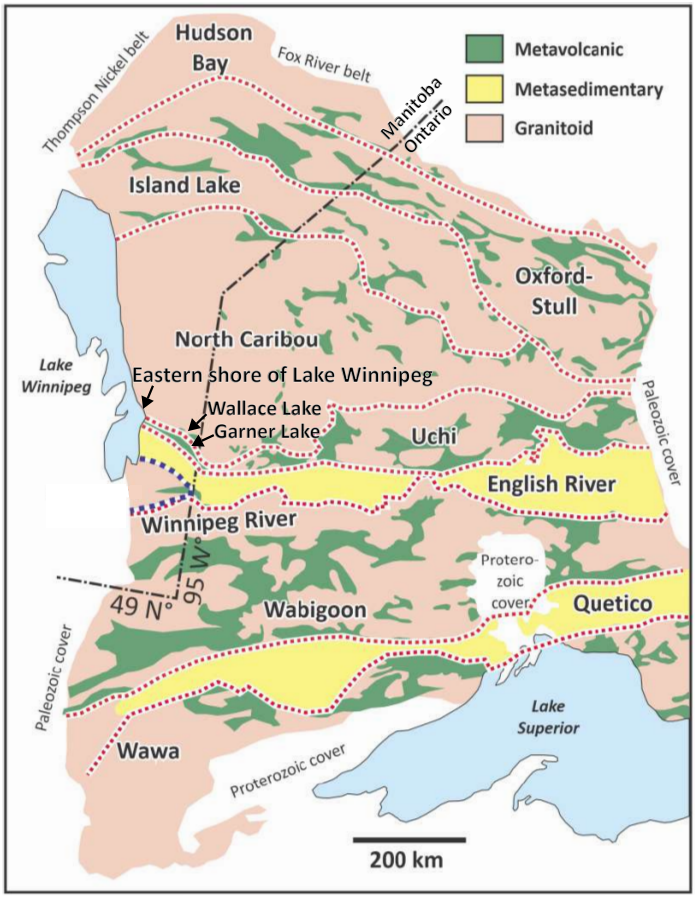


Figure GS2024-8-1: *Simplified geology of the northwestern Superior province from Martins et al. (2023). The black arrows indicate the locations of the three study areas and the red dashed lines represent the terrane and subprovince boundaries.*

Geological setting

The western Superior province can be divided into terranes and subprovinces that generally form large east-trending blocks (Figure GS2024-8-1). Terranes are defined by tectonic packages, whereas subprovinces are defined by lithological assemblages (Card and Ciesielski, 1986). The North Caribou terrane is considered to be the protocratonic nucleus of the western Superior craton, to which other terranes were accreted during the Neoarchean (Percival, 2007). Its southern margin consists of a 3.0 Ga tonalitic gneiss complex that is intruded by several different phases of granitoid plutons, the youngest of which was regional in scale and spanned 2.75–2.69 Ga (Corfu and Stone, 1998; Whalen et al., 2003). The tonalitic gneisses are nonconformably overlain by platform-rift deposits of the Lewis-Storey and Wallace assemblages, which are interpreted to record a plume-driven break-up event of Mesoarchean age (Sasseville and Tomlinson, 2000; Percival et al., 2006). These Mesoarchean units are juxtaposed against much younger Neoarchean supracrustal rocks forming part of the Uchi subprovince (Percival et al., 2006).

The Rice Lake greenstone belt in eastern Manitoba is part of the Uchi subprovince. Its boundary with the North Caribou terrane to the north is marked by the Wanipigow fault and it is bounded to the south by the English River subprovince. The Rice Lake greenstone belt consists primarily of Neoarchean supracrustal rocks that were accreted onto the southern margin of the North Caribou terrane (Percival et al., 2006). Mesoarchean intrusive and supracrustal rocks in the Garner Lake area were likewise accreted to the southern margin of the North Caribou terrane, as part of an older arc–back-arc complex (Anderson, 2013b). In the study area, volcaniclastic and epiclastic rocks are intruded by the Garner Lake intrusive complex. The intrusive complex consists of alternating layers of serpentinized peridotite and clinopyroxenite, overlain by gabbro (Anderson, 2013b). In the west, the top of the intrusive complex is marked by an angular unconformity overlain by younger volcaniclastic and epiclastic rocks. In the east, the contact is intrusive into older rhyolitic volcaniclastic rocks (Anderson, 2013b).

Lewis-Storey assemblage

The Lewis-Storey assemblage unconformably overlies a 3.0 Ga tonalitic gneiss and has previously been described as a platform-rift deposit consisting of basal arkosic grit, quartz arenite, komatiite, carbonate and iron formation (Percival et al., 2001). The basal arkosic grit has been interpreted to have formed through chemical weathering and slight downslope transport of

weathered tonalitic basement as a result of rift-related uplift (Percival et al., 2001, 2006). Alternatively, it has also been described as a cataclasite derived from the adjacent tonalite gneiss (Brown, 1981). The term 'grit' has generally been discontinued but refers to a sedimentary rock with angular clasts between 2 to 4 mm. In this report, the term 'arkosic grit' is used for consistency with the most recent geological map by Bailes and Percival (2005) and previous studies (e.g., Percival et al., 2001, 2006). Deposition of the quartz arenite, carbonate and iron formation is thought to reflect shallow-to-deeper water deposition as a result of thermal subsidence (Percival et al., 2001).

The Lewis-Story supracrustal sequence and its relationship to the underlying orthogneisses is shown in Figure GS2024-8-2 and described in the following sections from stratigraphic base to top. A stratigraphic section of a transect through the southern part of the study area is presented in Figure GS2024-8-3. Fieldwork along the shoreline revealed a consistent stratigraphy consisting of tonalitic gneiss (unit 1) overlain by arkosic grit (unit 2), quartz arenite (unit 4) and an ultramafic lava flow (unit 5). A mafic sill (unit 3) cuts the arkosic grit and can be traced for at least 2.5 km along the shoreline. In the northern part of the study area the sill has been subject to significantly more shear and forms a mylonite.

Stratigraphy

Tonalitic gneiss (unit 1)

The light brown to grey tonalitic gneiss of unit 1 (not shown) is medium to coarse grained and contains a characteristic blue quartz. The gneiss is generally weakly foliated but locally contains more intensely foliated zones. The gneiss is cut by fine-grained felsic and mafic dikes and rare granitic pegmatites; fine-grained felsic dikes are abundant near the nonconformity with the overlying Lewis-Storey assemblage. The gneiss contains heavily serpentinized ultramafic pods, which extend well to the east along strike (around 30 km) and range up to 5 km in length, as defined by aeromagnetic data (Natural Resources Canada, 1986). Four of these pods were investigated within the study area. Here

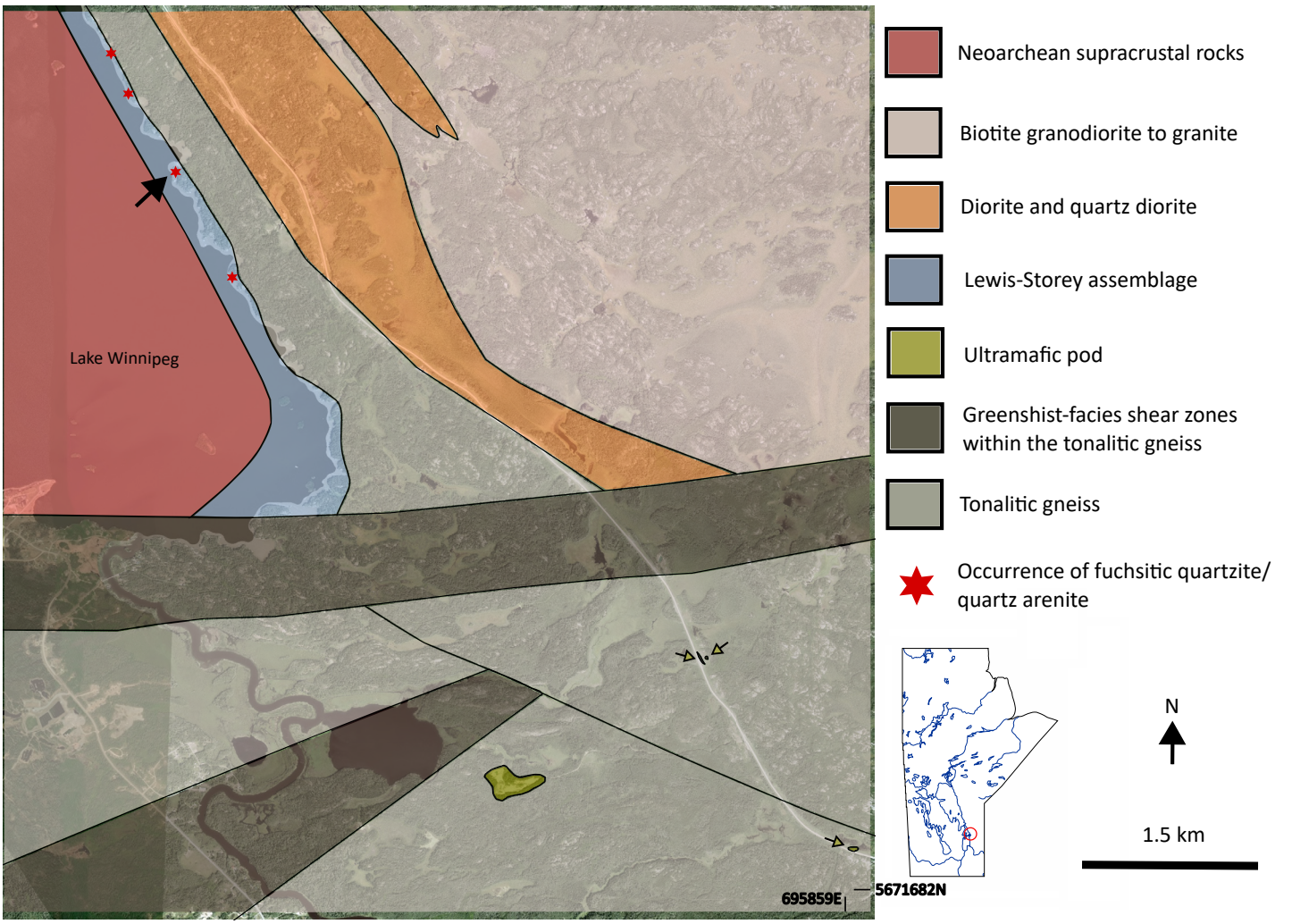


Figure GS2024-8-2: *Simplified bedrock geology of the Lewis-Storey assemblage area (modified from Bailes and Percival, 2005). The red stars indicate the locations of fuchsite-bearing quartzite/quartz arenite and the black arrow shows the location of Figure GS2024-8-3. Three small ultramafic pods are highlighted by green arrows. Inset map shows location of the study area (outlined in red). Corner co-ordinates are in UTM Zone 14, NAD83.*

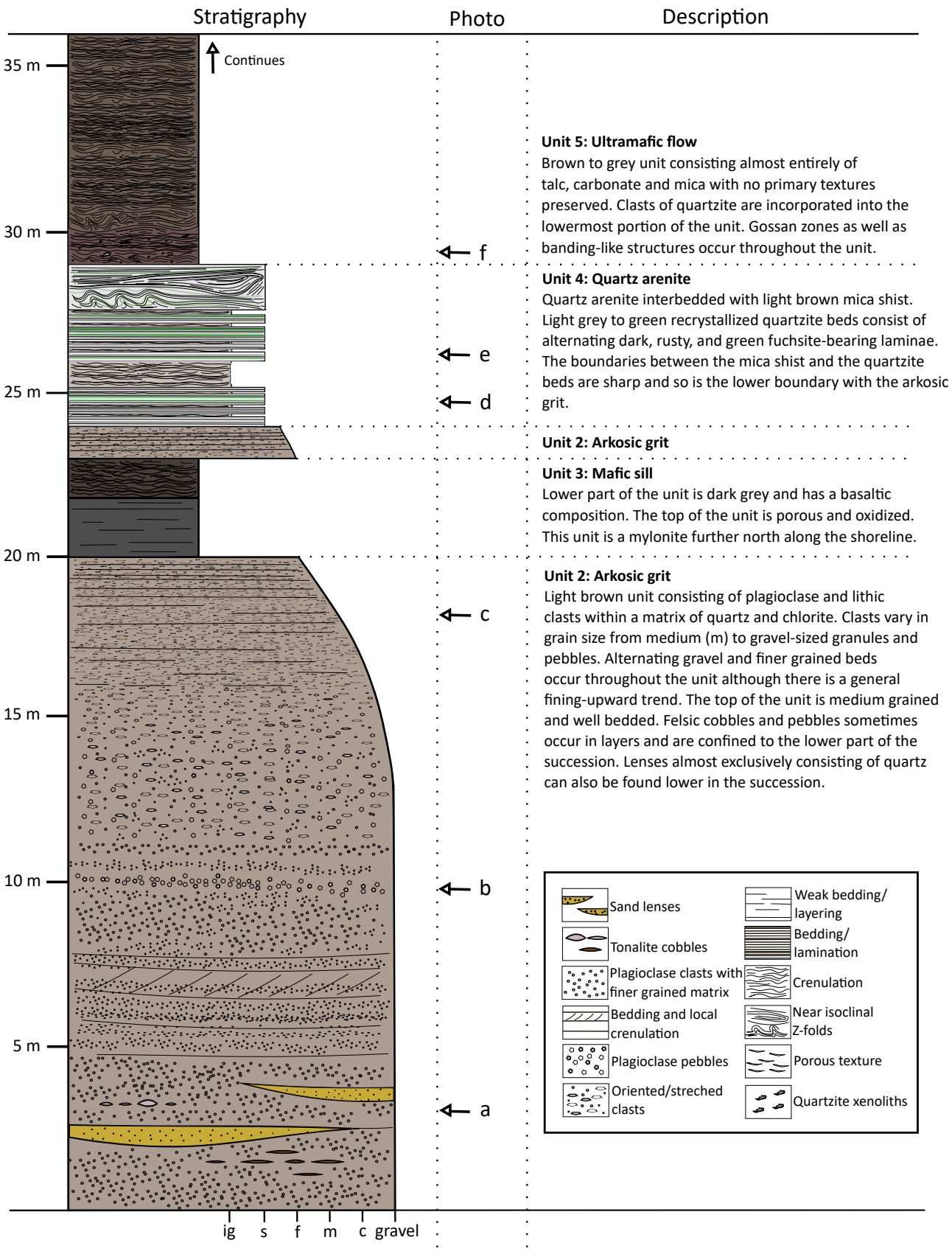


Figure GS2024-8-3: *Schematic stratigraphic section of the clastic sedimentary rocks of the Lewis-Storey assemblage. The location of the stratigraphic section is indicated on Figure GS2024-8-2 and the letters show the locations of the field photographs from Figure GS2024-8-4a–f. Abbreviations: c, coarse; f, fine; ig, igneous; m, medium; s, silt.*

the pods range from small (10 by 5 m) to relatively large (400 by 250 m). The pods contain several generations of serpentinite veins and there are little to no primary textures preserved in the small pods; however, the largest pod locally contained coarse-grained (up to 1 cm), mesh-textured olivine. The gneiss was observed to contain a reaction zone of biotite schist near one of the small pods. Here the gneiss is also intruded by two pegmatite veins that clearly crosscut the gneissosity.

Arkosic grit (unit 2)

The light brown arkosic grit of unit 2 (Figure GS2024-8-3) is rich in plagioclase and lithic fragments, which are surrounded by a matrix consisting of chlorite and quartz. The unit is textually immature with poorly sorted beds of medium- to pebble-sized clasts. The clasts are generally subangular and are locally oriented subparallel to the bedding plane, especially near the top of the unit. The unit becomes finer grained (clasts of 0.35–0.5 mm) and well bedded near the top.

Rare felsic cobbles occur near the bottom of the unit (Figure GS2024-8-4a). The cobbles are often boudinaged and appear in isolated layers, surrounded by finer grained matrix. Coarse and pebbly intervals (Figure GS2024-8-4b) are sometimes replaced by more well-sorted and finer grained beds with a relatively short lateral extension. Rare lenses rich in recrystallized quartz and up

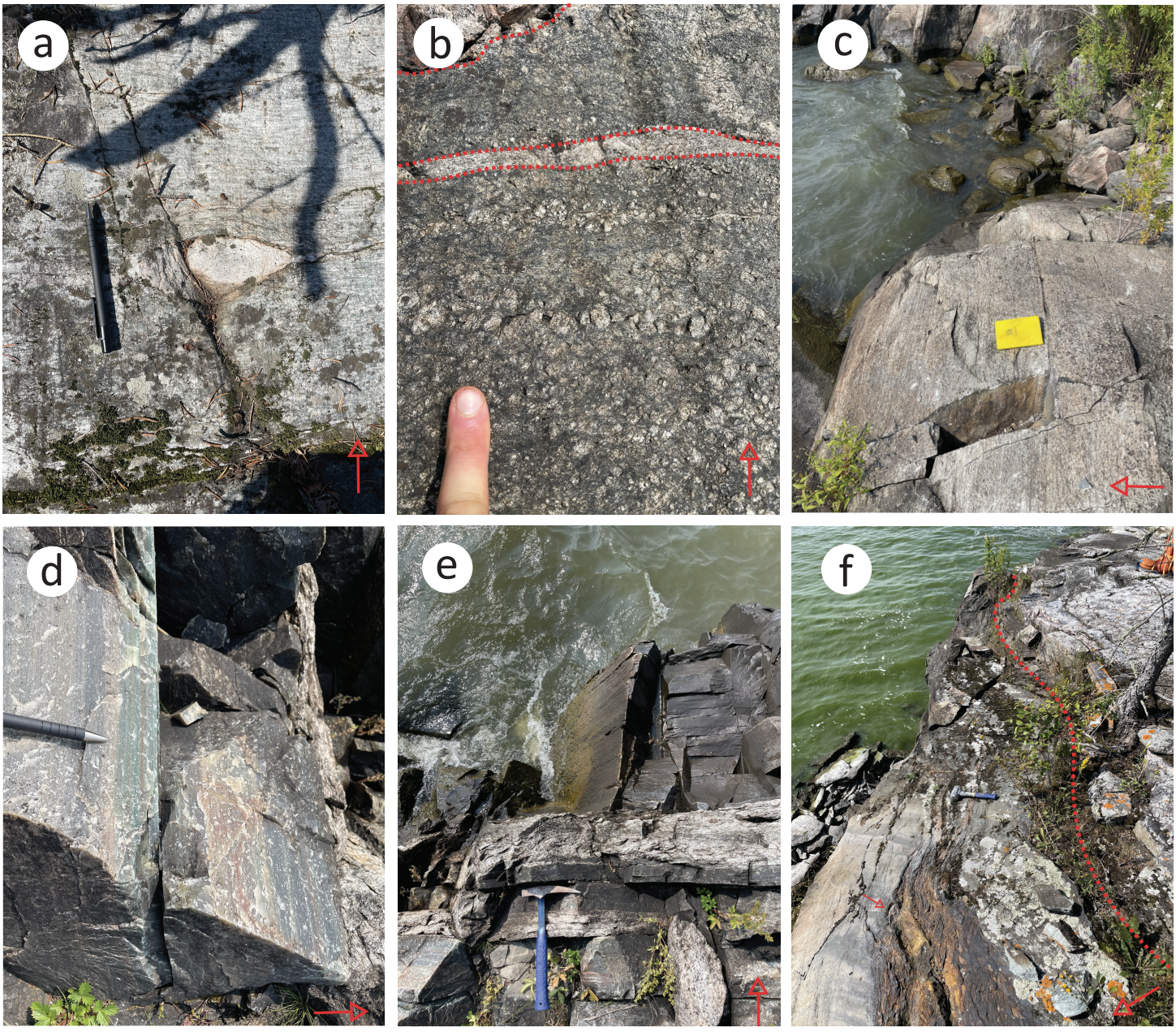


Figure GS2024-8-4: *Field photographs of the Lewis-Storey assemblage:* ***a)*** *arkosic grit with tonalitic cobble;* ***b)*** *grain size variations in arkosic grit, with felsic dikes outlined in red;* ***c)*** *well-bedded arkosic grit near the top of the unit;* ***d)*** *fuchsite-bearing quartzite bed;* ***e)*** *quartz arenite interbedded with mica schist;* ***f)*** *quartz arenite (right) overlain by an ultramafic lava flow (left), with contact marked by the red line and gossan zone highlighted by the small red arrow (bottom left). The red arrow at the bottom right of each panel indicates stratigraphic up-direction.*

to a few metres in length can also be found near the base of the unit.

Mafic rocks commonly crosscut and appear to intrude the arkosic grit. Some of the mafic dikes are laterally discontinuous and contain abundant small offshoots and dikelets. Fine-grained felsic dikes also intrude the unit, especially further north along the shoreline. In the northern part of the study area, the arkosic grit is more massive and cut by numerous felsic dikes, giving it an orthogneiss-like texture. The boundary with the underlying gneiss is thus difficult to confidently place. A potential boundary between the gneiss and arkosic grit is marked by a quartz-rich bed 40 cm thick, followed by a coarse- to medium-grained bedded interval 1.5 m thick that transitions into a coarse, pebbly layer, which is cut by abundant felsic and mafic dikes. This grades into the finer grained (clasts of 0.35–0.5 mm) and well-bedded sandstone at the top of the arkosic grit (Figure GS2024-8-4c).

Mafic sill (unit 3)

A mafic sill (unit 3; Figure GS2024-8-3) intrudes the arkosic grit in the southern part of the study area. The lower part of the sill is dark grey-green. The massive, fine-grained lower part of the sill sharply transitions into a brown, porous, crenulated zone, which marks the top of the sill. The lower boundary of the sill is undulose and locally cuts the foliation in the grit. Further north along the shoreline this mafic unit appears to transition into a mylonite containing boudinaged clasts of felsic material.

Quartz arenite (unit 4)

The light grey to green fuchsite-bearing quartz arenite unit 4 (Figure GS2024-8-3) predominantly consists of finely laminated quartzite beds with alternating dark and light laminae, and occasional green (fuchsitic) and orange-brown horizons (Figure GS2024-8-4d). The dark, green and orange-brown horizons contain scattered black grains, which are difficult to see due to the recrystallized nature of the quartzite beds. The quartz arenite is interbedded with mica schist (Figure GS2024-8-4e) that is internally layered with beds ranging between 2 to 5 cm in thickness. The mica schist intervals are usually thin (<30 cm) although thicker intervals up to 1 m also occur. The quartzite beds are typically thicker and more abundant than the mica schist. The boundary between the arkosic grit and quartz arenite is sharp, as are the boundaries between the quartzite beds and the mica schist. The top of the quartz arenite is locally characterized by near-isoclinal Z-folds occurring in a range of scales (metre to centimetre).

Ultramafic flow (unit 5)

The brown to grey ultramafic unit 5 (Figure GS2024-8-3) consists almost entirely of talc, carbonate and mica with no primary textures preserved. Clasts of quartzite are incorporated into the lowermost portion of the unit. Gossan zones as well as banding of uncertain origin or crenulations occur throughout the unit (Figure GS2024-8-4f). The lower contact with the quartzite is undulose.

Wallace assemblage

The supracrustal Wallace assemblage (Figure GS2024-8-1) consists of the Conley and Overload Bay formations. The metasedimentary Conley formation was examined on the northern shoreline of Wallace Lake, where it is strongly transposed on the northern limb of a map-scale syncline and ranges up to approximately 400 m in thickness. The Conley formation consists predominantly of sandstone and conglomerate capped by carbonates, iron formation and argillites (Fralick et al., 2008). The sandstone contains ca. 2.99 Ga detrital zircons and is cut by a 2.92 Ga felsic porphyry dike (Poulsen et al., 1996). These are thus the oldest supracrustal rocks in the Wallace Lake area and comparable in age to the quartz arenite of the Lewis-Storey assemblage. The Conley formation is overlain by komatiitic and mafic volcanic rocks and iron formation of the Overload Bay formation, which marks the top of the Wallace assemblage (Sasseville and Tomlinson, 2000; Sasseville et al., 2006).

Fieldwork was focused on the base of the Conley formation, which revealed a nonconformable lower boundary with tonalitic orthogneiss. This was overlain by sandstone interbedded with matrix-supported conglomerate overlain by pillowed basalt. An approximately 190 m long transect from the basal contact to the northern shoreline revealed a heterogeneous succession. Examples of the different lithologies are shown in Figure GS2024-8-5 and described below.

Stratigraphy

The contact between the tonalitic orthogneiss and the Conley formation (UTM Zone 14N, 756405E, 5659609N [NAD83]) was observed in several locations approximately 190 m from the northern shoreline of Wallace Lake. At one of these localities, a felsic dike cuts the lower part of the Conley formation. Near the contact abundant quartz veins also cut both the dike and the metasedimentary rocks (Figure GS2024-8-5a).

Further up the succession the metasedimentary rocks become more quartz rich. Coarse-grained, quartz- and feldspar-rich beds are locally interbedded with dark grey, fine-grained and laminated beds (Figure GS2024-8-5b, c). These are overlain by a matrix-supported cobble-boulder conglomerate (Figure GS2024-8-5d) approximately 50 m upsection and 65 m from the contact. The matrix is dark grey, fine grained and contains abundant biotite. The cobbles and boulders are generally subrounded and resemble the underlying basement. However, two types of boulders and cobbles can be identified: a light brown to grey, foliated, medium-grained rock; and a light grey, massive to weakly foliated, coarse-grained rock. The cobbles and boulders are concentrated in the middle of the conglomerate bed. The top of the bed is sharply overlain by a quartz-rich bed, which in turn, is sharply overlain by the dark grey, fine-grained, biotite-rich unit.

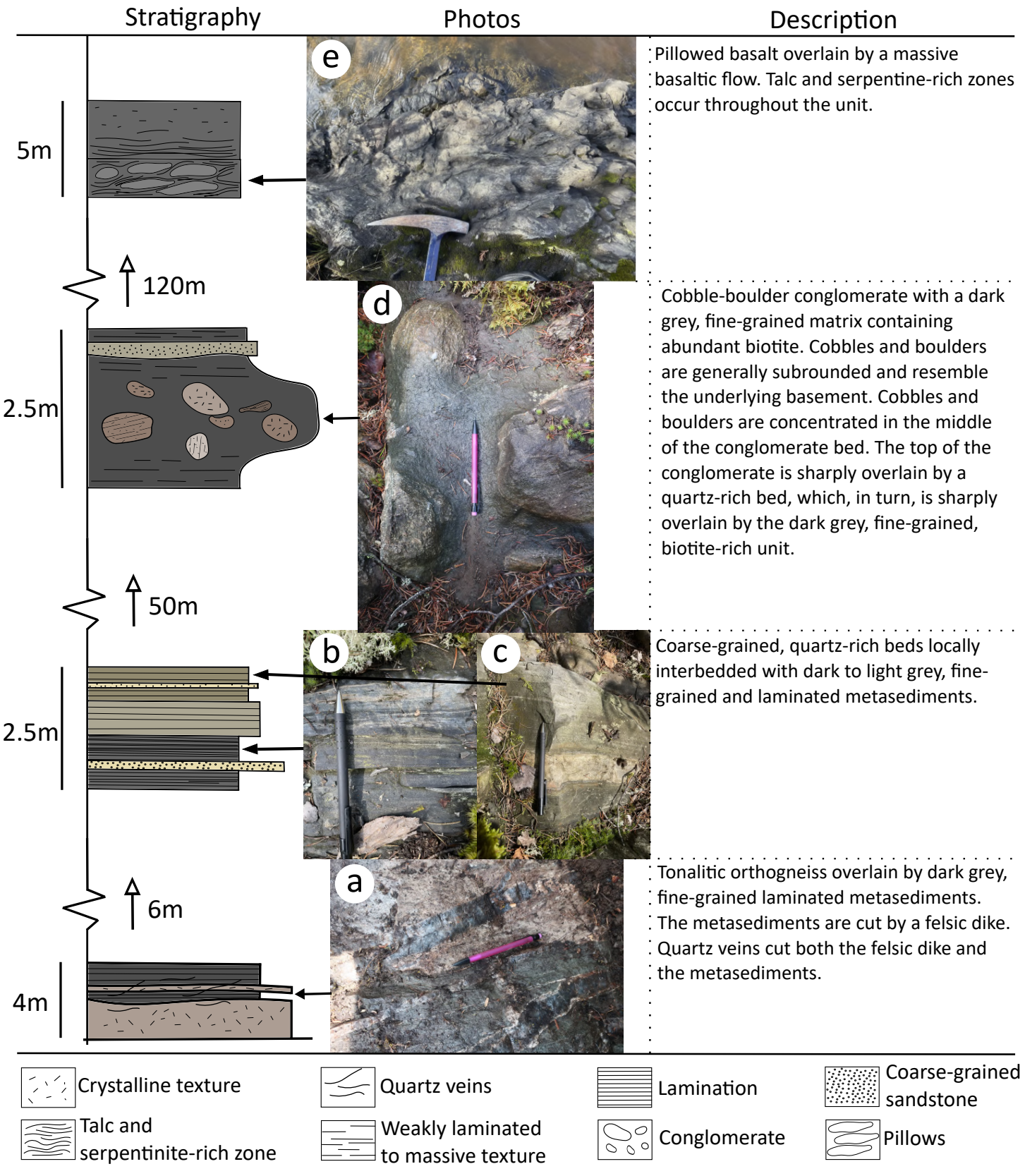


Figure GS2024-8-5: *Stratigraphic variation through the Conley formation, as observed in the Wallace Lake assemblage area:* ***a****) tonalitic orthogneiss overlain by laminated metasediments;* ***b)*** *coarse-grained quartz-rich beds;* ***c)*** *fine-grained, laminated metasediments;* ***d)*** *cobble-boulder conglomerate;* ***e)*** *pillowed basalt overlain by a massive basaltic flow.*

Pillowed basalt at the shoreline of Wallace Lake (756278E, 5659467N) is overlain by a massive basaltic flow (Figure 2024-8-5e). Pillowed basalt is also exposed on an island 200 m to the northwest, suggesting that this unit is relatively thick.

Garner Lake intrusive complex

The Garner Lake intrusive complex consists of a variety of lithologies. The base of the intrusion comprises alternating layers of serpentinized peridotite and pyroxenite. The top of the intrusion consists of layered gabbro cut by two generations of dikes: coarse-grained pegmatitic leucogabbro and fine-grained granitoid that contains xenoliths of leucogabbro.

The grey to light brown peridotite ranges from fine-grained, equiangular harzburgite (Figure GS2024-8-6a) to coarser grained harzburgite with oikocrystic pyroxene (Figure GS2024-8-6b). Contacts between the peridotite and pyroxenite are undulose. The pyroxenite is generally coarse grained and contains pseudomorphic hornblende as well as rare bronzite (orthopyroxene; Figure GS2024-8-6c). Internally the pyroxenite is quite heterogeneous with coarse-grained pegmatitic pods containing large amphiboles (up to 5 cm). Undulose boundaries between coarse- and fine-grained pyroxenite are also observed (Figure GS2024-8-6d). The coarser grained pyroxenite tends to have more pegmatitic pods. Although not found in situ, abundant boulders with large pyroxene crystals were found along the beach near the

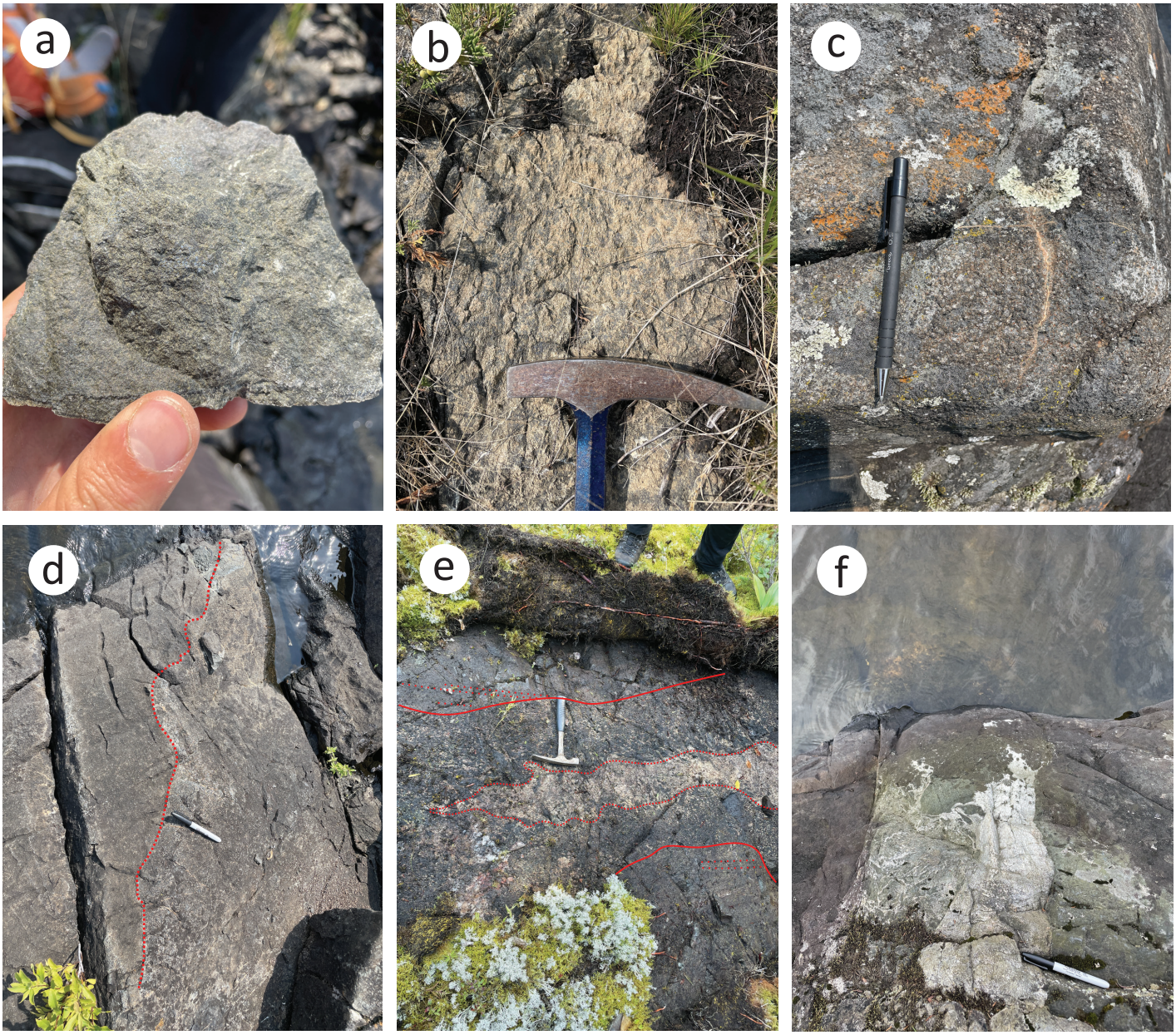


Figure GS2024-8-6: *Field photographs of the Garner Lake intrusive complex:* ***a)*** *fine-grained harzburgite;* ***b)*** *pyroxene oikocrysts in peridotite;* ***c)*** *coarse-grained pyroxenite;* ***d)*** *grain size variations within the pyroxenite (dotted line marks contact between coarse- and fine-grained pyroxenite);* ***e)*** *pegmatitic leucogabbro cutting a layered gabbro (layering indicated by the solid lines and contact with the leucogabbro by the dotted lines);* ***f)*** *fine-grained felsic dike cutting the layered gabbro.*

coarse-grained pyroxenite. One particular boulder contained hollow pyroxene crystals 25 cm long, which were altered to amphibole along the grain margins and surrounded by plagioclase.

Farther up in the complex, layered gabbro is cut by pegmatitic leucogabbro (Figure GS2024-8-6e). These pegmatite intrusions are locally zoned with a fine-grained centre surrounded by a coarse-grained zone in which grain size decreases slightly toward the margin of the dike. The pegmatite intrusions and layered gabbro are cut by fine-grained felsic dikes containing xenoliths of the surrounding gabbro (Figure GS2024-8-6f).

Discussion

The Lewis-Storey assemblage

The arkosic grit of the Lewis-Storey assemblage has been variously described as detritus shed from weathered tonalite, making it a sedimentary unit (e.g., Bailes and Percival, 2000; Percival et al., 2001, 2006), or a cataclasite derived from the adjacent tonalite gneiss (Brown, 1981). In places, the orthogneiss-like texture of the grit, the lack of a clear boundary with the adjacent orthogneiss and the evidence of shear in the overlying units (especially in the northern part of the study area), favour the latter. However, the presence of cobbles, sand lenses and grain-size variations throughout the unit point to a sedimentary origin. The overlying quartz arenite with which the underlying grit seems to be associated contains detrital zircons and is undoubtedly of clastic sedimentary origin.

Distinguishing primary and secondary features is challenging due to the pervasive effects of structural deformation and metamorphism. The features interpreted to be primary within the arkosic grit, including the cobbles, bedding, grain-size variations and sand lenses, could potentially be due to intense shearing of orthogneiss containing felsic dikes and later metamorphism. However, the laminae in the quartzite beds as well as the mica schist likely represent primary compositional differences. The mica schist may have been deposited as more feldspar-rich layers, clay-rich layers or even volcanic-ash units, which have since been altered to their present mica-rich composition. Thin sections and chemical analysis are needed to confidently determine the origin of the arkosic grit and the quartz arenite. Likely environments for Archean quartz arenites include a fluvial system or a shallow-marine environment (Donaldson and de Kemp, 1998), which is consistent with previous interpretations (Percival et al., 2001).

The Wallace assemblage

The Wallace assemblage is often correlated with the Lewis-Storey assemblage because of their similar age constraints and stratigraphy (e.g., Sasseville et al., 2006). However, the Conley formation is significantly thicker, more heterogeneous and lacks the fuchsite-bearing quartz arenite found at the eastern shore of Lake Winnipeg. Sasseville et al. (2006) noted that intrusive granitoid rocks have cut off the base of the Conley formation and that the contact relationship near the base of the formation was generally difficult to establish. However, the contact between the orthogneiss and the Conley formation is interpreted here as a nonconformity. The metasedimentary rocks directly overlie the orthogneiss and contain cobble-boulder conglomerate that includes orthogneiss clasts similar in appearance to the underlying orthogneiss. The heterogenous nature of the units suggests a dynamic depositional environment but overall reflects a deepening trend similar to that observed in the Lewis-Storey assemblage.

Economic considerations

Crustal architecture has a first-order control on the location of many major mineral systems. For example, orogenic gold deposits often occur proximal to the major transcrustal structures forming the faulted margins of successor basins within Archean greenstone belts (Thurston, 2015). Understanding the crustal architecture, nature and history of the western Superior province therefore has implications for understanding its mineral potential.

Mole et al. (2019) used Lu-Hf isotopes in zircon to generate ‘time-slice’ maps of the Yilgarn craton in Australia. This allowed them to identify both crustal-growth events and the cratonic architecture through time. They found that many older, thick, stable crustal blocks contained internal ‘ribbons’ and peripheral plateaus of juvenile crust. This framework provided pathways that localized later magmas and fluids leading to mineral endowment, and it was demonstrated that many gold and Ni-Cu systems could be correlated with the crustal architecture.

The North Caribou terrane is an old, thick and stable crustal block (e.g., Percival et al., 2006). Studying its early history through the detrital zircon and chromite record could reveal information about its crustal architecture and therefore the location of mineral deposits. Because detrital chromite can detect mafic and ultramafic crust in sedimentary source regions, it could potentially be used as an indicator mineral pointing to as yet unknown ultramafic systems that could host copper–nickel–platinum-group element (Cu-Ni-PGE) deposits.

Finally, knowledge about the early history of the western Superior province might also provide clues to understanding why the Rice Lake greenstone belt is less gold endowed than comparable and possibly correlated gold-producing regions (e.g., Red Lake). For example, if evidence from detrital zircon and chromite suggests that there was older crust predating the Mesoarchean 3 Ga events in the Rice Lake area, this could further support the importance of juvenile crust as a prerequisite for high-grade gold mineralization, focusing future exploration efforts.

Acknowledgments

The authors thank the Manitoba Geological Survey for logistical support, particularly C. Epp and P. Belanger, as well

as M. Rinne and X.M. Yang for reviewing earlier drafts of this report. They also thank J. Percival for constructive discussions and guidance with sampling locations. Fieldwork conducted for this report was funded by the European Union through the European Research Council (ERC) Starting Grant 101117373 awarded to P. Waterton (University of Copenhagen).

References

Anderson, S.D. 2013a: Geology and structure of the Garner–Gem lakes area, Rice Lake greenstone belt, southeastern Manitoba (parts of NTS 52L 11, 14); *in* Geology of the Garner–Gem lakes area, Rice Lake greenstone belt, southeastern Manitoba (parts of NTS 52L11, 14); Manitoba Mineral Resources, Manitoba Geological Survey, Geoscientific Report GR2013-1, Map GR2013-1-1, scale 1:20 000.

Anderson, S.D. 2013b: Geology of the Garner–Gem lakes area, Rice Lake greenstone belt, southeastern Manitoba (parts of NTS 52L11, 14); Manitoba Innovation, Energy and Mines, Manitoba Geological Survey, Geoscientific Report GR2013-1, 135 p.

Bailes, A.H. and Percival, J.A. 2000: Geology and structure of the North Caribou Terrane–Uchi Subprovince boundary in eastern Manitoba with emphasis on volcanic and volcaniclastic rocks of the Black Island assemblage, Manitoba; *in* Report of Activities 2000, Manitoba Industry, Trade and Mines, Manitoba Geological Survey, p. 161–174, URL <https://manitoba.ca/iem/geo/field/roa00pdfs/00gs-26.pdf> [September 2024].

Bailes, A.H. and Percival, J.A. 2005: Geology of the Black Island area, Lake Winnipeg, Manitoba (parts of NTS 62P1, 7 and 8); Manitoba Industry, Economic Development and Mines, Manitoba Geological Survey, Geoscientific Report GR2005-2, 33 p.

Barnes, S.J. and Roeder, P.L. 2001: The range of spinel compositions in terrestrial mafic and ultramafic rocks; Journal of Petrology, v. 42, no. 12, p. 2279–2302, URL <https://doi.org/10.1093/petrology/42.12.2279>.

Barnes, S.-J., Mansur, E.T., Maier, W.D. and Prevec, S.A. 2022: A comparison of trace element concentrations in chromite from komatiites, picrites, and layered intrusions: implications for the formation of massive chromite layers; Canadian Journal of Earth Sciences, v. 60, no. 2, p. 97–132, URL <https://doi.org/10.1139/cjes-2022-0064>.

Brown, A. 1981: Geology, Black Island, Lake Winnipeg, Manitoba; Geological Survey of Canada, Open File 812, 9 maps, scale 1:15 840.

Card, K. and Ciesielski, A. 1986: Subdivisions of the Superior province of the Canadian Shield; Geoscience Canada, v. 13, no. 1, p. 5–13.

Corfu, F. and Stone, D. 1998: Age, structure and orogenic significance of the Berens River composite batholiths, western Superior Province; Canadian Journal of Earth Sciences, v. 35, p. 1089–1109.

Dhuime, B., Hawkesworth, C.J., Delavault, H. and Cawood, P.A. 2017: Continental growth seen through the sedimentary record; Sedimentary Geology, v. 357, p. 16–32.

Donaldson, J.A. and de Kemp, E.A. 1998: Archaean quartz arenites in the Canadian Shield: examples from the Superior and Churchill Provinces; Sedimentary Geology, v. 120, no. 1–4, p. 153–176.

Fralick, P., Hollings, P. and King, D. 2008: Stratigraphy, geochemistry, and depositional environments of Mesoarchean sedimentary units in western Superior Province: implications for generation of early crust; *in* When Did Plate Tectonics Begin on Planet Earth?, K.C. Condie and V. Pease (ed.), Geological Society of America, Special Paper 440, p. 77–96, URL <https://doi.org/10.1130/2008.2440(04)>.

Garçon, M. 2021: Episodic growth of felsic continents in the past 3.7 Ga; Science Advances, v. 7, no. 39, 11 p., URL <https://doi.org/10.1126/sciadv.abj1807>.

Haugaard, R., Waterton, P., Ootes, L., Pearson, D.G., Luo, Y. and Konhauser, K. 2021: Detrital chromites reveal Slave craton's missing komatiite; Geology, v. 49, no. 9, p. 1079–1083.

Lipp, A., Shorttle, O., Sperling, E.A., Brocks, J., Cole, D., Crockford, P., Mouro, L., Dewing, K., Dornbos, S., Emmings, J.F., Farrell, U., Jarrett, A., Johnson, B.W., Kabanov, P., Keller, C.B., Kunzmann, M., Miller, A.J., Mills, N.T., O'Connell, B. and Yang, J. 2021: The composition and weathering of the continents over geologic time; Geochemical Perspectives Letters, v. 17, p. 21–26, URL <https://doi.org/10.7185/geochemlet.2109>.

Martins, T., Rinne, M.L., Breasley, C. and Adediran, H. 2023: Preliminary results from field investigations in the Bird River domain of the Archean Superior province, Manitoba (parts of NTS 52L5, 6, 11, 12); *in* Report of Activities 2023, Manitoba Economic Development, Investment, Trade and Natural Resources, Manitoba Geological Survey, p. 4–13. URL <https://manitoba.ca/iem/geo/field/roa23pdfs/GS2023-2.pdf> [September 2024].

Mole, D.R., Kirkland, C.L., Fiorentini, M.L., Barnes, S.J., Cassidy, K.F., Isaac, C., Belousova, E.A., Hartnady, M. and Thebaud, N. 2019: Time-space evolution of an Archean craton: a Hf-isotope window into continent formation; Earth-Science Reviews, v. 196, art. 102831, URL <https://doi.org/10.1016/j.earscirev.2019.04.003>.

Natural Resources Canada 1986: CAGDB–Manitoba (Flin Flon): Area 300 Bisset; *in* Geoscience Data Repository for Geophysical Data, Natural Resources Canada, Canadian Airborne Geophysical Database, URL <https://open.canada.ca/data/dataset/b2f6f681-4a35-543f-89f7-0356f86d5e5d> [September 2024].

O'Neil, J., Rizo, H., Reimink, J., Garçon, M. and Carlson, R.W. 2024: Earth's earliest crust; Elements, v. 20, no. 3, p. 168–173.

Percival, J. 2007: Eo- to Mesoarchean terranes of the Superior Province and their tectonic context; *in* Earth's Oldest Rocks, M.J. van Kranendok, R.H. Smithies and V.C. Bennett (ed.), Developments in Precambrian Geology, v. 15, p. 1065–1085, URL <doi.org/10.1016/S0166-2635(07)15084-2>.

Percival, J.A. and Whalen, J.B. 2000: Observations on the North Caribou terrane–Uchi Subprovince interface in western Ontario and eastern Manitoba; Geological Survey of Canada, Current Research, 2000-C15, 8 p.

Percival, J.A., Bailes, A. and McNicoll, V. 2001: Mesoarchean western margin of the Superior craton in the Lake Winnipeg area, Manitoba; Natural Resources Canada, Geological Survey of Canada, Current Research, 2001-C16, 19 p., URL <https://doi.org/10/4095/212697>.

Percival, J.A., McNicoll, V. and Bailes, A.H. 2006: Strike-slip juxtaposition of ca. 2.72 Ga juvenile arc and >2.98 Ga continent margin sequences and its implications for Archean terrane accretion, western Superior Province, Canada; Canadian Journal of Earth Sciences, v. 43, p. 895–927, URL <https://doi.org/10.1139/e06-039>.

Poulsen, K.H., Weber, W., Brommecker, R. and Seneshen, D.N. 1996: Lithostratigraphic assembly and structural setting of gold mineralization in the eastern Rice Lake greenstone belt, Manitoba; Geological Association of Canada–Mineralogical Association of Canada, Joint Annual Meeting, May 27–29, 1996, Winnipeg, Manitoba, Field Trip Guidebook A4, 106 p.

Sasseville, C. and Tomlinson, K.Y. 2000: Structure and stratigraphy of the Mesoarchean Wallace Lake greenstone belt, southeastern Manitoba; Geological Survey of Canada, Current Research 2000-C15, 8 p.

Sasseville, C., Tomlinson, K.Y., Hynes, A. and McNicoll, V. 2006: Stratigraphy, structure, and geochronology of the 3.0–2.7 Ga Wallace Lake greenstone belt, western Superior Province, southeast Manitoba, Canada; Canadian Journal of Earth Sciences, v. 43, p. 929–945.

Tang, M., Chen, K. and Rudnick, R.L. 2016: Archean upper crust transition from mafic to felsic marks the onset of plate tectonics; Science, v. 351, no. 6271, p. 372–375.

Thurston, P.C. 2015: Igneous rock associations 19. Greenstone belts and granite−greenstone terranes: constraints on the nature of the Archean world; Geoscience Canada, v. 42, no. 4, p. 437–484, URL <https://doi.org/10.12789/geocanj.2015.42.081>.

Whalen, J.B., Percival, J.A., McNicoll, V. and Longstaffe, F.J. 2003: Intra-oceanic production of continental crust in a Th-depleted ca. 3.0 Ga arc complex, western Superior Province, Canada; Contributions to Mineralogy and Petrology, v. 146, no. 1, p. 78–99.

GS2024-9

Spodumene-bearing pegmatites from the Cross Lake pegmatite field, east-central Manitoba: mineralogy and petrography descriptions (parts of NTS 63I12, 63J9)

by T. Martins, J. Janssens and P. Lenton[1]

In Brief:

- Petrographic descriptions from spodumene-bearing pegmatites from the Cross Lake pegmatite field are presented
- Archival detailed maps, geochemistry and station descriptions are also released with this report

Citation:
Martins, T., Janssens, J. and Lenton, P. 2024: Spodumene-bearing pegmatites from the Cross Lake pegmatite field, east-central Manitoba: mineralogy and petrography descriptions (parts of NTS 63I12, 63J9); *in* Report of Activities 2024, Manitoba Economic Development, Investment, Trade and Natural Resources, Manitoba Geological Survey, p. 77–84.

Summary

The Cross Lake pegmatite field in central Manitoba is a well-documented, lithium-rich pegmatite field of Archean age in the western Superior Province. This pegmatite field provides an excellent opportunity for the exploration and study of rare-element-bearing pegmatites, particularly the Li-enriched kind. Recently-cut polished thin sections of spodumene-bearing pegmatites from the Cross Lake pegmatite field were examined and are described in this report. Archival descriptions and outcrop maps of pegmatites from the Cross Lake pegmatite field are also being released in association with this report.

Introduction

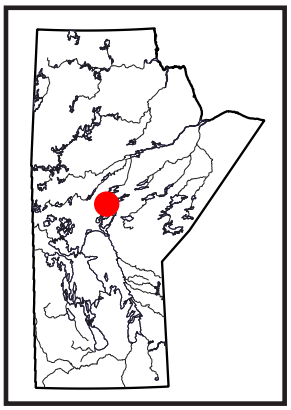
The Cross Lake greenstone belt was studied by the MGS in the 1980s (e.g., Corkery, 1983; Corkery et al., 1992). The Cross Lake pegmatite field was studied in detail by A. Anderson (1984) as part of an MSc. thesis, which was included in the MGS regional greenstone belt mapping project (Corkery, 1983; Corkery et al., 1992). Work by Anderson (1984) focused on the regional distribution and the geochemical, paragenetic and textural variations in the pegmatites and pegmatitic granites throughout the pegmatite field.

During the last few years, and due to increasing interest in hard-rock lithium resources associated with pegmatites (e.g., Kesler 2012; Gardiner et al., 2024; U.S. Geological Survey, 2024), the area has been the target of mineral exploration (e.g., Leeuwin Metals, 2024; Assessment File 63I8629, Manitoba Economic Development, Investment, Trade and Natural Resources). Lithium is considered critical for the green-energy transition and is included in the list of critical elements released by Canada (Government of Canada, 2024). Currently, Leeuwin Metals owns the rights to explore in this area (Leeuwin Metals, 2024).

This report summarizes the current knowledge of the Cross Lake pegmatite field and a detailed petrographic description of recently cut thin sections of the spodumene-bearing pegmatites. The associated Data Repository Item (Martins et al., 2024) includes unpublished detailed maps of selected pegmatite outcrops, along with station descriptions of MGS work from the 1980s.

Geological setting

The Cross Lake greenstone belt is flanked by the metaplutonic Molson Lake domain to the south and a largely metaplutonic terrane to the northwest (Figure GS2024-9-1). The northern contact is a major northeast-trending fault system with dextral strike-slip and a vertical component indicative of relative uplift of the northwest side (Breedveld, 1988). The southern contact is a much broader zone of deformation in which a number of east-southeast-trending dextral fault zones imbricate supracrustal rocks of the Pipestone Lake and Gunpoint groups and, to a lesser extent, Molson Lake domain plutonic rocks. This dextral strike-slip zone has a vertical component of south side up (Breedveld, 1988).



The Cross Lake greenstone belt is composed of supracrustal rocks and plutonic complexes. The supracrustal rocks in the belt can be subdivided into three groups: an older metavolcanic series, the Pipestone Lake group, is unconformably overlain by the metasedimentary-metavolcanic Gunpoint group, which is in turn overlain by the Cross Lake group. A more detailed description of the regional geology of this area, along with a relative sequence of geological events, is outlined in Corkery et al. (1992).

Cross Lake pegmatite field

The Cross Lake pegmatite field is located in the Cross Lake greenstone belt and contains numerous pegmatites of diverse geochemical affinity. This pegmatite field covers an area of about 200 km^2

[1] Manitoba Geological Survey (emeritus, deceased), Winnipeg, Manitoba

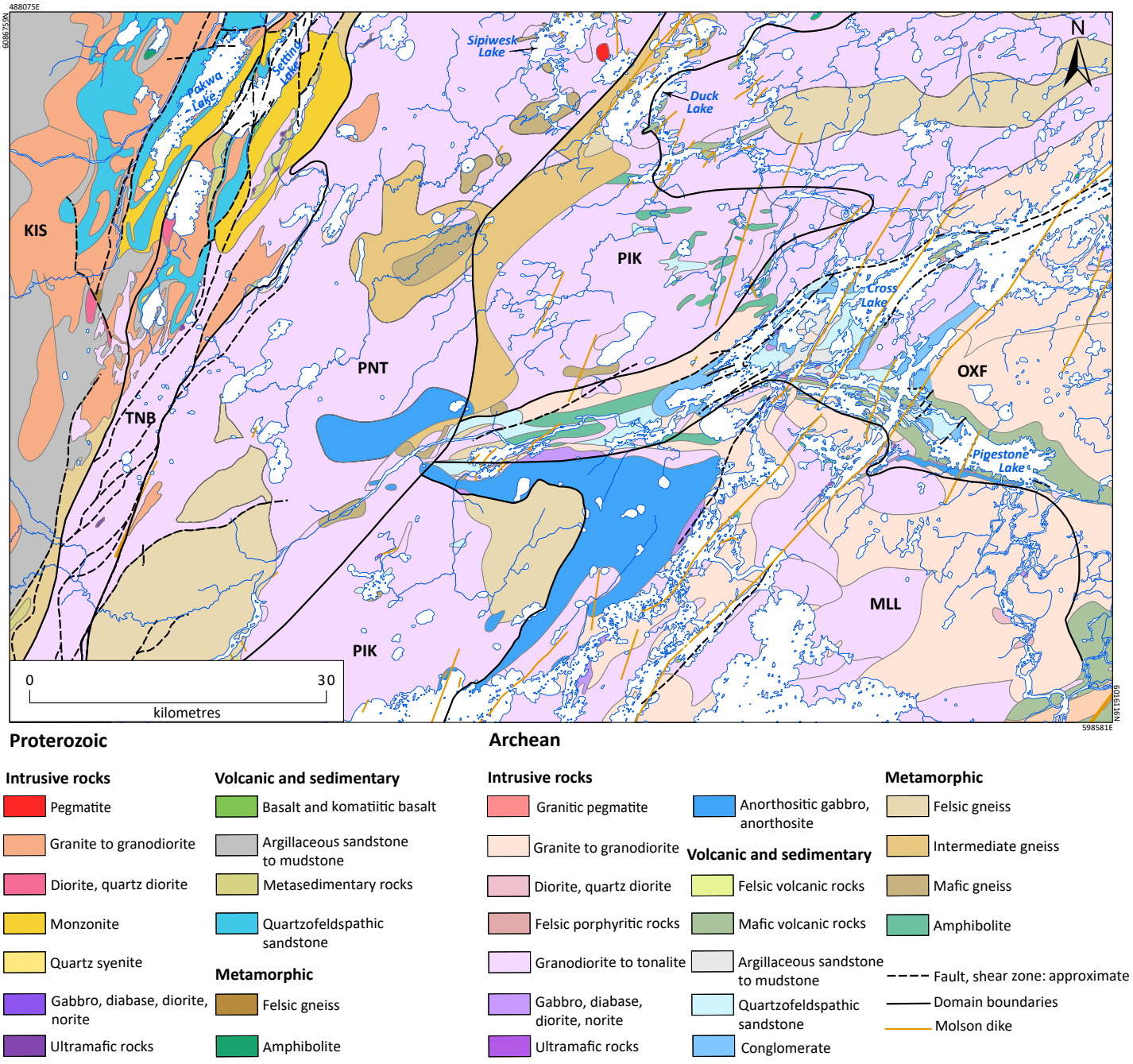


Figure GS2024-9-1: *Regional geology of the Cross Lake greenstone belt at 1:250 000 scale (geology from Manitoba Geological Survey, 2022). Domain abbreviations: KIS, Kisseynew; MLL, Molson Lake; OXF, Oxford; PIK, Pikwitonei; PNT, Paint Lake; TNB, Thompson nickel belt.*

that extends from the Minago River in the south to north of Cross Island (Figure GS2024-9-2). The pegmatites intrude amphibolite-facies supracrustal rocks, which parallel the axial trend of the belt. The pegmatites are en échelon and comprise narrow, linear, east- and northeast-trending zones parallel to the axial trend of the greenstone belt. A garnet-muscovite-tourmaline granite, interpreted to be comagmatic with the rare-element pegmatites, provided a U-Pb age between 2653 and 2634 Ma, interpreted as a likely age of intrusion (Corkery et al., 1992).

Anderson (1984) divided the pegmatite field into four major series. Each series consists of spatially and structurally related pegmatite bodies that present similar geochemical, paragenetic and textural characteristics. The same author suggested a progressive fractionation in an easterly direction, parallel to decreasing metamorphic grade of the hostrocks. Geochemical data indicate that the Minago and Southern series are genetically related (probably to a common source at depth) to mineralized Li-Be-Nb-Ta-Sn pegmatites recognized in the Southern series. The Northern series is geochemically distinct, interpreted to be derived from a separate source, and includes Be-Nb-Ta–mineralized pegmatites. The Nelson series was interpreted as consisting of anatectic bodies. Anderson et al. (2004) added that two petro-

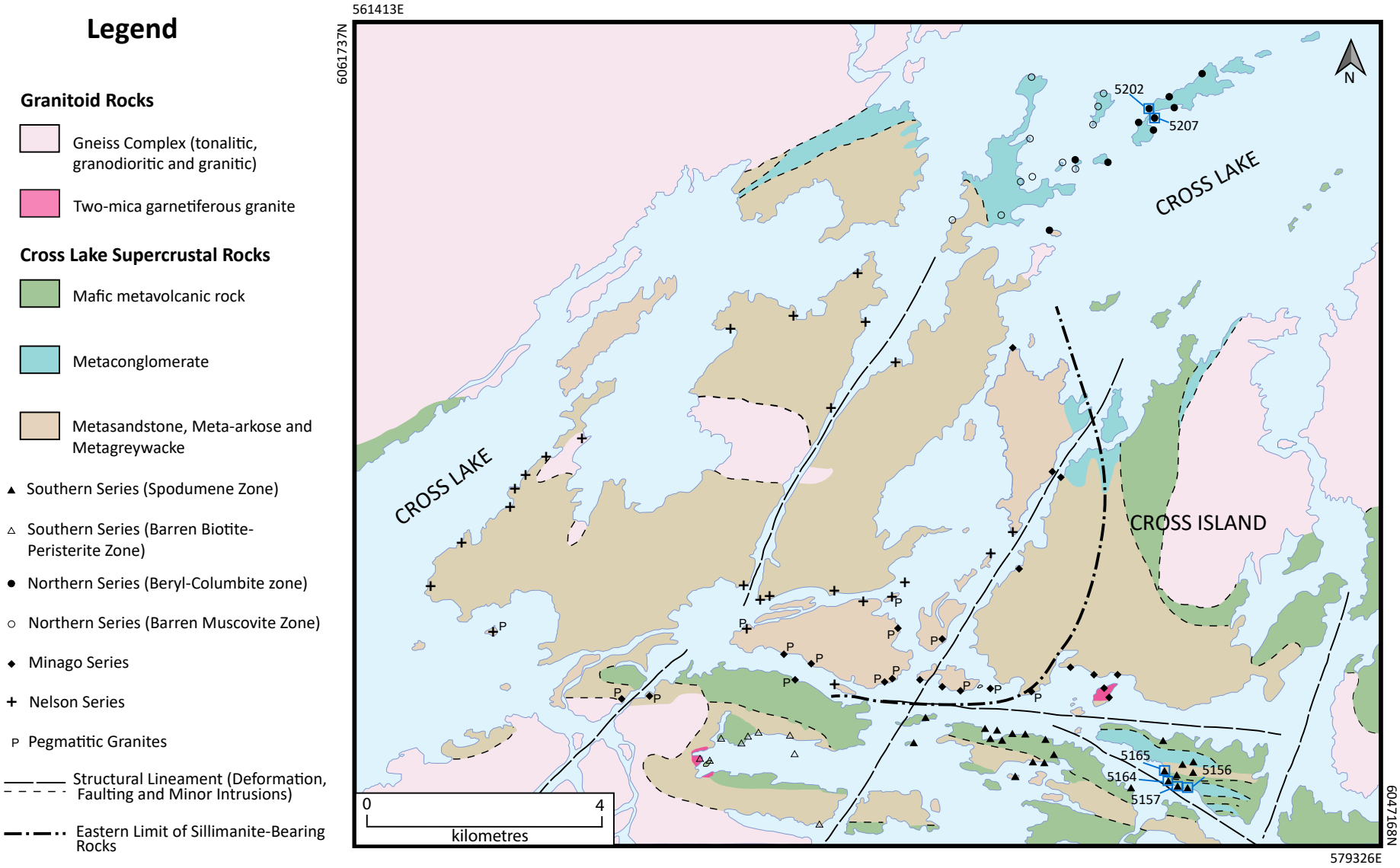


Figure GS2024-9-2: *Simplified geology of the Cross Lake pegmatite field, showing the different pegmatite groups defined by Anderson (1984). Locations of detailed pegmatite outcrop maps are marked by blue squares. Modified from Anderson (1984).*

genetic models are equally plausible: the series are the products of distinct granitic sources, or they are comagmatic and developed geochemical distinctions because of the heterogeneity of the parent melt.

Below is a summary of the characteristics of the pegmatites from each series. Detailed descriptions of the dikes' internal structure, mineral distribution, paragenesis and chemistry can be found in Anderson (1984).

Nelson series

This series consists of barren biotite-oligoclase-microcline-quartz-garnet pegmatite dikes. These pegmatites intrude the metapsammitic–pelitic rocks west of Cross Island (Figure GS2024-9-2). Additional minerals present include accessory blue apatite and schorl (black tourmaline).

Minago series

This group of pegmatites consists of a narrow linear zone of pegmatitic granite bodies (i.e., granite bodies composed mainly of quartz, feldspar and mica with a pegmatite texture, but lacking some features typical of other pegmatites in the area, such as graphic texture or internal zonation) and barren pegmatite dikes that outcrop intermittently from the Minago River to the southwestern shore of Cross Island (Figure GS2024-9-2). The main mineral assemblage of the pegmatitic granites and related pegmatites is microcline perthite, quartz, albite-oligoclase, biotite and muscovite. Graphic microcline perthite is most prevalent in the pegmatites and pegmatitic granites that constitute the eastern end of the Minago series but is absent or weakly developed in the bodies that lie farther west. Prevalent accessory mineral phases are garnet and schorl (black tourmaline), along with rare apatite, arsenopyrite and beryl.

Northern series

This series is composed of muscovite-bearing pegmatites that intruded the metasedimentary rocks north of Cross Island (Figure GS2024-9-2). The Northern series has been subdivided into a beryl-columbite pegmatite zone (Figure GS2024-9-3a) and a barren muscovite pegmatite zone (more common; Figure GS2024-9-3b). The internal zoning in the pegmatites of the Northern series is weakly developed. However, Anderson (1984) noted that the internal structure of the pegmatites of the barren muscovite zone evolves from a near texturally homogeneous muscovite+K-feldspar+quartz+plagioclase pegmatite to concentrically zoned bodies containing quartz cores. Figure GS2024-9-3b is a representation of the intermediate stage in the textural evolution of the barren muscovite pegmatite zone of the Northern series. Detailed description of this textural evolution can be found in Anderson (1984). The beryl-columbite pegmatites are the most fractionated members known in the Northern series.

Southern series

The pegmatites of the Southern series form an 8 km long belt south of Cross Island (Figure GS2024-9-2). They intrude the metavolcanic rocks and metasedimentary rocks south and east of the sillimanite zone of metamorphism. The series has been subdivided into two zones that are texturally and paragenetically distinct but spatially, structurally and geochemically related. These are the biotite-peristerite pegmatite zone and the spodumene pegmatite zone.

The biotite-peristerite pegmatite zone forms the western third of the southern series (Figure GS2024-9-2). Albitization and internal zonation are absent or weakly developed in the pegmatites of this zone. Figure GS2024-9-3c illustrates the mineral distribution and simple internal texture of the most evolved pegmatites in the biotite-peristerite zone of the Southern series. The characteristic mineral assemblage is biotite, peristerite, pale green apatite and rare ferrocolumbite.

The spodumene-bearing pegmatites are in a 5 km long, east-trending zone south of Cross Island that represents about two-thirds of the Southern pegmatite series (Anderson, 1984; Figure GS2024-9-2). These pegmatites are texturally complex, extensively albitized and paragenetically diverse. An idealized textural section of the spodumene-bearing pegmatites, representing zonation and characteristic mineralogy, can be found in Figure GS2024-9-3d. The spodumene pegmatites were fractured and boudinaged due to tensional stress, with fractures within the pegmatite that do not continue into the less competent hostrock. These pegmatites are irregular with complex apophyses (Anderson, 1984).

Pegmatite outcrop maps

P. Lenton (MGS emeritus, deceased) carried out detailed outcrop mapping of several of the pegmatite dikes from the Cross Lake pegmatite field (Figure GS2024-9-4) as part of an MGS regional mapping project in the 1980s (e.g., Corkery, 1983). Samples of mineral separates were also collected and will be studied at a later stage. Locations of the detailed maps are indicated in Figure GS2024-9-2. One example of a detailed pegmatite outcrop map is provided in this report (Figure GS2024-9-4). The complete set of detailed outcrop maps can be found in MGS Data Repository Item DRI2024013[2], together with a full collection of station maps and outcrop descriptions (Martins et al., 2024).

Petrographic descriptions

Recently made polished thin sections of the spodumene-bearing pegmatites (Southern series) from archival drillcore

[2] MGS Data Repository Item DRI2024013, containing the data or other information sources used to compile this report, is available online to download free of charge at https://manitoba.ca/iem/info/library/downloads/index.html, or on request from minesinfo@gov.mb.ca, or by contacting the Resource Centre, Manitoba Economic Development, Investment, Trade and Natural Resources, 360-1395 Ellice Avenue, Winnipeg, Manitoba R3G 3P2, Canada.

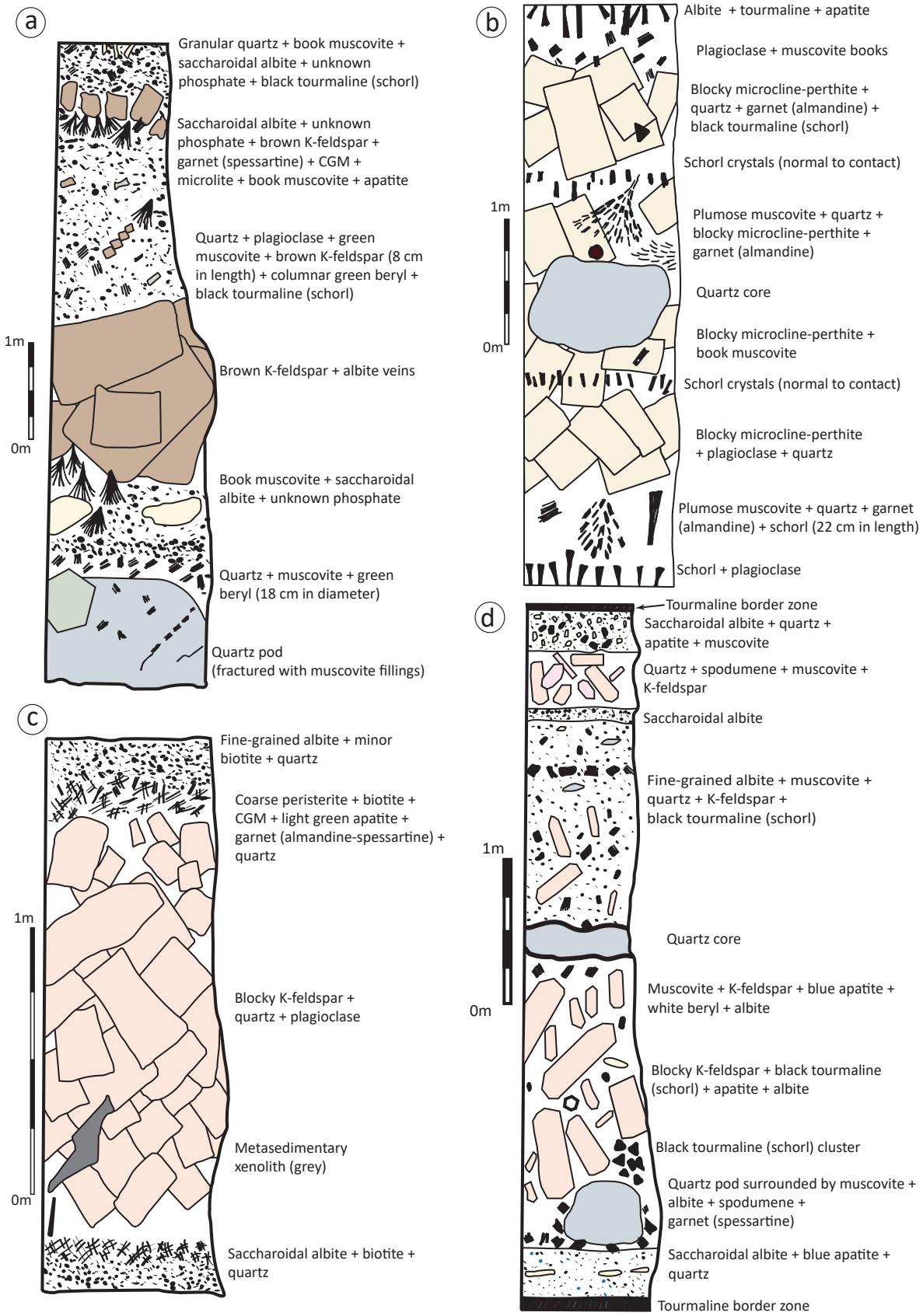


Figure GS2024-9-3*: Interpreted textural sections of the different pegmatite types at Cross Lake after Anderson (1984):* ***a)*** *beryl-columbite pegmatite of the Northern series, the most fractionated example;* ***b)*** *barren muscovite pegmatite of the Northern series, representing the intermediate stage in the textural evolution of the series;* ***c)*** *internal texture of the most evolved biotite-peristerite pegmatite of the Southern series;* ***d)*** *internal structure of a highly fractionated spodumene-bearing pegmatite of the Southern series. Abbreviations: CGM, columbite group mineral.*

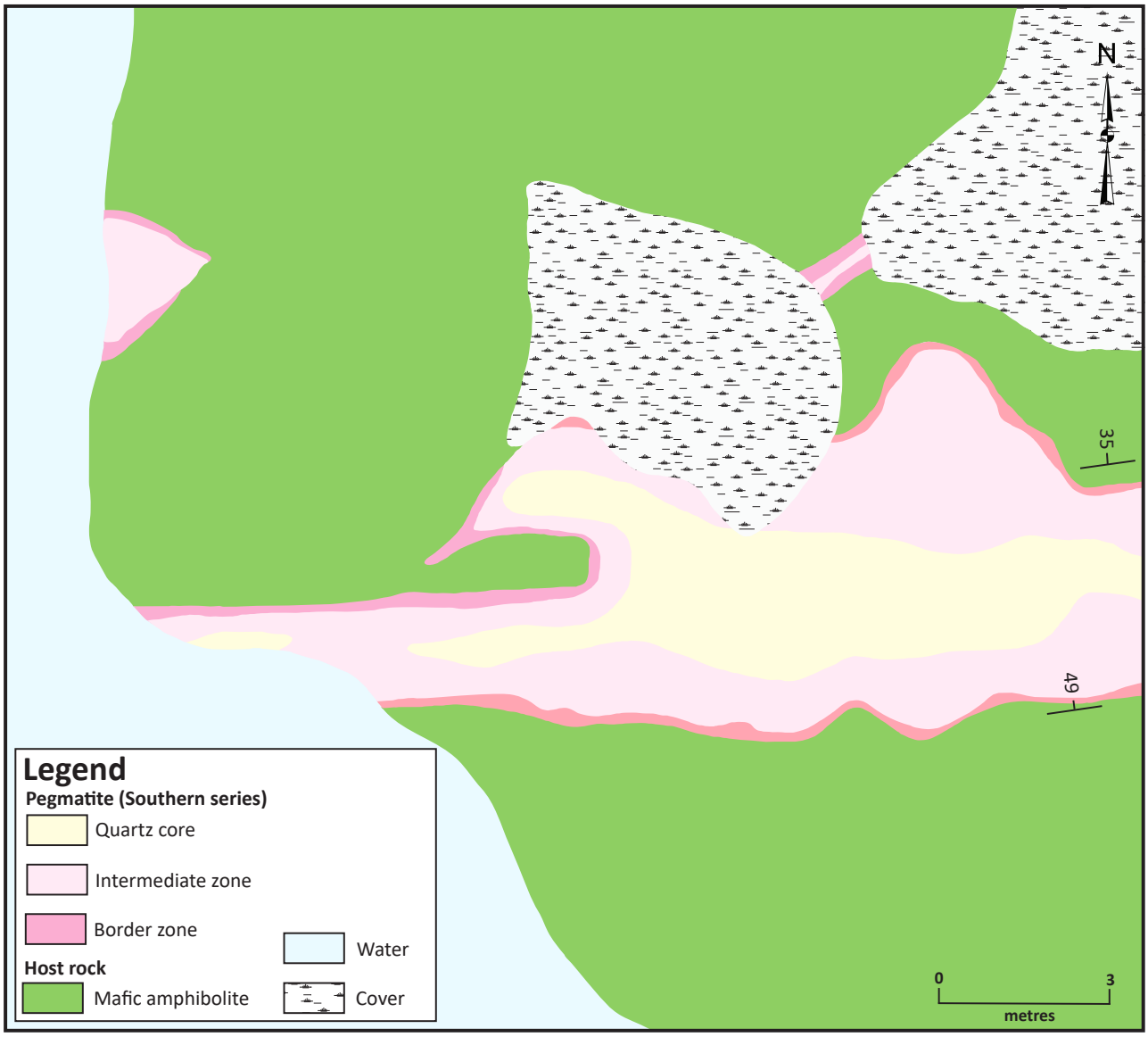


***Figure GS2024-9-4**: Example of a detailed outcrop map of a spodumene-bearing pegmatite dike from Cross Lake (station 5165 in Figure GS2024-9-2; UTM Zone 14, 575762E, 6048356N; map from DRI2024013).*

are described in detail in this section. Major minerals are quartz, plagioclase feldspar, K-feldspar, spodumene and muscovite. Accessory phases include a range of Ta-Nb-Mn-Fe oxides (columbite-group minerals [CGM], wodginite, ixiolite, tapiolite), tourmaline (unknown composition), apatite, zircon, amblygonite-montebrasite (Li-Al-F-OH phosphate series), triphylite-lithiophilite (Li-Fe-Mn phosphate series), garnet (unknown composition) and calcite. Beryl, arsenopyrite and löllingite were described by Anderson (1984) but were not observed during the current petrographic observations.

Quartz is interstitial to the other primary phases and often has undulatory extinction. Locally, it occurs in spodumene-quartz intergrowths, particularly at the edges of spodumene crystals. Plagioclase feldspar is present in all of the observed thin sections, occurring interstitially between the other primary phases. Anderson (1984) described albite of the cleavelandite habit occurring in the wall and intermediate zones of the spodumene-bearing pegmatites, associated with quartz, K-feldspar, pale green muscovite, spodumene, beryl, apatite and CGM. Very fine grained saccharoidal albite was recognized predominantly in association with quartz, muscovite and CGM, and locally replacing other primary mineral phases. Potassium-feldspar is interstitial with other major primary mineral phases. Locally, they can be perthitic, cloudy and have inclusions of other minerals (e.g., apatite, quartz). No graphic texture was observed in the current petrographic work.

Spodumene occurs as large laths with local fractures filled with late mica and plagioclase feldspar minerals. Very fine grained needles of spodumene occur throughout the thin section, growing at the edges of other minerals or surrounding and crosscutting earlier mineral phases (Figure GS2024-9-5a). Also observed are vermicular textures (Figure GS2024-9-5b) of spodumene and

quartz intergrowth, similar to what is described at the Tanco pegmatite as micro-SQUI by Breasley et al. (2022). Muscovite occurs in large crystals associated with spodumene, quartz and feldspar, and local kink bands are observed. Late fine-grained mica occurs in fractures of spodumene and feldspar. The large muscovite grains are zoned in backscattered electron (BSE) imagery, primarily due to variations in Cs and Rb contents (Figure GS2024-9-5c).

Columbite group minerals occur throughout the pegmatite but were more noticeable in the saccharoidal albite units. These minerals usually appear as needles or pear-shaped grains and can be found associated with other oxides (i.e., cassiterite, uraninite) only observed in BSE imagery (Figure GS2024-9-5d). Cassiterite can be found isolated or in association with CGMs, albite, quartz or muscovite. Bluish-green zoned tourmaline can form discrete grains or occur in association with apatite. Tourmaline is also observed as inclusions in spodumene. Tourmaline is more abundant in proximity to the country rock contacts but can be found in other areas of the pegmatite.

Apatite occurs as isolated crystals or associated with tourmaline, as described above (Figure GS2024-9-5a), and is most abundant near the pegmatite contacts. Zircon is metamict with radiation damage haloes in the surrounding minerals. Triphylite-lithiophilite and amblygonite-montebrasite are the main Li-bearing phosphate phases observed. Locally, amblygonite-montebrasite is replaced by calcite. Garnet is rare but was also observed in thin section, locally close to the contact with the country rock. Rare calcite occurs interstitially with quartz and feldspar. Late calcite, replacing other mineral phases and in veins in quartz, was also observed.

Economic considerations

Lithium is among the 34 minerals and elements that Canada considers critical for its potential to support Canada's economic growth and because of its direct role in the green revolution (Government of Canada, 2022). Rare-element pegmatites are a

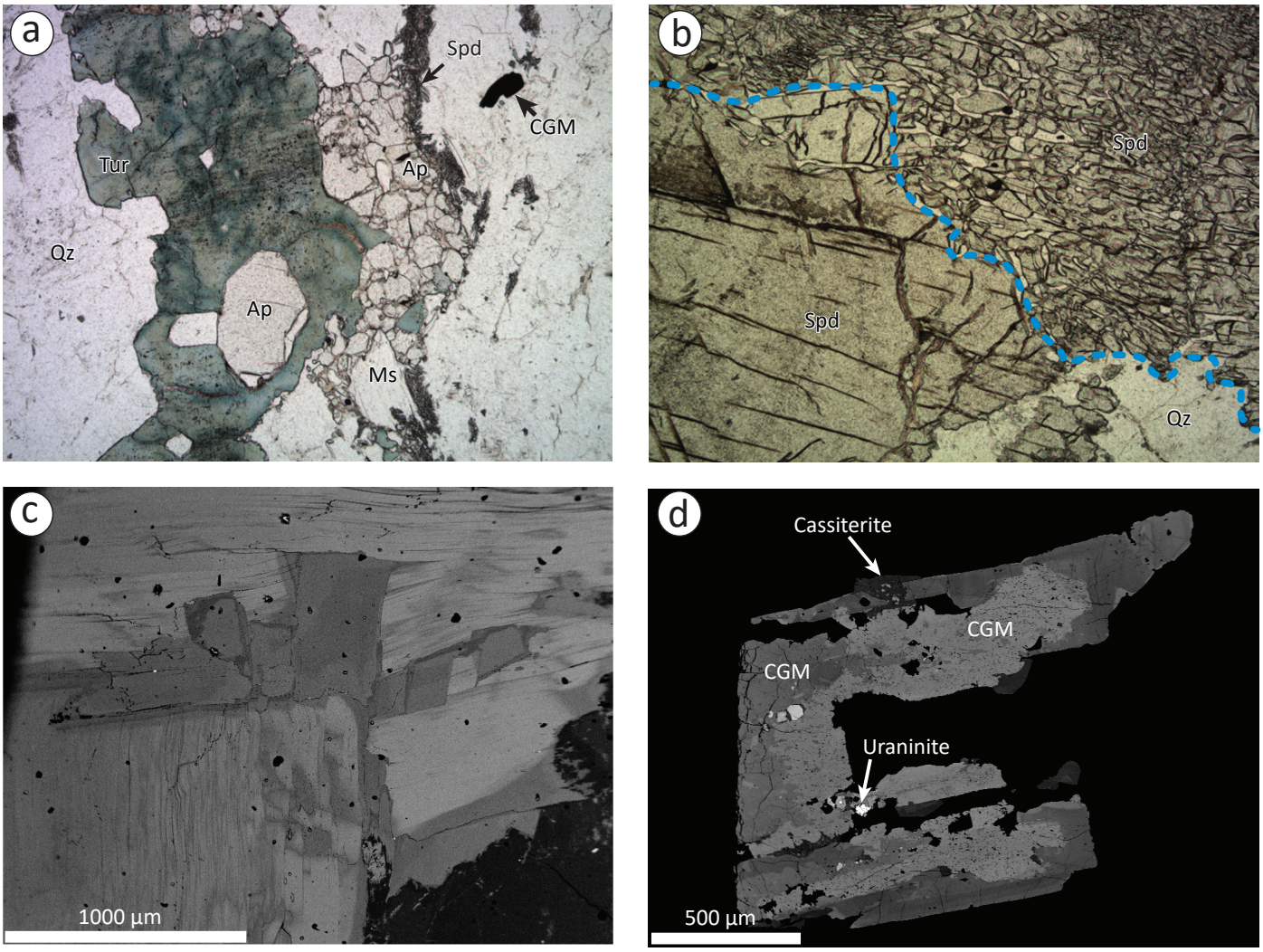


Figure GS2024-9-5*: Photo and electron micrographs of the studied thin sections of Li-bearing pegmatites:* ***a)*** *zoned tourmaline (Tur) associated with apatite (Ap), quartz (Qz) and muscovite (Ms). Fine grained spodumene (Spd) needles are observed surrounding feldspars, muscovite and quartz. Also visible is a columbite group mineral (CGM); plane polarized light;* ***b)*** *large spodumene (Spd) crystal (left) and vermicular intergrowth of spodumene and quartz (right); blue line highlights the difference between the two textures; plane polarized light;* ***c)*** *BSE image of a zoned muscovite, with lighter grey areas enriched in Rb and Cs;* ***d)*** *BSE image of a CGM in association with other oxides.*

source of hard-rock Li and are expected to continue to grow as an important source of this resource (U.S. Geological Survey, 2024). Manitoba plays an increasingly important role in the production of hard-rock Li because of the extraction and concentration of spodumene at the Tanco mine in the southeastern part of the province.

Based on mineral-chemistry indicators and element ratios, Anderson (1984) suggested that the most promising area for undiscovered mineralized pegmatites in the Cross Lake pegmatite field is on strike with, and east of, the spodumene pegmatite zone of the Southern series (Figure GS2024-9-2). The same author added that, if the aplite dikes on the north shore of Pipestone Lake are related to the Southern pegmatite series, more undiscovered pegmatites could exist between the known eastern limit of the spodumene-bearing pegmatites and Pipestone Lake. Given the possible easterly fractionation trend of the Southern pegmatite series, any additional pegmatites in the proposed target area would potentially be highly differentiated. However, this mineralization potential was not drill-tested. To the best of the current authors' knowledge, there are no surface exposures of pegmatites of the Southern series east of the current known extent.

Future work focusing on the lithium-bearing pegmatites includes detailed mineral characterization of mica and CGM, and multimineral geochronology studies. A better understanding and characterization of Li-bearing pegmatites in the Archean Superior Province further enhances Manitoba's potential as a Li producer.

Acknowledgments

The Leeuwin Metals team is thanked for collecting of the materials for the thin sections. A big thank you goes to the staff at Midland laboratories (C. Epp and P. Belanger) for retrieving the drillcore and facilitating the work. Thanks are also due to C. Couëslan and M. Rinne for critical reviews of previous versions of the manuscript. C. Steffano did the layout of the report. RnD Technical provided technical editing services.

References

Anderson, A. 1984: The geochemistry, mineralogy and petrology of the Cross Lake pegmatite field, central Manitoba; M.Sc. thesis, University of Manitoba, Winnipeg, Manitoba, 250 p., URL <http://hdl.handle.net/1993/29812> [October 2024].

Anderson, A.J., Tomascak, P.B. and Černý, P. 2004: Petrogenesis of the Cross Lake pegmatite field, central Manitoba; Geological Society of America, Abstracts with Programs. v. 36, no. 5, p. 4.

Breasley, C.M., Martins, T., Linnen, R.L. and Groat, L.A. 2022: Investigating textural and geochemical relations of lithium mineralization in the Tanco pegmatite, southeastern Manitoba (part of NTS 52L6); *in* Report of Activities 2022, Manitoba Natural Resources and Northern Development, Manitoba Geological Survey, p. 25–35, URL <https://manitoba.ca/iem/geo/field/roa22pdfs/GS2022-4.pdf> [October 2024].

Breedveld, M. 1988: A thermo-tectonic pilot study of the Cross Lake gneiss-greenstone terrane, Superior Province, Manitoba, Canada; Free University, Amsterdam, Institute of Earth Sciences, Internal Report.

Corkery, M.T. 1983: Cross Lake supracrustal investigation; *in* Report of Field Activities, 1983, Manitoba Energy and Mines, Mineral Resources Division, p. 32–45.

Corkery, M.T., Davis, D.W. and Lenton, P.G 1992: Geochronological constraints on the development of the Cross Lake greenstone belt, northwest Superior Province, Manitoba; Canadian Journal of Earth Sciences, v. 29, p. 2171–2185.

Gardiner, N.J., Jowitt, S.M. and Sykes, J.P. 2024: Lithium: critical, or not so critical?; Geoenergy, v. 2, URL <https://doi.org/10.1144/geoenergy2023-045> [October 2024].

Government of Canada 2022: Introducing Canada's Critical Minerals Strategy; Government of Canada, URL <https://www.canada.ca/en/campaign/critical-minerals-in-canada/canadas-critical-minerals-strategy.html> [October 2024].

Government of Canada 2024: Canada's critical minerals; Government of Canada, URL <https://www.canada.ca/en/campaign/critical-minerals-in-canada/critical-minerals-an-opportunity-for-canada.html> [October 2024].

Kesler, S.E., Gruber, P.W., Medina, P.A., Keoleian, G.A., Everson, M.P. and Wallington, T.J. 2012: Global lithium resources: relative importance of pegmatite, brine and other deposits; Ore Geology Reviews, v. 48, p. 55–69.

Leeuwin Metals 2024: Quarterly activities report for quarter ending 30 June 2024, 20 p., URL <https://wcsecure.weblink.com.au/pdf/LM1/02829925.pdf> [September 2024].

Manitoba Geological Survey 2022: New edition of the 1:250 000 scale Precambrian bedrock geology compilation map of Manitoba; Manitoba Economic Development, Investment, Trade and Natural Resources, Manitoba Geological Survey, GeoFile 3-2022, URL <https://manitoba.ca/iem/ info/libmin/geofile3-2022.zip> [August, 2024].

Martins, T., Janssens, J., Lenton, P., Corkery, T. and Anderson, A. 2024: Whole-rock geochemistry and interactive GIS map file from the Cross Lake pegmatite field (parts of NTS 63I3–6, 11–14, 63J1–3, 6–11, 14–16); Manitoba Economic Development, Investment, Trade and Natural Resources, Manitoba Geological Survey, Data Repository Item DRI2024013.

U.S. Geological Survey 2024: Lithium, U.S. Geological Survey, Mineral Commodity Summaries, p. 110–111, URL <https://pubs.usgs.gov/periodicals/mcs2024/mcs2024-lithium.pdf> [June 2024].

GS2024-10

Geological investigation of the Roberts Lake fault at Roberts Lake, north-central Manitoba (part of NTS 63J13)

by K.D. Reid

Summary

Metamorphic hydrothermal fluids and melts that form economically viable mineral deposits are often focused via reactivation of regional structures. Based on historical mapping and geological mapping at Roberts Lake, the history of the Roberts Lake fault is interpreted to have involved three phases. To begin, southwest-verging thrust faulting (D_{1a}) resulted in overturning of bedding in the sandstone, the development of S_1 fabrics and faulted contacts between units. Then, reactivation of the Roberts Lake fault (D_2) occurred, potentially associated with the formation of a later S_2 foliation and L_2 lineation. Last, a strike-slip fault (D_3) that merges with the Roberts Lake fault east of Roberts Lake extended to the Superior boundary zone. Regional aeromagnetic analysis identifies this late fault (D_3) as a possible translational extension of the Berry Creek shear zone east of Wekusko Lake and indicates that the earlier D_1/D_2 faults at Roberts Lake probably have deep-seated roots. Multiple reactivation of the Roberts Lake fault invariably played a role in the emplacement of orogenic gold and lithium-bearing pegmatites in the area.

In Brief:

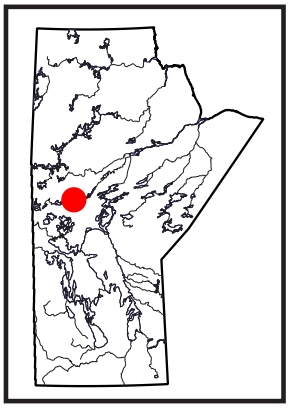
- The northeast dip of the D_1 and D_2 faults at Roberts Lake is interpreted to be related to southwest-verging thrust faulting that brought Roberts Lake basalts southwest over younger Missi group sediments
- Multiple reactivations of the Roberts Lake fault likely played a role in the emplacement of orogenic gold and lithium-bearing pegmatites in the area

Citation:
Reid, K.D. 2024: Geological investigation of the Roberts Lake fault at Roberts Lake, north-central Manitoba (part of NTS 63J13); *in* Report of Activities 2024, Manitoba Economic Development, Investment, Trade and Natural Resources, Manitoba Geological Survey, p. 85–91.

Introduction

The geological context of the rocks that lie between Wekusko Lake and the Superior boundary zone (Figure GS2024-10-1) is poorly understood, largely because of a lack of outcrop exposure and detailed geological mapping (Frarey, 1950; Bailes, 1985). The known presence of critical minerals (e.g., spodumene-bearing pegmatite) as well as base metals (e.g., volcanogenic copper-zinc) and precious metals (e.g., orogenic gold) has sparked exploration interest and research activity in the region.

In 2024, the Manitoba Geological Survey (MGS) continued targeted geological investigations at Roberts Lake (Figure GS2024-10-2) as part of a broader study to update the geology and tectonic setting of the rocks east of Wekusko Lake. Through previously completed mapping (e.g., Reid 2019, 2021, 2023) and review of historical geological maps, it has been shown that the rocks in the Roberts Lake area are lithologically diverse and structurally complex, thus inviting more focused attention. The particular emphasis of the current work is on verifying the geology as portrayed on the NATMAP compilation (Figure GS2024-10-2; NATMAP Shield Margin Project Working Group, 1998), which is largely compiled from Frarey (1950). Research objectives include examining the apparent position and vergence of the Roberts Lake fault with respect to mafic volcanic rocks on the northern side of the lake, and sandstone and mudstone on the southern side of the lake; investigating overturned bedding in Missi group sandstones directly south of the Roberts Lake fault; and reviewing the presence of mudstone rich in garnet and staurolite (interpreted as Burntwood group) along the southern shore of Roberts Lake. The work involved the review of outcrops at Roberts Lake and of historical maps (e.g., Stockwell, 1937; Frarey, 1950) as well as the analysis of data from light detection and ranging (LiDAR) and aeromagnetic surveys.



Regional geology of the East Wekusko area

The Paleoproterozoic Snow Lake subdomain is part of the Reindeer zone of the Trans-Hudson orogen in Manitoba (Lewry and Collerson, 1990). It is bounded by the Kisseynew domain to the north and the Superior boundary zone to the east (Figure GS2024-10-1). West of Reed Lake, volcanic rocks are interpreted as part of the Amisk collage (Lucas et al., 1996); Stern et al. (1995) suggested that stratigraphic and geochemical differences between the Snow Lake arc assemblage and volcanic rocks of the Amisk collage were likely the result of their having formed in distinct tectonic settings. The Snow Lake domain extends under younger Phanerozoic platform carbonate rocks to the south (Simard et al., 2010). The Snow Lake subdomain occurs as three structural panels bounded by the northeast-trending Berry Creek shear zone and Crowduck Bay fault (Figure GS2024-10-1). A northeast-trending panel of greywacke and mudstone 15–20 km wide that Ansdell et al. (1999) referred to as the Central Wekusko block (CWB) is separated from the Snow Lake arc assemblage (SLA) and the Herblet gneiss

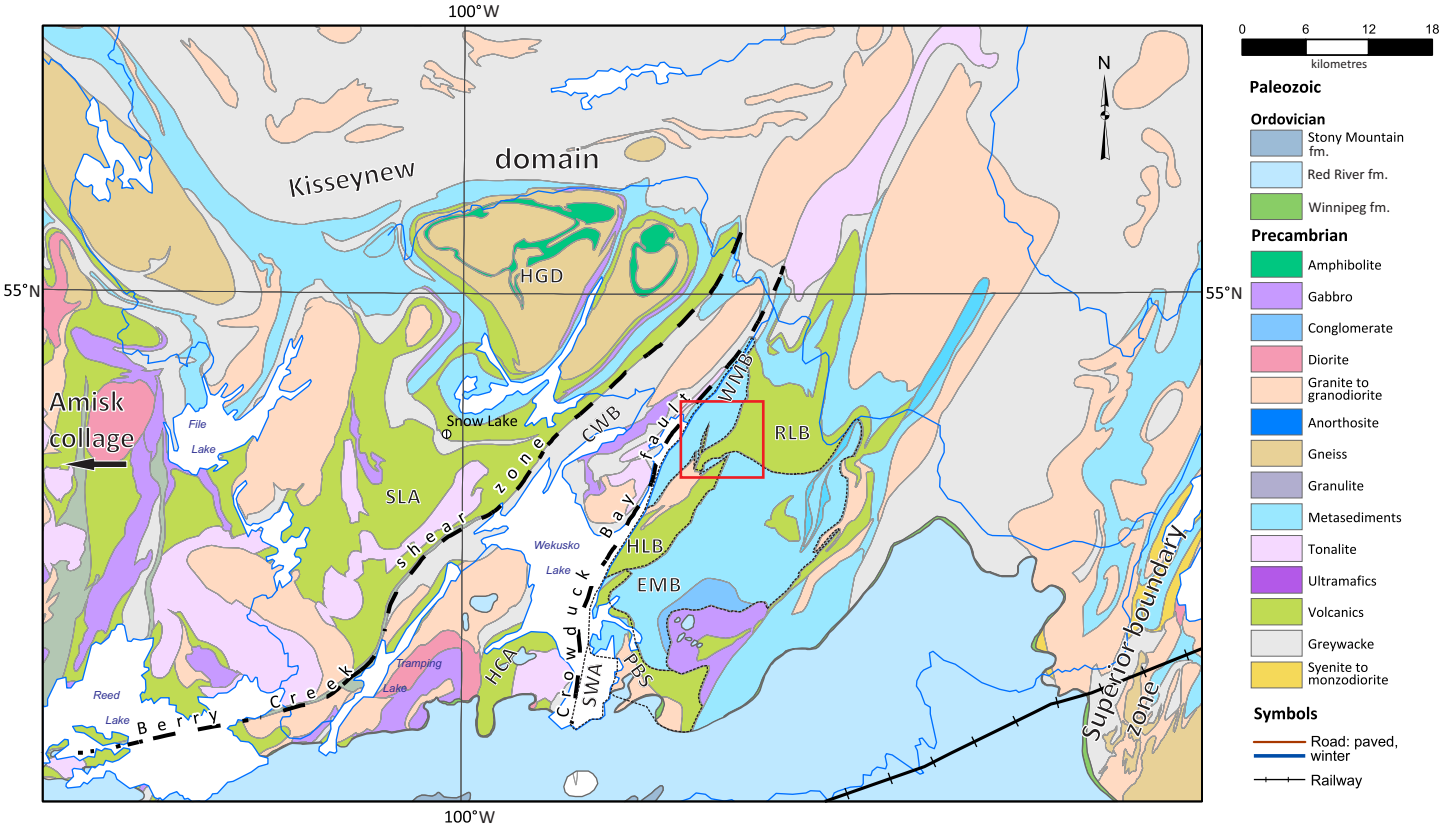


Figure GS2024-10-1: *Regional geology showing the Snow Lake domain, including the areas examined in 2024 (red polygon shows location of Figure GS2024-10-2) in north-central Manitoba (modified from Manitoba Geological Survey, 2022). Note the Kisseynew domain to the north, the Superior boundary zone to the east and Paleozoic cover rocks to the south. The Central Wekusko fault block (CWB), Eastern Missi fault block (EMB), Hayward Creek arc assemblage (HCA), Herb Lake fault block (HLB), Herblet gneiss dome (HGD), Puella Bay suite (PBS), Roberts Lake block (RLB), Snow Lake arc assemblage (SLA), South Wekusko assemblage (SWA) and Western Missi fault block (WMB) are shown relative to the Berry Creek shear zone and Crowduck Bay fault. Small dashed lines show the approximate boundaries of assemblages and structural blocks on the eastern side of Wekusko Lake.*

dome (HGD) by the Berry Creek shear zone (Figure GS2024-10-1). In the southwestern corner of the Wekusko Lake area, greywacke and mudstone are in structural contact with the Hayward Creek arc assemblage (HCA). Although no age determination is available for the Hayward Creek arc assemblage, it is thought to consist of ca. 1.89 Ga juvenile-arc rocks (Gilbert and Bailes, 2005).

The Crowduck Bay fault separates the CWB from rocks to the east and is considered a crustal-scale structure (Connors et al., 1999). Rocks east of the Crowduck Bay fault with similar lithostratigraphic elements are subdivided into fault-bounded blocks or assemblages (e.g., Connors et al., 1999; Gilbert and Bailes, 2005; Reid, 2021). These include ocean-floor basalts of the South Wekusko assemblage (SWA) and Roberts Lake block (RLB); evolved-arc volcanic rocks of the Puella Bay suite (PBS) and Herb Lake fault block (HLB); and fluvial-alluvial sedimentary rocks of the Western Missi fault block (WMB) and Eastern Missi fault block (EMB; Figure GS2024-10-1; e.g., Ansdell et al., 1999; Connors et al., 1999; Gilbert and Bailes, 2005; Reid, 2021).

The Roberts Lake area lies at the junction between rocks of the RLB, HLB, EMB and WMB (Figure GS2024-10-1). The map by Frarey (1950) indicates that a fault separates fluvial sandstone along the southern shore of Roberts Lake from pillowed basalt along the northern shore. Bedding measurements by Frarey (1950) in the Missi group sandstone and conglomerate south of Roberts Lake defined an upright synformal basin (Figure GS2024-10-2) but upon approaching the fault on Roberts Lake, the bedding is observed to be overturned. Connors et al. (1999, 2002) interpreted the Roberts Lake fault as a moderately dipping, south-verging thrust fault that places older basalt of MORB (mid-ocean–ridge basalt; unit F7a, Figure GS2024-10-2) affinity over younger sandstone and conglomerate. They also suggested that this thrusting is related to transpressional northwest-southeast shortening and the development of an extension lineation along the Crowduck Bay fault.

Field observations at Roberts Lake

A sequence of crossbedded feldspathic arenite (unit M3a, Figure GS2024-10-2) on the southern shore of Roberts Lake is overturned and youngs to the south (Figure GS2024-10-3a), consistent with the observations of Frarey (1950). With increasing biotite content in the sandstone, a bedding parallel cleavage S_0/S_1 is developed with an approximate strike of 300° and dip of

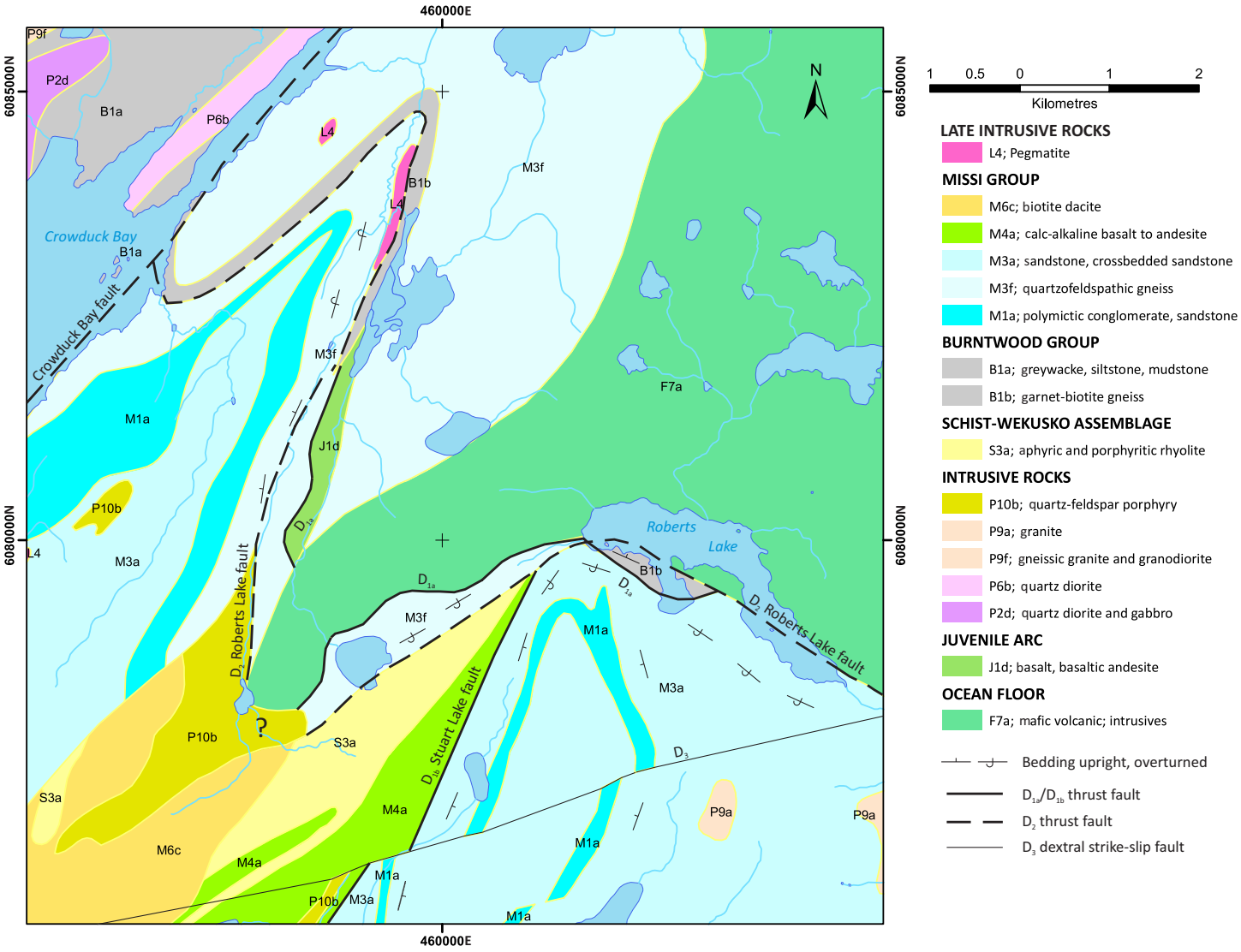


Figure GS2024-10-2: *Geology of the Roberts Lake study area, including the interpretation of fault generation (geology and unit codes from the NATMAP Shield Margin Project Working Group, 1998). Bedding measurements away from Roberts Lake are from Frarey (1950).*

38°, which is subsequently openly refolded, the axial plane forming an intersection lineation that trends 014° and plunges 64° (Figure GS2024-10-3b).

Directly north of the feldspathic arenite is a narrow (<100 m) unit of metamorphosed greywacke and mudstone rich in garnet and staurolite (unit B1b; Figure GS2024-10-2). The contact between the arenite and greywacke occurs between outcrops and is not exposed; however, it is believed to be relatively sharp, with no obvious increases in strain observed close to the contact (early S_1 brittle-ductile thrust?). Bedding in the greywacke and mudstone is defined by variations in garnet and staurolite content (Figure GS2024-10-3c). The local bedding strikes 282° and dips 39° and is characterized by reverse metamorphic grading (a transition from garnet-bearing sandy beds to coarse-grained beds with staurolite porphyroblasts), which is interpreted to indicate the unit youngs to the north. Close examination of quartz and biotite suggests an early S_1 foliation parallel to bedding S_0 that has been gently refolded, with 1–2 mm biotite books defining a crenulation cleavage S_2 that strikes 004° and dips 73°, nearly perpendicular to bedding S_0/S_1. This S_2 cleavage appears to gently anastomose around early formed garnet and staurolite porphyroblasts; it is considered analogous to the D_3 fabric described in Connors et al. (1999, 2002) and the D_4 fabric in Reid (2023).

The contact between the greywacke (unit B1b; Figure GS2024-10-2) and the Roberts Lake fault is not observed, but rocks on the promontory in the centre of Roberts Lake show evidence of increasing strain in the form of a carbonate-quartz-biotite-chlorite-sulphide–impregnated shear zone (Roberts Lake fault; Figures GS2024-10-2, 3d). This shear zone is a few metres wide and runs the length of the promontory, with a strike ranging from 334° to 353° and dips of 37° to 57°, while elongated streaks of carbonate within the shear zone trend 043° and plunge

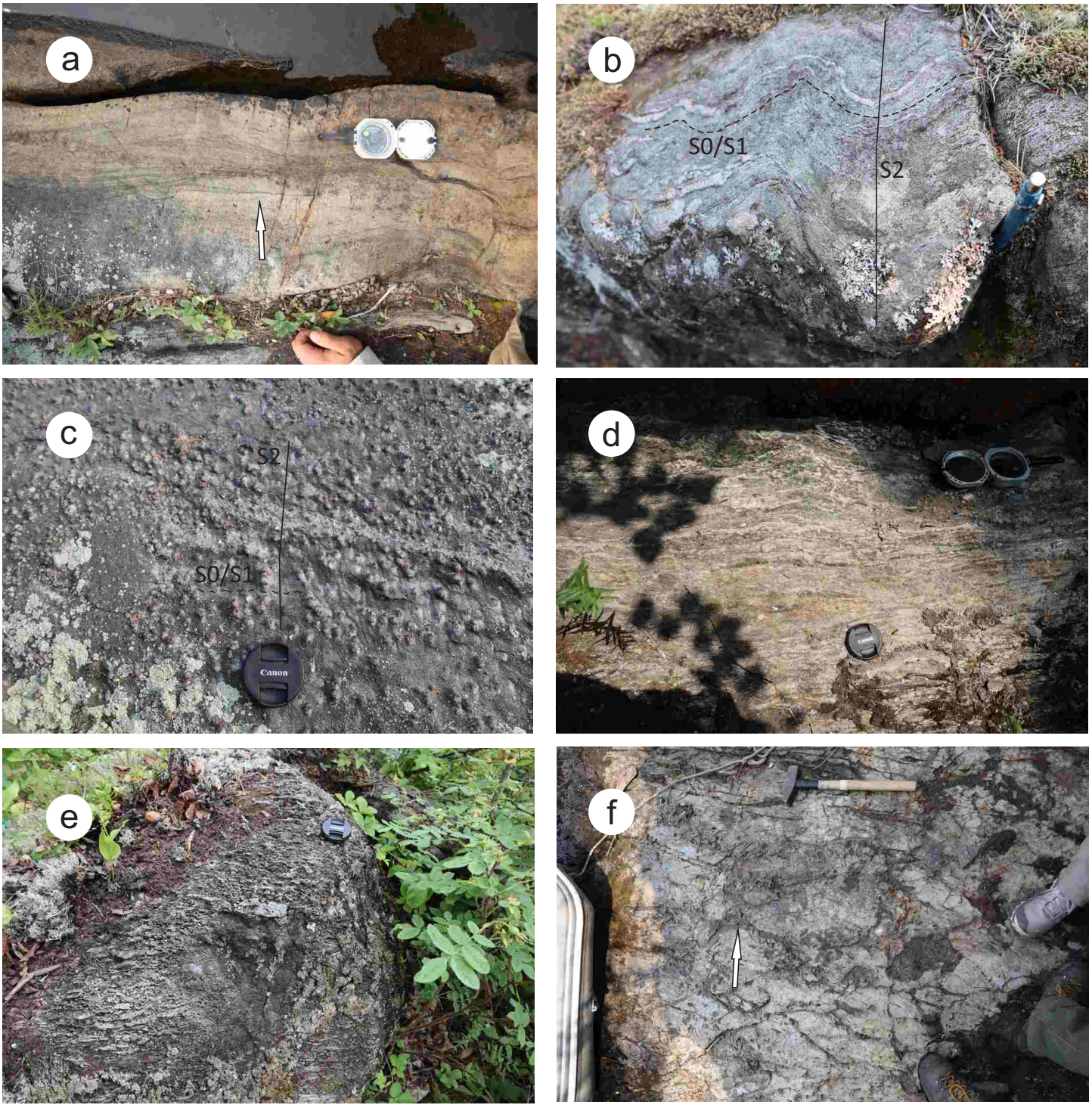


Figure GS2024-10-3: *Outcrop photographs from the Roberts Lake area:* ***a)*** *overturned crossbedded feldspathic arenite, with arrow indicating direction of stratigraphic younging (unit M3a; 461729E, 6079915N);* ***b)*** *feldspathic sandstone with increased biotite content showing S_0/S_1 refolded by F_2 (unit M3a; 461826E, 6079974N);* ***c)*** *porphyroblastic garnet greywacke with S_0/S_1 and later S_2 crenulation (unit B1b; 461826E, 6079974N);* ***d)*** *carbonate-quartz-biotite-chlorite-sulphide–impregnated D_2 deformation at the Roberts Lake fault (462566E, 6079709N);* ***e)*** *flattened (S_1) and lineated dacite lapilli in the hangingwall of the D_2 Roberts Lake fault (462883E, 6079496N);* ***f)*** *weakly flattened and sheared basalt with pillow selvages (arrow; unit F7a; 462391E, 6080419N). All co-ordinates are in UTM Zone 14, NAD83.*

48°. Directly in the hanging wall of the shear zone is a small unit containing lapilli-sized dacite clasts (Figure GS2024-10-3e), which have a distinct flattening (321°/47°) and lineation (036°/46°).

The northern side of Roberts Lake consists mainly of dark green, aphyric to very fine grained basalt with pillow selvages apparent in lower strain windows (unit 7Fa; Figure GS2024-10-3f). Measurements along the northern shore of pillow flattening/shearing show the strike ranging from 263° to 336° and the dip between 55° and 57°, while lineation in the basalt, defined by alignment of hornblende, trends 016–037° and plunges 51–55°.

Discussion

The geology at Roberts Lake (Figure GS2024-10-2) is relatively well represented by the mapping of Frarey (1950) and the NATMAP compilation (NATMAP Shield Margin Project Working Group, 1998). A unit of crossbedded feldspathic arenite along the southern side of Roberts Lake is consistently overturned and youngs to the southwest, whereas S_0/S_1 dips to the northeast. The adjacent narrow unit of garnet-staurolite–rich greywacke and mudstone has a similar S_0/S_1 cleavage dipping to the northeast but alternatively transitions to an upright structure that youngs to the northeast. The opposing facing directions across the contact between the two units would indicate that they were in fault contact prior to the development of the later north-striking S_2 cleavage. Along the northern side of Roberts Lake, S_1 manifests itself as pillow flattening and local shearing that dips to the northeast. A cleavage related to S_2 is less clearly developed in the mafic rocks; however, it is possible that the alignment of hornblende represents an intersection lineation formed at the intersection of the S_1 and S_2 cleavages.

Structural history of the Roberts Lake fault can be summarized in three phases:

1) The overturning of bedding in the sandstone; the development of S_1 fabrics in units M3a, B1b and F7a (Figure GS2024-10-2); and contacts between sandstone, greywacke and basalt are interpreted as being related to southwest-verging thrust faulting (D_{1a}; Figure GS2024-10-2) that brought (presumably) older Roberts Lake basalts of MORB affinity (unit F7a) southwest over younger Missi group sediments (unit M3a). The overturned bedding appears to be slightly folded around the synformal basin south of Roberts Lake, thus D_{1a} thrusting likely predates formation of the D_{1b} Stuart Lake fault (referred to as the Kiski fault; Connors et al. 1999). Reid (2024) interpreted the Stuart Lake anticline and fault to have formed synchronously with the emplacement of the Stuart Lake pluton at 1833.9 ±1.2 Ma, and D_1 thrust faulting at Roberts Lake is thus considered to have occurred concurrently with those events. The development of D_{1a} and D_{1b} faults as well as that of S_1 fabrics is considered to predate, or coincide with, peak metamorphic conditions and is analogous to the D_2 deformation events presented in Connors et al. (1999) and Reid (2023)
2) The carbonate-quartz-biotite-chlorite-sulphide-impregnated Roberts Lake Fault (D_2; Figure GS2024-10-2), another southwest-vergent structure, truncates the earlier D_{1a} and D_{1b} structures at the eastern and western ends of Roberts Lake as well as transecting various lithologies. The timing of this D_2 structure is less clear, but the lineation found within the fault is similar to the intersection lineation formed by S_1 foliation and F_2 fold hinges (Figure GS2024-10-3b); in addition, the lack of metamorphic recrystallization/annealing suggests that this fault postdates peak metamorphism. With the aid of LiDAR, aeromagnetic data and mapping by Frarey (1950), the D_2 Roberts Lake fault can be traced extending to Crowduck Bay, where it merges with, or is cut by, the Crowduck Bay fault (Figure GS2024-10-2). Overall, the D_2 Roberts Lake fault is considered to have been closely related to, or postdates, the D_3 deformation events described in Connors et al. (1999, 2002) and D_4 in Reid (2023).
3) Mapping by Frarey (1950) identified a brittle fault (D_3; Figure GS2024-10-2) with a component of dextral strike-slip movement that cuts the synformal basin south of Roberts Lake. It can be traced merging into the D_2 Roberts Lake fault east of Roberts Lake and extends east-northeast for approximately 50 km to the Superior Boundary zone. Interestingly, this fault not only has the same trend but also exhibits signs of the same late dextral movement as the crustal-scale Berry Creek shear zone to the west of Tramping Lake that can be traced for over 80 km to the west (Figure GS2024-10-4). The fact that the crustal-scale dextral movement along the Berry Creek shear zone west of Wekusko Lake appears to have translated into dextral movement east of Wekusko Lake along the late D_3 fault, to then merge with earlier D_1/D_2 thrust faults, suggests that the earlier D_1 and D_2 thrust faults were deeply rooted, as occurs in thick-skinned thrust systems (e.g., Pfiffner, 2017). Although no direct relationship between D_3 fault movement and lithium-bearing pegmatites has been observed, their sharp contacts and comb-like mineral texture indicate emplacement in dilatational structural sites while in the brittle-ductile to brittle environment (Silva et al., 2022; Reid, 2023). This occurred ca. 1780 ±8.1 Ma, based on analysis of columbite-group minerals in the Green Bay group pegmatites located a few kilometres northwest of Roberts Lake (Benn et al., 2019; Martins et al., 2019).

Economic considerations

Metamorphism and the development of regional structures play a significant role in the sourcing and focusing of hydrothermal fluids and melts that form economically viable mineral deposits such as the New Britannia gold mine, associated with the McLeod Road thrust (Rubingh et al., 2020), and the Tanco pegmatite, associated with the Bernic Lake shear zone (Kremer and Lin, 2006; Kremer, 2010). The combination of the metamorphic grade increasing northeast from Wekusko Lake and the structural complexity along the Roberts Lake fault is interpreted

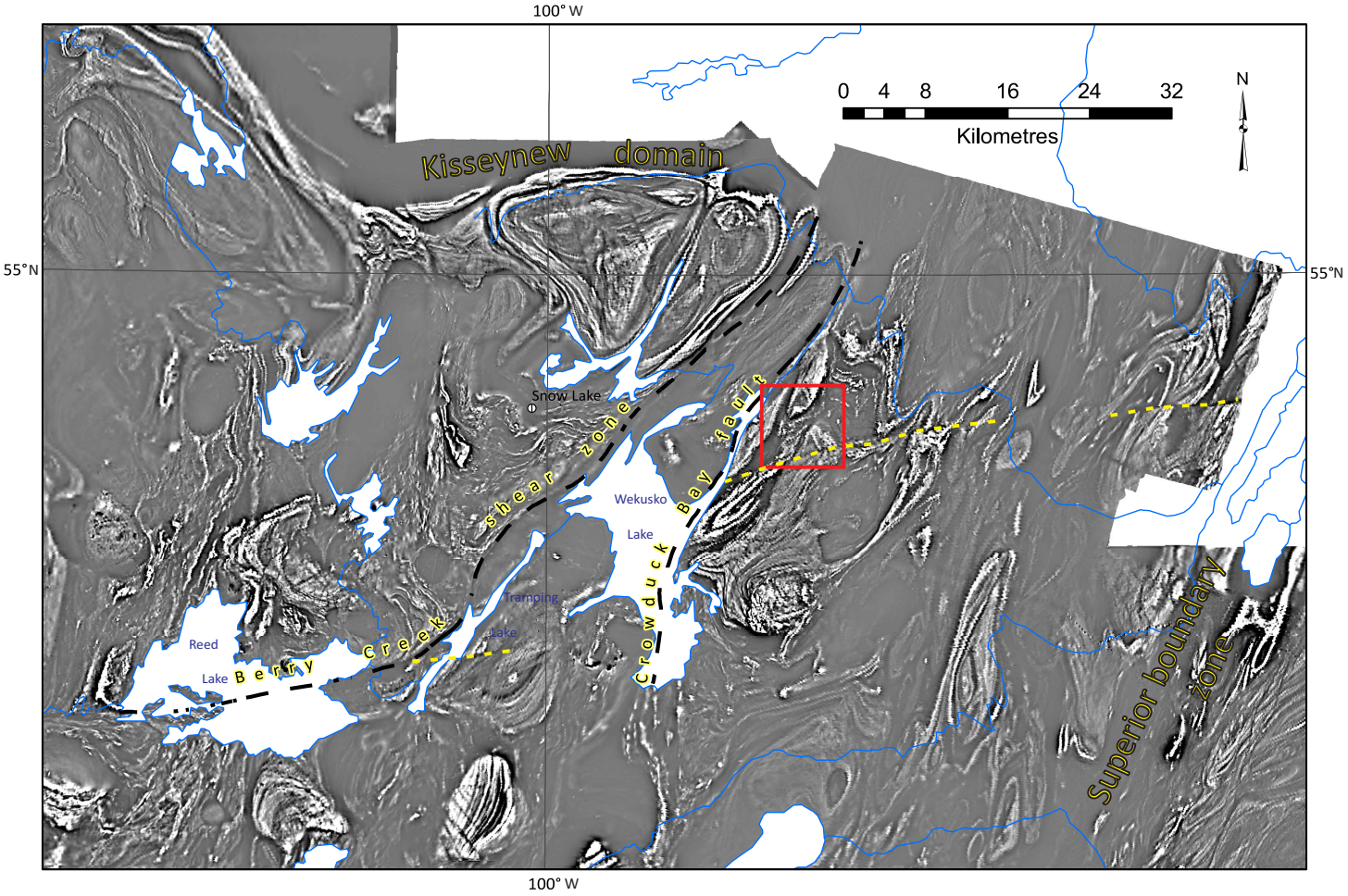


Figure GS2024-10-4: *Greyscale image showing the first vertical derivative of the magnetic field for the Snow Lake domain, data are from HudBay Minerals Inc. aeromagnetic compilation (unpublished, 2021) using data from two different survey systems: one pioneered by Spectrem Air, an airborne geophysics exploration company, and the VTEM™ (versatile time-domain electromagnetic) system developed by Geotech Ltd. Black dashed lines show the previous interpretations of the Berry Creek shear zone and Crowduck Bay fault, whereas the yellow dashed lines show the late dextral movements along the west-southwest-trending portion of the Berry Creek shear zone and the late dextral D_3 fault east of Wekusko Lake. Location of Figure GS2024-10-2 is indicated by the red polygon.*

as having played a role in the emplacement of orogenic gold and lithium-bearing pegmatites in the footwall and hangingwall of the structure (e.g., Stockwell, 1937; Benn et al., 2019; Silva et al., 2022). Southwest of Roberts Lake lie the Bachelor and McCafferty gold veins; these follow a D_1 axial plane that cuts rheologically competent felsic volcanic porphyry (see Stockwell, 1937). Alternatively, lithium-bearing pegmatites appear to postdate the D_1 and D_2 deformation events (D_2 and D_4 events; Reid, 2023) but may have been emplaced along pre-existing structures formed during the transition from brittle-ductile to brittle crustal levels, such as observed with the formation of the D_3 fault south of Roberts Lake. Interestingly, the Zoro and Violet-Thompson lithium-bearing pegmatite dikes (see Silva et al., 2022) occur in the hangingwall of the late crustal-scale brittle D_3 strike-slip fault, interpreted here to have roots that merge with the older D_1 and D_2 faults.

Acknowledgments

The author thanks A. Maki from Brandon University for providing enthusiastic field assistance, as well as C. Epp and P. Belanger for thorough logistical support. The author also thanks C. Couëslan and T. Martins for fruitful discussion and thorough reviews of this report.

References

Ansdell, K.M., Connors, K.A., Stern, R.A. and Lucas, S.B. 1999: Coeval sedimentation, magmatism, and fold-thrust belt development in the Trans-Hudson Orogen: geochronological evidence from the Wekusko Lake area, Manitoba, Canada; Canadian Journal of Earth Sciences, v. 36, p. 293–312.

Bailes, A.H. 1985: Geology of the Saw Lake area; Manitoba Energy and Mines, Geological Services Branch, Geological Report GR83-2, 47 p.

Benn, D., Martins, T. and Linnen, R.L. 2019: Interpretation of U-Pb isotopic dates of columbite-group minerals in pegmatites, Wekusko Lake pegmatite field, central Manitoba (part of NTS 63J13); *in* Report of Activities 2019, Manitoba Agriculture and Resource Development, Manitoba Geological Survey, p. 52–59, URL <https://manitoba.ca/geo/field/roa19pdfs/GS2019-5.pdf> [October 2024].

Connors, K.A., Ansdell, K.M. and Lucas, S.B. 1999: Coeval sedimentation, magmatism, and fold-thrust development in the Trans-Hudson orogen: propagation of deformation into an active continental arc setting, Wekusko Lake area, Manitoba; Canadian Journal of Earth Sciences, v. 36, p. 275–291.

Connors, K.A., Ansdell, K.M. and Lucas, S.B. 2002: Development of a transverse to orogen parallel extension lineation in a complex collisional setting, Trans-Hudson orogen, Manitoba, Canada; Journal of Structural Geology, v. 24, no. 1, p. 89–106, URL <https://doi.org/10.1016/S0191-8141(01)00051-7>.

Frarey, M.J. 1950: Crowduck Bay, Manitoba; Geological Survey of Canada, Map 987A, scale 1:63 360.

Gilbert, H.P. and Bailes, A.H. 2005: Geology of the southern Wekusko Lake area, Manitoba (NTS 63J12NW); Manitoba Industry, Economic Development and Mines, Manitoba Geological Survey, Geoscientific Map MAP2005-2, scale 1:20 000, URL <https://manitoba.ca/iem/info/libmin/MAP2005-2.pdf> [October 2024].

Kremer, P.D. 2010: Structural geology and geochronology of the Bernic Lake area in the Bird River greenstone belt, Manitoba: evidence for syn-deformational emplacement of the Bernic Lake pegmatite group; M.Sc. thesis, University of Waterloo, Waterloo, Ontario, 91 p.

Kremer, P.D. and Lin, S. 2006: Structural geology of the Bernic Lake area, Bird River greenstone belt, southeastern Manitoba (NTS 52L6): implications for rare element pegmatite emplacement; *in* Report of Activities 2006, Manitoba Science, Technology, Energy and Mines, Manitoba Geological Survey, p. 206–213.

Lewry, J.F. and Collerson, K.D. 1990: Trans-Hudson orogen: extent, subdivisions, and problems; *in* The Proterozoic Trans-Hudson Orogen of North America, J.F. Lewry and M.R. Stauffer (ed.), Geological Association of Canada, Special Publication 37, p. 1–14.

Lucas, S.B., Stern, R.A., Syme, E.C., Reilly, B.A. and Thomas, D.J. 1996: Intra-oceanic tectonics and the development of continental crust: 1.92–1.84 Ga evolution of the Flin Flon belt, Canada; Geological Society of America, Bulletin, v. 108, p. 602–629.

Manitoba Geological Survey 2022: New edition of the 1:250 000 scale Precambrian bedrock geology compilation map of Manitoba; Manitoba Natural Resources and Northern Development, Manitoba Geological Survey, GeoFile 3-2022, scale 1:250 000, URL <https://manitoba.ca/iem/info/libmin/geofile3-2022.zip> [October 2024].

Martins, T., Benn, D. and McFarlane, C. 2019: Laser-ablation inductively coupled plasma–mass spectrometry (LA-ICP-MS) analyses of columbite grains from Li-bearing pegmatites, Wekusko Lake pegmatite field (northeastern block), central Manitoba (part of NTS 63J13); Manitoba Agriculture and Resource Development, Manitoba Geological Survey, Data Repository Item DRI2019003, Microsoft® Excel® file, URL <https://manitoba.ca/iem/info/libmin/DRI2019003.xlsx> [September 2024].

NATMAP Shield Margin Project Working Group, 1998: Geology, NATMAP Shield Margin Project area, Flin Flon belt, Manitoba/Saskatchewan; Geological Survey of Canada, Map 1968A, 54 p., scale 1:100 000.

Pfiffner, O.A. 2017: Thick-skinned and thin-skinned tectonics: a global perspective; Geosciences, v. 7, no. 3, 89 p., URL <https://doi.org/10.3390/geosciences7030071>.

Reid, K.D. 2019: Bedrock geological mapping of the Puella Bay area (Wekusko Lake), north-central Manitoba (part of NTS 63J12); *in* Report of Activities 2019, Manitoba Agriculture and Resource Development, Manitoba Geological Survey, p. 42–51, URL <https://manitoba.ca/iem/geo/field/roa19pdfs/GS2019-4.pdf>[October 2024].

Reid, K.D. 2021: Results of bedrock geological mapping in the Stuart Bay–Chickadee Lake area (east of Wekusko Lake), north-central Manitoba (parts of NTS 63J12, 13); *in* Report of Activities 2021, Manitoba Agriculture and Resource Development, Manitoba Geological Survey, p. 29–39.

Reid, K.D. 2023: Geological investigations in the areas of Niblock Lake and Crowduck Bay (Wekusko Lake), north-central Manitoba (parts of NTS 63J13, 14); *in* Report of Activities 2023, Manitoba Economic Development, Investment, Trade and Natural Resources, Manitoba Geological Survey, p. 64–72.

Reid, K.D. 2024: New age constraints for volcanic and plutonic rocks southeast of Wekusko Lake, Manitoba; *in* GAC-MAC-PEG 2024 Brandon Meeting: Abstracts, Volume 47, Geoscience Canada, v. 51, p. 128, URL <https://doi.org/10.12789/geocanj.2024.51.211>.

Rubingh, K., Lafrance, B. and Gibson, H.L. 2020: A reinterpretation of the Snow Lake gold camp, Trans-Hudson Canada: the use of cleavages as markers to correlate structures across deformed terranes; Canadian Journal of Earth Sciences. v. 58, p. 610–639.

Silva, D., Martins, T., Groat, L. and Linnen, R. 2022: Preliminary observations on emplacement controls of pegmatite dikes from the Wekusko Lake pegmatite field, north-central Manitoba (parts of NTS 63J13, 14, 63O4); *in* Report of Activities 2022, Manitoba Natural Resources and Northern Development, Manitoba Geological Survey, p. 49–60, URL <https://manitoba.ca/iem/geo/field/roa22pdfs/GS2022-7.pdf> [October 2024].

Simard, R.-L., McGregor, C.R., Rayner, N. and Creaser, R.A. 2010: New geological mapping, geochemical, Sm-Nd isotopic and U-Pb data for the eastern sub-Phanerozoic Flin Flon belt, west-central Manitoba (parts of NTS 63J3-6, 11, 12, 14, 63K1-2, 7–10); *in* Report of Activities 2010, Manitoba Innovation, Energy and Mines, Manitoba Geological Survey, p. 69–87, URL <https://manitoba.ca/iem/geo/field/roa10pdfs/GS-6.pdf> [October 2024].

Stern, R.A., Syme, E.C., Bailes, A.H. and Lucas, S.B. 1995: Paleoproterozoic (1.90–1.86 Ga) arc volcanism in the Flin Flon belt, Trans-Hudson orogen, Canada; Contributions to Mineralogy and Petrology, v. 119, p. 117–141.

Stockwell, C.H. 1937: Gold deposits of Herb Lake area, northern Manitoba; Geological Survey of Canada, Memoir 208, 46 p.

GS2024-11

Geochronological update of sedimentary, volcanic and plutonic rocks in the Snow Lake area, north-central Manitoba (parts of NTS 63J13, 63K16)

by K.D Reid

In Brief:

- New ages for the Ham Lake and Wekusko Lake plutons will provide constraints on early deformation in the Snow Lake area
- Detrital zircons from greywacke on File Lake will provide information on provenance for the Burntwood group along the south flank of the Kisseynew basin

Citation:
Reid, K.D. 2024: Geochronological update of sedimentary, volcanic and plutonic rocks in the Snow Lake area, north-central Manitoba (parts of NTS 63J13, 63K16); *in* Report of Activities 2024, Manitoba Economic Development, Investment, Trade and Natural Resources, Manitoba Geological Survey, p. 92–97.

Summary

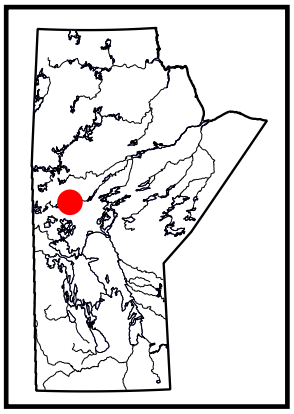
The broad economic mineral endowment of the Snow Lake region has made it the focus of extensive exploration and study for over a century. Throughout that period, detailed study and mapping have shown that various rocks in the Snow Lake area are in fact attributed to different lithotectonic assemblages (i.e., back-arc volcanic, arc volcanic, turbiditic greywacke) that may have formed in distinct tectonic environments during various time frames. Deformation and faulting related to the Trans-Hudson orogeny resulted in the juxtaposition of these assemblages. Attempts at placing absolute time constraints on both the formation of these assemblages and the subsequent deformation have been ongoing. The ongoing work has benefited from recent advances in U-Pb zircon geochronology that allow for more precise age determination using both laser-ablation inductively coupled plasma–mass spectrometry and isotope dilution–thermal ionization mass spectrometry. A rationale for resampling and dating certain igneous and sedimentary rocks of the Snow Lake area is presented in this report.

Introduction

As part of the multiyear program in the Snow Lake subdomain of the Reindeer zone of the Trans-Hudson orogen (THO) initiated in 2023 by the Manitoba Geological Survey (MGS), modern geochronological techniques were applied to rocks that have been well mapped but have poor or questionable absolute-age constraints. The core focus is centered around the File, Snow and Wekusko lakes areas (Figure GS2024-11-1). Thorough mapping campaigns have been carried out in these areas (e.g., Bailes, 1980; NATMAP Shield Margin Project, 1998; Gilbert and Bailes, 2005; Bailes and Galley, 2007) but, as much of the radiometric dating was completed in the 1980s and early 1990s, some ages are relatively imprecise. New geochronological sampling is briefly discussed in this report and, as more precise ages are obtained, the details will be released as Data Repository Items (DRI) and the implications of these results discussed in an Open File report (K.D. Reid, work in progress).

Geology of the File and Snow lakes areas

Rocks of the File, Snow and Wekusko lakes areas lie within the juvenile (internal) Reindeer zone of the THO, a collisional zone formed during the 2.0–1.8 Ga amalgamation of several oceanic arcs, back-arcs and Archean cratons to form the Laurentian supercontinent (Hoffman, 1988). This area encompasses the transition zone between the Snow Lake subdomain and the Kisseynew domain to the north (Figure GS2024-11-1). To the east, the Snow Lake subdomain is bounded by the Superior boundary zone, whereas to the south it continues under younger Phanerozoic platform carbonate rocks.



Volcanic rocks west of Reed Lake are considered part of the Amisk collage (Figure GS2024-11-1; Lucas et al., 1996). They are separated from the Snow Lake subdomain by the West Reed-North Star shear zone and from the Kisseynew domain by the Loonhead Lake fault. Stern et al. (1995) suggested that stratigraphic and geochemical differences between the Snow Lake arc assemblage and volcanic rocks of the Amisk collage were likely the result of their having formed in distinct tectonic settings.

The Loonhead Lake fault (LHLF) and the Snow Lake fault (SLF) are interpreted as thrust faults that developed during southwest-directed transport of greywacke and mudstone from the Kisseynew domain over the Snow Lake arc assemblage (SLA) and the Northeast Reed assemblage (NERA; Figure GS2024-11-1; Connors, 1996). The Loonhead Lake and Snow Lake faults are considered to have been potentially at one time a single thrust fault cut by the Ham Lake pluton (HLP; Figure GS2024-11-1). The Berry Creek shear zone separates the Snow Lake arc assemblage and the Herblet gneiss dome (HGD) from a northeast-trending panel of greywacke and mudstone 15–20 km wide referred to as the Central Wekusko block (CWB) by Ansdell et al. (1999; Figure GS2024-11-1). In the southwestern corner of the Wekusko Lake area, greywacke and mudstone are in structural contact with the Hayward

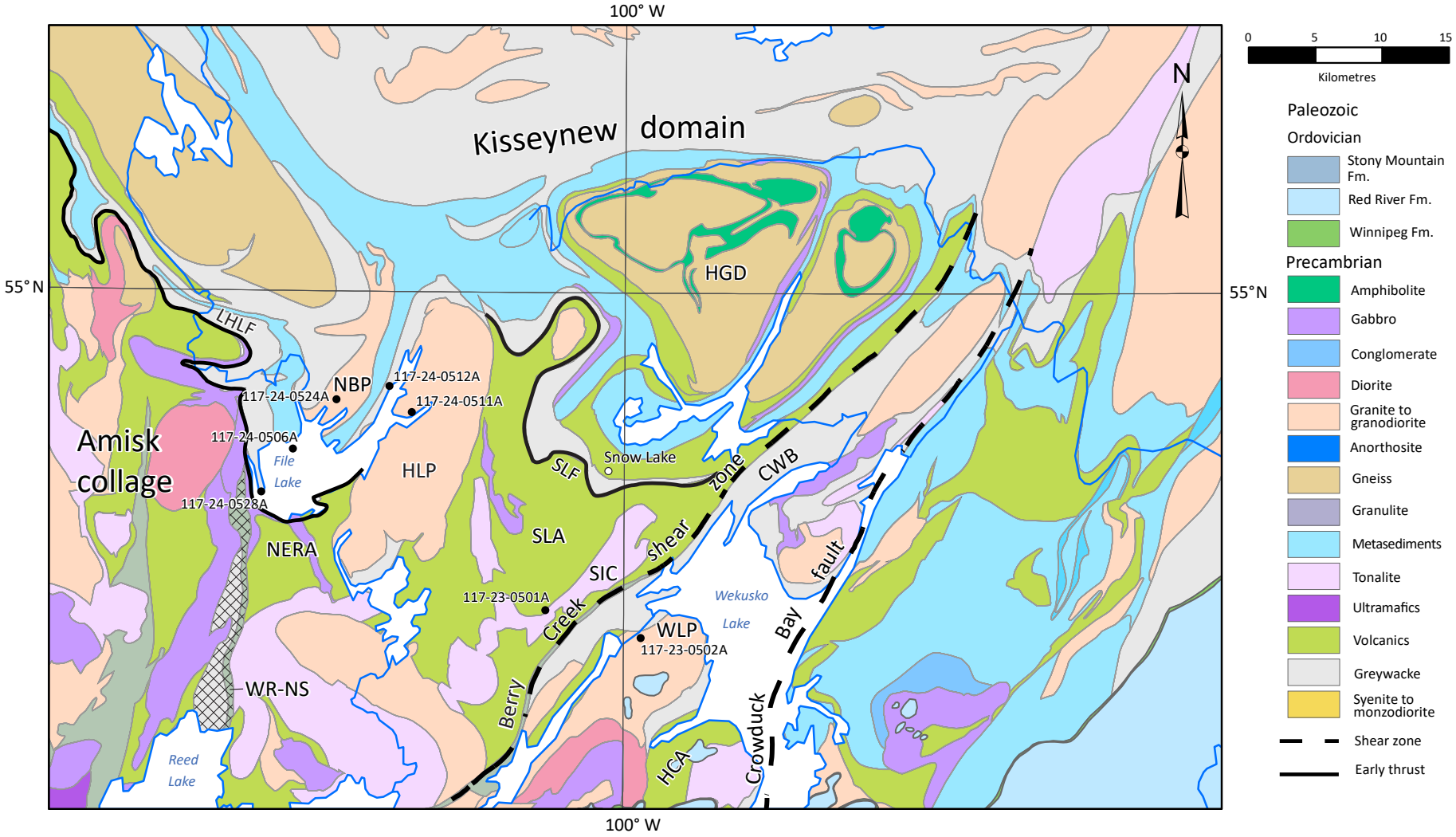


Figure GS2024-11-1: *Geology of the Snow Lake subdomain of the eastern Trans-Hudson orogen, modified from the 1:250 000 scale Precambrian bedrock geology map issued by the Manitoba Geological Survey (2022). Note the Kisseynew domain to the north and Paleozoic cover rocks to the south. The Central Wekusko fault block is shown relative to the Berry Creek shear zone and Crowduck Bay fault. Abbreviations: CWB, Central Wekusko fault block; HCA, Hayward Creek arc assemblage; HGD, Herblet gneiss dome; HLP, Ham Lake pluton; LHLF, Loonhead Lake fault; NBP, Nelson Bay rocks; NERA, Northeast Reed assemblage; SIC, Sneath intrusive complex; SLA, Snow Lake arc assemblage; SLF, Snow Lake fault; WLP, Wekusko Lake pluton; WR-NS, West Reed-North Star shear zone.*

Creek arc assemblage (HCA). Although no age determination is available for the Hayward Creek arc assemblage, it is thought to consist of ca. 1.89 Ga juvenile-arc rocks (Gilbert and Bailes, 2005).

Geochronological samples

Igneous rocks

Plutonic rocks

The Wekusko Lake granite (sample 117-23-0502A01; Figure GS2024-11-1) is a light grey to pink, massive, equigranular, medium-grained granite with biotite that is pseudomorphic after hornblende (Figure GS2024-11-2a). The intrusion was emplaced into mudstone and greywacke of the Burntwood group along the western side of Wekusko Lake, where the Burntwood group rocks are affected by two generations of folding: 1) an earlier isoclinal F_1 that transposes bedding and 2) a second generation of tight F_2 folding that refolds F_1. Map patterns show that emplacement of the granite body is synchronous with the second deformation event, as the main body intrudes into the nose of a northeast-trending F_2 fold but also has small protrusions cutting across F_2 folded limbs (Bailes and Galley, 2007). Zircon from the granite produced a discordant 1834 +8/-6 Ma age (Gordon et al., 1990), whereas a titanite fraction from the same granite yielded an age of 1841 ±5 Ma (David et al. 1996), which is within error of the zircon age. A new sample of the Wekusko Lake granite has been submitted to determine a more precise crystallization age and constrain the time of folding.

The Sneath Lake intrusive complex (SIC, Figure GS2024-11-1) occurs within the Anderson sequence volcanic rocks and presents many features of a high-level synvolcanic intrusion, including multiple intrusive phases, porphyritic character, columnar jointing, internal alteration and fragments of the distinctive Sneath megacrystic-quartz tonalite in the spatially associated Anderson-Stall rhyolite (Bailes and Galley, 2007). Although radiometric dating of a quartz-phyric–tonalite phase produced an age of 1886 +17/-9 Ma, within error of Chisel sequence rocks including the Stroud Lake felsic breccia at 1892 ±3 Ma (David et al., 1996) and the Richard Lake intrusive complex at 1889 +8/-6 Ma (Bailes et al., 1991), several questions remain unanswered. For example, were the Anderson sequence and Chisel sequence arcs formed at the same time and then structurally accreted together or was the Chisel sequence arc built on the Anderson sequence? A sample of Sneath Lake quartz-phyric tonalite (117-23-501A01; Figure GS2024-11-1) was collected and is being evaluated by Ballantyne et al. (2024) to help better understand the relationship between the volcanic rocks of the Anderson and Chisel sequences.

The Ham Lake pluton is an approximately 16 by 7 km, north-northeast-trending, massive granodiorite intrusion (Figure GS2024-11-1) that has a U-Pb zircon crystallization age of 1830 +27/–19 Ma (Gordon et al., 1990). It likely predates regional metamorphism (Bailes, 1980) and postdates F_1–F_2 folding and movement on the Loonhead Lake fault (Figure GS2024-11-1), which is interpreted by Connors (1996) as a major thrust fault that tectonically transported younger sedimentary rocks from the Kisseynew domain into the Snow Lake segment of the Flin Flon domain. A new sample (117-24-511A01, Figure GS2024-11-1, 2b) of the Ham Lake pluton was acquired to provide a more precise minimum age for the Loonhead Lake fault and associated thrusting of Burntwood group turbidites over the Flin Flon domain.

Rocks of probable volcanic origin

Harrison (1949) previously mapped Nelson Bay rocks (NBP, Figure GS2024-11-1) as foliated granite, but these were reinterpreted as a structural dome of predominantly recrystallized metavolcanic orthogneisses (Bailes, 1980). Additionally, a thin unit (<20 m thick) of fine-grained felsic orthogneiss occurs within the Missi group metasedimentary succession at File Lake; Bailes (1980) suggested it originally had been a felsic ash flow within the Missi sedimentary succession. Zwanzig and Bailes (2010) noted that the felsic rocks of the Nelson Bay dome structure and those within the Missi group shared geochemical similarities with the Cleunion rhyolite that occurs within the Missi group sediments further to the west. A sample from the Nelson Bay dome structure produced an age of 1832 ±2 Ma (David et al., 1996), indicating that these rocks are close in age to volcanic rocks observed elsewhere in the Missi group (e.g., Chickadee rhyolite 1836 ±1 Ma; Ansdell et al., 1999).

In the Nelson Bay area, the felsic rocks are light grey to pinkish grey, fine-grained, weakly granoblastic, with distinct layering that varies from centimetre- to metre-scale (Figure GS2024-11-2c). Structural measurements of this layering do support a domal structure; however, no features could be positively identified as pyroclastic or definitively volcanic in origin. At the northeastern end of Nelson Bay and within the Missi sediments at File Lake, the felsic rocks are nearly identical in appearance: both are siliceous, aphyric, laminated at the millimetre-scale, with a well-developed cleavage, and resemble tuffaceous rhyolite (Figure GS2024-11-2d, e). Samples from both locations (117-24-0524A01 and 117-24-0506A01, Figure GS2024-11-1) were collected for geochemical analyses and U-Pb zircon dating. The results should provide a basis for comparison with other Missi group volcanic stratigraphy (e.g., east of Wekusko Lake; see Reid et al. 2024) and help in determining minimum time constraints on observed deformation.

Original mapping by Bailes (1980) shows that the northeastern arm of File Lake contains a narrow band of mafic and felsic volcanic rocks (see units 14 and 14a in Bailes, 1980) that occurs within the Burntwood group. Re-examination of these outcrops revealed that rocks of probable volcanic origin are present, the most distinct of these being a monomictic mafic conglomerate/lapilli tuff and an adjacent aphyric rhyolite. Both mafic and felsic samples were collected for geochemical analysis, and a sample

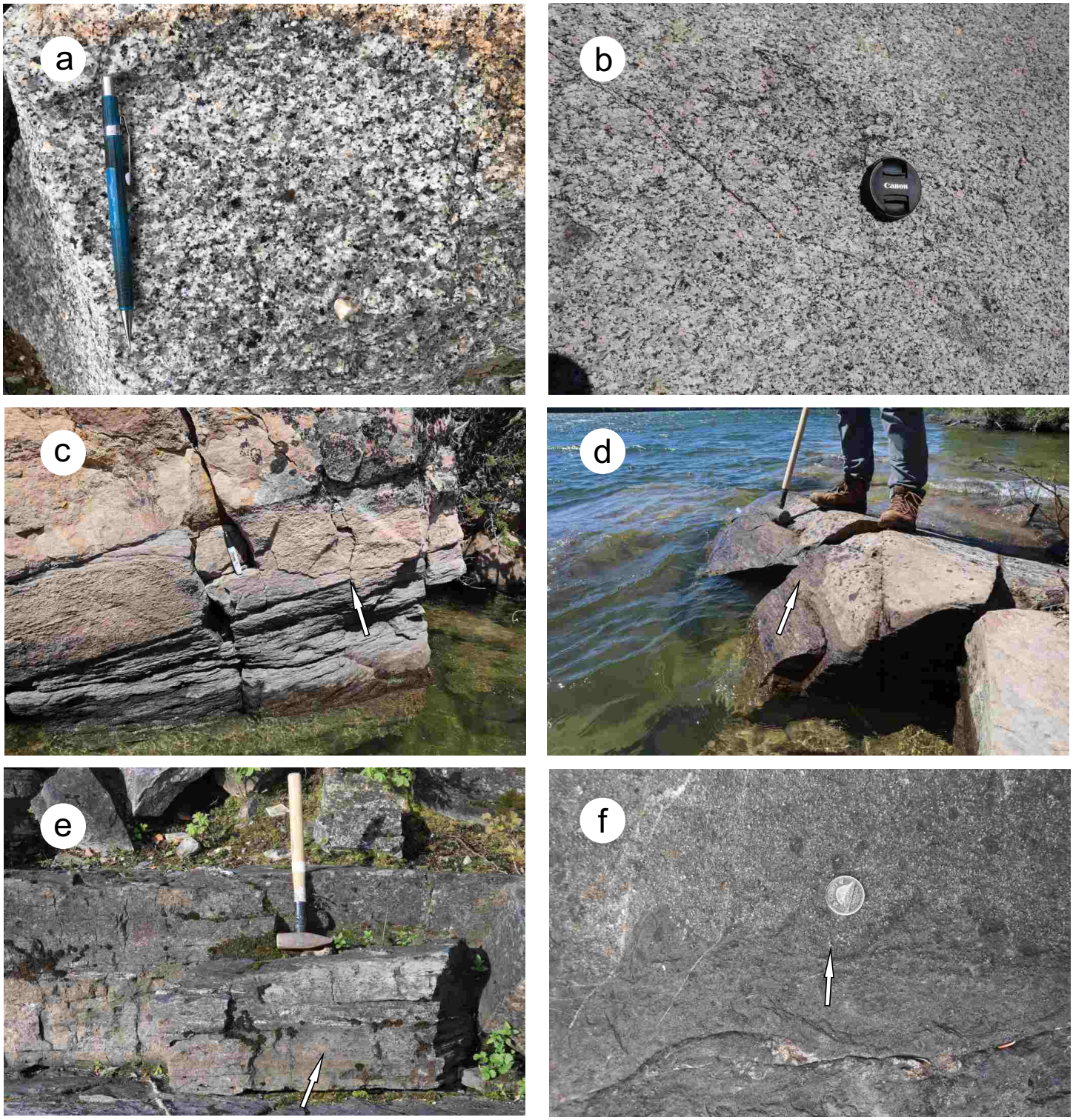


Figure GS2024-11-2: *Outcrop photographs from the Wekusko and File lakes areas:* ***a)*** *Wekusko Lake granite (436811E, 6069129N);* ***b)*** *very weakly foliated Ham Lake granite (420122E, 6086536N);* ***c)*** *centimetre- to metre-scale layered, fine-grained felsic volcanic rock from the Nelson Bay area at File Lake (arrow shows sharp contact between units; 413454E, 6086696N);* ***d)*** *millimetre- to centimetre-scale layered rhyolite at the northeastern end of Nelson Bay at File Lake (arrow points at layering; 414526E, 6087529N);* ***e)*** *millimetre- to centimetre-scale layered rhyolite within Missi group sandstone at File Lake (arrow points at layering; 411104E, 6083697N);* ***f)*** *soft sedimentary deformation (flame structures) at the contact between mud and sand bed (arrow) in the Burntwood group (408570E, 6080723N). All co-ordinates are in UTM Zone 14, NAD83.*

of the rhyolite (117-24-0512A01; Figure GS2024-11-1) was collected for radiometric dating.

Sedimentary rocks

Detailed mapping at File Lake by Bailes (1980) identified a 1000 m thick package of pebbly greywacke, greywacke and mudstone that was deposited by turbidity currents; these sediments were interpreted at the time to have been shed from the adjacent juvenile arc-volcanic rocks (Amisk group). However, analysis of detrital zircon from this package by David et al. (1996) revealed that the maximum age of sedimentation may be as young as ca. 1854 Ma at File Lake. A similar constraint on the maximum age of sedimentation was produced from greywacke and mudstone from the Wekusko Lake area, with the youngest concordant zircon yielding an age of 1859 ±7 Ma, which indicates the turbidites may be as much as 30 m.y. younger than the known age of juvenile-arc volcanism (e.g., Snow Lake arc assemblage ca.1.89 Ga). The small number of zircons used in the study by David et al. (1996) does not allow proper statistical comparison of provenance. A sandy bed sample (117-24-0528A01; Figure GS2024-11-2f) from the turbidite was collected at File Lake in 2024 to determine the overall provenance.

Discussion

Detailed field mapping of plutonic, volcanic and sedimentary rocks in the Snow Lake area (e.g., Bailes, 1980; Connors, 1996; Kraus and Williams, 1999; Bailes and Galley, 2007) has characterized the lithological and tectonic evolution of the region. However, many of the absolute age constraints for this region were obtained over 30 years ago and provided imprecise ages (e.g., 1830 +27/–19 Ma for the Ham Lake granite; Gordon et al., 1990). Advancements in sample preparation and treatment, as well as instrumentation, have shown that very accurate and precise ages can now be obtained from these rocks (e.g., 1833.9 ±1.2 Ma for the Stuart Lake granite; Reid, 2024). All new data and interpreted ages will be released in a DRI, as they become available, and the significance of these results will be discussed in an Open File report (K.D. Reid, work in progress).

A new absolute age constraint for the Sneath Lake tonalite will help gain a better understanding of the evolution of the juvenile Anderson sequence by allowing comparison with ages yielded by the arc-volcanic rocks of the Chisel sequence and will contribute to the work carried out by Ballantyne et al. (2024). Determining a precise crystallization age for the Ham Lake granite pluton will provide minimum constraints on the age of F_2 folding and the Loonhead Lake fault at File Lake. Similarly, an improved age determination for the Wekusko Lake pluton will provide constraints into F_2 folding in greywacke at Wekusko Lake. In addition to constraining the timing of deformation in the Snow Lake subdomain, precise ages for these plutons will also provide information on the evolution of successor-arc magmatism and allow comparison with known successor-arc volcanic rocks east of Wekusko Lake (e.g., Andsell et al, 1999; Reid, 2021). Building on the work by David et al. (1996), analysis of detrital zircon by laser ablation-inductively coupled plasma–mass spectrometry on the greywacke at File Lake will allow more thorough examination of the provenance of the greywacke at this location, relative to other greywacke units along the flank of the Kisseynew domain.

Economic considerations

Ore mineralizing events are often restricted to narrow windows of geological time and commonly associated with deformation and/or magmatic events. Therefore, it is important to understand geologically favourable time frames. For example, in the Snow Lake subdomain, orogenic gold mineralization is closely linked with early F_1 folding and thrust faulting such as those noted at the Nor-Acme anticline, Snow Lake thrust and McLeod Road thrust (Rubingh et al., 2020) but no absolute age constraints are available currently for these structures. Thrust faulting and folding extend into the File Lake area, where the Loonhead Lake fault is cut by the Ham Lake granite pluton, thus determination of the precise age of this pluton will help in establishing a minimum constraint on early deformation and allow comparison with the deformation/gold mineralizing time interval observed elsewhere in the Flin Flon domain (e.g., east of Wekusko Lake; Reid, 2021, 2024).

Acknowledgments

The author thanks M. Friesen and C. Couëslan for providing enthusiastic field assistance and fruitful discussion while at File Lake, as well as C. Epp and P. Belanger for thorough logistical support. The author would also like to thank M. Rinne and E. Yang for constructive reviews of this report.

References

Ansdell, K.M., Connors, K.A., Stern, R.A. and Lucas, S.B. 1999: Coeval sedimentation, magmatism, and fold-thrust development in the Trans-Hudson orogen: geochronological evidence from the Wekusko Lake area, Manitoba, Canada; Canadian Journal of Earth Sciences, v. 36, p. 293–312.

Bailes, A.H. 1980: Geology of the File Lake, Manitoba; Manitoba Department of Energy and Mines, Mineral Resources Division, Geological Report 78-1, 134 p.

Bailes, A.H. and Galley, A.G. 2007: Geology of the Chisel-Anderson lakes area, Snow Lake, Manitoba (NTS 63K16, 63J13); Manitoba Science, Technology, Energy and Mines, Manitoba Geological Survey, Geoscientific Map MAP2007-1, scale 1:20 000.

Bailes, A.H., Hunt, P.A. and Gordon, T.M. 1991: U-Pb zircon dating of possible synvolcanic plutons in the Flin Flon belt at Snow Lake, Manitoba; *in* Radiogenic Age and Isotopic Studies: Report 4, Geological Survey of Canada, Paper 90-2, p. 35–43, URL <https://doi.org/10.4095/131935>.

Ballantyne, S.M., Stewart, M., Reid, K.D., Anderson, M.O., Venturi, C. and Richardson, N. 2024: Research activities at the Lalor mine, Snow Lake, west-central Manitoba (part of NTS 63K16); *in* Report of Activities 2024, Manitoba Economic Development, Investment, Trade and Natural Resources, Manitoba Geological Survey, p. 98–103.

Connors, K.A. 1996: Unraveling the boundary between turbidites of the Kisseynew belt and volcano-plutonic rocks of the Flin Flon belt, eastern Trans-Hudson orogen, Canada; Canadian Journal of Earth Sciences, v. 33, p. 811–829.

David, J., Bailes, A.H. and Machado, N. 1996: Evolution of the Snow Lake portion of the Paleoproterozoic Flin Flon and Caisson belts, Trans-Hudson orogen, Manitoba, Canada; Precambrian Research, v. 80, p. 107–124.

Gilbert, H.P. and Bailes, A.H. 2005: Geology of the southern Wekusko Lake area, Manitoba (NTS 63J12NW); Manitoba Industry, Economic Development and Mines, Manitoba Geological Survey, Geoscientific Map MAP2005-2, scale 1:20 000, URL <https://manitoba.ca/iem/info/libmin/MAP2005-2.pdf> [October 2024].

Gordon, T.M., Hunt, P.A., Bailes, A.H. and Syme, E.C. 1990: U-Pb ages from the Flin Flon and Kisseynew belts, Manitoba: chronology of crust formation at an early Proterozoic accretionary margin; *in* The Early Proterozoic Trans-Hudson Orogen of North America, J.F. Lewry and M.R. Stauffer (ed.), Geological Association of Canada, Special Paper 37, p. 177–199.

Harrison, J.M. 1949: Geology and mineral deposits of the File-Tramping Lakes area, Manitoba; Geological Survey of Canada, Memoir 250, 92 p.

Hoffman, P.F. 1988: United plates of America, the birth of a craton: early Proterozoic assembly and growth of Laurentia; Annual Review of Earth and Planetary Sciences, v. 16, p. 543-603.

Kraus, J. and Williams, P.F. 1999: Structural development of the Snow Lake Allocthon and its role in the evolution of the southeastern Trans-Hudson Orogen in Manitoba, central Canada; Canadian Journal of Earth Sciences, v. 36, p. 1881–1899.

Lucas, S.B., Stern, R.A., Syme, E.C., Reilly, B.A. and Thomas, D.J. 1996: Intra-oceanic tectonics and the development of continental crust: 1.92–1.84 Ga evolution of the Flin Flon Belt, Canada; Geological Society of America, Bulletin, v. 108, p. 602–629.

Manitoba Geological Suvey 2022: New edition of the 1:250 000 scale Precambrian bedrock geology compilation map of Manitoba; Manitoba Natural Resources and Northern Development, Manitoba Geological Survey, GeoFile 3-2022, scale 1:250 000, URL <https://manitoba.ca/iem/info/libmin/geofile3-2022.zip> [October 2024].

NATMAP Shield Margin Project Working Group 1998: Geology, NATMAP Shield Margin Project area, Flin Flon belt, Manitoba/Saskatchewan; Geological Survey of Canada, Map 1968A, scale 1:100 000.

Reid, K.D. 2021: Bedrock geology of the Stuart Bay–Chickadee Lake area (east of Wekusko Lake), north-central Manitoba (parts of NTS 63J12, 13); Manitoba Agriculture and Resource Development, Manitoba Geological Survey, Preliminary Map PMAP2021-1, scale 1:15 000, URL <https://manitoba.ca/iem/info/libmin/PMAP2021-1.pdf> [September 2024].

Reid, K.D. 2024: New age constraints for volcanic and plutonic rocks southeast of Wekusko Lake, Manitoba; *in* GAC-MAC-PEG 2024 Brandon Meeting: Abstracts, Volume 47, Geoscience Canada, v. 51, p. 128, URL <https://doi.org/10.12789/geocanj.2024.51.211>.

Rubingh, K., Lafrance, B. and Gibson, H.L. 2020: A reinterpretation of the Snow Lake gold camp, Trans-Hudson Canada: the use of cleavages as markers to correlate structures across deformed terranes; Canadian Journal of Earth Sciences. v. 58, p. 610–639.

Stern, R.A., Syme, E.C., Bailes, A.H. and Lucas, S.B. 1995: Paleoproterozoic (1.90–1.86 Ga) arc volcanism in the Flin Flon belt, Trans-Hudson orogen, Canada; Contributions to Mineralogy and Petrology, v. 119, p. 117–141.

Zwanzig, H.V. and Bailes, A.H. 2010: Geology and geochemical evolution of the northern Flin Flon and southern Kisseynew domains, Kississing–File lakes area, Manitoba (parts of NTS 63K, N); Manitoba Innovation, Energy and Mines, Manitoba Geological Survey, Geoscientific Report GR2010-1, 135 p.

GS2024-12

Research activities at the Lalor mine, Snow Lake, west-central Manitoba (part of NTS 63K16)

by S.M. Ballantyne[1], M. Stewart[2], K.D. Reid, M.O. Anderson[1], C. Venturi[3] and N. Richardson[3]

In Brief:

- New geological studies are underway on the Snow Lake volcanogenic massive ore deposits as part of a doctoral study
- Summer 2024 fieldwork goals were to establish spatial and lithogeochemical relationships between the Lalor and 1901 deposits
- Results of this work will be incorporated into a 3-D geological model

Citation:
Ballantyne, S.M., Stewart, M., Reid, K.D., Anderson, M.O., Venturi, C. and Richardson, N. 2024: Research activities at the Lalor mine, Snow Lake, west-central Manitoba (part of NTS 63K16); *in* Report of Activities 2024, Manitoba Economic Development, Investment, Trade and Natural Resources, Manitoba Geological Survey, p. 98–103.

Summary

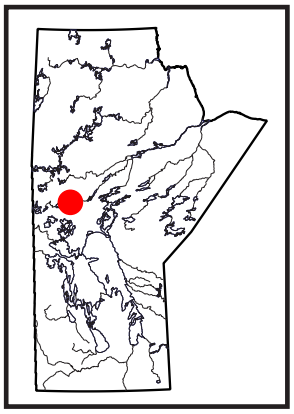
New geological studies on the volcanogenic massive sulphide orebodies of the Snow Lake area are underway as part of a doctoral study investigating the processes, geochemical signatures and resulting architecture of metal and sulphide remobilization in metamorphosed and deformed VMS deposits. This report summarizes the work done to date, with focus on fieldwork conducted in August 2024. The goals of the fieldwork included establishing the spatial relationships of the orebodies of the Lalor and 1901 deposits with hosting and neighbouring lithologies and deposit-scale faults, particularly the inferred Lalor-Chisel fault. Samples were collected for planned geochemical characterization of faults, detailed ore petrological work and geochronological uranium-lead dating. The results of this work will be incorporated into a 3-D geological model.

Introduction

The volcanogenic massive sulphide (VMS) deposits of the Snow Lake district in west-central Manitoba, owned and operated by Hudbay Minerals, have been the subject of many geological and economic studies (e.g., Bailes and Galley, 1999; Caté, 2016; Stewart, 2018). The wealth of base-metal deposits, active mining and mineral exploration, and complex geology with many open questions related to formation and postdepositional events continues to entice researchers pushing the envelope on our understanding of metamorphosed and deformed ancient VMS deposits. The Snow Lake arc assemblage (SLA) provides an ideal case study in understanding the geological controls on primary VMS mineralization and remobilization.

A doctoral study is being undertaken at the University of Toronto, in collaboration with Mount Royal University, the Manitoba Geological Survey and Hudbay Minerals Inc. This project is focused on understanding the processes, geochemical signatures and resulting architecture of metal and sulphide remobilization in metamorphosed and deformed VMS deposits. It seeks to determine the controls on grade and tonnage of mineralization, including primary mineralizing and upgrading processes and post-VMS deposit formation modifications related to metamorphism and deformation. The VMS deposits of the Snow Lake district are ideal case studies for exploring the proposed research questions. These orebodies are typical of ancient, modified VMS deposits, with excellent underground rock exposures and access to drillcore, and a substantial database replete with spatial data and geochemical results. This report summarizes the fieldwork completed in August of 2024, including drillcore stratigraphic logging and sampling, underground mapping and sampling, and surface sampling. Preliminary results are discussed, along with the next steps for this research project.

Geology of the Snow Lake arc assemblage



The Snow Lake arc assemblage (SLA) is part of the eastern Flin Flon belt in the Reindeer zone of the Trans-Hudson orogen in Manitoba (Figure GS2024-12-1). The SLA hosts eight known VMS deposits, interpreted to have formed from a single synvolcanic metalliferous hydrothermal system (Galley et al., 2007). The SLA is divided into the Chisel sequence, a series of mature arc-related volcanic rocks, and the Anderson sequence, which consists of primitive arc-related volcanics (Percival et al., 2004; Corrigan et al., 2009). This research project focuses mainly on the Chisel sequence and the VMS orebodies hosted within it. The Chisel sequence is divided into lower and upper sequences, and the VMS ore interval coincides with the transition between these units, marking a period of volcanic inactivity, subsidence, metal precipitation and ore accumulation (Bailes and Galley, 1996;

[1] Department of Earth Sciences, University of Toronto, Toronto, Ontario
[2] Department of Earth and Environmental Sciences, Mount Royal University, Calgary, Alberta
[3] Hudbay Minerals Inc., Toronto, Ontario

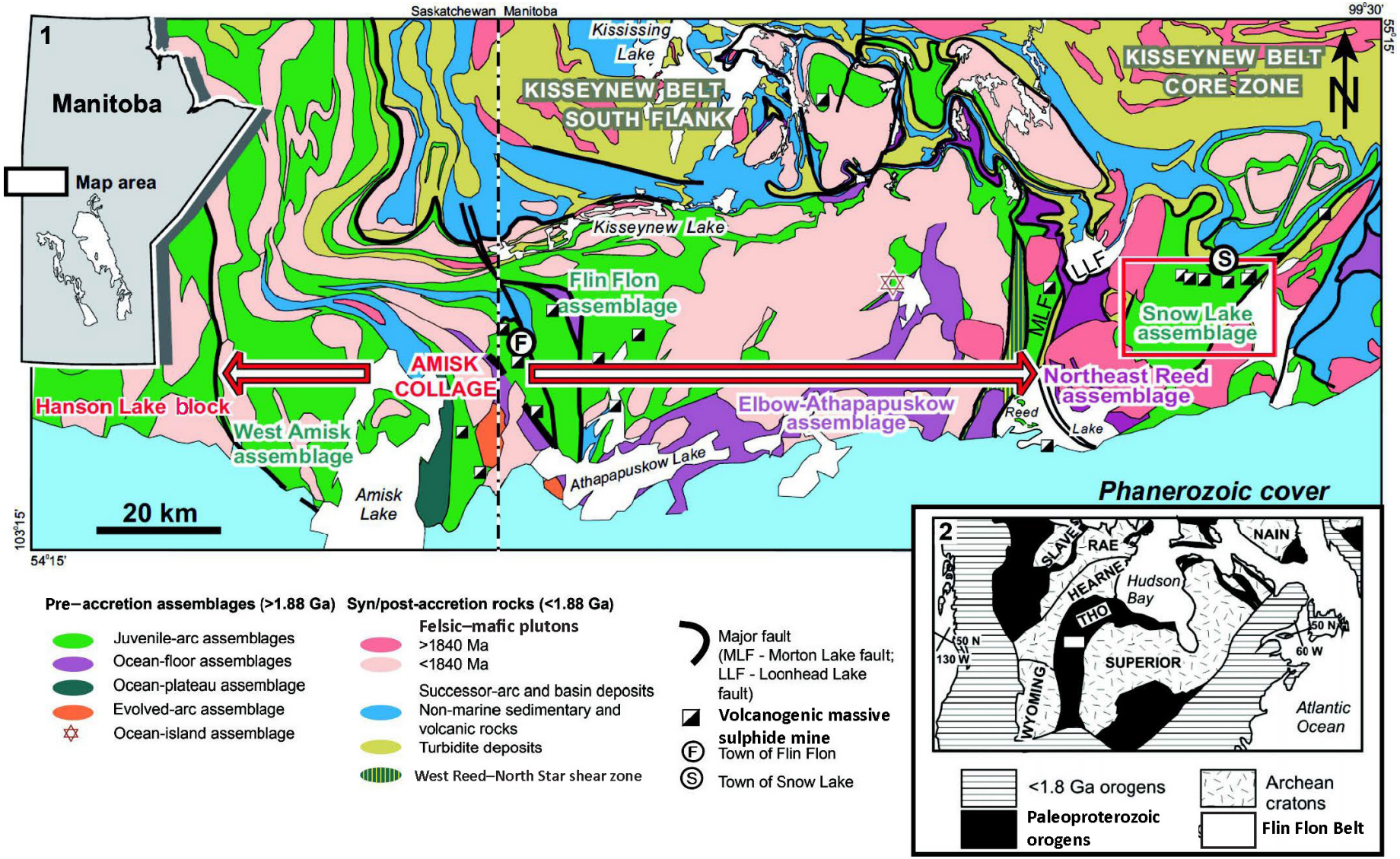


Figure GS2024-12-1: *Tectonostratigraphic assemblages of the Flin Flon Glennie complex, showing the Hanson Lake block in the west, the Amisk collage in the centre and the Snow Lake assemblage in the east. Inset map 1 indicates the map location within the province of Manitoba. Inset map 2 shows the location of the Flin Flon belt within the Trans-Hudson Orogen (modified by Stewart et al, 2018, after Syme et al., 1999).*

1999; Friesen et al, 2021). The rock assemblages and VMS mineralization formed via processes associated with volcanism and related hydrothermal activity as a pericratonic arc outboard of the Superior Craton ca. 1.92–1.88 Ga (David et al., 1996; Lucas et al., 1996; Corrigan et al., 2009). One of the goals of this study is to understand the depositional settings of the VMS ore lenses, comparing differences in the primary alteration, nature of remobilization and metal grades. This study focuses on the Lalor and 1901 deposits, as well as areas distal to these ore lenses at the same stratigraphic level.

Following VMS deposit formation, the SLA underwent four deformation events related to the closure of the Manikewan ocean and the Hudsonian orogen from 1.84 to 1.77 Ga (Kraus and Williams, 1998, 2001; Stewart et al., 2018). Phase equilibrium modelling indicates metamorphic conditions of 550–600°C and 4.5–5.5 kbar in the Snow Lake area (Lazzarotto et al., 2023), or peak almandine-amphibolite facies metamorphism, associated with the second deformation event ca. 1.81 Ga (Menard and Gordon, 1997). The spatial distribution of ore lenses in the SLA is interpreted to be primarily the result of isoclinal folding during transposition and thrust faulting that caused stacking of ore bodies (Caté et al., 2014; Caté, 2016; Stewart et al., 2018). Differentiating between primary and later faults related to accretion of VMS-hosting belts can reveal temporospatial relationships in ore-deposit formation, preservation and modification (Gibson et al., 1999; DeWolfe and Pittmann, 2018; Friesen et al., 2021). Characterizing faults in the SLA and the associations with ore lenses is a primary focus of this study.

2024 Fieldwork

Stratigraphic core logging and drillcore sampling

Preselected sections of five drillholes were stratigraphically logged and a total of 86 intervals were split, sampled and shipped to laboratories at the University of Toronto. The drillcore intersected several district-scale faults and shear zones, and targeted areas believed to intersect the inferred Lalor-Chisel fault (Figure GS2024-12-2). Characterizing this fault has remained elusive, despite numerous studies and its important spatial association to the VMS orebodies hosted in the SLA, which are generally in the footwall of the Lalor-Chisel fault. Orebodies of the 1901 deposit were also sampled, with the goal of comparing differences in metal content and mineral associations, and the nature of deformation (Figure GS2024-12-2a, b, c). The Lalor, 1901 and Chisel ore deposits appear similar in host rock, mineralization and alteration, although additional planned analyses will establish any similarities. Ore petrography of the samples collected from the 1901 deposit will be compared to previous studies on core from the Lalor deposit and from ore samples collected in this study from underground. Drillholes between the 1901 and Lalor deposit were also logged and sampled to aid in understanding the depositional setting distal to hydrothermal activity and the effects of metamorphism and deformation in regions with less alteration and sulphide content.

Underground mapping and sampling

A drift at the 950 level of the Lalor mine was mapped and sampled. This drift intersects several shear zones, metavolca-

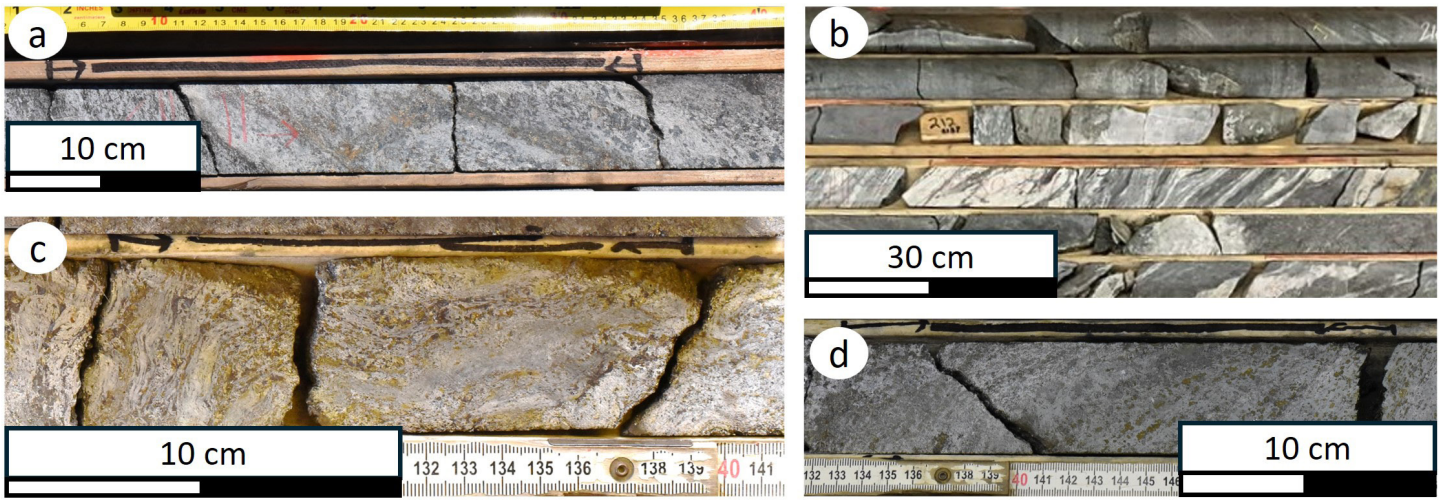


Figure GS2024-12-2: *Examples of the core that was relogged and sampled from Snow Lake, Manitoba; samples were collected and shipped to the University of Toronto for detailed description, petrographic work and additional analytical work:* ***a)*** *from drillhole NUX001, highly deformed sulphides plus gahnite that is likely part of the footwall to the 1901 deposit;* ***b)*** *from drillhole CH1925, shear zone distal to hydrothermal alteration, possibly the Lalor Chisel fault (to be confirmed with additional analyses and integration into the 3-D geological model);* ***c)*** *from drillhole CH1975, deformed and recrystallized sulphides in strongly altered and foliated rocks;* ***d)*** *examples of large grains of recrystallized pyrite and fine layers of deformed sulphides along foliation. Ore petrography on samples such as this, supplemented with electron backscatter diffraction (EBSD), is planned to investigate the timing and element distribution in remobilized sulphides.*

nic lithologies and five ore lenses. The foliation, contacts and shear zones are generally parallel and steeply (60–70 degrees) dipping toward the northeast. This drift runs approximately perpendicular to the strike of these features, allowing the spatial relationships and changes across section to be observed. In total, 19 samples were collected and their structural features recorded (examples shown in Figure GS2024-12-3). Sampling focused on testing variations in metal content through each of the lenses, and characterizing the hangingwall, footwall and deformed central parts of a large shear zone.

Sampling for U-Pb geochronology

Despite several attempts by previous researchers, a robust framework for the ages and duration of the ore-bearing volcanic sequences at Snow Lake has remained elusive, largely due to the low abundance of high-field-strength elements in the volcanic assemblages and the consequent lack of primary zircon (e.g., Stewart, 2018). To date, the only constraints available are from U-Pb zircon ages of two synvolcanic intrusions: Sneath Lake at 1886 +17/–9 Ma and the Richard Lake intrusive complex (RLIC) at 1889 +8/–9 Ma (Bailes et al., 1991). Xenocrystic zircons of the Stroud Lake felsic breccia, at the base of the Chisel sequence, have been dated at 1892 ±3 Ma (David et al., 1996). New surface samples from the RLIC were collected this year, with one targeting the same location as the published data of Bailes et al. (1991), and the other 1 km northeast. The collected RLIC samples are quartz-phyric tonalites (Figure GS2024-12-4). The Manitoba Geological Survey also collected samples for geochronological work during the summer of 2024. The first is a new surface sample of the Sneath Lake tonalite. The second consists of two intervals of core intersecting a relatively fresh gabbro intrusion, the Chisel pluton, thought to postdate volcanism but predate later deformation.

These samples have been sent to the University of Toronto's Jack Satterly Geochronology Laboratory. Under the guidance of Professor M. Hamilton, improved zircon-recovery techniques developed at the Satterly Lab since the last radiometric dating attempts at Snow Lake (methods that have proven highly successful in the Flin Flon district), and application of refined chemical-abrasion techniques in zircon dating for improved accuracy and precision, will be employed. The presence of other accessory phase chronometers (e.g., rutile, titanite, xenotime) will be assessed within selected assemblages to better constrain the thermal history of the district as it relates to the potential ore

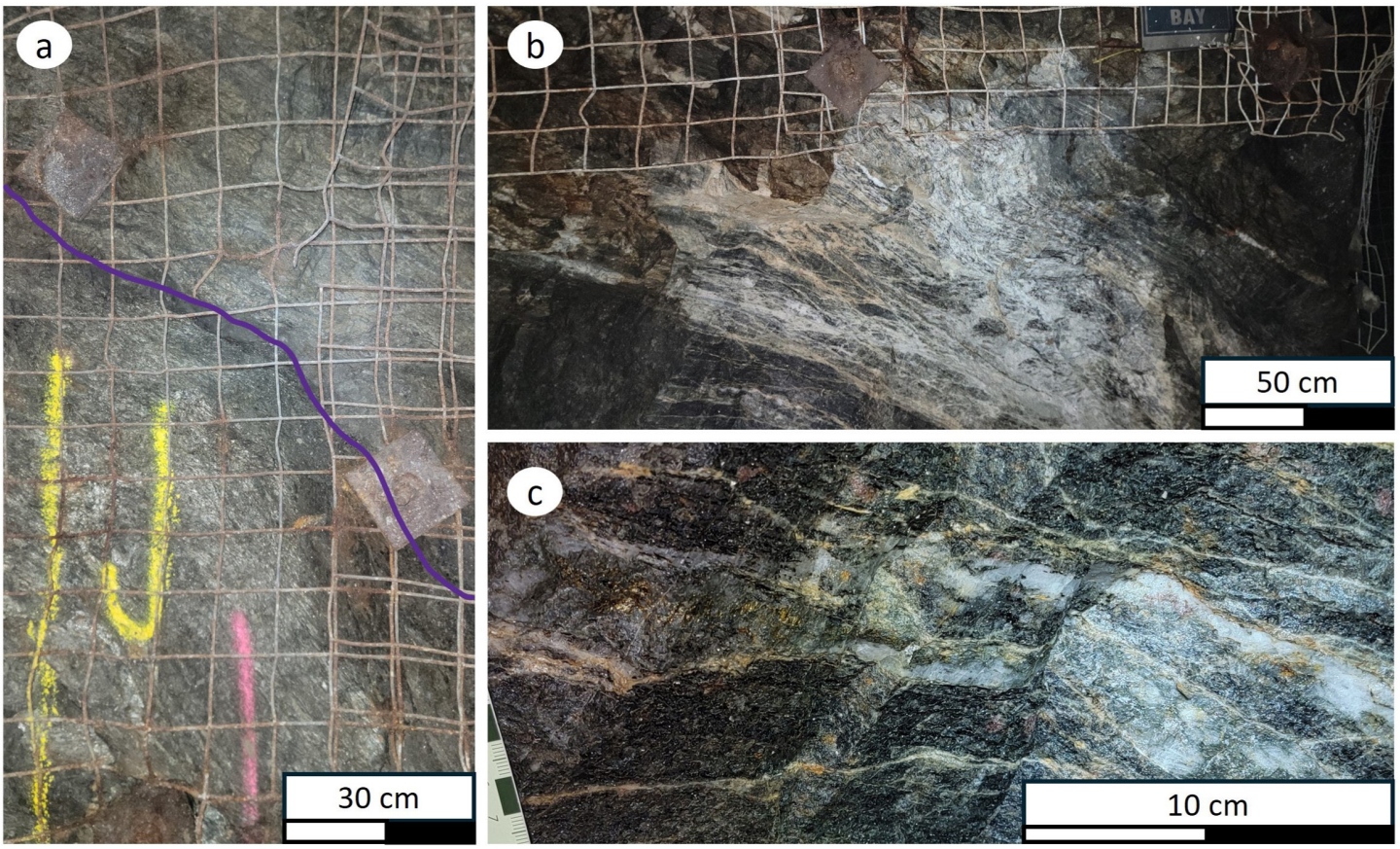


Figure GS2024-12-3: *Examples of the sample locations from a drift on the 950 level at the Lalor mine. Samples were collected and shipped to the University of Toronto for detailed description, petrographic work and additional analytical work:* ***a)*** *looking northwest, a sheared and undulating contact (purple line) between two ore lenses with significantly different metal grades;* ***b)*** *looking northwest, a wide (1–2 m) quartz-healed shear zone within one of the ore lenses; significant sulphide material occurs along the fractures, with evidence of recrystallization;* ***c)*** *close-up of the shear zone from image b, showing the sulphide-filled fractures.*

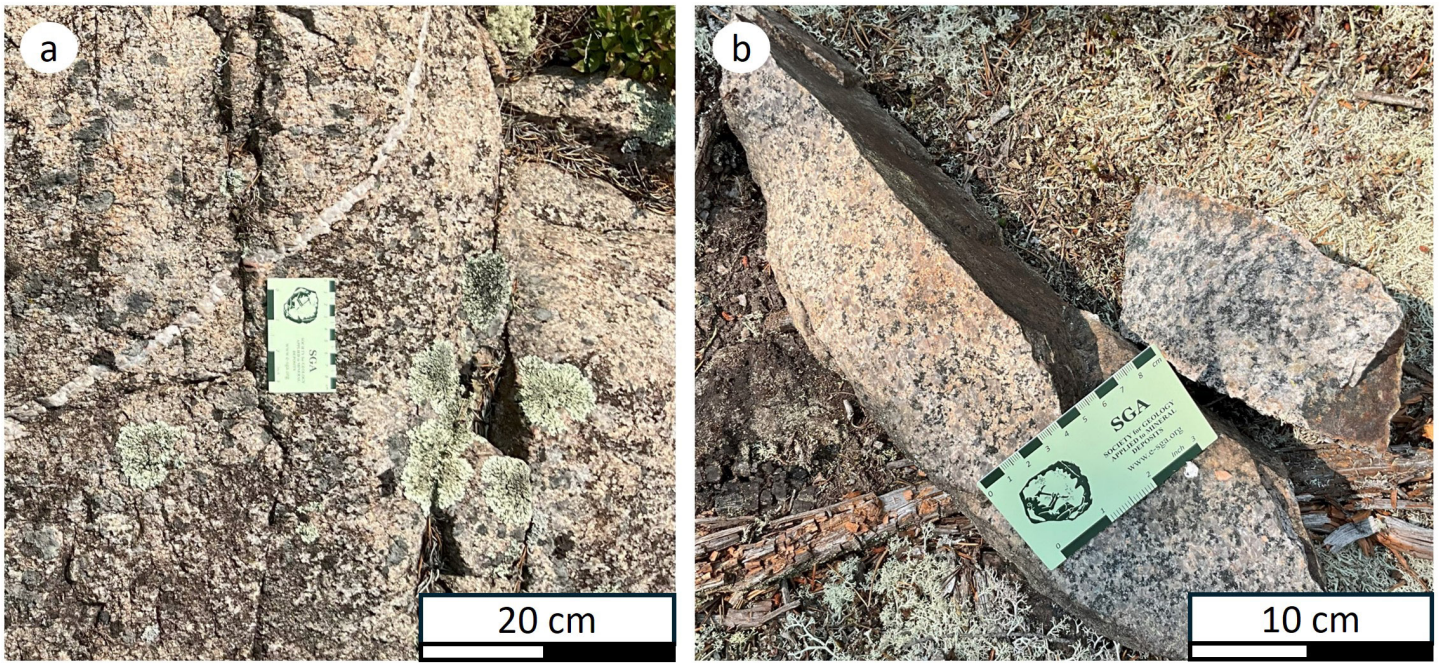


Figure GS2024-12-4: *Surface-sample locations in the Richard Lake intrusive complex, from* ***a)*** *near the existing data from Bailes 1886 +8/-9 Ma (Bailes et al., 1991), and* ***b)*** *1 km northeast of this location. New U-Pb dating may constrain the age of these synvolcanic tonalites.*

remobilization and upgrading process. The goal is to better constrain the existing dates for the RLIC and the Stroud Lake felsic breccia, and determine an age for the Chisel pluton.

Next steps

The 112 rock samples collected in the August 2024 site visit will be described in detail. Samples will be selected for thin-section petrography, and scanning electron microscopy (SEM) will be employed for understanding the gold chemical and mineral associations. Selected samples will be analyzed by electron microprobe and laser-ablation inductively coupled plasma–mass spectrometry (LA-ICP-MS) to examine microscale distributions and associations for gold, with the ultimate goal of linking a paragenetic sequence to primary metal enrichment and postdepositional upgrading and remobilization. Remobilization sequences under varying stress regimes, along with associated mineral and chemical changes, will be determined on some of the ore samples using electron backscatter diffraction (EBSD). The results will be integrated into a new 3-D geological model of the Snow Lake camp, often referred to as the Chisel basin. This geological model will incorporate a large drillcore database with geochemistry, produced by Hudbay Minerals, and new multivariate statistical analyses, with the goal of revealing novel spatial lithogeochemical associations. The findings from this work will verify and constrain the 3-D geological model.

Economic considerations

Volcanogenic massive sulphide deposits are significant sources of base metals, including zinc, copper and lead, as well as precious metals such as gold and silver. The development and deployment of electrified transportation and energy technologies is creating an ever-increasing demand for these metals from safe, reliable sources. The Snow Lake district has undergone continual VMS-related mineral exploration since the 1950s and has had seven producing VMS mines. The currently active Lalor mine produced 8.8 million tonnes of ore between 2012 and 2021 (Tavchandjian, 2021). A new deposit in the Snow Lake area, the 1901, is in currently the development phase. Expanding the understanding of the primary and postdepositional geological controls on spatial distribution, metal concentrations and associations, and of lithogeochemical signatures, could aid in creating new mineral exploration targets for VMS orebodies in the Snow Lake area, as well as other similar lithotectonic settings in Manitoba.

Acknowledgments

The authors thank everyone at the Hudbay exploration offices, Flin Flon core repository and Lalor mine. Special thanks go to J. Vickers for underground support at the Lalor mine. The authors are also grateful to M. Hamilton for guidance with the proposed U-Pb dating work.

References

Bailes, A. and Galley, A. 1996: Setting of Paleoproterozoic volcanic-hosted massive base metal sulphide deposits, Snow Lake; *in* EXTECH 1: A Multidisciplinary Approach to Massive Sulphide Research in the Rusty Lake–Snow Lake greenstone belts, Manitoba, G. Bonham-Carter, A.G. Galley and G.E.M. Hall (ed.), Geological Survey of Canada, Bulletin 426 p. 105–138.

Bailes, A.H. and Galley, A.G. 1999: Evolution of the Paleoproterozoic Snow Lake arc assemblage and geodynamic setting for associated volcanic-hosted massive sulphide deposits, Flin Flon Belt, Manitoba, Canada; Canadian Journal of Earth Sciences, v. 36, p. 1789–1805.

Bailes, A.H., Hunt, P.A. and Gordon, T.M. 1991: U-Pb dating of possible synvolcanic intrusions in the Flin Flon belt at Snow Lake, Manitoba; *in* Radiogenic Age and Isotopic Studies: Report 4, Geological Survey of Canada, Paper 90-2, p. 35–43.

Caté, A. 2016: Geology of the Paleoproterozoic Zn-Cu-Au Lalor volcanogenic massive sulphide deposit and its gold-rich lenses, Snow Lake, Manitoba; Ph.D. thesis, Université du Québec, Montréal, Québec, 384 p.

Caté, A., Mercier-Langevin, P., Ross, P.-S. and Simms, D. 2014: Structural controls on geometry and ore distribution in the Lalor auriferous VMS deposit, Snow Lake, west-central Manitoba (part of NTS 63K16): preliminary results from underground mapping; *in* Report of Activities 2014, Manitoba Mineral Resources, Manitoba Geological Survey, p. 104–115.

Corrigan, D., Pehrsson, S., Wodicka, N. and Kemp, E. 2009: The Palaeoproterozoic Trans-Hudson Orogen: a prototype of modern accretionary processes; Geological Society, London, Special Publications, v. 327, p. 457–479.

David, J., Bailes, A.H. and Machado, N. 1996: Evolution of the Snow Lake portion of the Palaeoproterozoic Flin Flon and Kisseynew belts, Trans-Hudson Orogen, Manitoba, Canada; Precambrian Research, v. 80, p. 107–124.

DeWolfe, Y.M. and Pittman, N. 2018: Subaqueous strombolian eruptions, and eruption-fed pyroclastic deposits in a Paleoproterozoic rifted-arc: Hidden formation, Flin Flon, Canada; Precambrian Research, v. 316, p. 48–65.

Friesen, V.C., DeWolfe, Y.M. and Gibson, H.L. 2021: Volcanic reconstruction and geochemistry of the Powderhouse formation in the Paleoproterozoic VMS-hosting Chisel sequence, Snow Lake, Manitoba, Canada; Canadian Journal of Earth Sciences, v. 58, p. 247–267.

Lazzarotto, M., Pattison, D.R.M., Gagné, S. and Couëslan, C.G. 2023: Metamorphic map of the Flin Flon domain, west-central Manitoba (parts of 63J, K, N, O); Manitoba Economic Development, Investment, Trade and Natural Resources, Manitoba Geological Survey, Geoscientific Paper GP2023-1, 35 p., 3 appendices, 1 map at 1:65 000 scale.

Lucas, S.B., Stern, R.A., Syme, E.C., Reilly, B.A. and Thomas, D.J. 1996: Intraoceanic tectonics and the development of continental crust: 1.92–1.84 Ga evolution of the Flin Flon Belt, Canada; GSA Bulletin, v. 108, p. 602–629.

Galley, A.G., Hannington, M.D. and Jonasson, I.R. 2007: Volcanogenic massive sulphide deposits; *in* Mineral Deposits of Canada: A Synthesis of Major Deposit-Types, District Metallogeny, the Evolution of Geological Provinces, and Exploration Methods, W.D. Goodfellow (ed.), Geological Association of Canada, Mineral Deposits Division, Special Publication No. 5, Ottawa, Ontario, p. 141–161.

Gibson, H.L., Morton, R.L. and Hudak, G.J. 1999: Submarine volcanic processes, deposits, and environments favorable for the location of volcanic-associated massive sulfide deposits; Reviews in Economic Geology, v. 8, p. 16–51.

Kraus, J. and Williams, P.F. 1998: Relationships between foliation development, porphyroblast growth and large-scale folding in a metaturbidite suite, Snow Lake, Canada; Journal of Structural Geology, v. 20, p. 61–76.

Kraus, J. and Williams, P.F. 2001: A new spin on 'non-rotating' porphyroblasts: implications of cleavage refraction and reference frames; Journal of Structural Geology, v. 23, p. 963–971.

Menard, T. and Gordon, T. 1997: Metamorphic P-T Paths from the eastern Flin Flon Belt and Kisseynew Domain, Snow Lake, Manitoba; The Canadian Mineralogist, v. 35, p. 1093–1115.

Percival, J.A., Whalen, J.B. and Rayner, N. 2004: Pikwitonei–Snow Lake, Manitoba transect (parts of NTS 63J, 63O and 63P), Trans-Hudson Orogen–Superior Margin Metallotect Project: initial geological, isotopic and SHRIMP U-Pb results; *in* Report of Activities 2004, Manitoba Industry, Economic Development and Mines, Manitoba Geological Survey, p. 120–134.

Rogers, J.J.W. and Santosh, M. 2002: Configuration of Columbia, a Mesoproterozoic Supercontinent; Gondwana Research, v. 5, p. 5–22.

Stewart, M.S. 2018: The volcanic and deformation history, geodynamic setting, and metallogenesis of the Chisel Sequence, Snow Lake, Manitoba, Canada; Ph.D. thesis, Laurentian University, Sudbury, Ontario, 293 p.

Stewart, M.S. Lafrance, B. and Gibson, H.L. 2018: Early thrusting and folding in the Snow Lake camp, Manitoba: tectonic implications and effects on volcanogenic massive sulfide deposits; Canadian Journal of Earth Sciences, v. 55, p. 935–957.

Syme, E.C., Lucas, S.B., Bailes, A.H. and Stern, R.A. 1999: Contrasting arc and MORB-like assemblages in the Paleoproterozoic Flin Flon Belt, Manitoba, and the role of intra-arc extension in localizing volcanic-hosted massive sulphide deposits; Canadian Journal of Earth Sciences, v. 36, p. 1767–1788.

Tavchandijian, O. 2021: NI 43-101 Technical (NI 43-101) report: Lalor and Snow Lake, Manitoba; Form 43-101F1 technical report prepared by Lalor and Snow Lake Operations, Manitoba, Canada, 200 p., URL <https://s23.q4cdn.com/405985100/files/doc_downloads/tech_reports/canada/Snow-Lake-and-Lalor-NI-43-101-Technical-Report_FINAL.pdf> [May 2024].

GS2024-13

Investigation of volcanic rocks along the eastern margin of the sub-Phanerozoic Thompson nickel belt, central Manitoba (part of NTS 63J3)

by C.G. Couëslan

In Brief:

- Four drillcores were relogged to determine the affinity of volcanic rocks reported by Hudson Bay Exploration and Development during the early 2000s
- A correlation with the Ospwagan group or the Winnipegosis komatiite belt would imply a potential for magmatic Ni-Cu deposits, while a juvenile-arc affinity could suggest a potential for VMS Cu-Zn
- Preliminary observations are largely inconclusive and samples will be submitted for further analytical work

Citation:
Couëslan, C.G. 2024: Investigation of volcanic rocks along the eastern margin of the sub-Phanerozoic Thompson nickel belt, central Manitoba (part of NTS 63J3); *in* Report of Activities 2024, Manitoba Economic Development, Investment, Trade and Natural Resources, Manitoba Geological Survey, p. 104–115.

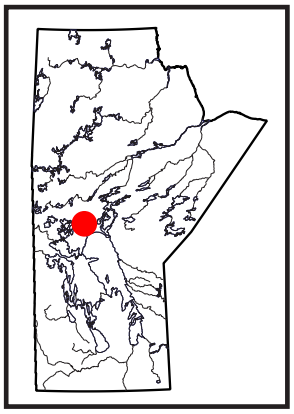
Summary

The geology of Precambrian rocks below the Phanerozoic strata of the Western Canada Sedimentary Basin remains poorly constrained in Manitoba. Several occurrences of volcanic rocks were reported by Hudson Bay Exploration and Development Company Limited (now HudBay Minerals Inc.) geologists during exploration for magmatic nickel-copper deposits along the eastern margin of the sub-Phanerozoic Thompson nickel belt in the early 2000s. The affinity of these volcanic rocks remains unknown. They could be related to the Ospwagan group of the Thompson nickel belt, the volcanic rocks of the Winnipegosis komatiite belt, or juvenile volcanic-arc rocks similar to those of the Tower deposit (located approximately 16 km to the south-southwest). Four drillcores were relogged to determine the affinity of the volcanic rocks. Preliminary observations are largely inconclusive. Samples will be submitted for petrographic thin sections, whole-rock lithogeochemistry, and Sm-Nd isotope geochemistry to help determine their affinity. A correlation with the Ospwagan group or the Winnipegosis komatiite belt would imply a potential for magmatic nickel-copper deposits, whereas a juvenile-arc affinity could suggest a potential for volcanogenic massive sulphide copper-zinc deposits.

Introduction

Exploration of the Precambrian basement underlying the Phanerozoic Western Canada Sedimentary Basin (sub-Phanerozoic) is exceedingly difficult. Exploration methods are entirely dependant on geophysical surveys and diamond drilling. There have been many successes with deposits discovered in the sub-Phanerozoic Flin Flon domain, Kisseynew domain, and Thompson nickel belt (TNB), which include magmatic nickel-copper (Ni-Cu; e.g., Minago and Namew Lake) and volcanogenic massive sulphide (VMS) copper-zinc (Cu-Zn; e.g., Limestone, Reed Lake, Talbot, Tower; Figure GS2024-13-1). Despite these successes, the geology of the sub-Phanerozoic Precambrian remains poorly constrained, with the extent and boundaries of the Flin Flon and Kisseynew domains, and TNB remaining a contentious issue (cf. NATMAP Shield Margin Project Working Group, 1998; Macek et al., 2006; McGregor, 2012; Reid, 2022). In addition, the Tower deposit, which is located along the eastern margin of the sub-Phanerozoic TNB, appears to share affinity with juvenile volcanic-arc rocks of the Trans-Hudson orogen. This suggests that juvenile rocks of the Reindeer zone could be thrust a significant distance east of the current Superior craton margin (Couëslan, 2018).

Several occurrences of volcanic rocks were reported by Hudson Bay Exploration and Development Company Limited (now HudBay Minerals Inc.) geologists during exploration for magmatic Ni-Cu deposits along the eastern margin of the sub-Phanerozoic TNB (Assessment Files 72992, 73174, 73553, 73648 and 94423, Manitoba Economic Development, Investment, Trade and Natural Resources, Winnipeg). The affinity of these volcanic rocks remains unknown. They could be related to the Bah Lake assemblage of the Ospwagan group of the TNB, the volcanic rocks of the Winnipegosis komatiite belt (WKB), or juvenile-arc rocks similar to those of the Tower deposit. A shared affinity with the Bah Lake assemblage or the WKB would imply a potential for magmatic Ni-Cu deposits, whereas a juvenile-arc affinity could suggest a potential for VMS Cu-Zn deposits. Three complete and one partial drillhole from the HudBay Minerals Inc. archives were relogged to determine the affinity of the volcanic rock occurrences. Twenty-two samples were collected for later petrographic, geochemical, and isotopic studies.



Regional geology

The investigated drillholes were collared near the boundary between the TNB and the WKB, and approximately 16 km north-northeast of the Tower deposit (Figure GS2024-13-1).

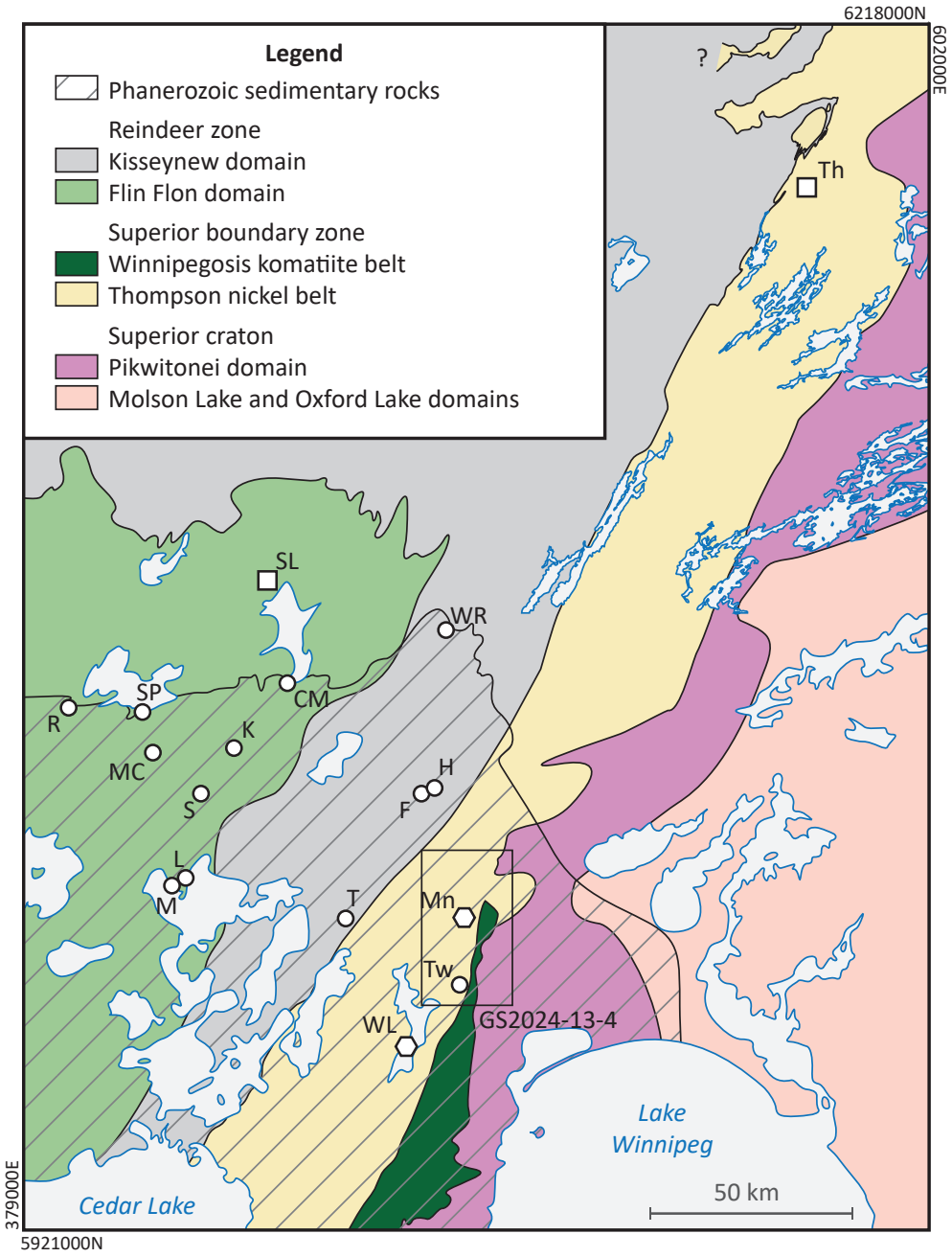


Figure GS2024-13-1: *Geological domains along the Superior boundary zone, central Manitoba (modified from Couëslan, 2020). Squares indicate the locations of towns/cities; circles and hexagons indicate the locations of sub-Phanerozoic volcanogenic massive sulphide deposits and magmatic nickel-copper deposits and occurrences, respectively. Box outlined in black shows location of Figure GS2024-13-4. Abbreviations: CM, Copperman; F, Fenton; H, Harmin; K, Kofman; L, Limestone; M, Moose; MC, McClarty; Mn, Minago; R, Reed; S, Sylvia; SL, Snow Lake; SP, Spruce Point; T, Talbot; Th, Thompson; Tw, Tower; WL, William Lake; WR, Watts River. All co-ordinates are in UTM Zone 14, NAD83.*

Thompson nickel belt (TNB)

The TNB forms a segment of the Superior boundary zone in Manitoba. In the sub-Phanerozoic, it is flanked to the northwest by the Kisseynew domain of the Reindeer zone of the Trans-Hudson orogen, and to the southeast by the WKB of the Superior boundary zone and the Pikwitonei domain of the Superior craton (Figure GS2024-13-1). The TNB is underlain largely by reworked Archean gneiss of the Pikwitonei domain, which is typically quartzofeldspathic, with enclaves of mafic to ultramafic rock. It is commonly migmatitic and characterized by complex internal structures that are the result of multiple generations of Archean and Paleoproterozoic deformation and metamorphism; clearly recognizable paragneiss is rare. The granulites of the Pikwitonei domain were exhumed and unconformably overlain by the Paleoproterozoic supracrustal rocks of the Ospwagan group (TNB) prior to intrusion of the Molson dike swarm and associated Ni-bearing ultramafic intrusions at ca. 1883 Ma (Bleeker, 1990; Zwanzig et al., 2007; Heaman et al., 2009; Scoates et al., 2017).

The Archean basement gneiss and Ospwagan group were subjected to multiple generations of deformation and metamorphic conditions, ranging from middle-amphibolite to lower-granulite facies, during the Trans-Hudson orogeny (Bleeker, 1990; Burnham et al., 2009; Couëslan and Pattison, 2012).

The dominant phase of penetrative deformation is D_2, which affected the Ospwagan group and ca. 1883 Ma magmatic rocks. This deformation phase resulted in the formation of F_2 nappe structures, which incorporated the underlying Archean gneiss. The nappe structures have been interpreted as either east verging (Bleeker, 1990; White et al., 2002) or southwest verging (Zwanzig et al., 2007; Burnham et al., 2009). The recumbent folds are associated with regionally penetrative S_2 fabrics. The D_2 phase of deformation is interpreted as the result of ca. 1830 to 1800 Ma convergence between the Superior craton margin and the Reindeer zone, and was accompanied, and outlasted, by prograde to peak regional metamorphism. The D_3 phase of deformation resulted in isoclinal folds with vertical to steeply southeast-dipping axial planes (Bleeker, 1990; Burnham et al., 2009). Mylonite zones with subvertical stretching lineations parallel many of the regional F_3 folds. Tightening of D_3 structures continued during D_4 deformation, and is characterized by localized retrograde greenschist metamorphism along northeast-striking, mylonitic, and cataclastic shear zones that commonly record southeast-side-up sinistral movement (Bleeker, 1990; Burnham et al., 2009).

Ospwagan group stratigraphy

The following summary of the Ospwagan group is sourced largely from Bleeker (1990) and Zwanzig et al. (2007). The Paleoproterozoic Ospwagan group unconformably overlies Archean basement gneiss in the TNB (Figure GS2024-13-2). The lowermost unit of the Ospwagan group is the siliciclastic Manasan forma-

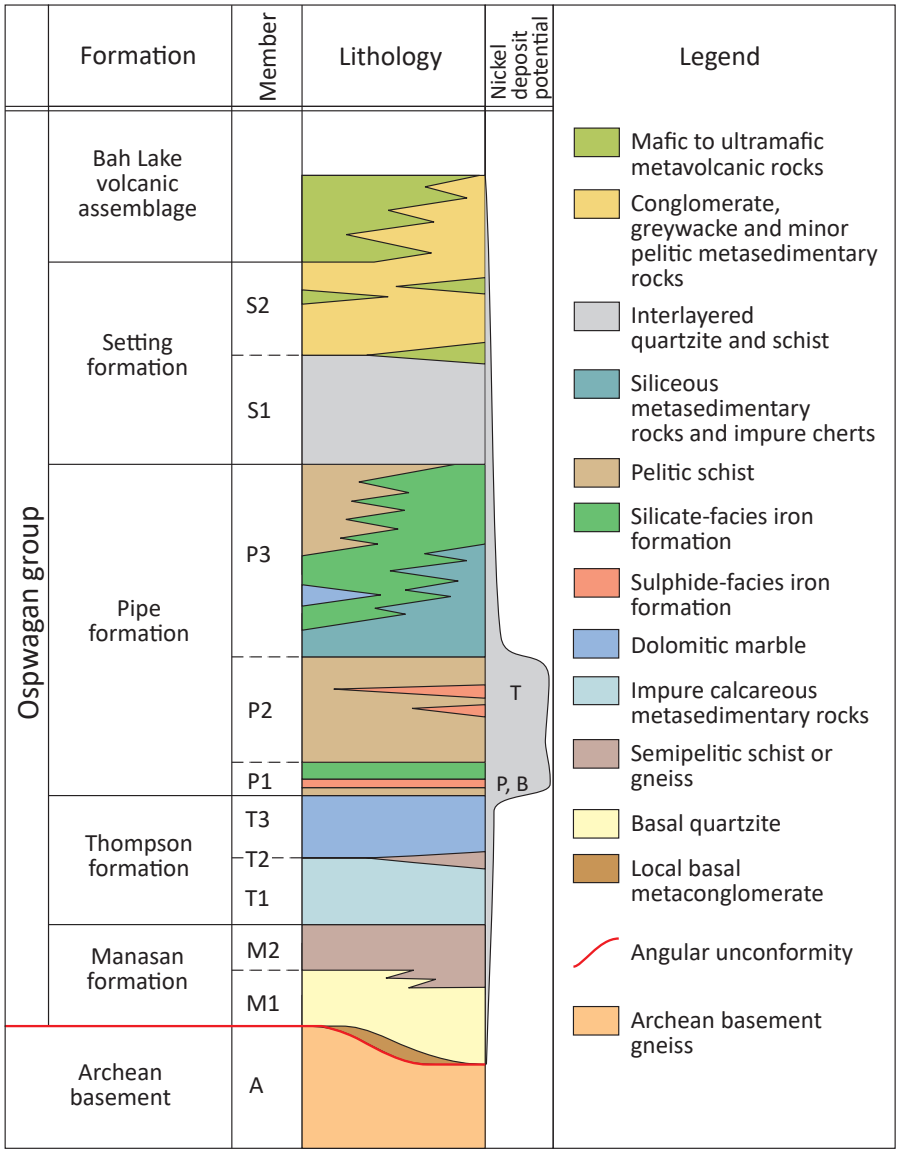


Figure GS2024-13-2: *Schematic lithostratigraphic section of the Ospwagan group (modified from Bleeker, 1990). Abbreviations: B, stratigraphic location of the Birchtree orebody; P, stratigraphic location of the Pipe II orebody; T, stratigraphic location of the Thompson orebody.*

tion, which fines upward from quartzite at the base to semipelite at the top. This siliciclastic system grades into the overlying calcareous sedimentary rocks of the Thompson formation. The Thompson formation consists of a variety of calcareous–siliceous rocks including chert, calcsilicate, and impure marble. It becomes increasingly calcareous toward the top and represents a transition from a siliciclastic-dominated to a carbonate-dominated system. The Manasan and Thompson formations are interpreted to represent a passive-margin sequence along the margin of the Superior craton.

The Pipe formation consists of a variety of pelitic and chemical sedimentary rocks including chert, iron formations, calcsilicate, and marble. Sulphidic rocks within the Pipe formation are the locus of the ore bodies at the Pipe II, Birchtree, and Thompson mines. The Pipe formation represents a mix of chemical sediments and fine to very fine siliciclastics that were deposited in either an open-marine environment (Zwanzig et al., 2007) or during the development of a foredeep basin (Bleeker, 1990).

The Setting formation represents a return to coarser clastic deposits. It consists of rhythmically interbedded quartzite and pelitic schist, thickly layered greywacke, and local beds grading from conglomeratic at the base to pelitic at the top. The Setting formation is interpreted to have been deposited by turbidity currents in a relatively deep marine environment, and may represent axial sedimentation within a foredeep basin (Bleeker, 1990) or possibly the onset of active tectonism and shallowing of the basin (Zwanzig et al., 2007).

At the top of the Ospwagan group is the Bah Lake assemblage, which consists of mafic to ultramafic volcanic rocks dominated by massive to pillowed basalt flows, with local picrite and minor synvolcanic intrusions. The Bah Lake assemblage is dominated by a high-Mg suite (similar to normal mid-ocean–ridge basalt; N-MORB) that occurs throughout much of the main TNB, and an incompatible-element–enriched suite (similar to enriched mid-ocean–ridge basalt; E-MORB) that occurs in the northwestern Setting Lake area and along the margin of the Kisseynew domain (Zwanzig, 2005). The enriched suite is interpreted to overlie the high-Mg suite; however, it is uncertain if this represents a stratigraphic or tectonic relationship. The Bah Lake assemblage could represent the onset of active rifting in the TNB (Zwanzig, 2005; Zwanzig et al., 2007) or magmatic activity within the foredeep (Bleeker, 1990).

Winnipegosis komatiite belt (WKB)

The WKB occurs along the eastern side of the sub-Phanerozoic Superior boundary zone in the Lake Winnipegosis–Cedar Lake area (Figure GS2024-13-1). It forms a 150 by 30 km greenstone belt adjacent to the TNB and occurs under 150–500 m of Phanerozoic cover (Hulbert et al., 1994; Pearson, 1996). Initially misidentified as Ospwagan group rocks, the mafic to ultramafic volcanic rocks of the WKB are distinctly younger (ca. 1870 Ma) than the volcanic rocks of the Ospwagan group (ca. >1890 Ma; Zwanzig, 2005; McGregor, 2012; Waterton et al., 2017). The WKB is subdivided into three volcanic packages: the western upper tholeiite suite, the central Winnipegosis komatiite suite, and the eastern Grand Island tholeiite suite (Figure GS2024-13-3; Lin et al., 1998; McGregor, 2012). Contacts between the three suites were initially interpreted as thrust faults; however, the contact between the Grand Island tholeiite suite and the Winnipegosis komatiite suite was later interpreted as stratigraphic by Cominco Ltd. geologists (Lucas et al., 1996). Little is known about the two tholeiite suites, which are characterized by indistinguishable MORB-like trace-element profiles. They could represent separate sequences derived from a similar magmatic source or they could represent thrust repetitions (Carlson, 2017).

The three supracrustal suites form a west-facing homoclinal sequence that rests unconformably on weathered Superior craton tonalite to granodiorite (Lin et al., 1998; McGregor, 2012). The sequence consists of a thin, discontinuous interval of tonalite-derived basal conglomerate and sandstone (Lucas et al., 1996; Waterton et al., 2017). This is overlain by a package of Fe-tholeiite flows <1 km thick, with thick sulphidic argillite interflow horizons (Grand Island tholeiite suite). The tholeiites are overlain by a sequence of clastic and chemical sedimentary rocks <500 m thick, which are dominantly carbonate at the base and become increasingly shale rich at the top, indicating a subsiding basin. The sedimentary rocks are overlain by a thick succession (<1 km) of komatiite that varies from thin sheet flows to ponded cumulate horizons (Winnipegosis komatiite suite). One drillhole intersected a basaltic sequence along the western margin of the WKB, which is referred to as the upper tholeiite suite. Gabbro and peridotite–dunite bodies intrude all of the above units (Pearson, 1996; McGregor, 2012). The overall stratigraphy of the WKB remains largely unknown.

Rocks of the WKB are characterized by subgreenschist- to greenschist-facies metamorphic assemblages (Waterton et al., 2017) and appear to extend northward to where komatiites of similar low-metamorphic grade are recognized east of the William Lake area (Lin et al., 1998). Recent studies suggest the komatiitic magmas were generated by a mantle plume deflected toward the margins of the Superior craton by a thick lithospheric keel and were emplaced within an evolving rift environment (Ciborowski et al., 2017; Waterton et al., 2017). The nature of the boundary between the TNB and WKB remains uncertain, but is assumed to be a fault (Lin et al., 1998).

Tower deposit

The following summary of the Tower deposit is sourced from Couëslan (2018). Tower is a juvenile-arc–hosted VMS deposit situated along the eastern margin of the sub-Phanerozoic TNB, close to the boundary with the WKB (Figure GS2024-13-1). The deposit is hosted in a sequence of variably altered mafic to felsic metavolcanic rocks, now represented by a variety of amphibolites, gneisses, and schists with middle-amphibolite–facies

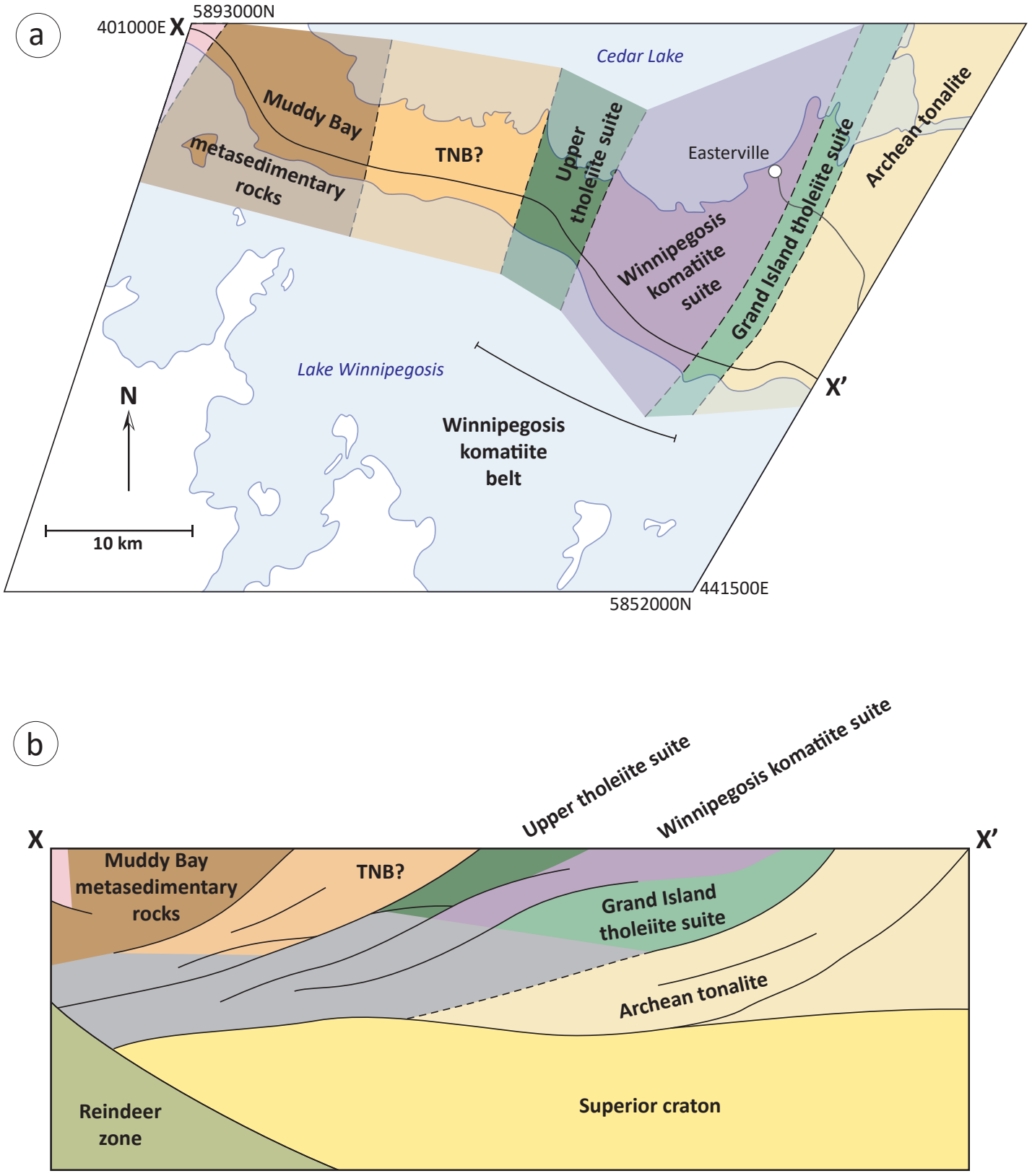


Figure GS2024-13-3: *Interpreted geology of the sub-Phanerozoic Superior boundary zone in the Lake Winnipegosis–Cedar Lake area of central Manitoba:* ***a)*** *map modified from Lucas et al. (1996);* ***b)*** *schematic interpretation of seismic data from LITHOPROBE transect S3B (line X–X'; adapted from Lucas et al., 1996; White et al., 2002). All co-ordinates are in UTM Zone 14, NAD83.*

assemblages. Lithogeochemistry suggests the sequence is dominantly mafic, with subordinate intermediate and felsic rocks. Zones of intense VMS-related hydrothermal alteration occur as muscovite-biotite, biotite-garnet, cummingtonite, and heterogeneous chlorite schists. The stratigraphy is intruded by mafic to ultramafic intrusions, and a juvenile granodiorite intrusion is present in the structural hangingwall to the deposit. The presence of felsic volcanic rocks with FII–FIIIa rhyolite geochemistry, local mafic rocks with boninitic affinity, and ultramafic rocks is suggestive of a rifted-arc environment. The rocks hosting the Tower deposit likely formed in an island-arc environment, within the Manikewan Ocean basin, at an unknown distance from the Superior craton margin. These juvenile-arc rocks were likely thrust onto the Superior craton during the Trans-Hudson orogeny and preserved as a klippe, or erosional remnant, approximately 30 km east (inboard) of the present-day craton margin.

Drillcore

Three complete drillholes and one partial drillhole that were collared near the boundary between the TNB and WKB, and roughly 16 km along strike from the Tower VMS deposit, were relogged. The drillholes were located on the compilation map of Macek et al. (2006) as an initial screening of the geological setting (Figure GS2024-13-4). Drillhole MRO-005 is interpreted to be within the TNB, in a region underlain by undivided Archean and Ospwagan group rocks. Farther north within the TNB, drillhole NIM-068 may be underlain by rocks of the Bah Lake volcanic assemblage. Drillholes MRO-006 and MRO-007 are located within the WKB, in a region underlain by mafic to ultramafic volcanic rocks and ultramafic intrusions. Thicknesses presented below are intersection widths, not true thickness. All Precambrian rocks in the drillcore are metamorphosed; however, the 'meta' prefix has been omitted for clarity.

Thompson nickel belt

MRO-005

The top of the Precambrian rocks in drillhole MRO-005 consists of 19 m of variably weathered ultramafic schist, which consists largely of clay, carbonate, chlorite, and pale green amphibole (Figure GS2024-13-5a). This is underlain by a 59 m intersection of interlayered pelite and iron formation (Figure GS2024-13-5b). The pelite forms beds <19 m thick, which are typically strongly foliated and well laminated. Local dark laminations are likely carbonaceous. Peak metamorphic assemblages contain quartz, plagioclase, muscovite, biotite, garnet, and staurolite, which is typical of the middle-amphibolite facies; however, much of the interval is retrogressed to weathered, with mafic minerals replaced by chlorite, clays, and iron oxides, and plagioclase replaced by epidote and clays. The pelite grades into a muscovite- and biotite-bearing siliceous sediment toward the bottom 5 m of the interval. The iron formation forms beds <8 m thick that are well layered to laminated and vary from strongly magnetic oxide- to nonmagnetic silicate-facies assemblages. Although garnet is typically well preserved, the remainder of iron-rich silicates are typically retrogressed to dark green chlorite or altered to brown clays. Preserved grunerite is relatively rare.

The pelite-iron formation package is underlain by a 3 m layer of graphitic and sulphidic schist (black shale). This is followed by 55 m of mafic volcanic rocks interbedded with subordinate impure chert and black shale (Figure GS2024-13-5c). The mafic volcanic rocks consist of relatively homogeneous amphibolite layers that likely represent massive flows or dikes, alternating with biotite-bearing, laminated beds that likely represent mafic tuff or possibly sheared flows. The impure chert occurs as well-laminated beds <4.5 m thick. It ranges from hornblende and biotite rich, with minor grunerite and garnet, to very siliceous, with minor amphibole and biotite. Although tentatively identified as impure chert, this unit could alternatively represent intermediate to felsic tuffaceous material. The black shale can occur as discrete layers within the basalt or in association with, and grading into, the impure chert.

The stratigraphy in MRO-005 could be interpreted as Pipe formation pelite and iron formation followed downhole by Bah Lake volcanic assemblage rocks, which would require that the stratigraphy is overturned (Figure GS2024-13-2). However, in this scenario Setting formation rocks are absent and seemingly replaced by black shale, which would indicate a detritus-starved basin. This would be in contrast with the high rates of sedimentation interpreted for the turbidite-derived Setting formation in the exposed parts of the TNB. In addition, the presence of interflow impure chert (or intermediate to felsic tuff) and black shale units is not typical of Bah Lake volcanic assemblage rocks in the exposed portions of the TNB. Black shale, or sulphidic argillite, is reported as thick interflow units associated with Fe-tholeiitic basalt in the Grand Island suite (McGregor, 2012). Iron formation and 'argillite' were also reported from a drillhole in the southern WKB, along strike from the Grand Island suite (Lin et al., 1998). However, the sequence in MRO-005 is metamorphosed to much higher grades than reported elsewhere for the WKB (typically subgreenschist to greenschist facies).

NIM-068

The Precambrian stratigraphy in drillcore NIM-068 begins with 9 m of variably weathered mafic volcanic rocks, followed by 155.5 m of basalt, with rare granitic pegmatite intrusions <1 m wide. The basalt varies from dark green and hornblende rich (Figure GS2024-13-5d) to grey-green, with minor hornblende and abundant tremolite and anthophyllite (Figure GS2024-13-5e). The lighter coloured layers become more abundant downhole and likely represent more magnesian bulk compositions. Local layers of well-laminated, biotite-bearing mafic tuff occur at the bottom of the interval and are <5 m thick. A 1.5 m mylonite zone is present approximately 110 m into the interval.

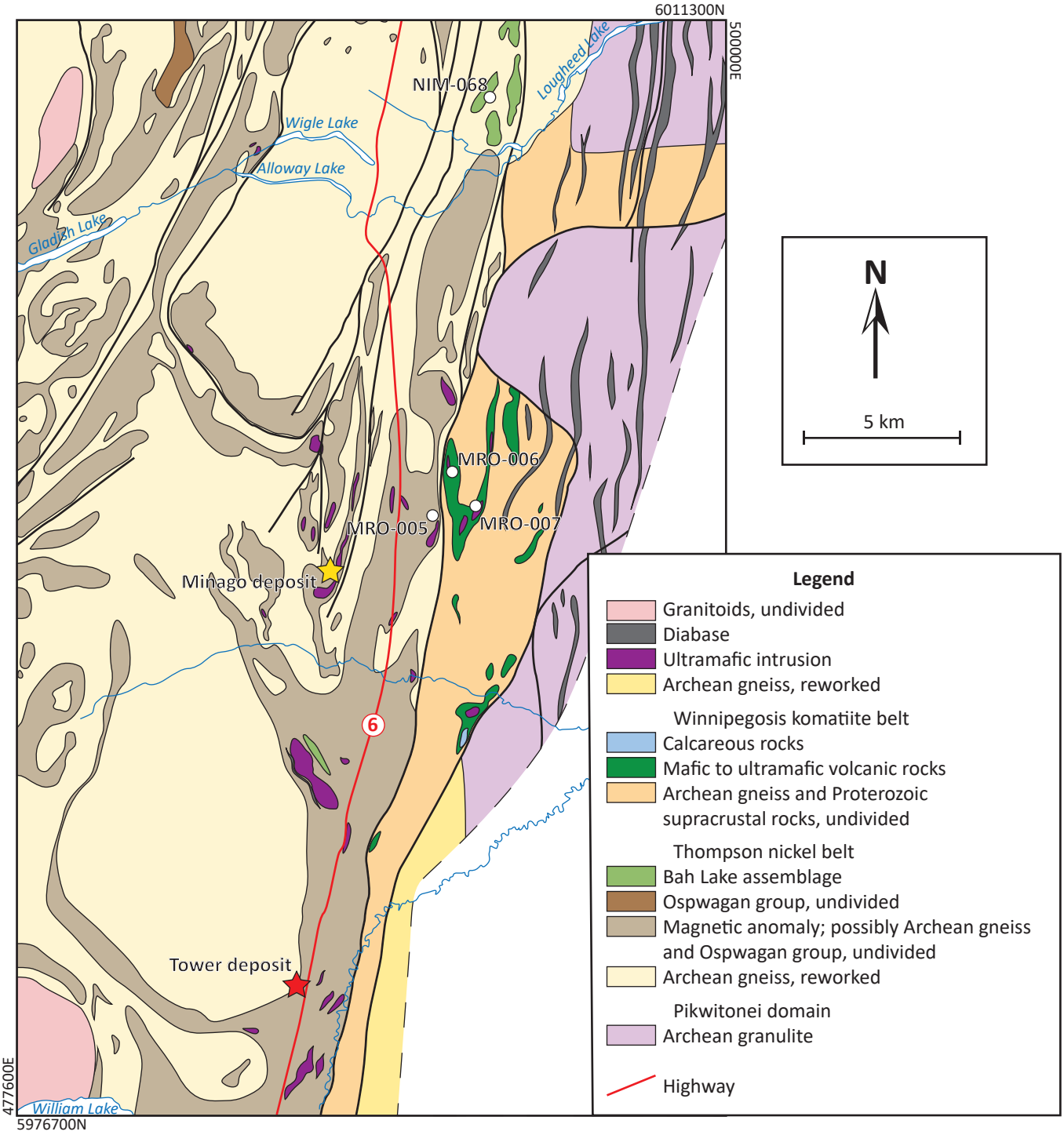


Figure GS2024-13-4: *Geology of the sub-Phanerozoic Thompson nickel belt in the Minago River area (modified from Macek et al., 2006). Circles indicate the locations of drillholes from this study; the red star indicates a volcanogenic massive sulphide deposit and the yellow star indicates a magmatic-nickel deposit. All co-ordinates are in UTM Zone 14, NAD83.*

The basalt is followed by a 15 m interval of peridotite that consists dominantly of serpentine, with minor anthophyllite and magnetite (Figure GS2024-13-5f). The peridotite contains local zones of ultramafic schist <2.5 m wide. The ultramafic schist typically consists of anthophyllite, with minor phlogopite; however, it can grade toward almost solid phlogopite. The peridotite is followed by 31 m of basalt grading into high-Mg basalt and mafic tuff toward the end of the interval. This is followed by a 4 m interval of graphite breccia, which consists of mafic tuff clasts in a matrix of graphite±subordinate pyrrhotite. The breccia varies from clast supported to matrix supported.

Underlying the breccia is an 18 m interval of picrite and mafic tuff interlayered on a scale <1.5 m (Figure GS2024-13-5g). The picrite is similar to the high-Mg basalt, but it is characterized

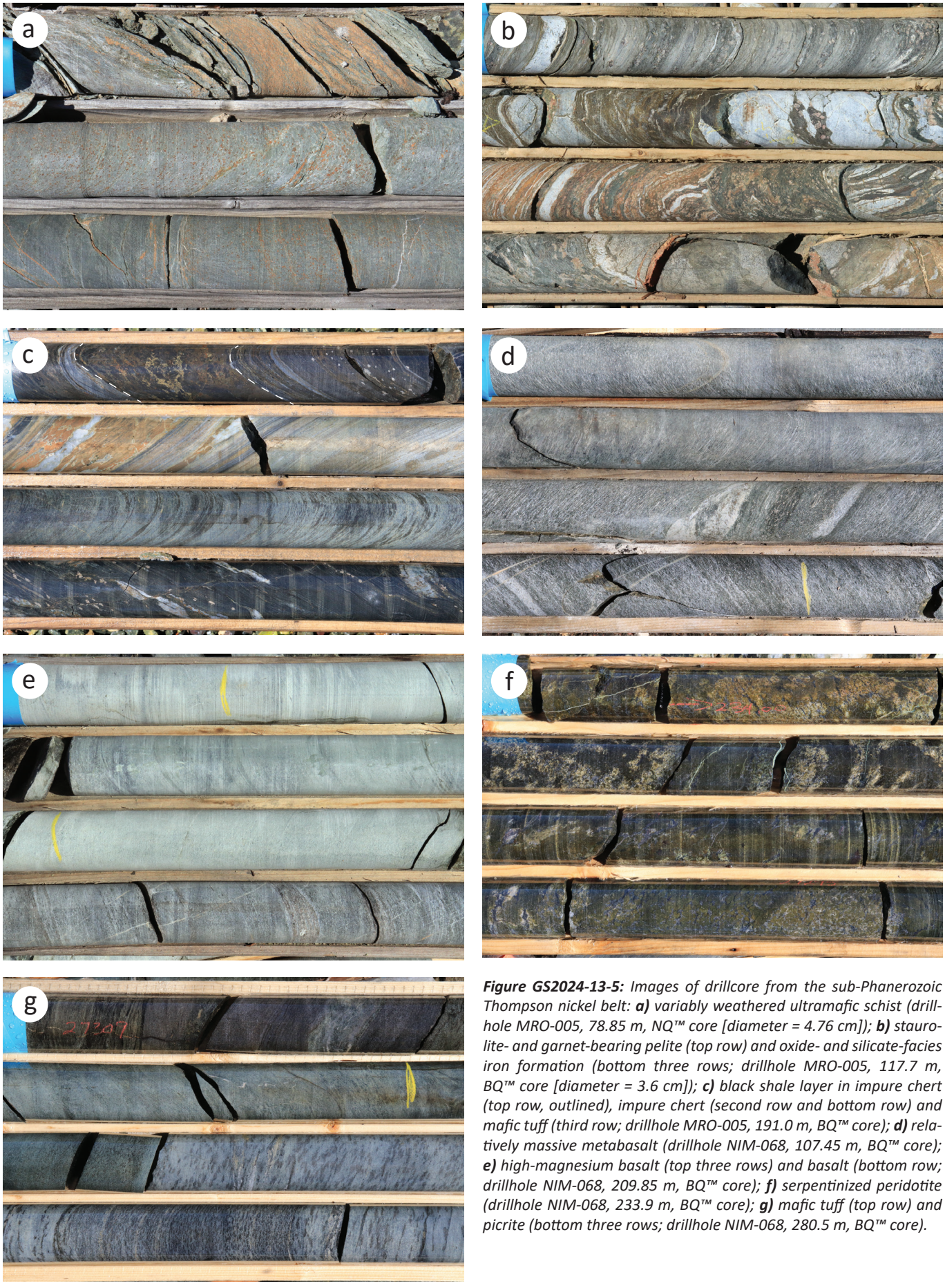


Figure GS2024-13-5: *Images of drillcore from the sub-Phanerozoic Thompson nickel belt:* ***a)*** *variably weathered ultramafic schist (drillhole MRO-005, 78.85 m, NQ™ core [diameter = 4.76 cm]);* ***b)*** *staurolite- and garnet-bearing pelite (top row) and oxide- and silicate-facies iron formation (bottom three rows; drillhole MRO-005, 117.7 m, BQ™ core [diameter = 3.6 cm]);* ***c)*** *black shale layer in impure chert (top row, outlined), impure chert (second row and bottom row) and mafic tuff (third row; drillhole MRO-005, 191.0 m, BQ™ core);* ***d)*** *relatively massive metabasalt (drillhole NIM-068, 107.45 m, BQ™ core);* ***e)*** *high-magnesium basalt (top three rows) and basalt (bottom row; drillhole NIM-068, 209.85 m, BQ™ core);* ***f)*** *serpentinized peridotite (drillhole NIM-068, 233.9 m, BQ™ core);* ***g)*** *mafic tuff (top row) and picrite (bottom three rows; drillhole NIM-068, 280.5 m, BQ™ core).*

by abundant flattened porphyroblasts of serpentinized olivine <5 mm across. This interval is intruded by a 4.5 m dike of grey, medium-grained biotite granite that contains trace amounts of garnet. The drillcore terminates in a 16 m interval of similar granite; however, it varies from grey to pink and contains local pegmatitic zones <40 cm thick.

The stratigraphy of drillcore NIM-068 consists almost entirely of mafic volcanic rocks, which makes interpreting the affinity difficult from hand sample observations alone. It is tentatively correlated with the Bah Lake assemblage, which is known to contain similar picritic rocks.

Winnipegosis komatiite belt

MRO-006

The top of the Precambrian rocks in drillcore MRO-006 consists of 32 m of relatively pure, grey to beige quartzite. The quartzite is foliated to mylonitic and contains trace amounts of oxide(s), minor amounts of intensely weathered feldspar, and minor zones of hematite staining (Figure GS2024-13-6a). The quartzite is relatively homogeneous, with local dark layers <5 cm thick that contain trace amounts of sulphide and biotite or chlorite. The quartzite is underlain by 106 m of dark green and variably sheared basalt (Figure GS2024-13-6b). The basalt is actinolite rich, with subordinate feldspar and local biotite. It is discontinuously layered on a scale <20 cm. Several metasomatized and sheared zones <2 m wide consist of a strongly foliated to protomylonitic, biotite-rich rock with local veinlets of quartz±feldspar (Figure GS2024-13-6c). Regularly spaced biotite-rich layers in lower strain basalt could represent pillow selvages. Toward the bottom of the interval, the basalt contains wispy epidote+quartz pods <2 cm thick and local carbonate veins <2 cm thick.

Strongly sheared granite intervals <26 m thick intrude the basalt and the basalt-quartzite contact. The granite is grey-brown to orange-green, protomylonitic to mylonitic, and consists of 30–40% quartzofeldspathic fragments <2 cm thick in a fine-grained biotite+quartz+feldspar matrix. The sheared granite contains local zones of hematization and chloritization, and (Fe-?) carbonate alteration. A single 14 m interval of sheared, garnet-bearing and biotite-rich quartzofeldspathic rock occurs toward the middle of the Precambrian section, and is bounded on both sides by sheared granite (Figure GS2024-13-6d). The rock is relatively homogeneous and could represent an interval of wacke, or possibly metasomatized basalt.

The affinity of the stratigraphy of drillcore MRO-006 is difficult to constrain because of its limited variability. The presence of quartzite in contact with mafic volcanic rocks could correlate with the Setting formation–Bah Lake assemblage transition in the Ospwagan group (Figure GS2024-13-2); however, the Setting formation quartzite is typically interlayered with pelite, which is not observed. Hornblende was not identified in hand sample, which could indicate greenschist-facies metamorphic assemblages typical of the WKB; however, confirmation of this observation requires further petrographic studies. Pure quartzite is not described from any part of the WKB stratigraphy.

MRO-007

The top of the Precambrian stratigraphy in drillcore MRO-007 consists of 11 m of regolith and intensely weathered basalt. This is followed by 58 m of ultramafic schist, with minor peridotite as intersections <7.5 m thick. The schist is silvery grey-brown and contains tan-weathering carbonate±serpentine pseudomorphs of olivine in a fine-grained groundmass of talc±anthophyllite (Figure GS2024-13-6e). The peridotite consists of serpentine with minor anthophyllite. Relict cumulate textures are locally preserved. Both the schist and the peridotite are strongly magnetic, with very fine-grained magnetite occurring in their respective groundmass.

The ultramafic rocks are followed by 150 m of basalt. The basalt occurs as fine-grained heterogeneous amphibolite that is plagioclase and actinolite rich, with minor hornblende. Local, coarse-grained homogeneous zones <9.5 m thick likely represent gabbro intrusions (Figure GS2024-13-6f). Sparse homogeneous zones grade into fine-grained amphibolite, which suggests they could represent massive flows. The amphibolite is discontinuously layered to laminated in places. The bottom 3.5 m of the unit is well laminated, which suggests it could represent a mafic tuff or strongly sheared basalt. The upper 3 m of the basalt, immediately below the ultramafic rocks, is brecciated, with locally intense veining of orange-weathering carbonate with or without a black acicular mineral that could be tourmaline.

The basalt is followed by 3 m of silicate-facies iron formation (Figure GS2024-13-6g). The iron formation is layered to laminated, with local chert beds up to 10 cm thick. Ferruginous layers are grunerite and biotite rich, with minor magnetite and trace amounts of sulphide. Below the iron formation is a 43 m interval of white to light grey quartzite. The quartzite is relatively pure, with trace amounts of muscovite, biotite, sulphide, and <7% feldspar. The rock is massive to thickly bedded, with local pyrite-rich laminations and dark laminations that likely contain biotite±sulphide±graphite. The quartzite becomes interlaminated with pelite over the last 40 cm of the interval (Figure GS2024-13-6h). The pelite is muscovite rich, with local brown-pink garnets. The remaining 265 m of core from this drillhole was unavailable at the time of logging.

The stratigraphic sequence in drillcore MRO-007 of basalt to iron formation to quartzite does not correlate well with the Ospwagan group (Figure GS2024-13-2). Moreover, a sequence containing iron formation and relatively pure quartzite is not described from any part of the WKB stratigraphy. In addition, the presence of hornblende within the basalt suggests a metamorphic assemblage transitional into the amphibolite facies, which would represent a higher metamorphic grade than previously interpreted for the WKB. It should be emphasized that the

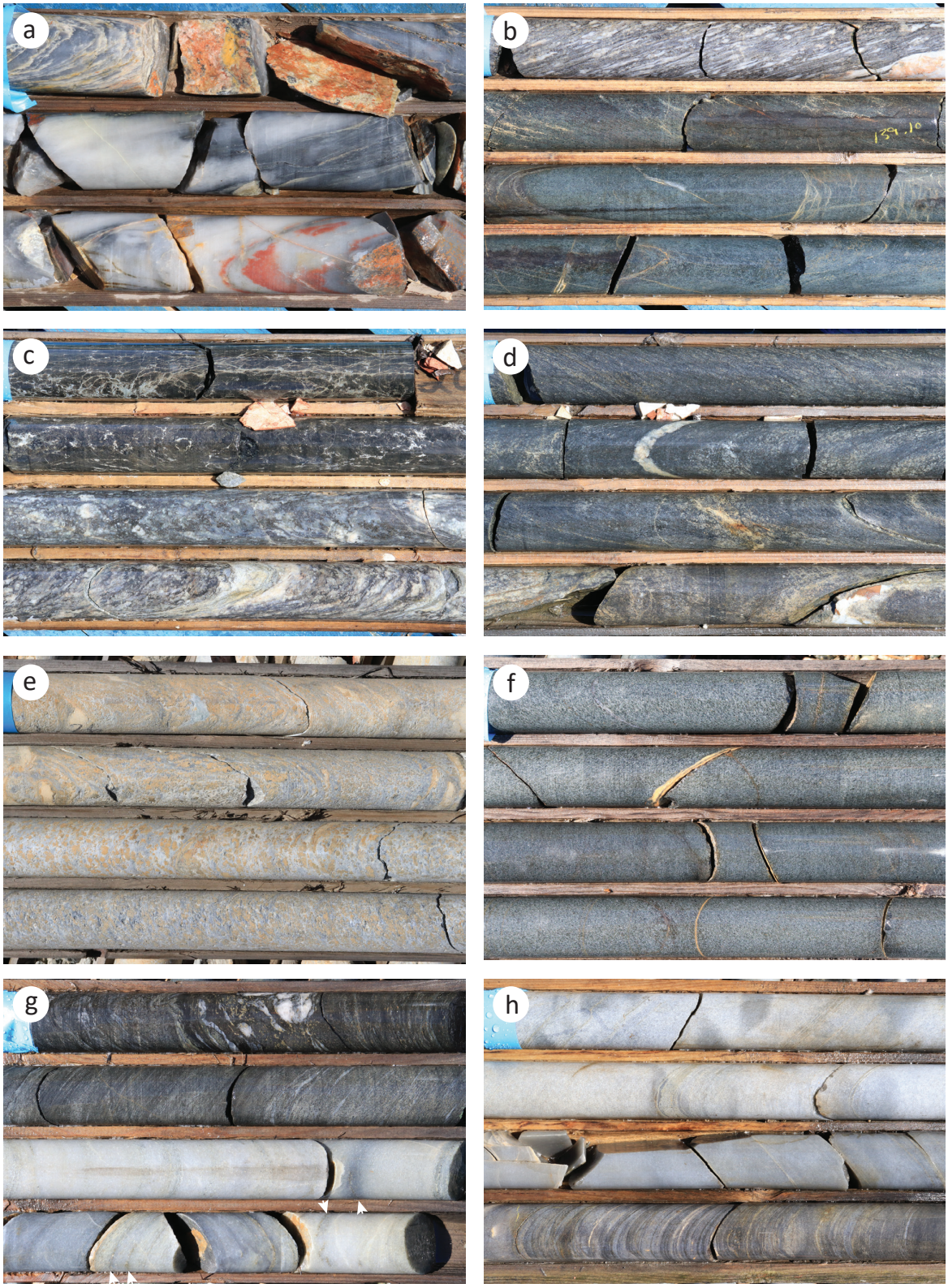


Figure GS2024-13-6: *Images of drillcore from the sub-Phanerozoic Winnipegosis komatiite belt:* ***a)*** *locally sheared quartzite with hematite staining (drillhole MRO-006, 104.7 m, NQ™ core [diameter = 4.76 cm]);* ***b)*** *protomylonitic granite (top row) and basalt (bottom three rows; drillhole MRO-006, 137.35 m, BQ™ core [diameter = 3.6 cm]);* ***c)*** *biotite-rich metasomatized rock with veinlets of quartz±feldspar (top two rows) and protomylonitic granite (bottom two rows; drillhole MRO-006, 205.75 m, BQ™ core);* ***d)*** *protomylonitic garnet-bearing and biotite-rich rock could represent sheared wacke or metasomatized basalt (drillhole MRO-006, 183.3 m, BQ™ core);* ***e)*** *talc-rich ultramafic schist (drillhole MRO-007, 116.5 m, BQ™ core);* ***f)*** *gabbro or possibly massive basalt (drillhole MRO-007, 157.8 m, BQ™ core);* ***g)*** *silicate-facies iron formation (top two rows) and quartzite with local sulphidic laminations (arrows, bottom two rows; drillhole MRO-007, 292.05 m, BQ™ core);* ***h)*** *quartzite (top three rows) and quartzite interlayered with pelite (bottom row, drillhole MRO-007, 332.5 m, BQ™ core).*

presence of the hornblende was identified in hand sample and requires further verification.

Economic considerations

Very little is known about the geology of the sub-Phanerozoic Superior boundary zone. Although its potential to host magmatic Ni-Cu deposits has been recognized for decades (Assessment Files 91655, 91731, 92282), its potential to host polymetallic VMS deposits is a relatively recent development (Assessment File 63G13256). The stratigraphy of the Ospwagan group and its importance for hosting Ni-deposits in the TNB is well established (Bleeker, 1990; Zwanzig et al., 2007). In contrast, the stratigraphy of the WKB and that of the juvenile volcanic-arc rocks hosting the Tower deposit remain largely unknown (Lin et al., 1998; Couëslan, 2018).

Determining the affinity of the volcanic rocks encountered in this study could have major implications for exploration in the sub-Phanerozoic Superior boundary zone. If it is determined that they share affinity with either the Bah Lake volcanic assemblage of the Ospwagan group (TNB) or the mafic to ultramafic volcanic rocks of the WKB, it could suggest potential for magmatic Ni-Cu deposits. If the volcanic rocks are correlative with the juvenile rocks that host the Tower deposit, it could suggest potential for Cu-Zn-Ag-Au VMS deposits and extend the area of known arc-affinity rocks in the area.

No obvious felsic or intermediate volcanic rocks, or VMS-related hydrothermal alteration, was recognized in the drillcore to correlate it with stratigraphy at the Tower deposit. Moreover, none of the logged drillcore could be unambiguously placed within Ospwagan group (TNB) or WKB stratigraphy. It is presumed that whole-rock lithogeochemistry and Sm-Nd isotope geochemistry, in combination with thin-section petrography, will help determine the affinity of the rock units described in this study. It is hoped that additional information can also be gathered from logging other drillcore in the area, if it becomes available.

Acknowledgments

Thanks to M. Friesen (University of Manitoba) and A. Maki (Brandon University) for providing excellent field assistance, as well as to M. Rinne and X.M. Yang for reviewing earlier drafts of the report. Special thanks to N. Richardson, C. Venturi, C. Henderson, W. Pachel, D. Fosseneuve, and B. Wesner of HudBay Minerals Inc. for their hospitality and providing access to the drillcore.

References

Bleeker, W. 1990: Evolution of the Thompson Nickel Belt and its nickel deposits, Manitoba, Canada; Ph.D. thesis, University of New Brunswick, Fredericton, New Brunswick, 400 p.

Burnham, O.M., Halden, N., Layton-Matthews, D., Lesher, C.M., Liwanag, J., Heaman, L., Hulbert, L., Machado, N., Michalak, D., Pacey, M., Peck, D.C., Potrel, A., Theyer, P., Toope, K. and Zwanzig, H. 2009: CAMIRO project 97E-02, Thompson Nickel Belt: final report, March 2002, revised and updated 2003; Manitoba Science, Technology, Energy and Mines, Manitoba Geological Survey, Open File OF2008-11, 434 p. plus appendices and GIS shape files for use with ArcInfo®.

Carlson, A. 2017: Geochemistry of mafic-ultramafic rocks in the Winnipegosis komatiite belt, Manitoba; M.Sc. research report, Laurentian University, Sudbury, Ontario, 48 p.

Ciborowski, T.J.R., Minifie, M.J., Kerr, A.C., Ernst, R.E., Baragar, B. and Millar, I.L. 2017: A mantle plume origin for the Paleoproterozoic circum-Superior large igneous province; Precambrian Research, v. 294, p. 189–213.

Couëslan, C.G. 2018: Geology of the Tower Cu-Zn-Ag-Au deposit, sub-Phanerozoic Superior boundary zone, central Manitoba (part of NTS 63G14); Manitoba Growth, Enterprise and Trade, Manitoba Geological Survey, Open File OF2018-4, 38 p.

Couëslan, C.G. and Pattison, D.R.M. 2012: Low-pressure regional amphibolite-facies to granulite-facies metamorphism of the Paleoproterozoic Thompson Nickel Belt, Manitoba; Canadian Journal of Earth Sciences, v. 49, p. 1117–1153.

Heaman, L.M., Peck, D. and Toope, K. 2009: Timing and geochemistry of 1.88 Ga Molson Igneous Events, Manitoba: insights into the formation of a craton-scale magmatic and metallogenic province; Precambrian Research, v. 172, p. 143–162.

Hulbert, L., Stern, R., Kyser, T.K., Pearson, J., Lesher, M. and Grinenko, L. 1994: The Winnipegosis komatiite belt central Manitoba; Manitoba Mining, Minerals, and Petroleum Convention 1994, November 20–23, 1994, Winnipeg, Manitoba, Program, p. 21.

Lin, S., Pacey, M., Theyer, P., Lenton, P., Macek, J., Peck, D., Zwanzig, H., Burnham, M., Keays, R., Lesher, M., Ferguson, I., Halden, N., Larocque, A., Bleeker, W., Broome, J., Lucas, S., White, D., Hulbert, L., Machado, N., Heaman, L. and Ansdell, K. 1998: Thompson nickel belt project; CAMIRO Project 97-E02, Annual Report – Year 1, 77 p. and appendices.

Lucas, S.B., White, D.J., Bleeker, W., Hajnal, Z., Lewry, J. and Weber, W. 1996: Crustal structure of the Superior Boundary Zone (Thompson Belt) from new Lithoprobe seismic reflection data; *in* Trans-Hudson Orogen Transect, Lithoprobe Report 55, p. 82–94.

Macek, J.J., Zwanzig, H.V. and Pacey, J.M. 2006: Thompson Nickel Belt geological compilation map, Manitoba (parts of NTS 63G, J, O, P and 64A and B); Manitoba Science, Technology, Energy and Mines, Manitoba Geological Survey, Open File Report OF2006-33, digital map on CD, URL <https://manitoba.ca/iem/info/libmin/OF2006-33.zip> [August 2023].

McGregor, C.R. 2012: GIS compilation of relogged sub-Phanerozoic Preccambrian exploration drillcore from the Thompson Nickel Belt, eastern Flin Flon Belt, and Winnipegosis Komatiite Belt (parts of NTS 63B, C, F, G, J, K); Manitoba Innovation, Energy and Mines, Manitoba Geological Survey, Open File OF2011-1, DVD.

NATMAP Shield Margin Project Working Group 1998: Geology, NATMAP Shield Margin Project area, Flin Flon belt, Manitoba/Saskatchewan; Geological Survey of Canada, Map 1968A, scale 1:100 000.

Pearson, J. 1996: Exploration, geophysics, and geology of the Winnipegosis basin, Thompson nickel belt, Manitoba Mining and Minerals Convention 1996, November 14–16, 1996, Winnipeg, Manitoba, Program, p. 39.

Reid, K.D. 2022: Preliminary interpretation of aeromagnetic data from poorly exposed and sub-Phanerozoic basement rocks east and southeast of Snow Lake, north-central Manitoba (parts of NTS 63F15, 16, 63G13, 14, 63J3–6, 11–14, 63K1, 2, 8, 9, 16, 63O3, 4); *in* Report of Activities 2022, Manitoba Natural Resources and Northern Development, Manitoba Geological Survey, p. 61–70.

Scoates, J.S., Scoates, J.R.F., Wall, C.J., Friedman, R.M. and Couëslan, C.G. 2017: Direct dating of ultramafic sills and mafic intrusions associated with Ni-sulfide mineralization in the Thompson nickel belt, Manitoba, Canada; Economic Geology, v. 112, p. 675–692.

Waterton, P., Pearson, D.G., Kjarsgaard, B., Hulbert, L., Locock, A., Parman, S. and Davis, B. 2017: Age, origin, and thermal evolution of the ultra-fresh ~1.9 Ga Winnipegosis Komatiites, Manitoba, Canada; Lithos, v. 268–271, p. 114–130.

White, D.J., Lucas, S.B., Bleeker, W., Hajnal, Z., Lewry, J.F. and Zwanzig, H.V. 2002: Suture-zone geometry along an irregular Paleoproterozoic margin: the Superior boundary zone, Manitoba, Canada; Geology, v. 30, p. 735–738.

Zwanzig, H.V. 2005: Geochemistry, Sm-Nd isotope data and age constraints of the Bah Lake assemblage, Thompson Nickel Belt and Kisseynew Domain margin: relation to Thompson-type ultramafic bodies and a tectonic model (NTS 63J, O and P); *in* Report of Activities 2005, Manitoba Industry, Economic Development and Mines, Manitoba Geological Survey, p. 40–53.

Zwanzig, H.V., Macek, J.J. and McGregor, C.R. 2007: Lithostratigraphy and geochemistry of the high-grade metasedimentary rocks in the Thompson Nickel Belt and adjacent Kisseynew Domain, Manitoba: implications for nickel exploration; Economic Geology, v. 102, p. 1197–1216.

GS2024-14

Bedrock mapping in the northwestern Burntwood Lake area, Kisseynew domain, west-central Manitoba (part of NTS 63N7)

by C.G. Couëslan and M.A. Friesen[1]

Summary

A mapping project in the northwestern arm of Burntwood Lake, accompanied by fieldwork for an honors thesis, was initiated in 2024 after the discovery of numerous carbonatite dikes within the Burntwood Lake syenite complex in 2023. Much of the area is underlain by migmatitic gneisses derived from Burntwood group wacke. The Burntwood group is intruded by quartz diorite and minor bodies of tonalite, which are locally orthopyroxene bearing. A heterogeneous clinopyroxene syenite pluton (the Burntwood Lake syenite complex) occurs in the centre of the mapping area. The syenite is intruded by a variety of carbonatite dikes, veins, and 'blows'. A variety of pegmatitic granite intrusions, ranging from centimetre-scale dikes to kilometre-scale bodies, occur throughout the study area and are likely derived from the partial melting of Burntwood group rocks. Two discrete, kilometre-scale bodies of porphyritic granite occur in the western and eastern portions of the map area. Sparse, centimetre- to metre-scale xenoliths and dikes of aplitic granite occur throughout the study area.

Burntwood group rocks are characterized by a northwest-striking S_1 gneissosity, which is moderately to steeply dipping to the northeast. Minor isoclinal folding of the gneissosity is accompanied by an axial planar, northwest-striking S_2 foliation, which is moderately to steeply dipping to the northeast. The S_2 fabric is well developed in all of the intrusive phases, except for some of the latest pegmatite and aplite dikes. The S_2 fabrics are cut by discrete, centimetre- to rarely metre-scale S_3 mylonitic shear zones, which are most abundant in the western portion of the study area. Peak metamorphic assemblages in the Burntwood group rocks consist of quartz–plagioclase–K-feldspar–garnet–cordierite–biotite±sillimanite±spinel, which is characteristic of the granulite facies for aluminous rocks.

Carbonatites from similar tectonic settings in California and China host several world-class rare-earth-element deposits, which suggests the Trans-Hudson alkaline-carbonatite igneous province could represent a new metallotect for rare-earth-element exploration in Manitoba. An apparent increase in the size and density of carbonatite intrusions proximal to an area of low ground in the northern part of the syenite complex suggests it could be underlain by relatively soft, carbonate-rich rocks. Although graphite was not found in any significant quantities, the high metamorphic grade of the area makes it ideally situated for the formation of high-value, large flake, or vein/lump graphite deposits.

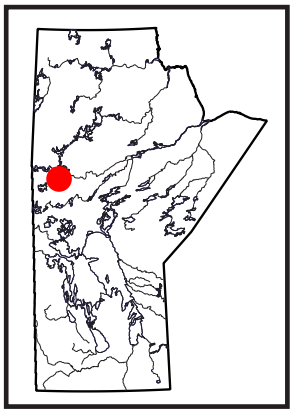
In Brief:

- The northwestern Burntwood Lake area is largely underlain by migmatite derived from Burntwood group wacke
- The Burntwood group is intruded by locally-derived pegmatitic granite, quartz diorite, tonalite, porphyritic granite, and a syenite-carbonatite complex
- The area could have potential for rare-earth element and graphite mineralization

Citation:
Couëslan, C.G. and Friesen, M.A. 2024: Bedrock mapping in the northwestern Burntwood Lake area, Kisseynew domain, west-central Manitoba (part of NTS 63N7); *in* Report of Activities 2024, Manitoba Economic Development, Investment, Trade and Natural Resources, Manitoba Geological Survey, p. 116–126.

Introduction

A scoping study of the Burntwood Lake syenite complex was initiated in the summer of 2023 following a forest fire that burned the area in 2022. The fire resulted in much better exposure than the last time the complex was visited in 2011, with significantly reduced lichen and moss cover (Martins et al., 2011). The improved exposure enabled a better understanding of the structural relations of different rock types, particularly in recessed areas. This led to the discovery of numerous carbonatite dikes, both in situ, and in displaced, locally derived material. These discoveries, coupled with their scientific and potentially economic importance, prompted additional work in July 2024, which included shoreline mapping of the northwestern arm of Burntwood Lake at a scale of 1:10 000 and fieldwork for an honours thesis at the University of Manitoba. This report is a summary of the preliminary findings.



Background

The Burntwood Lake syenite complex is located in the central Kisseynew domain, approximately 70 km north-northwest of the town of Snow Lake. The Kisseynew domain forms part of the internal zone of the Trans-Hudson orogen in Manitoba and is flanked by the Lynn Lake domain to the north, Flin Flon domain to the south, and Superior boundary zone to the east (Figure GS2024-14-1). The central Kisseynew domain is underlain by Burntwood group metagreywacke that is intruded by large plutons, sheets, and lenses of felsic to ultramafic rocks (Zwanzig, 2008). The Burntwood group was

[1] Department of Earth Sciences, University of Manitoba, Winnipeg, Manitoba

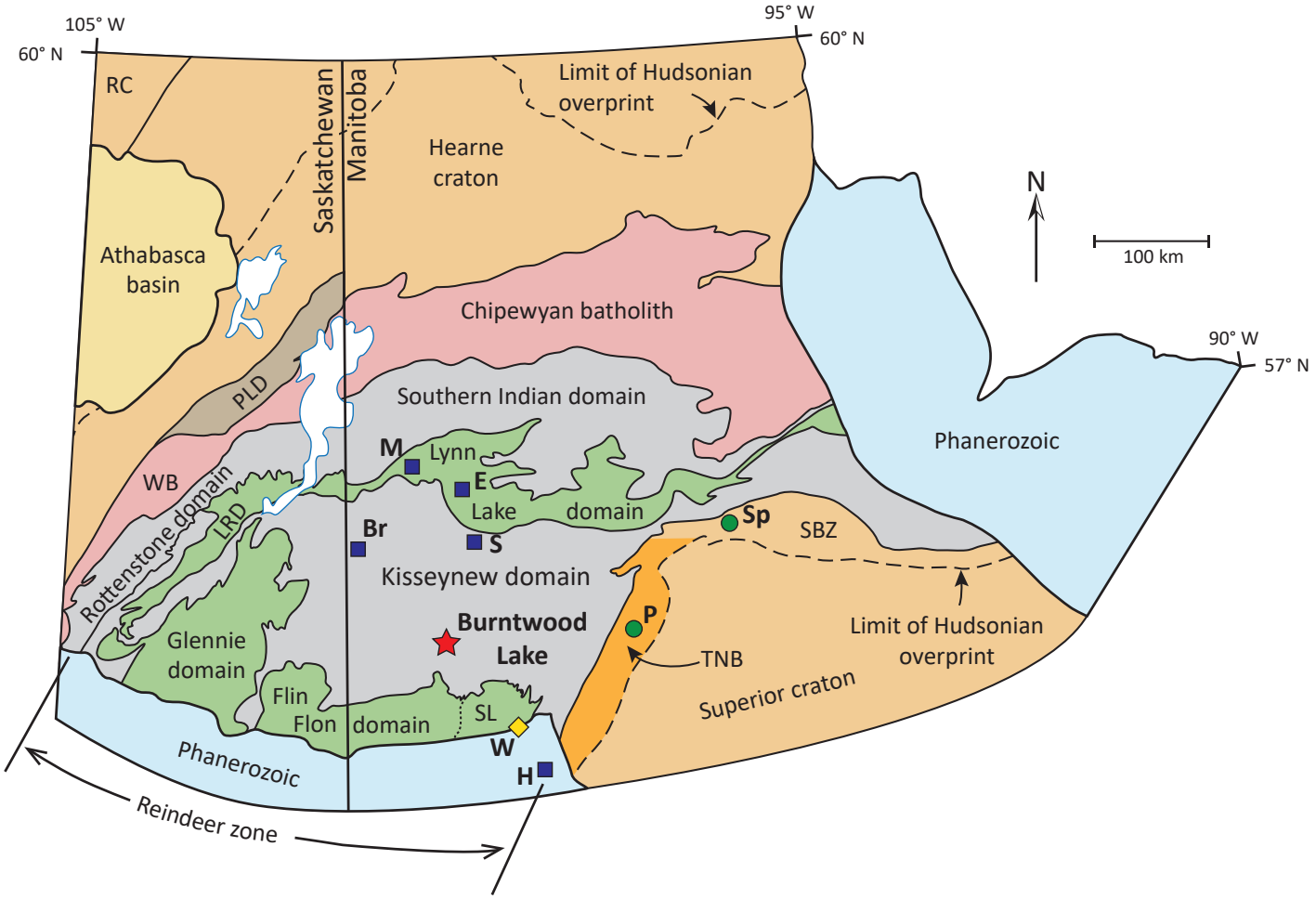


Figure GS2024-14-1: *Schematic map of major tectonic elements in the Manitoba–Saskatchewan segment of the Trans-Hudson orogen, west-central Manitoba (modified from Lewry et al., 1990; Maxeiner et al., 2021; Manitoba Geological Survey, 2022). The location of the Burntwood Lake syenite complex is indicated with a red star. Blue squares indicate the locations of high-potassium to shoshonitic syenite complexes in the Trans-Hudson orogen. Green circles indicate the locations of Paleoproterozoic, late-orogenic carbonatite magmatism in the Superior boundary zone. The yellow diamond indicates the location of anorogenic carbonatite magmatism. Abbreviations: Br, Brezden Lake; E, Eden Lake; H, Huzyk Creek; LRD, La Ronge domain; M, McVeigh Lake; P, Paint Lake; PLD, Peter Lake domain; RC, Rae craton; S, Suwannee River; SBZ, Superior boundary zone; SL, Snow Lake subdomain; Sp, Split Lake; TNB, Thompson nickel belt; W, Wekusko Lake; WB, Wathaman batholith.*

deposited between 1860 and 1840 Ma (Machado et al., 1999; Murphy and Zwanzig, 2021) into what has been variously interpreted as a back-arc, inter-arc or fore-arc basin (Ansdell et al., 1995; Zwanzig, 1997; Zwanzig and Bailes, 2010). The detritus was largely derived from the adjacent, juvenile magmatic arcs, as indicated by prominent, overlapping detrital zircon age peaks of 1870–1850 Ma in probability plots (Zwanzig and Bailes, 2010; Murphy and Zwanzig, 2021).

The Burntwood group is intruded by orthopyroxene-bearing, intermediate to mafic sheets and sills of the ca. 1825 Ma Touchbourne suite (Gordon et al., 1990; Zwanzig, 1990; Machado et al., 1999). This suite is postdated by coarsely inequigranular, garnetiferous tonalite to granodiorite, which are most abundant in the High Rock Lake area (Gordon et al., 1990; Zwanzig, 1990). Peraluminous granodiorite and granite are the most widespread igneous rocks in the central Kisseynew domain. They occur as segregations, sills, dikes, and irregular nebulitic bodies with inclusions of paragneiss (Gordon et al, 1990; Zwanzig, 1990). Other intrusions in the region include monzonite and syenite of the Trans-Hudson alkaline-carbonatite igneous province, melatonalite, and pegmatite (Baldwin et al., 1979; Gordon et al., 1990; Chakhmouradian et al., 2023).

The 'Trans-Hudson alkaline-carbonatite igneous province' consists of several syenite complexes of high-potassium calcalkaline to shoshonitic affinity, along with spatially associated carbonatite and lamprophyre dikes that occur within the Trans-Hudson orogen of Manitoba (Figure GS2024-14-1; Chakhmouradian et al., 2023). The Burntwood Lake (Martins et al., 2011; Chakhmouradian et al., 2023), Brezden Lake (Martins et al., 2012; Hnatiuk et al., 2022), Suwannee River (Martins and Couëslan, 2022), and Huzyk Creek (Couëslan, 2023) syenite plutons occur within the Kisseynew domain, whereas the Eden Lake (Mumin, 2002; Couëslan, 2005; Chakhmouradian et al., 2008) and McVeigh Lake (McRitchie, 1988) complexes occur within the Lynn Lake

domain. Granitoid rocks within these complexes typically range in composition from alkali-feldspar syenite (referred to as monzonite in some reports) to clinopyroxene melasyenite and leucocratic quartz syenite. Spatially associated lamprophyres have been reported at Brezden (Hnatiuk et al., 2022) and McVeigh (A.R. Chakhmouradian, pers. comm., 2023) lakes, and carbonatite dikes crosscutting syenites have been reported at Burntwood (Chakhmouradian et al., 2023), Brezden (Hnatiuk et al., 2022) and Eden lakes (Mumin, 2002; Couëslan, 2005; Chakhmouradian et al., 2008). The Hudsonian syenite complexes have been the subject of exploration for zirconium (Zr), rare-earth elements (REEs), thorium (Th), and uranium (U), with the majority of activities centered on Eden Lake, which hosts REE-rich apatite (up to 8 wt. % REEs) and late, hydrothermal REE-mineralization (McRitchie, 1989; Chakhmouradian et al., 2008; Mumin, 2010).

Rocks of the central Kisseynew domain attained upper-amphibolite– to granulite–facies metamorphic conditions. The migmatitic Burntwood group rocks contain zones of coarse, garnet- and cordierite-rich diatexite (Zwanzig, 2008). Gordon (1989) estimated peak metamorphic conditions of 750 ±50 °C and 5.5 ±1.0 kbar at ca. 1815 Ma for the central Kisseynew domain. However, estimated peak metamorphic conditions as high as 900 °C and 12 kbar at ca. 1800 Ma were reported by Growdon (2010). Large-scale, recumbent isoclinal folds predated peak metamorphism in this part of the domain and were subsequently refolded during the regional metamorphism (Gordon, 1989; Zwanzig, 2008).

Geology of the Burntwood Lake area

The Burntwood Lake area was last mapped in 1971 and 1972 (McRitchie, 1971; Baldwin and McRitchie, 1972; McRitchie, 1972). The area is underlain by Burntwood group wacke intruded by various igneous phases including gabbro, diorite, monzonite, granodiorite, granite, and syenite. Western portions of the Burntwood Lake area are characterized by northwest-striking metamorphic fabrics that consistently dip to the northeast. Metamorphic assemblages in the Burntwood group rocks are interpreted to be middle- to upper-amphibolite facies (McRitchie, 1971). The syenite intrusion of northwestern Burntwood Lake was later mapped in detail by McRitchie (1987), and revisited by Martins et al. (2011) and Chakhmouradian et al. (2023). The reader is referred to those publications for greater detail on the Burntwood Lake syenite complex.

Results of 2024 mapping

Mapping of the Burntwood Lake area in 2024 was restricted to the northwestern arm, in the vicinity of the syenite complex (Figure GS2024-14-2). The goal was to determine if additional syenite or carbonatite intrusions were present outside of the main plutonic complex. All rocks, except for some of the latest pegmatitic and aplitic intrusions, were deformed and subjected to at least amphibolite-facies metamorphic conditions. To improve the readability of the text, the 'meta-' prefix has been omitted from rock names.

Burntwood group

Burntwood group rocks underlie much of the Burntwood Lake area (Figure GS2024-14-2) and occur as a metatexite to diatexite that is typically intercalated with 20–80% pegmatitic granite. The metatexite is typically derived from more psammitic layers, whereas the diatexite is derived from more pelitic layers (Figure GS2024-14-3a, b). The psammitic layers are typically <1 m thick, fine to medium grained, and quartzofeldspathic with <20% biotite and <3% garnet. The layers contain rare pods of calcsilicate <20 cm thick that likely represent concretions (Figure GS2024-14-3a). The concretions appear to be plagioclase and/or amphibole rich, and locally scapolite bearing, with accessory amounts of garnet and a black, opaque mineral. The concretions can be partially epidotized.

The more pelitic layers are typically <3 m thick, medium to coarse grained, strongly foliated, and quartzofeldspathic, with 20–30% biotite, 5–7% garnet, and accessory graphite. The most pelitic layers can contain up to 20% cordierite, 15% garnet, and trace amounts of sillimanite. The cordierite is commonly pinitized. Outcrops can be dominated by psammitic or pelitic beds, and the composition of individual beds can be a gradation between the psammitic and pelitic end-members described above. Pods and discontinuous layers of in situ and in-source leucosome are typically <30 cm across and contain minor amounts of possibly peritectic cordierite and garnet. Garnet and cordierite in the leucosome commonly have biotite selvages/rims. Rose quartz forms rare pods <20 cm across.

Quartz diorite

A single outcrop of grey-weathering quartz diorite occurs in the northwestern part of the map area; however, similar intrusions of much greater extent (kilometre-scale) are reported from the northeastern and southwestern portions of the map area (Figure GS2024-14-2; Baldwin et al., 1979). The quartz diorite is brown on fresh surfaces, medium grained, and biotite and orthopyroxene bearing. The unit is relatively homogeneous and equigranular (Figure GS2024-14-3c), and is intruded by the pegmatitic granite. Contacts between the quartz diorite and granite are marked by the presence of medium- to very coarse-grained garnet. The quartz diorite could be correlative with the ca. 1825 Ma Touchbourne suite (Gordon et al., 1990; Zwanzig, 1990; Machado et al., 1999).

Tonalite

Sparse outcrops and metre-scale occurrences of tonalite occur throughout the map area (Figure GS2024-14-2). It varies from light grey to dark grey and is medium to coarse grained. The mafic mineral content is variable, with 5–20% biotite and locally minor amounts of garnet or a brown-weathering min-

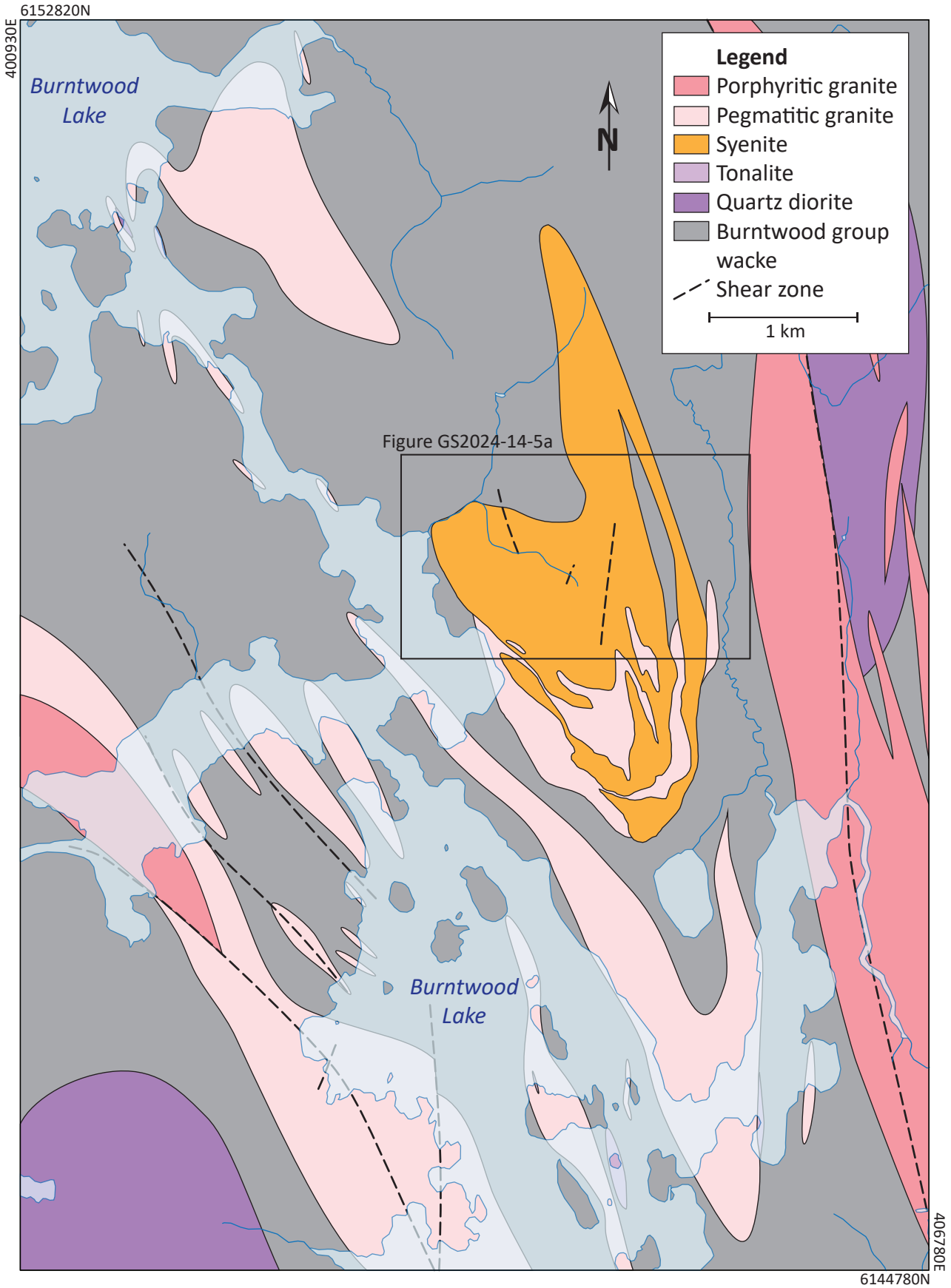


Figure GS2024-14-2: *Bedrock geology of the northwestern Burntwood Lake area, west-central Manitoba (simplified from Couëslan, 2024). Box outlined in black shows location of Figure GS2024-14-5a. Co-ordinates are in UTM Zone 14, NAD83.*

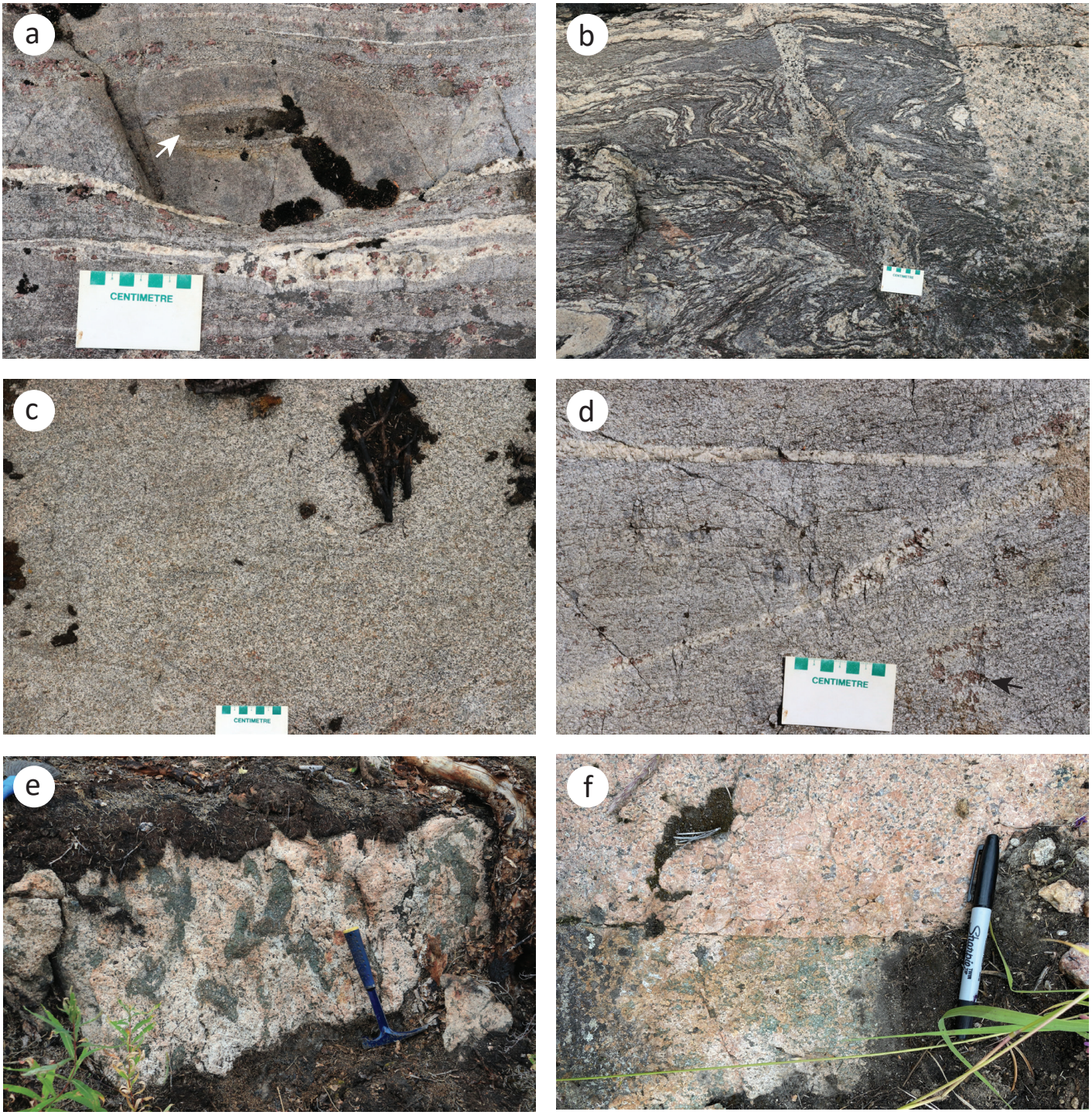


Figure GS2024-14-3: *Outcrop images from the northwestern Burntwood Lake area:* ***a)*** *Burntwood group metatexite consisting of more psammitic wacke, along with a calcsilicate concretion (arrow);* ***b)*** *Burntwood group diatexite consisting of more pelitic wacke;* ***c)*** *quartz diorite;* ***d)*** *tonalite with garnet clots (arrow) and crosscutting dikes of pegmatitic granite;* ***e)*** *syenite with clinopyroxene-rich clots and local diffuse bleaching;* ***f)*** *contact between quartz syenite (top half of image) and more melanocratic syenite.*

eral that could be orthopyroxene. Biotite locally forms clots, which gives the tonalite a spotted appearance. When present, garnet is evenly distributed as coarse clots (Figure GS2024-14-3d) associated with leucosome or pegmatite injection. The tonalite is intruded by pink pegmatite dikes <2 m across. Some occurrences of the tonalite, especially those suspected of being orthopyroxene bearing, could be related to the Touchbourne intrusive suite.

Syenite

The Burntwood Lake syenite complex occurs in the central portion of the map area (Figure GS2024-14-2). It is relatively het-

erogeneous and comprises several intrusive phases. The dominant syenite phase is medium to coarse grained, beige to brick red, and appears relatively leucocratic on weathered surfaces and melanocratic on fresh surfaces. The beige syenite is interpreted to contain a higher proportion of albite than the red syenite. The dominant mafic mineral is clinopyroxene, which forms euhedral to subhedral 0.1–1 cm crystals. Minor amphibole and biotite can be present and typically form rims around the clinopyroxene. The clinopyroxene also forms lenses and pods that are largely aligned with the regional foliation (Figure GS2024-14-3e). These segregations can contain a large proportion of apatite as well as accessory titanite and/or allanite. These mafic-rich pods are interpreted as cognate xenoliths and appear to become more abundant in the northern portion of the pluton, where they can lend a leopard-skin–like appearance to the syenite. The leopard-skin syenite locally displays a crude magmatic layering that is crosscut by the regional foliation. Sparse occurrences of porphyritic melasyenite consist of nearly equal proportions of biotite, clinopyroxene, and feldspar. The feldspar occurs as medium-grained polycrystalline pseudomorphs of K-feldspar prisms up to 3 cm long.

The main syenite is intruded by a quartz syenite, which is interpreted to be a more evolved phase of the pluton (Figure GS2024-14-3f). The quartz syenite is relatively leucocratic and consists dominantly of microcline and interstitial quartz, and locally approaches a granite composition. Mafic minerals in the quartz syenite consist predominantly of biotite. Beige aplite was observed at a few localities and can occur as discrete dikes <5 cm wide or as more pervasive intrusions. The aplite consists of microcline and quartz; its relationship to the quartz syenite is uncertain. The syenite is crosscut by microcline-rich pegmatite dikes that contain minor biotite and locally quartz cores. The composition of the pegmatite can range from quartz syenite to granite. Local 'pegmatoid dikes' of nearly solid microcline are also present and could be interpreted as cumulate material emplaced as crystal mushes or as hydrothermal veins. Diffuse, bleached zones occur throughout the northern part of the pluton and appear to overprint all silicate rocks in the complex (Figure GS2024-14-3e). This bleaching is caused by the albitization of microcline and appears to overprint the regional foliation, which becomes locally obscured. Additional details regarding the Burntwood Lake syenite complex can be found in Chakhmouradian et al. (2023).

Carbonatite

Carbonatites from the Burntwood Lake syenite complex are mineralogically and visually diverse. They can be fine to coarse grained and massive to foliated. The carbonatite varieties are provisionally subdivided into grey-white carbonatite and blue-grey carbonatite, based solely on the colour of the main carbonate mineral, which is typically calcite. Weathered surfaces of both varieties are typically crumbly and appear a light brown-beige with well-expressed cleavage. The carbonatite can contain variable amounts of apatite, clinopyroxene, and biotite. Accessory titanite, allanite, amphibole, and magnetite can be present. Syenite-derived xenoliths and xenocrysts can be abundant and typically increase in proportion toward the margin of the carbonatite (Figure GS2024-14-4a). Both biotite and amphibole may form reaction rims around clinopyroxene as well as the syenite-derived fragments.

The carbonatite forms discrete, centimetre- to metre-scale dikes and 'blows' (cf. Wilson and Head, 2007), and zones of diffuse veinlets (Figure GS2024-14-4b). The carbonatite intrusions are typically structurally controlled and can be found along the contacts of silicate rocks and along planes of weakness (Figure GS2024-14-4c). Exocontacts can appear either bleached, as a result of albitization, or melanocratic, due to enrichment in clinopyroxene (Figure GS2024-14-4b). Although grey-white carbonatite appeared to be the most common variety encountered during fieldwork in 2023, the blue-grey variety was more commonly observed during the 2024 field season. Additional information regarding the carbonatite can be found in Chakhmouradian et al. (2023).

All carbonatite discovered to date occurs in the northern part of the Burntwood Lake syenite complex; however, a single carbonate vein of uncertain affinity was located approximately 650 m southeast of the pluton. The vein is emplaced in Burntwood group wacke and truncated by a pegmatite dike. In addition to carbonate, it contains minor diopside and amphibole, and trace sulphide. Further work is required to determine if the carbonate vein is magmatic or hydrothermal/metamorphic in origin.

Pegmatitic granite

The pegmatitic granite occurs throughout the map area (Figure GS2024-14-2) and varies from centimetre-scale dikes to kilometre-scale intrusions. It is pink to white and varies from medium grained to pegmatitic. Contacts between medium-grained and pegmatitic zones are typically diffuse. Local exposures can be more equigranular. The granite contains minor biotite, and trace amounts of cordierite and garnet. The latter two minerals commonly occur as garnet-quartz and cordierite-quartz aggregates or pods <20 cm across (Figure GS2024-14-4d). These pods commonly occur as trains up to several metres long. The garnet is locally rimmed by biotite. The granite can be intercalated with up to 80% Burntwood group rocks in outcrop, and metre-scale xenoliths of psammitic wacke and schlieren of pelite are common (Figure GS2024-14-4e). These intrusions are interpreted as anatectic melts derived largely from the Burntwood group. The pegmatitic granite is intruded by, and intrusive into, the porphyritic granite, which suggests multiple episodes of emplacement.

Porphyritic granite

The porphyritic granite forms two discrete bodies in the western and eastern portions of the map area (Figure GS2024-14-2). It is pink to grey, coarse grained, and characterized by prismatic, twinned K-feldspar phenocrysts <0.5 by 1.5 cm. The

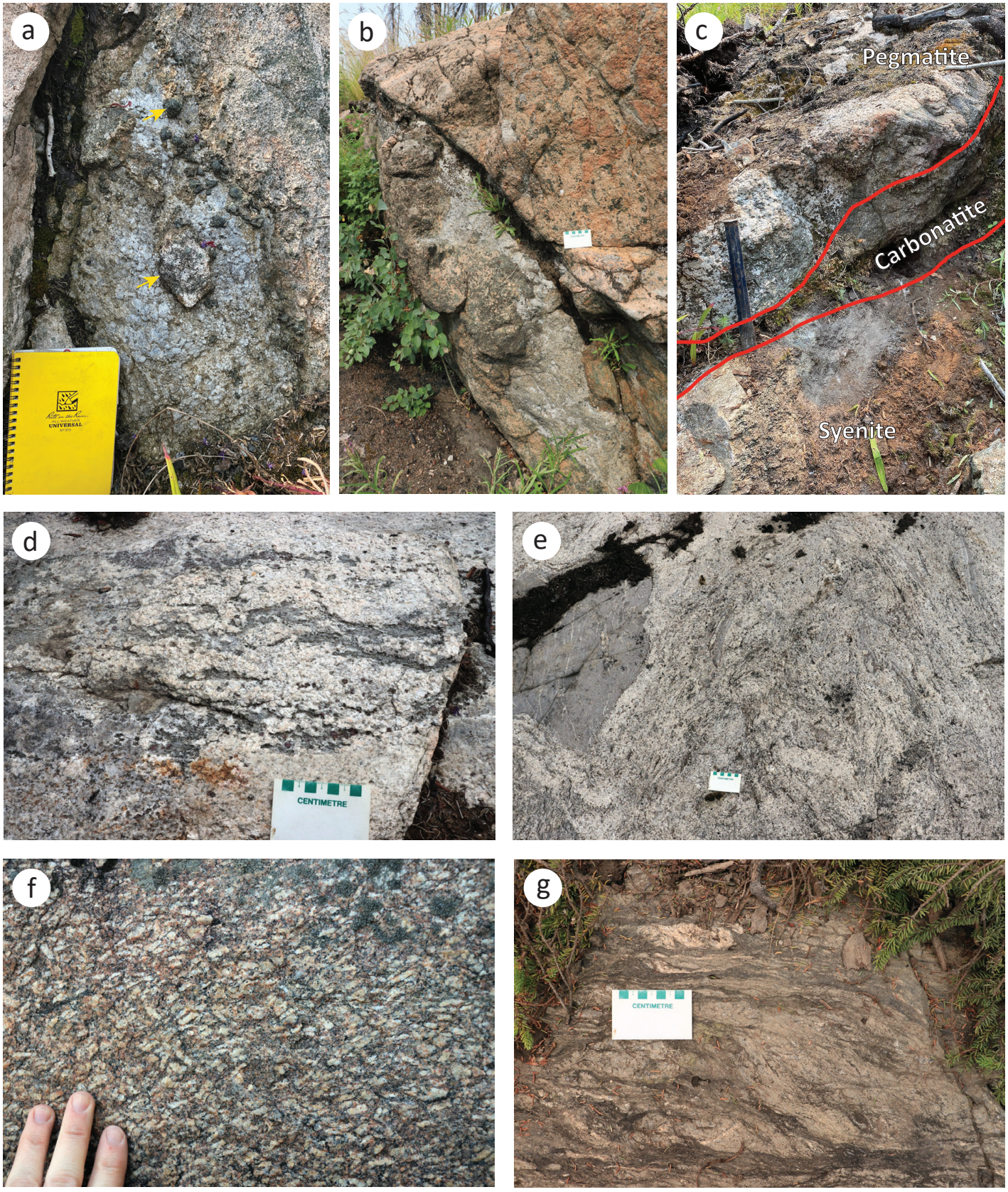


Figure GS2024-14-4: *Outcrop images from the northwestern Burntwood Lake area:* ***a)*** *blue-grey carbonatite with syenite-derived xenoliths and xenocrysts (arrows);* ***b)*** *carbonatite dike intruding syenite (note enrichment of clinopyroxene in the footwall exocontact and localized bleaching in the hangingwall);* ***c)*** *carbonatite dike that intruded along a syenite-pegmatite contact;* ***d)*** *trains of cordierite-quartz aggregates in pegmatitic granite;* ***e)*** *pegmatitic granite with xenoliths and schlieren derived from the Burntwood group;* ***f)*** *aligned K-feldspar phenocrysts in the porphyritic granite;* ***g)*** *mylonite derived from the Burntwood group, with entrained pegmatitic granite or leucosome.*

phenocrysts are aligned with the foliation, suggesting this could be a tectonic fabric (Figure GS2024-14-4f); this is supported by the local recrystallization of phenocrysts into augen. The granite locally has a seriate texture and can grade into zones of more equigranular granite; however, this could be the result of recrystallization during tectonic reworking. Minor biotite forms the dominant mafic mineral.

Aplitic granite

The aplitic granite is not an outcrop-forming unit, but occurs as sparse centimetre- to metre-scale xenoliths and dikes throughout the map area. It is pink to grey and contains trace to minor amounts of garnet and biotite. The garnet could be xenocrystic and commonly occurs as <1 cm clots that are rimmed by biotite. The aplite occurs as foliated, angular xenoliths in the pegmatitic granite and as rare massive dikes crosscutting the same unit, which suggests multiple episodes of emplacement.

Structural and metamorphic geology

Primary sedimentary layering (S_0) in the Burntwood group wacke has been transposed along a northwest-striking S_1 gneissosity that is moderately to steeply dipping to the northeast. Minor isoclinal folding of the gneissosity is accompanied by an axial planar northwest-striking S_2 foliation that is moderately to steeply dipping to the northeast. The S_2 foliation forms a regionally penetrative fabric that is well developed in all of the intrusive phases, except for some of the latest pegmatite and aplite dikes.

A primary S_0 igneous layering is locally developed within the syenite and is crosscut by the S_2 fabric. Diffuse zones of metasomatism (bleaching) within the syenite appear to overprint the S_2 foliation, suggesting it postdates the fabric development. The carbonatite varies from foliated to massive, which suggests that: 1) intrusions were emplaced before and after D_2, 2) some intrusions experienced static recrystallization after D_2, or 3) the fabric development is unrelated to the D_2 phase of deformation. Carbonatite dikes are locally emplaced along the S_2 foliation, suggesting that this plane of weakness was developing, or already developed, at the time of intrusion.

Discrete centimetre- to metre-scale, mylonitic D_3 shear zones are most abundant in the southwestern part of the map area (Figure GS2024-14-4g). The shear zones are dominantly sinistral and northwest-striking, and dip steeply to the northeast. Minor conjugate dextral shears are northeast-striking with steep dips. Regional S_2 fabrics wrap into these later D_3 structures.

Peak metamorphic assemblages observed in the Burntwood group wacke consist of quartz–plagioclase–K-feldspar–garnet–cordierite–biotite±sillimanite±spinel. The assemblage K-feldspar–garnet–cordierite is characteristic of granulite-facies metamorphism for aluminous rocks (Pattison et al., 2003). The majority of biotite grains appear to be part of the peak assemblage, which suggests that the incongruent melting reaction of this mineral was not surpassed. Granulite-facies peak metamorphic conditions could also be supported by the presence of orthopyroxene in the quartz diorite and locally in the tonalite. Orthopyroxene-bearing intrusions in this region have previously been interpreted as pre-peak metamorphic, which would imply a metamorphic, rather than magmatic, origin for the orthopyroxene (Gordon et al., 1990). Detailed petrographic studies will be required to corroborate this interpretation. Granulite-facies metamorphism is significantly higher than the middle- to upper-amphibolite–facies estimate of McRitchie (1971), and in broad agreement with the estimate of 750 ±50 °C and 5.5 ±1.0 kbar of Gordon (1989) for much of the central Kisseynew domain. Biotite is commonly observed as rims around garnet, and locally cordierite, in Burntwood group rocks and related granitoids, as well as rims around orthopyroxene in the quartz diorite and tonalite. This indicates some degree of retrogression, possibly under amphibolite-facies conditions.

Economic considerations

The Government of Canada has placed rare-earth elements (REEs) on its list of critical minerals (Natural Resources Canada, 2024). An increased demand for REEs, spurred on by the proliferation of low-carbon-footprint transportation, energy, and communication technologies, has created a need for new, economically viable REE deposits to sustain a reliable REE supply chain outside of the current producers, which are largely dependent on China (Cordier, 2024). Carbonatites are the most economically important source of light lanthanides (La-Eu) and host the largest known REE deposits, including Bayan Obo, Mianning-Dechang, and Weishan in China, and Mountain Pass in California, United States. The tectonic setting and geochemical characteristics of the rocks associated with these deposits are similar to those of the Trans-Hudson alkaline-carbonatite igneous province of Chakhmouradian et al. (2023), which includes the syenite-carbonatite complexes at Burntwood, Brezden, and Eden lakes (Figure GS2024-14-1). This represents a potential new metallotect for REE exploration.

There is an apparent increase in density and size of carbonatite intrusions around a low-lying area in the northern part of the Burntwood Lake syenite complex (Figure GS2024-14-5a, b). A ridge protruding into the southwestern end of the low ground contained a wide variety of carbonatite intrusions, with exposed areas of carbonate up to 10 m^2 that disappeared under cover in multiple directions. This could imply that the low ground, which encompasses an area of approximately 0.14 km^2, is underlain by more easily eroded, carbonate-rich rocks. It may be possible to test this hypothesis by using geophysical or soil/vegetation geochemical surveys.

Graphite is another mineral on the Government of Canada's critical minerals list (Natural Resources Canada, 2024). Some of its many uses include refractory applications, motor brushes, and steel making; however, higher valued coarse-grained graphite is used in high-temperature lubricants, and lithium battery and fuel



Figure GS2024-14-5: *Images of low ground in the northern part of the Burntwood Lake syenite complex:* ***a)*** *area outlined in Figure GS2024-14-2 with red stars indicating the locations of carbonatite intrusions and the extent of the syenite outlined in white;* ***b)*** *view looking east-northeast from the ridge protruding into the southwestern-end of the low ground and located between the two white arrows in (a).*

cell applications (Robinson et al., 2017). Several graphite deposits are hosted in Burntwood group rocks in the Kisseynew domain of Manitoba, including the Neuron claim (Callinex Mines Inc., 2014; Assessment File 63O15404, Manitoba Economic Development, Investment, Trade and Natural Resources, Winnipeg) and the Huzyk Creek graphite-vanadium property (Couëslan, 2020, 2022). The high metamorphic grade at Burntwood Lake makes it ideally situated for the formation of high-value, large-flake, or vein/lump graphite (Buseck and Beyssac, 2014). Although graphite was not found in any significant quantities during mapping, graphite-rich horizons are relatively soft and easy to erode, and are more likely to form negative relief than outcrops. The best way to explore for graphite mineralization would be using geophysical methods. Stratabound graphite-rich horizons should appear as relatively continuous, folded conductors, whereas vein or lump graphite could form more linear conductors coincident with shear zones. Graphite-rich mineralization is likely to have a relatively low magnetic response unless it is accompanied by significant pyrrhotite.

Acknowledgments

Sincere thanks to A.R. Chakhmouradian for guidance and discussions in the field and always pleasant company. Thanks to B. Gogal and J. Gogal of Gogal Sir Services for float plane and logistical support out of Snow Lake, and C. Epp and P. Belanger for logistical support out of Winnipeg. Thanks to T. Martins and K. Reid for reviewing earlier drafts of this report.

References

Ansdell, K.M., Lucas, S.B., Connors, K. and Stern, R.A. 1995: Kisseynew metasedimentary gneiss belt, Trans-Hudson orogen (Canada): back-arc origin and collisional inversion; Geology, v. 23, p. 1039–1043.

Baldwin, D.A. and McRitchie, W.D. 1972: Takipy Lake; Manitoba Department of Mines, Resources and Environmental Management, Mines Branch, Preliminary Map 1972G-10, scale 1:31 680.

Baldwin, D.A., Frohlinger, T.G., Kendrick, G., McRitchie, W.D. and Zwanzig, H.V. 1979: Geology of the Nelson House–Pukatawagan Region (Burntwood Project); Manitoba Department of Mines, Natural Resources and Environment, Mineral Resources Division, Geological Maps 78-3-1 to 78-3-22, scale 1:50 000.

Buseck, P.R. and Beyssac, O. 2014: From organic matter to graphite: Graphitization; Elements, v. 10, p. 421–426.

Callinex Mines Inc. 2014: Grades up to 60.38% carbon graphite confirmed at Callinex' Neuron property; Callinex Mines Inc., press release, April 25, 2014, URL <https://callinex.ca/grades-of-up-to-60-38-carbon-graphite-confirmed-at-callinex-neuron-property/> [October 2024].

Chakhmouradian, A.R., Mumin, A.H., Demény, A. and Elliott, B. 2008: Postorogenic carbonatites at Eden Lake, Trans Hudson Orogen (northern Manitoba, Canada): geological setting, mineralogy and geochemistry; Lithos, v. 103, p. 503–526.

Chakhmouradian, A.R., Couëslan, C.G. and Martins, T. 2023: The Burntwood Lake syenite complex revisited: the site of voluminous carbonatite magmatism in the Kisseynew domain, west-central Manitoba (part of NTS 63N7); *in* Report of Activities 2023, Manitoba Economic Development, Investment, Trade and Natural Resources, Manitoba Geological Survey, p. 40–51.

Cordier, D.J. 2024: Rare-earths; *in* Mineral Commodity Summaries 2024, U.S. Geological Survey, 212 p., URL <https://doi.org/10.3133/mcs2024>.

Couëslan, C.G. 2005: Geochemistry and petrology of the Eden Lake carbonatite and associated silicate rocks; M.Sc. thesis, University of Western Ontario, London, Ontario, 201 p.

Couëslan, C.G. 2020: Geology and interpretation of graphite- and vanadium-enriched drillcore from the Huzyk Creek property, sub-Phanerozoic Kisseynew domain, central Manitoba (NTS 63J6); Manitoba Agriculture and Resource Development, Manitoba Geological Survey, Geoscientific Paper GP2020-1, 29 p.

Couëslan, C.G. 2022: Affinity and petrogenesis of the Huzyk Creek metal-enriched graphite deposit: a metamorphosed metalliferous black shale in the Trans-Hudson orogen of Manitoba, Canada; The Canadian Mineralogist, v. 60, p. 853–880.

Couëslan, C.G. 2023: Age and petrology of zirconium- and light rare-earth element–enriched quartz monzonite in drillcore from the Huzyk Creek property, sub-Phanerozoic Kisseynew domain, central Manitoba (NTS 63J6); Manitoba Economic Development, Investment and Trade, Manitoba Geological Survey, Open File OF2023-2, 28 p.

Couëslan, C.G. 2024: Bedrock geology of the northwestern Burntwood Lake area, west-central Manitoba (part of NTS 63N7); Manitoba Economic Development, Investment, Trade and Natural Resources, Manitoba Geological Survey, Preliminary Map PMAP2024-1, scale 1:10 000.

Gordon, T.M. 1989: Thermal evolution of the Kisseynew sedimentary gneiss belt, Manitoba: metamorphism at an early Proterozoic accretionary margin; *in* Evolution of Metamorphic Belts, J.S. Daly, R.A. Cliff and B.W.D. Yardley (ed.), Geological Society, Special Publication 43, p. 233–243.

Gordon, T.M., Hunt, P.A., Bailes, A.H. and Syme, E.C. 1990: U-Pb ages from the Flin Flon and Kisseynew belts, Manitoba: chronology of crust formation at an Early Proterozoic accretionary margin; *in* The Early Proterozoic Trans-Hudson Orogen of North America, J.F. Lewry and M.R. Stauffer (ed.), Geological Association of Canada, Special Paper 37, p. 177–199.

Growdon, M.L. 2010: Crustal development and deformation of Laurentia during the Trans-Hudson and Alleghenian orogenies; Ph.D. thesis, Indiana University, Bloomington, Indiana, 221 p.

Hnatiuk, T., Couëslan, C.G., Chakhmouradian, A.R. and Martins, T. 2022: Preliminary results from targeted sampling of the Brezden Lake intrusive complex, west-central Manitoba (parts of NTS 64C4); *in* Report of Activities 2022, Manitoba Natural Resources and Northern Development, Manitoba Geological Survey, p. 42–48.

Lewry, J.F., Thomas, D.J., Macdonald, R. and Chiarenzelli, J. 1990: Structural relations in accreted terranes of the Trans-Hudson Orogen, Saskatchewan: telescoping in a collisional regime?; *in* The Early Proterozoic Trans-Hudson Orogen of North America, J.F. Lewry and M.R. Stauffer (ed.), Geological Association of Canada, Special Paper 37, p. 75–94.

Machado, N., Zwanzig, H. and Parent, M. 1999: U–Pb ages of plutons, sedimentation, and metamorphism of the Paleoproterozoic Kisseynew metasedimentary belt, Trans-Hudson Orogen (Manitoba, Canada); Canadian Journal of Earth Sciences, v. 36, p. 1829–1842.

Manitoba Geological Survey 2022: Bedrock geology of Manitoba; Manitoba Natural Resources and Northern Development, Manitoba Geological Survey, Open File OF2022-2, scale 1:1 000 000.

Martins T. and Couëslan, C.G. 2022: Critical minerals scoping study of the Suwannee River syenite intrusion, west-central Manitoba (part of NTS 64B4); *in* Report of Activities 2022, Manitoba Natural Resources and Northern Development, Manitoba Geological Survey, p. 36–41.

Martins, T., Couëslan, C.G. and Böhm, C.O. 2011: The Burntwood Lake alkali-feldspar syenite revisited, west-central Manitoba (part of NTS 63N8); *in* Report of Activities 2011, Manitoba Innovation, Energy and Mines, Manitoba Geological Survey, p. 79–85.

Martins, T., Couëslan, C.G. and Böhm, C.O. 2012: Rare metals scoping study of the Brezden Lake intrusive complex, western Manitoba (part of NTS 64C4); *in* Report of Activities 2012, Manitoba Innovation, Energy and Mines, Manitoba Geological Survey, p. 115–123.

Maxeiner, R., Ashton, K., Bosman, S., Card, C., Kohlruss, D., Marsh, A., Morelli, R. and Slimmon, W. 2021: Notes to accompany the new 2021 edition of the 1:1 000 000-scale geological map of Saskatchewan; Saskatchewan Geological Survey, Miscellaneous Report 2021-2, 20 p.

McRitchie, W.D. 1971: Burntwood Lake area (63N-7E, -8 and part of 10E); *in* Summary of Geological Field Work 1971, Manitoba Department of Mines, Resources and Environmental Management, Mines Branch, Geological Paper GP6/71, p. 30–33.

McRitchie, W.D. 1972: Burntwood Lake; Manitoba Department of Mines, Resources and Environmental Management, Mines Branch, Preliminary Map 1972G-11, scale 1:31 680.

McRitchie, W.D. 1987: Burntwood Lake syenite; *in* Report of Field Activities 1987, Manitoba Energy and Mines, Minerals Division, p. 65–69.

McRitchie, W.D. 1988: Alkaline intrusions of the Churchill Province Eden Lake (64C/9) and Brezden Lake (64C/4); *in* Report of Field Activities 1988, Manitoba Energy and Mines, Minerals Division, p. 5–11.

McRitchie, W.D. 1989: Ground scintillometer reconnaissance of the Eden Lake aegerine-augite monzonite; *in* Report of Field Activities 1989, Manitoba Energy and Mines, Minerals Division, p. 7–12.

Mumin, A.H. 2002: Discovery of a carbonatite complex at Eden Lake (NTS 64C9); *in* Report of Activities 2002, Manitoba Industry, Trade and Mines, Manitoba Geological Survey, p. 187–197.

Mumin, H. 2010: The Eden Lake rare metal (REE, Y, U, Th, phosphate) carbonatite complex Manitoba–updated report; *in* NI 43-101 technical report prepared for Medallion Resources Ltd, p. 87–94.

Murphy, L.A. and Zwanzig, H.V. 2021: Geology of the Wuskwatim–Granville lakes corridor, Kisseynew domain, Manitoba (parts of NTS 63O, P, 64A–C); Manitoba Agriculture and Resource Development, Manitoba Geological Survey, Geoscientific Report GR2021–2, 94 p.

Natural Resources Canada 2024: Critical minerals in Canada; Natural Resources Canada, URL <https://www.canada.ca/en/campaign/critical-minerals-in-canada/critical-minerals-an-opportunity-for-canada.html> [September 2024].

Pattison, D.R.M., Chacko, T., Farquhar, J. and McFarlane, C.R.M. 2003: Temperatures of granulite-facies metamorphism: constraints from experimental phase equilibria and thermobarometry corrected for retrograde exchange; Journal of Petrology, v. 44, p. 867–900.

Robinson, G.R., Jr., Hammarstrom, J.M. and Olson, D.W. 2017: Graphite; *in* Critical Mineral Resources of the United States—Economic and Environmental Geology and Prospects for Future Supply, K.J. Schulz, J.H. DeYoung, Jr., R.R. Seal II and D.C. Bradley (ed.), U.S. Geological Survey, Professional Paper 1802, p. J1–J24.

Wilson, L. and Head, J.W., III 2007: An integrated model of kimberlite ascent and eruption; Nature, v. 447, p. 53–57.

Zwanzig, H.V. 1990: Kisseynew gneiss belt in Manitoba: stratigraphy, structure, and tectonic evolution; *in* The Early Proterozoic Trans-Hudson Orogen of North America, J.F. Lewry and M.R. Stauffer (ed.), Geological Association of Canada, Special Paper 37, p. 95–120.

Zwanzig, H.V. 1997: Comments on "Kisseynew metasedimentary gneiss belt, Trans-Hudson orogen (Canada): back-arc origin and collisional inversion" by Ansdell et al., 1995 (Geology, v. 23, p. 1039–1043); Geology, v. 25, p. 90–91.

Zwanzig, H.V. 2008: Correlation of lithological assemblages flanking the Kisseynew Domain, Manitoba (parts of NTS 63N, 63O, 64B, 64C): proposal for tectonic/metallogenic subdomains; *in* Report of Activities 2008, Manitoba Science, Technology, Energy and Mines, Manitoba Geological Survey, p. 38–52.

Zwanzig, H.V. and Bailes, A.H. 2010: Geology and geochemical evolution of the northern Flin Flon and southern Kisseynew domains, Kississing-File lakes area, Manitoba (parts of NTS 63K, N); Manitoba Innovation, Energy and Mines, Manitoba Geological Survey, Geoscientific Report GR2010-1, 135 p.

GS2024-15

Thompson Facility and Compound core recovery project, east-central Manitoba (parts of NTS 64A1, 8): year two

by C.G. Couëslan

Summary

A project initiated in 2023 to salvage diamond-drillcore at the Manitoba Geological Survey's Thompson Facility and Compound was completed during the 2024 field season. The drillcore that remained to be salvaged was from an advanced exploration project in the Assean Lake area. Four drillholes were selected for recovery based on their length and their spatial distribution along the trend of mineralization.

In Brief:

- A project was initiated in 2023 to salvage diamond-drillcore that has been stored outdoors at the Manitoba Geological Survey's Thompson Facility and Compound
- Four drillholes were selected for recovery from the Assean Lake area based on length and spatial distribution along a trend of gold mineralization
- The core was restacked in cross piles, roofed with salvaged core boxes, and covered with tarps

Citation:
Couëslan, C.G. 2024: Thompson Facility and Compound core recovery project, east-central Manitoba (parts of NTS 64A1, 8): year two; *in* Report of Activities 2024, Manitoba Economic Development, Investment, Trade and Natural Resources, Manitoba Geological Survey, p. 127–128.

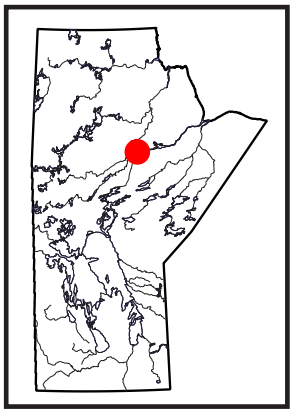
Project introduction and progress

A project initiated in 2023 to salvage diamond-drillcore stored outdoors at the Manitoba Geological Survey's Thompson Facility and Compound was completed during the 2024 field season. The drillcore boxes are in varying states of decay, with much of the core in danger of becoming lost. Drillcore from 75 holes was recovered during the first summer of the project (Couëslan, 2023b). All of the remaining drillcore was from an advanced gold exploration project in the Assean Lake area that ran from 2001 to 2004 (Assessment files 74035 and 74112, Manitoba Economic Development, Investment, Trade and Natural Resources, Winnipeg). During two weeks in July and August of 2024, the Assean Lake core was inventoried and four drillholes were selected for recovery based on length and their spatial distribution along the trend of mineralization. Core from a fifth drillhole (HT-01-3) from the Assean Lake project was recovered the previous year (Couëslan, 2023a).

The selected drillcore was removed from the cross piles and laid out. The core was washed and damaged boxes were either fixed or replaced. Missing, damaged or illegible core box labels were replaced with metal DYMO® tags. Core recovery from the four drillholes was close to 100% with very few pieces being lost because of core box collapse. The drillcore was restacked so that individual drillholes were organized within a single cross pile, rather than being distributed across several piles. The cross piles were roofed with salvaged core boxes and covered with tarps. A list of the drillcore recovered in 2023 and 2024 can be found in Data Repository Item DRI2024009[1] (Couëslan, 2024).

Economic considerations

Archived drillcore is often used by industry geologists to evaluate the mineral potential of an area, and can be a determining factor in whether or not investment dollars are spent in Manitoba. In addition, core can be used by geologists from surveys and academia to further the understanding of the geology of Manitoba, which can, in turn, open up areas to new exploration activities and targets. It is hoped that the drillcore recovered from this project can be moved to a secure indoor storage facility where it will continue to be available to geologists wishing to learn more about the geology and mineral potential of the Assean Lake area.



Acknowledgments

Thanks to M. Friesen (University of Manitoba) and A. Maki (Brandon University) for providing excellent field assistance, and C. Epp and T. Kennedy for logistical support. Thanks to M. Nicolas and J. Rentz for reviewing drafts of this report.

References

Couëslan, C.G. 2023a: Salvaged diamond-drillcore at the Thompson Facility and Compound, from east-central Manitoba (NTS 54C, 63P, 64A); Manitoba Economic Development, Investment, Trade and Natural Resources, Manitoba Geological Survey, Data Repository Item DRI2023006, Microsoft® Excel® file.

[1] MGS Data Repository Item DRI2024009, containing the data or other information sources used to compile this report, is available online to download free of charge at https://manitoba.ca/iem/info/library/downloads/index.html, or on request from minesinfo@gov.mb.ca, or by contacting the Resource Centre, Manitoba Economic Development, Investment, Trade and Natural Resources, 360-1395 Ellice Avenue, Winnipeg, Manitoba R3G 3P2, Canada.

Couëslan, C.G. 2023b: Thompson Facility and Compound core recovery project, east-central Manitoba (parts of NTS 54C, 63P, 64A); *in* Report of Activities 2023, Manitoba Economic Development, Investment, Trade and Natural Resources, Manitoba Geological Survey, p. 90–92.

Couëslan, C.G. 2024: Salvaged diamond-drillcore at the Thompson Facility and Compound, east-central Manitoba (parts of NTS 54C, 63P, 64A): updated; Manitoba Economic Development, Investment, Trade and Natural Resources, Manitoba Geological Survey, Data Repository Item DRI2024009, Microsoft® Excel® file.

GS2024-16

New uranium-lead zircon dates from the Lynn Lake greenstone belt, northwestern Manitoba (part of NTS 64C14): implications for diverse granitoid magmatism and gold mineralization

by X.M. Yang

In Brief:

- Two new precise U-Pb zircon dates establish the timing of syn- to post-Sickle granitoid intrusions, each with distinct geochemical traits
- The Motriuk Lake quartz diorite shows an adakitic signature, while the Little Brightsand Lake leucogranite is highly fractionated
- Syn- to post-Sickle adakitic granitoids reflect post-arc magmatism and track gold mineralization

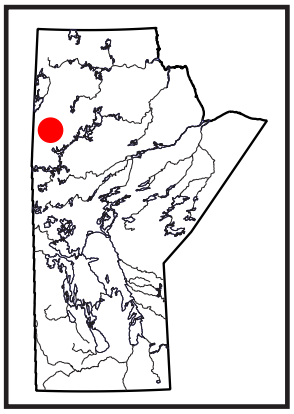
Citation:
Yang, X.M. 2024: New uranium-lead zircon dates from the Lynn Lake greenstone belt, northwestern Manitoba (part of NTS 64C14): implications for diverse granitoid magmatism and gold mineralization; *in* Report of Activities 2024, Manitoba Economic Development, Investment, Trade and Natural Resources, Manitoba Geological Survey, p. 129–144.

Summary

This report presents two new high-precision CA-ID-TIMS (chemical abrasion–isotope dilution–thermal ionization mass spectrometry) U-Pb zircon dates for two important granitoid intrusions from the Lynn Lake greenstone belt of the Paleoproterozoic Trans-Hudson orogen, northwestern Manitoba. Geochronological sampling was guided by detailed bedrock geological mapping and crosscutting relationships, which effectively constrained the temporal sequence of the dated granitoid intrusions relative to the surrounding country rocks. The leucogranite of the Little Brightsand Lake pluton, dated at 1848.3 ±2.7 Ma, intrudes the Zed Lake group greywacke, which is comparable to the Sickle group sedimentary rocks. This provides not only a precise crystallization (and/or emplacement) age of the leucogranite but also establishes a minimum deposition age for the Zed Lake group greywacke. The quartz diorite of the Motriuk Lake pluton, dated at 1849.4 ±1.3 Ma, cuts the Wasekwan group supracrustal package and displays an adakitic signature in its whole-rock geochemical composition, characteristic of post-arc slab failure granitoids. Geochemically, the Motriuk Lake quartz diorite is more primitive than the Little Brightsand Lake leucogranite. The two intrusions, while distinct in geochemical composition, are identical in age within their uncertainties and are therefore interpreted to be derived from distinct sources and emplaced in different geodynamic settings. The Motriuk Lake quartz diorite likely formed by post-arc magmatism triggered by slab break-off due to terrane collision during the Trans-Hudson orogeny, whereas the Little Brightsand Lake leucogranite originated from anatexis (or partial melting) of crustal materials. These new age data provide strong evidence for lithostratigraphic correlation, particularly for the period ca. 1857–1847 Ma in the region, and have significant implications for the understanding of diverse granitoid magmatism and its genetic link to orogenic gold mineralization in the Lynn Lake greenstone belt of the Paleoproterozoic Trans-Hudson orogen.

Introduction

In 2024, the Manitoba Geological Survey (MGS) continued its multiyear bedrock geological mapping program in the Paleoproterozoic Lynn Lake greenstone belt (LLGB), within the Trans-Hudson orogen of northwestern Manitoba. The objective of the fieldwork conducted in the summer of 2024 was to collect additional field data in support of the program's ultimate goal of updating 1:50 000 scale bedrock geology maps of the belt. This has involved examining key sites, continuing the ongoing compilation of existing data and incorporating newly acquired bedrock mapping information. Bulk-rock samples (n = 29) were collected from key exposures examined this past summer for further laboratory work. New field observations are highlighted below, in particular from the occurrences of diverse granitoid intrusions, which provide critical insights into the geodynamic evolution of the LLGB and genesis of the various types of economic mineralization at specific stages of the Trans-Hudson orogeny:



- A diorite stock cuts the Ralph Lake conglomerate, which is then cut by feldspar porphyry dikes.
- A leucogranite intrusion, part of the Little Brightsand Lake pluton, intrudes greywacke of the Zed Lake group.
- The Motriuk Lake pluton cuts the Wasekwan group volcanic and volcaniclastic to sedimentary sequence.
- A garnet-bearing S-type granodiorite phase in the Zed Lake pluton, cut by leucogranite dikes, has been identified.
- Muscovite-tourmaline pegmatite dikes cut volcano-sedimentary rocks of the Wasekwan group.

Based solely on the crosscutting relationships observed in the field, the Little Brightsand Lake granitoid intrusion in this report can be interpreted as postdating deposition of the Zed Lake group greywacke and the Motriuk Lake pluton as postdating Wasekwan group. The feldspar

porphyry dike and muscovite-tourmaline pegmatite dikes might be part of the Late intrusive suite that appear to be discrete in occurrence and do not show a certain connection with any large granitoid plutons (Yang, 2019, 2021a, 2023a; Yang and Beaumont-Smith, 2015, 2017). This study uses high-resolution, chemical-abrasion, isotope dilution–thermal ionization mass spectrometry (CA-ID-TIMS) U-Pb zircon geochronology to date the Motiuk Lake and Little Brightsand Lake plutons. The former cuts through the Wasekwan group (Yang, 2019), and the latter intrudes the Zed Lake group (Yang, 2021a). The new data provide a key piece of evidence for lithostratigraphic correlation in the region, geodynamic evolution, occurrences of diverse granitoid magmatism and their genetic linkages with potential economic mineralization, such as orogenic gold and rare metals or critical minerals. A revised tectonic model is proposed to demonstrate the geodynamic processes recorded in diverse granitoid intrusions and associated mineralization potential of the LLGB.

General geology

The LLGB, an important element of the Paleoproterozoic Trans-Hudson orogen (THO; Hoffman, 1988; Lewry and Collerson, 1990; Zwanzig, 2004; Ansdell, 2005; Corrigan et al., 2007, 2009; Zwanzig and Bailes, 2010; Corrigan, 2012), is endowed with several styles of economic mineralization, such as volcanogenic massive sulphide (VMS) zinc-copper (Zn-Cu), magmatic nickel-copper-cobalt (Ni-Cu-Co) and orogenic gold (Au; see Figure GS2024-16-1), as well as rare-earth elements and niobium hosted in the Eden Lake carbonatite complex (e.g., Mumin, 2002; Chakhmouradian et al., 2008). Mining in the Lynn Lake greenstone belt has historically contributed significantly to Manitoba's economy and continues to remain a primary focus for mineral exploration companies.

The LLGB is bounded to the north by the Southern Indian domain and flanked to the south by the Kisseynew domain (Gilbert et al., 1980; Gilbert, 1993; Zwanzig and Bailes, 2010; Martins et al., 2022). It is composed of two east- to northeast-trending, steeply dipping belts (Figure GS2024-16-1) consisting of various supracrustal rocks of the Wasekwan group that were intruded by granitoid plutons of the 1.891–1.870 Ga Pool Lake intrusive suite (Manitoba Energy and Mines, 1986; Baldwin et al., 1987; Turek et al., 2000; Beaumont-Smith and Böhm, 2002; Beaumont-Smith et al., 2006), which is believed to be pre-Sickle (e.g., Yang and Beaumont-Smith, 2015; Yang, 2023a). The Wasekwan group consists of a variety of volcanic rocks, including basalt, andesite, dacite, rhyolite and related volcaniclastic rocks, along with sedimentary rocks. Younger, molasse-type sedimentary rocks of the Sickle group (>1.836 Ga; see Lawley et al., 2020) unconformably overlie the Wasekwan group and the Pool Lake intrusive suite. Based on their crosscutting relationships with the Sickle group, the granitoid intrusions in the LLGB are divided into three intrusive suites: pre-Sickle, syn- to post-Sickle and late intrusions (Milligan, 1960; Yang and Beaumont-Smith, 2015, 2017; Yang and Lawley, 2018, 2024a; Yang, 2019, 2021a, 2023a). The supracrustal rocks and the granitoid rocks of the LLGB experienced peak amphibolite-facies metamorphism ca. 1.83–1.81 Ga (Lawley et al., 2020, 2023). The lithostratigraphic column of the supracrustal sequence, including the Wasekwan and Sickle groups (as well as the Ralp Lake and Zed Lake groups, interpreted by some authors as comparable with the Sickle group; see Gilbert et al., 1980; Syme, 1985; Gilbert, 1993; Lawley et al., 2020, 2023), and their relationships with three intrusive suites of granitoid plutons and/or intrusions, are illustrated in Figure GS2024-16-2, which also highlights various styles of economic mineralization within the LLGB.

Significant differences in the geology and geochemistry of the northern and southern belts of the LLGB (Gilbert et al., 1980; Syme, 1985; Zwanzig et al., 1999; Beaumont-Smith, 2008; Glendenning et al., 2015) may reflect regional differences in tectonic settings obscured by structural transposition of multiple deformation events (D_1–D_6; Zwanzig, 2000; Anderson and Beaumont-Smith, 2001; Beaumont-Smith and Böhm, 2002, 2003, 2004; Jones et al., 2006). The northern and southern belts contain disparate volcanic assemblages that were later structurally juxtaposed, likely representing a tectonic collage (Zwanzig et al., 1999) formed by northward subduction, followed by contraction and underthrusting of the Kisseynew domain beneath the LLGB during terminal collision (White et al., 2000). Note that this report uses the term 'Wasekwan group' to consist with publications released previously by the MGS (e.g., Gilbert et al., 1980; Gilbert, 1993; Syme, 1985; Baldwin et al., 1987; Beaumont-Smith and Böhm, 2002, 2003, 2004; Beaumont-Smith, 2008; Yang, 2023a, 2023b and references therein).

Field observations and historical drilling records indicate the presence of disseminated to massive sulphides (e.g., sphalerite, chalcopyrite, pyrrhotite) in the Wasekwan supracrustal rocks, including the Fox VMS Zn-Cu ore deposit (Gilbert et al., 1980; Fedikow and Gale, 1982; Baldwin, 1989; Ferreira, 1993; Yang and Beaumont-Smith, 2015, 2016; Yang, 2022, 2023b). These sulphide minerals, regardless from strata-bounded VMS deposits or country rocks, may have played an important role in the formation of magmatic Ni-Cu-Co ore deposits hosted in mafic-ultramafic intrusions (e.g., the Lynn Lake deposit; Figures GS2024-16-1 and -2) via providing external sulphur required for triggering sulphide saturation in tholeiitic (or calcic) gabbroic magmas (Yang, 2023b). Orogenic gold deposits in the LLGB, either intrusion-hosted or epigenic, are controlled mostly by D_2 shear zones, although the intersections of D_3 or D_4 structures with D_2 faults could be favourable settings for Au further enrichment (i.e., chemical-structural traps; Beaumont-Smith and Böhm, 2004; Jones et al., 2006; Yang and Beaumont-Smith, 2015; Hastie et al., 2018; Lawley et al., 2020, 2023). Multiple phases of gold (Au) mineralization occurred up to 80 Myr after the peak of metamorphism (Figure GS2024-16-2), potentially as a result of the exhumation of the THO (see Lawley et al., 2023).

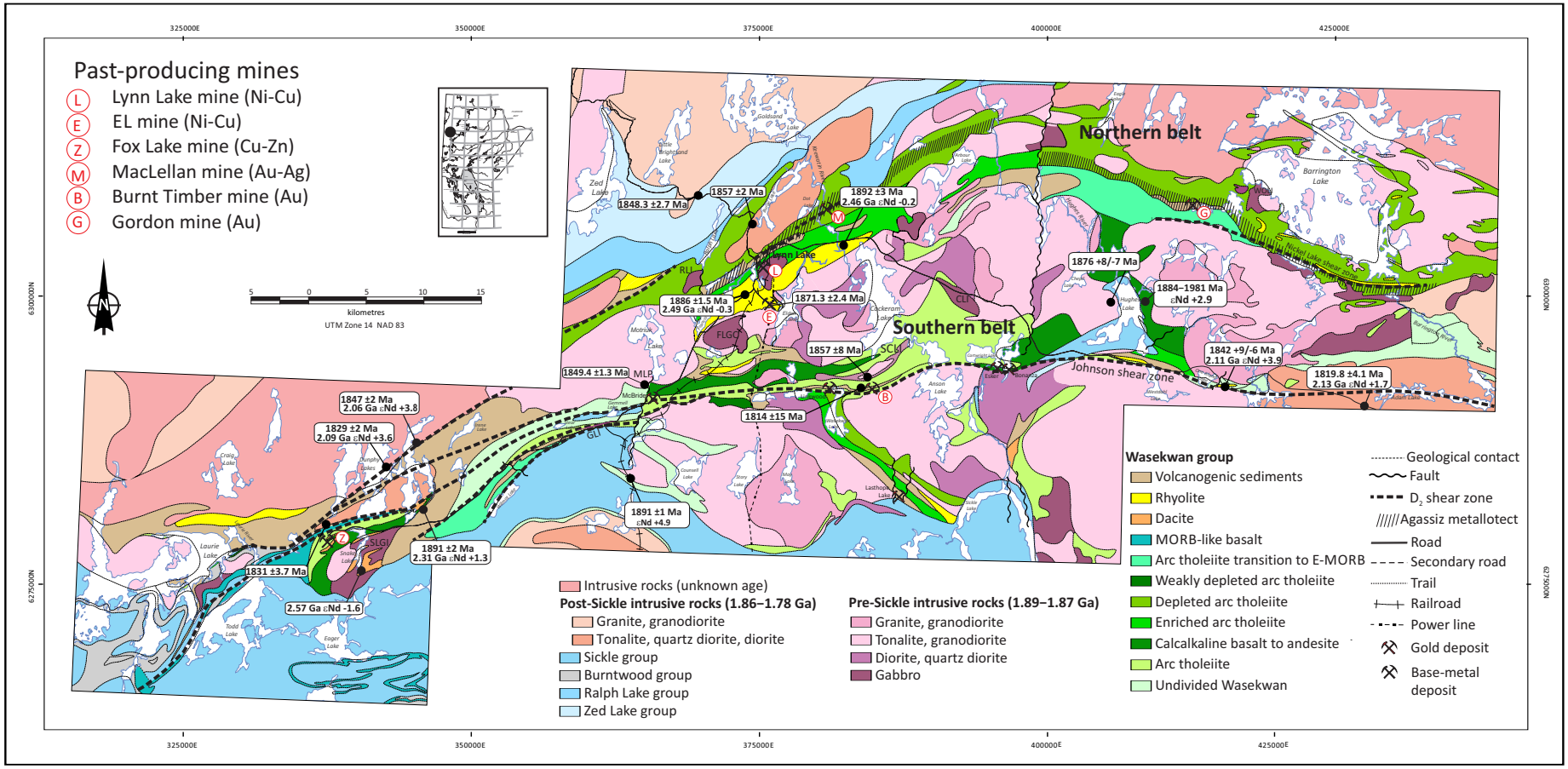


Figure GS2024-16-1: *Regional geology with uranium-lead zircon ages and neodymium isotopic compositions of the Lynn Lake greenstone belt (modified and compiled from Gilbert et al., 1980; Manitoba Energy and Mines, 1986; Gilbert, 1993; Zwanzig et al., 1999; Turek et al., 2000; Beaumont-Smith and Böhm, 2002, 2003, 2004; Beaumont-Smith et al., 2006; Jones et al., 2006; Beaumont-Smith, 2008; Yang and Beaumont-Smith, 2015, 2016, 2017; Lawley et al., 2020, 2023; Yang, 2022, 2023b). Abbreviations: CLI, Cartwright Lake intrusion; FLGC, Fraser Lake gabbro complex; GLI, Gemmell Lake intrusion; MLP, Motriuk Lake plug; MORB, mid-ocean–ridge basalt; RLI, Ralph Lake intrusion; SCLI, Southern Cockeram Lake intrusion; SLGI, Snake Lake gabbro intrusion; WOLI, White Owl Lake intrusion.*

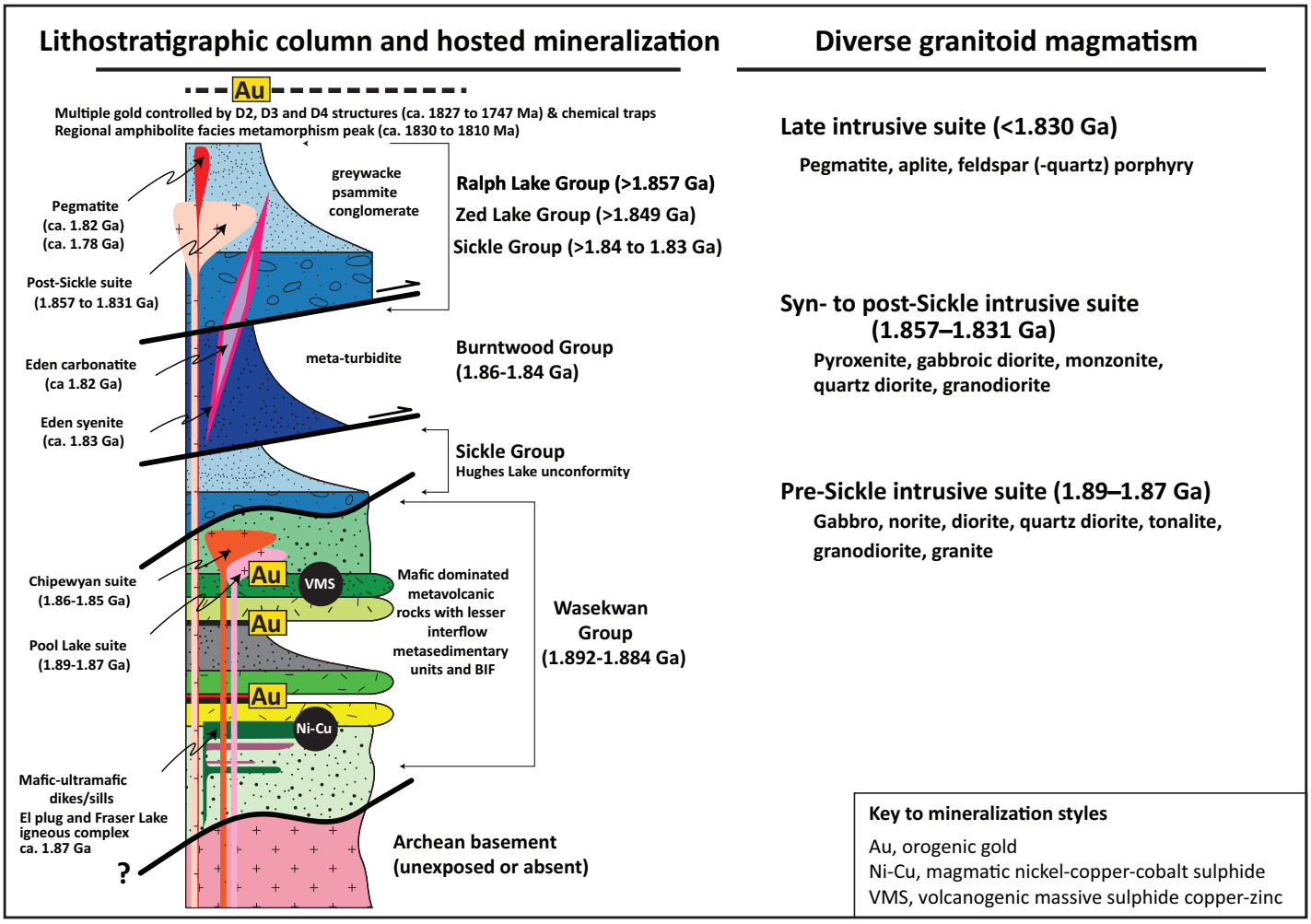


Figure GS2024-16-2: *Schematic lithostratigraphic column of the Lynn Lake greenstone belt, intruded by three suites of various styles of granitoid intrusions and related (or) hosted mineralization based on the field relationships, detailed bedrock geological mapping, new and published U-Pb zircon geochronological data (modified after Lawley et al., 2020, 2023; Yang, 2019, 2023a; this study). Abbreviation: BIF, banded iron formation.*

Sample descriptions

Two granitoid samples were dated to establish precise age constraints on the timing of their crystallization and/or emplacement. One sample (111-19-350A01) is a quartz diorite collected from the Motriuk Lake pluton that cuts the supracrustal sequence of the Wasekwan group (Yang, 2019). This quartz diorite is massive, medium-grained, moderately to weakly foliated and equigranular, displaying relatively high magnetic susceptibility (MS) values of up to 7.6 × 10^{-3} SI indistinguishable from normally oxidized magnetite-series and normal I-type granites elsewhere (Chappell and White, 1974, 1992, 2001; Ishihara, 1977, 1981, 2004; Yang, 2023a). It consists of 5-10% quartz (~3–4 mm), 60-70% plagioclase laths (3–5 mm), and 15–20% amphibole with diffuse crystal edges (2–5 mm; Figure GS2024-16-3a), and accessory minerals including Fe-Ti oxides, zircon, titanite, and apatite.

The other sample dated in this study is a leucogranite (111-21-154A01) that was collected from the Little Brightsand Lake pluton intruding the Zed Lake group greywacke (Yang, 2021a). This leucogranite is medium- to coarse-grained, massive, equigranular and locally porphyritic, having low MS value of 0.054 × 10^{-3} SI, much similar to reduced ilmenite series and S-type granites (Chappell and White, 1974, 1992, 2001; Ishihara, 1977, 1981, 2004; Yang, 2023a). It consists of 25–35% anhedral quartz (2–4 mm), 55–60% subhedral to euhedral feldspar (2–4 mm), 4–5% biotite and about ~1% muscovite (Figure GS2024-16-3b). The contact between the greywacke and the leucogranite is sharp and wavy to irregular, and concentrates biotite aggregates on the greywacke side, typical of contact metamorphism caused by the leoucogranite intrusion (Yang, 2021a). The leucogranite becomes finer in grain size as it approaches the contact with the Zed Lake greywacke. It occurs as dikes and/or veins that seem to have been emplaced along S_2 foliations, which are folded into 'Z' shapes and boudinaged together with quartz veins containing pyrite (Figure GS2024-16-3c, d). This suggests that the leucogranite is syn-kinematic and likely influenced by trans-compression during terrane collision.

Geochemical attributes

Granitoid samples from the Motriuk Lake and Little Brightsand Lake plutons exhibit distinctly different geochemical char-

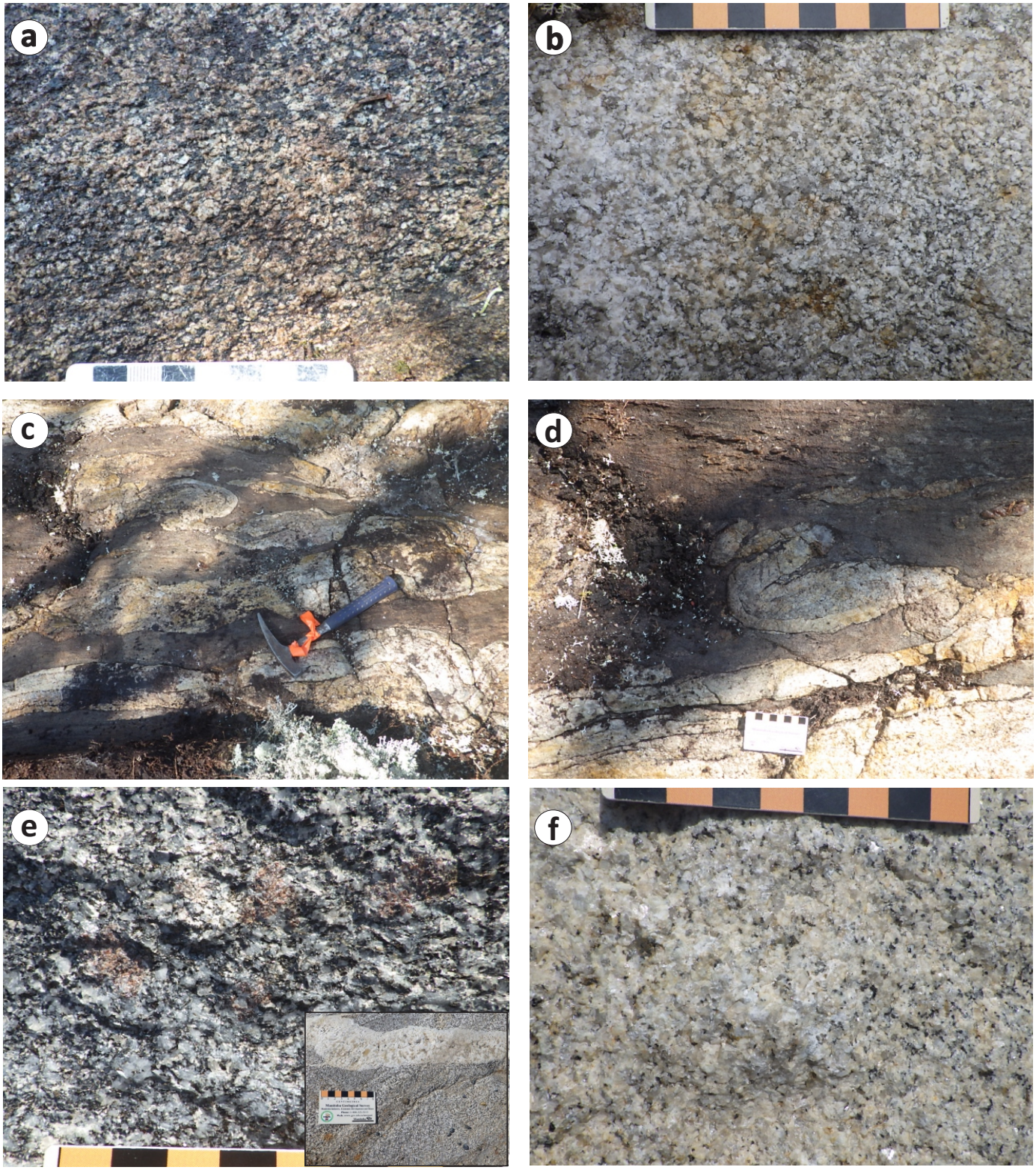


Figure GS2024-16-3: *Field photos of granitoid rocks showing textural features and field relationships, and the rocks sampled for precise U-Pb zircon age determination:* ***a)*** *medium-grained quartz diorite from the Motriuk Lake pluton (UTM Zone 14, 365250E, 6292311N, NAD 83);* ***b)*** *massive, equigranular, medium- to coarse-grained leucogranite from the Little Brightsand Lake pluton (UTM 369166E; 6308570N) with MS value of 0.054 × 10^{-3} SI;* ***c)*** *the leucogranite dikes and/or veins cut the Zed Lake greywacke that has higher MS value of 0.348 × 10^{-3} (UTM 365250E, 6292311N);* ***d)*** *the leucogranite dikes and veins are folded (e.g., as 'Z'-shaped fold) and boudinaged. UTM co-ordinates are the same as the exposure of (c); hammer handle points north;* ***e)*** *medium-grained garnet-bearing granodiorite (MS value of 0.44 × 10^{-3}) from the Zed Lake pluton (UTM 363768E, 6314725N), which is cut by a medium- to coarse-grained leucogranite dike as shown by inset photo in the lower right corner; note that reddish garnet presents mainly as garnet + biotite + feldspar aggregates, although discrete garnet crystals are also evident; and* ***f)*** *medium- to coarse-grained leucogranite (MS value of 0.041 × 10^{-3}) UTM locality is the same as (e).*

acteristics (Figure GS2024-16-4; the data from Yang, 2020, 2021b, 2024). The Motriuk Lake samples have relatively lower and varied SiO_2 contents and range from diorite to granodiorite and granite, according to the total alkalis versus silica (TAS) classification diagram (Figure GS2024-16-4a) proposed by Middlemost (1994). These samples display a mainly calcalkaline affinity, with one exception that is calcic or tholeiitic based on the Rittmann serial index (σ <1.2; Yang, 2007). They are mainly metaluminous, as indicated by the Shand index diagram (Figure GS2024-16-4b) and less evolved in geochemical composition, as suggested by lower τ[1] values (22.1–53.0). Additionally, the Motriuk Lake samples show high Sr/Y (>40) and La/Yb (>20) ratios (Figure GS2024-16-4c), which are characteristic of adakite-like granitoids and/or sanukitoids (Shirey and Hanson, 1984; Martin et al., 2005, 2009; Richards and Kerrich, 2007; Yousefi and Lentz, 2024) or slab-failure granitoids (Hildebrand et al., 2018; Yang and Lawley, 2018, 2024a, 2024b; Whalen and Hildebrand, 2019).

The granitoid samples from the Little Brightsand Lake pluton are exclusively situated in the granite field on the TAS diagram and are predominantly calcic in magmatic affinity (Figure GS2024-16-4a). They are classified as peraluminous granites based on the Shand index (Figure GS2024-16-4b). All four samples display low La/Yb ratios (<20) and an exceptionally wide range of Sr/Y ratios, from 6 to 1436, with some values plotting beyond the scale of Figure GS2024-16-4c. These geochemical signatures suggest the significant presence of feldspar cumulates in the rocks. This is supported further by their calcic (or tholeiitic) magmatic affinity combined with highly evolved geochemical characteristics, as indicated by their high SiO_2 concentrations (73.4 wt. % to 74.5 wt. %) and high τ values (54.4 to 241.4).

U-Pb zircon dating

Precise U-Pb zircon ages from episodic granitoid magmatism is crucial in understanding the geodynamic settings recorded by granitoids in mountain belts, such as the Paleozoic Appalachian Mountains (e.g., Frisch et al., 2011), the Paleoproterozoic Trans-Australian Orogen (Gibson et al., 2024), and the Paleoproterozoic Trans-Hudson orogen (Beaumont-Smith and Böhm, 2002; Beaumont-Smith et al., 2006; Yang and Lawley, 2018). A variety of genetic types of granitoids have been identified thus far in the LLGB of the Manitoban THO, such as volcanic arc I-type, intra-arc extensional A-type, and adakite-like (or adakitic) granitoids intrusions as well as collisional S-type granites (Yang, 2019, 2021a, 2023a; Yang and Lawley, 2018, 2024a, 2024b; see Figure GS2024-16-3a to -3f). As mentioned above, these diverse granitoids can be grouped into pre-Sickle, syn- to post-Sickle and late intrusive suites (Figure GS2024-16-2).

Methods

U-Pb zircon geochronological analysis was performed at the Jack Satterly Geochronology Laboratory, the University of Toronto, Ontario (Canada), using chemical abrasion- isotope dilution-thermal ionization mass spectrometry (CA-ID-TIMS) dating techniques with high precision. Whole-rock samples are initially crushed and ground into powder, followed by heavy mineral separation using a Wilfley table and further purification through density and magnetic separations. Zircon, the target mineral, is selected manually under a binocular microscope to ensure the freshest and least altered grains are chosen (see Hamilton, 2022).

The selected zircon grains undergo chemical abrasion to remove radiation-damaged areas, following a modified procedure after Mattinson (2005). This involves annealing the grains at 900°C for two days and etching them in hydrofluoric acid. The chemically abraded grains are then dissolved, and uranium (U) and lead (Pb) are isolated using anion exchange columns as described by Krogh (1973). The isotopic compositions of Pb and UO_2 are analyzed using a VG354 mass spectrometer with a Daly collector, following the methodology outlined by Gerstenberger and Haase (1997).

The mass spectrometer data is processed using the UtilAge program developed by D. Davis, with corrections for initial ^{230}Th disequilibrium in zircon applied to the $^{206}Pb/^{238}U$ ages, assuming a Th/U ratio in the magma of 4.2 (Hamilton, 2022). Common Pb is assigned to procedural blank, and initial Pb above 1 picogram is corrected using the Pb evolution model by Stacey and Kramers (1975). The analytical results are tabulated in Table GS2024-16-1. The Concordia curve is plotted using the Isoplot 3.71 Add-In for MS Excel® program (Ludwig, 2009), incorporating uncertainties in uranium decay constants (Jaffey et al., 1971). Ages are reported with a 95% confidence level, and complex cases are discussed in detail (below).

Results

Quartz diorite (sample 111-19-350A01) from the Motriuk Lake pluton

Abundant zircon crystals were yielded from least magnetic fraction of the heavy mineral concentrate from the quartz diorite sample 111-19-350A01. These zircon crystals are nearly pure, fine-grained, and dominated by colourless to very pale yellow, clear to slightly clouded, short to elongate (up to 5:1) prismatic morphologies, commonly with cracks. These features are common for magmatic zircons (Corfu et al., 2003). Four pristine zircon crystals (see inset photos a and b of Figure GS2024-16-5) were selected for U-Pb chemical and isotope analysis. Minor molybdenite is present in the mineral separates, as is well-formed dark and pale titanite in the more magnetic fractions.

[1] $\tau = (Al_2O_3 - Na_2O)/TiO_2$, unit in wt. %. τ was proposed by (Grasso, 1968), that is termed Gottini index and can be used readily for describing degree of magmatic differentiation (Yang, 2007). A higher τ value signifies a greater level of differentiation.

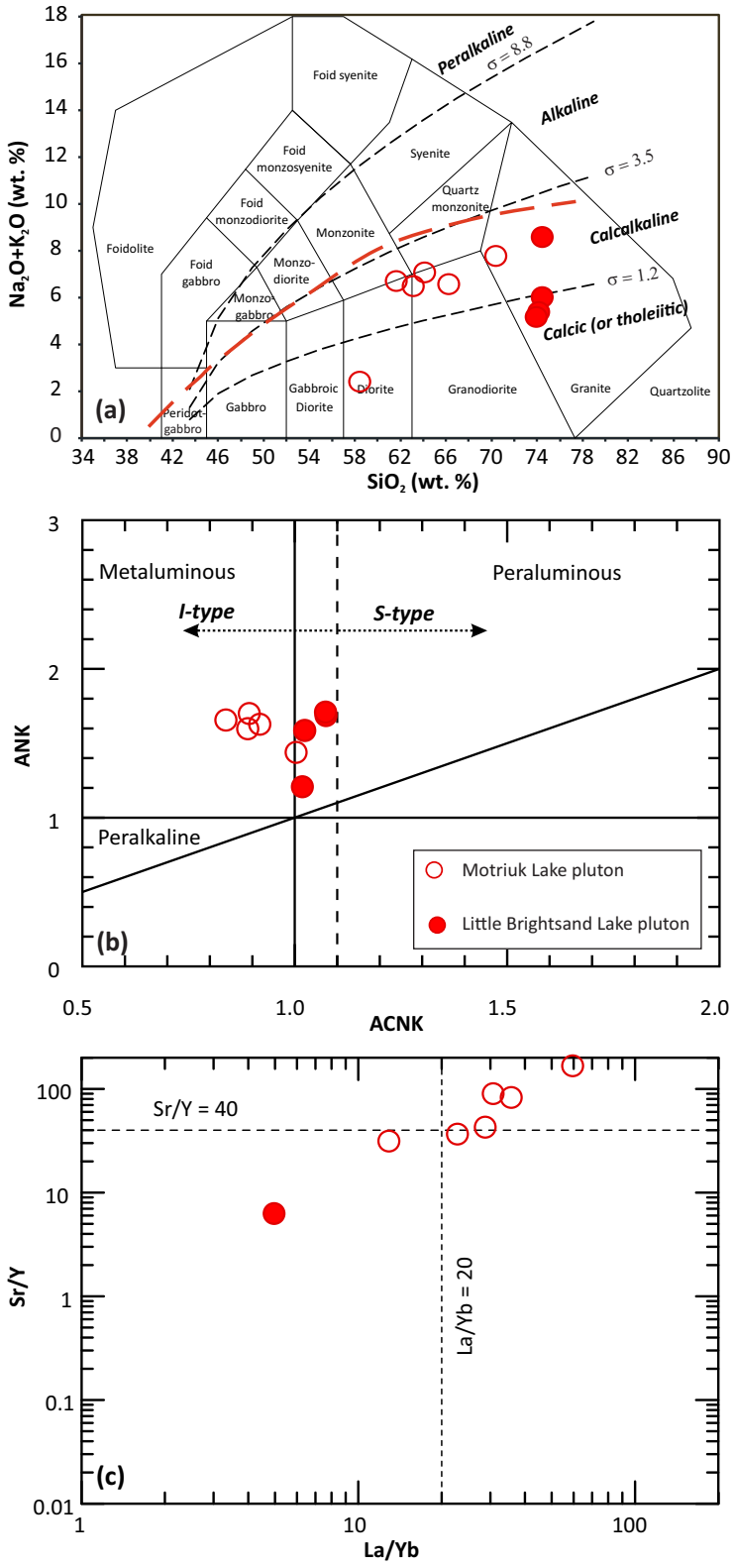


Figure GS2024-16-4: *Geochemical characteristics of granitoid rocks:* ***a****) total alkalis versus SiO_2 diagram (TAS; after Middlemost, 1994); dashed lines labeled σ values indicate the boundaries between calcic (σ ≤ 1.2), calc-alkaline (1.2 < σ < 3.5), alkaline (3.5 < σ < 8.8), and peralkaline series (8.8≤ σ) (after Yang, 2007); σ denotes the Rittmann Serial index, and σ = $(Na_2O + K_2O)^2/(SiO_2 - 43)$, unit in wt. % (Rittmann, 1962, 1973); red dashed line is boundary of subalkaline and alkaline volcanic rocks (Irvine and Barager, 1971).* ***b****) Shand index plot based on ANK versus ACNK (after Maniar and Piccoli, 1989); ACNK = molar $Al_2O_3/(CaO+Na_2O+K_2O)$, ANK = molar $Al_2O_3/(Na_2O + K_2O)$; vertical dashed line is ACNK = 1.1 discriminating S- from I-type granites (after Chappell and White, 1974, 2001).* ***c****) Sr/Y versus La/Yb ratios for discrimination of adakites from arc rocks (after Richards and Kerrich, 2007); note that three samples from the Little Brightsand Lake pluton plot out of Y-axis as they have Sr/Y ratios of 647 to 1436 but low La/Yb (<20), suggestive of the occurrence of significant amounts of feldspar cumulates (data sources: Yang, 2020, 2021b, 2024).*

Table GS2024-16-1: Chemical abrasion–isotope dilution–thermal ionization mass spectrometry (CA-ID-TIMS) U-Pb isotopic data for zircons in the granitoids samples from the Lynn Lake greenstone belt.

Sample/ Fraction	Description	U (ppm)	Th/U	Pb^1 (pg)	Pb_c (pg)	$^{206}Pb/^{204}Pb$	$^{207}Pb/^{235}U$	±2σ	$^{206}Pb/^{238}U$	±2σ	Corr. Coeff. (rho)	$^{207}Pb/^{206}Pb$	±2σ	$^{207}Pb/^{235}U$	±2σ	$^{206}Pb/^{238}U$	±2σ	$^{207}Pb/^{206}Pb$	±2σ	Disc. (%)
Motriuk Lake quartz diorite (sample 111-19-350A01; UTM Zone 14, 365250E, 6292311N, NAD 83)																				
Z1	1 clr, cls, flat, shrt pr; incl	310	0.456	108.7	0.50	13046	5.17896	0.01922	0.332161	0.000866	0.7439	0.113082	0.000281	1849.2	3.2	1848.8	4.2	1849.5	4.5	0.0
Z2	1 clr, cls, el (2.5:1) pr; incl	271	0.430	47.86	0.35	8271	5.17568	0.01297	0.331983	0.000679	0.9111	0.113071	0.000120	1848.6	2.1	1848.0	3.3	1849.3	1.9	0.1
Z3	1 clr, cls, brkn el pr, crkd; dk incl	171	0.480	62.36	11.27	338	5.19269	0.08079	0.332697	0.001238	0.6804	0.113199	0.001508	1851.4	13.3	1851.4	6.0	1851.4	24.2	-0.0
Z4	1 clr, cls, crkd flat pr	340	0.439	138.0	1.28	6521	5.17664	0.01334	0.332008	0.000676	0.9102	0.113083	0.000126	1848.8	2.2	1848.1	3.3	1849.5	2.0	0.1
Little Brightsand Lake leucogranite (sample 111-21-154A01; UTM Zone 14369166E, 6308570N, NAD 83)																				
Z1	1 c-e, cls-grey brkn needle, tip	40	0.046	13.1	1.00	888	5.22109	0.03818	0.335048	0.001152	0.6689	0.113019	0.000636	1856.1	6.2	1862.8	5.6	1848.5	10.2	-0.9
Z2	2 cls, cls flat/el, crkd pr	52	0.040	16.8	0.92	1224	5.18501	0.06047	0.332469	0.003484	0.9242	0.113109	0.000505	1850.2	9.9	1850.3	16.9	1850.0	8.1	-0.0
Z3	1 c-e, cls-grey, brkn, el, oz pr	124	0.087	40.3	0.78	3393	5.17291	0.01705	0.332030	0.000844	0.8565	0.112994	0.000195	1848.2	2.8	1848.2	4.1	1848.1	3.1	-0.0
Z4	1 clr, cls, crkd, flat, brkn, el pr tip	44	0.051	14.1	1.40	682	5.18691	0.04715	0.333003	0.001147	0.6481	0.112969	0.000830	1850.5	7.7	1852.9	5.5	1847.7	13.3	-0.3

Notes:
All analyzed zircon fractions represent best optical quality (crack, inclusion, and core free), freshest (least altered) available grains. All zircons were chemically abraded.
Abbreviations: anh, anhedral; brkn, broken; c-e, cloudy-etched; cld, clouded/turbid; clr, clear; cls, colourless; crkd, cracked; dk, dark; dt, doubly-terminated; el, elongate; eq, equant; ext, exterior/outermost; fctd, faceted; frag, fragment(s); gl, glassy; incl, mineral or melt inclusion(s); irr, irregular; lrg/med/sm, larger/medium/smaller; oz, oscillatory-zoned; pbr, pale brown; pr, prism/prismatic; shrp, sharp; shrt, short; skel, skeletal; sl rnd, slightly rounded; Z, zircon.
Pb^T is total amount (in picograms) of Pb.
Pb_C is total measured common Pb (in picograms) assuming the isotopic composition of laboratory blank: 206/204 - 18.49 ±0.4%; 207/204 - 15.59 ±0.4%; 208/204 - 39.36 ±0.4%.
Pb/U atomic ratios are corrected for spike, fractionation, blank, and, where necessary, initial common Pb; $^{206}Pb/^{204}Pb$ is corrected for spike and fractionation.
Th/U is model value calculated from radiogenic $^{208}Pb/^{206}Pb$ ratio and $^{207}Pb/^{206}Pb$ age, assuming concordance.
Disc. (%) - per cent discordance for the given $^{207}Pb/^{206}Pb$ age.
Uranium decay constants are from Jaffey et al. (1971).

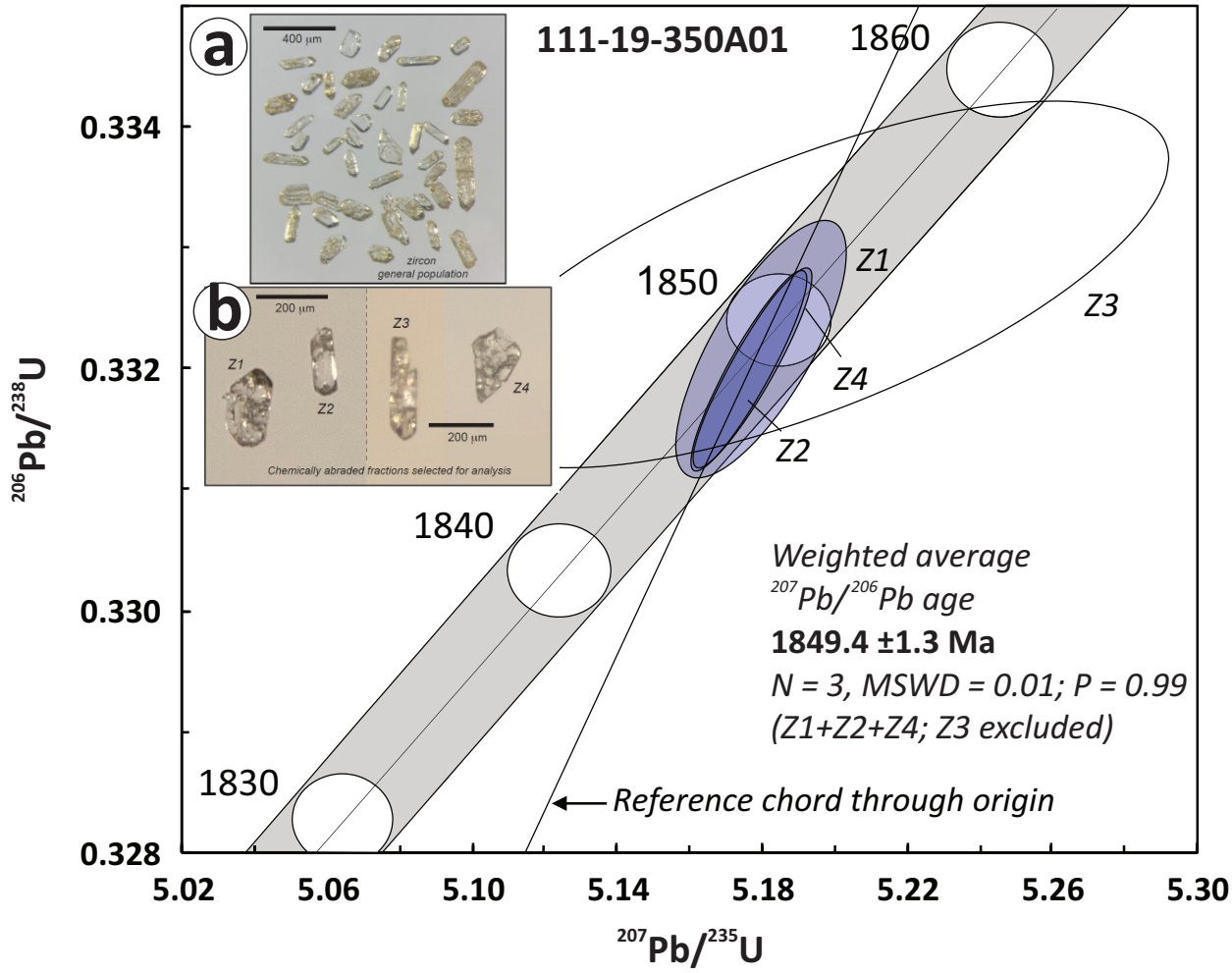


Figure GS2024-16-5: *Concordia diagram of CA-ID-TIMS U-Pb zircon age data for quartz diorite sample from the Motriuk Lake pluton in the Lynn Lake greenstone belt. Inset photos show population of zircons recovered from the sample* ***(a)*** *and chemical abraded and analysed zircon grains* ***(b)****. Abbreviations: MSWD, mean squares of weighted deviates; N, number of analyses; P, probability.*

U-Pb isotopic results are presented for the analyzed four single grain zircon fractions in Table GS2024-16-1 and plot on Figure GS2024-16-5. The data points for all fractions are concordant and overlapping, although the results for Z3 are imprecise due to elevated common Pb, likely resulting from the presence of micro-inclusions in it. Nevertheless, calculated $^{207}Pb/^{206}Pb$ ages for all four analyses range narrowly between 1849.3 and 1851.4 Ma, and between 1849.3 and 1849.5 Ma when excluding Z3. A weighted average age calculated for Z1, Z2 and Z4 gives 1849.4 ±1.3 Ma (MSWD = 0.01; P = 99%). This age is considered a robust age for the timing of crystallization and/or emplacement of the quartz diorite. This age certainly fits within the intermediate age interval of felsic plutonism in the Lynn Lake greenstone belt (e.g., 1857 to 1847 Ma; Figure GS2024-16-2). It is also similar to the older age for the northeast Dunphy Lakes hornblende tonalite, at 1847 ±2 Ma reported by Beaumont-Smith and Böhm (2003). Note that Beaumont-Smith and Böhm (2003) also reported a slightly younger age of ca. 1843 Ma for a rhyodacite sample collected from One Island Lake to east of the LLGB (see Figure GS2024-16-1), that seems to be product of a distinct episode of magmatism from the Motriuk Lake adakitic plutonism.

Leucogranite (sample 111-21-154A01) from the Little Brightsand Lake pluton

This leucogranite sample gave a good recovery of zircon grains, with the population dominated by elongate, colourless to pale- and medium-yellow, clear to clouded, frequently cracked crystals (see inset photos a and b in Figure GS2024-16-6).

A total of four fractions were analyzed from this sample, each comprising 1 or 2 grains; the results are all overlapping and mostly concordant (Table GS2024-16-1; Figure GS2024-16-6). Most of the zircon crystals appear to be relatively low in U (much like the whole rock) and nonradiogenic for Pb, so that the individual analyses have slightly expanded error ellipses, but the $^{207}Pb/^{206}Pb$ ages are all very consistent between 1847.7 and 1850.0 Ma. The analyzed zircons are also very depleted in Th, giving uniformly low Th/U ratios between 0.04 and 0.09 (Table GS2024-16-1). Collectively, all four analyses yield a weighted

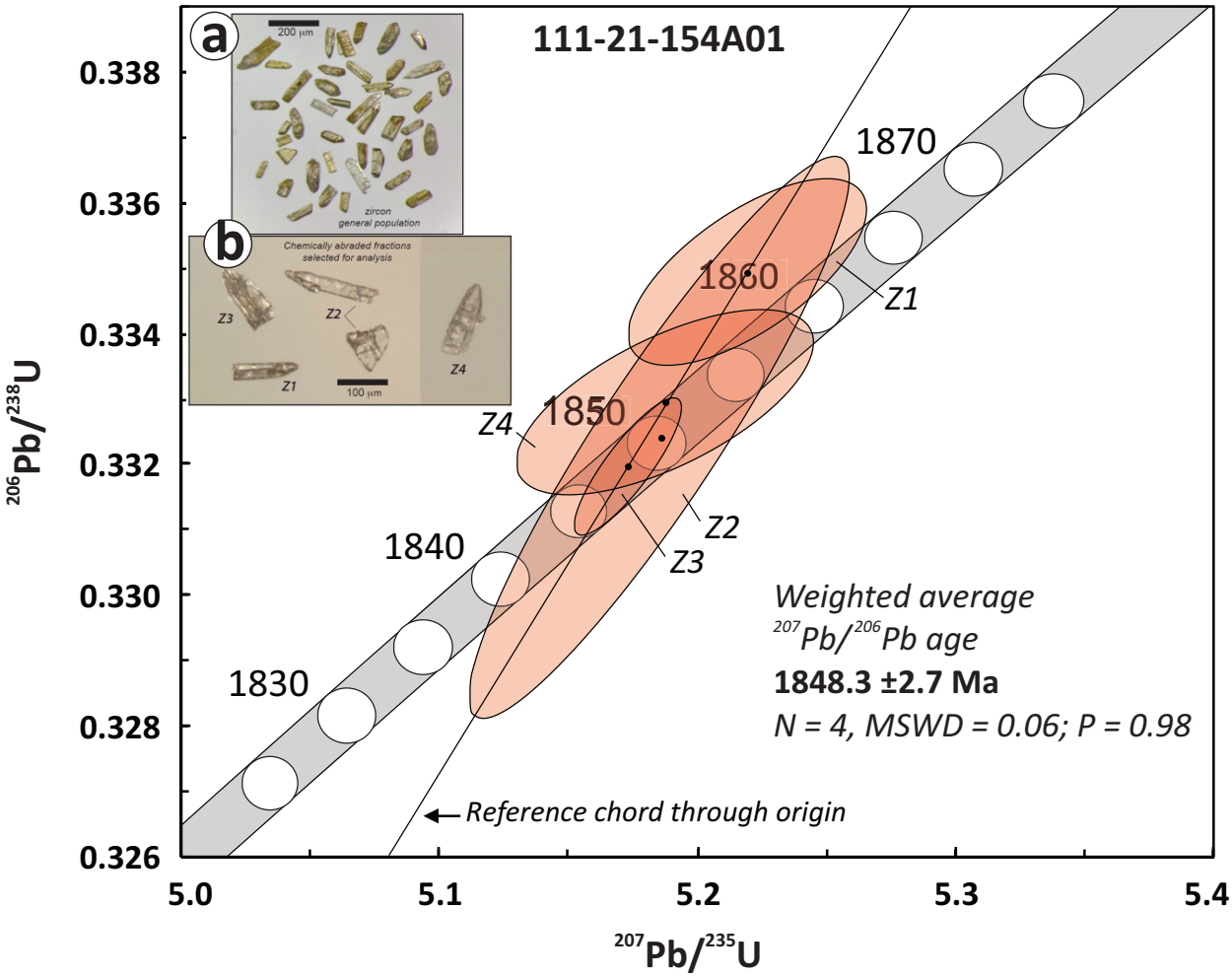


Figure GS2024-16-6: *Concordia diagram of CA-ID-TIMS U-Pb zircon age data for the granite sample collected from the Little Brightsand Lake pluton in Ralph Lake mapping area (Yang, 2021a), Lynn Lake greenstone belt. Inset photos show population of zircons recovered from the sample* ***(a)*** *and chemical abraded zircon grains* ***(b)****. Abbreviations: MSWD, mean squares of weighted deviates; N, number of analyses; P, probability.*

average $^{207}Pb/^{206}Pb$ age of 1848.3 ±2.7 Ma (MSWD = 0.06; P = 98%). This age is statistically identical within error to the new age presented above for sample 111-19-350A01 (1849.4 ±1.3 Ma) but is younger than the 1857 ±2 Ma Burge Lake pluton (Beaumont-Smith et al., 2006) that cuts the Ralph Lake group conglomerate (Yang and Beaumont-Smith, 2015).

Interpretation and geological significance

The U-Pb zircon age of 1849.4 ±1.3 Ma for the quartz diorite of the Motriuk Lake pluton is interpreted as the timing of its crystallization and/or emplacement, which intrudes the Wasekwan group supracrustal package. This quartz diorite exhibits an adakitic geochemical signature (Yang and Lawley, 2024b; this study), geochemically consistent with post-arc slab failure granitoids described by Whalen and Hildebrand (2019). It is less evolved than the leucogranite in the Little Brightsand pluton. The adakitic intrusions are interpreted as products of post-arc magmatism, based on the tectonic model proposed by Hildebrand et al. (2018) and supported by observations from this study. Notably, Zwanzig (2024) uses slab failure granitoid intrusions as indicators of terrane accretion to collisions during the tectonic evolution of the THO. Regardless of how the rocks are termed, the discovery of adakitic granitoids in the LLGB holds significant implications for gold mineralization, as several auriferous quartz-sulphide vein systems hosted in quartz diorite (e.g., McBride, Finlay McKinlay; see Yang, 2019) are located near the Motriuk Lake pluton. Similar spatial associations between adakitic intrusions and gold deposits have been observed at the Gordon Au mine adjacent to the Farley Lake stock, and at the McLellan Au-Ag mine alongside the Burge Lake pluton (see Yang and Lawley, 2018, 2024a, 2024b).

The U-Pb zircon age of 1848.3 ±2.7 Ma for the leucogranite of the Little Brightsand Lake pluton is interpreted as the timing of its crystallization (and/or emplacement) within the Zed Lake group greywacke. This age also establishes a minimum deposition age for the Zed Lake greywacke. It has been postulated that the Sickle group sedimentary rocks are comparable in stratigraphic position and/or in age to the Zed Lake group greywacke (Gilbert et al., 1980; Syme, 1985; Gilbert, 1993; Yang and Beau-

mont-Smith, 2015; Lawley et al., 2020, 2023). If this is the case, the precise U-Pb zircon age reported here could indicate that the Sickle group deposition interval is not as well constrained as the narrow time interval of ca. 1.84-1.83 Ma interpreted by Lawley et al. (2020, 2023; Figure GS2024-16-2).

The reason for the relatively low Th/U ratios in zircon (Table GS2024-16-1) from the Little Brightsand Lake granite is unclear. If this granite crystallized from a peraluminous melt that was co-crystallizing high-Th monazite, low Th/U ratios in zircon precipitating from the melt would be expected. However, the geochemistry of this granite argues against such a scenario, consistent with the fact that there is no monazite observed. Rather, it appears to indicate the presence of cumulative feldspars from highly evolved granites. Zircon with Th/U ratios of <0.1 is common mostly in low-temperature and low-pressure metamorphic rocks and/or due to alteration itself (*see* Rubatto, 2017). If the granite melt formed by anatexis (or partial melting) of metamorphic rocks in the crust, it may have resulted in crystallization of zircon with such low Th/U ratios. Alternatively, highly evolved granite involved in Th-rich phases, such as monazite, allanite, could also leads to formation of zircon with low Th/U ratio. However, these accessory minerals are not evident in the leucogranite.

Tectonic model

A revised model of the tectonic evolution of the LLGB and adjacent domains/terranes is illustrated in Figure GS2024-16-7. This model considers the episodic and diverse granitoid magmatism of various genetic types (Figure GS2024-16-2), supported by precise U-Pb zircon age constraints. The tectonic evolution recorded in the LLGB is characterized by volcanic arc I-type granitoids, A-type granitoids associated with intraoceanic extension due to slab roll-back, and adakitic granitoids (e.g., the Farley Lake quartz diorite stock, the Burge Lake pluton, the Motriuk Lake pluton, the Dunphy Lakes batholith, and the Fox mine intrusion; see Yang and Lawley, 2024a, 2024b, and this study) formed by partial melting of prior metasomatized depleted mantle triggered by slab break-off due to terrane collision. Terrane collision is indicated by the presence of S-type granitoids as described this past summer (Figure GS2024-16-3e; e.g., Yang et al., 2019; Yang, 2023a) but this finding needs to be backed up by precise U-Pb zircon geochronology, whole-rock geochemistry and tracer Sm-Nd isotopes. More importantly, this shift in geodynamic settings, in response to crust-mantle interactions through trans-crustal structures (e.g., the Nickel Lale shear zone, Johnson shear zone; Figure GS2024-16-1), particularly during specific stages, may have led to economic mineralization. Examples include arc I-type intrusions associated with porphyry Cu-Au-Mo (cf. Richards and Kerrich, 2007; Sun et al., 2010; Yousefi and Lentz, 2024), A-type granites associated with U, Nb, and rare-earth elements (Whalen et al., 1987; Eby, 1990, 1992; Bonin, 2007), adakitic intrusions associated with Au (Cu) (Lin and Beakhouse, 2013; Whalen and Hildebrand, 2019), and collisional S-type granites associated with critical metals, such as Li, Ta, Cs, and Sn (see Yang et al., 2019; Yang and Lawley, 2024a and references therein). Association of S-types granites with pegmatite-hosted Li, Ta, Cs and Sn mineralization is currently not known in the LLGB. Further work is needed to establish this connection.

The ca. 1.857 (i.e., Burge Lake pluton; Beaumont-Smith, 2006) to 1.831 Ga (i.e., Fox mine intrusion; Turek et al., 2000), episodic adakite-like granitoid intrusions in the LLGB were formed as results of post-arc magmatism (Yang and Lawley, 2024b; this study), and likely indicates opposing subduction polarity (Figure GS2024-16-7); an older southward subduction; and an younger northward subduction. The current model proposal is consistent with the views of Corrigan et al. (2009) and Corrigan (2012), although their studies did not report the occurrences of adakitic granitoid intrusions. The arc magmatic activity

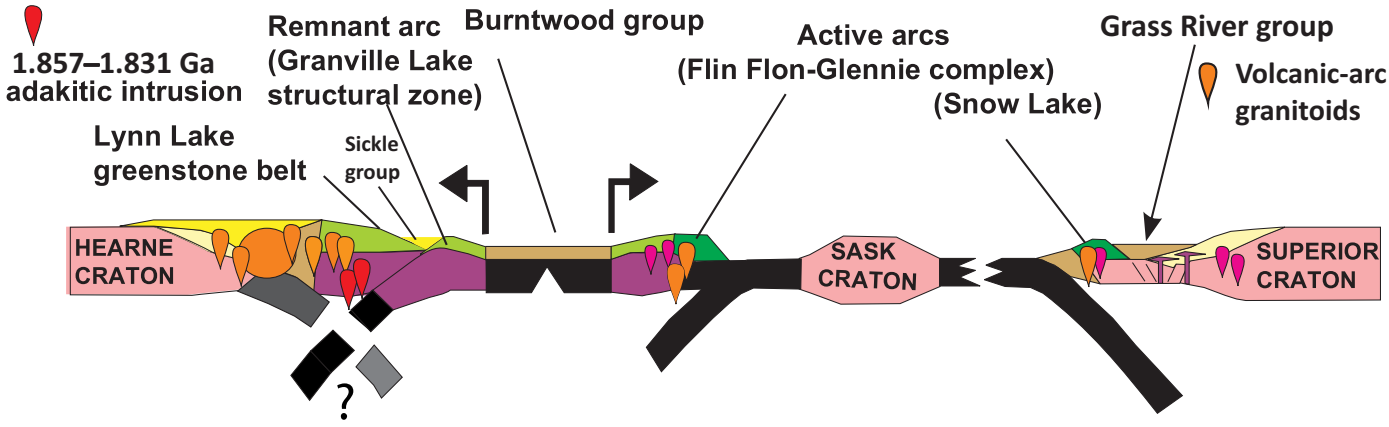


***Figure GS2024-16-7**: A revised tectonic model of the Lynn Lake greenstone belt (modified from Corrigan et al., 2007, 2009; Zwanzig and Bailes, 2010 and with results from this study). Slab break-off (dark grey) occurs as a result of terrane collision between a continental block and an oceanic arc, following an earlier southward subduction. A second slab break-off event (black) is caused by terrane collision, possibly between a continental arc and an oceanic arc, following a later northward subduction.*

produced the 1.891 to 1.870 Ga Pool Lake intrusive suite, the pre-Sickle intrusions (Figure GS2024-16-2; Baldwin et al., 1987; Turek et al., 2000; Beaumont-Smith and Böhm, 2002; Beaumont-Smith et al., 2006; Manitoba Agriculture and Resource Development, 2021; Yang, 2023a). Geochemical and Nd isotopic analyses suggest that these adakitic granitoids may have originated from the partial melting of previously metasomatized mantle by subduction-related melts and/or fluids. This process was triggered by the upwelling of hot asthenospheric mantle due to slab roll-back and break-off events that were likely the consequences of terrane amalgamation or collision (Yang and Lawley, 2024a, 2024b).

The shifts of tectonic settings likely reflect a geodynamic response to deep mantle processes, creating an extensional setting within the uplifting orogen and leading to the formation of syn-orogenic basins filled with molasse-type sediments, such as the Sickle group polymictic conglomerate and arkosic sandstone. Concurrently, the exhumation of the Trans-Hudson orogen triggered gold mineralization (Lawley et al., 2023). Although the adakitic intrusions were emplaced before the onset of gold mineralization, auriferous fluids driven by magmatism would have flowed along the same deep faults where the intrusions occurred. As a result, these adakitic intrusions may serve as valuable indicators for targeting potential orogenic gold mineralization in the Lynn Lake greenstone belt and beyond in the Trans-Hudson orogen.

The syn-orogenic sedimentary basin filled by the Sickle group sediments represents a surface expression and response to deep geodynamic processes within the lithosphere of the orogenic belts (e.g., Lawley et al., 2020, 2023; Yang and Lawley, 2024a, 2024b; Gibson et al., 2024). Such model of a basin formation is attributed to extension, driven by slab roll-back and/or slab break-off, which induced magmatism represented by adakite-like granitoid intrusions (as well as A-type granites) simultaneously and may have initiated the flow of ore fluids into favourable structural-chemical traps, leading to gold mineralization in the Lynn Lake greenstone belt.

The field observations presented in this report along side the geochronology results suggest that the Sickle group was deposited during a longer time interval and may have been not only limited to the time interval of greater than ca. 1.84–1.83 Ga (Lawley et al., 2020, 2023). Alternatively, although the Sickle group in the LLGB is thought equivalent in depositional ages to the Ralph Lake and Zed Lake groups sedimentary rocks, the latter two were thought to deposit as part of the Southern Indian domain (SID; Manitoba Energy and Mines, 1986) and may not be correlated directly to the Sickle group. The boundary between the LLGB and the SID is represented by the Ralph Lake shear zone, where the Ralph Lake conglomerate and greywacke are thrusted over the Wasekwan group of the LLGB (e.g., Yang, 2021b).

Economic considerations

Syn- to post-Sickle group adakitic granitoid intrusions exhibit distinct geochemical characteristics compared to the highly differentiated leucogranites dated in this study, despite their synchronous occurrence within the LLGB. This difference underscores the diversity of post-arc granitoid magmatism linked to the geodynamic evolution of the Trans-Hudson orogen. The 1849.4 ±1.3 Ma quartz diorite of the Motriuk Lake pluton, an adakitic intrusion, likely formed through partial melting of a metasomatized mantle, triggered by slab break-off following terrane (i.e., arc-continent) collision. This together with other adakitic intrusions are considered to create favourable conditions for orogenic gold mineralization (see Yang and Lawley, 2024a, 2024b), which could be longer lived than what is interpreted by other authors. In the LLGB, three major orogenic Au deposits (Figure GS2024-16-1) are situated nearby adakite-like intrusions (Glendenning et al., 2015; Hastie et al., 2018; Lawley et al., 2020, 2023), suggesting a potential linkage with gold metallogenesis.

In contrast, the 1848.3 ±2.7 Ma leucogranite of the Little Brightsand Lake pluton, which displays a highly evolved geochemical signature, is likely the result of strong fractionation of parental magmas derived from partial melting of crustal materials under relatively reduced redox conditions. A critical factor that needs to be considered in mineral exploration for intrusion-related ore deposits is the current erosion level of the granite intrusions, when investigating and exploring for granitoid intrusion-related mineral deposits (Yang, 2023a). This can be assessed by estimating their emplacement depth and/or crystallization pressure (e.g., Yang, 2017; Yang et al., 2021). More work is required to evaluate potential of granitic pegmatite-hosted rare metals (or critical metals: lithium, tantalum, cesium) mineralization associated with the S-type granodiorite that was identified this past summer in the Zed Lake pluton.

Acknowledgments

The author thanks S. Tetteh providing enthusiastic field assistance, as well as C. Epp and P. Belanger for thorough logistical support and cataloguing and processing of the samples; J. Janssens for assistance in compiling DRI2024011[2]; and A. Martin, H. Adediran and G. Keller for technical support. C.J.M. Lawley and M.G. Houlé of the Geological Survey of Canada are gratefully acknowledged for their collaborations during the course of this study. M. Hamilton is gratefully acknowledged for providing high quality U-Pb zircon data via an analytical contract with the MGS. The manuscript has benefited greatly from constructive reviews by T. Martins and K. Reid, technical editing by R.F. Davie,

[2] MGS Data Repository Item DRI2024011, containing the data or other information sources used to compile this report, is available online to download free of charge at https://manitoba.ca/iem/info/library/downloads/index.html, or on request from minesinfo@gov.mb.ca, or by contacting the Resource Centre, Manitoba Economic Development, Investment, Trade and Natural Resources, 360-1395 Ellice Avenue, Winnipeg, Manitoba R3G 3P2, Canada.

and report layout by C. Steffano. Alamos Gold Inc. and Corazon Mining Ltd. are gratefully acknowledged for providing various supports.

References

Anderson, S.D. and Beaumont-Smith, C.J. 2001: Structural analysis of the Pool Lake–Boiley Lake area, Lynn Lake greenstone belt (NTS 64C/11); *in* Report of Activities 2001, Manitoba Industry, Trade and Mines, Manitoba Geological Survey, p. 76–85, URL <https://manitoba.ca/iem/geo/field/roa01pdfs/01gs-12.pdf> [November 2019].

Ansdell, K.M. 2005: Tectonic evolution of the Manitoba-Saskatchewan segment of the Paleoproterozoic Trans-Hudson Orogen, Canada; Canadian Journal of Earth Sciences, v. 42, p. 741–759.

Baldwin, D.A. 1989: Mineral deposits and occurrences in the Lynn Lake area, NTS 64C/14; Manitoba Energy and Mines, Geological Services, Mineral Deposit Series Report No. 6, 130 p., URL <https://manitoba.ca/iem/info/libmin/MDS6.zip> [September 2023].

Baldwin, D.A., Syme, E.C., Zwanzig, H.V., Gordon, T.M., Hunt, P.A. and Stevens, R.P. 1987: U-Pb zircon ages from the Lynn Lake and Rusty Lake metavolcanic belts, Manitoba: two ages of Proterozoic magmatism; Canadian Journal of Earth Sciences, v. 24, p. 1053–1063.

Beaumont-Smith, C.J. 2008: Geochemistry data for the Lynn Lake greenstone belt, Manitoba (NTS 64C11-16); Manitoba Science, Technology, Energy and Mines, Manitoba Geological Survey, Open File OF2007-1, 5 p., URL <https://manitoba.ca/iem/info/libmin/OF2007-1.zip> [October 2021].

Beaumont-Smith, C.J. and Böhm, C.O. 2002: Structural analysis and geochronological studies in the Lynn Lake greenstone belt and its gold-bearing shear zones (NTS 64C10, 11, 12, 14, 15 and 16), Manitoba; *in* Report of Activities 2002, Manitoba Industry, Trade and Mines, Manitoba Geological Survey, p. 159–170, URL <https://manitoba.ca/iem/geo/field/roa02pdfs/GS-19.pdf> [October 2021].

Beaumont-Smith, C.J. and Böhm, C.O. 2003: Tectonic evolution and gold metallogeny of the Lynn Lake greenstone belt, Manitoba (NTS 64C10, 11, 12, 14, 15 and 16), Manitoba; *in* Report of Activities 2003, Manitoba Industry, Economic Development and Mines, Manitoba Geological Survey, p. 39–49, URL <https://manitoba.ca/iem/geo/field/roa03pdfs/GS-06.pdf> [October 2021].

Beaumont-Smith, C.J. and Böhm, C.O. 2004: Structural analysis of the Lynn Lake greenstone belt, Manitoba (NTS 64C10, 11, 12, 14, 15 and 16); *in* Report of Activities 2004, Manitoba Industry, Economic Development and Mines, Manitoba Geological Survey, p. 55–68, URL <https://manitoba.ca/iem/geo/field/roa04pdfs/GS-06.pdf> [October 2021].

Beaumont-Smith, C.J., Machado, N. and Peck, D.C. 2006: New uranium-lead geochronology results from the Lynn Lake greenstone belt, Manitoba (NTS 64C11-16); Manitoba Science, Technology, Energy and Mines, Manitoba Geological Survey, Geoscientific Paper GP2006-1, 11 p, URL <https://manitoba.ca/iem/info/libmin/GP2006-1.pdf> [October 2021].

Bonin, B. 2007: A-type granites and related rocks: evolution of a concept, problems and prospects; Lithos, v. 97, p. 1–29.

Chakhmouradian, A.R., Mumin, A.H., Demény, A. and Elliott, B. 2008: Postorogenic carbonatites at Eden Lake, Trans-Hudson Orogen (northern Manitoba, Canada): geological setting, mineralogy and geochemistry; Lithos, v. 103, p. 503–526.

Chappell, B.W. and White, A.J.R. 1974: Two contrasting granite types; Pacific Geology, v. 8, p. 173–174.

Chappell, B.W. and White, A.J.R. 1992: I- and S-type granites in the Lachlan Fold Belt; Transactions of the Royal Society of Edinburgh: Earth Sciences, v. 83, p. 1–26.

Chappell, B.W. and White, A.J.R. 2001: Two contrasting granite types: 25 years later; Australian Journal of Earth Sciences, v. 48, p. 489–499.

Corfu, F., Hahnchar, J.M., Hoskin, P.W.O. and Kinny, P. 2003: Atlas of zircon textures; Reviews in Mineralogy and Geochemistry, v. 53, p. 469–500.

Corrigan, D. 2012: Paleoproterozoic crustal evolution and tectonic processes: insights from the LITHOPROBE program in the Trans-Hudson orogen, Canada, Chapter 4; *in* Tectonic Styles in Canada: The LITHOPROBE Perspective, J.A. Percival, F.A. Cook and R.M. Clowes (ed.), Geological Association of Canada, Special Paper 49, p. 237–284.

Corrigan, D., Galley, A.G. and Pehrsson, S. 2007: Tectonic evolution and metallogeny of the southwestern Trans-Hudson Orogen; *in* Mineral Deposits of Canada: A Synthesis of Major Deposit-Types, District Metallogeny, the Evolution of Geological Provinces, and Exploration Methods, W.D. Goodfellow (ed.), Geological Association of Canada, Mineral Deposits Division, Special Publication 5, p. 881–902.

Corrigan, D., Pehrsson, S., Wodicka, N. and de Kemp, E. 2009: The Palaeoproterozoic Trans-Hudson Orogen: a prototype of modern accretionary processes; *in* Ancient Orogens and Modern Analogues, J.B. Murphy, J.D. Keppie, and A.J. Hynes (ed.), Geological Society of London, Special Publications, v. 327, p. 457–479.

Eby, G.N. 1990: The A-type granitods: a review of their occurrence and chemical characteristics and speculations on their petrogenesis; Lithos, v. 26, p. 115–134.

Eby, G.N. 1992: Chemical subdivision of the A-type granitoids: petrogenetic and tectonic implications; Geology, v. 20, p. 641–644.

Fedikow, M.A.F. and Gale, G.H. 1982: Mineral deposit studies in the Lynn Lake area; *in* Report of Field Activities 1982, Manitoba Department of Energy and Mines, Mineral Resources Division, p. 44–54, URL <https://manitoba.ca/iem/geo/field/rfa1982.pdf> [October 2022].

Ferreira, K.J. 1993: Mineral deposits and occurrences in the Laurie Lake area, NTS 64C/12; Manitoba Energy and Mines, Geological Services, Mineral Deposit Series Report No. 9, 101 p., URL <https://manitoba.ca/iem/info/libmin/MDS9.zip> [September 2022].

Frisch, W., Meschede, M. and Blakey, R. 2011: Plate tectonics: Continental drift and mountain building. Springer, Heidelberg, 212 p.

Gerstenberger, H. and Haase, G. 1997: A highly effective emitter substance for mass spectrometric Pb isotope ratio determinations; Chemical Geology, v. 136, p. 309–312.

Gibson, G.M., Champion, D.C. and Doublier, M.P. 2024: The Paleoproterozoic Trans-Australian Orogen: Its magmatic and tectonothermal record, links to northern Laurentia, and implications for supercontinent assembly; Geological Society of America Bulletin, URL <https://doi.org/10.1130/B36255.1>.

Gilbert, H.P. 1993: Geology of the Barrington Lake–Melvin Lake–Fraser Lake area; Manitoba Energy and Mines, Geological Services, Geological Report GR87-3, 97 p., URL <https://manitoba.ca/iem/info/libmin/GR87-3.zip> [October 2021].

Gilbert, H.P., Syme, E.C. and Zwanzig, H.V. 1980: Geology of the metavolcanic and volcaniclastic metasedimentary rocks in the Lynn Lake area; Manitoba Energy and Mines, Mineral Resources Division, Geological Paper GP80-1, 118 p., URL <https://manitoba.ca/iem/info/libmin/GP80-1.zip> [October 2021].

Glendenning, M.W.P., Gagnon, J.E. and Polat, A. 2015: Geochemistry of the metavolcanic rocks in the vicinity of the MacLellan Au-Ag deposit and an evaluation of the tectonic setting of the Lynn Lake greenstone belt, Canada: evidence for a Paleoproterozoic-aged rifted continental margin; Lithos, v. 233, p. 46–68.

Grasso, V.G. 1968: The TiO_2 frequency in volcanic rocks; Geologische Rundschau, v. 57, p. 930–935.

Hamilton, M.A. 2022: Report on U-Pb CA-ID-TIMS geochronology of Archean and Proterozoic rock units in support of Manitoba Geological Survey bedrock mapping programs, 2018-2022; Jack Satterly Geochronology Laboratory, Department of Earth Sciences, University of Toronto, Toronto, Ontario, 51 p.

Hastie, E.C.G., Gagnon, J.E. and Samson, I.M. 2018: The Paleoproterozoic MacLellan deposit and related Au-Ag occurrences, Lynn Lake greenstone belt, Manitoba: an emerging, structurally controlled gold camp; Ore Geology Reviews, v. 94, p. 24–45.

Hildebrand, R.S., Whalen, J.B. and Bowring, S.A. 2018: Resolving the crustal composition paradox by 3.8 billion years of slab failure magmatism and collisional recycling of continental crust; Tectonophysics, v. 734–735, p. 69–88.

Hoffman, P.H. 1988: United plates of America, the birth of a craton: Early Proterozoic assembly and growth of Laurentia; Annual Reviews of Earth and Planetary Sciences, v. 16, p. 543–603.

Irvine, T.N. and Baragar, W.R.A. 1971: A guide to the chemical classification of the common volcanic rocks; Canadian Journal of Earth Sciences, v. 8, p. 523–548.

Ishihara, S. 1977: The magnetite-series and ilmenite-series granitic rocks; Mining Geology, v. 27, p. 293–305, URL <https://doi.org/10.11456/shigenchishitsu1951.27.293>.

Ishihara, S. 1981: The granitoid series and mineralization; Economic Geology, 75th Anniversary Volume, p. 458–484, URL <https://doi.org/10.5382/AV75.14>.

Ishihara, S. 2004: The redox state of granitoids relative to tectonic setting and Earth history: the magnetite-ilmenite series 30 years later; Earth and Environmental Science Transactions of the Royal Society of Edinburgh, v. 95, p. 23–33, URL <https://doi.org/10.1017/S0263593300000894>.

Jaffey, A.H., Flynn, K.F., Glendenin, L.E., Bentley, W.C. and Essling, A.M. 1971: Precision measurement of half-lives and specific activities of ^{235}U and ^{238}U; Physical Review, v. 4, p. 1889–1906.

Jones, L.R., Lafrance, B. and Beaumont-Smith, C.J. 2006: Structural controls on gold mineralization at the Burnt Timber Mine, Lynn Lake Greenstone Belt, Trans-Hudson Orogen, Manitoba; Exploration and Mining Geology, v. 15, p. 89–100.

Krogh, T.E. 1973: A low contamination method for hydrothermal decomposition of zircon and extraction of U and Pb for isotopic age determinations; Geochimica et Cosmochimica Acta, v. 37, p. 485–494.

Lawley, C.J.M., Yang, X.M., Selby, D., Davis, W., Zhang, S., Petts, D.C. and Jackson, S.E. 2020: Sedimentary basin controls on orogenic gold deposits: new constraints from U-Pb detrital zircon and Re-Os sulphide geochronology, Lynn Lake greenstone belt, Canada; Ore Geology Reviews, v. 126, art. 103790, URL <https://doi.org/10.1016/j.oregeorev.2020.103790>.

Lawley, C.J.M., Schneider, D.A., Camacho, A., McFarlane, C.R.M., Davis, W.J. and Yang, X.M. 2023: Post-orogenic exhumation triggers gold mobility in the Trans-Hudson orogen: new geochronology results from the Lynn Lake Greenstone Belt, Manitoba, Canada; Precambrian Research, v. 395, art. 107127, URL <https://doi.org/10.1016/j.precamres.2023.107127>.

Lewry, J.F. and Collerson, K.D. 1990: The Trans-Hudson Orogen: extent, subdivisions and problems; in The Early Proterozoic Trans-Hudson Orogen of North America, J.F. Lewry and M.R. Stauffer (ed.), Geological Association of Canada, Special Paper 37, p. 1–14.

Lin, S. and Beakhouse, G.P. 2013: Synchronous vertical and horizontal tectonism at late stages of Archean cratonization and genesis of Hemlo gold deposit, Superior craton, Ontario, Canada; Geology, v. 41, p. 359–362.

Ludwig, K.R. 2009: User's manual for Isoplot 3.71 a geochronological toolkit for Excel; Berkeley Geochronological Center Special Publication 4, 72 p.

Maniar, P.D. and Piccoli, P.M. 1989: Tectonic discrimination of granitoids; Geological Society of America Bulletin, v. 101, p. 635–643.

Manitoba Agriculture and Resource Development 2021: Lynn Lake, Manitoba (NTS 64C14); Manitoba Agriculture and Resource Development, Manitoba Geological Survey, Lynn Lake Bedrock Compilation Map 64C14, scale 1:50 000, URL <https://manitoba.ca/iem/info/libmin/lynn_lake_compilation_2021.zip> [October 2021].

Manitoba Energy and Mines 1986: Granville Lake, NTS 64C; Manitoba Energy and Mines, Minerals Division, Bedrock Geology Compilation Map 64C, scale 1:250 000, URL <https://manitoba.ca/iem/info/libmin/bgcms/bgcms_granville_lake.pdf> [October 2022].

Martin, H., Smithies, R.H., Rapp, R., Moyen, J.-F. and Champion, D. 2005: An overview of adakite, tonalite–trondhjemite–granodiorite (TTG), and sanukitoid: relationships and some implications for crustal evolution; Lithos, v. 79, p. 1–24.

Martin, H., Moyen, J.-F. and Rapp, R. 2009: The sanukitoid series: magmatism at the Archaean-Proterozoic transition; Earth and Environmental Science Transactions of The Royal Society of Edinburgh, v. 100, Special Issue 1-2, p. 15–33.

Martins, T., Rayner, N., Corrigan, D. and Kremer, P. 2022: Regional geology and tectonic framework of the Southern Indian domain, Trans-Hudson orogen, Manitoba; Canadian Journal of Earth Sciences, v. 59, p. 371–388, URL <https://doi.org/10.1139/cjes-2020-0142>.

Mattinson, J. 2005: Zircon U-Pb chemical abrasion (CA-TIMS) method: Combined annealing and multi-step partial dissolution analysis for improved precision and accuracy of zircon ages; Chemical Geology, v. 220, p. 47–66.

Middlemost, E.A.K. 1994: Naming materials in the magma/igneous rock system; Earth-Science Reviews, v. 37, p. 215–224.

Milligan, G.C. 1960: Geology of the Lynn Lake district; Manitoba Department of Mines and Natural Resources, Mines Branch, Publication 57-1, 317 p.

Mumin, A.H. 2002: Discovery of a carbonatite complex at Eden Lake (NTS 64C9), Manitoba; *in* Report of Activities 2002, Manitoba Industry, Trade and Mines, Manitoba Geological Survey, p. 187–197, URL <https://manitoba.ca/iem/geo/field/roa02pdfs/GS-21.pdf> [August 2024].

Richards, J.P. and Kerrich, R. 2007: Special paper: Adakite-like rocks: their diverse origins and questionable role in metallogenesis; Economic Geology, v. 102, p. 537–576.

Rittmann, A. 1962: Volcanoes and their activity; Wiley, New York, USA, 305 p.

Rittmann, A. 1973: Stable mineral assemblages of igneous rocks; Springer-Verlag, Berlin, Germany, 262 p.

Rubatto, D. 2017: Zircon: the metamorphic mineral; Reviews in Mineralogy & Geochemistry, v. 83, p. 297–328.

Shirey, S.B. and Hanson, G.N. 1984: Mantle derived Archaean monzodiorites and trachyandesites; Nature, v. 310, p. 222–224.

Stacey, J.S. and Kramers, J.D. 1975: Approximation of terrestrial lead isotope evolution by a two-stage model; Earth and Planetary Science Letters, v. 26, p. 207–221.

Sun, W.D., Ling, M.X., Yang, X.Y., Fan, W.M., Ding, X. and Liang, H.Y. 2010: Ridge subduction and porphyry copper-gold mineralization: an overview; Science China Earth Sciences, v. 53, p. 475–484.

Syme, E.C. 1985: Geochemistry of metavolcanic rocks in the Lynn Lake Belt; Manitoba Energy and Mines, Geological Services, Geological Report GR84-1, 84 p., 1 map, 1:100 000 scale.

Turek, A., Woodhead, J. and Zwanzig H.V. 2000: U-Pb age of the gabbro and other plutons at Lynn Lake (part of NTS 64C); *in* Report of Activities 2000, Manitoba Industry, Trade and Mines, Manitoba Geological Survey, p. 97–104, URL <https://manitoba.ca/iem/geo/field/roa00pdfs/00gs-18.pdf> [October 2021].

Whalen, J.B. and Hildebrand, R.S. 2019: Trace element discrimination of arc, slab failure, and A-type granitic rocks; Lithos, v. 348–349, art. 105179.

Whalen, J.B., Currie, K.L. and Chappell, B.W. 1987: A-type granites: geochemical characteristics, discrimination and petrogenesis; Contributions to Mineralogy and Petrology, v. 95, p. 407–419.

White, D.J., Zwanzig, H.V. and Hajnal, Z. 2000: Crustal suture preserved in the Paleoproterozoic Trans-Hudson orogeny, Canada; Geology, v. 28, p. 527–530.

Yang, X.M. 2007: Using the Rittmann Serial Index to define the alkalinity of igneous rocks; Neues Jahrbuch für Mineralogie, v. 184, p. 95–103.

Yang, X.M. 2017: Estimation of crystallization pressure of granite intrusions; Lithos, v. 286–287, p. 324–329, URL <https://doi.org/10.1016/j.lithos.2017.06.018>.

Yang, X.M. 2019: Preliminary results of bedrock mapping in the Gemmell Lake area, Lynn Lake greenstone belt, northwestern Manitoba (parts of NTS 64C11, 14); *in* Report of Activities 2019, Manitoba Agriculture and Resource Development, Manitoba Geological Survey, p. 10–29, URL <https://manitoba.ca/iem/geo/field/roa19pdfs/GS2019-2.pdf> [October 2021].

Yang, X.M. 2020: Bedrock geochemical data of the Gemmell Lake area, Lynn Lake greenstone belt, northwestern Manitoba (parts of NTS 64C11, 14); Manitoba Agriculture and Resource Development, Manitoba Geological Survey, Data Repository Item DRI2020009, Microsoft® Excel® file.

Yang, X.M. 2021a: Bedrock mapping at Ralph Lake, Lynn Lake greenstone belt, northwestern Manitoba (part of NTS 64C14): preliminary results and geological implications; *in* Report of Activities 2021, Manitoba Agriculture and Resource Development, Manitoba Geological Survey, p. 40–58, URL <https://manitoba.ca/iem/geo/field/roa21pdfs/GS2021-5.pdf> [November 2021].

Yang, X.M. 2021b: Bedrock geochemical data of the Ralph Lake area, Lynn Lake greenstone belt, northwestern Manitoba (parts of NTS 64C14); Manitoba Agriculture and Resource Development, Manitoba Geological Survey, Data Repository Item DRI2021021, Microsoft® Excel® file.

Yang, X.M. 2022: Preliminary results of bedrock geological mapping in the Fox mine–Snake Lake area, Lynn Lake greenstone belt, northwestern Manitoba (part of NTS 64C12); *in* Report of Activities 2022, Manitoba Natural Resources and Northern Development, Manitoba Geological Survey, p. 71–86, URL <https://manitoba.ca/iem/geo/field/roa22pdfs/GS2022-9.pdf> [November 2022].

Yang, X.M. 2023a: Progress report on the study of granitoids in Manitoba: petrogenesis and metallogeny; Manitoba Economic Development, Investment and Trade, Manitoba Geological Survey, Open File OF2022-3, 119 p., URL <https://manitoba.ca/iem/info/libmin/OF2022-3.zip> [March 2023].

Yang, X.M. 2023b: Field relationships, geochemical characteristics and metallogenic implications of gabbroic intrusions in the Paleoproterozoic Lynn Lake greenstone belt, northwestern Manitoba (parts of NTS 64C10–12, 14–16); *in* Report of Activities 2023, Manitoba Economic Development, Investment, Trade and Natural Resources, Manitoba Geological Survey, p. 73–89, URL <https://manitoba.ca/iem/geo/field/roa23pdfs/GS2023-9.pdf> [November 2023].

Yang, X.M. 2024: Geochemical data of bulk-rock samples collected in the 2022 and 2023 field seasons from the Lynn Lake greenstone belt, northwestern Manitoba (parts of NTS 64C10–12, 14–16); Manitoba Economic Development, Investment, Trade and Natural Resources, Manitoba Geological Survey, Data Repository Item DRI2024011, Microsoft® Excel® file.

Yang, X.M. and Beaumont-Smith, C.J. 2015: Granitoid rocks in the Lynn Lake region, northwestern Manitoba: preliminary results of reconnaissance mapping and sampling; *in* Report of Activities 2015, Manitoba Mineral Resources, Manitoba Geological Survey, p. 68–78, URL <https://manitoba.ca/iem/geo/field/roa15pdfs/GS-5.pdf> [October 2021].

Yang, X.M. and Beaumont-Smith, C.J. 2016: Geological investigations in the Farley Lake area, Lynn Lake greenstone belt, northwestern Manitoba (part of NTS 64C16); *in* Report of Activities 2016, Manitoba Growth, Enterprise and Trade, Manitoba Geological Survey, p. 99–114, URL <https://manitoba.ca/iem/geo/field/roa16pdfs/GS-9.pdf> [October 2021].

Yang, X.M. and Beaumont-Smith, C.J. 2017: Geological investigations of the Wasekwan Lake area, Lynn Lake greenstone belt, northwestern Manitoba (parts of NTS 64C10, 15); *in* Report of Activities 2017, Manitoba Growth, Enterprise and Trade, Manitoba Geological Survey, p. 117–132, URL <https://manitoba.ca/iem/geo/field/roa17pdfs/GS2017-11.pdf> [October 2021].

Yang, X.M. and Lawley, C.J.M. 2018: Tectonic setting of the Gordon gold deposit, Lynn Lake greenstone belt, northwestern Manitoba (parts of NTS 64C16): evidence from lithogeochemistry, Nd isotopes and U-Pb geochronology; *in* Report of Activities 2018, Manitoba Growth, Enterprise and Trade, Manitoba Geological Survey, p. 89–109, URL <https://manitoba.ca/iem/geo/field/roa18pdfs/GS2018-8.pdf> [October 2021].

Yang, X.M. and Lawley, C.J.M. 2024a: Rapid switch in geodynamic setting revealed by episodic granitoid magmatism in the Lynn Lake greenstone belt of Paleoproterozoic Trans-Hudson Orogen, Manitoba, Canada; Lithos, v. 470–471, art. 107534, URL <https://doi.org/10.1016/j.lithos.2024.107534>.

Yang, X.M. and Lawley, C.J.M. 2024b: Adakite-like granitoid intrusions in the Paleoproterozoic Lynn Lake greenstone belt, northwestern Manitoba, Canada: Implications for geodynamic setting and gold mineralization [abstract]; Geological Association of Canada–Mineralogical Association of Canada and the 10th International Symposium on granitic pegmatites, Joint Annual Meeting, Brandon, Manitoba, May 19–22, 2024, Program with Abstracts; Geoscience Canada, v. 51, p. 127, URL <https://doi.org/10.12789/geocanj.2024.51.211>.

Yang, X.M., Drayson, D. and Polat, A. 2019: S-type granites in the western Superior Province: a marker of Archean collision zones; Canadian Journal of Earth Sciences, v. 56, p. 1409-1436, URL <https://doi.org/10.1139/cjes-2018-0056>.

Yang, X.M., Lentz, D.R. and Chi, G. 2021: Ferric-ferrous iron oxide ratios: Effect on crystallization pressure of granites estimated by Qtz-geobarometry; Lithos, v. 380-381, art. 105920, URL <https://doi.org/10.1016/j.lithos.2020.105920>.

Yousefi, F. and Lentz D.R. 2024: Formation of high-silica adakites and their relationship with slab break-off: implications for generating fertile Cu-Au-Mo porphyry systems; Geoscience Frontiers, v. 15, art. 101927, URL <https://doi.org/10.1016/j.gsf.2024.101927>.

Zwanzig, H.V. 2000: Geochemistry and tectonic framework of the Kisseynew Domain–Lynn Lake belt boundary (part of NTS 63P/13); *in* Report of Activities 2000, Manitoba Industry, Trade and Mines, Manitoba Geological Survey, p. 91–96, URL <https://manitoba.ca/iem/geo/field/roa00pdfs/00gs-17.pdf> [October 2021].

Zwanzig, H. 2024: Tectonic model of the Paleoproterozoic western Trans-Hudson Orogen [abstract]; Geological Association of Canada–Mineralogical Association of Canada and the 10th International Symposium on granitic pegmatites, Joint Annual Meeting, Brandon, Manitoba, May 19–22, 2024, Program with Abstracts; Geoscience Canada, v. 51, p. 128, URL <https://doi.org/10.12789/geocanj.2024.51.211>.

Zwanzig, H.V. and Bailes, A.H. 2010: Geology and geochemical evolution of the northern Flin Flon and southern Kisseynew domains, Kississing–File lakes area, Manitoba (parts of NTS 63K, N); Manitoba Innovation, Energy and Mines, Manitoba Geological Survey, Geoscientific Report GR2010-1, 135 p., URL <https://manitoba.ca/iem/info/libmin/GR2010-1.zip> [October 2021].

Zwanzig, H.V., Syme, E.C. and Gilbert, H.P. 1999: Updated trace element geochemistry of the ca. 1.9 Ga metavolcanic rocks in the Paleoproterozoic Lynn Lake belt; Manitoba Industry, Trade and Mines, Geological Services, Open File Report OF99-13, 46 p., URL <https://manitoba.ca/iem/info/libmin/OF99-13.zip> [October 2020].

GS2024-17

Initial results from a long-period magnetotelluric survey in the Flin Flon, Snow Lake and The Pas area, west-central Manitoba (NTS 63F, G, J, K, parts of 63B, I, N)

by B.F.W. Chase[1], J. Marks, A. Williamson[1], A. Maki[2], K. Moshtaghian[1] and M.J. Unsworth[1]

In Brief:

- Long-period magnetotelluric data was collected and will be used to produce a 3-D resistivity model of the lithosphere
- Conductive anomalies in the 3-D resistivity model will be interpreted using the mineral systems framework

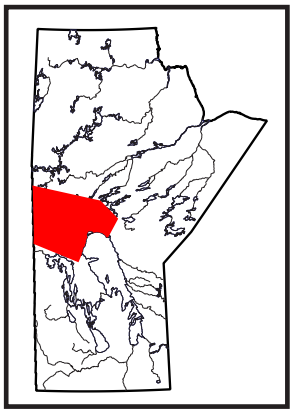
Citation:
Chase, B.F.W., Marks, J., Williamson, A., Maki, A., Moshtaghian, K. and Unsworth, M.J. 2024: Initial results from a long-period magnetotelluric survey in the Flin Flon, Snow Lake and The Pas area, west-central Manitoba (NTS 63F, G, J, K, parts of 63B, I, N); *in* Report of Activities 2024, Manitoba Economic Development, Investment, Trade and Natural Resources, Manitoba Geological Survey, p. 145–152.

Summary

The Manitoba Geological Survey, in collaboration with the University of Alberta, is developing a model of the lithospheric structure beneath the province of Manitoba. Information about deep lithospheric structure cannot be obtained from drilling and requires deep sounding geophysical exploration. One of the most useful methods for this task is magnetotelluric exploration, which uses natural low-frequency electromagnetic signals to determine the electrical resistivity structure of the Earth to depths in excess of 200 km. A long-period magnetotelluric survey was conducted at 22 stations in June and July of 2024 in west-central Manitoba. The new data will be combined with long-period magnetotelluric data previously collected in Saskatchewan to produce a 3-D resistivity model of the lithosphere of the Trans-Hudson orogen beneath west-central Manitoba and central Saskatchewan. This 3-D resistivity model will improve the understanding of the factors that control the spatial distribution of mineralization and may also guide future exploration in the region.

Introduction

The crystalline basement rocks of Manitoba are part of the eastern margin of the Trans-Hudson orogen (THO) and include the boundary with the Superior craton (Figure GS2024-17-1). This part of Laurentia was assembled during the closure of the Manikewan Ocean in the Proterozoic, 1.9–1.8 Ga (Whitmeyer and Karlstrom, 2007). Lithotectonic units mapped in this region include the Flin Flon belt (FFB; part of the Flin Flon–Clearwater domain), the Kisseynew domain, the Superior boundary zone (SBZ) and several domains of the Superior province (i.e., Superior craton; Figure GS2024-17-1). The FFB is one of a series of volcano-sedimentary belts within the THO and includes a series of arc and oceanic-island basalts and successor-arc plutons (Lewry and Collerson, 1990; Conners et al., 1999; Syme et al., 1999; Whalen et al., 1999). It is commonly linked to the Glennie domain in Saskatchewan, and both are interpreted to have a similar tectonic origin (Clowes and Roy, 2021). The FFB is one of the most well-endowed volcanogenic massive-sulphide districts on Earth (Syme et al., 1999). The Kisseynew domain is the largest component of the THO in Saskatchewan and Manitoba and consists of metasedimentary and intrusive supracrustal units that are interpreted to have been deposited in a back-arc basin (Ansdell et al., 1995; Zwanzig et al., 2007). The Kisseynew domain formed over the FFB–Glennie domain crust, which was undergoing extension as a result of northward-directed subduction zone retreat (Clowes and Roy, 2021). The Kisseynew domain underwent tectonic collapse and thickening during accretion of the Sask and Superior cratons ca. 1.84 Ga (Ansdell et al., 1995; White et al., 2005). The SBZ is largely composed of supracrustal Paleoproterozoic continental rift margin rocks that first intruded through and were deposited on the attenuated edge of the Superior craton from 1.880 to 1.865 Ga, and these rocks were then later intruded by granitoids during terminal ocean closure, 1.836–1.726 Ga (Bleeker, 1990; Machado, 1990; Weber, 1990; Bleeker et al., 1995). The Thompson nickel belt is a prolific mining district located within the SBZ. The Superior province defines the eastern margin of the THO and is composed of a series of Archean blocks accreted together before ca. 2.6 Ga and separated by major structures or changes in metamorphic gradient (Percival et al., 2006, 2012).



The current understanding of the deep lithospheric structure of the THO is derived from geophysical studies that have used seismic, magnetotelluric (MT) and potential field exploration methods (e.g., Jones et al., 2005; White et al., 2005). In the THO, previous studies have been limited in their depth of exploration to within the crust, providing limited information about the lithospheric mantle. Another limitation of these studies is that they have generally used 2-D approaches to data analysis,

[1] Department of Physics, University of Alberta, Edmonton, Alberta
[2] Brandon University, Brandon, Manitoba

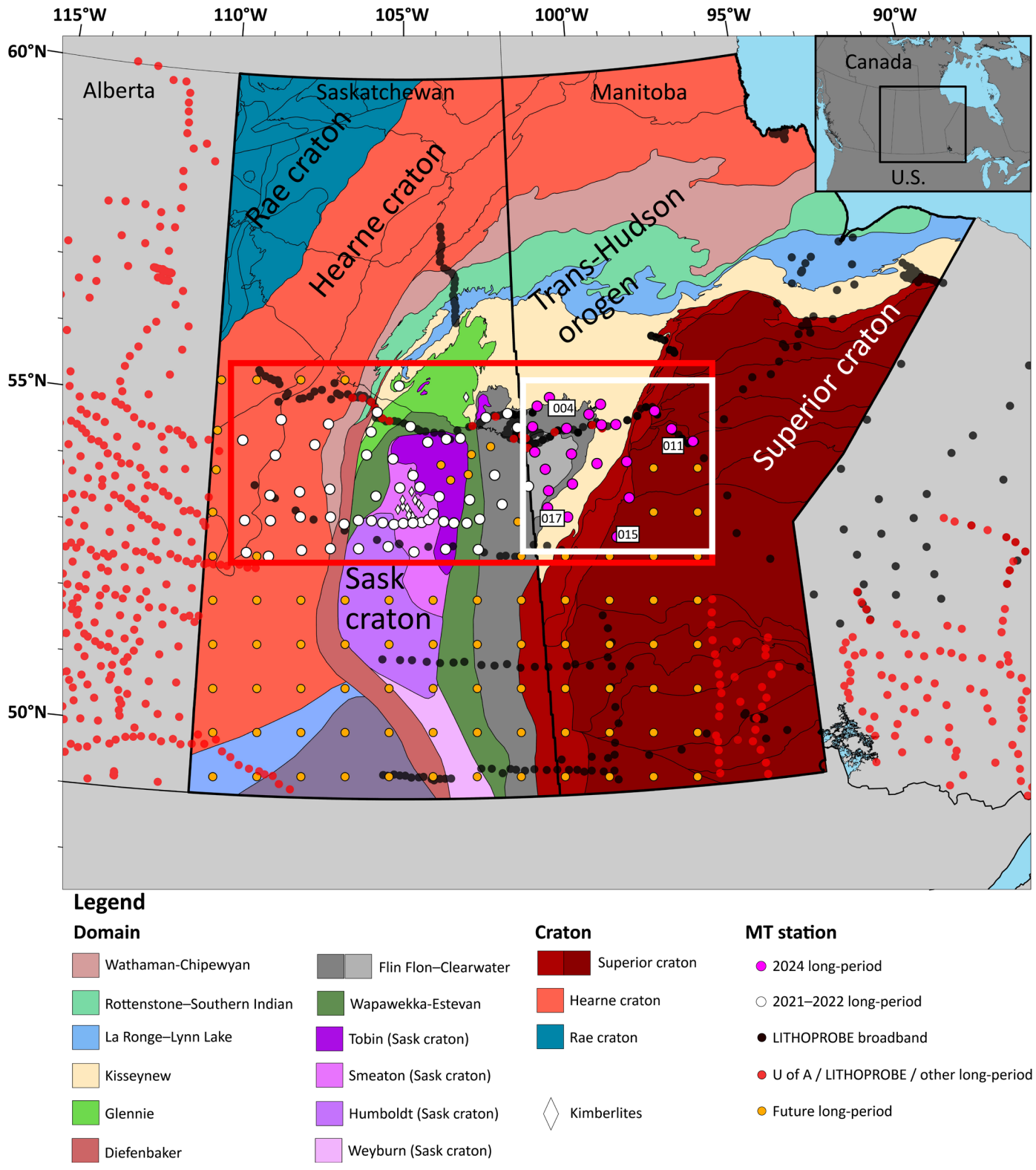


Figure GS2024-17-1: *Lithotectonic units of Manitoba and Saskatchewan. The Trans-Hudson orogen is composed of the various lithotectonic units between the Hearne and Superior cratons. Thin black lines indicate the boundaries of the domains within the Superior, Hearne and Rae cratons. Magnetotelluric (MT) data coverage is shown for the region (University of Alberta, unpublished data, 2024). Note that the LITHOPROBE or U of A long-period stations in Alberta represent stations where the data were collected for the LITHOPROBE program or by the University of Alberta (U of A), whereas in the rest of Canada, data were collected for the LITHOPROBE program or other programs. Data from the stations inside the red box will be used to create a 3-D resistivity model of the lithosphere of the Trans-Hudson orogen in this area. The white box defines the new long-period magnetotelluric (LMT) survey area shown in Figure GS2024-17-3. The numbered boxes correspond to the LMT stations displayed in Figure GS2024-17-4. Manitoba lithotectonic units modified after Manitoba Geological Survey (2022). Saskatchewan lithotectonic units modified after Saskatchewan Energy and Resources (2021).*

which provides limited information about the along-strike variability of the structure of the THO in Canada (e.g., White et al., 2002). In past studies, the structural complexity of the THO has led to differing interpretations of fundamental features, such as polarity of subduction (e.g., White et al., 2002). In the United States, the use of deep-imaging, whole-lithosphere–scale, geophysical methods in 3-D have helped improve the understanding of the structure of the southern THO (lat. 43–49°N). These data have highlighted that the structural complexity observed at shallow depths in the crust may have developed during late-stage deformation and may also overprint earlier structures at greater depth (e.g., Ye et al., 2019; Bedrosian and Finn, 2021). To improve the understanding of the THO in Canada, 3-D geophysical datasets that can produce images of the entire lithosphere are required.

The new long-period magnetotelluric (LMT) dataset described in this report addresses this goal and offers the ability to image the deep structure around regional mineral deposits and mining districts. The MT method is ideal for this task, given its sensitivity to common ore-related minerals and its ability to delineate regions altered by the passage of mineralizing fluids, which both often present as conductive anomalies (e.g., Heinson et al., 2018; Kirkby et al., 2022; Chase and Unsworth, 2024). Identified conductors can be interpreted within the mineral systems framework to efficiently select areas for continued mineral exploration (McCuaig et al., 2010; McCuaig and Hronsky, 2014).

There are two questions that the 2024 LMT dataset will address:

- What is the electrical resistivity structure of the eastern margin of the THO and adjacent area of the Superior craton?
- Are the low resistivity anomalies mapped with MT spatially associated with the occurrence of mineral deposits?

Previous studies

Geophysical studies of the deep lithospheric structure of the THO have taken place since the 1980s through the LITHOPROBE program (Clowes et al., 1999). The LITHOPROBE program collected multiple seismic reflection, seismic refraction and MT profiles across the THO (Figure GS2024-17-1). Critically, the seismic datasets were used to delineate terrane boundaries and determine the direction of subduction during closure of the Manikewan Ocean (e.g., Ansdell, 2005; White et al., 2005). The MT datasets were used in a similar manner and identified an extension of the North American Central Plains (NACP) conductor, a crustal anomaly that is related to the suture zone observed in the THO both in the United States and Canada (Jones et al., 2005; Bedrosian and Finn, 2021). The MT data also showed that the NACP conductor occurred beneath the La Ronge gold belt (central Saskatchewan), suggesting a connection between the conductor and mineral deposits (Jones et al., 2005). The LMT data collected in 2021–2022 (Figure GS2024-17-1), revealed a similar conductor beneath the Flin Flon region and suggested that regional-scale conductors were associated with a major conductor in the lithospheric mantle beneath the Sask craton (Chase and Unsworth, 2024).

Introduction to the magnetotelluric method

In mineral exploration, airborne or ground-based electromagnetic (EM) surveys are routinely used to locate electrically conductive anomalies related to mineralization (Simpson and Bahr, 2005). In these methods, the depth of investigation is limited by the skin depth, which is defined as

$$\delta = \frac{503}{\sqrt{\sigma f}} \quad (1)$$

where δ is the skin depth (metres), is the electrical conductivity (the inverse of resistivity) of the Earth (siemens/metre), and is frequency (hertz) and the reciprocal of the period (seconds). These methods use a transmitter to generate the signals and the depth of investigation is typically limited to a few hundred metres.

For deeper imaging, it is most efficient to use natural low-frequency EM signals as they increase the depth of investigation (Equation 1), which is what is used during an MT survey. The MT method is similar to controlled-source EM methods but with some important distinctions. The first is that the MT method uses natural EM signals. At frequencies above 1 hertz (Hz), these signals come from global lightning activity, and below 1 Hz they are primarily generated by interactions between solar wind and the magnetosphere (Simpson and Bahr, 2005). The MT data are transformed during processing into the frequency domain to give apparent resistivity curves, which show the resistivity of the subsurface as a function of frequency. The frequencies collected in MT exploration are typically in the range of 10 000–0.0001 Hz (or 0.0001–10 000 seconds). In comparison, controlled-source EM methods use signals in the frequency range 100 000–100 Hz. This makes the MT method capable of imaging deeper structures than controlled-source EM methods. Magnetotelluric exploration uses three distinct frequency bands, depending on the target depth. The first is audio magnetotellurics (AMT), which has the frequency range of 10 000–1 Hz, and is useful for imaging the near surface, usually to depths of <1–2 km. The second is broadband magnetotellurics (BBMT), which has the frequency range of 1000–0.001 Hz, and is useful for imaging the crust and upper mantle. The final is LMT, which has a frequency range of 1–0.0001 Hz, and is capable of imaging the entire lithosphere. Long-period magnetotelluric data were collected for the 2024 study described in this report.

In the field, MT instruments record two orthogonal electric field components and three orthogonal magnetic field components as a function of time (Figure GS2024-17-2). In LMT systems, the magnetic fields are recorded with a single three-component sensor, whereas in BBMT and AMT systems they are recorded using three different sensors. The MT method is an ideal regional exploration tool that can be used to investigate mineral systems

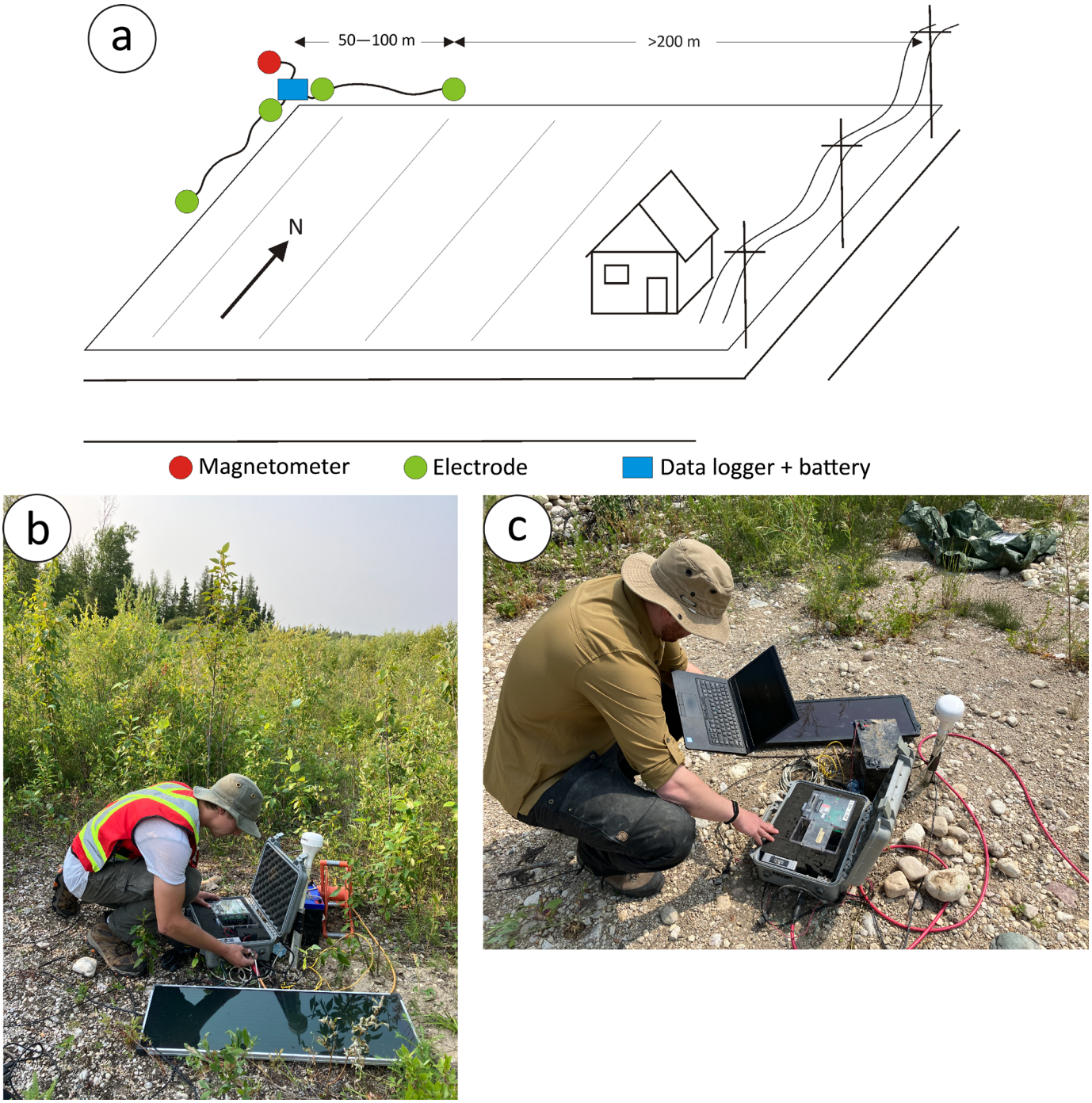


Figure GS2024-17-2: a) *Layout of a long-period magnetotelluric (LMT) station. Installation only requires digging 4–6 temporary holes in the ground to a depth of 30–40 cm. The station typically occupies an area that is up to 100 by 100 m in size;* ***b, c)*** *Examples of a LMT system (Narod Geophysics Ltd.'s Narod Intelligent Magnetotelluric System [NIMS]) being deployed in the field in Manitoba.*

on a range of spatial scales. This includes deposit- to lithospheric-scale studies that image the pathways taken by the fluids that formed a mineral deposit.

Magnetotelluric fieldwork

In the summer of 2024, LMT data were recorded at 22 stations in west-central Manitoba with an average station spacing of 50–70 km (Figure GS2024-17-3). At each location, the LMT station recorded data for 10–15 days. The data were recorded with Narod Geophysics Ltd.'s Narod Intelligent Magnetotelluric System (NIMS) LMT instruments. Following best practices for LMT data collection, the electrodes were buried 30–40 cm below the surface to avoid the effects of daily temperature variations and precipitation. Bentonite was placed in the electrode holes to improve electrical contact with the ground. Stations were time synchronized using GPS in order to allow for comparison of the time-series data and the removal of noise. Stations were installed at least 0.5–1 km away from major infrastructure to minimize

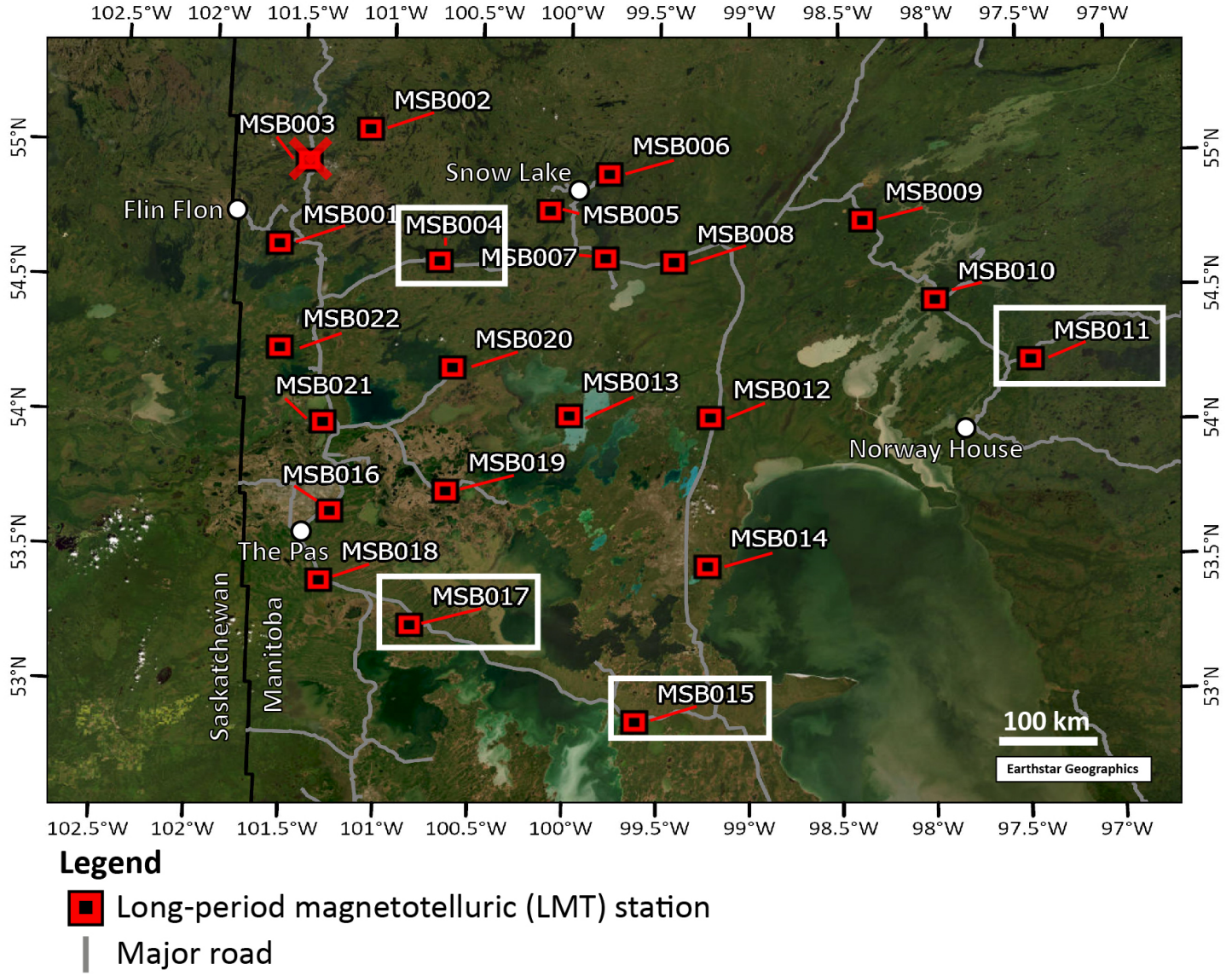


Figure GS2024-17-3: *Distribution of the long-period magnetotelluric (LMT) stations installed in 2024 in west-central Manitoba. The red X on station MSB003 indicates that it was excluded from the 3-D inversion process due to poor data quality. White boxes correspond to the LMT stations in Figure GS2024-17-4. Basemap was created using ArcGIS® software by Esri. ArcGIS® and ArcMap™ are the intellectual property of Esri and are used herein under license. Copyright © Esri. All rights reserved. For more information about Esri software, please visit <https://esri.ca/>.*

cultural noise. Each station produced 100–220 Mb of time-series data.

Magnetotelluric data analysis

After data processing, reliable apparent resistivity curves were obtained in the period range 5–10 000 s. Data from one station (MSB003, Figure GS2024-17-3) were not used due to poor quality because of equipment failure. Figure GS2024-17-4 provides examples of data from the 2024 LMT survey. At each of these stations, the resistivity from the shallow data (high frequency) is in the range 100–10 000 ohm-metre (Ω•m; Figure GS2024-17-4), as expected in a shield environment with crystalline upper crustal rocks. Data from stations MSB004 and MSB011 show similar resistivity values but MSB004 has slightly lower values, likely reflecting a more conductive lithosphere within the THO (Figure GS2024-17-4a). Data from station MSB011, the farthest east, show the highest resistivity values, likely due to it being located on the Superior craton (Figure GS2024-17-4b). The decreasing resistivity values exhibited at longer periods are likely associated with conductive features in the region. Stations MSB015 and MSB017 are located along the southern margin of the survey area and the data show evidence of a conductor at mid-periods (Figure GS2024-17-4c, d). A 2-D or 3-D resistivity structure is indicated by the XY and YX curves diverging as a function of frequency. If the resistivity structure was 1-D, the curves would be coincident.

The LMT data were measured as a function of frequency and need to be converted into a resistivity model as a function

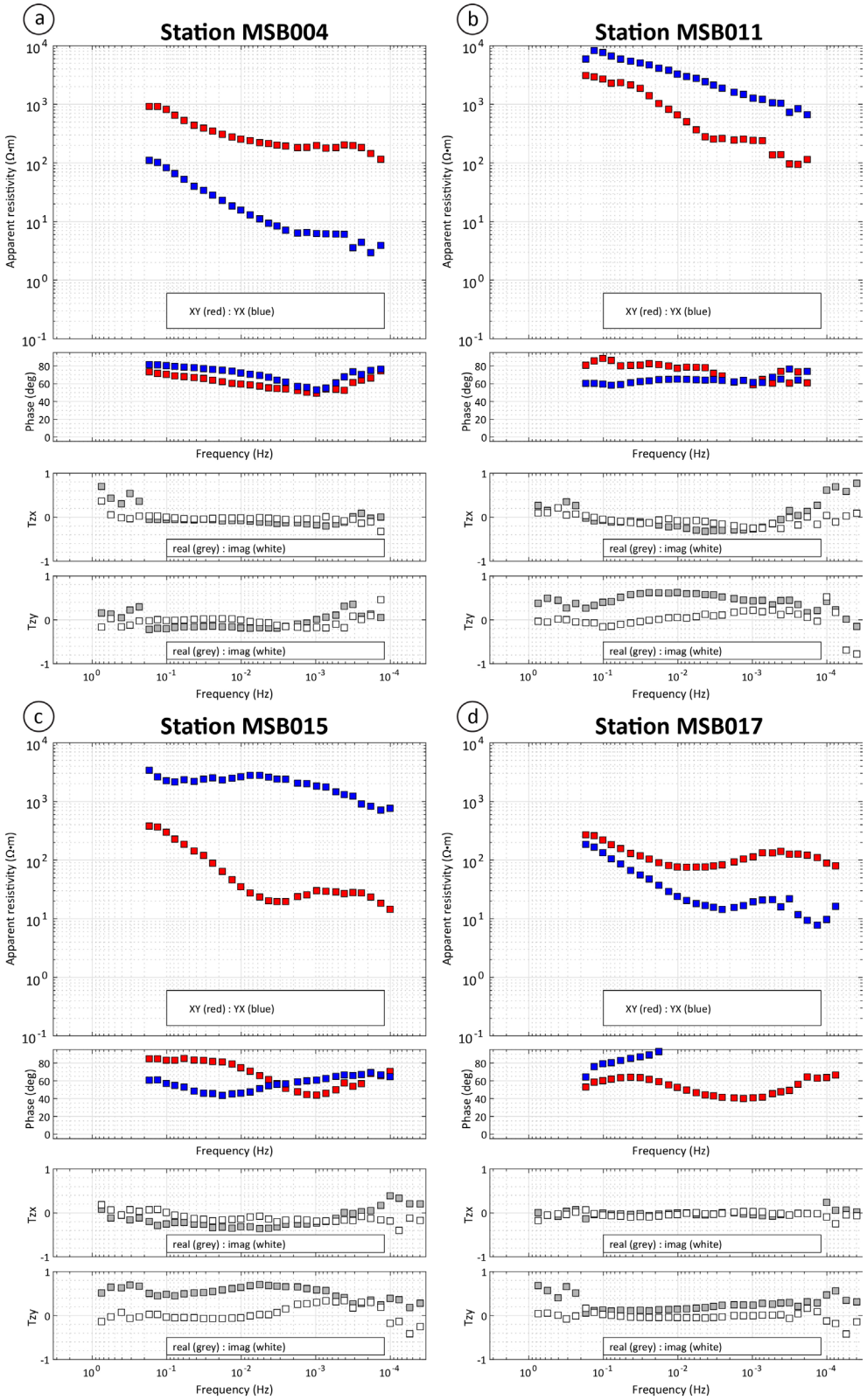


Figure GS2024-17-4: *Apparent resistivity and phase curves as a function of frequency for four long-period magnetotelluric (LMT) stations installed as part of this study:* ***a)*** *station MSB004;* ***b)*** *station MSB011;* ***c)*** *station MSB015;* ***d)*** *station MSB017. The apparent resistivity curves are obtained from the ratio of components of the electric and magnetic field measurements. The X and Y correspond to measurements of these fields in the north-south and east-west directions, respectively. Red curves are the traverse electric mode, which is highly sensitive to conductive features. Blue curves are the transverse magnetic mode, which is sensitive to both resistors and conductors, but the latter less so than the transverse electric mode. The functions labelled Tzy and Tzx are the components of the tipper (T) and are computed from the ratio of vertical (z) to horizontal (x and y) magnetic field components. The tipper is highly sensitive to conductive features. The real and imaginary (imag) components of the tipper are the in-phase and quadrature components, respectively. The locations of the stations chosen are shown in Figures GS2024-17-1 and -3. Abbreviations: Ω•m, ohm-metre; deg, degree; Hz, hertz.*

of depth and horizontal distance using a process called inversion. The LMT data collected in Manitoba show some 3-D characteristics (Figure GS2024-17-4) thus a 3-D inversion approach must be used. The 3-D inversion models are produced using the ModEM (Modular system for Electromagnetic inversion) algorithm of Kelbert et al. (2014). Computer resources are provided by the Digital Research Alliance of Canada. Some initial inversions have been completed and resulting models show that a number of crustal conductors are located in the central portion of the new data grid approximately 30–80 km east of The Pas. A major lithospheric conductor is also present beneath the Snow Lake mining district; it is similar to those observed by Chase and Unsworth (2024) beneath the mining districts around Flin Flon and La Ronge.

Future work

The inversion of the new LMT data collected in Manitoba is still in progress. The planned research will combine the 2024 LMT data with the LITHOPROBE (Jones et al., 2005) and Chase and Unsworth (2024) MT datasets. The integrated dataset will be inverted to produce a resistivity model that includes as much of the previously collected data as possible. The resulting 3-D resistivity model will be evaluated with a sensitivity analysis to determine which model features are required. This will be followed by a systematic interpretation of the 3-D resistivity model. Conductive anomalies in this model will be quantitatively interpreted to determine the cause. Anomalies present in the crust will be evaluated using data from regional geology maps and drillcore and geophysical data, allowing for a better understanding of the structural controls related to their formation and how they may relate to regional mineralization. The 3-D resistivity model will be interpreted within the mineral systems framework (e.g., McCuaig et al., 2010; McCuaig and Hronsky, 2014) to determine the factors that control the spatial distribution of mineralization. In the long term, it is planned to extend the LMT survey across southern Manitoba and Saskatchewan (Figure GS2024-17-1). This grid of LMT stations can then be combined with the EarthScope MT array in the contiguous United States (Murphy et al., 2023). This will produce a 3-D resistivity model of the lithosphere of the entire THO, which will improve tectonic evolution models for North America.

Economic considerations

The MT resistivity model developed by Chase and Unsworth (2024) for central Saskatchewan shows the presence of several major lithosphere conductors beneath Flin Flon and the La Ronge gold belt. These conductors are connected to an underlying conductive anomaly located in lithospheric mantle beneath the Sask craton. These conductors were interpreted to be due to the presence of sulphide minerals and graphite films deposited by past episodes of fluid flow in the lithosphere. These sulphide minerals may contain economically important base and precious metals (e.g., Tomkins and Evans, 2015; Walters et al., 2020). Ultimately, these conductors may explain why economic mineralization is concentrated beneath the La Ronge gold belt and Flin Flon. The new LMT data suggest that a conductor is present in the study area in Manitoba and appears to have a similar nature to the previously reported conductors in Saskatchewan. This may suggest there are regional whole-lithosphere controls on the distribution of mineralization in this region of the THO. Additional conductors were detected beneath the thin Phanerozoic sedimentary cover both east of The Pas and in Saskatchewan (Chase and Unsworth, 2024). These may indicate additional zones of mineralization that have not been previously investigated.

Acknowledgments

The authors thank the Manitoba Geological Survey for logistical support and K. Reid, T. Martins, T. Kennedy and G. Keller are acknowledged for logistical support, assistance in survey planning and communication with local communities about the survey. The authors thank T. Hodder, K. Reid and T. Martins for reviews of this report. C. Steffano is thanked for the layout of the report. C. Epp and P. Belanger are thanked for their assistance with vehicle and equipment maintenance. RnD Technical is thanked for technical editing assistance.

References

Ansdell, K.M. 2005: Tectonic evolution of the Manitoba-Saskatchewan segment of the Paleoproterozoic Trans-Hudson orogen, Canada; Canadian Journal of Earth Sciences, v. 42, no. 4, p. 741–759, URL <https://doi.org/10.1139/e05-035>.

Ansdell, K.M., Lucas, S.B., Connors, K. and Stern, R.A. 1995: Kisseynew metasedimentary gneiss belt, Trans-Hudson orogen (Canada): back-arc origin and collisional inversion; Geology, v. 23, no. 11, p. 1039–1043, URL <https://doi.org/10.1130/0091-7613(1995)023<1039:KMGBTH>2.3.CO;2>.

Bedrosian, P.A. and Finn, C.A. 2021: When Wyoming became superior: oblique convergence along the southern Trans-Hudson orogen; Geophysical Research Letters, v. 48, no. 13, art. e2021GL092970, URL <https://doi.org/10.1029/2021GL092970>.

Bleeker, W. 1990: New structural-metamorphic constraints on Early Proterozoic oblique collision along the Thompson nickel belt, northern Manitoba; *in* The Early Proterozoic Trans-Hudson Orogen of North America, J.F. Lewry and M.R. Stauffer (ed.), Geological Association of Canada, Special Paper 37, p. 57–74.

Bleeker, W., Nagerl, P. and Machado, N. 1995: The Thompson nickel belt, Manitoba: some new U-Pb ages; Geological Association of Canada–Mineralogical Association of Canada, Joint Annual Meeting, May 17–19, 1996, Victoria, British Columbia, Program with Abstracts, v. 20, p. A8.

Chase, B.F.W. and Unsworth, M.J. 2024: Magnetotelluric evidence for the formation of the layered Sask Craton by flat slab subduction; Earth and Planetary Science Letters, v. 647, art. 119027, URL <https://doi.org/10.1016/j.epsl.2024.119027>.

Clowes, R.M. and Roy, B. 2021: Crustal structure of the metasedimentary Kisseynew domain and bounding volcanic–plutonic domains, Trans-Hudson orogen, Canada; Canadian Journal of Earth Sciences, v. 58, no. 3, p. 268–285, URL <https://doi.org/10.1139/cjes-2020-0062>.

Clowes, R., Cook, F., Hajnal, Z., Hall, J., Lewry, J., Lucas, S. and Wardle, R. 1999: Canada's LITHOPROBE Project (collaborative, multidisciplinary geoscience research leads to new understanding of continental evolution); Episodes Journal of International Geoscience, v. 22, no. 1, p. 3–20, URL <https://doi.org/10.18814/epiiugs/1999/v22i1/002>.

Connors, K.A., Ansdell, K.M. and Lucas, S.B. 1999: Coeval sedimentation, magmatism, and fold-thrust development in the Trans-Hudson orogen: propagation of deformation into an active continental arc setting, Wekusko Lake area, Manitoba; Canadian Journal of Earth Sciences, v. 36, no. 2, p. 275–291, URL <https://doi.org/10.1139/e98-090>.

Heinson, G., Didana, Y., Soeffky, P., Thiel, S. and Wise, T. 2018: The crustal geophysical signature of a world-class magmatic mineral system; Scientific Reports, v. 8, art. 10608, URL <https://doi.org/10.1038/s41598-018-29016-2>.

Jones, A.G., Ledo, J. and Ferguson, I.J. 2005: Electromagnetic images of the Trans-Hudson orogen: the North American Central Plains anomaly revealed; Canadian Journal of Earth Sciences, v. 42, no. 4, p. 457–478, URL <https://doi.org/10.1139/e05-018>.

Kelbert, A., Meqbel, N., Egbert, G.D. and Tandon, K. 2014: ModEM: a modular system for inversion of electromagnetic geophysical data; Computers & Geosciences, v. 66, p. 40–53, URL <https://doi.org/10.1016/j.cageo.2014.01.010>.

Kirkby, A., Czarnota, K., Huston, D.L., Champion, D.C., Doublier, M.P., Bedrosian, P.A., Duan, J. and Heinson, G. 2022: Lithospheric conductors reveal source regions of convergent margin mineral systems; Scientific Reports, v. 12, no. 1, art. 8190, URL <https://doi.org/10.1038/s41598-022-11921-2>.

Lewry, J.F. and Collerson, K.D. 1990: Trans-Hudson orogen: extent, subdivisions, and problems; *in* The Early Proterozoic Trans-Hudson Orogen of North America, J.F. Lewry and M.R. Stauffer (ed.), Geological Association of Canada, Special Paper 37, p. 1–14.

Machado, N. 1990: Timing of collisional events in the Trans-Hudson orogen: evidence from U-Pb geochronology for the New Quebec orogen, the Thompson belt and the Reindeer zone (Manitoba and Saskatchewan); *in* The Early Proterozoic Trans-Hudson Orogen of North America, J.F. Lewry and M.R. Stauffer (ed.), Geological Association of Canada, Special Paper 37, p. 433–441.

Manitoba Geological Survey 2022: Bedrock geology of Manitoba; Manitoba Natural Resources and Northern Development, Manitoba Geological Survey, Open File OF2022-2, scale 1:1 000 000.

McCuaig, C.T. and Hronsky, J.M.A. 2014: The mineral system concept: the key to exploration targeting; *in* Building Exploration Capability for the 21st Century, K.D. Kelly and H.C. Golden (ed.), Special Publication of the Society of Economic Geologists, v. 18, p. 153–175.

McCuaig, T.C., Beresford, S. and Hronsky, J. 2010: Translating the mineral systems approach into an effective exploration targeting system; Ore Geology Reviews, v. 38, no. 3, p. 128–138, URL <https://doi.org/10.1016/j.oregeorev.2010.05.008>.

Murphy, B.S., Bedrosian, P. and Kelbert, A. 2023: Geoelectric constraints on the Precambrian assembly and architecture of southern Laurentia; *in* Laurentia: Turning Points in the Evolution of a Continent, S.J. Whitmeyer, M.L. Williams, D.A. Kellett and B. Tikoff (ed.), Geological Society of America, Memoir 220, p. 203–220, URL <https://doi.org/10.1130/2022.1220(13)>.

Percival, J.A., Sanborn-Barrie, M., Skulski, T., Stott, G.M., Helmstaedt, H. and White, D.J. 2006: Tectonic evolution of the western Superior Province from NATMAP and Lithoprobe studies; Canadian Journal of Earth Sciences, v. 43, no. 7, p. 1085–1117, URL <https://doi.org/10.1139/e06-062>.

Percival, J.A., Skulski, T., Sanborn-Barrie, M., Stott, G.M., Leclair, A.D., Corkery, M.T. and Boily, M. 2012: Geology and tectonic evolution of the Superior Province, Canada; *in* Tectonic Styles in Canada: the LITHOPROBE Perspective, J.A. Percival, F.A. Cook and R.M. Clowes (ed.), Geological Association of Canada, Special Paper 49, p. 321–378.

Saskatchewan Energy and Resources 2021: Geological domains for the province of Saskatchewan, CSRS NAD83 Zone 13; *in* Mining and Petroleum GeoAtlas, Saskatchewan Ministry of Energy and Resources, URL <https://gisappl.saskatchewan.ca/Html5Ext/index.html?viewer=GeoAtlas> [September 2022].

Simpson, F. and Bahr, K. 2005: Practical Magnetotellurics; Cambridge University Press, Cambridge, England, 254 p.

Syme, E.C., Lucas, S.B., Bailes, A.H. and Stern, R.A. 1999: Contrasting arc and MORB-like assemblages in the Paleoproterozoic Flin Flon belt, Manitoba, and the role of intra-arc extension in localizing volcanic-hosted massive sulphide deposits; Canadian Journal of Earth Sciences, v. 36, no. 11, p. 1767–1788, URL <https://doi.org/10.1139/e98-084>.

Tomkins, A.G. and Evans, K.A. 2015: Separate zones of sulfate and sulfide release from subducted mafic oceanic crust; Earth and Planetary Science Letters, v. 428, p. 73–83, URL <https://doi.org/10.1016/j.epsl.2015.07.028>.

Walters, J.B., Cruz-Uribe, A.M. and Marschall, H.R. 2020: Sulfur loss from subducted altered oceanic crust and implications for mantle oxidation; Geochemical Perspective Letters, v. 13, p. 36–41, URL <https://doi.org/10.7185/geochemlet.2011>.

Weber, W. 1990: The Churchill-Superior boundary zone, southeast margin of the Trans-Hudson orogen: a review; *in* The Early Proterozoic Trans-Hudson Orogen of North America, J.F. Lewry and M.R. Stauffer (ed.), Geological Association of Canada, Special Paper 37, p. 41–55.

Whalen, J.B., Syme, E.C. and Stern, R.A. 1999: Geochemical and Nd isotopic evolution of Paleoproterozoic arc-type magmatism in the Flin Flon belt, Trans-Hudson orogen, Canada; Canadian Journal of Earth Sciences, v. 36, no. 2, p. 227–250, URL <https://doi.org/10.1139/e98-026>.

White, D.J., Lucas, S.B., Bleeker, W., Hajnal, Z., Lewry, J.F. and Zwanzig, H.V. 2002: Suture-zone geometry along an irregular Paleoproterozoic margin: the Superior boundary zone, Manitoba, Canada; Geology, v. 30, no. 8, p. 735–738, URL <https://doi.org/10.1130/0091-7613(2002)030<0735:SZGAAI>2.0.CO;2>.

White, D.J., Thomas, M.D., Jones, A.G., Hope, J., Németh, B. and Hajnal, Z. 2005: Geophysical transect across a Paleoproterozoic continent–continent collision zone: the Trans-Hudson orogen; Canadian Journal of Earth Sciences, v. 42, no. 4, p. 385–402, URL <https://doi.org/10.1139/e05-002>.

Whitmeyer, S.J. and Karlstrom, K.E. 2007: Tectonic model for the Proterozoic growth of North America; Geosphere, v. 3, no. 4, p. 220–259, URL <https://doi.org/10.1130/GES00055.1>.

Ye, G., Unsworth, M., Wei, W., Jin, S. and Liu, Z. 2019: The lithospheric structure of the Solonker suture zone and adjacent areas: crustal anisotropy revealed by a high-resolution magnetotelluric study; Journal of Geophysical Research: Solid Earth, v. 124, no. 2, p. 1142–1163, URL <https://doi.org/10.1029/2018JB015719>.

Zwanzig, H.V., Macek, J.J. and McGregor, C.R. 2007: Lithostratigraphy and geochemistry of the high-grade metasedimentary rocks in the Thompson nickel belt and adjacent Kisseynew domain, Manitoba: implications for nickel exploration; Economic Geology, v. 102, no. 7, p. 1197–1216, URL <https://doi.org/10.2113/gsecongeo.102.7.1197>.

GS2024-18

Rock volatiles analysis of drill cuttings to evaluate the helium and hydrocarbon prospectivity of southwestern Manitoba (parts of NTS 62F2, K3)

by M.P.B. Nicolas, C.M. Smith[1] and M.P. Smith[1]

In Brief:

- Volatile analysis of legacy drill cuttings was done on three oil wells
- Results indicates zones prospective for helium and show indicators of unexplored, active hydrocarbon systems in the Devonian-age strata

Citation:
Nicolas, M.P.B., Smith, C.M. and Smith, M.P. 2024: Rock volatiles analysis of drill cuttings to evaluate the helium and hydrocarbon prospectivity of southwestern Manitoba (parts of NTS 62F2, K3); *in* Report of Activities 2024, Manitoba Economic Development, Investment, Trade and Natural Resources, Manitoba Geological Survey, p. 153–163.

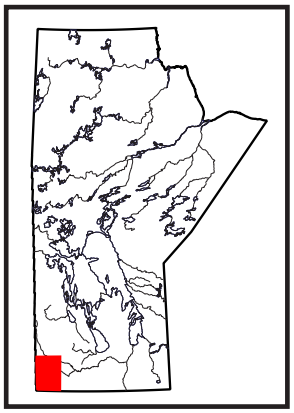
Summary

The helium and hydrocarbon prospectivity of southwestern Manitoba was evaluated using the Rock Volatiles Stratigraphy (RVS) system. Drill cuttings from three legacy oil wells (L.S. 9, Sec. 6, Twp. 2, Rge. 26, W 1st Mer. [abbreviated 9-6-2-26W1], 16-29-12-29W1 and 1-25-4-23W1) were analyzed for a wide range of volatile compounds, including C1–C10 hydrocarbons, carbon dioxide, water and helium. Two of the wells were originally sampled in 2023, and in 2024 were sampled farther upsection, for complete profiles from the Precambrian up to the Lodgepole Formation. A new well, located farther to the east at 1-25-4-25W1, was sampled from the Precambrian to the Lodgepole Formation. All three wells show signs of potential helium accumulations and indicate a complex active helium system in the subsurface, which is affected by structural and stratigraphic controls. Hydrocarbon signatures within all three wells indicate an active oil system in Devonian strata, with evidence for migration, as well as potential for bypassed pay in the areas. Results from this study indicate a considerable untapped potential, including significant helium presence in southwestern Manitoba and indicators of unexplored, active hydrocarbon systems in formations below current oil-producing horizons.

Introduction

A review of helium occurrences in southwestern Manitoba oil and gas wells by Nicolas (2018) and Nicolas et al. (2023b) indicated the presence of a helium system in southwestern Manitoba (Figure GS2024-18-1). Traditional gas analyses conducted on samples collected downhole in oil and gas wells are the most common way to measure gases from a reservoir. The Rock Volatiles Stratigraphy (RVS) system provides a postdrilling option to measure and evaluate the residual volatile fraction trapped in drilled cuttings or core. Nicolas et al. (2023b) conducted RVS analysis on a series of drill-cutting samples from three oil and gas wells, with samples collected from the Precambrian, upsection to either the Silurian Interlake Group or the Devonian Dawson Bay Formation. The positive results reported in Nicolas et al. (2023b) led to a new suite of samples being collected for rock volatiles analysis in 2024. The Manitoba Geological Survey (MGS), again in partnership with Advanced Hydrocarbon Stratigraphy, Inc. (AHS), studied the volatile fraction of fluids in drill cuttings from three oil wells (Table GS2024-18-1) drilled in the Paleozoic. By measuring fluid, gas, hydrocarbon, rock and reservoir properties it is possible to evaluate for helium prospectivity in Manitoba, and provide insights into local hydrocarbon systems.

Nicolas et al. (2023b) described the benefits and limitations of RVS analysis and compared the results to previous studies. Subsequent core studies, such as those described in Smith et al. (2022, 2023, 2024), have reinforced the correlation between RVS helium values and those observed in gas tests.



Methodology

Drill cuttings from three historical petroleum exploration wells in southwestern Manitoba were sampled for testing by the RVS system. The three wells sampled for this study are 1) Corex Coulter Prov. 100/09-06-002-26W1/00 (oil and gas well licence 2610, Manitoba Economic Development, Industry, Trade and Natural Resources, Winnipeg) in 9-6-2-26W1; 2) ASM-BTO et al Kirkella Prov. 100/16-29-012-29W1/00 (oil and gas well licence 2532) in 16-29-12-29W1; and 3) Tundra Dand 100/01-25-004-23W1/00 (oil and gas well licence 4859) in 1-25-4-23W1 (Figure GS2024-18-1). Sampling intervals were restricted to the available cuttings in storage; the sampling interval was ~6 m (20 ft.) for the well at 16-29-12-29W1 and 5 m for the wells at 9-6-2-26W1 and 1-25-4-23W1 (Table GS2024-18-1).

[1] Advance Hydrocarbon Stratigraphy, Inc., Tulsa, Oklahoma

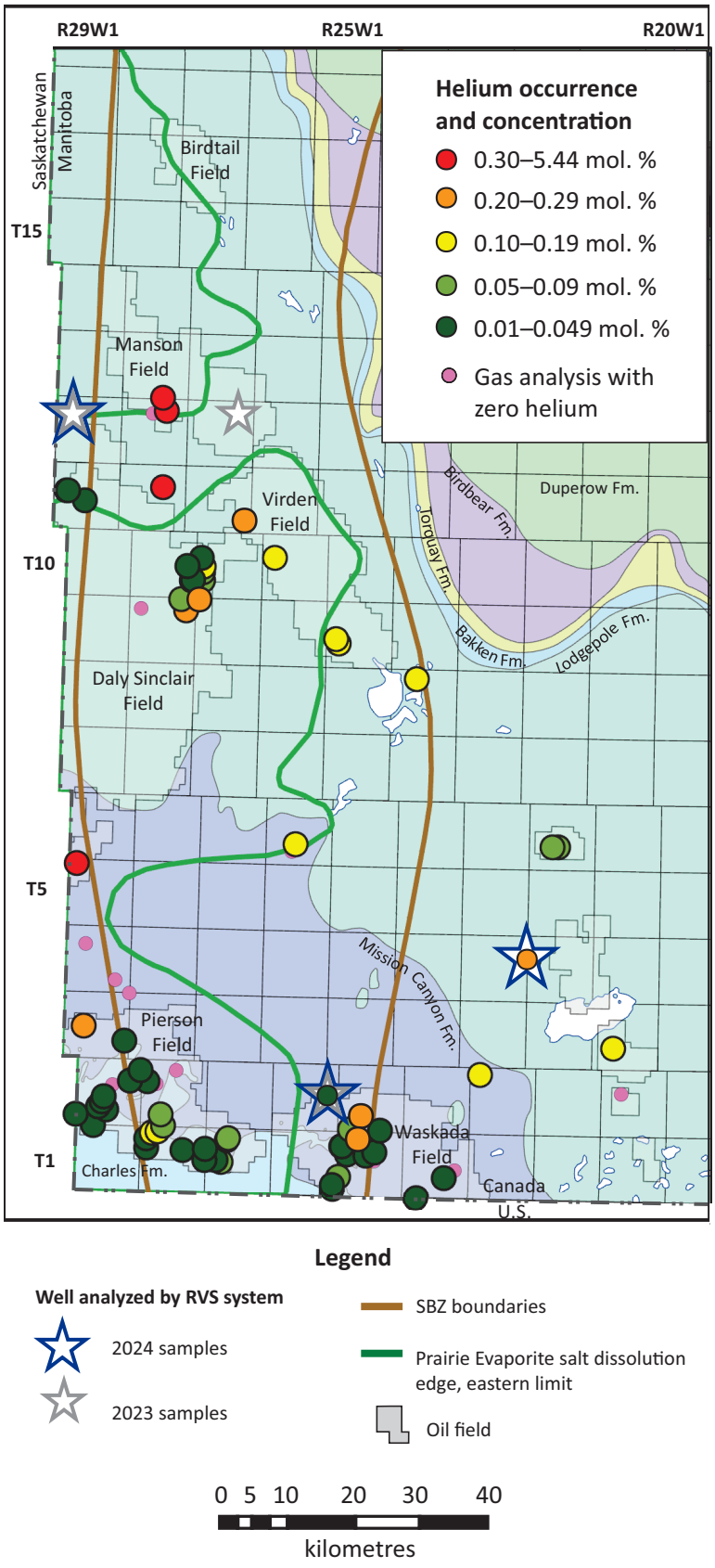


Figure GS2024-18-1: *Paleozoic bedrock geology of southwestern Manitoba showing the formational subcrop edges (modified after Nicolas et al., 2010). Also shown are the 1) locations of wells sampled in 2023 and 2024 and analyzed by the Rock Volatiles Stratigraphy (RVS) system and 2) distribution of gas analyses and helium occurrences (modified from Nicolas, 2018). Select oil fields are labelled (Nicolas, 2023). Abbreviation: SBZ, Superior boundary zone.*

Table GS2024-18-1: List of wells sampled in southwestern Manitoba.

Unique well identifier (UWI)	Licence number	Easting (Zone 14, NAD83)	Northing (Zone 14, NAD83)	Year drilled	Total depth (m TVD)	Sample depth range (m TVD)	Sample interval	Stratigraphy	Comments
100/09-06-002-26W1/00	2610	358365.58	5440090.64	1979	1986.0	1485–1160	5 m	Dawson Bay Fm. to Lodgepole Fm.	Salt-gel drilling mud used in deeper section; drilled with mill-tooth drill bit
100/16-29-012-29W1/00	2532	327790.04	5546621.49	1974	1664.2	1356–765	~6 m (20 ft.)	Interlake Gp. to Lodgepole Fm.	Salt-gel drilling mud used below 589 m; drilled with mill-tooth drill bit
100/01-25-004-23W1/00	4859	394906.57	5464921.23	2000	1670.0	1655–815	5 m	Precambrian to Lodgepole Fm.	Drilled with PDC drill bit

Abbreviations: PDC, polycrystalline diamond compact; TVD, true vertical depth.

The wells at 9-6-2-26W1 and 16-29-12-29W1 were sampled and analyzed in 2023 and were then sampled farther upsection (from the shallowest 2023 sample) in 2024. The well at 1-25-4-23W1 was added to the 2024 study, with samples collected from the Precambrian to the Lodgepole Formation. One of the wells sampled in 2023, the well at 13-24-12-27W1 (oil and gas well licence 10911), was not resampled in 2024. For consistency, and to allow stratigraphic comparisons, all wells were sampled through the section, from the Precambrian basement up to the lower Lodgepole Formation. Selection of the new well was based on the availability of Precambrian samples at a depth of ≥1500 m, good quality drill cuttings and sample recovery possible at ~5 m intervals continuously from the Precambrian up through to the Lodgepole Formation. The geographic location of the new well was also considered, as a location away from the effects of the sub-Phanerozoic Superior boundary zone (SBZ) and the salt dissolution of the Prairie Evaporite was preferred. The rationale to select a well located away from any major structural disturbances was to allow for comparison with those that occur in areas with known structural features.

The samples were sent to the AHS laboratory in Tulsa, Oklahoma, for analysis by their proprietary cryotrap mass spectrometer (CT-MS) system specially designed to analyze for C1–C10 hydrocarbons, helium, formation water, CO_2, sulphur gases, organic acids and mechanical strength. Smith et al. (2022) found that more than 40 volatile compounds can be measured from core samples, but that less compounds could be reliably analyzed from drill cuttings. Table GS2024-18-2 shows the list of compounds and rock properties analyzed from drill cuttings for this study.

Each sample consisted of 3 g of drill cuttings from each interval, starting with the vial at the maximum sample depth identified for that well. Each well was then sampled upsection, up to the lower Lodgepole Formation, ensuring a minimum of 100 samples was collected for a given well.

The same analytical methods were applied to these samples as those described in Nicolas et al. (2023b), with the exception for how the mechanical strength was measured. In 2023, the mechanical strength was measured using an automated system to measure the thickness of the sample container after a crushing force had been applied. Due to concerns about the automated system, AHS manually measured the thickness of the crushed sample containers with vernier calipers in 2024.

Table GS2024-18-2: Generalized list of compounds and rock properties analyzed by the Rock Volatiles Stratigraphy system on drill cuttings in this study. Data Repository Item DRI2024008 (Nicolas et al., 2024) provides details on compounds, properties, proxies and calculations.

Compounds	Rock properties
Methane	Mechanical strength
Ethane	Permeability proxy
Propane	Hydrocarbon liquid volume
Butanes	Hydrocarbon gas volume
Pentanes	Total water
Benzene	Equivalent oil production
C6 naphthenes	Equivalent gas production
Hexanes	Gas-oil ratio (GOR)
Toluene	
C7 naphthenes	
Heptanes	
C8 aromatics	
C8 naphthenes	
Octanes	
C9 naphthenes	
Nonanes	
C10 naphthenes	
Decanes	
CO_2	
Helium	
Nitrogen	
Formic acid	
Acetic acid	
SO- (sulphate proxy)	

Rock Volatiles Stratigraphy results and interpretation

The entirety of the RVS data is available in Data Repository Item DRI2024008 (Nicolas et al., 2024)[2]. There is a significant amount of information that can be extracted from the RVS data. This report focuses only on the data used to evaluate helium and hydrocarbon prospectivity, but also on select data for other fluids, such as organic acids, water and CO_2, as they provide information about the overall fluid dynamics of the system. To allow more accurate comparison between the 2023 and 2024 datasets, mechanical strength was remeasured for samples from the wells at 9-6-2-26W1 and 1-25-4-23W1. The data corrections for these two wells are in Nicolas et al. (2024); the mechanical strength for 16-29-12-29W1 was not remeasured.

The drill bit used and drilling mud composition can affect the results and these factors need to be considered when interpreting RVS data (Nicolas et al., 2023b). Table GS2024-18-1 lists the drill bit used for each well analyzed in this study. Polycrystalline diamond compact (PDC) drill bits, commonly used to drill modern wells, shear and grind the rock to a much finer grain size, destroying much of the macro- and microporosity, compared to mill-tooth bits, such as tricone/rock/cable tool diamond-drill bits, typical of older technologies. For RVS analysis, larger drill cuttings are preferred as rock morphology has not been overly compromised and sample handling has been minimal thus the escape of volatiles from pore spaces has been minimized.

Oil and gas well at 9-6-2-26W1 (licence 2610)

Drill cuttings collected from the well at 9-6-2-26W1 were sampled from 1485 m true vertical depth (TVD), near the base of the Burr Member of the Dawson Bay Formation, up to 1160 m TVD, in the basal limestone facies of the Scallion Member of the Lodgepole Formation. The drill cuttings from this well were generated using a mill-tooth drill bit. Figure GS2024-18-2 shows the data logs for select analyses, including helium, as they relate to stratigraphy. For a comprehensive discussion of the results below 1485 m TVD, see Nicolas et al. (2023b).

Helium

Smith et al. (2022) stated that a reading above 0.7 nanomol (nmol) helium on a RVS log indicates a potential economic accumulation of helium. The comparison of drill cuttings between wells drilled with different drill bits (i.e., mill-tooth bits versus PDC bits) in Nicolas et al. (2023b) indicated that this threshold is better applied to wells with drill cuttings the size of coarse-grained sand to pebbles. A lower threshold is needed for wells with drill cuttings the size of medium to coarse sand. The well at 9-6-2-26W1 has large enough drill cuttings to use the 0.7 nmol helium threshold.

Above 1485 m TVD, helium values show a positive response in the Dawson Bay Formation (1490 m TVD) with a peak at the top of the Burr Member before decreasing to the middle of the Harris Member of the Souris River Formation (1400 m TVD). The helium values drop upsection, indicating a break in the helium system (i.e., no further upward migration of helium), until the top of the Torquay Formation is reached, where the values peak at 0.92 nmol; the Upper Member of the overlying Bakken Formation may be acting as a seal to the helium system below. In this well, the highly organic shales of the Upper Member of the Bakken Formation might even be contributing helium to the system (Nicolas et al., 2023b), further increasing the helium accumulation at this stratigraphic level. Overall, the helium distribution throughout the section in this well is variable but consistently present. This indicates an active helium migration system, which, despite being constrained by tight rock units in places, has sufficient migration pathways that transect many stratigraphic boundaries. This suggests a structural control on fluid movement, such as an efficient fracture network or nearby faults.

Hydrocarbons

Above 1400 m TVD, the helium values decrease to near background levels and there is a noticeable increase in CO_2 and hydrocarbon gas volume levels upsection. This depth also coincides with a sudden increase in formic acid levels and the beginning of a decline in hydrocarbon liquid volumes. This break may indicate an oil–gas transition zone.

Also of note is a marked occurrence of high CO_2, near zero to low helium values, and distinct high formic acid and sulphate values constrained within the Souris River Formation to lower Duperow Formation. This, together with a variable interbedded lithology typical of these formations, suggests a complex stratigraphic and depositional environment influencing the fluids.

An observation from the 2023 results (below 1485 m TVD; Figure GS2024-18-2; Nicolas et al., 2023b), which has not been previously reported, is the correlation of the responses from two drillstem tests (DST) with the responses on the profiles. Drillstem test 1 was at 1535–1520 m TVD, at the top of the Winnipegosis Formation, and DST 3 was at 1602–1596 m TVD, at the top of the Interlake Group. The results of DST 1 in the Winnipegosis Formation indicate a fair to good initial blow followed by a steady flow throughout the test, and results of DST 3 in the Interlake Group indicate a strong steady air blow throughout the test (oil and gas well licence 2610). Correlation of the DST 1 depths with the RVS log shows the helium values are moderately low, but the hydrocarbon response is high. The total water is capped at this depth giving it a high total water content, which coincides with moderately high hydrocarbon liquid volumes, and a sudden spike in acetic acid. These responses may coincide with the oil-water

[2] MGS Data Repository Item DRI2024008, containing the data or other information sources used to compile this report, is available online to download free of charge at https://manitoba.ca/iem/info/library/downloads/index.html, or on request from minesinfo@gov.mb.ca, or by contacting the Resource Centre, Manitoba Economic Development, Investment, Trade and Natural Resources, 360-1395 Ellice Avenue, Winnipeg, Manitoba R3G 3P2, Canada.

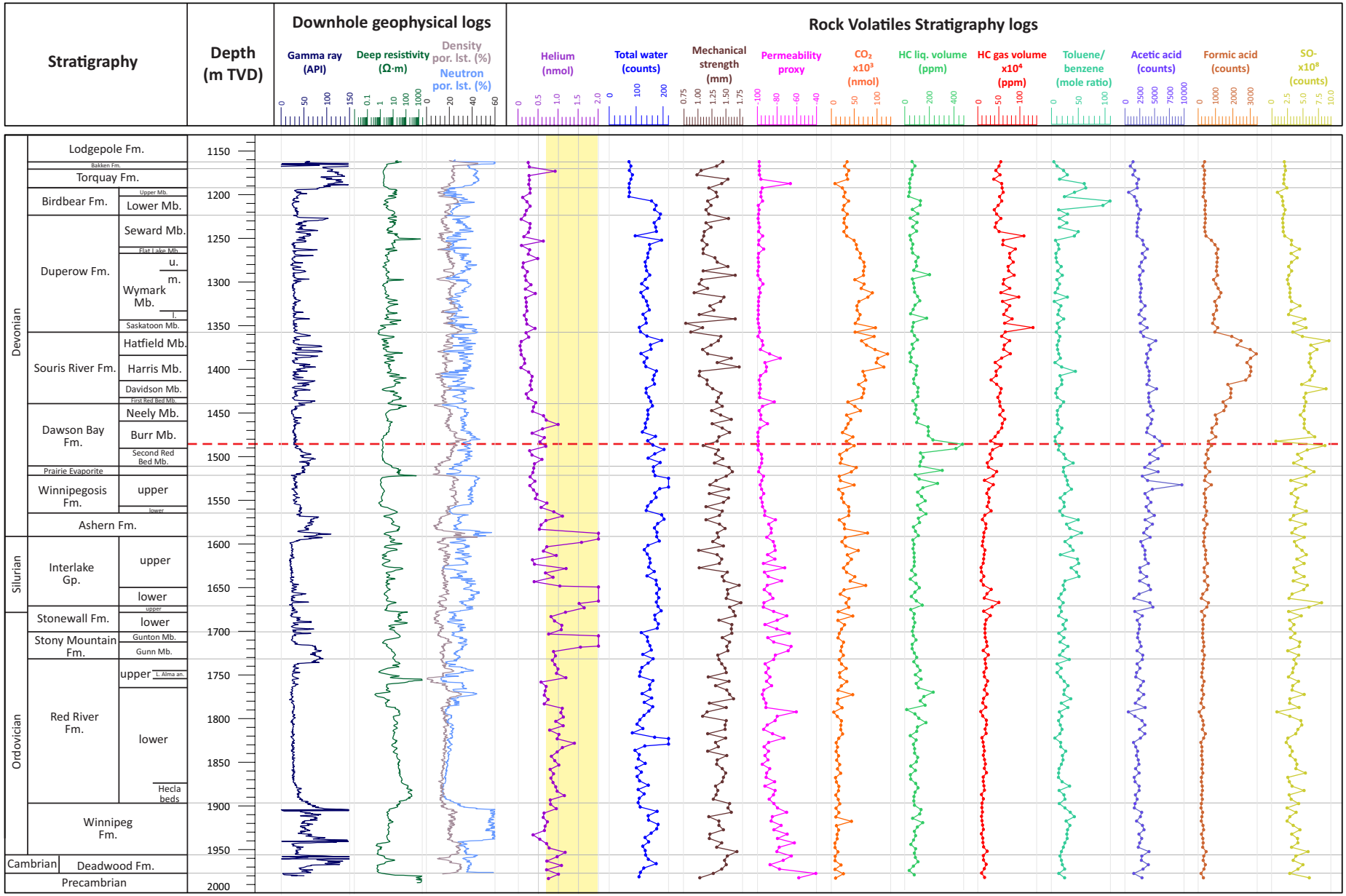


Figure GS2024-18-2: *Stratigraphy and Rock Volatiles Stratigraphy data logs for the oil and gas well at L.S. 9, Sec. 6, Twp. 2, Rge. 26, W 1st Mer. (9-6-2-26W1, southwestern Manitoba), including select downhole geophysical logs. Samples were collected at 5 m intervals. The red dashed line indicates the break between the 2023 data reported in Nicolas et al. (2023a, b) and the new 2024 data (above the red dashed line). Yellow highlighted area on the helium track shows values ≥0.7 nanomoles (nmol). Mechanical strength of the sample increases from left to right on the mechanical strength log; the permeability proxy log indicates increased permeability from left to right. Abbreviations: HC, hydrocarbon; L. Alma an., Lake Alma anhydrite; l., lower; liq., liquid; por. lst., porosity of limestone; m., middle; TVD, true vertical depth; u., upper.*

contact for the hydrocarbon system occurring within the Dawson Bay Formation. Therefore, the DST may have been done too low in the section to show positive oil results. For DST 3, the corresponding depths coincide with very high helium values, a CO_2 peak and a good permeability index reading, but with unremarkable hydrocarbon liquid and gas volumes. This indicates that the strong steady air flow from this test was likely due to the helium and CO_2 accumulated at this depth.

In the Burr Member of the Dawson Bay Formation, the hydrocarbon liquid volume on the RVS logs shows a dramatic increase with a corresponding increase in hydrocarbon gas volumes, indicating the presence of hydrocarbons (Figure GS2024-18-2). The low toluene/benzene ratio indicates that there has been limited migration of hydrocarbons out the system, which suggests an oil trap nearby. This could be a potential oil exploration interval in this area.

Oil and gas well at 16-29-12-29W1 (licence 2532)

Drill cuttings collected from the well at 16-29-12-29W1 were sampled from 1360 m TVD, in the lower Interlake Group, up to 765 m TVD, in the basal limestone facies of the Scallion Member of the Lodgepole Formation. The drill cuttings from this well were generated using a mill-tooth drill bit. Figure GS2024-18-3 shows the data logs for select analyses, including helium, as they relate to stratigraphy. For a comprehensive discussion of the results below 1360 m TDV, see Nicolas et al. (2023b).

Helium

The helium system in this well shows a break at 1365 m TVD, just below the 2023–2024 sample boundary, where the values drop to near zero. Two isolated helium-rich zones occur upsection from this break. The first occurs in the Winnipegosis Formation as a thin helium show, where the thick salt of the Prairie Evaporite above acts as a barrier to the helium migrating upward from the lower Paleozoic section. The second occurs from 1025 to 985 m TVD and extends from the Hatfield Member of the Souris River Formation to the lower Wymark Member of the Duperow Formation. The helium system in this well is constrained to the lower Paleozoic formations.

Hydrocarbons

The 1025–985 m TVD interval coincides with a high hydrocarbon liquid volume and corresponding low water content within the Hatfield Member of the Souris River Formation to the middle Wymark Member of the Duperow Formation. The base of this section, at 1025 m TVD, also coincides with a marked change in acetic acid and formic acid values and a sharp increase in sulphate values. The change likely corresponds to an oil-water contact that is partly controlled by stratigraphic and lithological variations.

There were DSTs conducted on this well at 771–763 m TVD and 781–774 m TVD, coinciding with the Bakken Formation. These intervals returned poor results with no oil or gas shows. The RVS results for hydrocarbon indicators support these findings, indicating no active oil system in these tested formations (Figure GS2024-18-3). However, farther down the section, in the interval from the middle Dawson Bay to upper Souris River formations, there are high liquid hydrocarbon volumes in combination with the anomalously high toluene/benzene values, and a slight drop in water content. This indicates that there is likely an active oil system through this section with some ongoing migration that is worth exploring within this well or at nearby locations.

Oil and gas well at 1-25-4-23W1 (licence 4859)

Drill cuttings collected from the well at 1-25-4-23W1 were sampled from 1655 m TVD, in the Precambrian, up to 815 m TVD, in the Scallion Member of the Lodgepole Formation. Figure GS2024-18-4 shows the data logs for select analyses, including helium, as they relate to stratigraphy.

Helium

The drill cuttings from this well were generated using a PDC drill bit. These finer grained drill cuttings will still yield valuable results in volatile analysis, but the results will be significantly attenuated due to the loss of macropores during drilling. Comparing the volatile analysis profile to those of the wells at 9-6-2-26W1 and 16-29-12-29W1 will be difficult, therefore it is recommended that only general trends of volatile results be compared when necessary. Additionally, the threshold of 0.7 nmol helium as the lower economic limit cannot be applied to this well, however, values occurring above the threshold do indicate very high helium values.

The helium system in this well is consistently distributed throughout the section, with several distinctive high peaks. However, there is a clear break where helium values drop to zero above the Bakken–Lodgepole formation contact. This indicates that, despite the high permeability of the Lodgepole Formation, the shale of the Upper Member of the Bakken Formation is a very effective seal for helium.

Aside from the isolated peaks, the section from the Red River Formation to the middle Stonewall Formation shows elevated helium values, consistent with the profiles in the other wells analyzed. Within this section, the highest helium values occur between the Stony Mountain Formation and the Stonewall Formation, where the system is capped by the tight t-marker unit. This suggests an active helium system may extend farther east, away from structural disturbances. After the helium peak in the Stonewall Formation, the helium values decrease gradually in the lower Interlake Group. This gradual decrease in helium values upsection in the lower Interlake Group is also observed in the well at 16-29-12-29W1 (Figure GS2024-18-3), which is in contrast to the wells at 9-6-2-26W1 (Figure GS2024-18-2) and 13-24-12-27W1 (Nicolas et al., 2023b).

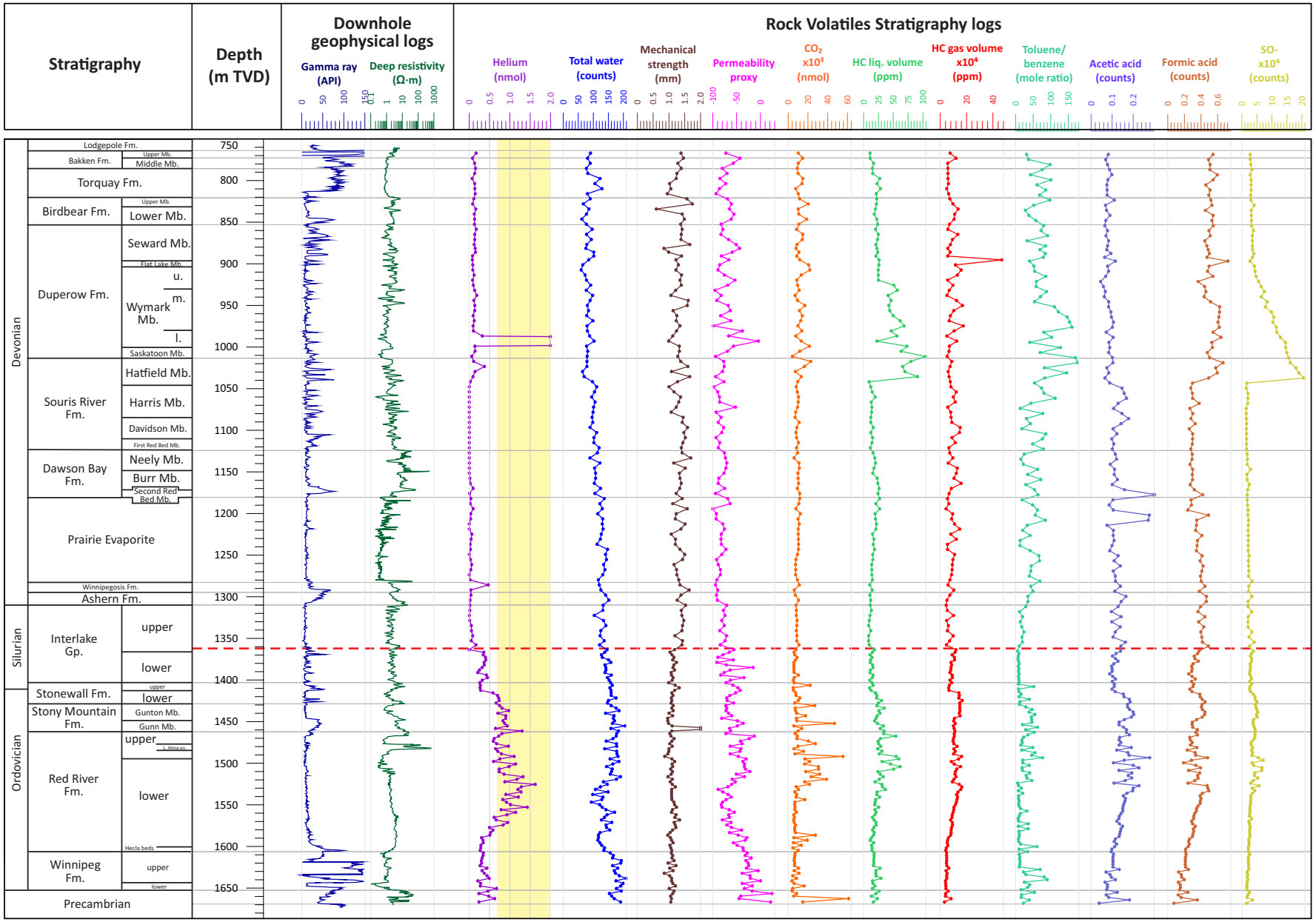


Figure GS2024-18-3: *Stratigraphy and Rock Volatiles Stratigraphy (RVS) data logs for the well at L.S. 16, Sec. 29, Twp. 12, Rge. 29, W 1st Mer. (16-29-12-29W1, southwestern Manitoba), including select downhole geophysical logs. Samples above 1360 m TVD were collected at ~6 m (20 ft.) intervals; samples below 1360 m TVD were collected at ~3 m (10 ft.) intervals. The red dashed line indicates the break between the 2023 data reported in Nicolas et al. (2023a, b) and the new 2024 data (above the red dashed line). Yellow highlighted area on the helium track shows values ≥0.7 nanomoles (nmol). Mechanical strength of the sample increases from left to right on the mechanical strength log; the permeability proxy log indicates increased permeability from left to right. Abbreviations: HC, hydrocarbon; l., lower; L. Alma an., Lake Alma anhydrite; liq., liquid; m., middle; TVD, true vertical depth; u., upper.*

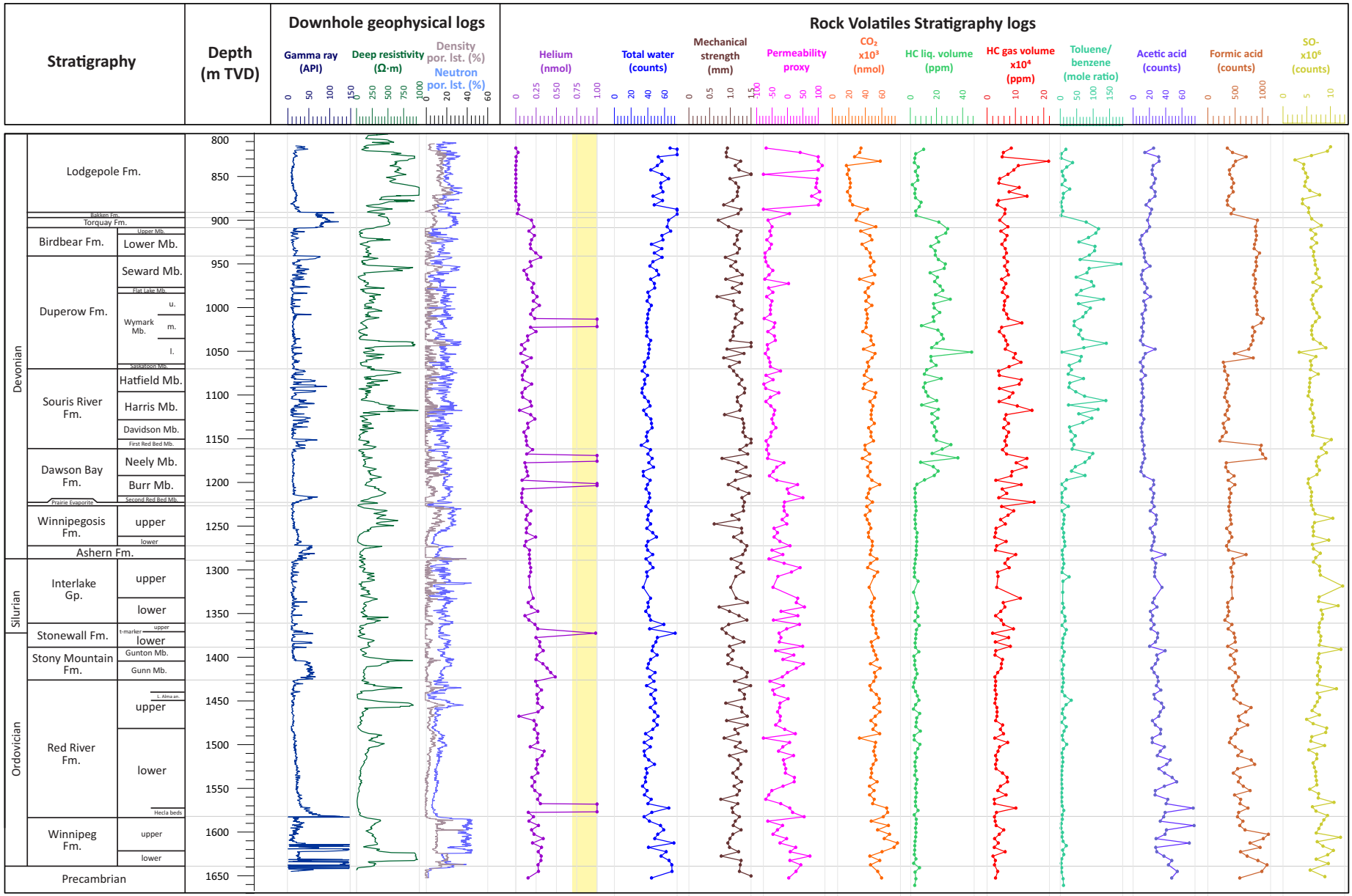


Figure GS2024-18-4: *Stratigraphy and Rock Volatiles Stratigraphy (RVS) data logs for the oil and gas well at L.S. 1, Sec. 25, Twp. 4, Rge. 23, W 1st Mer. (1-25-4-23W1, southwestern Manitoba), including select downhole geophysical logs. Samples were collected at 5 m intervals. Yellow highlighted area on the helium track shows values ≥0.7 nanomoles (nmol). Mechanical strength of the sample increases from left to right on the mechanical strength log; the permeability proxy log indicates increased permeability from left to right. Abbreviations: HC, hydrocarbon; L. Alma an., Lake Alma anhydrite; l., lower; liq., liquid; por. lst., porosity of limestone; m., middle; TVD, true vertical depth; u., upper.*

Four other peaks were noted in the section, at the base of the Red River Formation, at the top of two of the members of the Dawson Bay Formation, and at the top of the middle Wymark Member of the Duperow Formation. Each of these are coincident with known occurrences of tighter lithologies, commonly, but not exclusively, anhydrite may be acting as a seal, contributing to the trapping and accumulation of helium in these stratigraphic horizons (Smith et al., 2023).

Hydrocarbons

In the section from the Neely Member of the Dawson Bay Formation (~1195 m TVD), continuously up to the base of the Bakken Formation (~900 m TVD), the hydrocarbon liquid volumes are significantly higher than anywhere else in the section. Overall, this section also has high toluene/benzene ratios, lower permeability and low acetic acid values. Within this section, the formic acid shows two blocky signatures, a small one at the bottom of this zone and one starting at 1060 m TVD depth. The latter also coincides with a further increase in hydrocarbon liquid volumes and toluene/benzene values. This indicates two separate hydrocarbon-bearing intervals, a thin one at 1195–1155 m TVD, and a much thicker one at 1060–900 m TVD. The bottom interval coincides with a helium peak, as well as slightly elevated hydrocarbon gas volumes, and the top of the lowest interval coincides with the First Red Bed Member of the Souris River Formation. This member is likely forming a localized cap for this hydrocarbon system, preventing or limiting the upward migration of fluids. The lack of a clear break of RVS values between the two intervals suggests the two intervals may be connected to some degree and the interval between them (1155–1060 m TVD) is acting as a pinch point, slowing down the fluids' migration upward. The higher interval (1060–900 m TVD) is quite thick and indicates hydrocarbons have migrated through this Devonian strata. The increase in water content upsection and no coinciding acetic acid and formic acid response to indicate an oil-water contact, suggests this interval may be waterlogged. Therefore, searching for oil updip from this location may prove to be a good exploration strategy.

The helium peak at 1015 m TVD also coincides with a small increase in hydrocarbon gas volumes and low hydrocarbon liquid volumes, as well as very low permeability. This low permeability may provide insight into the pore space size and the ability for the rock to hold onto the water and helium more tightly in small pore spaces. This becomes an interesting observation when considering the small size of the drill cuttings for this well. It is possible that the fine-grained cuttings from this well show a trend normally masked by the stronger signature of the coarse-grained drill cuttings. Consequently, nanoporosity may have a larger role in the system than previously thought.

This well produced oil from the Lodgepole Formation for a short time but was quickly deemed uneconomic and abandoned (oil and gas well licence 4859). The RVS results indicate little hydrocarbon liquids in the Lodgepole Formation and a high water content. The low toluene/benzene ratios do not support upward migration of oil to supply this small oil accumulation, suggesting oil migration in the Lodgepole Formation of this area is driven by lateral fluid flow along porous Mississippian strata. This supports the model of local stratigraphic trapping of hydrocarbons (Klassen, 1996). The high hydrocarbon gas volumes are unexpected and may be an artifact of the smaller drill cuttings and preservation of nanoporosity.

Discussion

Helium

A comparison of all the volatile profiles indicates that the well at 9-6-2-26W1 has the most prospective helium profile, with helium values never going below a baseline or falling below detection and consistently being high, particularly from the Deadwood to Winnipegosis formations. This may indicate that helium can migrate through the entire studied section. The 1-25-4-23W1 well is the only well with a sample from the Lodgepole Formation, providing insight farther upsection. The results suggest that there is helium throughout the system below the Lodgepole Formation, but the helium values drop to below detection above the Bakken Formation. This may indicate that the Bakken Formation serves as break in the regional helium cap, and that any helium present above is driven by a different helium system. Analysis results reported in Nicolas (2018) also indicate very low to no helium in the Lodgepole Formation, but they also showed the helium system returns higher in the section in the Mission Canyon and Amaranth formations. Testing farther upsection, throughout the Mississippian strata and beyond, could help better understand the relationship—if any exists—between the lower Paleozoic strata and the Mississippian and above strata.

The presence of helium throughout the sampled sections in all the wells is interesting, as several sealing units are present, and the volume of helium required to infiltrate a section several hundred metres thick over a vast area is substantial. This points to a complex helium system affected by both horizontal and vertical migration. The consistent occurrence of helium in the Red River and Winnipeg formations, as seen in RVS logs and gas analyses, suggests local generation of helium from a deeper widespread source, such as the Precambrian basement. Radioactive decay within the granitic basement results in the upward diffusion of gases into the porous Winnipeg and Red River formations and they are sealed locally by tight mudstone and anhydrite in the upper parts of the section. All the profiles for the Winnipeg Formation show a high water content, which may be related to the porous and permeable nature of the interbedded sand units within the formation. This would therefore affect the ability of the helium to accumulate within the lower Winnipeg Formation; the helium would be forced to diffuse out and upsection to the Red River Formation, which supports the presence of overall higher helium values in this formation.

In comparison, the seemingly random nature of the high helium occurrences and peaks above the Red River Formation suggests a more complex system, with influences from a combination of stratigraphic factors, porosity variations, structural elements and fracture networks (and faults?). These seemingly random accumulations occur most often in the Dawson Bay to Duperow formations—this corresponds to an approximately 300 m thick interval with helium prospectivity in the Devonian section.

Thick evaporitic units are considered the best seals for helium, and the only well in this study with a thick section of salt preserved is at 16-29-12-29W1. Interestingly, this is also the only well to have a strong helium system break, just below the Prairie Evaporite. The presence of the Prairie Evaporite may therefore play an important role in the helium system, not only from a sealing perspective, but also from a structural perspective. When the Prairie Evaporite is absent, there is evidence for multistage dissolution upsection, and extensive fracture networks both above and below, which are responsible for the enhanced water flow needed to dissolve the thick halite package. It is no coincidence that the preferential dissolution of the Prairie Evaporite follows the SBZ; this Precambrian crustal suture has caused Phanerozoic-aged faulting, fracturing and stratal disturbances, both syn- and postdeposition (e.g., McCabe, 1959; Dietrich and Bezys, 1998; Nicolas, 2012; Nicolas and Yang, 2022).

Nicolas (2018) indicated that the Bakken Formation may be both a source (upper shale member) and reservoir (middle sandstone member) for helium. The Upper Member of the Bakken Formation is a highly organic shale often with a high gamma-ray signature on geophysical logs. There is variability in the gamma-ray readings on logs, from being high (>250 API) to low (<100 API), that has been shown to be related to the geographic location within the basin (Nicolas, 2012). In this study, the well at 9-6-2-26W1 has a very high gamma-ray response (>350 API) with a corresponding high helium value (0.27 nmol), the well at 16-29-12-29W1 has a high gamma-ray response (~300 API) with a moderate helium value (0.18 nmol), and the well at 1-25-4-23W1 has a lower gamma-ray response (~100 API) and low helium value (~0.01 nmol). It is uncertain whether there is a predictive correlation between the gamma-ray signature of the Bakken Formation and the helium values. With the limited data from this study, this is more of an observation, but is worth tracking to see if the helium self-sourcing ability of the Bakken Formation is related to its gamma-ray signature, which indicates the radioactive decay of the shale and subsequent contribution of helium to the system.

Since 2023, core studies at AHS have further reinforced the theory that rock properties exert a strong control on the helium retained in the rock sample. This study supports this theory as seen in the volatile profiles, where trends in helium-rich zones are similar in all of the wells. Smith et al. (2023, 2024) show further evidence that the residual helium in the rock samples can be quantitatively related to the helium that would be observed in a gas test. Although most RVS studies were conducted on core samples, using this information to extrapolate to drill cuttings and calibrate the RVS results to compensate for the size of the drill cuttings would be a useful tool when evaluating newer wells. Helium is present in the 1-25-4-23W1 drill cuttings, despite absolute abundances being significantly less than those observed in the other two wells, and the well being drilled with newer technology drill bits. The data support that this is likely an artefact of sample type and not the true helium concentrations in the subsurface.

Hydrocarbons

The hydrocarbon story for these wells is also interesting. The well at 1-25-4-23W1 produced oil from the Lodgepole Formation, whereas DSTs at the other wells showed no oil. However, the liquid hydrocarbon volumes on the profiles indicate that

- the 9-6-2-26W1 well has a strong signature in the Burr Member of the Dawson Bay Formation;
- the 16-29-12-29W1 well has a strong signature from the Hatfield Member of the Souris River Formation to the middle Wymark Member of the Duperow Formation; and
- the 1-25-4-23W1 well has a strong signature in the upper Dawson Bay Formation to the base of the Bakken Formation.

All these zones, which are located in stratigraphic intervals below the current oil-producing horizons in Manitoba, may represent unexplored hydrocarbon reservoirs that have not been adequately tested. The petroleum technical well file for 1-25-4-23W1 indicates a live oil show within the Dawson Bay Formation (oil and gas well licence 4859). Although the presence of economic accumulations of oil may or may not be present, at a minimum, the toluene/benzene profiles indicate oil migrating through the system in all these wells. Notably, the 16-29-12-29W1 well has the highest liquid hydrocarbon volumes in combination with anomalously high toluene/benzene values, when compared to the same section in the other wells, indicating an active hydrocarbon system through the Souris River and Duperow formations in this area.

Future work and recommendations

Future work with this project will include sampling neighbouring wells that have been drilled with different technologies to make a series of direct comparisons on RVS signatures. This will also allow for the potential tracking of shallower sealing features.

Although not currently part of the immediate scope, recommended work includes sampling through the Mississippian up to the lower Jurassic to further understand the helium system above the Bakken Formation. Sampling wells within active oil fields, as well as far away from the oil field system (east of Rge. 20W1 and north of Twp. 17), would provide a broader context for the regional helium migration patterns and their relationship to structural controls.

Economic considerations

The RVS data from three Manitoba wells indicate a considerable untapped potential, including significant helium presence in the deeper subsurface of southwestern Manitoba. Since these helium shows are not associated with large producing oil and gas pools, helium produced from these zones would be classified as green helium, making it a highly attractive target for investment and exploration, particularly in the growing market for environmentally sustainable resources. The RVS data also show indicators of active hydrocarbon systems in unexplored horizons that are deeper than the current oil-producing horizons in Manitoba, offering an additional upside, thus positioning the region for resource development.

Acknowledgments

The authors would like to thank M. Yurkowski from the Saskatchewan Geological Survey for her good discussions and insights into the helium systems in the Williston Basin. P. Fulton-Regula and P. Fraino are also acknowledged for their critical review of this report.

References

Dietrich, J.R. and Bezys, R.K. 1998: Basement-sedimentary cover relationships along the Churchill-Superior Boundary Zone, southwestern Manitoba; *in* Eighth International Williston Basin Symposium, J.E. Christopher, D.F. Gilboy, D.F. Paterson and S.L. Bend (ed.), Saskatchewan Geological Survey, Special Publication 13, p. 175.

Klassen, H.J. 1996: An overview of the regional geology and petroleum potential, Lodgepole Formation, southwestern Manitoba; Manitoba Energy and Mines, Petroleum and Energy Branch, Petroleum Open File POF 15-96, 42 p.

McCabe, H.R. 1959: Mississippian Stratigraphy of Manitoba; Manitoba Department of Mines and Natural Resources, Mines Branch, Winnipeg, Publication 58-1, 99 p.

Nicolas, M.P.B. 2012: Stratigraphy and regional geology of the Late Devonian-Early Mississippian Three Forks Group, southwestern Manitoba (NTS 62F, part of 62G, K); Manitoba Innovation, Energy and Mines, Manitoba Geological Survey, Geoscientific Report GR2012-3, 92 p.

Nicolas, M.P.B. 2018: Summary of helium occurrences in southwestern Manitoba; *in* Report of Activities 2018, Manitoba Growth, Enterprise and Trade, Manitoba Geological Survey, p. 110–118.

Nicolas, M.P.B. 2023: Manitoba's designated oil fields and pools 2023; Manitoba Economic Development, Investment and Trade, Manitoba Geological Survey, URL <https://manitoba.ca/iem/petroleum/f_p_codes/poolbook_2023.pdf> [October 2024].

Nicolas, M.P.B. and Yang, C. 2022: Stratigraphy and distribution of the potash-bearing members of the Devonian Prairie Evaporite, southwestern Manitoba (parts of NTS 62F, K); *in* Report of Activities 2022, Manitoba Natural Resources and Resource Development, Manitoba Geological Survey, p. 87–95.

Nicolas, M.P.B., Matile, G.L.D., Keller, G.R. and Bamburak, J.D. 2010: Phanerozoic geology of southern Manitoba; Manitoba Innovation, Energy and Mines, Manitoba Geological Survey, Stratigraphic Map SM2010-1, 2 sheets, scale 1:600 000.

Nicolas, M.P.B., Smith, C.M. and Smith, M.P. 2023a: Rock Volatiles Stratigraphy data from drill cuttings from three oil wells in southwestern Manitoba (parts of NTS 62F2, K3); Manitoba Economic Development, Investment, Trade and Natural Resources, Manitoba Geological Survey, Data Repository Item DRI2023014, Microsoft® Excel® file.

Nicolas, M.P.B., Smith, C.M. and Smith, M.P. 2023b: Volatiles analysis of drill cuttings to evaluate the helium prospectivity of southwestern Manitoba (parts of NTS 62F2, K3); *in* Report of Activities 2023, Manitoba Economic Development, Investment, Trade and Natural Resources, Manitoba Geological Survey, p. 93–104.

Nicolas, M.P.B., Smith, C.M. and Smith, M.P. 2024: Rock Volatiles Stratigraphy data from drill cuttings from four oil wells in southwestern Manitoba (parts of NTS 62F2, K3); Manitoba Economic Development, Investment, Trade and Natural Resources, Manitoba Geological Survey, Data Repository Item DRI2024008, Microsoft® Excel® file.

Smith, C.M., Gordon, P.S., Smith, T.M. and Smith, M.P. 2024: Advanced novel analysis of helium in legacy cores from nine wells having known helium contents: an attempt to develop a helium exploration and production tool; Canadian Energy Geoscience Association–Canadian Society of Exploration Geophysicists, Annual Convention (GeoConvention 2024), June 17–19, 2024, Calgary, Alberta, abstract, URL <https://geoconvention.com/wp-content/uploads/abstracts/2024/107588-advanced-novel-analyses-of-helium-in-legacy-cores.pdf> [September 2024].

Smith, C., Smith, M.P., Gordon, P.S., Smith, T.M., Flynn, J., Kohlruss, D. and Yurkowski, M.M. 2023: Understanding the subsurface helium system of Saskatchewan with a focus on traps/seals via volatiles analysis of helium and other compounds in legacy cores; *in* The Rocky Mountain Association of Geologists, North American Helium Conference, Program Book, March 22–23, 2023, Westminster, Colorado, p. 50–51.

Smith, C.M., Smith, M., Gordon, P., Smith, T., Flynn, J., Priddell, T. and Yurkowski, M. 2022: Rock volatiles analyses of the B.A. Saskatchewan Landing Core — detailed fluid, reservoir, and cap rock insights from the C1-C10 hydrocarbons, organic acids, CO_2, formation water, helium, various sulfur gases, and mechanical strength: implications for helium system analysis; *in* Twenty-Ninth Williston Basin Petroleum Conference, Dr. Don Kent Core Workshop Volume, Saskatchewan Geological Society, Special Publication No. 27, p. 1–9.

GS2024-19

Geologic hydrogen in the Williston and Hudson Bay basins, southwestern and northeastern Manitoba (parts of NTS 53, 54, 62, 63)

by M.P.B. Nicolas

In Brief:

- Manitoba has the right geological conditions to support an active hydrogen system
- Hydrogen generation by radiolysis and rock-water interactions are the dominant sources, with potential in both basins

Citation:
Nicolas, M.P.B. 2024: Geologic hydrogen in the Williston and Hudson Bay basins, southwestern and northeastern Manitoba (parts of NTS 53, 54, 62, 63); *in* Report of Activities 2024, Manitoba Economic Development, Investment, Trade and Natural Resources, Manitoba Geological Survey, p. 164–171.

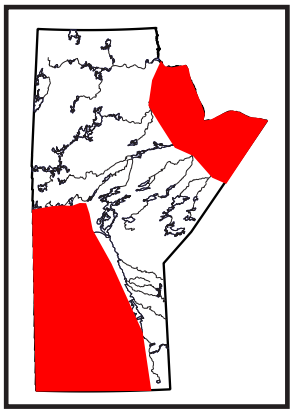
Summary

Geologic hydrogen, also referred to as white, gold, natural or free hydrogen, is formed by natural processes and can occur in potentially economic accumulations in the subsurface but has been largely overlooked as a resource. This reconnaissance study focused on hydrogen potential within the sedimentary strata of the Williston and Hudson Bay basins. Geologic hydrogen is formed by several reactions, including radiolysis and rock-water interactions related to serpentinization and iron oxidation of Precambrian rocks—with serpentinization theorized to be the best source of geologic hydrogen. Potential Precambrian hydrogen generation sources were identified by mapping drillholes reported to have basement lithologies with the potential to generate hydrogen from a rock-water interaction. To further define the area of these potential sources, the drillholes were mapped in combination with total field magnetic anomaly data. A compilation of gas analyses results from government petroleum technical well files indicated very low concentrations of hydrogen, with only 10 analyses having hydrogen concentrations of >1 mol. % and two of those with values of ~8 mol. %. The highest values come from wells producing from the Bakken Formation, suggesting the high values may be the product of radiolysis, a result of the radioactive decay of the highly organic shale. These occurrences of low hydrogen concentrations and prejudice in overlooking hydrogen during gas analyses in the past have resulted in potential reporting errors, and may have resulted in bypassing occurrences.

Introduction

Hydrogen, the first element in the periodic table, is an odourless, colourless, highly reactive, mobile and light element that occurs as the molecule H_2 in gas form. Geologic hydrogen, also referred to as white, gold, natural or free hydrogen, is formed by natural processes and can occur in potentially economic accumulations in the subsurface, although its use as a naturally occurring clean fuel resource has been largely overlooked until recently. As a chemical, hydrogen is used in many industrial applications, such as ammonia production and hydrocarbon refining, and is an important clean fuel in space rockets and other propulsion systems (Sukumaran, 2024).

The reactivity and diffusibility of hydrogen has led to the belief that economic accumulations are not possible. In the geological environment, hydrogen is formed as a byproduct of several reactions, including rock-water interactions (e.g., the oxidation of Fe^{2+}-bearing minerals and serpentinization of ultramafic rocks), weathering, decomposition of organic matter and natural water hydrolysis (Lin et al., 2005; Warr et al., 2019). The development of geological models to better understand these hydrogen systems and how the models can be used to predict its viability as a reliable resource and its economic boundaries is still in its infancy. The determination of an economic threshold for hydrogen production from the subsurface is ambiguous, but with an increasing demand for clean hydrogen fuel, these limits are being studied.



In order to understand the geologic hydrogen system in strata of the Williston and Hudson Bay basins in Manitoba, potential bedrock sources of hydrogen were identified and oil and gas wells with reported concentrations of hydrogen were reviewed.

Geological models

As a foundation, lessons can be learned by applying the concepts and methodologies used for petroleum exploration in sedimentary basins to exploring for geologic hydrogen, such as identifying a significant source, migration pathways, porous reservoirs and tight seals. Sedimentary basins, including the Williston Basin, have a long history of oil and gas exploration and production, therefore, there is a good understanding of the migration-reservoir-seal systems in this basin. The challenge is in identifying a significant hydrogen source.

Jackson et al. (2024) indicated that the most efficient hydrogen generator in the geological environment is serpentinization, but other popular generators being considered are iron-rich rock–water interactions and radiolysis, where water is decomposed by natural radiation. In Manitoba, the best geological setting for these processes to occur are in the Canadian Shield, particularly in greenstone belts, which form the complex fabric of the Precambrian basement of the Williston Basin.

Radiolysis

The natural radioactive decay of uranium, thorium and potassium will breakdown water to form helium and hydrogen, with large accumulations taking hundreds of millions of years to form (Broadhead, 2005). Based on the radiolysis formation model, the areas of helium potential discussed in Nicolas (2018) and Nicolas et al. (2023, 2024) would also be areas of potential for geologic hydrogen. The helium atom is smaller than the hydrogen molecule, making any seal tight enough to trap helium also sufficient to trap hydrogen thus allowing it to accumulate, notwithstanding the reactivity of hydrogen. In Manitoba, granitic basement rocks and highly radioactive shales would be the best geological environments to produce hydrogen by radiolysis.

Rock-water interactions

Serpentinization is seen as the most effective process for hydrogen production but it requires metamorphic conditions of between 200 and 300 °C and higher pressures than those seen in most undeformed sedimentary basins. Therefore, any hydrogen found within these sedimentary basins must have migrated into the strata from deeper sources. Hydrogen generation by serpentinization is geologically instantaneous, occurring over hundreds of thousands to one million years (Rüpke and Hasenclever, 2017). At points in the past, Precambrian greenstone belts within continental crust have been exposed to these conditions and likely contain enough remnant olivine to activate serpentinization at a later date via deep groundwater circulating through old and reactivated faults and fractures (Jackson et al., 2024). Through these processes, hydrogen generation can occur anew, initially migrating in an aqueous phase, followed by the upward migration in a gas phase to be trapped in the porous sedimentary strata above. Exsolution of hydrogen into a gas-rich phase would occur as the pressure and temperature decreases.

Oxidation of iron-rich rocks in the Precambrian basement is another source of hydrogen but with lower yields than that from serpentinization (Jackson et al., 2024). Iron formations are the best target in this case, but other iron-rich sulphide deposits are not to be discounted, including Mississippi Valley–type (MVT) deposits within the sedimentary strata.

Hydrogen sources

Identifying local sources of hydrogen is an important step in evaluating the hydrogen potential of a region. This can be done by identifying where rock types most likely to generate hydrogen would occur. For this study, a digital compilation of all the drillholes that penetrated the Precambrian in Manitoba prior to 2013 (McGregor, 2013) was reviewed. This compilation includes core and drill cuttings descriptions from industry and government reports. These descriptions were filtered for the following keywords: serpentinized (including serpentine), iron (iron formation, iron sulphide, iron-rich), olivine and ultramafic (including dunite, peridotite, komatiite). From this, a subset of drillholes—and potential hydrogen generating sites—emerged (Figures GS2024-19-1, -2).

Williston Basin

The first obvious trend in the Williston Basin (Figure GS2024-19-1) is the overall higher density of drillhole occurrences in the northwestern part of the map area; this is directly related to the mineral exploration drilling where the Phanerozoic cover is relatively thin. In the northwestern area, there are two separate high-density clusters: an east-west cluster along the northern basin edge resulting from exploration programs related to the sub-Phanerozoic extension of the metalliferous Flin Flon domain and its greenstone belts, and a northeast-southwest cluster related to the sub-Phanerozoic extension of the Thompson nickel belt and the Superior boundary zone (SBZ).

Given the abundance of iron-bearing units, sulphides and serpentinized units in the northern region, natural hydrogen is likely to have been generated but dissipated long ago. It is more likely that recent hydrogen generation would come from oxidation of iron formations. The Phanerozoic cover is fairly thin, well jointed and often karsted, suggesting that any natural hydrogen would degas to surface and not accumulate, although it is not unheard of to have gases trapped at shallow depths. Using the helium system as a model, a minimum depth of approximately 500 m (Broadhead, 2005) would be a preferred depth to ensure higher reservoir pressures for better trapping and economic accumulation.

Even though the southern half of the map has markedly less data points, some faint patterns do emerge. The Uchi, Bird River and Winnipeg River domains show the highest occurrences of drillholes with lithology keywords, in addition to an interesting occurrence of serpentine/serpentinized occurrences near or along these domain boundaries, as well as the SBZ. These crustal domain junctions are known to cause faulting and fracturing in the strata above and enhance fluid flow. The large crustal suture of the SBZ—the most significant sub-Phanerozoic Precambrian feature in the Williston Basin in Manitoba—is responsible for the development of the oil fields in the south, and has numerous documented faults and fractures and stratal disturbances (McCabe, 1959; Bezys et al., 1996, 1997; Dietrich and Bezys, 1998; Nicolas, 2012). Post-basin–formation hydrothermal systems and large networks of saline water fractures have also been documented; these create the much-needed deep migration pathways required to tap into ancient networks and deep fluids.

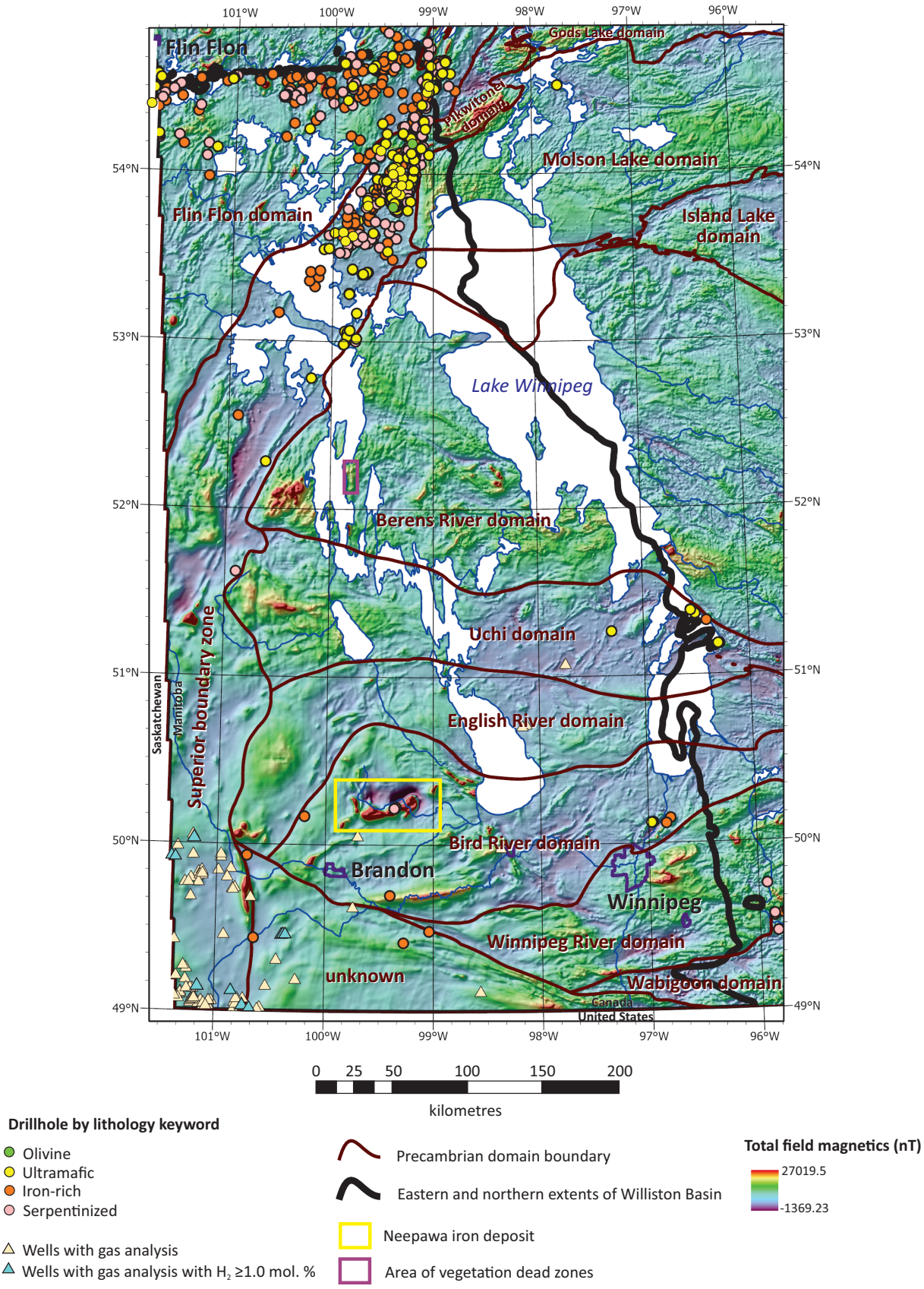


Figure GS2024-19-1: *Shaded total field magnetic anomaly map of the Williston Basin in southwestern Manitoba (Manitoba Economic Development, Investment, Trade and Natural Resources, 2024a) showing the Precambrian domain boundaries as drawn by McGregor (2013), and the distribution of drillholes with records that included the following lithology keywords (from McGregor, 2013): serpentinized (including serpentine), iron (including iron formation, iron sulphide, iron-rich), olivine and ultramafic (including dunite, peridotite, komatiite). Abbreviation: nT, nanotesla.*

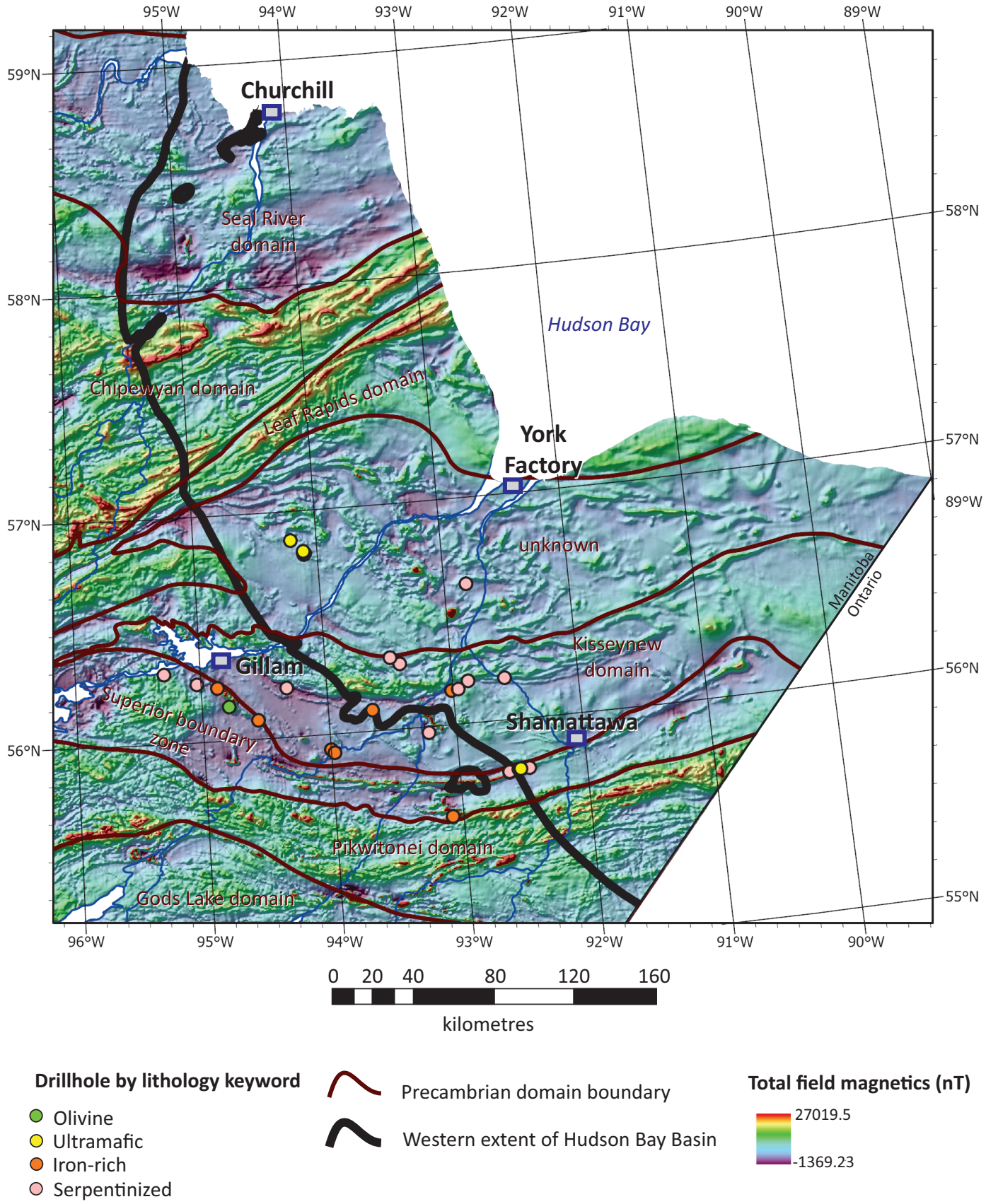


Figure GS2024-19-2: *Shaded total field magnetic anomaly map of the Hudson Bay Basin in northeastern Manitoba (Manitoba Economic Development, Investment, Trade and Natural Resources, 2024a) showing the Precambrian domain boundaries as drawn by McGregor (2013), and the distribution of drillholes with records that included the following lithology keywords (from McGregor, 2013): serpentinized (including serpentine), iron (including iron formation, iron sulphide, iron-rich), olivine and ultramafic (including dunite, peridotite, komatiite). Abbreviation: nT, nanotesla.*

The abundance of documented occurrences of serpentinized rocks points to the possibility of renewed serpentinization within the SBZ at depth, invigorated by hot and warm hydrothermal systems (Bezys et al., 1997; Grasby et al., 2009). Considering these theories, the SBZ and areas around crustal domain boundaries would serve as the best potential natural hydrogen sources and pathways. The migration through a network of pores, fractures and faults into the sedimentary strata above, with its porous reservoirs and multiple sealing units, provide for the rest of the hydrogen system requirements.

Overlying the drillholes with lithology keywords on a total field magnetic anomaly map, single sites (drillholes) become much larger source areas. High magnetic values would align with most of the rock types selected by the lithology search and likely correlate to sub-Phanerozoic greenstone belts, as expected, but would also show broader areas of high magnetic susceptibility, such as iron formations. The best example of this is the iron formation occurrence around the town of Neepawa (Figure GS2024-19-1) in Twp. 14 to 15, Rge. 13 to 16, W 1st Mer., which not only has a documented iron deposit but also has a strong magnetic signature outlining the area. From an iron-oxidation play perspective, this could serve as a large natural hydrogen point source. Despite the theorized low hydrogen yield by oxidation reactions, the size of the iron deposit and the time factor (up to 450 million years) favour its potential for hydrogen production. Drilling records for three wells drilled into this deposit do not mention any gas kicks while drilling but do mention several very porous horizons encountered in the Paleozoic section above the deposit (oil and gas well licence 1, Manitoba Economic Development, Investment, Trade and Natural Resources, Winnipeg).

Hudson Bay Basin

The lithological keyword search turned up a few favourable drillholes in a concentrated area of the onshore portion of the Hudson Bay Basin (i.e., the Hudson Bay Lowland; Figure GS2024-19-2). The dominant lithologies identified were iron formations and serpentinized rocks. In the sub-Phanerozoic cover, many of these lithological occurrences are clustered along the edges of the SBZ and the Kisseynew domain, or along major magnetic changes. All lithologies in question were from drillholes that had a Phanerozoic thickness of less than 115 m, meaning that any residual hydrogen released from rock-water interactions would have quickly dissipated to the atmosphere due to a lack of sealing units in the strata above. However, due to the scarcity of exploration drillholes in the Hudson Bay Lowland, including the northeastern extension of the SBZ and Kisseynew domain, more hydrogen-generating lithologies may occur below the Phanerozoic cover, with the thicker sedimentary strata providing more storage space and potential sealing units (Nicolas et al., 2024). Sources for hydrogen in the Hudson Bay Basin in Manitoba could also be from radiolysis of uranium-, thorium- and potassium-bearing bedrock, analogous to the helium system in the Williston Basin, and would be more likely to occur in the northeast where the strata is thicker.

Evidence for hydrogen occurrences

Documented natural hydrogen occurrences are rare and historically did not garner any interest thus finding historical records that mention hydrogen is challenging. This historical disinterest in natural hydrogen caused a prejudice in the way gas samples were collected and analyzed (Zgonnik, 2020). Unless a sample was expected to contain high hydrogen concentrations, the analytical method of gas chromatography commonly used hydrogen as the carrier gas thus hydrogen could not be detected in the sample (Zgonnik, 2020). Hydrogen only becomes more noticeable and noteworthy when concentrations exceed 10% by volume and it becomes flammable (Zgonnik, 2020).

Hydrogen occurrences in the subsurface can only be identified through a gas analysis test, but as mentioned above, the gas chromatography methods used are usually biased against hydrogen. Gas analysis conducted on samples from subsurface fluids is done through drillstem tests, or sampling at the wellhead or battery site. There are 101 gas analyses reported in Manitoba's petroleum technical well files for the Williston Basin, many of which have hydrogen measured (Manitoba Economic Development, Investment, Trade and Natural Resources, 2024b; Nicolas, 2024[1]); there are no gas analyses available for wells in the Hudson Bay Basin. Most gas analyses reported trace to very low hydrogen concentrations. These low concentrations were affected by sample flushing and by the hydrogen reacting readily with hydrocarbons (Hand, 2023) as these analyses were generally run on hydrocarbon-rich samples. Only 10 wells reported hydrogen values of >1 mol. %, with three of those having higher than average values (L.S. 13, Sec. 26, Twp. 12, Rge. 28, W 1st Mer. [abbreviated 13-26-12-28W1], 5-20-11-29W1 and 6-20-11-29W1, with values of 8.49, 3.28 and 7.99 mol. %, respectively); all of these wells were producing from the Middle Member of the Mississippian Bakken Formation. The Bakken Formation has been identified as a potential helium source due to its radioactive highly organic shale beds (Nicolas, 2018; Nicolas et al., 2023, 2024), therefore, it may be possible that the hydrogen measured here is a product of radiolysis. Whether these higher concentrations are a function of residual hydrogen from the flushing process in the gas chamber, or they are representative of naturally occurring hydrogen, it is uncertain, since other gas analyses of samples from the Bakken Formation do not show such high concentrations. All three of these gas analyses come from wells located around Twp. 11 to 12, Rge. 28 to 29W1, coinciding with the Kirkella Field, an area

[1] MGS Data Repository Item DRI2024012, containing the data or other information sources used to compile this map/report, is available online to download free of charge at https://manitoba.ca/iem/info/library/downloads/index.html, or on request from minesinfo@gov.mb.ca, or by contacting the Resource Centre, Manitoba Economic Development, Investment, Trade and Natural Resources, 360-1395 Ellice Avenue, Winnipeg, Manitoba R3G 3P2, Canada.

known for structural disturbances and high helium occurrences (Nicolas, 2018; Nicolas et al., 2023, 2024). The other seven analyses with >1 mol. % hydrogen occur in the Mississippian Mission Canyon Formation and Virden Member of the Lodgepole Formation in the Pierson, Waskada and Souris Hartney oil fields. The Waskada and Souris Hartney oil fields, like the Kirkella Field, are also known for their complex structural disturbances, including multistage salt collapse caused by fluid movement through deep fracture systems. In particular, the Waskada Field falls along the eastern boundary of the SBZ suggesting the deep fractures that penetrate to the Precambrian basement are the result of lithospheric flexure along this large crustal suture. These deep fractures provide the ideal scenario for hydrogen generated in the Precambrian to move upward into the sedimentary strata.

Hydrogen dead zones

Surface seeps of hydrogen have been documented worldwide, many of them referred to as eternal fires (Zgonnik, 2020; Sukumaran, 2024). When hydrogen occurs below ignition concentrations (below 10% by volume), vegetation dead zones—also known as fairy circles—can occur around surficial hydrogen seeps. Searching for hydrogen from the 'top-down' requires looking for the presence of fairy circles, then investigating the subsurface for the source—a common hydrogen exploration method.

In Manitoba, there are recorded circular vegetation dead zones that occur on the east side of Lake Winnipegosis, across the lake from Duck Bay (Figure GS2024-19-1). D. Berk (pers. comm., 2008) showed the author photos of these dead zones, which occurred on his mineral exploration mining claim; the assessment file for this claim includes mention of "vegetation dead or kill zones" (Assessment File 74929, Manitoba Economic Development, Investment, Trade and Natural Resources, Winnipeg). The assessment file for this claim also mentions faulting and bedrock movement and includes results from a soil gas hydrocarbon geochemistry survey. There was no mention of hydrogen in the results or discussion, but the presence at depth of a volcanogenic massive-sulphide (VMS) deposit was suggested; a theory that is also supported by the results of a magnetic geophysical survey. Unfortunately, there was no deep drill program executed on this claim to verify the presence of VMS deposits at depth, or MVT deposits or kimberlites–which were also a consideration. On the mining claim site, significant bedrock disturbances were observed, including brecciated carbonate units with a blue-grey clay matrix and zebra-textured dolomite (similar to hydrothermal dolomite) in vertical fractures (D. Berk, pers. comm., 2008). This all suggests that there were fluids moving through the system in the past. The fact that there are vegetation dead zones in modern day, suggests ongoing processes. Although it is uncertain if hydrogen degassing is the cause, it should not be too quickly discounted as a possibility without thorough investigation. If buried iron-rich deposits are not the source, then perhaps investigating kimberlite intrusions as the source is worthwhile, as these intrusions, which can have the correct metamorphic conditions for serpentinization, can release high volumes of hydrogen (Zgonnik, 2020).

Hydrogen production of the future

Zgonnik (2020) lists several locations worldwide that have hydrogen production directly from Precambrian wells. This brings to question the opportunity for hydrogen production in Manitoba directly from Precambrian wells, either collared directly on the Precambrian shield rocks or through the Phanerozoic sequence of the Williston and Hudson Bay basins. The benefit of the sedimentary basin is the extra space to migrate and store hydrogen long term in porous sedimentary reservoirs. Storage of hydrogen, over the long term, can include a porous reservoir with a good seal, but recent work by Truche et al. (2018) suggests hydrogen may be adsorbed onto water-saturated clays and trapped below the surface, a theory Yurkowski et al. (2024) is investigating in Saskatchewan. These clay alteration haloes over hydrogen-producing deposits may be an important play type to consider in the future (Truche et al., 2018).

Future recommendations

Currently industry is not exploring for geologic hydrogen in Manitoba; however, it is clear that exploration opportunities do exist. Future gas analyses conducted on fluids from oil and gas wells (through drillstem tests or sampling at the wellhead or battery site) should consider testing for hydrogen to ensure accurate results going forward. Current exploration for helium in deeper horizons than those accessed for oil and gas production may yield insights into the potential for deeper hydrogen resources in the short term. Known deep-sourced fluids in the Phanerozoic cover could be potential conduits for hydrogen generated by serpentinization or iron oxidation, with migration and entrapment opportunities nearby.

Outside of the sedimentary basins, exploration into the Precambrian shield is also a possibility, with some successes reported globally (Zgonnik, 2020). Artificial intelligence and optical character recognition methods applied to mineral exploration assessment files may assist in this venture, as there may be records of hydrogen gas pockets encountered during drilling programs or hydrogen seeps observed in mine workings.

Economic considerations

Hydrogen is a clean-burning fuel and is seen as an important energy source for the future. As hydrogen has been overlooked throughout history, geologic hydrogen systems are poorly characterized and the understanding of the mechanisms of formation is still mostly theoretical—much work is still needed. Once the economic potential of geologic hydrogen is fully understood, it will revolutionize the energy sector. However, until such time, purposeful and mindful observations of hydrogen occurrences is important, no matter how low or high the concentrations.

Occurrences of hydrogen in gas analyses from oil and gas wells in Manitoba are very low, but this may be a result of analytical blindless to hydrogen and is not indicative of any hydrogen anomalies. Gas analyses of samples from nonhydrocarbon-bearing strata are required to verify for hydrogen; such tests are more likely to come from future green helium test wells, or perhaps hydrogen test wells.

Even though there are no clear indications of accumulated hydrogen in Manitoba records, the Precambrian basement rocks underlying the Williston Basin strata do have the right lithologies to form hydrogen under the right conditions. The Hudson Bay Basin hydrogen potential is not well constrained due to lack of data, but should not be discounted. Overall, Manitoba has good potential to support a hydrogen system, as it has good potential sources, migration pathways, reservoirs and seals required for accumulations.

Acknowledgments

The author would like to thank S. Bergen from the University of Manitoba for her assistance in compiling the gas compositions, M.M. Nicolas from the University of Manitoba for her library support, and M. Yurkowski from the Saskatchewan Geological Survey for her good discussions and innovative research. C. Couëslan and E. Enaworu are acknowledged for their critical review of this report.

References

Bezys, R.K., Fedikow, M.A.F., Bamburak, J.D. and Abercrombie, H.J. 1997: Geological setting of Prairie-type Au mineralization, Mafeking Quarry, west central Manitoba 1996 work (NTS 63C); Manitoba Energy and Mines, Preliminary Map 1997P-1, scale 1:5000.

Bezys, R.K., Fedikow, M.A.F. and Kjarsgaard, B.A. 1996: Evidence of Cretaceous(?) volcanism along the Churchill-Superior boundary zone, Manitoba (NTS 63G/4); *in* Report of Activities 1996, Manitoba Energy and Mines, Minerals Division, p. 122–126.

Broadhead, R. 2005: Helium in New Mexico - geologic distribution, resource demand, and exploration possibilities; New Mexico Geology, v. 27, p. 93–101.

Dietrich, J.R. and Bezys, R.K. 1998: Basement-sedimentary cover relationships along the Churchill-Superior boundary zone, southwestern Manitoba; Eighth International Williston Basin Symposium, October 19–21, 1998, Regina, Saskatchewan, abstract, p. 175.

Grasby, S.E., Bezys, R.K. and Beauchamp, B. 2009: Silica chimneys formed by low-temperature brine spring discharge; Astrobiology, v. 9, p. 931–941.

Hand, E. 2023: Hidden hydrogen; Science, v. 379, p. 630–636.

Jackson, O., Lawrence, S.R., Hutchinson, I.P., Stocks, A.E., Barnicoat, A.C. and Powney, M. 2024: Natural hydrogen: sources, systems and exploration plays; Geoenergy, v. 2, p. 1–9.

Lin, L.H., Slater, G.F., Sherwood Lollar, B., Lacrampe-Couloume, G. and Onstott, T.C. 2005: The yield and isotopic composition of radiolytic H_2, a potential energy source for the deep subsurface biosphere; Geochimica et Cosmochimica Acta, v. 69, p. 893–903.

Manitoba Economic Development, Investment, Trade and Natural Resources 2024a: Geoscience service; *in* GIS Map Gallery, Manitoba Economic Development, Investment, Trade and Natural Resources, Manitoba Geological Survey, URL <https://rdmaps.gov.mb.ca/Html5Viewer/index.html?viewer=MapGallery_Geology.MapGallery> [September 2024].

Manitoba Economic Development, Investment, Trade and Natural Resources 2024b: Petroleum technical well files; *in* GIS Map Gallery, Manitoba Economic Development, Investment, Trade and Natural Resources, Mining, Oil and Gas Branch, URL <https://manitoba.ca/iem/petroleum/gis/technical.html> [September 2024].

McCabe, H.R. 1959: Mississippian stratigraphy of Manitoba; Manitoba Mines and Natural Resources, Mines Branch, Publication 58-1, 99 p.

McGregor, C.R. 2013: Digital compilation of sub-Phanerozoic Precambrian geology in Manitoba; Manitoba Innovation, Energy and Mines, Manitoba Geological Survey, Open File Report OF2012-2, DVD-ROM.

Nicolas, M.P.B. 2012: Stratigraphy and regional geology of the Late Devonian-Early Mississippian Three Forks Group, southwestern Manitoba (NTS 62F, part of 62G, K); Manitoba Innovation, Energy and Mines, Manitoba Geological Survey, Geoscientific Report GR2012-3, 92 p.

Nicolas, M.P.B. 2018: Summary of helium occurrences in southwestern Manitoba; *in* Report of Activities 2018, Manitoba Growth, Enterprise and Trade, Manitoba Geological Survey, p. 110–118.

Nicolas, M.P.B. 2024: Compilation of gas compositions from oil and gas wells in southwestern Manitoba (NTS 62G12, 62K3, parts of 62F); Manitoba Economic Development, Investment, Trade and Natural Resources, Manitoba Geological Survey, Data Repository Item DRI2024012, Microsoft® Excel® file.

Nicolas, M.P.B., Smith, C.M. and Smith, M.P. 2023: Volatiles analysis of drill cuttings to evaluate the helium prospectivity of southwestern Manitoba (parts of NTS 62F2, K3); *in* Report of Activities 2023, Manitoba Economic Development, Investment, Trade and Natural Resources, Manitoba Geological Survey, p. 93–104.

Nicolas, M.P.B., Smith, C.M. and Smith, M.P. 2024: Rock volatiles analysis of drill cuttings to evaluate the helium and hydrocarbon prospectivity of southwestern Manitoba (parts of NTS 62F2, K3); *in* Report of Activities 2024, Manitoba Economic Development, Investment, Trade and Natural Resources, Manitoba Geological Survey, p. 153–163.

Rüpke, L.H. and Hasenclever, J. 2017: Global rates of mantle serpentinization and H_2 production at oceanic transform faults in 3-D geodynamic models; Geophysical Research Letters, v. 44, p. 6726–6734.

Sukumaran, P.V. 2024: Geological hydrogen: a new carbon-free, clean energy vector; Journal of Geological Society of India, v. 100, no. 3, p. 447–450.

Truche, L., Joubert, G., Dargent, M., Martz, P., Cathelineau, M., Rigaudier, T. and Quirt, D. 2018: Clay minerals trap hydrogen in the Earth's crust: evidence from the Cigar Lake uranium deposit, Athabasca; Earth and Planetary Science Letters, v. 493, p. 186–197.

Warr, O., Giunta, T., Ballentine, C.J. and Sherwood Lollar, B. 2019: Mechanisms and rates of ^{4}He, ^{40}Ar, and H_2 production and accumulation in fracture fluids in Precambrian Shield environments; Chemical Geology, v. 530, art. 119322.

Yurkowski, M., Flynn, J., Gilbert, M., Bosman, S., Maxeiner, R. and Card, C. 2024: Hydrogen and helium: is there an analogue relationship in Saskatchewan's uranium deposits?; Canadian Energy Geoscience Association–Canadian Society of Exploration Geophysicists, Annual Convention (GeoConvention 2024), June 17–19, 2024, Calgary, Alberta, abstract, URL <https://geoconvention.com/wp-content/uploads/abstracts/2024/104290-saskatchewans-hydrogen-potential1.pdf> [September 2024].

Zgonnik, V. 2020: The occurrence and geoscience of natural hydrogen: a comprehensive review; Earth-Science Reviews, v. 203, p. 1–51.

GS2024-20

Pore space resource potential of the Paleozoic sequence in the Hudson Bay Basin, northeastern Manitoba (parts of NTS 53N, O, 54A–F, K, L)

by M.P.B. Nicolas

In Brief:

- Hudson Bay Lowland has potential for oil, helium, natural hydrogen and lithium brines, low enthalpy geothermal heat, but limited stratigraphic potential for geologic storage of CO_2
- Resource assessments are not available for these pore spaces resources, but should still be considered as a future opportunity in land-use planning

Citation:
Nicolas, M.P.B. 2024: Pore space resource potential of the Paleozoic sequence in the Hudson Bay Basin, northeastern Manitoba (parts of NTS 53N, O, 54A–F, K, L); *in* Report of Activities 2024, Manitoba Economic Development, Investment, Trade and Natural Resources, Manitoba Geological Survey, p. 172–180.

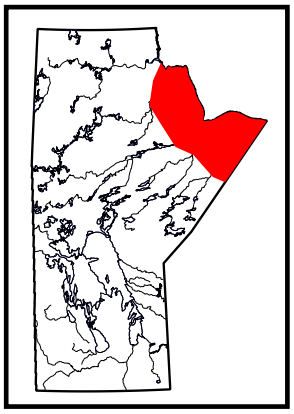
Summary

Exploration and studies conducted in the Hudson Bay Basin have been focused on hydrocarbons with no attention to other subsurface pore space resources and commodities. Commodities such as helium, geologic hydrogen and metal (lithium) brines, as well as resources such as carbon capture and storage and geothermal energy all have potential within this basin. Yet, the geological understanding of this large basin is insufficient to inform of their true potential for formal resource assessments. Despite this, datasets collected through multijurisdictional studies support an active hydrocarbon system in the Hudson Bay Basin, both offshore and onshore, and the potential for onshore oil accumulations in northeastern Manitoba is very good. Using the geological framework and models of the basin, predictions for other pore space resources can be deduced and there is considered to be good potential for accumulations of helium, geologic hydrogen and metal (lithium) brines. Furthermore, low enthalpy, localized geothermal heat is possible whereas deep geologic carbon storage is considered to be limited at this time.

Introduction

Pore space resource refers to a resource or commodity that is stored in and extracted from fluids within pore spaces of subsurface rocks, often within sedimentary basins. These resources can include hydrocarbons, dissolved metals, dissolved or exsolved gases, storage space and stored thermal energy. Historically, sedimentary basins are best known for their hydrocarbon resources, which has informed subsurface geological models. A societal shift in focus to reducing emissions, combined with the emergence of new commodity requirements, has prompted renewed geological evaluation and exploration of these sedimentary basins. Hydrocarbon-focused exploration, while still important, is now occurring in parallel with exploration for new commodities within the same sedimentary basins, but often in different strata and with different exploration models. Commodities such as helium, geologic hydrogen (also known as natural, white, gold or free hydrogen) and metal (lithium) brines are the focus of current exploration. These exploration activities are being informed by geological models and the fundamental knowledge used for oil exploration to inform new models and identify new exploration targets both within and outside of the usual oil fields. Commodifying pore space itself is at the forefront, with the rise in carbon capture and storage (CCS) projects seeking subsurface geological reservoirs as disposal sites. Additionally, extracting energy for heat or electrical generation from deep, subsurface warm and hot saline fluids is also a 'commodity' gaining momentum in the pore space resource sector.

The Western Canada Sedimentary Basin (WCSB) is undergoing this pore space transformation, but more remote basins lag behind. It is under this broad context of pore space resources that the Hudson Bay Basin (HBB) has not yet been evaluated, historically having only been assessed for its hydrocarbon potential. This report will discuss its general potential for pore space resources, including hydrocarbons, helium, geologic hydrogen, metal brines, geothermal energy and CCS.



Geological setting

The HBB of northeastern Manitoba consists of a thick sequence (up to ~900 m) of Paleozoic carbonate and clastic sedimentary rocks (Figure GS2024-20-1). Roughly centred in the modern Hudson Bay, the HBB is the largest Phanerozoic basin in Canada, with an area of ~820 000 km^2, and the least explored and understood basin in North America (Lavoie et al., 2013). The sedimentary rocks preserved and exposed onshore were deposited during the Paleozoic era (roughly 250 to 550 million years ago) in a shallow tropical marine environment. This marine environment resulted in the deposition of organic-bearing argillaceous carbonate and shale beds interbedded with thick carbonate strata

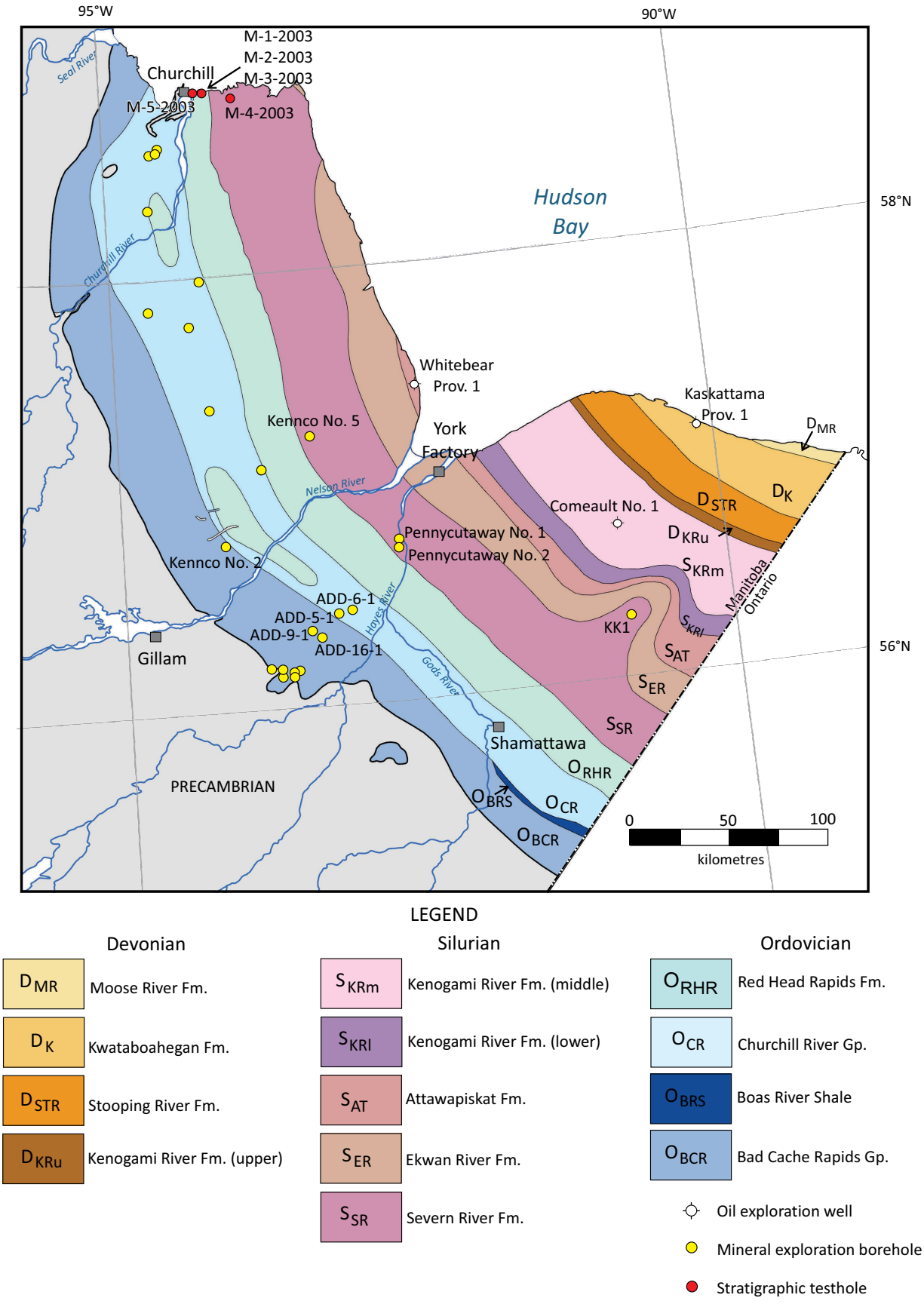


Figure GS2024-20-1: *Bedrock geology of the Hudson Bay Basin in northeastern Manitoba, showing locations of exploration and stratigraphic test drillholes. Only wells/boreholes/testholes with core available are labelled, with shortened names; see Nicolas and Lavoie (2010) for list of full names and cored intervals.*

during periods of reefal growth and the deposition of evaporitic sequences during periods of restricted and arid conditions (Nelson, 1964; Sanford et al., 1968; Cumming, 1971; Norford, 1971; Norris, 1993; Lavoie et al., 2013). This depositional environment is prospective for hydrocarbons and the development of reservoirs and conditions conducive to other pore space commodities, such as helium, geologic hydrogen, metal brines, geothermal energy and CCS reservoirs.

Hydrocarbon exploration history

Hydrocarbon (petroleum) exploration was first attempted in the HBB (onshore and offshore) from approximately 1964 to 1972, then renewed interest followed in the mid 1980s. Between these bouts of exploration a total of nine exploration oil and gas wells were drilled, five of them were drilled offshore in the centre of the basin and four of them were drilled onshore (three in Manitoba and one in Ontario; Nicolas and Lavoie, 2010; Nicolas and Armstrong, 2017), and seismic surveys were conducted in the centre of the basin (Lavoie et al., 2013). By 1990, the industry and the Geological Survey of Canada (GSC) had gathered a total of 96 000 linear-km of deep and shallow seismic data. Difficulties in acquiring seismic data in Hudson Bay resulted in much of the data to be of poor quality. Even though no commercial discoveries of oil or gas resulted from the drilling (according to the methods of the time), traces of oil and gas and bitumen-impregnated rocks were reported from all of the offshore wells, as well as minor traces in some onshore wells (Nicolas and Lavoie, 2012a; Lavoie et al., 2013). A quantitative resource evaluation concluded that the HBB has an estimated oil potential of 818 Mb (130×10^6 m^3) and gas potential of 3.2 Tcf (90×10^9 m^3; Procter et al., 1984). Unfortunately, the lack of economic success resulted in industry discontinuing their exploration of the HBB, and although there has been occasional industry interest since the 1980s, no advanced exploration has occurred.

Recent research

From 2008–2018, the Geological Survey of Canada led the Geo-mapping for Energy and Minerals (GEM) and GEM-2 programs, which included the successful Hudson Bay and Foxe Basins Project (2008–2013) and Hudson–Ungava Project (2014–2018), to study the geology and hydrocarbon potential of these northern sedimentary basins. Over the course of 10 years, the GEM Energy research team included geoscientists from the federal government, provincial and territorial governments (Manitoba, Ontario, Quebec and Nunavut) and Canadian universities. This team reviewed archival data, reinterpreting data using new geoscientific theories and techniques, and acquired new data from which to verify the hydrocarbon prospectivity of these basins. This work concluded that these basins have excellent hydrocarbon prospectivity (Lavoie et al., 2013, 2019, 2022). Although no new resource estimate was completed during this research, a new resource estimate would most certainly be higher than that calculated by Procter et al. (1984) since hydrocarbon resource evaluations have significantly changed. A qualitative assessment published by Hanna et al. (2018) supports the high hydrocarbon potential of the basin.

The potential for a sedimentary basin to host economic conventional hydrocarbon accumulations is based on the presence of multiple independent elements: a mature source rock rich in organic matter, a porous reservoir capped by a seal and trapping mechanism(s), and timing for fluids to charge the pore space within the reservoir. These studies demonstrated that the HBB has all the geological conditions for hydrocarbon systems to exist, including mature and diverse source rocks, attractive reservoirs and efficient traps and seals (Lavoie et al., 2013, 2019, 2022).

Hudson Bay Basin hydrocarbon potential

To date, study results support an active hydrocarbon system in the HBB, both offshore and onshore, favouring the accumulation of oil but not as much natural gas (Nicolas and Lavoie, 2012a, b). Evidence of migration pathways includes fractures in core that are lined with migrated oil residue (Nicolas and Lavoie, 2010) and the presence of hydrothermal dolomite (identified in the Churchill area; Nicolas and Lavoie, 2012a). Potential reservoir targets were identified in porous strata in all the oil exploration core and in some mineral exploration borehole core (Suchy and Stearn, 1993; Eggie et al., 2014), including clastic beds of the Bad Cache Rapids Group and Silurian reefs of the Severn River and Attawapiskat formations. Lastly, faults identified in the field and in geophysical datasets along with stratigraphic relationships indicate the potential presence of the traps needed for a conventional hydrocarbon system. The areas with the best potential for subsurface accumulations of oil in Manitoba are outlined in Figure GS2024-20-2a and shown vertically in Figure GS2024-20-3.

Within this oil potential area, the prospectivity of oil accumulations is primarily in Devonian and Silurian strata and increases across the region from the southwestern edge of the oil potential area outlined in Figure GS2024-20-2a, toward the northeast, along the Hudson Bay shoreline.

Oil and gas potential areas

An evaluation of the oil and gas potential in the HBB is based on the geological depositional environment, lithology, stratigraphy and subsurface depths. This is achieved through a general ranking for northeastern Manitoba, which is displayed in Figure GS2024-20-2a and shown in a vertical distribution in Figure GS2024-20-3. The southwestern corner of the HBB is considered an oil-rich basin, and is not expected to generate large volumes of natural gas (Nicolas and Lavoie, 2012a).

Rank 3—good potential

Areas with a rank 3 potential contain porous carbonate rocks of the Silurian Severn River Formation (lower units) at minimum depths (~400 m vertical depth) for there to be enough lithostatic pressure to contain oil within a given oil trap scenario, as well

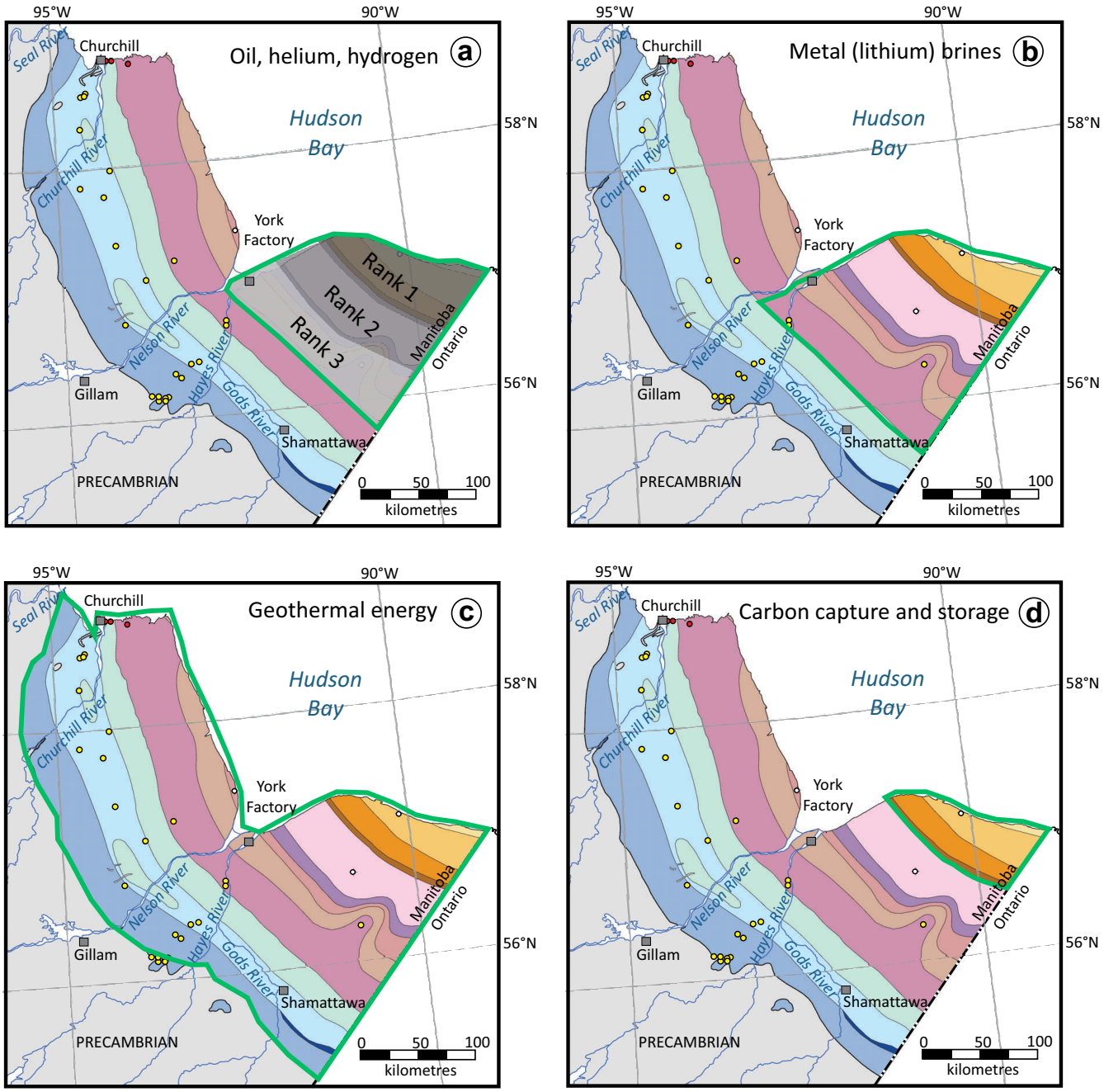


Figure GS2024-20-2: *Prospective areas in the southwestern Hudson Bay Basin are outlined in green for* ***a)*** *oil, helium and hydrogen with ranked areas (rank 1 is excellent, rank 2 is very good and rank 3 is good);* ***b)*** *metal (lithium) brines;* ***c)*** *geothermal energy; and* ***d)*** *carbon capture and storage. See Figure GS2024-20-1 for legend.*

as for unconventional biogenic gas accumulations, which would be accessible with present day technology (Figure GS2024-20-3). The term unconventional here refers to hydrocarbon reservoirs that have much lower porosity and permeability than the traditional (conventional) reservoirs, which require special drilling techniques and stimulation strategies to achieve economic sustainability.

Rank 2—very good potential

Areas with a rank 2 potential meet all the criteria of rank 3 areas, as well as 1) increased strata thicknesses and depth for the porous limestone reservoirs, 2) increased lithostatic pressure to contain larger oil accumulations within any given oil trap scenario, and 3) addition of more porous carbonate beds as a result of the northeastern dip of the strata, allowing more units to occur within the minimum depth zone for economical oil accumulations (middle units of the Silurian Severn River Formation; Figure GS2024-20-3). This area also has evidence of structural disturbances, which increases the probability of complex oil trapping systems. The best unconventional target formations are at greater depths, which translate to better gas generation since at these depths the rock can withstand more rigorous extrac-

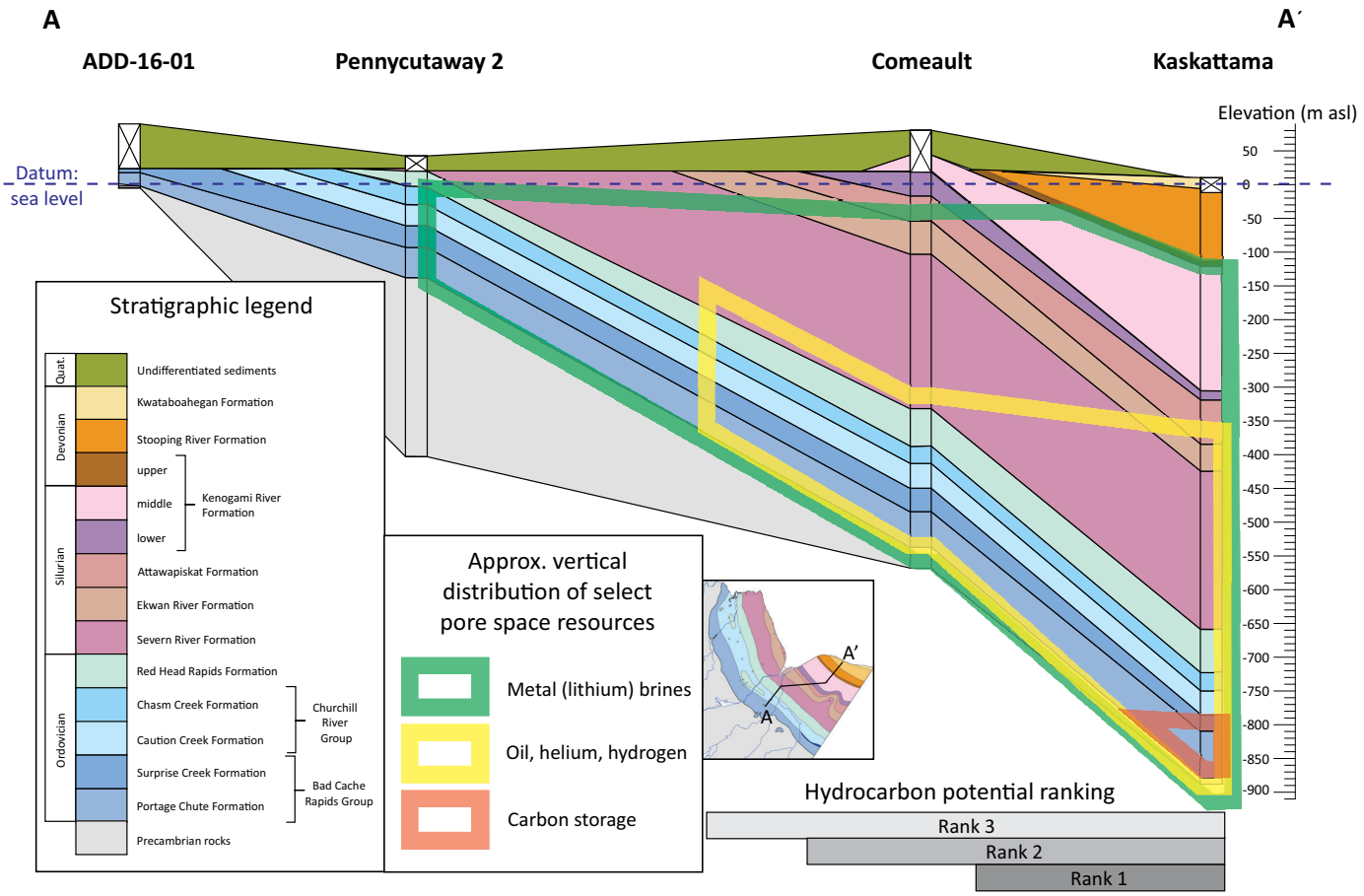


Figure GS2024-20-3: *Structural cross-section A-A' showing the approximate vertical depth and stratigraphic distribution of selected pore space resources. The hydrocarbon potential ranking corresponds to the ranking map shown in Figure GS2024-20-2; rank 1 is excellent, rank 2 is very good and rank 3 is good. Inset map shows the location of the cross-section in northeastern Manitoba (see Figure GS2024-20-1 for legend). Full borehole or well names: ADD-16-01, Arctic Star Diamond Corp. ADD-16-01 borehole (Assessment File 74259, Manitoba Economic Development, Investment, Trade and Natural Resources, Winnipeg); Pennycutaway 2, Selco/Hudson Bay Mining and Smelting Pennycutaway 2 borehole (Assessment File 91728); Comeault, Houston Oils et al. Comeault Prov. No. 1 well (oil and gas well licence 2337, Manitoba Economic Development, Investment, Trade and Natural Resources, Winnipeg); Kaskattama, Sogepet Aquitaine Kaskattama Prov. No. 1 well (oil and gas well licence 2168). White boxes with a cross indicate lost core or no core recovered. Abbreviations: Approx., approximately; Quat., Quaternary.*

tion techniques. Geochemical analyses from core within this zone indicate multiple thin (~1–15 cm) zones with high organic contents, and visual evidence of oil migration through fractures (as seen by bitumen staining along naturally fractured horizons; Nicolas and Lavoie, 2010, 2012a).

Rank 1—excellent potential

Areas with a rank 1 potential meet all the criteria of rank 2 and 3 areas; in addition, the porous formations mentioned above are situated at greater depths, with additional porous carbonate units added to the stratigraphic section, including the upper units of the Silurian Severn River, Ekwan River and Attawapiskat formations (Figure GS2024-20-3). Within rank 1, the Attawapiskat Formation has the best reservoir potential due to its high porosity and permeability and occurrence of large reefal structures capped with the tight carbonate and mudstone rocks of the Kenogami River Formation. The abundance of organic-rich beds increases in this area (Surprise Creek Formation of the Bad Cache Rapids Group and Red Head Rapids Formation), as does their subsurface depth. This area is also located along the shelf-break location of the paleo-HBB, which is traditionally the most prospective region within a hydrocarbon-bearing sedimentary basin. Geochemical analyses suggest these beds may have been heated and buried deep enough through their geological history to have produced hydrocarbons (Nicolas and Lavoie, 2012a; Lavoie et al., 2013). If not suitable as source rocks for conventional hydrocarbon systems, then these beds have potential for unconventional hydrocarbons. There is a significant increase in sediment thickness (~300 m) and thus burial depths of the strata between the rank 2 (very good) and rank 1 (excellent) areas, which increases their prospectivity.

Potential for other pore space resources

Exploration and studies conducted on the HBB have been focused on hydrocarbons with no attention to other subsurface resources and commodities. Commodities such as helium, geo-

logic hydrogen and metal (lithium) brines and resources such as CCS and geothermal energy all have varying degrees of potential within this basin, but there is a lack of geological knowledge to gauge the prospectivity of these commodities in the HBB.

Using the same rationale outlined for hydrocarbon potential, a similar exercise can be applied to other pore space resources, with some key differences that are resource specific. Oil generation and source rock geochemistry are not a factor for these other commodities, instead commodity-specific considerations for helium, geologic hydrogen and lithium brine are needed, such as a source of natural radioactive decay for helium and radiolysis for hydrogen (Zgonnik, 2020) and lithium-enriched clays for lithium brine (Bishop and Robbins, 2023). For geothermal resources an increased crustal heat flow is required and for CCS reservoirs need to be situated at a minimum depth of 800 m.

The HBB of northeastern Manitoba does have the geological conditions, including conduits for the migration of gas, porous reservoirs and seals, that are needed to create an economic deposit of helium. Helium occurrences have been identified in the Williston Basin of southeastern Manitoba (Nicolas, 2018; Nicolas et al., 2023) in strata that are correlative to Silurian and Ordovician rocks in the HBB. The Precambrian basement composition underlying the HBB (favouring granitic rocks in places) and the occurrence of clastic sedimentary units with high gamma-ray readings (e.g., shale, sandstone) are excellent sources of helium. The Surprise Creek and Red Head Rapids formations have high gamma-ray responses (Nicolas and Armstrong, 2017), increasing toward the basin centre (Lavoie et al., 2013). Several lineaments related to fracture networks (Nicolas and Clayton, 2015) and basement structures, such as the Winisk River fault and one area currently being studied on the northeastern edge the Kaskattama highland (Craven et al., 2017), provide the conduits for fluid flow. Porous strata of the Severn River and Portage Chute formations occur within the preferred helium reservoir intervals of 500–1500 m depth (Brown, 2010). Particularly efficient seals for helium are evaporitic units, but low permeable carbonate and shale beds can also be good sealing beds. The Red Head Rapids Formation contains salt beds, increasing in thickness towards the centre of the basin, which can serve as a perfect seal for the small helium atom.

There have been no helium or hydrogen measurements conducted on any of the wells in the HBB, however, modern techniques, such as rock volatiles analysis (Nicolas et al., 2023, 2024), have been developed that measure helium concentrations throughout a stratigraphic section. This type of sampling and analysis would be required on the core available to more accurately evaluate the helium potential of the HBB. Since this analysis has not been completed, the entire area outlined for hydrocarbon potential in Figures GS2024-20-2a and -3 could serve as a proxy for a 'good' helium potential.

The understanding of the geological processes that form hydrogen in the subsurface are poorly understood but are receiving rejuvenated interest (Zgonnik, 2020; Jackson et al., 2024). Considering the known association of hydrogen with helium occurrences (Ellis, 2024; Yurkowski et al., 2024), helium targets may also be considered as hydrogen targets; however, the reactivity of hydrogen versus inert helium results in some important differences to consider, specifically in the range of geological environments in which they may occur (Zgonnik, 2020; Ellis, 2024; Jackson et al., 2024;). Despite the scarcity of data available for the HBB, Nicolas (2024) conducted a high level evaluation of hydrogen potential. Overall, it is challenging to confidently indicate where geologic hydrogen may occur in the HBB, therefore, using the prospective area outlined for helium as a maximum area for hydrogen prospectivity is recommended (Figure GS2024-20-2a).

Metal (lithium) brines

Metal brines refer to deep subsurface saline groundwater with elevated concentrations of dissolved metals. The chemistry of saline groundwater in the HBB is poorly documented and there is limited knowledge of the hydrostratigraphy of the HBB. Deep subsurface brines enriched in lithium have been discovered in the WCSB and exploration is currently being undertaken in Saskatchewan (Jensen, 2016; Jensen and Rostron, 2018) and Manitoba (Xtract Lithium, 2024). The source of the lithium in the WCSB is uncertain, but theories include rock-water interactions with lithium-enriched clay layers (Bishop and Robbins, 2023) and episodic erosion of lithium-bearing minerals and/or lithium-rich surface waters flowing from the Canadian Shield into the basin (Nicolas, 2017). Although untested, these same mechanisms and aquifer-specific metal enrichments are just as likely to occur in the HBB, especially within similar porous rocks. The economics of metal brines are less sensitive to depth requirements and more reliant on groundwater chemistry, aquifer characteristics and hydrostatic pressures to ensure reliable production. Based on these factors, the potential area for metal (lithium) brines is larger compared to the designated potential areas for hydrocarbons and helium. The entire Silurian Severn River Formation extent is included in the prospective area since depth is not a limiting factor. This area of potential includes the Red Head Rapids Formation, its argillaceous beds could act as possible aquitards to constrain the brines, and other Ordovician carbonate beds, which could serve as potential metal sources as well as reservoirs. Figure GS2024-20-2b shows the metal (lithium) brine prospectivity map and its distribution at depth is shown in Figure GS2024-20-3.

Geothermal energy

The HBB is considered a cool sedimentary basin, with no anomalous heat flow and low geothermal potential. Geothermal potential is limited to direct heat or heat exchange (Grasby et al., 2012), which can be considered for local/household use. Given the remoteness of the communities in the HBL and their current reliance on diesel fuel for heat, tapping into this low enthalpy but

consistent and reliable source of heat stored in the bedrock underlying these communities may be worth considering. Using these types of geothermal systems, the entire distribution of the carbonate strata of the HBB could be considered as a potential area for this geothermal resource, although targeted studies would be required to test this potential. The HBB does not have the potential for geothermal energy for the purposes of electrical generation or large-scale heating infrastructure. Figure GS2024-20-2c shows the area for consideration for low enthalpy geothermal heat.

Carbon capture and storage

The potential to store carbon (as CO_2) in the HBB succession of northeastern Manitoba is very limited. The only formation with sufficient porosity at depths of >800 m is the Ordovician Portage Chute Formation of the Bad Cache Rapids Group. These constraints leave the most prospective area in the HBB to a narrow region that is approximately equivalent to the aerial distribution of the Devonian Stooping River, Kwataboahegan and Moose River formations (Figure GS2024-20-2d). Here, the porous carbonates of the Portage Chute Formation occur at sufficient depths (Figure GS2024-20-3) for deep geologic carbon storage as part of a CCS system. However, this is a remote area with no anthropogenic CO_2 point sources nearby to feed such an operation at this time and the geology remains untested for this type of operation.

Discussion

Only three exploratory wells that penetrate the entire sedimentary section have ever been drilled in this area of Manitoba; therefore, it is not possible to conduct a true resource assessment for any commodity. However, to put the HBB into perspective, the northeastern flank of the Williston Basin in southwestern Manitoba is significantly smaller than the HBB (~182 000 km^2, which is 22% of the size of the entire HBB) and more than 25 dry holes were drilled in southwestern Manitoba before the first oil pool was discovered. The HBB has only nine exploratory oil wells, with three of those in Manitoba.

Geoscientists have a good understanding of hydrocarbon systems, making geoscientific investigations of frontier basins easier to evaluate with limited data. When evaluating for other nonconventional resources, such as the pore space resources discussed herein, the confidence in the prospectivity is reduced significantly. Thus, geologists must rely on foundational understanding of the basin and its stratigraphy as the best tool to developing a prospectivity map for a region, especially one as remote as the HBB, until exploration for a specific pore space resource is conducted.

Economic considerations

The reassessment of the hydrocarbon potential of the HBB using modern technology and reintegrating old and new data through a modern lens has significantly helped to better understand this remote basin. What was once thought as a large area without hydrocarbon potential has now been reinterpreted as a highly prospective frontier area. Successful exploration in northern Manitoba brings significant positive economic impact and development, particularly for northern communities. The coast of Hudson Bay, including the deepwater port at Churchill and connecting rail line, allows access to major markets. Thus, successful hydrocarbon exploration and understanding of other pore space commodities available in the HBB would benefit all of Manitoba.

The assessment of other pore space resources, such as helium, geologic hydrogen and metal (lithium) brines, is difficult given the lack of data currently available, but by applying the knowledge gained from previous reassessments of hydrocarbons, it is possible to extrapolate and conclude that the potential does exist. As technology advances and economic conditions improve, these resources could become a viable exploration target of the future, adding further value to the region. Geothermal energy for use in direct heat and heat exchange systems may be possible to develop at the household scale. However, carbon capture and deep geologic storage potential in the Hudson Bay Basin is extremely limited. From an economic opportunity perspective, and in the broader land-use planning of this northern region, knowing the pore space resource potential, its benefits and limitations, is important in the decision-making process.

Acknowledgments

The author would like to acknowledge D. Lavoie, formerly of the Geological Survey of Canada, the leader of the Hudson Bay and Foxe Basins Project and the Hudson–Ungava Project of the Geo-mapping for Energy and Minerals programs (GEM, 2008-2013; GEM-2, 2013–2020) and the extended GEM Energy team for their extensive support in researching and understanding the geology and hydrocarbon potential of the Hudson Bay Basin. The author thanks P. Fraino and T. Hodder for their critical review of this report.

References

Bishop, B.A. and Robbins, L.J. 2023: Overview of potential lithium sources in the WCSB; Canadian Energy Geoscience Association–Canadian Society of Exploration Geophysicists, Annual Convention (GeoConvention 2023), May 15–17, 2023, Calgary, Alberta, abstract, 4 p., URL <https://geoconvention.com/wp-content/uploads/abstracts/2023/91590-overview-of-potential-lithium-sources-in-the-wcsb.pdf> [September 2024].

Brown, A. 2010: Formation of high helium gases: a guide for explorationists; American Association of Petroleum Geologists, AAPG Convention, April 11–14, 2010, New Orleans, Louisiana, abstract, URL <https://www.searchanddiscovery.com/documents/2010/80115brown/ndx_brown.pdf> [September 2024].

Craven, J.A., Ferguson, I.J., Nicolas, M.P.B., Zaprozan, T., Hodder, T.J., Roberts, B.R. and Clarke, N. 2017: Report of activities for the ground geophysical survey across the Kaskattama highlands, Manitoba: GEM-2 Hudson-Ungava Project; Geological Survey of Canada, Open File 8321, 34 p.

Cumming, L.M. 1971: Ordovician strata of the Hudson Bay Lowlands in northern Manitoba; *in* Geoscience Studies in Manitoba, A.C. Turnock (ed.), Geological Association of Canada, p. 189–197.

Eggie, L.A., Pietrus, E., Ramdoyal, A. and Chow, N. 2014: Diagenesis of the Lower Silurian Ekwan River and Attawapiskat formations, Hudson Bay Lowland, northern Manitoba (parts of NTS 54B, F, G); *in* Report of Activities 2014, Manitoba Mineral Resources, Manitoba Geological Survey, p. 161–171.

Ellis, G.S. 2024: Mapping geologic hydrogen resource prospectivity; Canadian Energy Geoscience Association–Canadian Society of Exploration Geophysicists, Annual Convention (GeoConvention 2024), June 17–19, 2024, Calgary, Alberta, abstract, URL <https://geoconvention.com/wp-content/uploads/abstracts/2024/104118-mapping-geologic-hydrogen-resource-prospectivity.pdf> [September 2024].

Grasby, S.E., Allen, D.M., Bell, S., Chen, Z., Ferguson, G., Jessop, A., Kelman, M., Ko, M., Majorowics, J., Moore, M., Raymond, J. and Therrien, R. 2012: Geothermal energy resource potential of Canada; Geological Survey of Canada, Open File 6914, 322 p.

Hanna, M.C., Lister, C.J., Kublik, K., Kung, L.E., McCarthy, W.M., McDannell, K.T. and Jassim, Y. 2018: Qualitative petroleum resource assessment of western Hudson Bay, Foxe Channel, and Repulse Bay, Manitoba, Nunavut, Ontario, and Quebec; Geological Survey of Canada, Open File 8434, 31 p.

Jackson, O., Lawrence, S.R., Hutchinson, I.P., Stocks, A.E., Barnicoat, A.C. and Powney, M. 2024: Natural hydrogen: sources, systems and exploration plays; Geoenergy, v. 2, p. 1–9.

Jensen, G.K.S. 2016: Results from the 2016 field season for the brine sampling project: investigating the mineral potential of brines in Saskatchewan; *in* Summary of Investigations 2016, Volume 1, Saskatchewan Geological Survey, Saskatchewan Ministry of Economy, Miscellaneous Report 2016-4.1, Paper A-3, p. 7.

Jensen, G.K.S. and Rostron, B.J. 2018: Investigating the mineral potential of brines in Saskatchewan: new results from the brine sampling project for 2018; *in* Summary of Investigations 2018, Volume 1, Saskatchewan Geological Survey, Saskatchewan Ministry of Energy and Resources, Miscellaneous Report 2018-4.1, Paper A-5, p. 8.

Lavoie, D., Pinet, N., Dietrich, J., Zhang, S., Hu, K., Asselin, E., Chen, Z., Bertrand, R., Galloway, J., Decker, V., Budkewitsch, P., Armstrong, D., Nicolas, M.P.B., Reyes, J., Kohn, B.P., Duchesne, M.J., Brake, V., Keating, P., Craven, J. and Roberts, B. 2013: Geological framework, basin evolution, hydrocarbon system data and conceptual hydrocarbon plays for the Hudson Bay and Foxe basins, Canadian Arctic; Geological Survey of Canada, Open File 7363, 210 p.

Lavoie, D., Pinet, N., Zhang, S., Reyes, J., Jiang, C., Ardakani, O.H., Savard, M.M., Dhillon, R.S., Chen, Z., Dietrich, J.R., Hu, K., Craven, J.A., Roberts, B., Duchesne, M.J., Brake, V.I., Huot-Vezina, G., Galloway, J.M., McCracken, A.D., Asselin, E., Decker, V., Beauchemin, M., Nicolas, M.P.B., Armstrong, D.K. and Hahn, K.E. 2019: Hudson Bay, Hudson Strait, Moose River, and Foxe basins: synthesis of research activities under the Geomapping for Energy and Minerals (GEM) programs 2008-2018; Geological Survey of Canada, Open File 8507, 76 p.

Lavoie, D., Pinet, N., Zhang, S., Reyes, J., Jiang, C., Ardakani, O.H., Savard, M.M., Dhillon, R.S., Chen, Z., Dietrich, J.R., Hu, K., Craven, J.A., Roberts, B., Duchesne, M.J., Brake, V.I., Huot-Vezina, G., Galloway, J.M., McCracken, A.D., Asselin, E., Decker, V., Beauchemin, M., Nicolas, M.P.B., Armstrong, D.K. and Hahn, K.E. 2022: Hudson Bay, Hudson Strait, Moose River, and Foxe basins: synthesis of research activities under the Geomapping for Energy and Minerals (GEM) programs 2008-2018; *in* Sedimentary Basins of Northern Canada: Contributions to a 1000 Ma Geological Journey and Insight on Resource Potential, D. Lavoie and K. Dewing (ed.), Geological Survey of Canada, Bulletin 609, p. 37–76.

Nelson, S.J. 1964: Ordovician stratigraphy of northern Hudson Bay Lowland, Manitoba; Geological Survey of Canada, Bulletin 108, 36 p.

Nicolas, M.P.B. 2017: Preliminary investigation of the potential for lithium in groundwater in sedimentary rocks in southwestern Manitoba; *in* Report of Activities 2017, Manitoba Growth, Enterprise and Trade, Manitoba Geological Survey, p. 183–190.

Nicolas, M.P.B. 2018: Summary of helium occurrences in southwestern Manitoba; *in* Report of Activities 2018, Manitoba Growth, Enterprise and Trade, Manitoba Geological Survey, p. 110–118.

Nicolas, M.P.B. 2024: Geologic hydrogen in the Williston and Hudson Bay basins, southwestern and northeastern Manitoba (parts of NTS 53, 54, 62, 63); *in* Report of Activities 2024, Manitoba Economic Development, Investment, Trade and Natural Resources, Manitoba Geological Survey, p. 164–171.

Nicolas, M.P.B. and Armstrong, D.K. 2017: Update on Paleozoic stratigraphic correlations in the Hudson Bay Lowland, northeastern Manitoba and northern Ontario; *in* Report of Activities 2017, Manitoba Growth, Enterprise and Trade, Manitoba Geological Survey, p. 133–147.

Nicolas, M.P.B. and Clayton, B.W. 2015: Lineament mapping of the Hudson Bay Lowland using remote-sensing methods, northeastern Manitoba (parts of NTS 53 N, O, 54); *in* Report of Activities 2015, Manitoba Mineral Resources, Manitoba Geological Survey, p. 89–93.

Nicolas, M.P.B. and Lavoie, D. 2010: Hudson Bay and Foxe Basins Project: update on a Geo-mapping for Energy and Minerals program (GEM) initiative, northeastern Manitoba (part of NTS 54); *in* Report of Activities 2010, Manitoba Innovation, Energy and Mines, Manitoba Geological Survey, p. 186–192.

Nicolas, M.P.B. and Lavoie, D. 2012a: Oil shale and reservoir rocks of the Hudson Bay Lowland, northeastern Manitoba (part of NTS 54); *in* Report of Activities 2012, Manitoba Innovation, Energy and Mines, Manitoba Geological Survey, p. 124–133.

Nicolas, M.P.B. and Lavoie, D. 2012b: RockEval™ 6 results from Paleozoic core samples from the Hudson Bay Lowland, northeastern Manitoba (part of NTS 54); Manitoba Innovation, Energy and Mines, Manitoba Geological Survey, Data Repository Item DRI2012002, Microsoft® Excel® file.

Nicolas, M.P.B., Smith, C.M. and Smith, M.P. 2023: Volatiles analysis of drill cuttings to evaluate the helium prospectivity of southwestern Manitoba (parts of NTS 62F2, K3); *in* Report of Activities 2023, Manitoba Economic Development, Investment, Trade and Natural Resources, Manitoba Geological Survey, p. 93–104.

Nicolas, M.P.B., Smith, C.M. and Smith, M.P. 2024: Rock volatiles analysis of drill cuttings to evaluate the helium and hydrogen prospectivity of southwestern Manitoba (parts of NTS 62F2, K3); *in* Report of Activities 2024, Manitoba Economic Development, Investment, Trade and Natural Resources, Manitoba Geological Survey, p. 153–163.

Norford, B.S. 1971: Silurian stratigraphy of northern Manitoba; *in* Geoscience Studies in Manitoba, A.C. Turnock (ed.), Geological Association of Canada, p. 199–207.

Norris, A.W. 1993: Hudson platform - geology; Chapter 8 *in* Sedimentary Cover of the Craton in Canada, D.F. Stott and J.D. Aitken (ed.), Geological Survey of Canada, Geology of Canada, no. 5, p. 653–700.

Procter, R.M., Taylor, G.C. and Wade, J.A. 1984: Oil and natural gas resources of Canada 1983; Geological Survey of Canada, Paper 83-31, 59 p.

Sanford, B.V., Norris, A.W., Bostock, H.H. and Bell, R.T. 1968: Geology of the Hudson Bay Lowlands: Operation Winisk; Geological Survey of Canada, Paper 67-60, 46 p.

Suchy, D.R. and Stearn, C.W. 1993: Lower Silurian reefs and post-reef beds of the Attawapiskat Formation, Hudson Bay Platform, northern Ontario; Canadian Journal of Earth Sciences, v. 30, p. 575–590.

Xtract Lithium Corp. 2024: Xtract project; Xtract Lithium Corp., URL <https://xtractlithium.com/xtract-project-2/> [September 2024].

Yurkowski, M., Flynn, J., Gilbert, M., Bosman, S., Maxeiner, R. and Card, C. 2024: Hydrogen and helium: is there an analogue relationship in Saskatchewan's uranium deposits?; Canadian Energy Geoscience Association–Canadian Society of Exploration Geophysicists, Annual Convention (GeoConvention 2024), June 17–19, 2024, Calgary, Alberta, abstract, URL <https://geoconvention.com/wp-content/uploads/abstracts/2024/104290-saskatchewans-hydrogen-potential1.pdf> [September 2024].

Zgonnik, V. 2020: The occurrence and geoscience of natural hydrogen: a comprehensive review; Earth-Science Reviews, v. 203, p. 1–51.

GS2024-21

Compilation of saline water analysis data from oil and gas wells, southwestern Manitoba (NTS 62F, G, J, K, N)

by E. Enaworu and M.P.B. Nicolas

Summary

In 2023, the Manitoba Geological Survey initiated the compilation of water analysis data from subsurface saline aquifers in the Williston Basin of southwestern Manitoba. This report focuses on the compilation of saline water analysis data extracted from technical well files for 298 oil and gas wells in southwestern Manitoba. Derived directly from water analysis reports, the compilation includes many fields of information, including location information, stratigraphy, salinity, pH, specific gravity, water resistivity, total dissolved solids, composition and much more. Each water analysis data entry was carefully assessed for quality and accuracy. Once completed, this dataset will inform future hydrogeological studies and the resultant mapping will inform regulatory decisions, land-use planning and future pore space resource exploration, including critical minerals, geothermal energy and carbon capture and storage.

In Brief:

- Saline water analysis data from oil and gas wells spanning 75 years has been compiled into a user-friendly digital format
- This data will inform hydrogeological evaluation of saline water aquifers

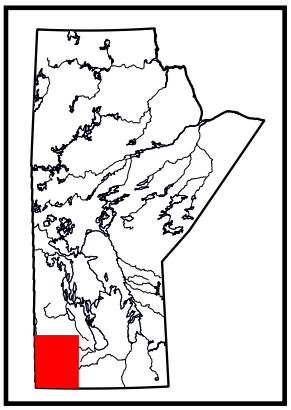
Citation:
Enaworu, E. and Nicolas, M.P.B. 2024: Compilation of saline water analysis data from oil and gas wells, southwestern Manitoba (NTS 62F, G, J, K, N); *in* Report of Activities 2024, Manitoba Economic Development, Investment, Trade and Natural Resources, Manitoba Geological Survey, p. 181–184.

Introduction

Data compilation for saline aquifers is key to understanding their prospect, uses and limitations and industrial applications. Recently, there has been an increased demand for the compilation and evaluation of data on brines within saline aquifers, due to the potential for their use as storage sites for carbon dioxide (CO_2), geothermal energy, sources of lithium and in the secondary recovery of hydrocarbons. As a result of this demand, in 2023, the Manitoba Geological Survey (MGS) initiated a project to compile water analysis data from oil and gas well operations. Within the deep subsurface sedimentary formations of the Williston Basin in southwestern Manitoba, there are many saline aquifers that occur at varying depths and with salinity concentrations that vary by formation and location (Grasby and Betcher, 2002; Nicolas, 2017; Nicolas and Grasby, 2018).

Companies exploring for or producing oil and gas in Manitoba are required to submit all the technical well information to the provincial regulator for official filing and the information is made available to the public after a confidentiality period has ended. When a company collects and analyzes water samples from their well, the laboratory results are submitted and then added to the petroleum technical well file for that well (Manitoba Economic Development, Investment, Trade and Natural Resources, 2024). These water samples are collected from drillstem tests (DST), wellheads and battery sites. The water analysis reports ensuing are a good public source of information from which to begin a compilation.

These water analyses provide valuable information that can be used to help evaluate the hydrogeology and reservoir parameters of the aquifers. These reports are of variable digital quality and only available in Adobe Acrobat® portable document format (PDF), most of which were created by scanning paper documents up to 75 years old. The poor quality of the older reports and the variability in the information contained within each report prevented the use of automated digital scanning for data extraction. Therefore, in order to compile the water chemistry information, a manual extraction of information and entry into a database was required.



The objective of this project is to extract and compile all the information from water analysis reports into a new publicly accessible database. The outcome will be in a user-friendly digital format that will be updated regularly.

Geology and hydrogeology

The Williston Basin consists of stratigraphic sequences from the Paleozoic to Cenozoic eras. The Paleozoic formations in the subsurface in southwestern Manitoba consist dominantly of limestone, dolostone and evaporites (Nicolas and Barchyn, 2008). The Mesozoic formations consist of shale, red siltstone and sandstone whereas the Cenozoic section comprises silty and fine sandy shale (Corkery, 1996).

Hydrostratigraphic flow analysis models were developed by Palombi (2008) for the northeastern portion of the Williston Basin. Palombi (2008) observed large differences in the type of formation waters in the saline aquifers and identified four different water compositions based on their ion chemistry. These four water compositions are 1) calcium, 2) sodium chloride brines, 3) calcium sulphate freshwaters and 4) sodium sulphate brackish waters. Palombi and Rostron (2006) indicated that there are significant differences in the density and composition of waters in these saline aquifers.

The flow direction of these saline waters differs across formations, with a flow direction from east to northeast for Mesozoic aquifers, west to east for Mississippian aquifers, updip to the northeast for lower Paleozoic aquifers, and upward movement for Jurassic saline aquifers. At the margins of the basin, the flow is vertical, whereas in the centre of the basin it is horizontal (Palombi, 2008). A major hydrological divide occurs in Manitoba, extending roughly in a northwest–southeast trend along and through Lake Winnipegosis and Lake Manitoba. This divide separates the subsurface freshwaters to the east from the subsurface saline aquifer waters to the west (Grasby and Betcher, 2002).

Methodology

A four-phase approach was adopted to perform this data compilation (Figure GS2024-21-1). The first phase consisted of obtaining the well information and licence numbers of the oil and gas wells in the Williston Basin, searching for the well files using the licence number, and downloading the well files in PDF. The second phase consisted of searching for the saline water analysis data within the PDF documents, splitting the saline water analysis data from the other well data using Adobe® Acrobat Pro software and extracting the data from the PDF document and entering it into a Microsoft® Excel® spreadsheet. The third phase consisted of storing the extracted data securely in a Microsoft Excel spreadsheet, checking the spreadsheet to ensure that it is robust enough to accommodate variants of the data and quality checking the data for any errors introduced during the extraction process. The fourth phase will consist of the final compilation process and the preparation of a MGS GeoFile digital publication.

All water analysis reports found for these wells were extracted to individual PDF files. Data from each file was then entered into a spreadsheet, one row per analysis. The following information from each analysis was captured: oil and gas well licence number, unique well identifier (UWI), location, well name, DST number, sample identification, oil field name, depth intervals tested, subsurface formation assigned at the time of sampling, geological age, nature of liquid, total solids in parts per million (ppm), primary salinity, secondary salinity, primary alkalinity, secondary alkalinity, chloride salinity, sulphate salinity, pH, specific gravity (sg), density, water resistivity (R_w), total dissolved solids (TDS), resistivity index, hardness, turbidity and total concentration (in ppm).

Results

The search through the well files returned 298 oil and gas well licences with water analysis reports. Each of these reports was extracted from the well files and their chemistry information recorded in a Microsoft Excel spreadsheet. Figure GS2024-21-2 shows the locations of these 298 oil and gas wells.

Phases one, two and three of this saline water compilation project are now complete, and phase four is estimated to be completed in the winter of 2024–2025.

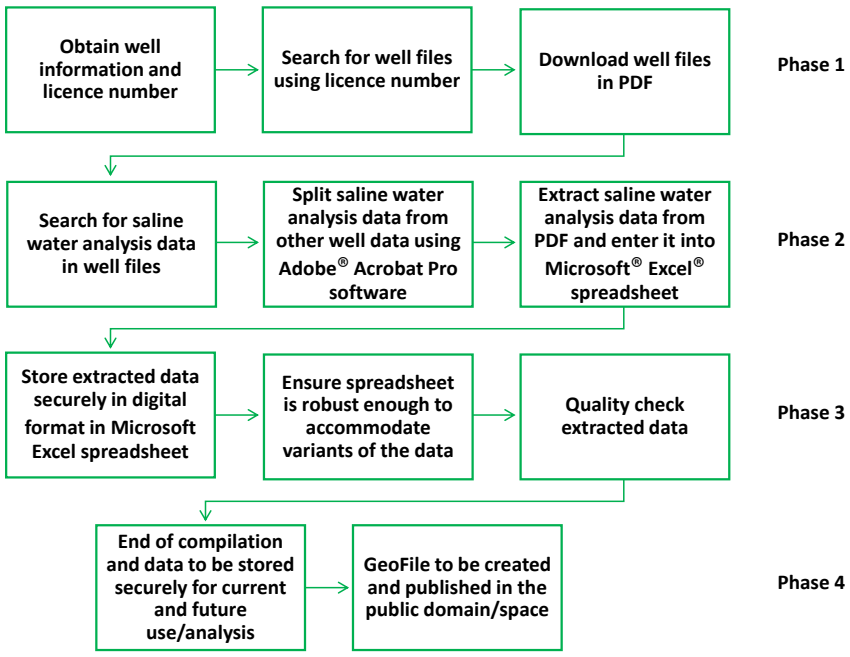


Figure GS2024-21-1: *Steps and workflow method used in the saline water analysis data compilation.*

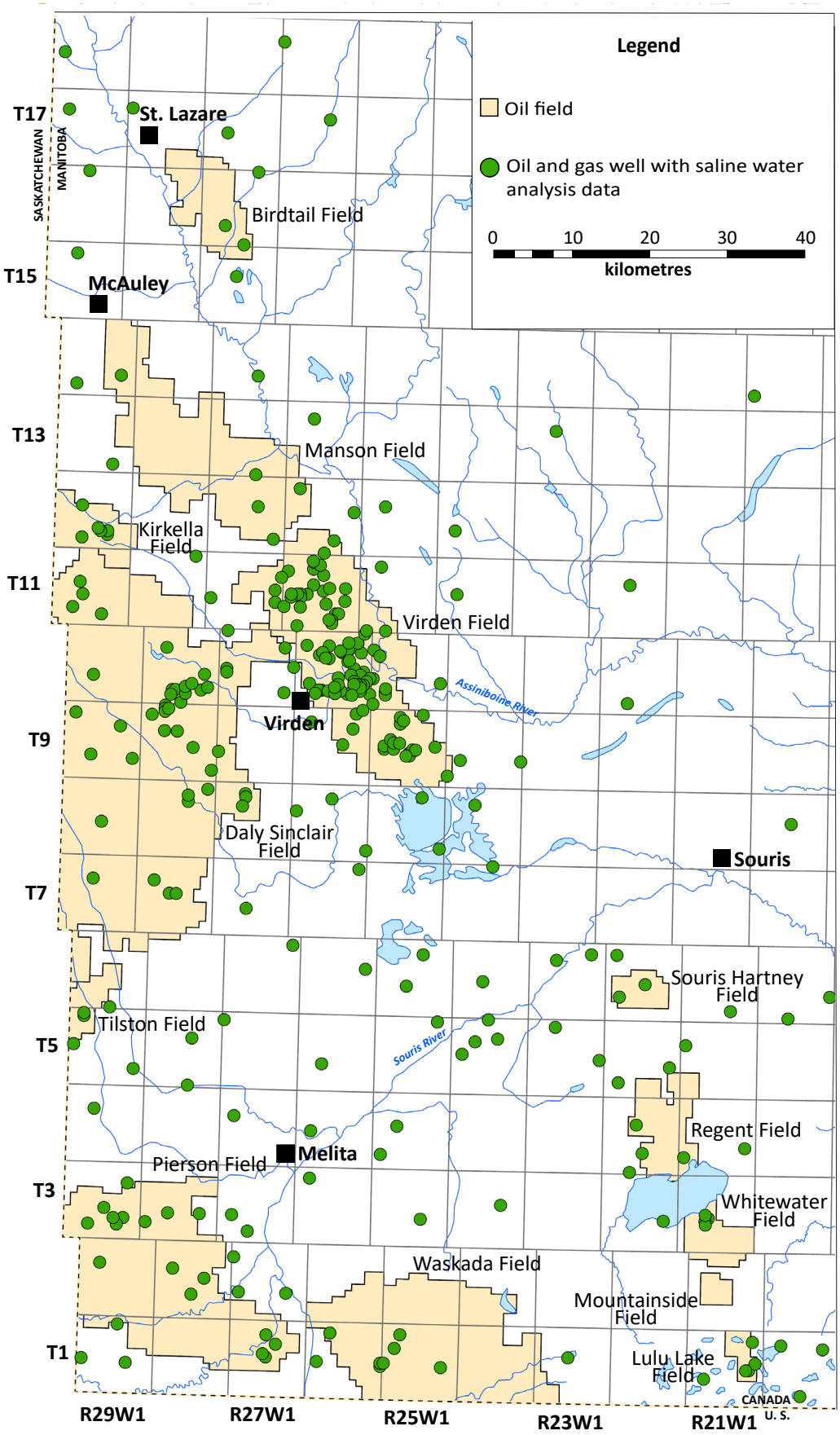


Figure GS2024-21-2: *Locations of oil fields and oil and gas wells with saline water analysis data in southwestern Manitoba. Oil field locations from Nicolas (2023) and well locations from Manitoba Economic Development, Industry, Trade and Natural Resources (2024).*

Future work

The fourth and final phase of this project is to finalize the compilation of the dataset and prepare it for publication. As new water analyses are submitted, the database will be updated and released to the public annually, or as needed. This compilation will have the following characteristics:

- uniquely structured to accommodate different formats of water analysis data
- robust, user-friendly and flexible enough to accommodate the integration of additional datasets
- each well point can be plotted according to location (DLS), geological period, stratigraphic formations, UWI, oil and gas licence number, etc.
- can be easily updated and converted into multiple formats
- can easily be imported into various software for further analysis

Products and maps derived from this saline water database will be produced by the MGS in the years to come and will further inform the hydrogeological framework of Manitoba's deep subsurface waters.

Economic considerations

As the green economy expands, more resources are required to fill the gap. Pore space resources are poised to fill that space and have become increasingly more important in the energy and mineral industry. One of those resources is the saline aquifers within the sedimentary basins in Manitoba. These saline aquifers include metal-rich brines. These brines are potential sources of dissolved metals and nonmetals, including lithium, magnesium, calcium, bromine and iodine, for use in a variety of industrial applications such as battery production, metallurgy, agriculture and medicine. Additionally, these brines can also be a source of geothermal heat and key targets for carbon capture and storage (CCS). The documentation and evaluation of the hydrogeology and saline aquifer characteristics of the subsurface brines in Manitoba is required to inform regulatory and exploration decisions and resource and land-use planning.

Acknowledgments

The authors would like to thank A. Abdelrahman and S. Sidhu (Mining, Oil and Gas Branch) and H. Adediran for their assistance with data access and software support, and P. Fulton-Regula for her thorough review of this report.

References

Corkery, M.T. 1996: Geology and landforms of Manitoba; *in* The Geography of Manitoba: Its Land and Its People, J. Welsted, J. Everitt and C. Stadel (ed.), University of Manitoba Press, Winnipeg, Manitoba, p. 11–30.

Grasby, S.E. and Betcher, R.N. 2002: Regional hydrogeochemistry of the carbonate rock aquifer, southern Manitoba; Canadian Journal of Earth Sciences, v. 39, p. 1053–1063.

Manitoba Economic Development, Investment, Trade and Natural Resources 2024: Petroleum technical well files; *in* GIS Map Gallery, Manitoba Economic Development, Investment, Trade and Natural Resources, Mining, Oil and Gas Branch, URL <https://manitoba.ca/iem/petroleum/gis/technical.html> [September 2024].

Nicolas, M.P.B. 2017: Preliminary investigation of the potential for lithium in groundwater in sedimentary rocks in southwestern Manitoba; *in* Report of Activities 2017, Manitoba Growth, Enterprise and Trade, Manitoba Geological Survey, p. 183–190.

Nicolas, M.P.B. 2023: Manitoba's designated oil fields and pools 2023; Manitoba Economic Development, Investment and Trade, Manitoba Geological Survey, 63 p., URL <https://manitoba.ca/iem/petroleum/f_p_codes/poolbook_2023.pdf> [October 2024].

Nicolas, M.P.B. and Barchyn, D. 2008: Williston Basin Project (Targeted Geoscience Initiative II): summary report on Paleozoic stratigraphy, mapping and hydrocarbon assessment, southwestern Manitoba; Manitoba Science, Technology, Energy and Mines, Manitoba Geological Survey, Geoscientific Paper GP2008-2, 21 p.

Nicolas, M.P.B. and Grasby, S.E. 2018: Lithium concentrations in brine springs near Lake Winnipegosis, west-central Manitoba (parts of NTS 63C, 62N16, 62O12, 13); *in* Report of Activities 2018, Manitoba Growth, Enterprise and Trade, Manitoba Geological Survey, p. 119–124.

Palombi, D.D. 2008: Regional hydrogeological characterization of the northeastern margin in the Williston Basin; M.Sc. thesis, University of Alberta, Edmonton, Alberta, 196 p.

Palombi, D.D. and Rostron, B.J. 2006: Regional hydrochemistry of Lower Paleozoic aquifers in the northern portion of the Williston Basin, Saskatchewan–Manitoba; *in* Saskatchewan and Northern Plains Oil & Gas Symposium 2006, C.F. Gilboy and S.G. Whittaker (ed.), Saskatchewan Geological Society, Special Publication 19, p. 201–209.

GS2024-22

Distribution of the lithological units of the Winnipeg Formation, southern Manitoba (NTS 62F–K, N–P)

by V.L. Markstrom

Summary

Silica sand is a mineral with many industrial uses, including the production of silicon metal, which is on Canada's critical minerals list. In Manitoba, the purest and highest quality sand for economic development is derived from the Ordovician Winnipeg Formation. Due to increased interest in Manitoba's silica sand, the formation is being re-examined by the Manitoba Geological Survey. Within the Winnipeg Formation, the Carman Sand is of particular interest due to its high purity and quality, making it an excellent source of proppant sand. Isopach and structure maps were created for the Winnipeg Formation, including for the upper unit, the Carman Sand and the lower unit. The Winnipeg Formation is thickest in southern Manitoba, measuring 75 m, and gradually thins northward, with a sharp decrease in thickness toward the eastern edge of the Williston Basin, to <1 m. This pattern is observed in both the upper and lower units, although each unit shows spatial variability in thickness. The upper unit is thickest in the southwest measuring 75 m, whereas the lower unit is the thickest in south-central Manitoba measuring 53.4 m. The Carman Sand is restricted to a small area in the south. Most of the Carman Sand exceeds 20 m in thickness, with certain areas of the lens reaching up to 34.7 m near the City of Steinbach. Based on the structural maps, the Winnipeg Formation and all its lithological units dip toward the southwestern corner of the province. To the northeast, the Winnipeg Formation ascends to the surface along the boundary of the Williston Basin where it outcrops periodically. These trends allow to better constrain the thickness and distribution of the Winnipeg Formation, which is essential for future economic development.

In Brief:

- Mapping of the lithological units of the Winnipeg Formation in southern Manitoba shows variability in distribution of sand
- Map of the Carman sand outlines area for high-quality silica sand exploration

Citation:
Markstrom, V.L. 2024: Distribution of the lithological units of the Winnipeg Formation, southern Manitoba (NTS 62F–K, N–P); *in* Report of Activities 2024, Manitoba Economic Development, Investment, Trade and Natural Resources, Manitoba Geological Survey, p. 185–191.

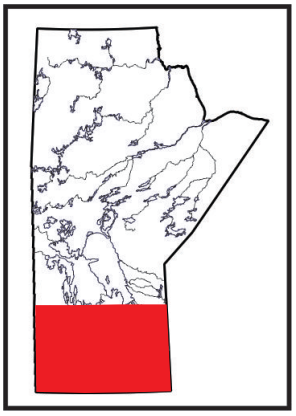
Introduction

Due its high quality, the silica sand derived from the Ordovician Winnipeg Formation can be used for a variety of industrial applications, including solar panels and proppant sand. Both the upper and lower units contain silica sand, but only the lower unit has been quarried in Manitoba to date. The extracted sand was primarily used to produce glass (Watson, 1985). Renewed interest in the high-quality silica sand of the Winnipeg Formation has resulted in exploration near the community of Seymourville and east of the City of Steinbach. Within the upper unit of the Winnipeg Formation, there is a decametres-thick horizon of unconsolidated silica sand, the Carman Sand (Figure GS2024-22-1), which has recently gained more attention as a potential source for proppant sand due to its optimal grain size, well-sorted nature, and sphericity and strength of the grains. Though the Winnipeg Formation has been studied in the past, renewed exploration has provided data from new drillholes and samples to study this unique formation.

The objectives of this study are to

1) map and re-evaluate the distribution of the Ordovician Winnipeg Formation and its lithological units across southern Manitoba;
2) highlight the difference between the spatial distribution of the upper and lower units;
3) map the basal sandstone bed of the lower unit and re-examine its economic potential; and
4) constrain the extent of the Carman Sand to help support future economic development.

Presented in this report are the preliminary isopach maps of the Winnipeg Formation, providing a visual presentation of its distribution and the difference between the spatial distribution of the lithological units.



Previous work

A report on the Ordovician stratigraphy of the Lake Winnipeg area was published by Baillie (1952), and included descriptions of outcrops of the Winnipeg Formation in the Hecla, Black Island and Punk Island area. In this report, Baillie (1952) informally divided the Winnipeg Formation into upper and lower units. The first comprehensive subsurface study was published by Andrichuk (1959),

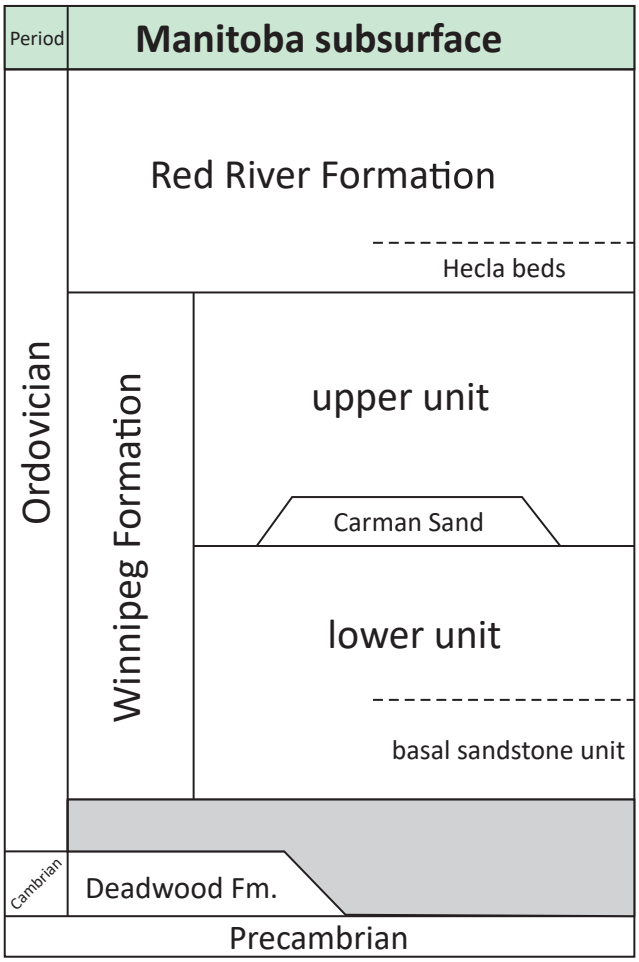


Figure GS2024-22-1: *Stratigraphic column of the lower Paleozoic in the subsurface of southern Manitoba.*

who constructed isopach and lithofacies maps for both units and identified the Carman Sand lens. Vigrass (1971) further studied the lithofacies of the Winnipeg Formation in Manitoba and Saskatchewan, providing detailed lithological descriptions and depositional environments for each unit. McCabe (1978) published a thorough investigation into the oil reservoir potential of the Cambrian Deadwood Formation and Ordovician Winnipeg Formation for southwestern Manitoba. This study included an extensive series of isopach and structure maps as well as a summary of the Cambrian–Ordovician paleogeography. The economic potential of silica sand was described by Watson (1985) who summarized the history, lithology and lithogeochemistry of various silica sand sources in Manitoba, including the lower unit of the Winnipeg Formation. Gale et al. (1993) examined the lithogeochemistry of lower unit samples taken from Black Island, recording the distribution of impurities after industrial processing. The most recent publication (Lapenskie, 2016) included an investigation of two Winnipeg Formation outcrops along the northern edge of the Williston Basin and an assessment of the lithogeochemistry of samples of the lower unit from three sites across Manitoba.

Regional geology and stratigraphy

The Winnipeg Formation is composed of interbedded quartz-rich sandstone and arenaceous shale, which were deposited in the Williston Basin during the Middle Ordovician. The formation is thickest in southern Manitoba, reaching up to 75 m, and pinches out to the north (McCabe, 1978). The Winnipeg Formation unconformably overlies the Precambrian basement except in the southwestern corner of the province, where it overlies the Cambrian Deadwood Formation (Figure GS2024-22-1). The Winnipeg Formation is conformably overlain by the Ordovician Red River Formation (McCabe, 1978). The basal beds of the Red River Formation, called the Hecla beds, represent a gradational change between the two formations (McCabe, 1978).

The Winnipeg Formation has been subdivided into upper and lower units. The lower unit is characterized by a basal single-blanket sandstone that extends throughout the Williston Basin and is thickest (4.6 m) in southern Manitoba (McCabe, 1978). This basal sandstone is capped by a thick layer of shale, which is then overlain by transitions of discontinuous sandstone (Figure GS2024-22-2a). The lower unit was deposited in shallow marine, intertidal to deltaic environments during the early stages of a transgressive cycle (Vigrass, 1971). The upper unit consists of a basal shale bed that transitions into a sequence of interbedded sand-shale layers trending northward (McCabe, 1978). It has been interpreted to be deposited in offshore to nearshore environments (McCabe, 1978). The Carman Sand occurs within the upper unit and has been described as a vestigial offshore sandbar (Vigrass, 1971). The Carman Sand consists of a fine- to medium-grained, well-sorted, well-rounded silica sand that is unconsolidated (Figure GS2024-22-2b).

The lithogeochemistry of the Winnipeg Formation sand differs between lithofacies and spatially within the Williston Basin. The SiO_2 concentration within the lower unit varies with the highest content of 95.2–98.9% occurring near Seymourville (Watson, 1985; Lapenskie, 2016). However, samples of the lower unit collected from other sites had values as low as 61.1% SiO_2 (Lapenskie, 2016). The lithogeochemistry of the Carman Sand is not currently available.

The Winnipeg Formation outcrops along a thin north-south-trending margin at the eastern edge of the Williston Basin roughly following the boundary of the Precambrian shield. Outcrops of the lower unit are documented near Seymourville, including Grindstone Point, Hecla, Punk Island and Black Island. Disseminated boulders of the lower unit can be found in the Victoria Beach area. The Winnipeg Formation outcrops along the northern edge of the Williston Basin as well, specifically around the Wekusko Lake to Athapapuskow Lake area, west-central Manitoba (Lapenskie, 2016).

Methodology

Well and drillcore data from the Williston Basin Targeted Geoscience Initiative (TGI) database (TGI Williston Basin Working

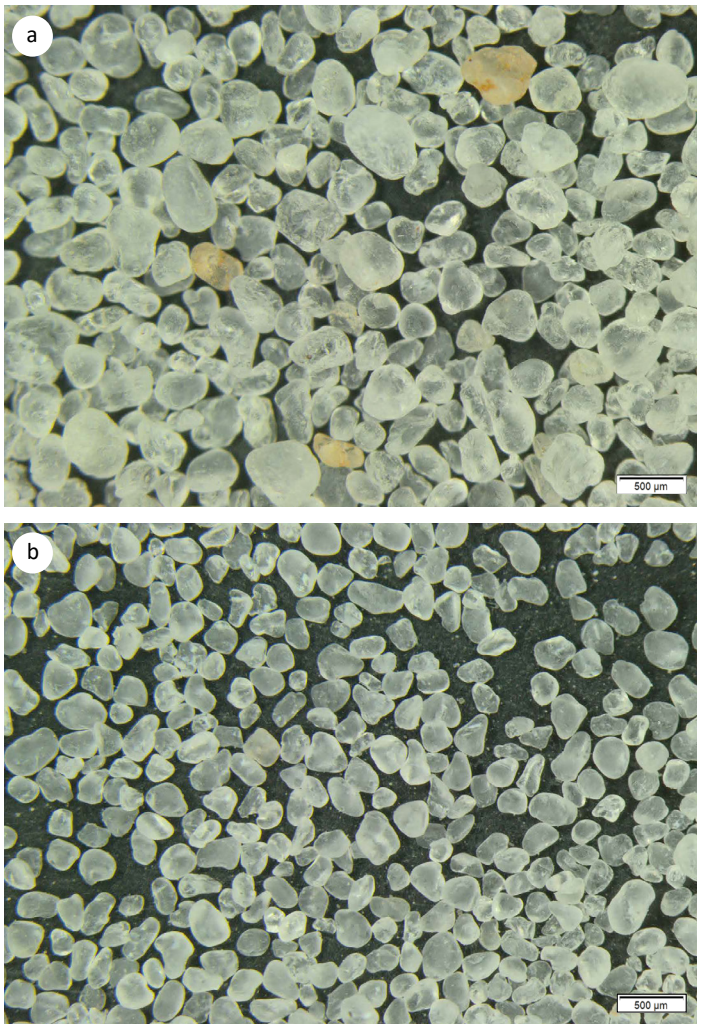


Figure GS2024-22-2: *Winnipeg Formation sand from* ***a)*** *the lower unit and* ***b)*** *the Carman Sand; note the abundant well-sorted, well-rounded silica grains in the Carman Sand.*

Group, 2008c) and the Manitoba Stratigraphic Database (MSD; Bezys and Conley, 1998) as well as borehole data extracted from assessment files in the Integrated Mining and Quarrying System (iMaQs; Manitoba Economic Development, Investment, Trade and Natural Resources, 2024) were compiled into a single dataset for this study. A series of isopach and structure maps were created using this dataset and were cropped to the Phanerozoic eastern edges of the Williston basin and to the region of interest (Twp. 1–30, Rge. 10E1–25W1) to focus on the area around the Carman Sand. Each map was computer generated using the Natural Neighbor tool in Esri® ArcGIS Pro. An isopach map of the upper unit without the Carman Sand data was constructed to identify the spatial boundary of the lens. A polygon of this area was made and then used to raster the maps of the Carman Sand to better constrain the sandbody.

Results

The Winnipeg Formation is thickest in the southern area of the province and has a distinctive east-west-trending lobate shape. The thickest section of the Winnipeg Formation is 75 m thick, northeast of the town of Melita. There are also thick areas of the Winnipeg Formation near the town of Ste. Rose du Lac. The Winnipeg Formation gradually thins toward the north but along the southeastern edge of Williston Basin it thins sharply. The isopach maps of the Winnipeg Formation constructed for this study are consistent with previously published TGI maps (TGI Williston Basin Working Group, 2008a).

For the lower unit, the thickest area occurs in south-central Manitoba close to the eastern boundary of the Williston Basin (Figure GS2024-22-3). The lower unit is 53.4 m thick south of the City of Winnipeg, with thick areas also occurring near the community of St. Marks and the town of Ste. Rose du Lac. There is distinctive thinning of the lower unit near the boundary of the overlying Carman Sand. The lower unit gradually thins along the edge of the Williston Basin except for the southeastern corner where it thins out abruptly.

The upper unit of the Winnipeg Formation thickens toward the southwestern corner of the province with the thickest (~75 m) near the town of Melita (Figure GS2024-22-4). The unit gradually thins to 5 m thick toward the edge of the Williston Basin. The upper unit also thins around the Carman Sand boundary and is particularly thin in patches south of the City of Winnipeg.

The Carman Sand is an asymmetrical teardrop-shaped lobe that trends east-west and narrows significantly toward the west (Figure GS2024-22-5). The lens is located exclusively in the south-central area of the province (Twp. 2–10, Rge. 8E1–16W1). Most of the lens is >20 m thick but can reach up to 34.7 m toward the eastern edge of the lobe, south of the City of Steinbach. There is a small patch of the Carman Sand approximately 33.4 m thick east of the local urban district of Ninette. The lens thins out along the northern and eastern boundaries but seems to abruptly truncate along the southwestern boundary.

The structure maps show that the Winnipeg Formation, its upper unit, the Carman Sand and its lower unit all dip toward the southwestern corner of the province. The Winnipeg Formation ascends to the surface toward the northern and eastern edges of the Williston Basin. The lower unit outcrops along this boundary, however, the Carman Sand pinches out before reaching the surface. The structure maps constructed for this project were consistent with previous research and didn't significantly differ from the TGI maps (TGI Williston Basin Working Group, 2008b).

Discussion

The isopach map of the Winnipeg Formation in this study is similar to previous research (McCabe, 1978) but by isolating each unit, clearer spatial differences between the upper and lower units, as well as the Carman Sand are apparent. Notably, the thickest part of the lower unit and the Carman Sand spatially coincide. However, the upper unit is thickest toward the southwestern portion of the province, where the Carman Sand pinches out. It is currently unclear if the thickened area of the lower unit

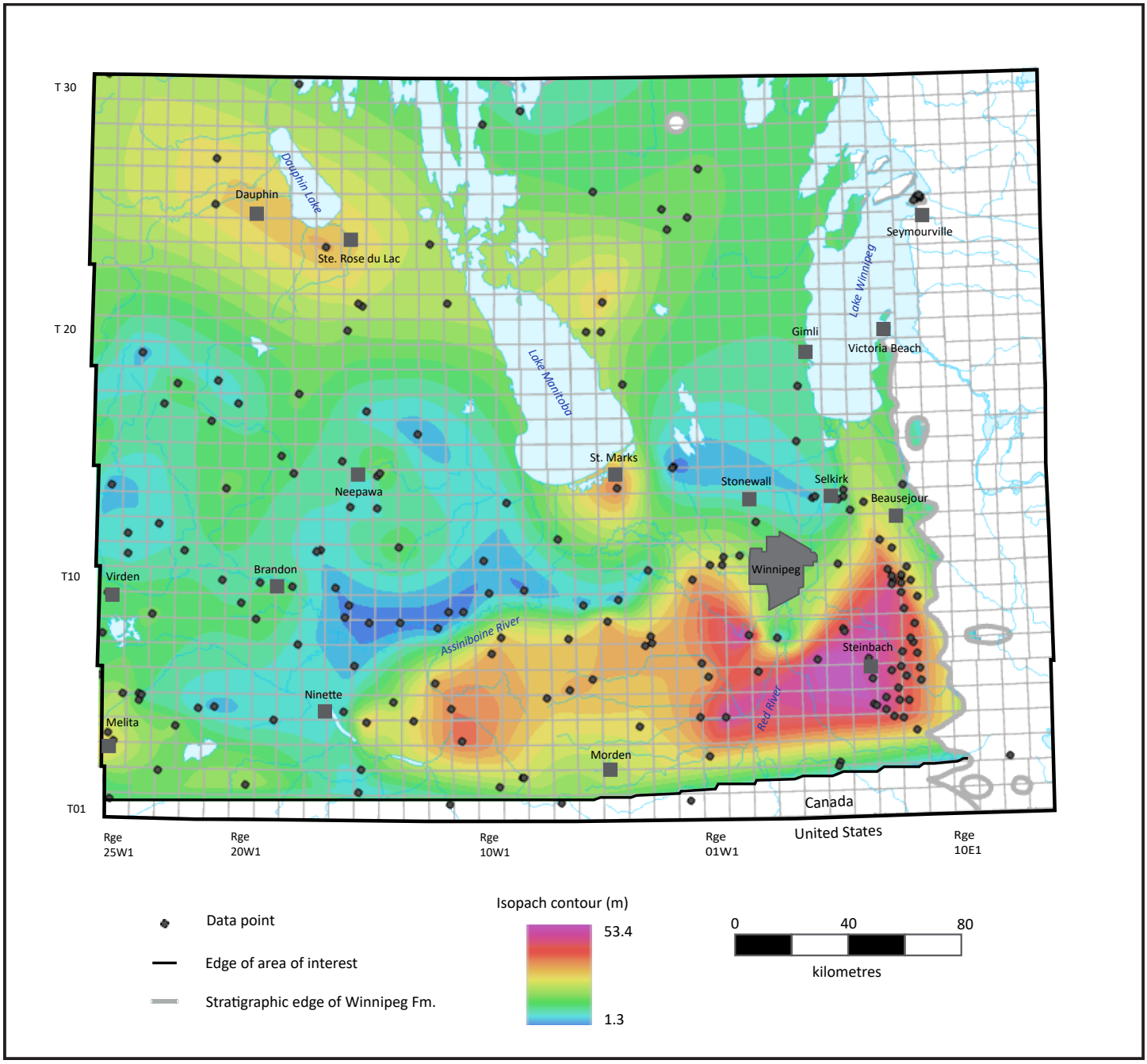


Figure GS2024-22-3: *Isopach map of the lower unit of the Winnipeg Formation in southern Manitoba. This preliminary map was constructed using a computer-generated model constrained to the project dataset. Data points from TGI Williston Basin Working Group (2008c). Basemap was created using ArcGIS® software by Esri. ArcGIS® is the intellectual property of Esri and is used herein under license. Copyright © Esri. All rights reserved. For more information about Esri software, please visit <https://esri.ca/>.*

was also deposited as a vestigial sandbar, as proposed for the Carman Sand (Vigrass, 1971), or if there are other structural controls from the Precambrian basement affecting the spatial distribution of the Winnipeg Formation. The Carman Sand appears to be consistently more than 20 m thick, with the thickest area (34.7 m) toward the eastern edge of the lens near the City of Steinbach. The Carman Sand also thickens to 33.7 m at the western edge of the lens but is spatially smaller than the thickened area along the eastern edge.

Future work

Refined mapping and lithological control of the Carman Sand toward the western edge of its distribution is required to confirm its spatial distribution across southern Manitoba. With this additional data, a more detailed isopach map for the Carman Sand will be constructed. This map will help identify new areas of economic potential for high-quality silica sand. Further work characterizing the sand quality and lithogeochemistry of the Carman Sand will also be done. The basal sandstone bed of the lower unit

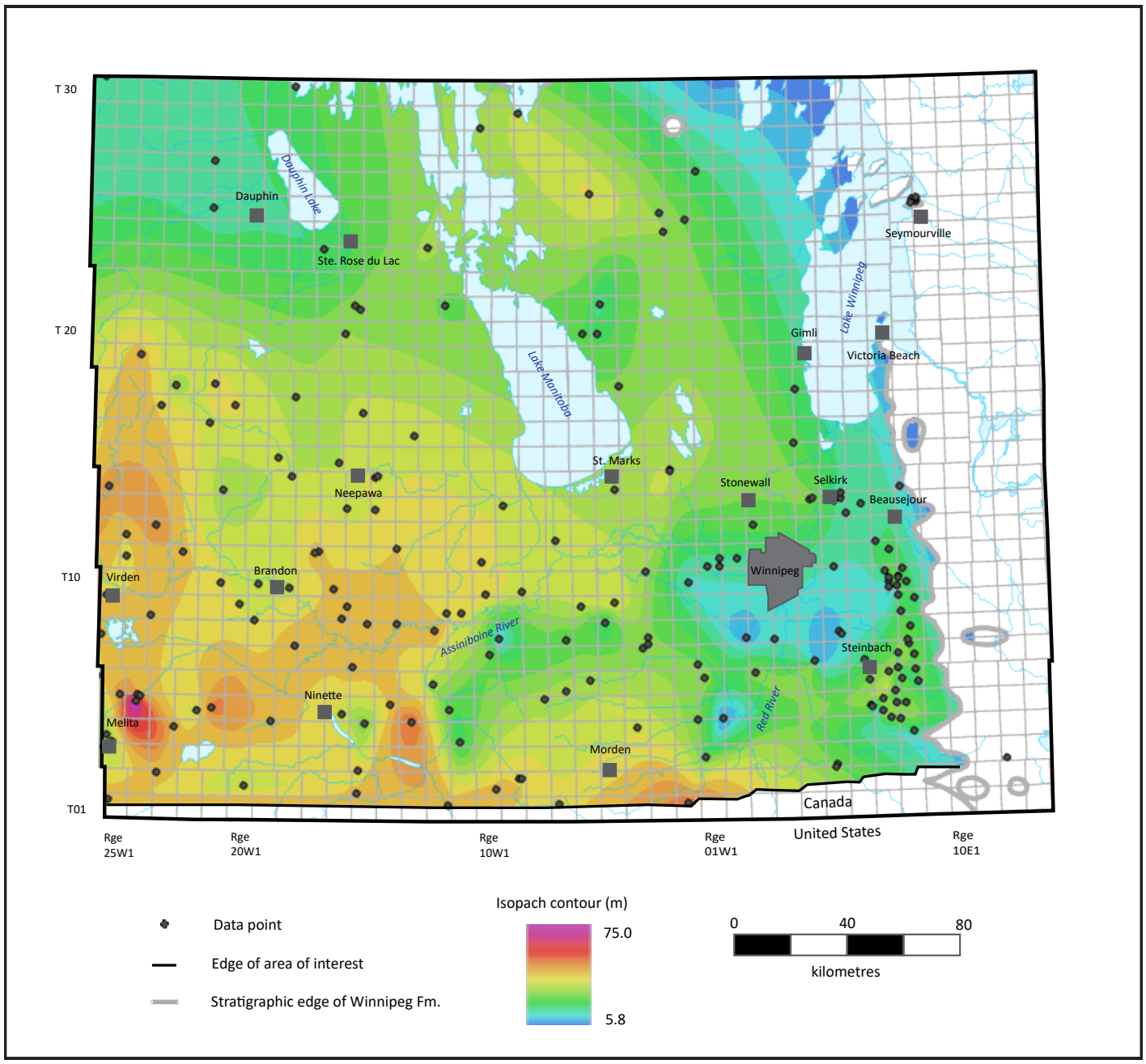


Figure GS2024-22-4: *Isopach map of the upper unit (including the Carman Sand) of the Winnipeg Formation in southern Manitoba. This preliminary map was constructed using a computer-generated model constrained to the project dataset. Data points from TGI Williston Basin Working Group (2008c). Basemap was created using ArcGIS® software by Esri. ArcGIS® is the intellectual property of Esri and is used herein under license. Copyright © Esri. All rights reserved. For more information about Esri software, please visit <https://esri.ca/>.*

is another potential economic source of silica sand and will be mapped to re-examine its distribution across Manitoba.

Economic considerations

Historically, the Winnipeg Formation has been extracted for glass production. However, silica sand has a wide range of industrial applications. In particular, recent development of the lower unit has focused on extracting this resource for solar panel production. The economic potential of the Carman Sand has also garnered interest. The high purity and quality of silica sand from the Carman Sand makes it an excellent candidate for producing high-quality proppant sand, which is currently in demand. As shown in this report, the distribution of the Carman Sand is irregular, therefore new mapping is needed to expand and refine the occurrence of this high-quality silica sand resource.

Acknowledgments

The author would like to thank M. Nicolas for sharing her knowledge of the Winnipeg Formation and Manitoba Phanero-

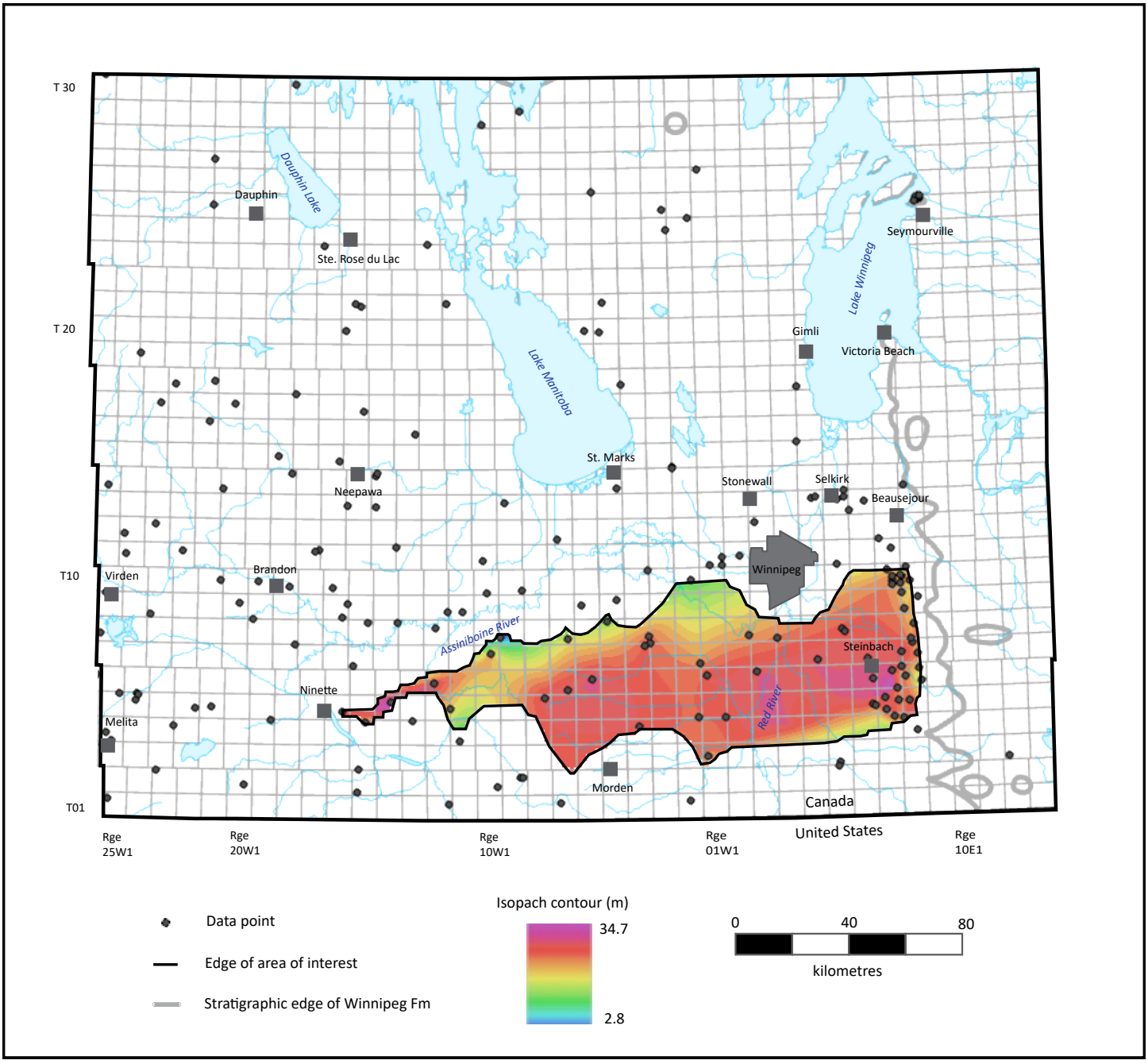


Figure GS2024-22-5: *Isopach map of the Carman Sand of the Winnipeg Formation in southern Manitoba. This preliminary map was constructed using a computer-generated model constrained to the project dataset. Data points from TGI Williston Basin Working Group (2008c). Basemap was created using ArcGIS® software by Esri. ArcGIS® is the intellectual property of Esri and is used herein under license. Copyright © Esri. All rights reserved. For more information about Esri software, please visit <https://esri.ca/>.*

zoic geology, and H. Adediran for his help in constructing all the maps for this report. Reviews of this report were provided by P. Fraino and M. Nicolas.

References

Andrichuk, J.M. 1959: Ordovician and Silurian stratigraphy and sedimentation in southern Manitoba; American Association of Petroleum Geologists Bulletin, v. 43, no. 10, p. 2333–2398.

Baillie, A.W. 1952: Ordovician geology of Lake Winnipeg and adjacent areas, Manitoba; Manitoba Department of Mines and Natural Resources, Mines Branch, Publication 51-6, 64 p., URL <https://1592.sydneyplus.com/genieplus/final/Download.aspx?template=Catalog&field=Website&record=1baecc28-514c-40b7-804c-f619fe735ebc&showSave=False&repeat=a1dfd2d2-9ecb-42ff-91c1-e3ce5c35d635> [October 2024].

Bezys, R.K. and Conley, G.G. 1998: Manitoba stratigraphic database and the Manitoba stratigraphic map series; Manitoba Energy and Mines, Geological Services, Open File Report OF98-7, CD-ROM.

Gale, G.H., Halden, N.M. and Mejia, S. 1993: High purity silica studies-geochemical and mineralogical studies of Winnipeg Formation silica sands; *in* Report of Activities 1993, Manitoba Energy and Mines, Minerals Division, p. 146–148.

Lapenskie, K. 2016: Preliminary investigations into the high-purity silica sand of the Winnipeg Formation, southern Manitoba; *in* Report of Activities 2016, Manitoba Growth, Enterprise and Trade, Manitoba Geological Survey, p. 176–180.

Manitoba Economic Development, Investment, Trade and Natural Resources 2024: iMaQs, Manitoba's Integrated Mining and Quarrying System; Manitoba Economic Development, Investment, Trade and Natural Resources, URL <https://manitoba.ca/iem/mines/imaqs/index.html> [September 2024].

McCabe, H.R. 1978: Reservoir potential of the Deadwood and Winnipeg formations, southwestern Manitoba; Manitoba Department of Mines, Resources and Environmental Management, Mineral Resources Division, Geological Paper GP78-3, 54 p.

TGI Williston Basin Working Group 2008a: Ordovician Winnipeg Formation: isopach contour; Manitoba Science, Technology, Energy and Mines, Manitoba Geological Survey, Stratigraphic Map SM2008-OW-I, scale 1:1 000 000, URL <https://manitoba.ca/iem/geo/willistontgi/mapfiles/pdfs/055_ord_winnipeg_fm_iso.pdf> [October 2024].

TGI Williston Basin Working Group 2008b: Ordovician Winnipeg Formation: structure contour; Manitoba Science, Technology, Energy and Mines, Manitoba Geological Survey, Stratigraphic Map SM2008-OW-S, scale 1:1 000 000, URL <https://manitoba.ca/iem/geo/willistontgi/mapfiles/pdfs/055_ord_winnipeg_fm_str.pdf> [October 2024].

TGI Williston Basin Working Group 2008c: Williston Basin TGI database, lower Paleozoic data; Manitoba Science, Technology, Energy and Mines, Manitoba Geological Survey, URL <https://manitoba.ca/iem/geo/willistontgi/database.html> [October 2024].

Vigrass, L.W. 1971: Depositional framework of the Winnipeg Formation in Manitoba and eastern Saskatchewan; *in* Geoscience Studies in Manitoba, A.C. Turnock (ed.), Geological Association of Canada, Special Paper 9, p. 225–234.

Watson, D.M. 1985: Silica in Manitoba; Manitoba Energy and Mines, Geological Services, Economic Geology Report ER84-2, 35 p.

GS2024-23

Preliminary observations from the Manson Field's Reston-Amaranth-Lodgepole oil reservoir, southwestern Manitoba (part of NTS 62K)

by P.J. Fulton-Regula

Summary

The Reston-Amaranth-Lodgepole pool in the Manson Field produces oil from a continuous reservoir spanning the Mississippian Lodgepole Formation to the Jurassic Lower Melita Member of the Melita Formation in Manitoba. The Manson Field currently has 101 producing oil wells and a total cumulative production of 888 223 m^3 of oil. Producing formations within this reservoir are primarily the Mississippian Lodgepole Formation and Middle Jurassic Reston Formation mudstone, wackestone and packstone intervals. Other productive intervals include siliceous layers and sandstone sequences.

The rocks in this interval display sedimentary, postdepositional, diagenetic and structural characteristics that suggest enhanced fluid movement and faulting may have influenced the reservoir thickness, composition, sulphide precipitation, oil location and the potential for local oil generation. Unusual features observed in the core include isolated sandstone units, breccia zones, anhydrite dissolution, siliceous layers, sulphide precipitation and enhanced porosity development. Further work will be conducted to better understand this reservoir, the structural regime of the area and the potential for critical minerals and new oil accumulations within the sedimentary succession of Manitoba.

In Brief:

- Oil production is predominantly from the Lodgepole and Reston formations, with some production from the Amaranth and Melita formations
- Observations include evidence for enhanced fluid movement in proximity to a north-northwest trending lineament and siliceous breccia zones

Citation:
Fulton-Regula, P.J. 2024: Preliminary observations from the Manson Field's Reston-Amaranth-Lodgepole oil reservoir, southwestern Manitoba (part of NTS 62K); *in* Report of Activities 2024, Manitoba Economic Development, Investment, Trade and Natural Resources, Manitoba Geological Survey, p. 192–199.

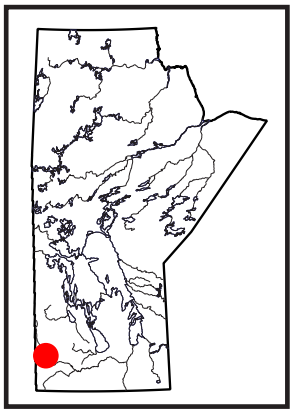
Introduction

The first oil discovery in the Manson Field was in 2009 (oil and gas well licence 7114, Manitoba Economic Development, Investment, Trade and Natural Resources, Winnipeg) in L.S. 12, Sec. 24, Twp. 13, Rge. 29 W 1st Mer. (abbreviated 12-24-13-29W1) in the Bakken Formation to Torquay Formation (Bakken-Torquay oil pools). In 2011, oil was discovered farther to the east and higher in the stratigraphic section in the well at 1-34-12-27W1 (oil and gas well licence 8288). Due to uncertainties in the geophysical log signatures, this productive interval was originally interpreted as the Mississippian Lodgepole Formation. After extensive core examination, the interpretation of the reservoir interval was revised and expanded upsection to include the Triassic to Jurassic Amaranth Formation and the Jurassic Reston Formation. However, it was clear that the reservoir and geology in this area was unusual and complex, and required further study.

There are currently 101 producing wells in the Reston-Amaranth-Lodgepole pools in the Manson Field with a cumulative oil production of 888 223 m^3 (Manitoba Economic Development, Investment, Trade and Natural Resources, unpublished data, 2024).

This study was undertaken to better understand the unique geology of the Reston-Amaranth-Lodgepole pools in the Manson Field. The objectives of this study are to

1) describe the lithological characteristics of the reservoir targets in the eastern extension of the Manson Field;
2) correlate core to geophysical log signatures to map the extent of reservoir units;
3) calibrate geophysical logs and create type sections to inform stratigraphic assignment of the reservoir and field-pool coding designations;
4) understand the depositional and postdepositional history of the Manson Field and how that history translates to other areas of Manitoba; and
5) understand the potential for further oil accumulations and critical mineral deposits.



Methodology

Between 2015 and 2024, 51 drillcore from Twp. 12 to 13 and Rge. 26 to 27W1 were examined (Figure GS2024-23-1). The core came from the Whitewater Lake Member of the Lodgepole Formation to the Lower Melita Member of the Melita Formation. These core were chosen based on the amount of core available within the formations of interest, their location within the study area and their avail-

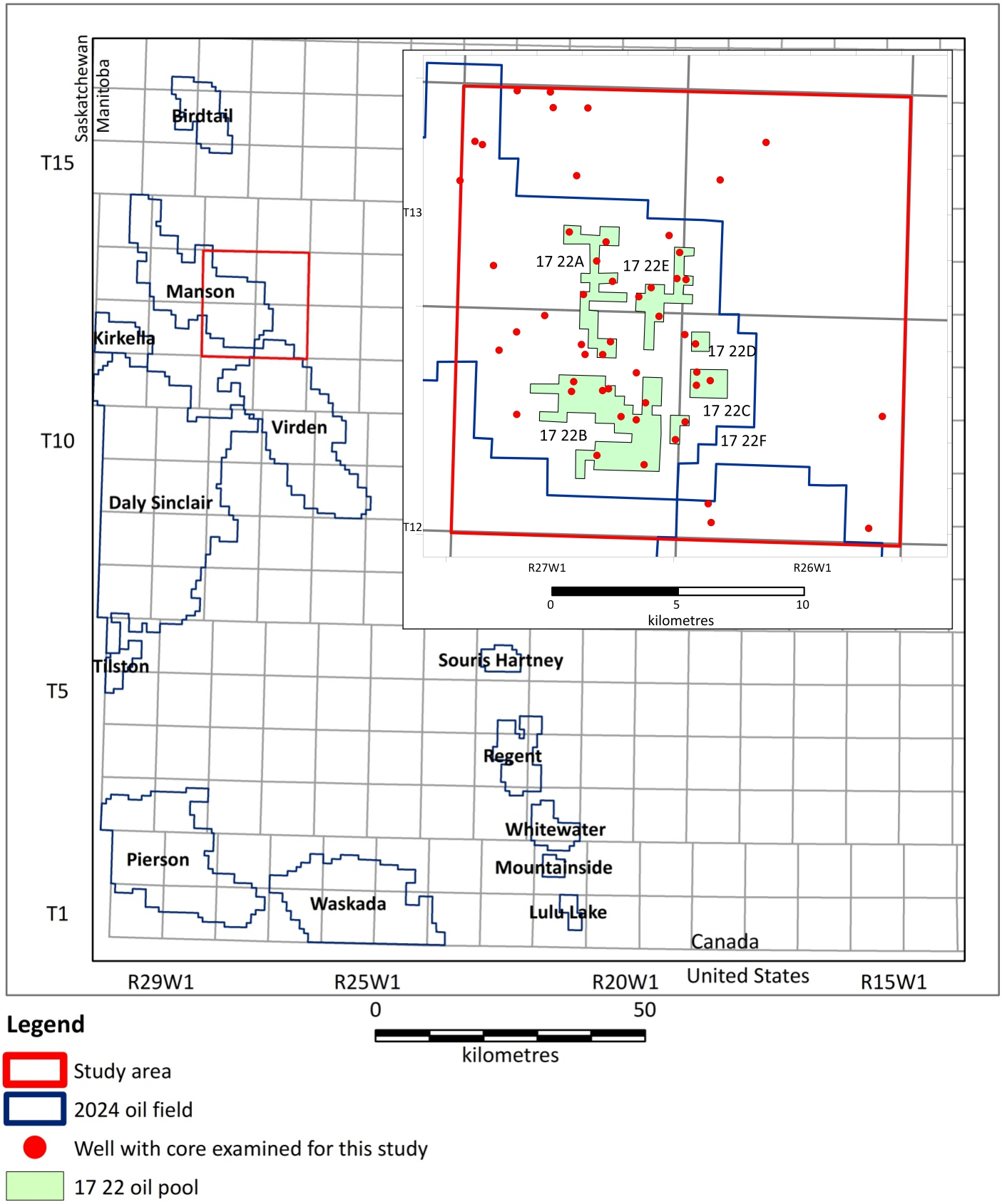


Figure GS2024-23-1: *Locations of the Manitoba oil fields, with the project area outlined in red (P.J. Fulton-Regula,* Manitoba's Designated Oil Fields and Pools 2024 (NTS 62F1–3, 6–11, 14–16, 62K1–3, 6–8)*, work in progress, 2024). Inset map shows the Reston-Amaranth-Lodgepole pools (17 22 field-pool codes; P.J. Fulton-Regula,* Manitoba's Designated Oil Fields and Pools 2024 (NTS 62F1–3, 6–11, 14–16, 62K1–3, 6–8)*, work in progress, 2024) and bottom-hole locations of wells with core examined for this study (geoLOGIC systems ltd., 2024).*

ability for viewing at the Manitoba Geological Survey Midland Sample and Core Library (Winnipeg, Manitoba). Core were thoroughly described and photographed.

Results

Lithological characteristics

Lodgepole Formation

In the study area, the Lodgepole Formation is characterized by the presence of a variably fossiliferous, yellow, pink, maroon and light grey, crystalline, calcareous wackestone to packstone, with occasional fine-grained, black laminations and zoned siliceous layers and nodules. Fossils present include crinoids, solitary corals, gastropods and brachiopods. Rare anhydrite layers occur at the top of the formation; these were identified in the wells at 3-34-12-27W1 and 3-30-12-26W1.

In the well at 13-10-13-27W1, the Whitewater Lake Member underlies the Flossie Lake Member of the Lodgepole Formation. The Whitewater Lake Member consists of a light green, silty, calcareous mudstone and wackestone and light pink and beige calcareous packstone, with anhydrite, dark grey nodular siliceous clasts, white siliceous layers, brachiopods and crinoids. In the well at 6-3-13-27W1, where the overlying Flossie Lake Member is absent, the Whitewater Lake Member is composed of yellow and beige mudstone with zoned white chalky- to black-rimmed siliceous layers, and siliceous fracture infill. It is overlain by pink and grey layered, calcareous mudstone with occasional brachiopods. Porosity is intergranular to intercrystalline and >10% fracture porosity within siliceous layers. Oil staining occurs in the wackestone and siliceous layers.

Where the Flossie Lake Member is present, it is a highly variable, layered, cream, pink, yellow, beige and grey, dolomitic mudstone, wackestone or packstone with anhydrite layers, and includes *Ophiomorpha*, solitary corals, brachiopods and crinoids. Also present are siliceous layers that are yellow with orange rims at the top of the member, with the layers becoming white and more homogeneous with increasing depth. Porosity is intergranular to intercrystalline and fracture oil staining was observed in light beige mudstone to wackestone. No sulphides were noted in the Flossie Lake Member where anhydrite is present. Where the Flossie Lake Member does not have anhydrite, the siliceous layers are generally white to grey with black rims, porosity is >10% vuggy and mouldic with fractures, often with oil staining and sulphides.

The contact between the Lodgepole Formation and the Amaranth Formation in Manitoba is recognized as an unconformable surface; it can be a sharp marker on geophysical well logs.

Lower Amaranth Member, Amaranth Formation

The Lower Amaranth Member of the Amaranth Formation is up to 5 m thick and consists of a nonfossiliferous, grey to beige and red, layered, dolomitic mudstone to siltstone, which contains zoned grey to black siliceous layers and clasts. Rare red siliceous layers occur in places. Porosity is vuggy, fracture and mouldic around siliceous layers; no obvious porosity was recorded in the mudstone of the Lower Amaranth Member. Oil staining around siliceous layers and clasts is common. In certain areas, the Lower Amaranth Member is green, with occasional slickensides on surfaces, and brecciated siliceous layers that occur as rubble in core.

With decreasing red colour and increasing anhydrite upsection, the Lower Amaranth Member has a gradational contact with the Upper Amaranth Member. To maintain consistency across pre-existing stratigraphic datasets and to respect the geophysical log pick in Nicolas (2009), this contact has been placed beneath the first anhydrite layer seen in geophysical logs, where present.

Upper Amaranth Member, Amaranth Formation

The Upper Amaranth Member of the Amaranth Formation is up to 38 m thick, and consists of nonfossiliferous, bedded, beige calcareous to green dolomitic mudstone, with dominantly grey to white, occasionally yellow and orange, crystalline anhydrite or gypsum. The anhydrite and gypsum are massive at the base of the member, becoming beds and nodules in grey to beige calcareous mudstone near the top. This mudstone can have siltstone and fine-grained black laminations; zoned grey to black siliceous layers; dispersed, zoned, grey to black, siliceous clast layers; and pink gypsum. Where anhydrite and gypsum are absent, the mudstone is dolomitic and often appears as green rubble with residual siliceous layers and clasts, and slickensides on surfaces.

Porosity is generally <0.1% intercrystalline to pinpoint, but also <10% vuggy and fracture within and around siliceous layers and clasts. Oil staining occurs in association with vuggy and fracture porosity. Sulphides were noted around interpreted anhydrite clasts, along bedding planes, in nodules and lining vugs and fractures.

For this report, the top of the Upper Amaranth Member of the Amaranth Formation is characterized by the first appearance of evaporitic, massive anhydrite beds. This is a good geophysical log marker, however, this pick becomes difficult to make when evaporites are not present in the section. Current work suggests that there may be a gradational contact between the grey and beige calcareous mudstone of the Reston Formation and the beige calcareous and green dolomitic mudstone of the Amaranth Formation.

Reston Formation

In the study area, the Reston Formation is a 0.3–52.5 m thick, light beige to light grey and green, nonfossiliferous, calcareous mudstone to medium-grained calcareous sandstone. At the base of the formation, it is often dolomitized with zoned grey to black siliceous layers and nodules. These layers and nodules were brecciated and worked to varying degrees upsection to produce breccia, conglomerate with angular to rounded clasts, subangular to subrounded pebble layers (often noted at a distance from the

siliceous layers) and grey chert sandstone with rounded grains (at the top of formation).

Porosity in the grey chert sandstone beds is primarily intergranular, <2%, whereas the siliceous layers and breccia exhibit vuggy, fracture and mouldic porosity. Oil staining is associated with 0.01–2% intergranular and <5% fracture porosity. Sulphides were noted within fractures, along bedding contacts and crosscutting bedding. Additionally, slickensides were noted in a green mudstone with siliceous clast rubble.

In the study area, the top of Reston Formation was picked in core at a light beige to light grey and green, nonfossiliferous, calcareous mudstone to medium-grained calcareous sandstone. This core pick corresponds to the geophysical log signature seen in Nicolas (2009). The Reston Formation has a conformable gradational contact with the Melita Formation.

Lower Melita Member, Melita Formation

In the study area, the Lower Melita Member of the Melita Formation is 46–205 m thick and is composed of greenish-grey to brown, beige and black, calcareous mudstone or shale with conchoidal fractures, as well as bivalve packstone, calcareous siltstone, and brown and grey sandstone. The mudstone can contain occasional bivalves, muscovite mica flakes, wood and swelling clays.

Toward the base of the Lower Melita Member, the grey to white and green sandstone to siltstone and mudstone typically form fining-upward cycles. These cycles show reworking of the siliceous layers from angular siliceous breccia in a mud matrix, through conglomerate to fine-grained, crossbedded sandstone to siltstone (with rounded grains) and mudstone. The siliceous layers, breccia and conglomerate can exhibit <10% vuggy and fracture porosity and in the sandstone, <5% intergranular porosity. Oil staining has been noted in the sandstone.

Higher in the section the variably consolidated, noncalcareous, brown sandstone can contain bivalves, muscovite mica flakes, sulphides, lignite and wood fragments. Porosity is intergranular, <10%, and the sandstone can have a faint petroleum smell. It is uncertain if the brown colour in this sandstone is due to oil staining.

Fining-upward sequences in the Lower Melita Member were recorded in 12 wells. The full sequence was not always observed due to core availability and distance from competent siliceous layers, but in general the sequence starts at the base with siliceous layers, breccia and conglomerate, and grades vertically to sandstone and then mudstone. Coarsening-upward sequences, from mudstone to sandstone, were recorded in two wells. Additional work is required to better categorize the units within this formation, map their extent and characterize their relationship with the underlying Reston Formation.

Preliminary observations from core

Siliceous layers

In the study area, five siliceous layers were identified from the Lodgepole Formation to the Lower Melita Member. These siliceous layers, which are chalky in places, exhibit colour zoning from black (or rarely red) to grey and brown (when oil stained), orange, yellow and beige to white. The colour zoning noted was typically observed as a light core to a darker rim. Where anhydrite was present in the Lodgepole Formation, siliceous layers and nodules were yellow with orange rims. Where the anhydrite was absent from the Lodgepole to Melita formations, the siliceous layers and nodules were typically white to grey with dark grey or black rims.

These siliceous layers exhibit varying degrees of brecciation. Where anhydrite is present in the Lodgepole Formation, these layers were not brecciated. Where the anhydrite is absent from the Lodgepole Formation to the Lower Melita Member, the siliceous layers exhibit varying degrees of brecciation. A progression from zoned siliceous layers (base of unit) to breccia with angular fragments, conglomerate with subangular to subrounded clasts, subrounded pebble layers (often noted at a distance from siliceous layers) and grey chert sandstone with rounded grains (top of unit) was noted.

Further work is required to understand their genesis and to map these layers in the study area.

Evidence for dissolution, recrystallization and remobilization

In the study area, there is evidence for enhanced fluid movement throughout the section studied, including

- inconsistent dolomitization, overprinting of the original texture and recrystallization in the mudstone, wackestone and packstone of the Amaranth and Reston formations and some parts of the Lodgepole Formation;
- absence of anhydrite in the Lodgepole and Amaranth formations;
- stylolites in the Lodgepole Formation where anhydrite is absent;
- vuggy and fracture porosity development in brecciated siliceous layers;
- vuggy and mouldic porosity development in the Lodgepole Formation;
- euhedral and crosscutting vein sulphides associated with siliceous layers of the Lodgepole, Amaranth and Reston formations;
- crosscutting sulphides in the light grey, laminated mudstone to siltstone of the Reston Formation; and
- bleaching of the Lodgepole Formation siliceous layers near fractures containing sulphides.

Local structure—evidence for faulting and subsidence

The core in the study area also records

- fining- and coarsening-upward cycles from the Amaranth to Melita formations;
- anhydrite and gypsum missing from the Amaranth Formation and Flossie Lake Member of the Lodgepole Formation;
- local thickening, thinning and nondeposition of portions of the Amaranth, Reston and Melita formations;
- slickensides on core surfaces;
- locally deposited 1 cm thick lignite and paleosol layers in the Lower Melita Formation; and
- green colouration in the mudstone and sandstone of the Amaranth and Reston formations.

Further, core logging results have revealed a north-north-west- to south-southeast-trending lineament between areas where the Amaranth Formation contains anhydrite or gypsum and where the Amaranth Formation is missing anhydrite and gypsum. In Figure GS2024-23-2, this lineament is plotted over the Reston Formation isopach contour map showing a thickened Reston Formation section striking along and to the west of this lineament. This lineament is currently interpreted as a fault. Further work is required to fully understand the extent of this structure and related subsidence and its relationship to other observed structures and core features.

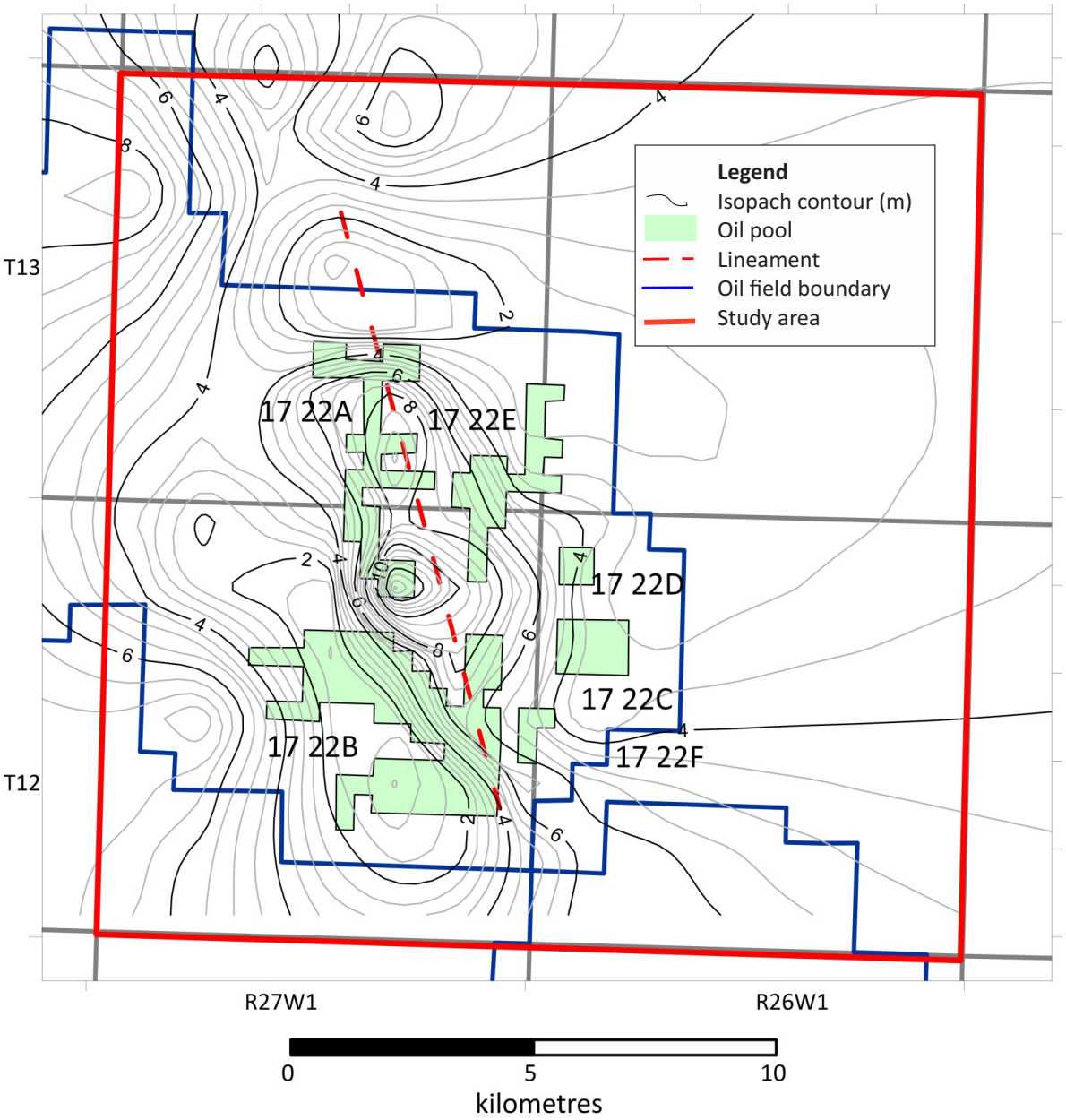


Figure GS2024-23-2: *Isopach contour map of the Reston Formation in the study area; contour interval is 0.5 m. Red dashed line indicates location of lineament separating the area where the Amaranth Formation is missing anhydrite and gypsum, on the west side, from the area where the Amaranth Formation contains anhydrite or gypsum, on the east side.*

Sulphides

In the study area, sulphides were noted from the Lodgepole Formation to Melita Formation. Preliminary interpretations indicate primary sulphide laminations occur from the Lodgepole Formation to Reston Formation, primary anhedral sulphide nodules occur in the Amaranth Formation, and synsedimentary sulphide layers and anhedral nodules occur in the Lower Melita Member of the Melita Formation. Secondary sulphides crosscut bedding and occur at bedding contacts and in fractures within brecciated siliceous layers in the Lodgepole, Amaranth and Reston formations. Euhedral sulphides were noted in the Amaranth Formation.

Reservoir units and oil production

Three main reservoir units have been identified in the Reston-Amaranth-Lodgepole pools of the Manson Field (Table GS2024-23-1):

1) mudstone, wackestone and packstone layers with intercrystalline to vuggy and mouldic porosity; these include Lodgepole Formation calcareous mudstone, wackestone and packstone intervals and Reston Formation calcareous mudstone with porosities of >2%
2) chert sandstone of the Reston Formation and brown sandstone of the Lower Melita Member of the Melita Formation with intergranular interpreted porosity, >5%
3) siliceous layers in the Lodgepole, Amaranth, Reston and Melita formations with interpreted vuggy and fracture porosity, >10%

The productive oil perforation distribution (Table GS2024-23-1) and faulting suggest that oil is primarily produced in the mudstone, wackestone and packstone intervals of the Lodgepole and Reston formations; and oil is also being produced from siliceous layers in the Amaranth, Reston and Melita formations and from sandstone in the Reston and Melita formations.

Table GS2024-23-2 lists the oil production by pool for the Reston-Amaranth-Lodgepole pools. Most oil production from the Reston-Amaranth-Lodgepole pools occurs in pools 17 22A and 17 22B, where anhydrite is absent from the Amaranth Formation. Limited oil has been produced from pools 17 22C–F where anhydrite is present in the Amaranth Formation.

Discussion and preliminary interpretations

Figure GS2024-23-2 shows the lineament interpreted as a fault between the Amaranth Formation that contains anhydrite or gypsum, on the east side, and the Amaranth Formation where the anhydrite and gypsum are missing, on the west side. This fault coincides with a thickening of the overlying Reston Formation, suggesting the dissolution of Amaranth Formation anhydrite in association with the fault resulted in the overlying Reston Formation infilling a depression on the Amaranth Formation surface.

The productive oil perforation distribution, shown in Table GS2024-23-1, suggests that oil is produced from mudstone, wackestone and packstone intervals of the Lodgepole and Reston formations; siliceous layers in the Amaranth, Reston and Melita formations; and sandstone of the Reston Formation and the

Table GS2024-23-1: Total perforation count in well casing separated by member/unit and oil pool designation for the Reston-Amaranth-Lodgepole pools of the Manson Field (Manitoba Economic Development, Investment, Trade and Natural Resources, unpublished data, 2024).

Formation	Unit	Field-pool code						Total perforations
		17 22A	17 22B	17 22C	17 22D	17 22E	17 22F	
Melita	Brown sandstone	0	0	0	1	0	0	1
	Siliceous layer	0	0	0	1	0	0	1
Reston	Undifferentiated	17	14	1	10	2	3	47
	Chert sandstone	1	0	0	0	0	0	1
	Siliceous layer	9	3	0	7	0	0	19
Amaranth	Upper Amaranth Mb.	0	0	0	0	0	0	0
	Siliceous layer	1	0	0	0	0	1	2
	Lower Amaranth Mb.	0	0	0	0	0	0	0
	Siliceous layer	0	0	0	0	0	0	0
Lodgepole	Undifferentiated	14	47	0	2	0	5	68

Table GS2024-23-2: The cumulative oil production by pool for the Reston-Amaranth-Lodgepole pools as of July 8, 2024 (Manitoba Economic Development, Investment, Trade and Natural Resources, unpublished data, 2024).

Field-pool code	17 22A	17 22B	17 22C	17 22D	17 22E	17 22F	Total
Number of wells	22	57	2	11	7	2	101
Average production by well (m^3)	6 215	11 689	445	5 508	3 315	277	8 794
Total production (m^3)	136 735	666 250	891	60 591	23 202	554	888 223

Lower Melita Member of the Melita Formation. Table GS2024-23-2 indicates that larger cumulative oil production comes from pools 17 22A and 17 22B, both of which occur where the Amaranth Formation anhydrite is absent (Figure GS2024-23-2). Smaller cumulative production has been achieved where the Amaranth Formation anhydrite is present. However, pools 17 22A and 17 22B have also been in production for longer than pools 17 22C–17 22F, so caution is required when interpreting these results. Although oil production from the Lodgepole Formation is common in the surrounding area, rare perforations in the Amaranth, Reston and Melita formations indicate oil production from stratigraphically higher formations may be possible where there is faulting, dissolution and subsidence. Further work is required to assess the source of this oil and its association with potential faulting.

The following characteristics suggest a diagenetic history of enhanced fluid flow in the study area:

- dissolution of anhydrite
- presence of synsedimentary sulphides
- presence of secondary sulphides crosscutting bedding and in fractures within brecciated siliceous layers
- bleaching of siliceous layers around fractures containing sulphides

Further work is necessary to determine the association of enhanced fluid flow with faulting, and if there is an associated increase in heat flow that may have resulted in local oil generation from mudstone and the emplacement of critical minerals.

In general, the depositional and diagenetic features observed in the Manson Field, from the Lodgepole to Melita formations, record a complex history of structural and fluid movement. Missing stratigraphic units, abrupt lithological changes with the deposition of siliceous layers, fining- and coarsening-upward sequences and sudden variations in formation thickness, all suggest a dynamic landscape of collapse, relative uplift and fluid movement during the deposition of the Amaranth, Reston and Melita formations. These processes may have played a role in new oil migration pathways, reservoir development and trapping features within the Manson Field.

Future work

This ongoing study has highlighted the need for the following work:

- update the Reston-Amaranth-Lodgepole pool name to include the Lower Melita Member of the Melita Formation
- correlate core picks of formation and unit contacts to surrounding uncored wells within and outside the study area using core-log correlation
- study the type sections of the Reston and Melita formations and determine how they differ from the sections in the Manson Field
- create updated isopach maps for the Lower Melita Member of the Melita Formation, Reston Formation, Amaranth Formation, Flossie Lake and Whitewater Lake members of the Lodgepole Formation, and map the distribution and thickness of the siliceous layers and sandstone in order to ascertain the extent and timing of faulting and how these relate to diagenetic processes in the study area
- update the Lodgepole Formation subcrop map, review the rock types in the formation and explore diagenetic processes, siliceous layer deposition and sulphide precipitation
- create normalized plots to properly assess oil production in relation to subsidence
- conduct Rock-Eval and total organic carbon (TOC) analyses of the Lower Melita Member mudstone to investigate its oil-generating potential
- conduct X-ray fluorescence (XRF) analysis of sulphides, siliceous layers and white minerals for critical minerals
- analyze thin sections of core samples to understand mineral textures and relationships, and explore the diagenetic history of this reservoir
- review and correlate the available porosity, permeability and oil density data for the oil reservoir, and cross-reference with the described lithologies

Economic considerations

Primary and secondary sulphides were noted in the study area in the Lodgepole, Amaranth, Reston and Melita formations. Further work is required to confirm the type and quantity of this mineralization and identify where critical minerals may be prospective in the sedimentary section of Manitoba.

The Manson Field hosts an oil reservoir that occurs in the youngest identified stratigraphic oil-containing horizon in Manitoba. Though oil in the Reston-Amaranth-Lodgepole pools is primarily produced in the Lodgepole and Reston formations, oil is also being produced higher in the stratigraphic section in proximity to an interpreted fault. This production suggests additional oil resources may be present higher in the section around faults and opens up the possibility of a new oil-play type in Manitoba.

Acknowledgments

The author would like to thank C. Epp and P. Belanger at the Manitoba Geological Survey Midland Sample and Core Library (Winnipeg, Manitoba); S. Tetteh and A. Maki (summer students) for their help with preparing the core for viewing and photographing the core; and M. Nicolas and J. Bamburak (Manitoba Geological Survey [emeritus]) for their geological support in this work. Thank you to the company geologists active in this area for seeing value in cutting cores and providing their ideas on this oil reservoir. This report was built on the work of others, thank you for increasing the understanding of this economically important

area. The author acknowledges P. Fraino and M. Nicolas for their thorough review of this report.

References

geoLOGIC systems ltd. 2024: geoSCOUT version 8.3.0.0; geoLOGIC systems ltd., URL <https://www.geologic.com/products/geoscout/> [September 2024].

Nicolas, M.P.B. 2009: Williston Basin Project (Targeted Geoscience Initiative II): summary report on Mesozoic stratigraphy, mapping and hydrocarbon assessment, southwestern Manitoba; Manitoba Science, Technology, Energy and Mines, Manitoba Geological Survey, Geoscientific Paper GP2009-1, 19 p.

GS2024-24

Reconnaissance-scale Quaternary geology investigations to support lithium exploration in southeastern Manitoba (parts of NTS 52L, M, 62P, 63A)

by T.J. Hodder and O.B. Lian[1]

In Brief:

- Investigating the glacial dispersal of detritus from known Li-bearing pegmatites in the Bird River area using multiple parameters
- Reconnaissance-scale sampling of till from Bloodvein to Pointe du Bois

Citation:
Hodder, T.J. and Lian, O.B. 2024: Reconnaissance-scale Quaternary geology investigations to support lithium exploration in southeastern Manitoba (parts of NTS 52L, M, 62P, 63A); *in* Report of Activities 2024, Manitoba Economic Development, Investment, Trade and Natural Resources, Manitoba Geological Survey, p. 200–208.

Summary

Quaternary geology investigations were conducted in southeastern Manitoba to map paleo–ice-flow indicators, collect till samples and document the surficial sediments. This study aims to document the till composition down-ice of known Li-bearing pegmatites in the Bird River area and investigate the potential for additional Li-bearing pegmatites in the region. The 2024 field season focused on completing a reconnaissance-scale sampling transect from the First Nation community of Bloodvein to Pointe Du Bois. Preliminary results from till samples collected in 2022–2023 indicate that spodumene recovery in till accurately reflects the location of known Li-bearing pegmatites in the Bird River area. There are at least six phases of paleo-ice flow, with the dominant ice-flow direction toward the southwest to west-southwest (230–250°). This study will provide guidance on till prospecting in Manitoba for Li-bearing pegmatites and a framework for understanding dispersal patterns in southeastern Manitoba.

Introduction

Geological surveys in Canada are conducting studies to better understand Li-bearing pegmatites and improve exploration methods to find new occurrences, including till prospecting best practices (Hagedorn and Beckett-Brown, 2023; Brushett et al., 2024; McClenaghan et al., 2024). As part of this initiative, the Manitoba Geological Survey (MGS) is conducting a multidisciplinary Precambrian and Quaternary geology project focusing on the Bird River area of the Superior province in southeastern Manitoba (Hodder and Martins, 2023; Martins et al., 2023). In 2024, the scope of the Quaternary geology-based fieldwork expanded to include a reconnaissance-scale study of the till composition between the First Nation community of Bloodvein and Pointe du Bois (Figure GS2024-24-1).

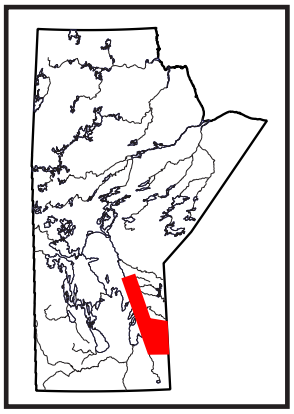
The goals of the Quaternary geology component of this study area are to

- map paleo–ice-flow indicators to assist reconstructions of the glacial history, which in turn guides till prospecting studies;
- assess the suitability of till-matrix geochemistry and indicator minerals to characterize the dispersal of detritus from known Li-bearing pegmatites in the Cat Lake area; and
- collect till samples at a reconnaissance-scale to gauge the prospectivity of the region for additional Li-bearing pegmatites.

Methods

A total of 140 field stations were visited over a 14-day period in 2024 to document the Quaternary sediments, collect till samples and measure the orientation of ice-flow indicators, bringing the total number of field stations visited from 2022–2024 to 279. The surficial materials at each field station were investigated by means of a hand-dug shovel hole, a Dutch auger (1.2 m long) hole, gravel pit or roadcut/trailcut exposure.

The primary goal of till sampling in 2024 was to collect samples (where possible) at a reconnaissance-scale (approximately every 5–7 km) using road access, from the First Nation community of Bloodvein to Pointe Du Bois (Figure GS2024-24-1). In addition, further till sampling was conducted around the Eagle and F.D. No. 5 Li-bearing pegmatites in the Cat Lake area to better constrain dispersal patterns from these known Li occurrences and further investigate the elevated gold grain counts in till sampled in 2022 and 2023 (Hodder, 2024b). Lastly, till previously sampled along the east-side road contained two spodumene grains that were confirmed by Raman spectroscopy (Hod-



[1] University of the Fraser Valley, Abbotsford, British Columbia

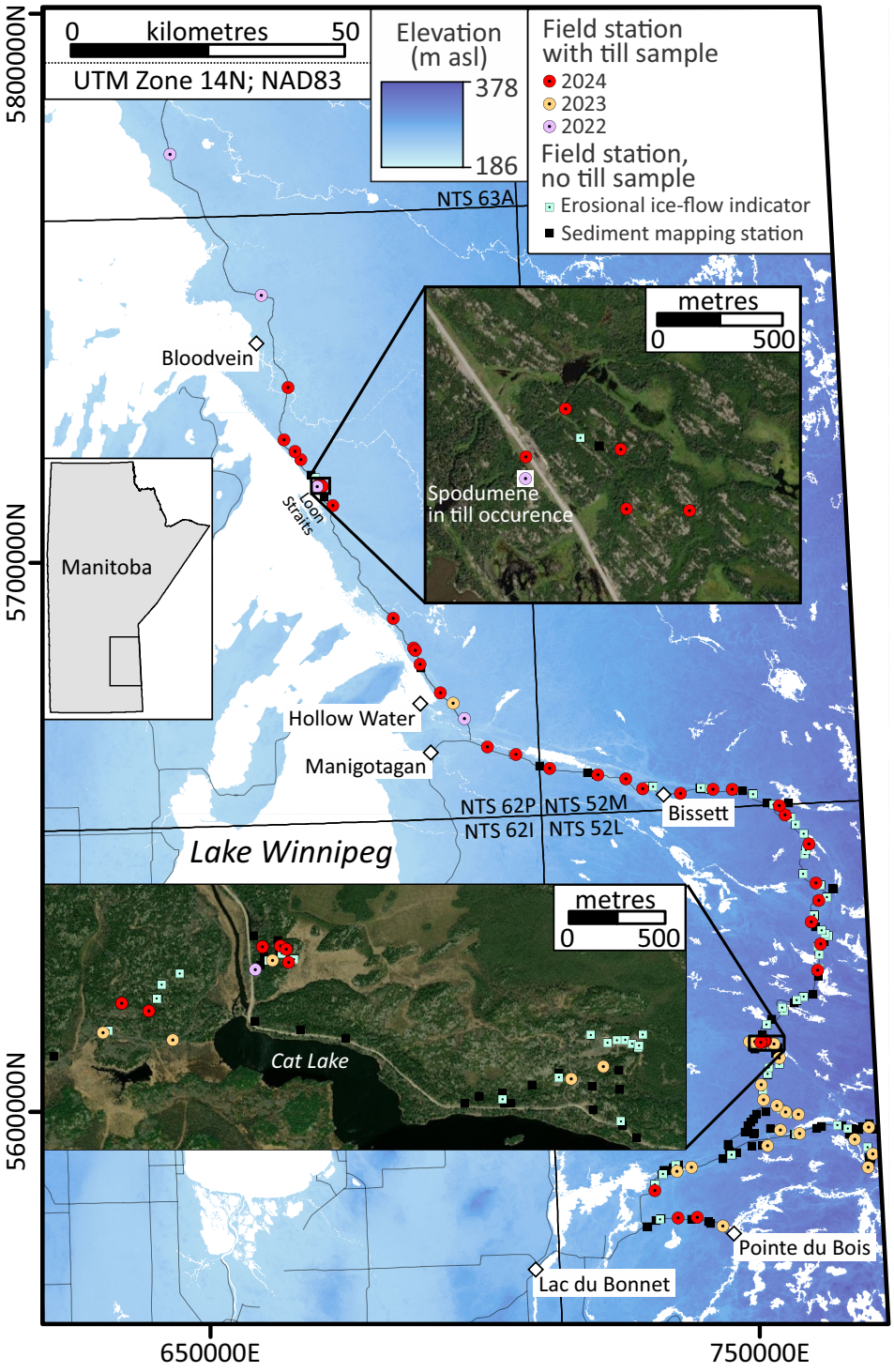


Figure GS2024-24-1: *Location of stations visited in southeastern Manitoba as part of this study. Background elevation data is provided by Earth Observation Research Center and Japanese Aerospace Exploration Agency (2022). Basemap imagery was created using ArcGIS® software by Esri. ArcGIS® and ArcMap™ are the intellectual property of Esri and are used herein under license. Copyright © Esri. All rights reserved. For more information about Esri software please visit <https://esri.ca/>.*

der and Martins, 2023; Hodder, 2024b). This was unexpected since there are no known Li-bearing pegmatites in the area and the potential for Li mineralization is considered to be low with no known occurrences in the region (Rinne, 2023a, b); however, till-matrix Li and Cs values are elevated in the region (Hodder and Martins, 2023). To further assess the lithium potential of the region, follow-up till sampling was conducted in the vicinity of the spodumene in till occurrence east of Loon Straits (Figure GS2024-24-1).

Till samples were collected at 41 stations during the 2024 field season at depths ranging from 0.3 to 3.7 m below the natural land surface, adding to the 29 till samples collected in

2022 and 2023 (Hodder and Martins, 2023; Hodder, 2024b, c). At each site, a smaller ~2–3 kg sample and a larger ~14–16 kg sample were collected from diamicton interpreted as till (Evans, 2018). Unmodified C-horizon till is the preferred sample material (n = 23 of 41), though in cases of thin till where C-horizon diamicton was not present or of limited thickness, samples collected consist of a mix of B- and C-horizon diamicton (n = 17 of 41) or B-horizon diamicton (n = 1 of 41). At one site, samples of both the B- and C-horizon till were taken to compare the matrix geochemistry. The 2–3 kg till samples were split for archival purposes at the MGS Midland Sample and Core Library (Winnipeg, Manitoba) and will be analyzed for matrix grain size and geochemistry. The 14–16 kg samples were submitted to Overburden Drilling Management Limited (Ottawa, Ontario) for gold counts and indicator-mineral analyses (metamorphic massive-sulphide–indicator minerals [MMSIMs®] and lithium-indicator minerals), as well as the recovery of clasts for lithological classification.

Erosional paleo–ice-flow indicators, such as striae, grooves, crescentic gouges and chattermarks, were mapped at bedrock outcrops within the study area. The relative-age relationships at outcrops that exhibited multiple paleo–ice-flow indicators were deciphered using the crosscutting and outcrop relationships of facets and striae (McMartin and Paulen, 2009; e.g., Figure GS2024-24-2). A clast-fabric measurement in till was completed at one stratigraphic section along the east-side road, where the long-axes orientation (trend and plunge) of 32 elongated clasts, defined by a minimum 1.5:1.0 ratio of the a-axis (longest) to the b-axis (middle), were measured. These elongated clasts tend to rotate within the till matrix and orient parallel to the overlying glacier's shear stress direction (Holmes, 1941; Hicock et al., 1996).

Preliminary results

Till sampling in 2024

The entire study area was inundated by glacial Lake Agassiz following retreat of the Laurentide Ice Sheet from southeastern Manitoba (Fisher and Breckenridge, 2022; Gauthier et al., 2022). This large proglacial lake remobilized fine-grained material (clay, silt and sand) in till deposits, leaving a lag at the surface that consists of interlocked cobble- to boulder-sized clasts. To access unmodified till, the lag surface needs to be excavated and the proportion of silt and clay within the sediment needs to be assessed. In many areas with thin till cover, the extent of post-glacial modification was extensive, and the till was completely eroded, or entirely reworked leaving a clast lag and/or sandy gravel (~0.1–0.7 m thick). Where possible, roadcuts or trailcuts were used to sample till below the lag surface at depth and till was most commonly found encountered on the lee-side of bedrock outcrops (e.g., Figure GS2024-24-3a, b). At the station scale, there is significant spatial variability of till preservation and careful attention to elevation and vegetation, specifically investigating both the high and low terrains, is necessary to increase till sampling efficiency.

Spodumene and Li concentrations in till

In the Bird River area, spodumene {$LiAlSi_2O_6$} grains were recovered from till samples collected in 2022–2023 down-ice of known Li-bearing pegmatites (Figure GS2024-24-4a, b; Hodder, 2024b). The recovery of spodumene in glacial sediment provides a clear reflection of the known mineralization in the area. Problematically, the concentration of Li values in the till-matrix from the same samples is not elevated above background values (Figure GS2024-24-4a, b; Hodder, 2024c). The three highest values of Li in till matrix are all situated up-ice of known Li-related surface occurrences (Figure GS2024-24-4b). Following receipt of the 2024 analytical results, a more detailed analysis of the till composition will be conducted to further examine the relationships between spodumene grain recovery, different size fractions of till-matrix analyzed, analytical digestions used and pathfinder elements.

Ice-flow history

Erosional ice-flow indicators were mapped at 49 field stations during the 2024 field season (Hodder, 2024a[2]). Striations and grooves account for the majority of documented erosional paleo–ice-flow indicators, with minor observations of crescentic gouges and chattermarks. Six phases of ice flow are interpreted based on relative-age relationships observed in the study area (Figure GS2024-24-5). The erosional record is dominated by south-southwest to west-southwest trending paleo–ice-flow indicators that were formed during the final two phases of ice flow that the region experienced (phases e and f) and outcrops in the region are typically moulded toward the southwest. However, there are older ice-flow events that can be deciphered within the erosional record. These include ice-flow events toward the west to west-northwest (phase a, 260–285°), south to south-southwest (phase b, 180–196°), west-southwest (phase c, 252–260°) and east-southeast to south-southeast (phase d, 105–155°). Relative age-relationships indicate that phase a is older than phases c, d, e and f. In the field, no relative-age relationships were observed between phases a and b, or between phase b and phases c and d. This complicates resolving the relative-age relationship between some of these older ice-flow events. Future work will synthesize these observations with previous studies to provide a regional ice-flow reconstruction (Henderson, 1994; Gauthier and Hodder, 2020; Matile et al., 2023).

[2] MGS Data Repository Item DRI2024010, containing the data or other information sources used to compile this report, is available online to download free of charge at https://manitoba.ca/iem/info/library/downloads/index.html, or on request from minesinfo@gov.mb.ca, or by contacting the Resource Centre, Manitoba Economic Development, Investment, Trade and Natural Resources, 360-1395 Ellice Avenue, Winnipeg, Manitoba R3G 3P2, Canada.

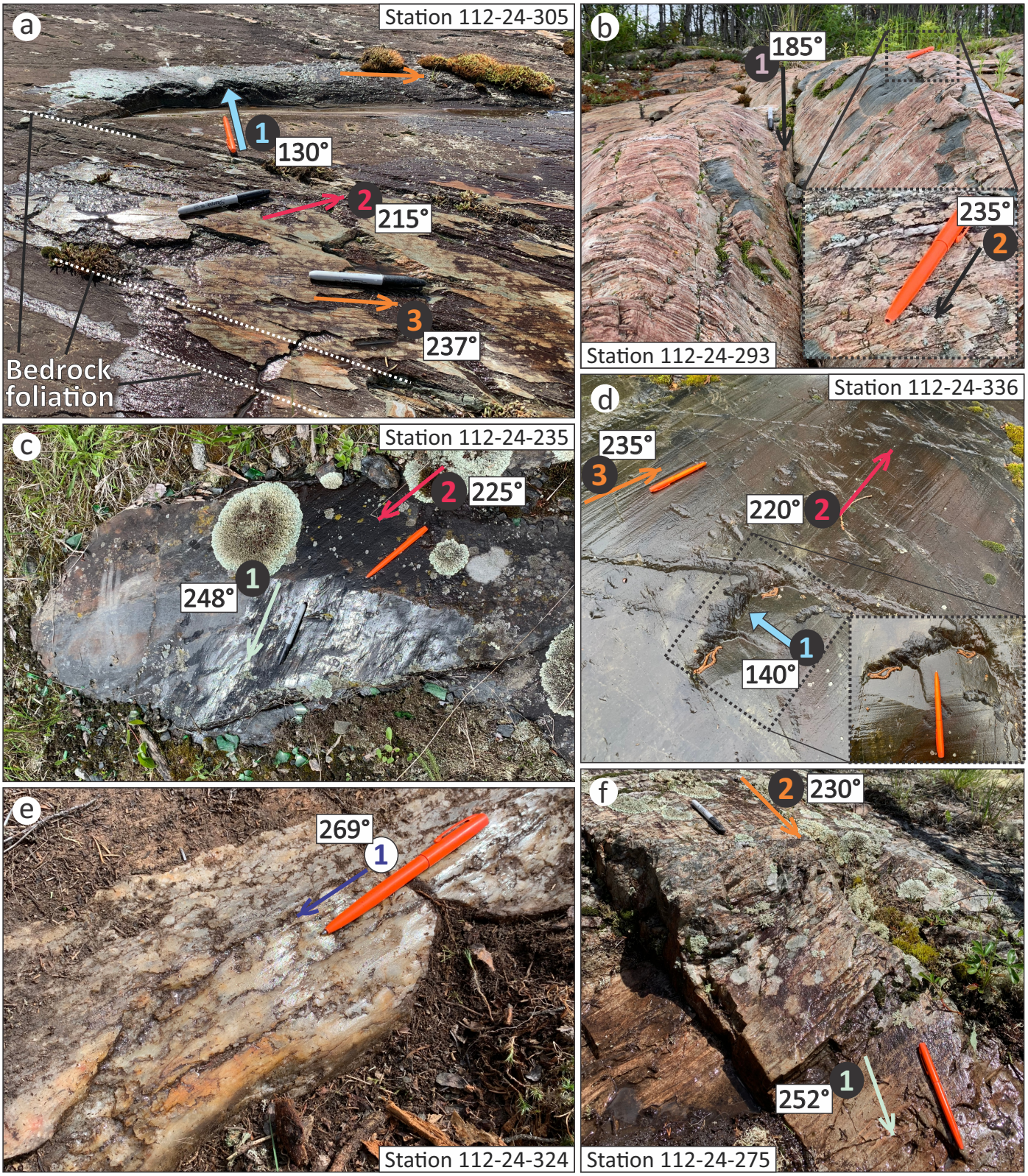


Figure GS2024-24-2: *Examples of erosional ice-flow indicators and the relative age-relationships observed in the study area:* ***a)*** *an older southeast-trending (130°) crescentic gouge is preserved on the upper surface of an outcrop where southwest-trending (215°) striations are crosscut by west-southwest-trending (237°) striations;* ***b)*** *south-trending (185°) striations and grooves are preserved on a protected trough from later southwest-trending (235°) striations and grooves;* ***c)*** *west-southwest-trending striations (248°) are preserved on a protected facet from later southwest-trending (225°) striations;* ***d)*** *an older southeast-trending (140°) crescentic gouge is preserved on the upper surface of an outcrop where southwest-trending striations and grooves (220°) are crosscut by southwest-trending (235°) striations and grooves;* ***e)*** *west-trending (269°) striations are preserved on a protected step from west-southwest-trending (239°) grooves on the uppermost surface of the outcrop (not shown);* ***f)*** *west-southwest-trending (252°) striations are preserved on a protected step from southwest-trending (230°) striations.*



Figure GS2024-24-3: *Examples of field stations where unmodified till was sampled:* ***a)*** *roadcut at station 112-24-249 where till below the clast lag was sampled at depth; the white arrows indicate boulders that form a lag surface over the till deposit;* ***b)*** *aerial and ground view of the roadcut at station 112-24-231 where till was sampled on the lee-side (southwest side, down-ice) of a prominent bedrock outcrop. Basemap imagery in (b) was created using ArcGIS® software by Esri. ArcGIS® and ArcMap™ are the intellectual property of Esri and are used herein under license. Copyright © Esri. All rights reserved. For more information about Esri software please visit <https://esri.ca/>. Abbreviation: R, bedrock.*

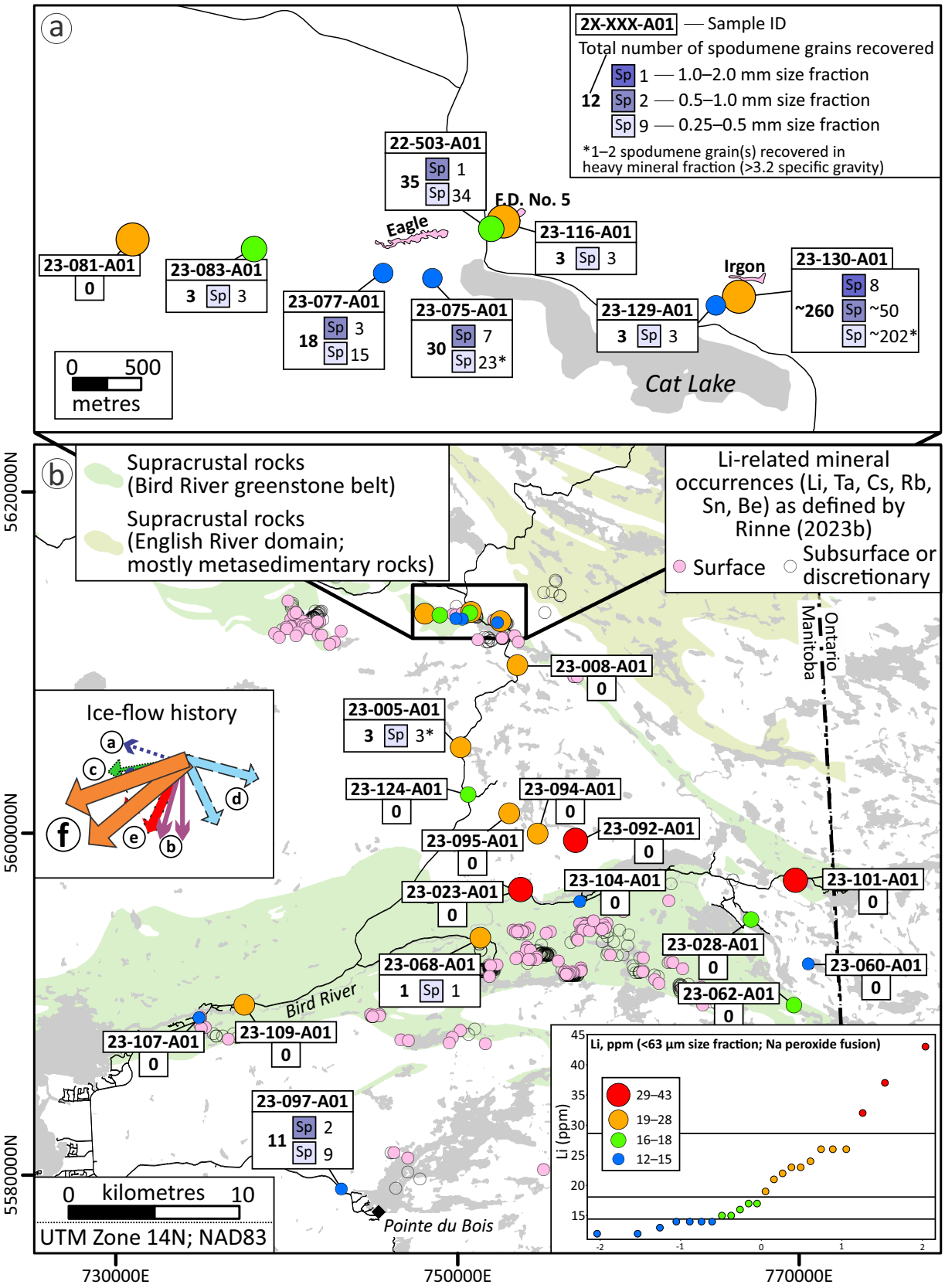


Figure GS2024-24-4: *Till-matrix spodumene counts (0.25–2.0 mm size fraction) and lithium concentrations (<63 µm size fraction) for samples analyzed in 2023 from the Bird River area:* ***a)*** *till samples around Li-bearing pegmatites (pink polygons) in the Cat Lake area, location shown in b);* ***b)*** *regional-scale till samples in the Bird River greenstone belt area. Till-composition data presented are available in Hodder (2024b, c). For clarity, the background geology (modified from Manitoba Geological Survey, 2022) has been simplified to show only supracrustal-dominant and mafic-intrusive units (i.e., approximate greenstone belt outlines).*

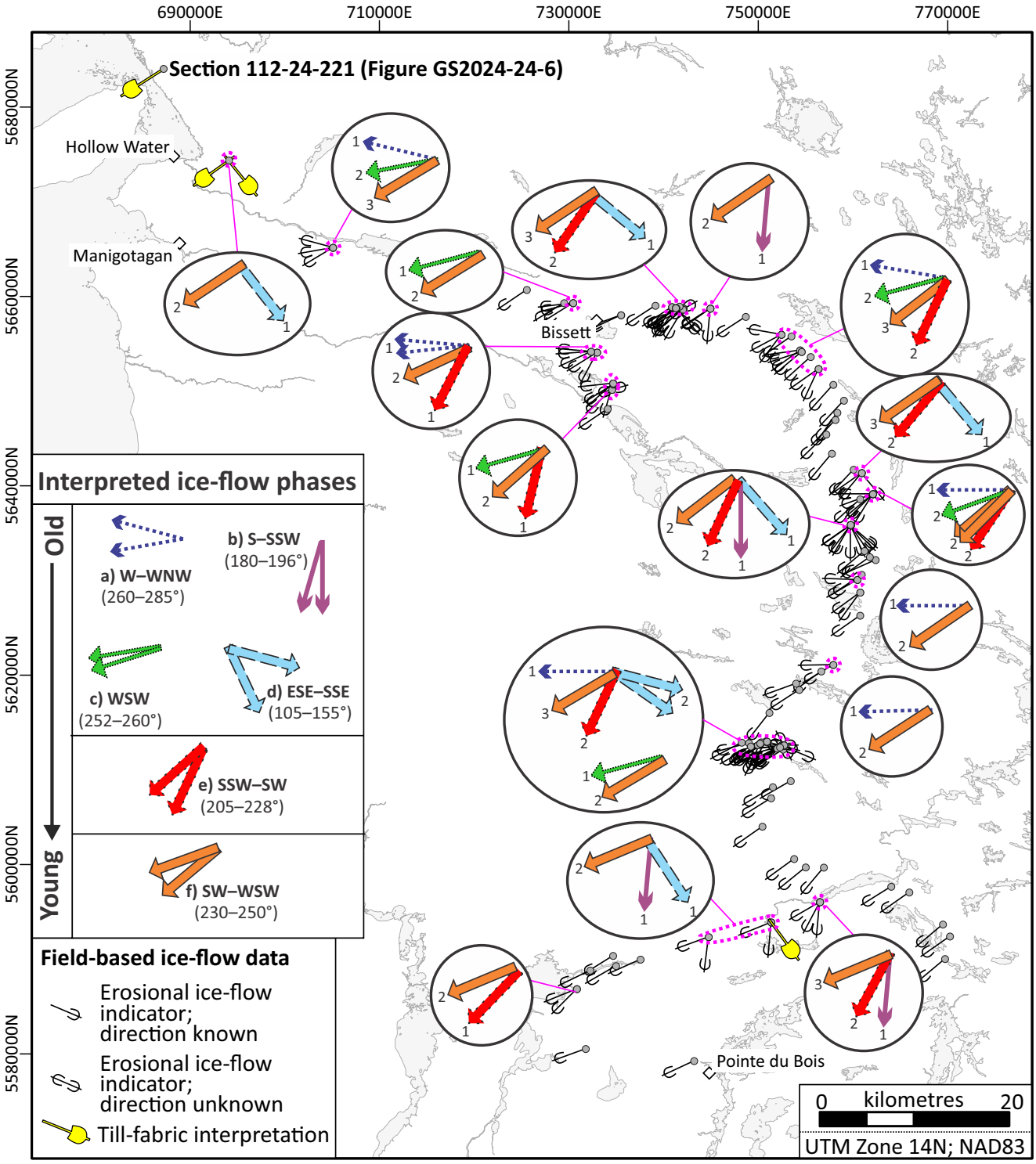


Figure GS2024-24-5: *Ice-flow–indicator data (relative-age relationships indicated) and an interpretation of the ice-flow phases in the study area.*

Importance of Quaternary stratigraphy

Erosional ice-flow indicators provide a relative-age relationship of ice-flow events but provide no indication of absolute timing. To assess the absolute timing of these ice-flow events, sorted sediments that were deposited during ice-free periods (underlying the glacial sediment) are an important stratigraphic constraint. These subtill stratigraphic beds can be dated using radiocarbon (if organics are present) or with optical dating of mineral grains. Understanding the timing of ice-flow events is important for improving spatiotemporal reconstructions of glacial dispersal, which in turn guides till prospecting.

Along the east-side road, two sites have subtill sorted sediments preserved on the lee-side (southwest side) of prominent bedrock outcrops. These sorted sediments are interpreted to

have been deposited during an ice-free period, possibly in a nearshore lacustrine depositional environment. At section 112-24-221 (Figure GS2024-24-6), there is ≥4.5 m of sand and gravel underlying till that drapes an undulating bedrock surface. Sand with crossbedding or horizontal bedding was sampled for optical dating to determine the timing of sediment deposition (Figure GS2024-24-6). The overlying till, qualitatively similar to the typical surficial till sampled across the study area, has a clast fabric that is interpreted to have formed by southwest-trending ice flow. As such, the southwest-trending clast fabric is tentatively correlated to the youngest mapped erosional ice-flow phase (phase f; Figure GS2024-24-5).

Economic considerations

Spodumene was successfully recovered from till sampled down-ice of known Li-bearing pegmatite occurrences in 2022

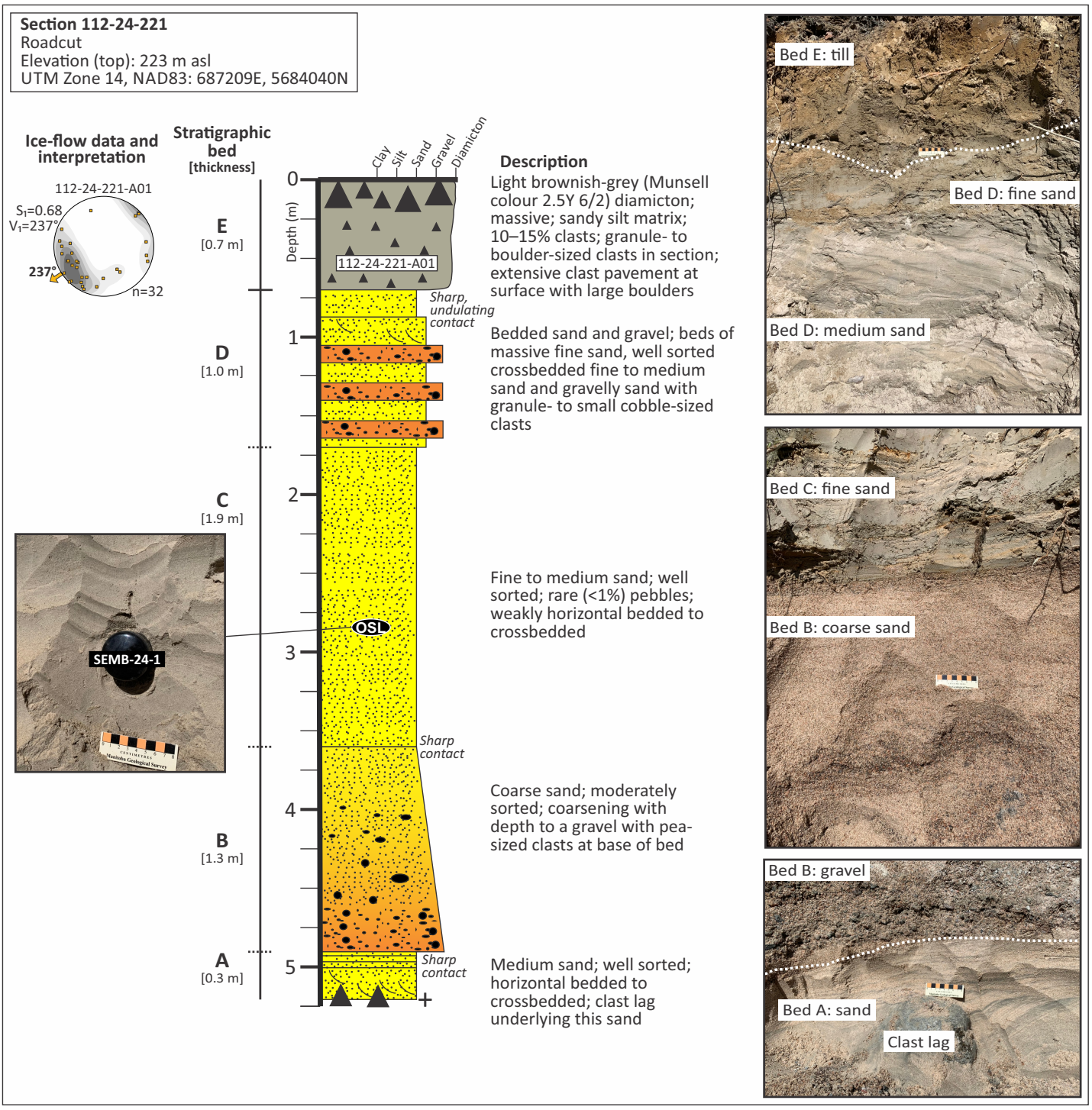


Figure GS2024-24-6: *Quaternary stratigraphy at section 112-24-221. See Figure GS2024-24-5 for location in the study area. Abbreviations: OSL, optically stimulated luminescence sample site; S_1, principal eigenvalue; SEMB-24-1, sample number; V_1, principal eigenvector.*

and 2023 (Hodder et al., 2024b). This highlights the effectiveness of indicator-mineral counts for identifying regions with Li-bearing pegmatites, which can be applied elsewhere in the province. Fieldwork in 2024 sampled till for lithium-indicator minerals at a reconnaissance-scale between the First Nation community of Bloodvein and Pointe du Bois, which will provide insight into the potential for lithium mineralization across this region. Furthermore, the 2022–2023 recovery of gold, euxenite, parisite, scheelite, molybdenite, chromitite and gahnite from till samples (Hodder et al., 2024b) reflects the region's diverse mineral potential, including critical minerals, that is being further evaluated with the analyses of the 2024 till samples.

Acknowledgments

The authors thank S. Bergen, A. Martin and J. Kristoff for field assistance. Logistical support from C. Epp and P. Belanger is appreciated. M. Gauthier and M. Nicolas are thanked for reviewing this report.

References

Brushett, D.M., Beckett-Brown, C.E., McClenaghan, M.B., Paulen, R.C., Rice, J.M., Haji Egeh, A. and Pelchat, P. 2024: Till geochemical data for the Brazil Lake pegmatite area, southwest Nova Scotia (NTS 21-A/04, 20-O/16 and 20-P/13): samples collected in 2020, 2021, and 2022; Geological Survey of Canada, Open File 9148, 35 p.

Earth Observation Research Center and Japanese Aerospace Exploration Agency 2022: ALOS Global Digital Surface Model; Earth Observation Research Center and Japanese Aerospace Exploration Agency, ALOS World 3D - 30m, URL <https://www.eorc.jaxa.jp/ALOS/en/dataset/aw3d30/aw3d30_e.htm> [March 2022].

Evans, D.J.A. 2018: Till: A Glacial Process Sedimentology; John Wiley & Sons Ltd, Chichester, United Kingdom, 400 p., URL <https://doi.org/10.1002/9781118652541>.

Fisher, T.G. and Breckenridge, A. 2022: Relative lake level reconstructions for glacial Lake Agassiz spanning the Herman to Campbell levels; Quaternary Science Reviews, v. 294, art. 107760.

Gauthier, M.S. and Hodder, T.J. 2020: Surficial geology mapping from Manigotagan to Berens River, southeastern Manitoba (parts of NTS 62P1, 7, 8, 10, 15, 63A2, 7); *in* Report of Activities 2020, Manitoba Agriculture and Resource Development, Manitoba Geological Survey, p. 41–46.

Gauthier, M.S., Breckenridge, A. and Hodder, T.J. 2022: Patterns of ice recession and ice stream activity for the MIS 2 Laurentide Ice Sheet in Manitoba, Canada; Boreas, v. 51, p. 274–298.

Hagedorn, G.W. and Beckett-Brown, C.E. 2023: Till sampling and surficial mapping in the Georgia Lake area, northwestern Ontario; *in* Summary of Field Work and Other Activities, 2023, Ontario Geological Survey, Open File Report 6405, p. 23-1 to 23-9.

Henderson, P.J. 1994: Surficial geology and drift composition of the Bissett-English Brook area, Rice Lake greenstone belt, southeastern Manitoba; Geological Survey of Canada, Open File 2910, 43 p.

Hicock, S.R., Goff, J.R., Lian, O.B. and Little, E.C. 1996: On the interpretation of subglacial till fabric; Journal of Sedimentary Research, v. 66, p. 928–934.

Hodder, T.J. 2024a: Field-based ice-flow–indicator data collected during the 2023 and 2024 field seasons in southeastern Manitoba (parts of NTS 52L, M, 62P); Manitoba Economic Development, Investment, Trade and Natural Resources, Manitoba Geological Survey, Data Repository Item DRI2024010, Microsoft® Excel® file.

Hodder, T.J. 2024b: Gold and indicator-mineral data derived from glacial sediments (till) in southeastern Manitoba (parts of NTS 52L, 62P, 63A); Manitoba Economic Development, Investment, Trade and Natural Resources, Manitoba Geological Survey, Data Repository Item DRI2024004, Microsoft® Excel® file.

Hodder, T.J., 2024c: Till-matrix geochemistry data from the 2022–2023 field seasons in southeastern Manitoba (parts of NTS 52L, 62P, 63A); Manitoba Economic Development, Investment, Trade and Natural Resources, Manitoba Geological Survey, Data Repository Item DRI2024003, Microsoft® Excel® file.

Hodder, T.J. and Martins, T. 2023: Current Quaternary geology investigations in southeastern Manitoba and implications for mineral exploration (parts of NTS 52L, 62P, 63A); *in* Report of Activities 2023, Manitoba Economic Development, Investment, Trade and Natural Resources, Manitoba Geological Survey, p. 105–119.

Holmes, C.D. 1941: Till fabric; Geological Society of America, Bulletin 52, p. 1299–1354.

Manitoba Geological Survey 2022: New edition of the 1:250 000 scale Precambrian bedrock geology compilation map of Manitoba; Manitoba Natural Resources and Northern Development, Manitoba Geological Survey, GeoFile 3-2022, scale 1:250 000.

Martins, T., Rinne, M.L., Breasley, C. and Adediran, H. 2023: Preliminary results from field investigations in the Bird River domain of the Archean Superior province, Manitoba (parts of NTS 52L5, 6, 11, 12); *in* Report of Activities 2023, Manitoba Economic Development, Investment, Trade and Natural Resources, Manitoba Geological Survey, p. 4–13.

Matile, G.M., Thorleifson, L.H., Hodder, T.J. and Martin, A.B. 2023: Field-based ice-flow data collected during the 1998 NATMAP II field season, southeastern Manitoba (parts of NTS 52L, 62I); Manitoba Economic Development, Investment and Trade, Manitoba Geological Survey, Data Repository Item DRI2023002, Microsoft® Excel® file.

McClenaghan, M.B., Brushett, D.M., Beckett-Brown, C.E., Paulen, R.C., Rice, J.M. and White, C.E. 2024: Indicator-mineral signatures of the Brazil Lake lithium-cesium-tantalum pegmatites, southwest Nova Scotia (parts of NTS 20-O/16, 20P/13, 21A/04, and 21B/01); Geological Survey of Canada, Open File 9189, 57 p.

McMartin, I. and Paulen, R.C. 2009: Ice-flow indicators and the importance of ice-flow mapping for drift prospecting; *in* Application of Till and Stream Sediment Heavy Mineral and Geochemical Methods to Mineral Exploration in Western and Northern Canada, R.C. Paulen and I. McMartin (ed.), Geological Association of Canada, Short Course Notes 18, p. 15–34.

Rinne, M.L. 2023a: Progress report on the Manitoba Mineral Deposits Database; *in* Report of Activities 2023, Manitoba Economic Development, Investment, Trade and Natural Resources, Manitoba Geological Survey, p. 1–3.

Rinne, M.L. 2023b: Updates to the Manitoba Mineral Deposits Database; Manitoba Economic Development, Investment, Trade and Natural Resources, Manitoba Geological Survey, GeoFile 5-2023, Microsoft® Excel® file.

GS2024-25

Quaternary site data, till composition and ice-flow indicators between the North Knife River and the Seal River, and in the Gross Lake area, far northeastern Manitoba (parts of NTS 54L10–15, 54M5, 6, 12)

by M.S. Gauthier and S. Bergen[1]

In Brief:

- Surficial mapping west and northwest of Churchill
- Collection of till samples to determine provenance and till-exploration potential, including for diamonds, gold, lithium and other critical minerals
- Collection of ice-flow data to reconstruct the glacial history and aid till exploration
- Update of the relative sea level history

Citation:
Gauthier, M.S. and Bergen, S. 2024: Quaternary site data, till composition and ice-flow indicators between the North Knife River and the Seal River, and in the Gross Lake area, far northeastern Manitoba (parts of NTS 54L10–15, 54M5, 6, 12); *in* Report of Activities 2024, Manitoba Economic Development, Investment, Trade and Natural Resources, Manitoba Geological Survey, p. 209–218.

Summary

Quaternary geology fieldwork, including till sampling and ice-flow–indicator mapping, was conducted in a 2700 km^2 area between the North Knife River and the Seal River, and in a 865 km^2 area around Gross Lake, far northeastern Manitoba (parts of NTS 54L10–15, 54M5, 6, 12) to infill gaps within existing mapping. A total of 66 two kilogram till samples were collected for grain-size, geochemical (<63 µm size fraction) and clast-lithology (2–8 mm size fraction) analyses. At 55 of these 66 sample sites, an additional 14–16 kg was collected for indicator-mineral analysis. In addition, eight marine shell samples were collected for radiocarbon dating, to update the postglacial rebound (isostatic uplift) history.

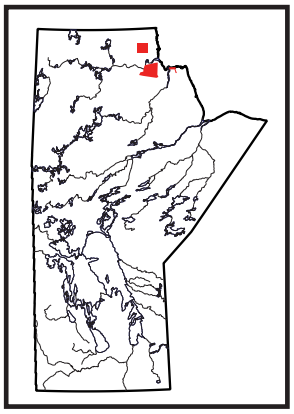
Introduction

This report presents a summary of activities related to three weeks of fieldwork undertaken west and northwest of Churchill, Manitoba, in the summer of 2024. Quaternary geology investigations included site characterization (sedimentology, geomorphology, type and thickness of glacial sediments) and collection of representative till samples for compositional analysis. Ice-flow indicators were mapped to augment the current understanding of the regional ice-flow history. Geological observations, sampling of till and/or measurements of ice-flow indicators were recorded at 185 stations, which includes 10 sections along the North Knife and South Knife rivers and 12 road-accessible sites near Churchill. The objectives of this study are to

- conduct 1:50 000 scale surficial geology mapping;
- collect till samples to assess the composition and provenance of the till;
- map paleo–ice-flow indicators to assist reconstructions of the glacial history; and
- collect organic material (shell or wood) for radiocarbon dating in order to update the postglacial rebound (isostatic uplift) history.

Bedrock geology

The study area is underlain by Paleozoic limestone and dolostone of the Hudson Bay Basin in the east and Proterozoic and Archean metasedimentary, metavolcanic and plutonic rocks of the Precambrian shield in the west (Figure GS2024-25-1; Anderson et al., 2010; Manitoba Geological Survey, 2022). Within the Gross Lake area, there is one mineral occurrence of rare earth elements (REE) ~5.4 km southeast of Gross Lake (Böhm et al., 2020; Rinne, 2024). There are no reported mineral occurrences within the North Knife River to Seal River area; however, drilling immediately to the north has identified multiple mineral occurrences within the Archean gabbro and mafic volcanics that outcrop along the Seal River (Rinne, 2024).



Quaternary history

The study area was previously mapped in the late 1980s (1:250 000 scale, Dredge and Nixon, 1981, 1982). More recent detailed mapped has been conducted to the west of the study area (1:50 000 scale, Trommelen and Campbell, 2012b; Trommelen, 2014c; Gauthier, 2016b). Most of the North Knife River to Seal River area is poorly drained, with variable organic cover underlain by permafrost. The study area was glaciated multiple times by ice flowing from multiple migratory domes of the Laurentide Ice Sheet (Dredge and Nixon, 1992; Gauthier et al., 2019). The glaciers left behind a palimpsest landscape (Figure GS2024-25-2) dominated by ice-transverse crevasse ridges and ribbed

[1] University of Manitoba, Winnipeg, Manitoba

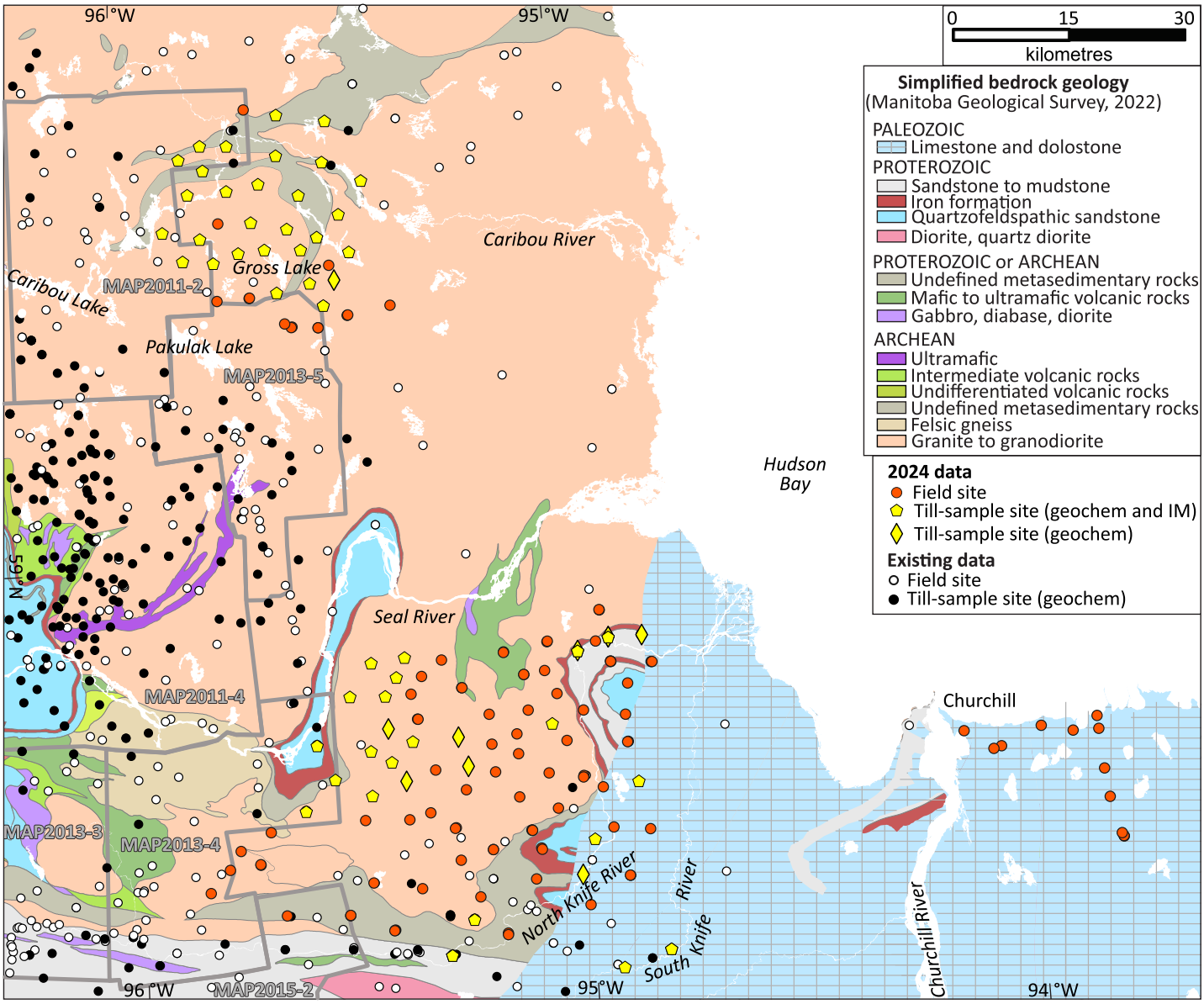


Figure GS2024-25-1: *Field sites and till sample sites overlying the bedrock geology of far northeastern Manitoba (Manitoba Geological Survey, 2022). Grey outlined polygons and MAPxxxx-x refers to the Manitoba Geological Survey map and publication number, respectively (Trommelen and Campbell, 2012a, b; Trommelen, 2014a–c; Gauthier, 2016b). Datum is NAD83. Abbreviations: geochem, geochemical analysis; IM, indicator-mineral analysis.*

moraine ridges (Trommelen et al., 2014) and ice-parallel streamlined landforms, eskers and meltwater channels (Trommelen et al., 2012). During and post deglaciation, the area was covered by the Tyrrell Sea to ~175 m above sea level (asl) along the Caribou River, ~150 m asl along the North Knife River and 140–150 m asl along the Churchill River (Dredge and Nixon, 1992; Gauthier et al., 2020; McMartin et al., 2022). As the sea regressed, it formed numerous small beach ridges (Figure GS2024-25-2).

Methods

Truck- and helicopter-supported fieldwork was undertaken over 21 days in July–August, 2024, based out of the town of Churchill. A total of 185 field sites were visited to ground-truth the surficial geology mapping, collect till samples and map ice-flow indicators (Figure GS2024-25-1). The surficial material at each field station was investigated by means of a hand-dug shovel hole, a Dutch auger (1.2 m long) hole and/or a natural sediment exposure.

The 66 collected till samples will be split for archiving at the Manitoba Geological Survey Midland Sample and Core Library (Winnipeg, Manitoba), and then analyzed for grain size, matrix geochemistry (<63 µm size fraction) and clast lithology. An additional 14–16 kg till sample was collected for indicator-mineral analysis at 55 sample sites. These samples were submitted to Overburden Drilling Management Limited (Ottawa, Ontario) in collaboration with the Geological Survey of Canada. They will

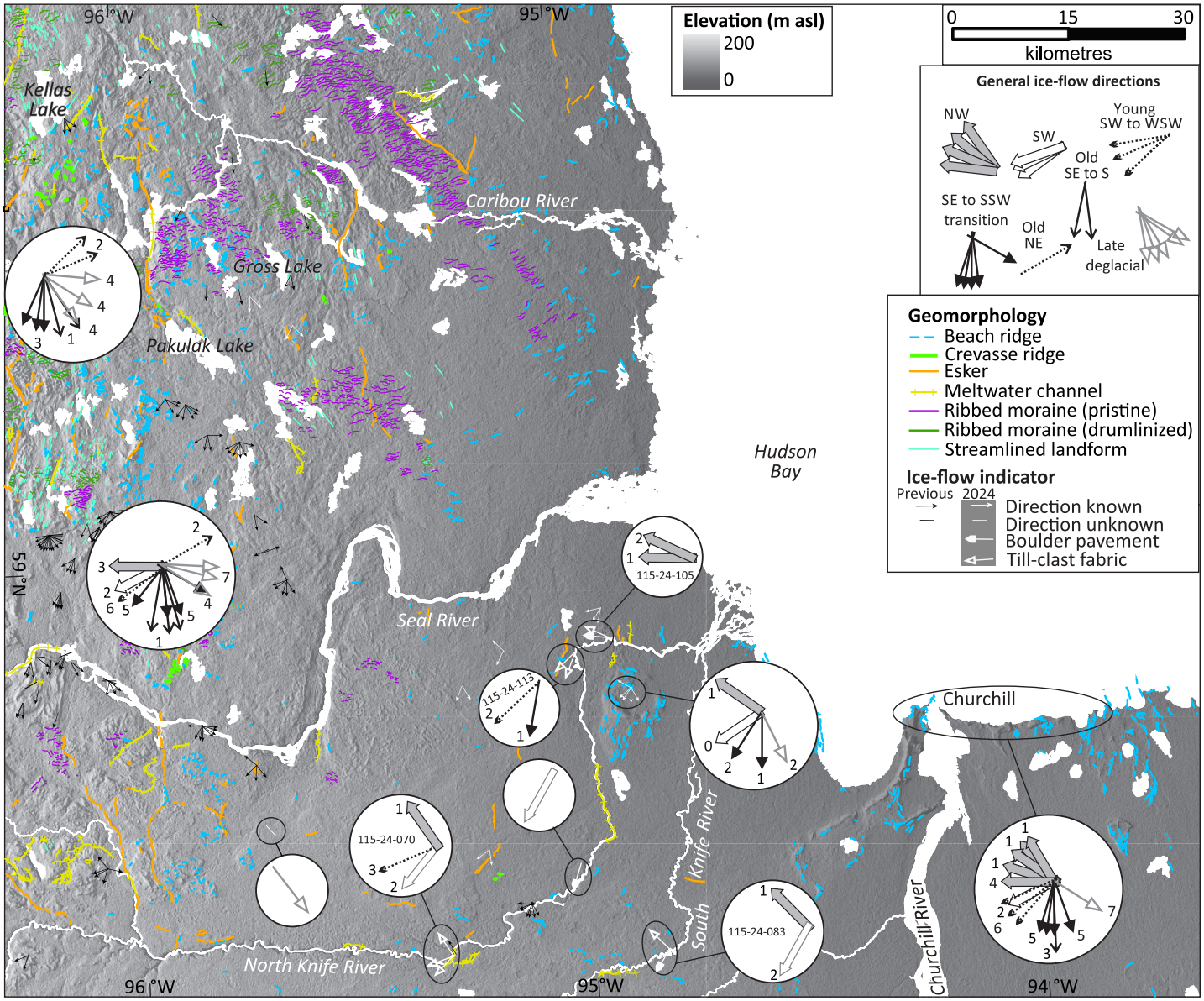


Figure GS2024-25-2: *Geomorphology and ice-flow indicators mapped in the far northeast of Manitoba, from this study and previous work (Trommelen and Ross, 2011; Trommelen, 2015; Gauthier, 2019, 2022). Indicators are denoted by relative age when observed either upsection (till fabrics) or by crosscutting relationships (erosional field-based ice-flow indicators). Locations of till-fabric analyses indicated (site 115-24-XX). Background hillshade is generated from a Shuttle Radar Topography Mission digital elevation model (U.S. Geological Survey, 2014). Datum is NAD83.*

be analyzed for metamorphosed massive-sulphide–indicator minerals (MMSIMs®), kimberlite-indicator minerals (KIM), lithium-indicator minerals (LIM) and visible gold.

Ice-flow data were obtained from erosional ice-flow indicators observed in the field, or by measuring the long-axes orientation, or fabric, of clasts within till. The long-axis orientation of elongated clasts were measured, as such clasts tend to rotate within the fine-grained till matrix and orient parallel to the overlying glacier's shear stress direction (Holmes, 1941). Elongated clasts are defined as having a minimum ratio of 1.5:1.0 of lengths of their longest axis to their second-longest axis. The orientations (trend and plunge) of a minimum sampled population of 25 elongated clasts were measured in situ for a statistically valid result. Lodged boulders in till, with parallel striae on their polished upper surface, were also measured when present.

Preliminary surficial geology

Bedrock

Bedrock is near surface in most of the study area. Problematically, the bedrock often exists as boulder fields (Figure GS2024-25-3a) or frost-shattered broken rock draped by variable organics or modern lake sediments (felsenmeer, Figure GS2024-25-3b, c). Intact bedrock is rare and is actively shattering or being heaved by frost (Figure GS2024-25-3d, e). These rubble areas are identified as bedrock based on the angular to



Figure GS2024-25-3: *Bedrock in the study area often outcrops as monolithic boulder fields* ***(a)*** *or angular blocks termed felsenmeer* ***(b)*** *that may be covered by organics* ***(c)****. 'Intact' bedrock outcrops are actively shattering or being heaved by frost* ***(d, e)****. Due to the same frost action, till-derived boulder fields look similar to rubble bedrock but contain rocks of different lithologies that may be more rounded* ***(f)****.*

subangular boulder edges and their monolithic nature (Dredge and Nixon, 1992). Careful attention in the field is needed to separate rubble bedrock from till-derived boulder fields, which contain rocks of different lithologies with angular to subrounded edges (Figure GS2024-25-3f).

Glaciomarine and marine

Glaciers depress the surface of the Earth, and how the Earth responds to this loading and subsequent unloading (deglaciation) is a process called glacial isostatic adjustment. Glacial ice was present in the Churchill area as late as 8000 cal. years BP, meaning that there were complex interactions between the ice and the Tyrrell Sea waters on its eastern side (Dredge and Nixon, 1992; Gauthier et al., 2020; McMartin et al., 2022). The land was still depressed once the glaciers melted, and marine sediments were deposited far inland; up to ~150 m above modern sea level along the North Knife River and ~175 m asl west of the Gross Lake area (McMartin et al., 2022). The North Knife River–Seal River and Gross Lake study areas are between 20–135 m asl and 70–150 m asl, respectively, meaning that most of the landscape was beneath the Tyrrell Sea for a long time. To assess how long the land took to rebound, eight marine shell samples were collected from ~21–87 m asl. Twigs were collected near the base of fluvial sands, within a peat bed overlying marine sediment at 48 m asl, to date the minimum age of marine regression at that site along the North Knife River. Three samples near Churchill were collected to provide more accurate dates than the current 1960 and 1970s conventional dates on bulk samples (Craig, 1969; McNeely and Brennan, 2005; Gauthier, 2023a). Combining this new data with other radiocarbon dates in the area will provide a better assessment of the relative sea level history for the region (Gauthier, 2016a; Simon et al., 2016; Lambeck et al., 2017).

Glaciomarine to marine sediments include completely reworked and redistributed till turned into gravelly sand (Figure GS2024-25-4a), sand or gravel beach ridges (Figure GS2024-25-4b), littoral sand, intertidal silt and clast-poor diamict (Figure GS2024-25-4c–f). The glaciomarine to marine diamict, also termed stony pelite (Dredge and Nixon, 1992), is a massive, matrix-supported, very poorly sorted, silty-clayey diamict with 3–25% clasts that are granule- to small cobble-sized. The clasts may be randomly distributed throughout, or only near the surface due to permafrost action. Dredge and Nixon (1992) note that the stony pelite has an uncertain origin and can be interpreted as permafrost-mixed marine sediments and till, glaciomarine sediments, and/or deepwater marine sea-ice detritus, like that observed on the sea floor in modern Hudson Bay. Regardless of origin, these sites must be avoided during till prospecting, as the sediments are unrelated to the underlying bedrock. Several previously sampled 'tills' are actually marine diamicts and will be removed from existing till-data compilations (Gauthier, 2019, 2024, samples AN356713, AN360213, AN361513).

Tills

The study area is draped by a massive, matrix-supported, overconsolidated, generally olive-brown diamict with a sandy-silt or silty-sand matrix (Figure GS2024-25-5a, d). An older highly overconsolidated diamict(s) with blocky structure and oxidation staining along the joints was studied at section 115-24-070 along the North Knife River (Figure GS2024-25-2). There is a pre-existing till sample from this section (Gauthier, 2019, AN345913; Gauthier and Godbout, 2023), though the new work shows there are actually three tills within the 5.4 m of exposed diamict—interpreted to have been deposited by ice with very different flow directions (Figure GS2024-25-2).

Washed tills

Till prospecting programs must be careful to sample unmodified till whenever possible. Till in the study area was washed by the glacial to postglacial Tyrrell Sea waves, which may have caused removal of the fine-textured size fraction, or remobilization and partial sorting of the surface sediments (Figure GS2024-25-5). Wave washing can leach the water-soluble elements from the sediments and hence lead to a decreased elemental concentration than might have been there originally (Randour, 2018). Alternatively, if sampling the sand-size fraction for heavy minerals, then the concentration of these heavier minerals within a sample volume may be increased.

It is still possible to find 'good till' that hasn't been modified within the wave-washed terrain. Till prospecting programs must look for active or inactive mud boils (frost boils) that are bringing / have brought unmodified (typically siltier) sediment up from below. Mud boils are rare (Figure GS2024-25-6a, b), but can be spotted from the air. If mud boils are not found, its often possible to dig down amongst the boulders and wave-washed surface sediments to find unoxidized siltier C-horizon diamict at depth (Figure GS2024-25-6c).

Ice-flow history

Erosional field-based ice-flow indicators

New erosional ice-flow measurements were obtained from striations, grooves, chattermarks, crescentic gouges and fractures at eight field sites in 2024. More bedrock outcrops were visited, but all surfaces were weathered and/or frost shattered. The new data confirms the existing complex ice-flow history summarized in Figure GS2024-25-2 and discussed in detail within Gauthier et al. (2019).

Till-clast fabric analyses

Previous stratigraphic studies along the North Knife and South Knife rivers did not measure till fabrics nor investigate the tills in detail (Dredge and Nixon, 1992; Trommelen, 2015; Gauthier, 2019). New till-based stratigraphies in northeastern Manitoba have shown the importance of this data, especially where

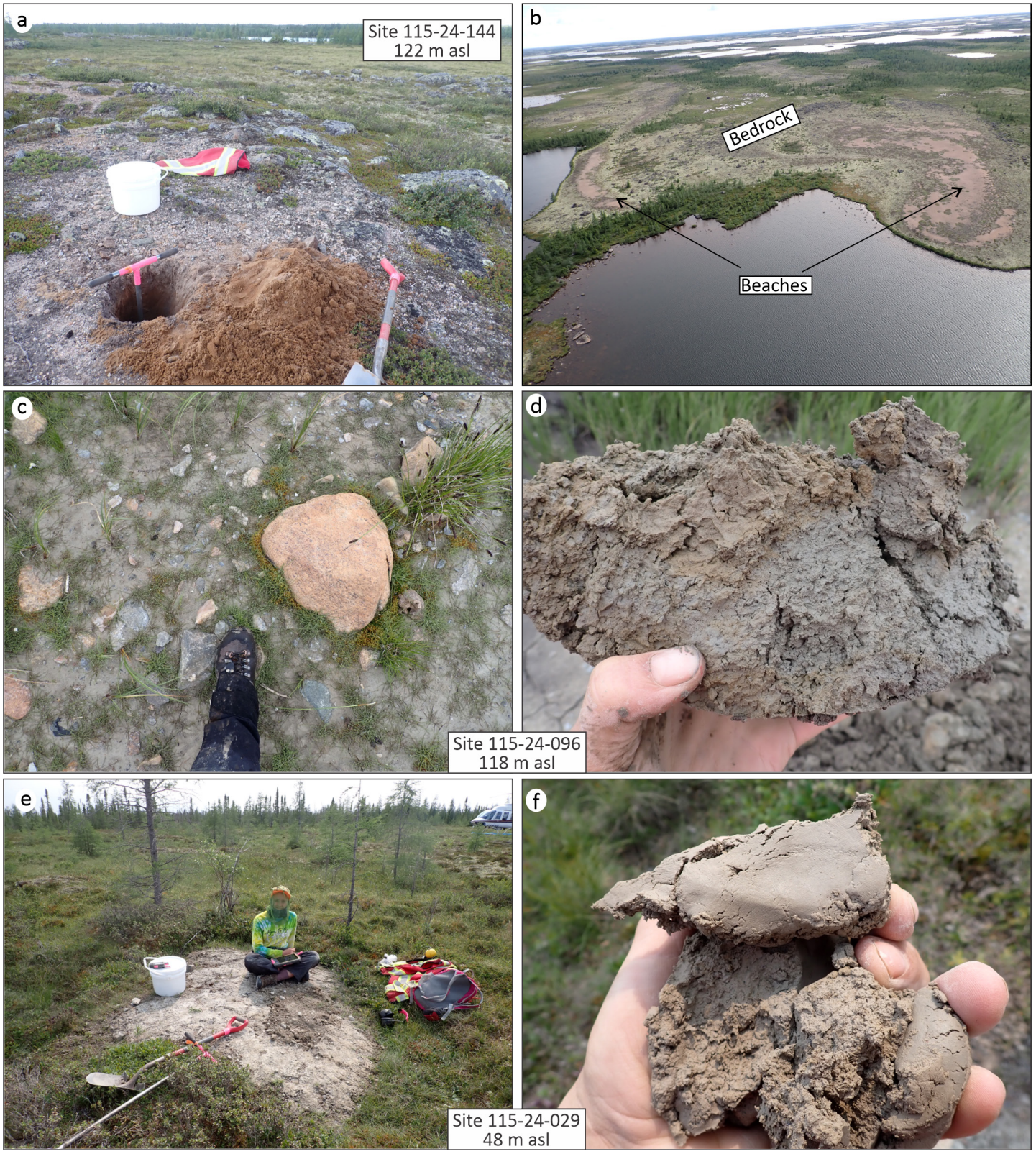


Figure GS2024-25-4: *Glaciomarine to marine sedimentation in the study area includes reworked and redistributed till turned into gravelly sand with no remaining fines* ***(a)****, sand to gravel beach ridges* ***(b)*** *and silt to silty clay diamict* ***(c–f)****.*

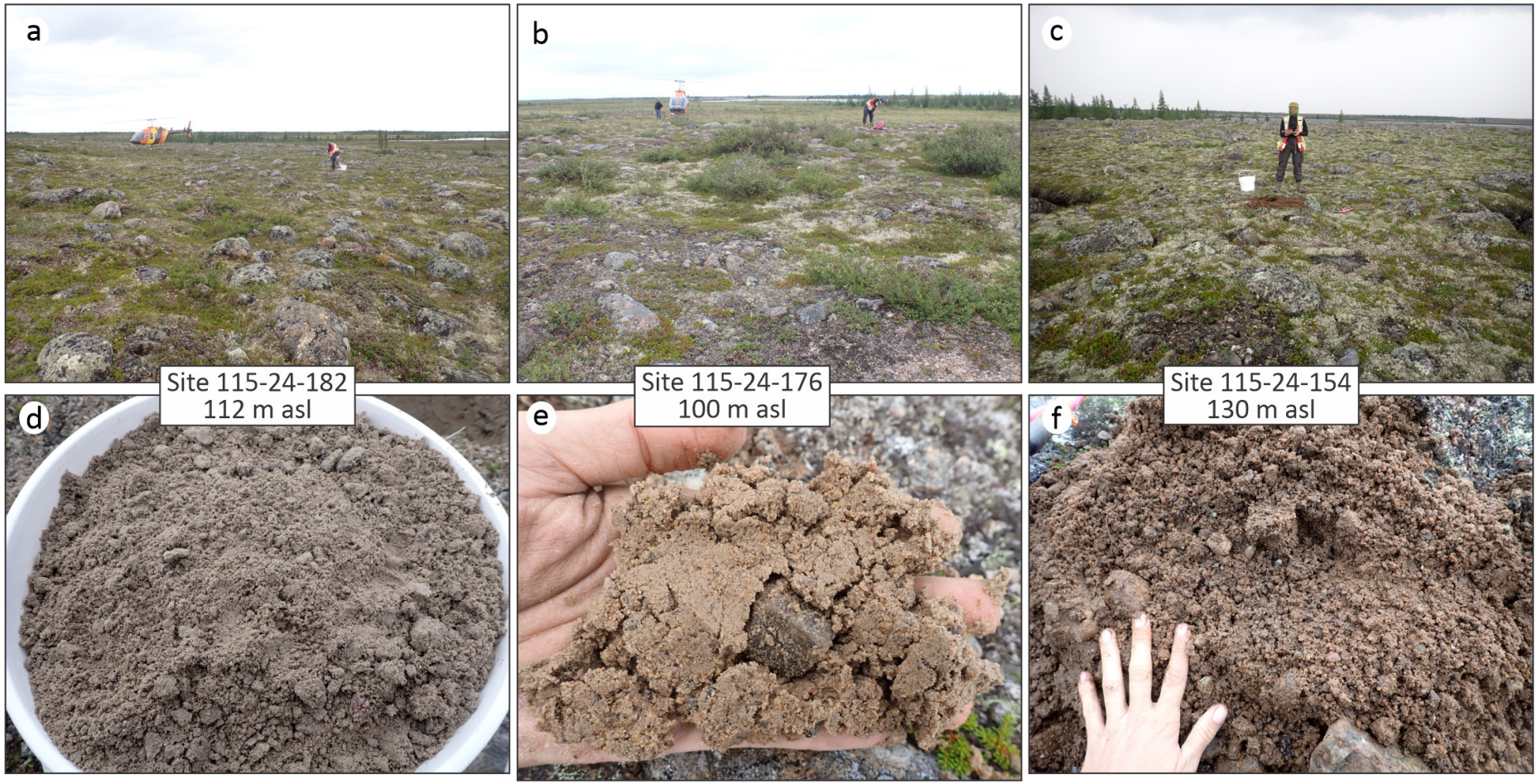


Figure GS2024-25-5: *The intensity of Tyrrell Sea wave washing was variable throughout the study area, and not controlled by elevation. Wave washing may have removed fines from the till, leaving behind just sand and clean clasts* ***(b, e)*** *compared to unmodified diamict* ***(a, d)****, or may have redistributed the surface sediments resulting in the formation of gravelly sand to sandy gravel* ***(c, f)****. Site 115-24-182 has ~60% boulders at surface and unwashed till. Site 115-24-176 has ~80% boulders at surface and sand with 10–15% clasts. Site 115-24-154 has ~60% boulders at surface, with 0.5 m of sand that has 40–60% clasts over ≥0.2 m of sand that has 0–5% clasts.*

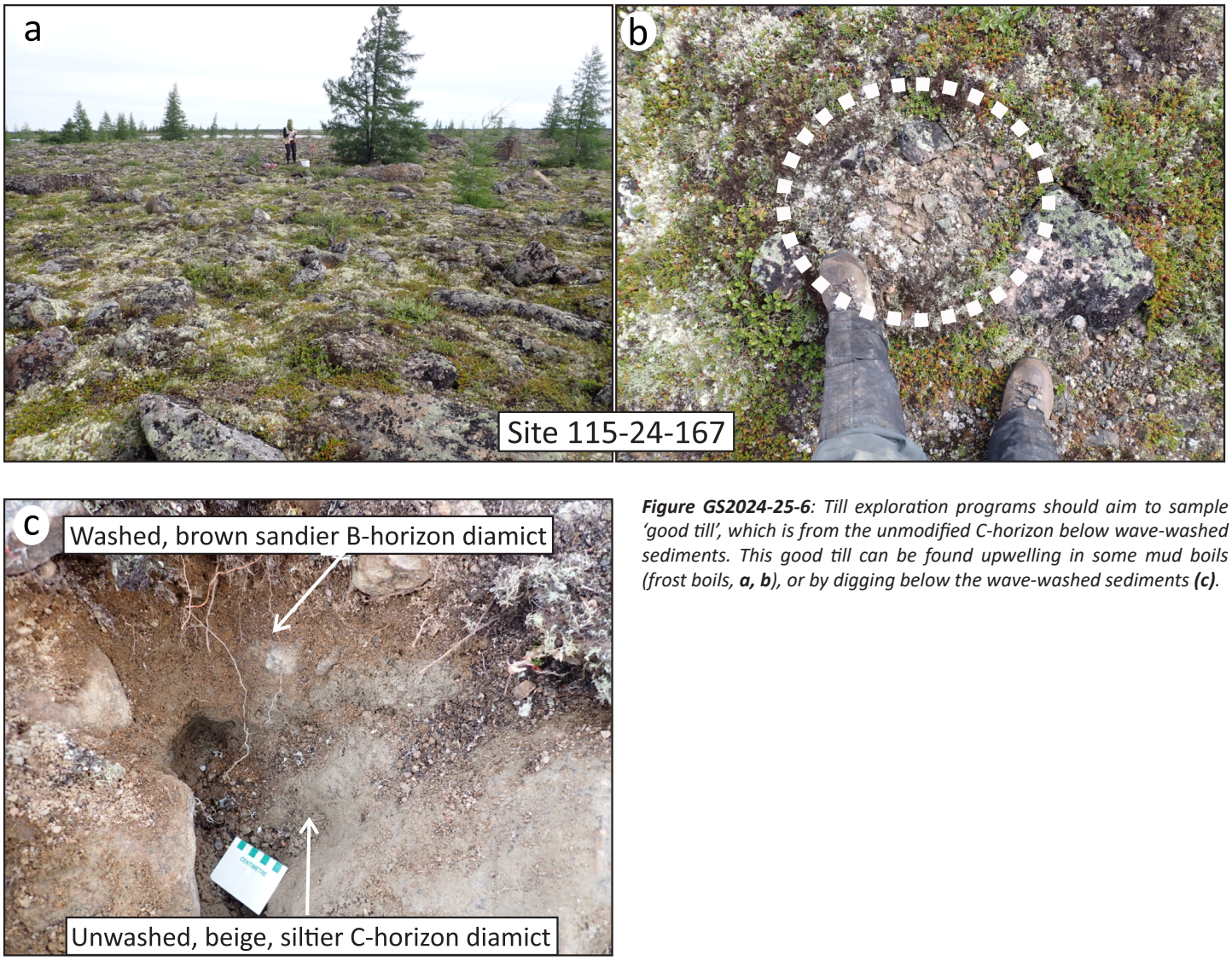


***Figure GS2024-25-6**: Till exploration programs should aim to sample 'good till', which is from the unmodified C-horizon below wave-washed sediments. This good till can be found upwelling in some mud boils (frost boils, **a, b**), or by digging below the wave-washed sediments **(c)**.*

tills appear qualitatively similar (Gauthier et al., 2024; Hodder et al., 2024). As such, five sections were studied using the new methodology and till-clast fabrics were measured at four of the sections (Figure GS2024-25-2). These sections expose ~8–14 m of glacial and postglacial sediments.

An ice-flow event can be erosional, depositional or both. As such, determining which specific ice-flow directions were responsible for till provenance is ongoing. Calcareous detritus was glacially dispersed for distances up to ~40 km west-northwest of the Paleozoic carbonate bedrock, roughly as far as the Seal River (Figure GS2024-25-1). The North Knife River to Seal River study area is within this dispersal pattern, and previously sampled tills contained 5–15% total carbonate in the <63 um size fraction (Gauthier, 2023b). The Gross Lake study area tills may contain trace reworked (inherited) carbonate—to be confirmed by this study. The carbonate dispersal pattern bears little relationship to deglacial ice-flow orientations (Gauthier et al., 2022), requiring most of the detritus to have been transported during earlier west- and northwest-trending ice-flow phases (Trommelen et al., 2013; McMartin et al., 2016; Gauthier et al., 2019). A study just to the west showed that tills contain a complex mix of local- (<15 km) and continental-scale (350–600 km) detritus, with palimpsest dispersal patterns (Trommelen et al., 2013).

Future work

Ongoing surficial geology analyses will focus on 1:50 000 scale surficial mapping, as well as tracing lithological indicators from known bedrock source areas. The latter will be conducted by clast-lithology counts, indicator-mineral counts and geochemical analysis of the collected till samples. Radiocarbon dating results will be added to existing data, to determine updated relative sea level histories for the area.

Economic considerations

Manitoba's far northeast is a remote and largely unexplored frontier, with a variable thickness of sediment covering much of the bedrock. Results from this study will contribute to an

improved understanding of the Quaternary surface sediments, subsurface stratigraphy, glacial history and till provenance in the areas west and northwest of Churchill. This is necessary to support habitat mapping, carbon estimates, land-use planning, infrastructure development, aggregate-resource identification and mineral exploration.

Acknowledgments

The authors thank F. Roberts of Prairie Helicopters Ltd. for his good nature and calm flying. The Churchill Northern Studies Centre provided accommodations. Indicator-mineral analyses are funded by Geological Survey of Canada's Geo-mapping for Energy and Minerals, GeoNorth program (GEM-GeoNorth; Natural Resources Canada). Logistical support was provided by C. Epp throughout the project.

References

Anderson, S.D., Böhm, C.O. and Syme, E.C. 2010: Precambrian geology of the Seal River region, Manitoba (parts of 54L, M, 64I, P); Manitoba Innovation, Energy and Mines, Manitoba Geological Survey, Preliminary Map PMAP2010-1, scale 1:175 000.

Böhm, C.O., Anderson, S.D., Syme, E.C., Carlson, A.R. and Murphy, L.A. 2020: Whole-rock geochemistry compilation of the Seal River–Great Island area, southeast Hearne craton margin, northern Manitoba (parts of NTS 54L, M, 64I, P); Manitoba Agriculture and Resource Development, Manitoba Geological Survey, Data Repository Item DRI2020030, Microsoft® Excel® file.

Craig, B.G. 1969: Late glacial and postglacial history of the Hudson Bay region; *in* Earth Science Symposium on Hudson Bay, P.J. Hood (ed.), Geological Survey of Canada, Paper 68-53, p. 63–77.

Dredge, L.A. and Nixon, F.M. 1981: Surficial geology, Churchill, Manitoba; Geological Survey of Canada, Preliminary Map 4-1980, scale 1:250 000.

Dredge, L.A. and Nixon, F.M. 1982: Surficial geology, Caribou River, Manitoba; Geological Survey of Canada, Preliminary Map 5-1980, scale 1:250 000.

Dredge, L.A. and Nixon, F.M. 1992: Glacial and environmental geology of northeastern Manitoba; Geological Survey of Canada, Memoir 432, 80 p.

Gauthier, M.S. 2016a: Postglacial lacustrine and marine deposits, far northeastern Manitoba (parts of NTS 54E, L, M, 64I, P); Manitoba Mineral Resources, Manitoba Geological Survey, Geological Paper GP2015-1, 37 p., 4 appendices.

Gauthier, M.S. 2016b: Surficial geology of the North and South Knife lakes area (east-half), Manitoba (parts of NTS 54L4, 5, 12 and 64I1, 8, 9); Manitoba Mineral Resources, Manitoba Geological Survey, Geoscientific Map MAP2015-2, scale 1:100 000.

Gauthier, M.S. 2019: Till composition, stratigraphy, ice-flow indicator data and glacial history of the North Knife River–Churchill River region, Manitoba (parts of NTS 54L, 64I); Manitoba Agriculture and Resource Development, Manitoba Geological Survey, Geoscientific Paper GP2019-1, 41 p., 14 appendices.

Gauthier, M.S. 2022: Digital compilation of surficial point and line features for Manitoba, including ice-flow data; Manitoba Natural Resources and Northern Development, Manitoba Geological Survey, GeoFile 1-2022, 5 p.

Gauthier, M.S. 2023a: Manitoba radiocarbon ages; Manitoba Economic Development, Investment and Trade, Manitoba Geological Survey, GeoFile 6-2023, Microsoft® Excel® file.

Gauthier, M.S. 2023b: Manitoba till-matrix geochemistry compilation: total carbonate of the silt plus clay (<63 µm) size-fraction; Manitoba Economic Development, Investment, Trade and Natural Resources, Manitoba Geological Survey, GeoFile 7-2023, Microsoft® Excel® file.

Gauthier, M.S. 2024: Manitoba till-matrix geochemistry compilation: silt plus clay (<63 µm) size fraction by inductively coupled plasma–mass spectrometry after an aqua-regia or modified aqua-regia digestion; Manitoba Economic Development, Investment, Trade and Natural Resources, Manitoba Geological Survey, GeoFile 2-2024, Microsoft® Excel® file.

Gauthier, M.S. and Godbout, P.M. 2023: Till-matrix geochemistry reanalyses data from far northeastern and far northwestern Manitoba (parts of NTS 54E, F, L; 64J, K, N and O); Manitoba Economic Development, Investment and Trade, Manitoba Geological Survey, Data Repository Item DRI2023007, Microsoft® Excel® file.

Gauthier, M.S., Breckenridge, A. and Hodder, T.J. 2022: Patterns of ice recession and ice stream activity for the MIS 2 Laurentide Ice Sheet in Manitoba, Canada; Boreas, v. 51, no. 2, p. 274–298.

Gauthier, M.S., Hodder, T.J., Dalton, A.S., Lian, O.B., Schaarschmidt, M., Ross, M., Väliranta, M. and Finkelstein, S.A. 2024: Preservation of probable MIS 7 deglacial and nonglacial deposits near the edge of the Hudson Bay Lowland in Manitoba, Canada; Canadian Journal of Earth Sciences, Just-IN manuscript, URL <https://doi.org/10.1139/cjes-2024-0019>.

Gauthier, M.S., Hodder, T.J., Ross, M., Kelley, S.E., Rochester, A. and McCausland, P. 2019: The subglacial mosaic of the Laurentide Ice Sheet; a study of the interior region of southwestern Hudson Bay; Quaternary Science Reviews, v. 214, p. 1–27.

Gauthier, M.S., Kelley, S.E. and Hodder, T.J. 2020: Lake Agassiz drainage bracketed Holocene Hudson Bay Ice Saddle collapse; Earth and Planetary Science Letters, v. 554, no. 15, p. 116372.

Hodder, T.J., Gauthier, M.S., Ross, M., Kelley, S.E., Lian, O.B., Dalton, A.S. and Finkelstein, S.A. 2024: Unravelling the fragmented sediment–landform assemblage in an area of thick Quaternary sediment, western Hudson Bay Lowland, Canada; Canadian Journal of Earth Sciences, e-First, URL <https://doi.org/10.1139/cjes-2024-0018>.

Holmes, C.D. 1941: Till fabric; Bulletin of the Geological Society of America, v. 52, p. 1299–1354.

Lambeck, K., Purcell, A. and Zhao, S. 2017: The North American Late Wisconsin ice sheet and mantle viscosity from glacial rebound analyses; Quaternary Science Reviews, v. 158, p. 172–210.

Manitoba Geological Survey 2022: New edition of the 1:250 000 scale Precambrian bedrock geology compilation map of Manitoba; Manitoba Natural Resources and Northern Development, Manitoba Geological Survey, GeoFile 3-2022, scale 1:250 000.

McMartin, I., Dredge, L.A., Grunksy, E. and Pehrsson, S.J. 2016: Till geochemistry in west-central Manitoba: interpretation of provenance and mineralization based on glacial history and multivariate data analysis; Economic Geology, v. 111, no. 4, p. 1001–1020.

McMartin, I., Gauthier, M.S. and Page, A.V. 2022: Updated post-glacial marine limits along western Hudson Bay, central mainland Nunavut and northern Manitoba; Geological Survey of Canada, Open File 8921, 19 p.

McNeely, R. and Brennan, J. 2005: Geological Survey of Canada revised shell dates; Geological Survey of Canada, Open File 5019, 530 p.

Randour, I. 2018: Géologie quaternaire de la région de Wager Bay, Nunavut: cartographie, datation de rivages marins et impacts de l'invasion marine sur la géochimie des sédiments glaciaires; M.Sc. thesis, Université du Québec à Montréal, Montréal, Quebec, 144 p.

Rinne, M.L. 2024: Updates to the Manitoba Mineral Deposits Database; Manitoba Economic Development, Investment, Trade and Natural Resources, Manitoba Geological Survey, GeoFile 5-2024, Microsoft® Excel® file.

Simon, K.M., James, T.S., Henton, J.A. and Dyke, A.S. 2016: A glacial isostatic adjustment model for the central and northern Laurentide Ice Sheet based on relative sea level and GPS measurements; Geophysical Journal International, v. 205, p. 1618–1636.

Trommelen, M.S. 2014a: Surficial geology of the Dechanhooledezay River area, Manitoba (parts of NTS 64I9, 10, 15, 16); Manitoba Mineral Resources, Manitoba Geological Survey, Geoscientific Map MAP2013-3, scale 1:50 000.

Trommelen, M.S. 2014b: Surficial geology of the Pady Lake area, Manitoba (parts of NTS 54L12, 13, 64I9, 16); Manitoba Mineral Resources, Manitoba Geological Survey, Geoscientific Map MAP2013-4, scale 1:50 000.

Trommelen, M.S. 2014c: Surficial geology of the Schoenthaler Lake area, Manitoba (parts of NTS 54L13, 54M4, 5); Manitoba Mineral Resources, Manitoba Geological Survey, Geoscientific Map MAP2013-5, scale 1:50 000.

Trommelen, M.S. 2015: Surficial geology, till composition, stratigraphy and ice-flow indicator data, Seal River–North Knife River area, Manitoba (parts of NTS 54L, M, 64I, P); Manitoba Mineral Resources, Manitoba Geological Survey, Geoscientific Paper, GP2013-2, 27 p., 11 appendices.

Trommelen, M.S. and Campbell, J.E. 2012a: Surficial geology, Sosnowski Lake, Manitoba; Geological Survey of Canada, Canadian Geoscience Map 43 and Manitoba Innovation, Energy and Mines, Manitoba Geological Survey, Geoscientific Map MAP2011-4, scale 1:50 000.

Trommelen, M.S. and Campbell, J.E. 2012b: Surficial geology, Stubner Lake, Manitoba; Geological Survey of Canada, Canadian Geoscience Map 41 and Manitoba Innovation, Energy and Mines, Manitoba Geological Survey, Geoscientific Map MAP2011-2, scale 1:50 000.

Trommelen, M.S. and Ross, M. 2011: Far North Geomapping Initiative: palimpsest bedrock macroforms and other complex ice-flow indicators near Churchill, northern Manitoba (part of NTS 54L16); *in* Report of Activities 2011, Manitoba Innovation, Energy and Mines, Manitoba Geological Survey, p. 29–35.

Trommelen, M.S., Ross, M. and Campbell, J.E. 2012: Glacial terrain zone analysis of a fragmented paleoglaciological record, southeast Keewatin sector of the Laurentide Ice Sheet; Quaternary Science Reviews, v. 40, p. 1–20.

Trommelen, M.S., Ross, M. and Campbell, J.E. 2013: Inherited clast dispersal patterns: implications for paleoglaciology of the SE Keewatin sector of the Laurentide Ice Sheet; Boreas, v. 42, no. 3, p. 693–713.

Trommelen, M.S., Ross, M. and Ismail, A. 2014: Ribbed moraines in northern Manitoba, Canada: characteristics and preservation as part of a subglacial deformation mosaic near the core regions of ice sheets; Quaternary Science Reviews, v. 87, p. 135–155.

U.S. Geological Survey 2014: USGS EROS archive - digital elevation - Shuttle Radar Topography Mission (SRTM) 1 arc-second global; U.S. Geological Survey, 30 m cell, zipped hgt format, URL <https://doi.org/10.5066/F7PR7TFT>.

GS2024-26

Geophysical imaging of a buried gravel deposit in the Rural Municipality of Taché, southeastern Manitoba (part of NTS 62H15)

by J.W. Rentz, J. Marks, A. Frederiksen[1] and R. Guerard[1]

Summary

The Manitoba Geological Survey, in collaboration with the University of Manitoba, carried out a geophysical investigation of a buried gravel deposit at an active gravel pit, within the Rural Municipality of Taché, with the goal of better understanding the characteristics of the deposit. These included the thickness of the deposit, the lateral extent, thickness of overburden cover and, if possible, variations in the deposit structure. The survey used a combination of techniques including direct-current resistivity, ground-penetrating radar, electromagnetic induction and total magnetic intensity. Of these, only direct-current resistivity and ground-penetrating radar yielded useable results. The surveys were able to delineate a subsurface resistive structure that is approximately 10 m thick, buried beneath a less resistive layer 2–5 m thick. Results from the surveys were not extensive enough to fully delineate the deposit. Future work will include additional geophysical surveys and ground-truthing prior to expanding the study to investigate other buried deposits.

In Brief:

- Investigation of a buried gravel deposit in the RM of Taché was done using geophysics to assist in the understanding of the deposit
- Interpretation of geophysical results provide details on stratigraphy, depth, and deposit extent

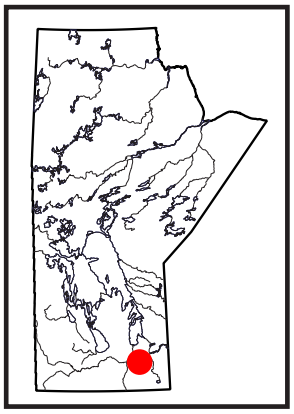
Citation:
Rentz, J.W., Marks, J., Frederiksen, A. and Guerard, R. 2024: Geophysical imaging of a buried gravel deposit in the Rural Municipality of Taché, southeastern Manitoba (part of NTS 62H15); *in* Report of Activities 2024, Manitoba Economic Development, Investment, Trade and Natural Resources, Manitoba Geological Survey, p. 219–225.

Introduction

Manitoba sand and gravel resources are commonly identified using fieldwork, in combination with remotely sensed imagery and elevation models. These methods work well when aggregate is visible at the surface, or forms easily identifiable landforms known to contain sand and gravel (e.g., eskers, beach ridges, fans). Interestingly, parts of southeastern Manitoba are host to gravel deposits that do not have a surface expression and are often covered by >0.5 m of overburden (Matile and Conley, 1979a–d; Gauthier and Hodder, 2023). As such, it can be difficult to map the lateral extent of existing known buried deposits, and to predict the location of additional buried aggregate resources. Several of the pits in southeastern Manitoba contain buried aggregate deposits that are at least 20 m thick, hence buried gravel has the potential to be a significant future source of aggregate. Given that the Winnipeg Metropolitan Region may be largely depleted of useable aggregate resources by as early as 2026 (The UMA Group, 1976), identifying new resources is of utmost importance. To gain a better understanding, a buried aggregate deposit in the Monominto gravel pit in the Rural Municipality of Taché (Figure GS2024-26-1) was analyzed using various geophysical techniques. The objectives of this study are to see which geophysical techniques work best to image the site's subsurface geology, attempting to answer questions about overburden thickness and both the lateral and vertical extent of the buried aggregate deposit.

Study area

The Monominto gravel pit (deposit 2318, Matile and Conley, 1979d) is located 2.5 km east of the Red River lowland in southeastern Manitoba, in an area with till and shallow glaciolacustrine sediments at the surface (Matile and Conley, 1979d; Matile, 2004). The area is relatively low lying (Figure GS2024-26-1) and well drained. The current gravel pit is approximately 1300 m long, averaging 250 m in width, and has been dug as a rough rectangle striking to the southeast. The pit is currently owned by the Rural Municipality (R.M.) of Taché and has been in operation since the 1970s. Aggregate from this site was most recently used for the rehabilitation of Provincial Trunk Highway 12, attesting to the high quality and importance of the buried deposit.



One area of the pit (site 118-23-010, Figure GS2024-26-1), visited in 2023, consists of 1.4 m of massive matrix-supported diamict with a clayey sandy silt matrix and 15% clasts overlying 1.2 m of crossbedded fine- to medium-grained sand, which is underlain by >1 m of sandy gravel with 40–60% clasts (Figure GS2024-26-2a–d; Gauthier and Rentz, 2024). The sandy gravel is currently being extracted from up to ~10 m below the water table (A. Brandt, pers. comm., 2023). At approximately

[1] Department of Earth Sciences, University of Manitoba, Winnipeg, Manitoba

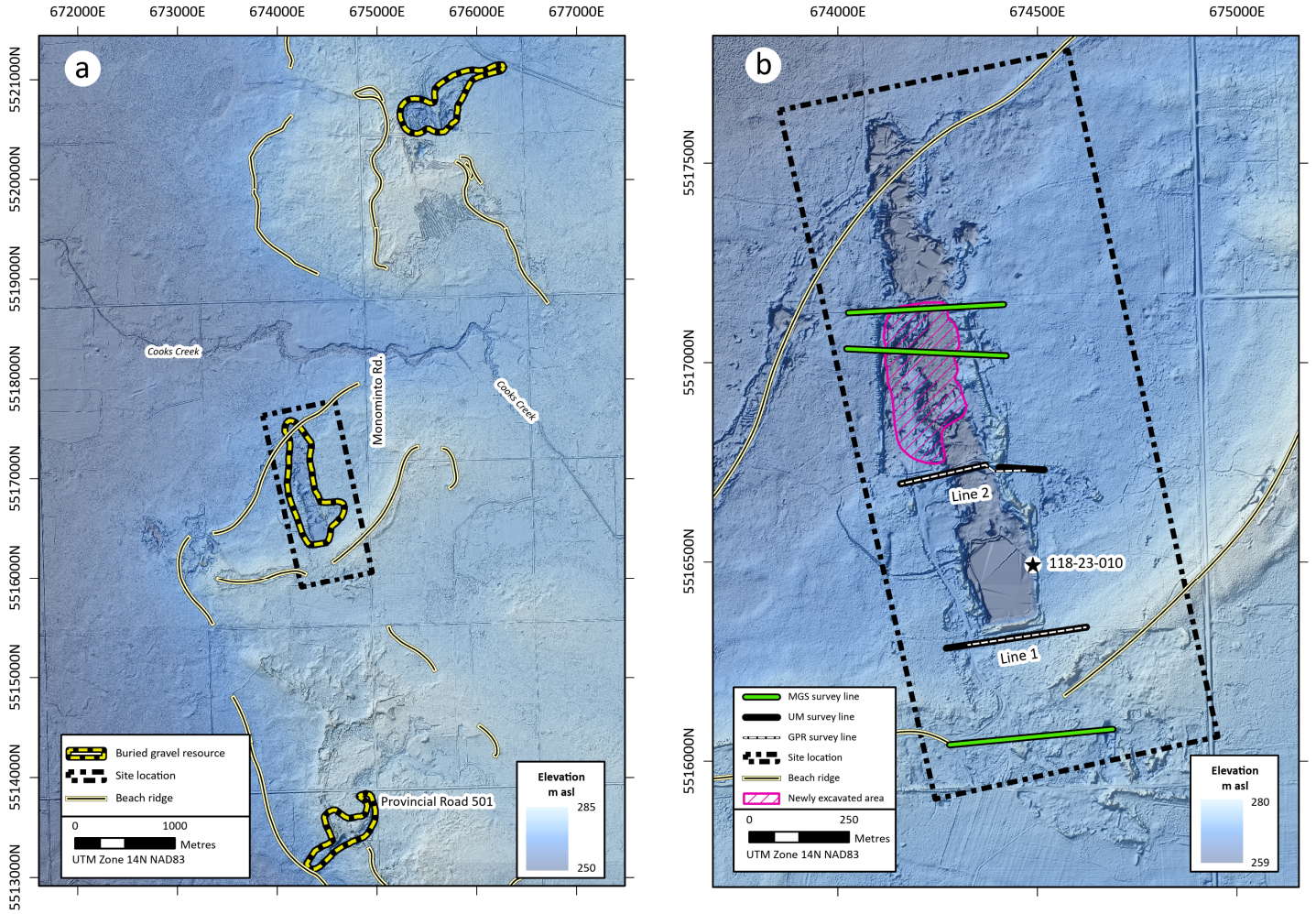


Figure GS2024-26-1: *Light detection and ranging (LiDAR) image with a background hillshade image (ATLIS Geomatics Inc., 2016, 2018) of the study area:* ***a)*** *site location (Sec. 28, Twp. 9, Rge. 7, E 1st Mer.) as well as the locations of nearby aggregate pits excavated into buried gravel deposits;* ***b)*** *locations of both the University of Manitoba (UM) and Manitoba Geological Survey (MGS) geophysical survey lines. Star indicates the site of stratigraphic section 118-23-010. Abbreviations: GPR, ground-penetrating radar; m asl, metres above sea level.*

3 m below the water table there is a cemented gravel layer that is approximately 0.6 m thick (Diamond Construction & Gravel Ltd., pers. comm., 2024).

Methods

Geophysical surveys took place in two phases. In May 2024, the first phase was undertaken by the University of Manitoba (UM) in collaboration with the Manitoba Geological Survey (MGS). In August 2024, the second phase was undertaken by MGS staff using resistivity equipment; see Marks and Rentz (2024) for details on geophysical methods. In the first phase, two transects were conducted transverse to the existing pit (Figure GS2024-26-1b). The first line was located approximately 25–30 m south of the southern extent of the pit, and the second located across the middle of the pit (Figure GS2024-26-1b). Line 2 follows a road and dips down approximately 3.5 m where gravel was extracted, before moving back up to the same elevation. These two locations were chosen to examine the stratigraphy beyond the pit's current extent (line 1), examine the depth and stratigraphy of the known gravel pit (line 2), and act as a geophysical control line for resistivity values. Geophysical techniques used included direct-current resistivity (DC-resistivity), ground-penetrating radar (GPR), electromagnetic induction and total magnetic intensity. A summary of the common uses and limitations of the techniques are given in Table GS2024-26-1.

Direct-current resistivity

Two resistivity lines were surveyed using an Iris Instruments Syscal Junior Resistivity Metre in a dipole-dipole configuration. Each of the lines consisted of three 115 m spreads of 24 electrodes with an electrode spacing of 5 m. Additionally, a 15 m horizontal overlap was applied to the lines after each set of readings. The raw data was processed by removing erroneous values and by adding elevation data to each of the 5 m stations using a digital elevation model (ATLIS Geomatics Inc., 2016). The processed data was then inverted using the Geotomo Software Res2DInv software package using a least squares method with a maximum of seven iterations and a root-mean-square convergence of <5%.

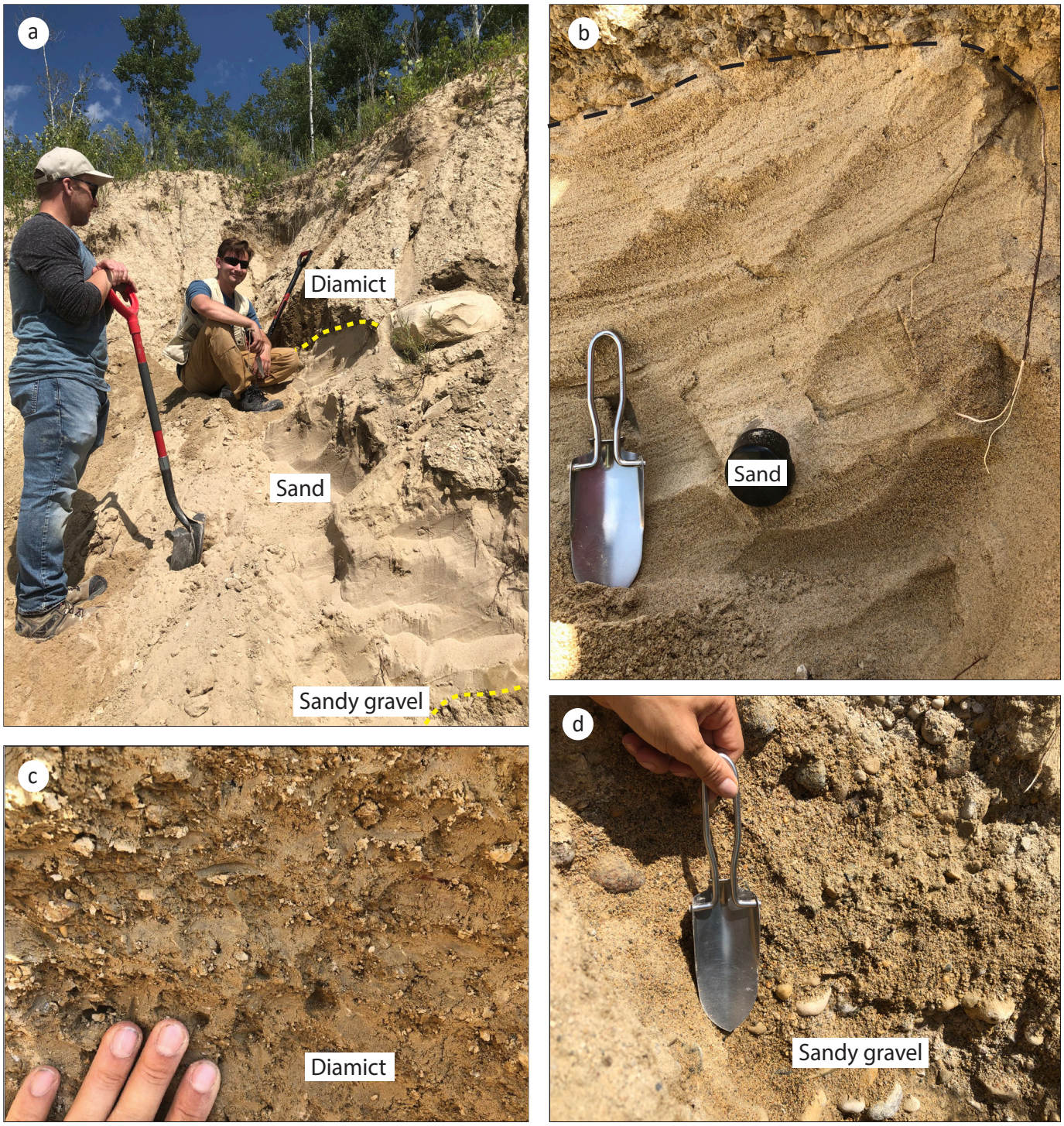


Figure GS2024-26-2: *Quaternary stratigraphy at site 118-23-010, southeastern Manitoba:* ***a)*** *overview of the stratigraphic section;* ***b)*** *close-up of crossbedded fine- to medium-grained sand;* ***c)*** *close-up of diamict with clayey sandy silt matrix;* ***d)*** *close-up of sandy gravel shown in a). See Figure GS2024-26-1 for location of site.*

A model cell width of 2.5 m (half the electrode spacing) was also used along with a horizontal weighting filter to optimize data fitting.

Ground-penetrating radar

A GPR survey was conducted using a Geophysical Survey Systems, Inc. (GSSI) SIR 3000 system along both lines 1 and 2. Line 1 was surveyed using a frequency of 400 megahertz (MHz) and line 2 was surveyed using a frequency of 200 MHz. The difference in frequencies relates to the ability of the GPR's electromagnetic waves to reach different depths—generally, the lower the frequency, the deeper the instrument can read. However, a lower frequency will also result in a lower resolution. The 400 MHz frequency was used to characterize the overburden at surface,

Table GS2024-26-1: Common uses and limitations of the geophysical instruments used in this study. Abbreviations: DC, direct-current; GPR, ground-penetrating radar.

Instrument	Uses	Common limitations
DC-resistivity	Mapping aggregate resources	Different materials may have the same resistivity
	Mapping stratigraphy	Influenced by near-surface groundwater
	Determining depth to bedrock	Influenced by conductive groundwater
	Determining depth to water table	Poor contact between electrodes and ground may result in inaccurate readings
		Interference by subsurface metal objects
Ground penetrating radar	Mapping stratigraphy	Poor contact between GPR system and ground surface can interfere with the radar waves
	Mapping of subsurface features such as faults and bedding	High conductivity soils may limit the survey depth
	Archaeological mapping	Large subsurface cobbles and boulders may interfere with the radar waves
Electromagnetic induction	Mapping ground conductivity, which can be used to evaluate soil types	Complex stratigraphy is not easily mapped due to the weighting of layers versus depth
	Mapping aggregate resources	Data can be unreliable in highly conductive and highly resistive soils
		Interference by subsurface metal objects
Total magnetic intensity	Identifying geological structures	Interference by metal objects
	Mapping subsurface lithology	Penetration depth may be variable
	Identifying mineral resources	Not commonly used in aggregate exploration

whereas the 200 MHz frequency was used to characterize the gravel deposit's depth and structure in an area where the overburden had been stripped away. Additionally, a dielectric constant of 6 was used for depth determination. Typical dielectric constants for sand and gravel range from 3 (dryer conditions) to 6 (more saturated conditions), as the survey was conducted in the spring a dielectric constant of 6 was used for both survey lines.

Electromagnetic induction and total magnetic intensity

Electromagnetic induction and total magnetic intensity surveys were completed along line 1. Using a 10 m coil spacing, a Geonics Limited EM-34-3 instrument was used to map the ground conductivity in both the horizontal and vertical dipoles. A Gem Systems GSM-19 Overhauser magnetometer/gradiometer was used to measure the magnetic intensity of the subsurface to capture any magnetic anomalies that may exist within a resistive layer.

Preliminary results

Four geophysical techniques were tested along the UM lines 1 and 2. Of the techniques used, the most useful data was provided by the DC-resistivity survey followed by the GPR survey, whereas neither the electromagnetic induction nor the total magnetic intensity surveys provided very useable data. The lack of useable data is likely because a) the apparent conductivity of the electromagnetic induction readings consists of a weighted-average response over the exploration depth and in this case the readings may have been masked by the overburden (McNeill, 1980; Fitterman and Labson, 2005; Rentz et al., 2021) and b) magnetic material was not sufficiently abundant within the stratigraphic column for total magnetic intensity to be effective.

Direct-current resistivity

There is an extensive subsurface resistive deposit of linear continuity, ~400–4039 ohm-metre (Ω•m), across most of line 1 (Figure GS2024-26-3). The resistive layer of interest appears to reside between 5 and 15 m below ground surface with at least 10 m of depth extent, if not more. There is a similar extensive subsurface resistive deposit of linear continuity, ~400–4039 Ω•m across most of line 2 (Figure GS2024-26-3). Again, the resistive layer of interest is approximately 10 m thick and is located approximately 2–4 m below a less resistive layer.

Ground-penetrating radar

The low frequency ground-penetrating radar survey on line 2 provided useful data, whereas the high frequency survey on line 1 did not. The line 2 profile shows a potential stratigraphic contact approximately 3–6 m below ground surface (Figure GS2024-26-4a, b).

Future work

Since the initial DC-resistivity survey did not fully capture the lateral extent of the anomalies, an additional DC-resistivity

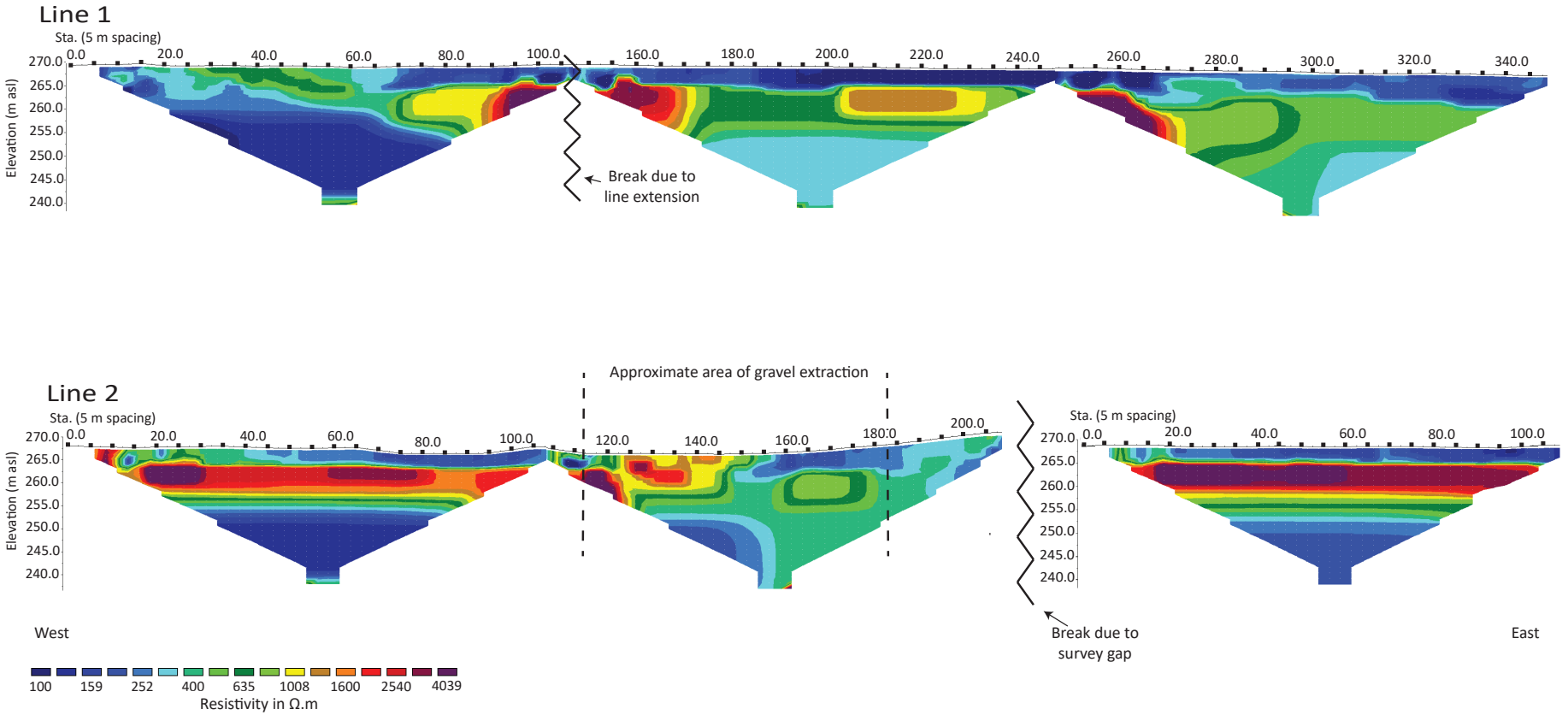


Figure GS2024-26-3: *Inversion results of the direct-current resistivity survey along both lines 1 and 2, Monominto gravel pit, southeastern Manitoba. See Figure GS2024-26-1 for location of lines. Abbreviations: Ω•m, ohm-metre; m asl, metres above sea level; Sta., station.*

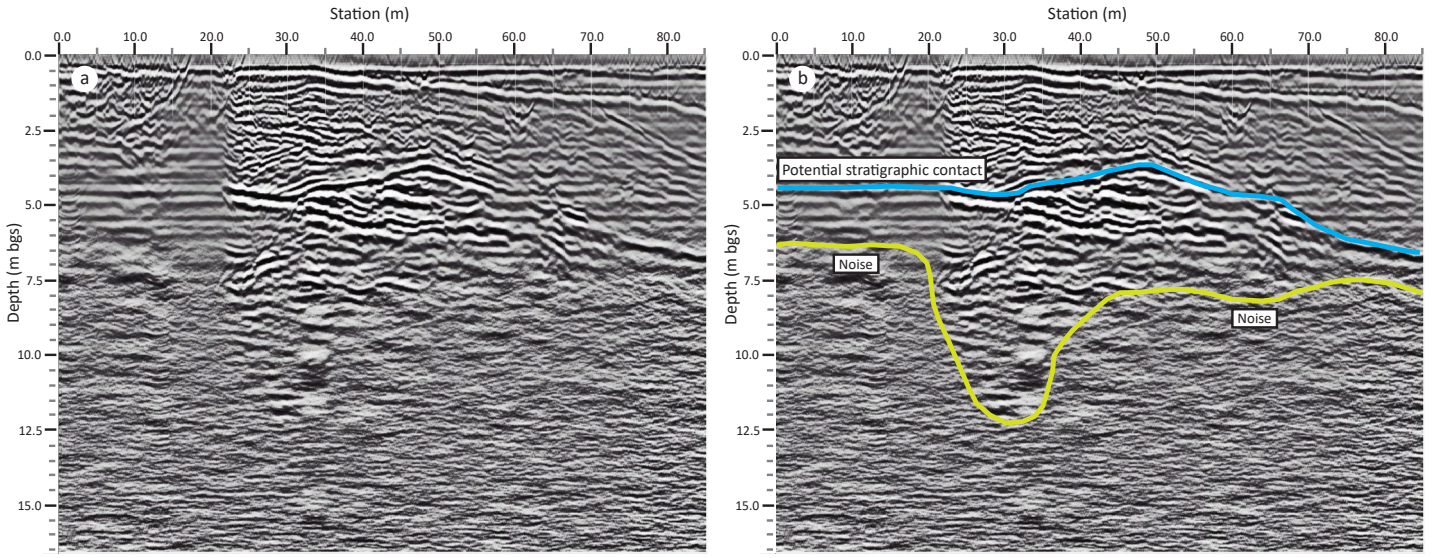


Figure GS2024-26-4: *Ground-penetrating radar (GPR) survey results from the eastern part of survey line 2, Monominto pit, southeastern Manitoba:* ***a)*** *unannotated GPR results (200 megahertz frequency);* ***b)*** *annotation of potential stratigraphic contact. Yellow line indicates limit of resolution. See Figure GS2024-26-1 for location of line 2. Abbreviation: bgs, below ground surface.*

survey was completed by the MGS in August 2024 (Marks and Rentz, 2024). The next steps are to reconcile and interpret the results of all of the geophysical surveys and integrate them with field observations.

Economic considerations

Aggregate is an essential resource for road construction, foundation construction and railroad base and concrete/asphalt formation. The increasing demand for aggregate, especially from the Winnipeg Metropolitan Region, dictates that additional resources need to be identified. Past estimations predicted that high-quality aggregate deposits within the metropolitan region may be depleted as early as the year 2026, therefore, it is imperative that new and existing aggregate resources are fully identified to facilitate future growth in the metropolitan region.

Acknowledgments

The authors thank the University of Manitoba's Clayton H. Ridell Faculty of Environment, Earth, and Resources for their support with this project, with a special thanks to M. Serzu for his enthusiastic field support. The authors would like to acknowledge M. Gauthier for her critical review of this report.

References

ATLIS Geomatics Inc. 2016: Cooks Creek LiDAR DEM; Manitoba Infrastructure, URL <https://mli.gov.mb.ca/dems/index_external_lidar.html> [June 2023].

ATLIS Geomatics Inc. 2018: Seine River and Rat River watersheds LiDAR DEM; Manitoba Infrastructure, URL <https://mli.gov.mb.ca/dems/index_external_lidar.html> [June 2023].

Fitterman, D.V. and Labson, V.F. 2005: Electromagnetic induction methods for environmental problems; *in* Near-Surface Geophysics, Investigations in Geophysics, D.K. Butler (ed.), Society of Exploration Geophysicists, Investigations in Geophysics Series No. 13, p. 301–356.

Gauthier, M.S. and Hodder, T.J. 2023: Quaternary site data, till composition and ice-flow indicators in the Roseau River area, southeastern Manitoba (parts of NTS 62H2, 7); Manitoba Economic Development, Investment and Trade, Manitoba Geological Survey, Open File OF2023-3, 10 p., 8 appendices, URL <https://manitoba.ca/iem/info/libmin/OF2023-3.zip> [September 2024].

Gauthier, M.S. and Rentz, J. 2024: 2023 aggregate field visits: Quaternary site data, composition, and ice-flow indicators from gravel pits in southern Manitoba (parts of NTS 62H15, I13, P5); Manitoba Economic Development, Investment, Trade and Natural Resources, Manitoba Geological Survey, Data Repository Item DRI2024007, Microsoft® Excel® file, 1 appendix, URL <https://manitoba.ca/iem/info/libmin/DRI2024007.zip> [September 2024].

Marks, J. and Rentz, J.W. 2024: Preliminary results of a multi-electrode resistivity survey of a buried gravel deposit in the Rural Municipality of Taché, southeastern Manitoba (part of NTS 62H15); *in* Report of Activities 2024, Manitoba Economic Development, Investment, Trade and Natural Resources, Manitoba Geological Survey, p. 226–232.

Matile, G.L.D. 2004: Surficial geology, Steinbach, Manitoba; Geological Survey of Canada, Map 2056A and Manitoba Industry, Economic Development and Mines, Manitoba Geological Survey, Geoscientific Map MAP2003-8, scale 1:100 000, URL <https://manitoba.ca/iem/info/libmin/MAP2003-8.pdf> [August 2024].

Matile, G.L.D. and Conley, G.G. 1979a: Quaternary geology and sand and gravel resources of the Rural Municipality of Hanover; Manitoba Department of Energy and Mines, Mineral Resources Division, Municipality Map AR80-4, scale 1:50 000, URL <https://manitoba.ca/iem/info/libmin/AR80-4.pdf> [September 2024].

Matile, G.L.D. and Conley, G.G. 1979b: Quaternary geology and sand and gravel resources of the Rural Municipality of Springfield; Manitoba Department of Energy and Mines, Mineral Resources Division, Municipality Map AR80-1, scale 1:50 000, URL <https://manitoba.ca/iem/info/libmin/AR80-1.pdf> [June 2023].

Matile, G.L.D. and Conley, G.G. 1979c: Quaternary geology and sand and gravel resources of the Rural Municipality of Ste. Anne; Manitoba Department of Energy and Mines, Mineral Resources Division, Municipality Map AR80-3, scale 1:50 000, URL <https://manitoba.ca/iem/info/libmin/AR80-3.pdf> [September 2024].

Matile, G.L.D. and Conley, G.G. 1979d: Quaternary geology and sand and gravel resources of the Rural Municipality of Tache; Manitoba Department of Energy and Mines, Mineral Resources Division, Municipality Map AR80-2, scale 1:50 000, URL <https://manitoba.ca/iem/info/libmin/AR80-2.pdf> [June 2023].

McNeill, J.D. 1980: Electromagnetic terrain conductivity measurement at low induction numbers; Geonics Limited, Technical Note TN 6, 13 p., URL <https://geonics.com/pdfs/technicalnotes/tn6.pdf> [September 2024].

Rentz, J.W., Sri Ranjan, R., Ferguson, I.J. and Holländer, H.M. 2021: Effects of salinity and water content on apparent conductivity in an alluvial setting in the Canadian Prairies; Environmental Earth Sciences, v. 80, no. 93, p. 1–26.

The UMA Group 1976: Aggregate resources of the Winnipeg region; Manitoba Mines, Resources and Environmental Management, Mineral Resources Division, Open File Report 77/4, URL <https://manitoba.ca/iem/info/libmin/OF77-4.pdf> [June 2023].

GS2024-27

Preliminary results of a multi-electrode resistivity survey of a buried gravel deposit in the Rural Municipality of Taché, southeastern Manitoba (part of NTS 62H15)

by J. Marks and J.W. Rentz

In Brief:

- Multi-electrode resistivity imaging was successful at resolving anomalies correlating to typical sand and gravel resistivity values
- Resistivity imaging may assist in delineating buried gravel deposits, and may allow for more precise aggregate mining techniques

Citation:
Marks, J. and Rentz, J.W. 2024: Preliminary results of a multi-electrode resistivity survey of a buried gravel deposit in the Rural Municipality of Taché, southeastern Manitoba (part of NTS 62H15); *in* Report of Activities 2024, Manitoba Economic Development, Investment, Trade and Natural Resources, Manitoba Geological Survey, p. 226–232.

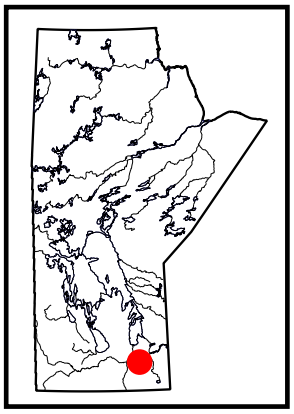
Summary

A series of multi-electrode resistivity transects were collected by the Manitoba Geological Survey over the Monominto gravel pit as part of an ongoing project to update Manitoba's remaining aggregate resources. The objective of this study was to conduct a resistivity survey over a known shallow-buried aggregate deposit to better understand the deposit geometry for future extraction, and document the resistivity signature of this deposit to guide future aggregate exploration. The preliminary results of this resistivity survey indicate the ability to resolve relatively resistive anomalous features (300–4039 ohm-metre) in the subsurface. These features are interpreted to represent buried sand and gravel, as they strongly correspond to typical sand and gravel resistivity ranges. Future work will investigate the cause of the relatively low resistivity anomalies in transect 1 and will add geological constraints to inversion models to investigate the potential artifacts present in transect 2.

Introduction

The Manitoba Geological Survey (MGS) recently began updating its provincial aggregate resource maps, which have remained mostly unchanged since the mid-1990s (Rentz, 2023). One aspect of this work is to identify shallow-buried gravel deposits and further develop exploration techniques for these types of deposits. For this reason, a known buried gravel deposit was selected for a subsurface resistivity analysis with the objective of identifying the geometry and resistivity characteristics of the gravel deposit, which will guide ongoing deposit extraction and future aggregate exploration projects. The University of Manitoba (UM), in collaboration with the MGS, previously collected two transects of resistivity data over the same gravel deposit as part of their field school program (Rentz et al., 2024; Figure GS2024-27-1). This study focuses on three new transect locations, which were chosen to expand upon this pre-existing data.

The selected gravel pit, informally named the Monominto gravel pit, is located within the Rural Municipality (R.M.) of Taché in southeastern Manitoba, ~30 km east-southeast of Winnipeg (Figure GS2024-27-1), and has been in operation since the 1970s. Around that time, the deposit was characterized as sand and gravel overlain by silt till of varying thickness, and active pits exposed 1.5–4 m of gravel, with no mining occurring below the water table (Matile and Conley, 1979a, b). The Monominto pit is currently operated by the R.M. of Taché. Most of the pit area has been excavated to ~262 m asl, which is ~1 m above the water table, but sandy gravel is currently being extracted up to ~10 m below the water table (Rentz et al., 2024).



Methodology and survey design

The Monominto gravel pit is approximately 1300 m long, 250 m wide and is oriented north-northwest–south-southeast (340–160°). Three resistivity transects were surveyed approximately perpendicular to the pit orientation, extending beyond the current east-west pit boundaries (Figure GS2024-27-1). Transects are 415 m long and comprise four lines (datasets) of 24 electrodes at 5 m station spacing, with a 15 m horizontal overlap between adjacent lines. The equipment used to gather data was an IRIS Instruments Syscal Junior Switch-24, used in a dipole-dipole configuration.

The raw resistivity data were processed using IRIS Instruments Prosys II software. Processing steps included

- removal of data points with erroneous resistivity values or relatively high standard deviations,
- shifting electrode stations horizontally to achieve continuity between adjacent lines, and
- adding elevation data to electrode stations using a high-resolution dataset collected in 2014 (ATLIS Geomatics Inc., 2016).

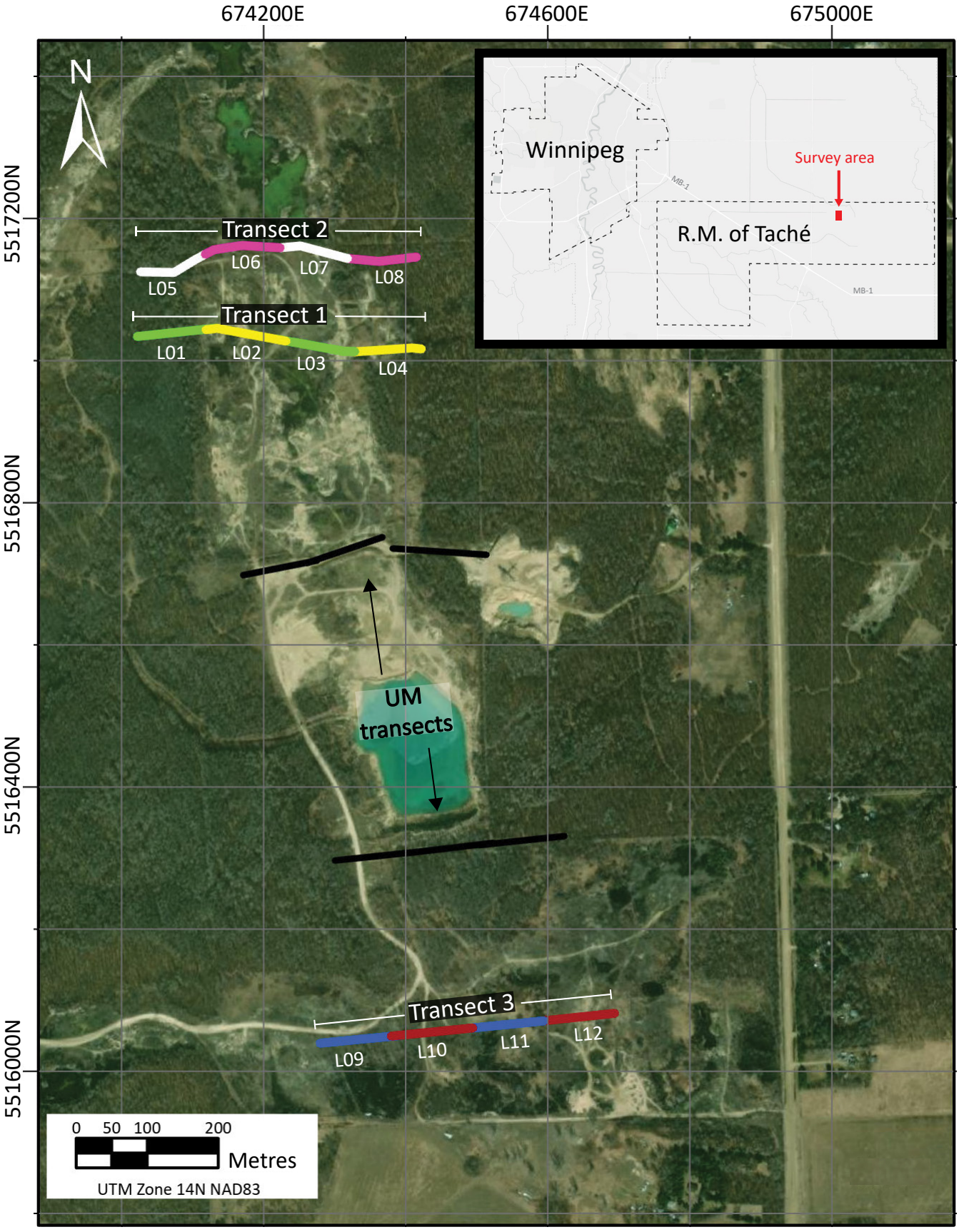


Figure GS2024-27-1: *Locations of resistivity transects over the Monominto gravel pit within Sec. 28, Twp. 9, Rge. 7, E 1st Mer., southeastern Manitoba. Coloured lines indicate where data were collected by the Manitoba Geological Survey in August 2024. Black lines indicate where data were collected by the University of Manitoba (UM) in May 2024. Satellite imagery from Esri® (2021). Abbreviations: L, line; R.M., Rural Municipality.*

Finally, the data were imported into the Geotomo Software Res2DInv software package and inverted using a least squares method. To prevent overfitting the data, an iteration maximum of seven and root-mean-square (RMS) convergence threshold of <5% was selected. Additionally, the model cell width was set to half the unit electrode spacing to help manage large resistivity variations at the surface, and a horizontal weighting filter was applied to some datasets to optimize data fit.

Preliminary results

Transect 1

Both lines L01 and L04 show an ~8 m thick linear resistive anomaly at ~260 m asl. In line L01, this anomaly occurs from stations 10 to 75 and has a resistivity range of 400–2540 ohm-metre (Ω•m; T1-A in Figure GS2024-27-2), whereas in line L04, it occurs from stations 330 to 375 with a resistivity range of 1008–4039 Ω•m (T1-B in Figure GS2024-27-2). In both lines, this linear resistive anomaly trends to the surface with a resistivity range of 400–1600 Ω•m (T1-C and T1-D in Figure GS2024-27-2). In contrast, the linear resistive anomaly is less resolved in lines L02 and L03, appearing sporadically and with a significantly lower resistivity range of 252–800 Ω•m (T1-E in Figure GS2024-27-2).

Transect 2

The results from transect 2 show three distinct resistive anomalies (Figure GS2024-27-3). The first anomaly occurs from stations 15 to 75, is ~10 m thick from ~250 to 260 m asl and has a resistivity range of 400–1600 Ω•m (T2-A in Figure GS2024-27-3). At station 55, this anomaly's thickness changes to ~3 m thick and it is shallower, from ~259 to 262 m asl. The second anomaly occurs from stations 125 to 250 and is characterized as two east-west-trending resistive anomalies, segmented vertically by an ~5 m wide conductive trend. The top of this anomaly has a resistivity range of 400–3200 Ω•m (T2-B in Figure GS2024-27-3), whereas the bottom has a relatively lower resistivity range of 400–1300 Ω•m (T2-C in Figure GS2024-27-3). Lastly, the third anomaly is a highly resistive body that occurs from stations 260 to 360 (T2-D in Figure GS2024-27-3). This feature is ~8 m thick from 257 to 265 m asl and has a resistivity range of 400–4039 Ω•m.

Transect 3

Transect 3 results show a resistive anomaly from stations 170 to 400 (Figure GS2024-27-4). This anomaly occurs from ~240 to 260 m asl, varies in thickness from 10 to 20 m and increases in resistivity from west to east within a range of 300–4039 Ω•m (T3-A in Figure GS2024-27-4). This feature is continuous across lines L10, L11 and L12, with a change in the intensity of the resistivity between lines L10 and L11, from ~635 to ~320 Ω•m, respectively (T3-B and T3-C in Figure GS2024-27-4). However, the similarity of the geometry and depth increases confidence that the anomaly is continuous between the lines. To determine if this anomaly exists to the east, two additional datasets were collected adjacent to line L12 (data processing is still in progress thus the data are not shown in this report). Preliminary analysis of this data indicates no subsurface resistive anomalies, suggesting the resistive anomaly in transect 3 terminates abruptly near station 400.

Discussion

Table GS2024-27-1 shows typical resistivity ranges of earth materials, compared with the resistivity ranges of anomalies from this study. Most anomalies correspond well to typical sand and gravel resistivity values and provide confidence that sand and gravel deposits are resolved as relatively resistive features within a more conductive medium.

In transect 1, the results in lines L02 and L03 show unexpectantly low resistivity values (T1-E in Figure GS2024-27-2), as most of the stations are within an area where sand and gravel is known to extend ~10 m deeper than the current pit elevation (Rentz et al., 2024). One possible theory for this resistivity signature is that the water table is influencing the measurements at this location. The water table is measured to be 0.6 m below the ground surface at station 220. More research will be necessary before any definite conclusions can be drawn. Additionally, sand and gravel is observed at the surface on line L04 near stations 330 to 350, which may explain why the anomaly at depth trends toward the surface at this location (T1-D in Figure GS2024-27-2). Conversely, the western part of line L01 (stations 0–60) occurs within a densely forested area, with no sand and gravel observed at the surface. It is unknown why the resistivity trends toward the surface in this area (T1-C in Figure GS2024-27-2); it may be related to electrode-ground contact.

It is unclear if the imaged conductive feature that bisects the second anomaly in transect 2 (between T2-B and T2-C in Figure GS2024-27-3) is a real geological feature, or an artifact created from the inversion process. This highlights a need to add geological constraints to future iterations, which may improve the subsurface model.

Economic considerations

Aggregate mining is a vital part of Manitoba's economy as it provides essential materials for the construction of buildings, roadways, railways and bridges. Multi-electrode resistivity imaging can assist in accurately delineating buried gravel deposits and allow for more precise, noninvasive exploration techniques, which in turn increases efficiency and reduces exploration costs. With the increasing scarcity of aggregate resources within the Winnipeg Metropolitan Region, it is imperative to be able to effectively identify shallow-buried aggregate resources and map the buried extent of known deposits using innovative approaches.

Acknowledgments

The authors acknowledge M. Serzu, A. Fredrickson and I. Ferguson from the University of Manitoba for allowing access to

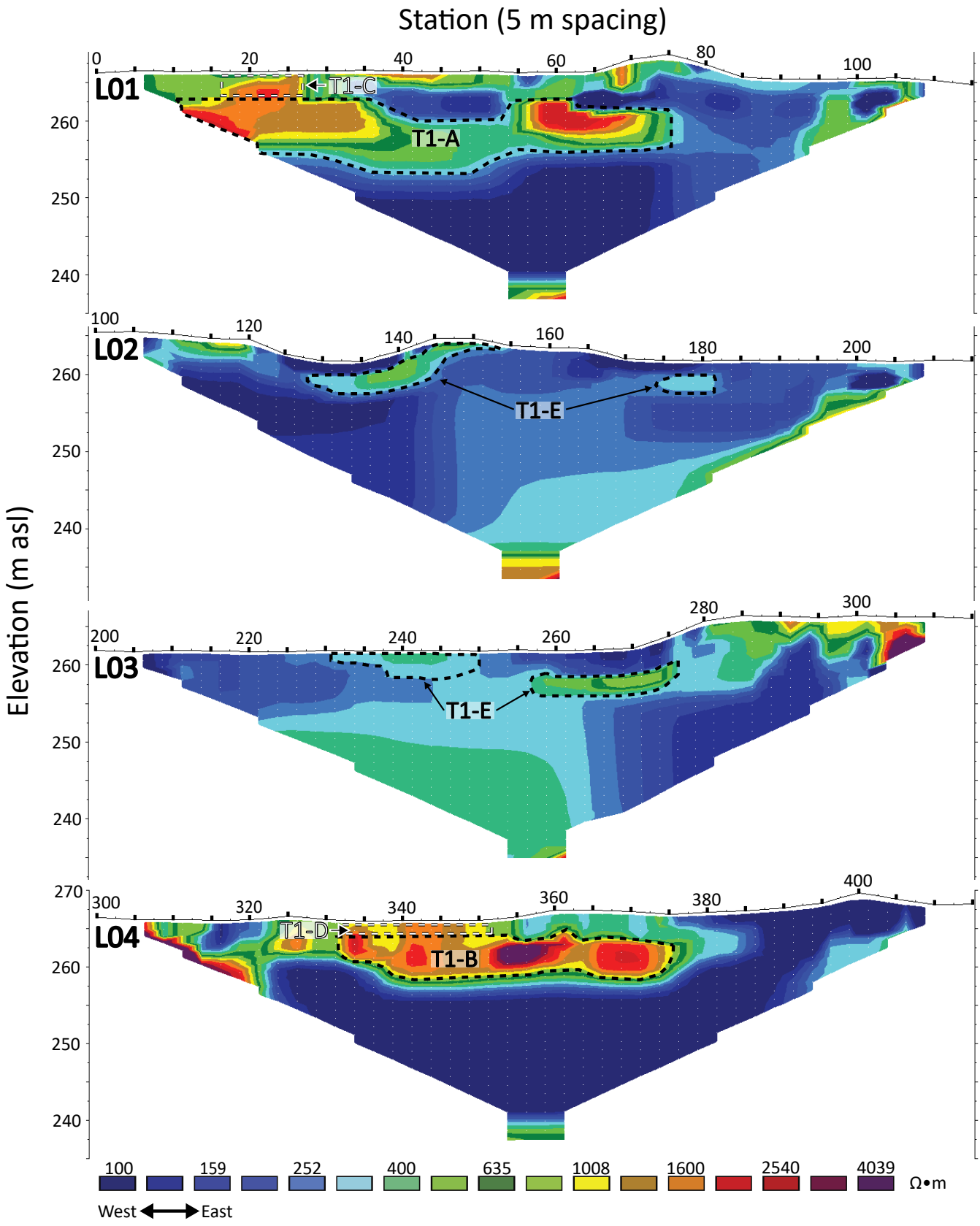


Figure GS2024-27-2: *Inversion results for transect 1 showing a resistivity cross-section with elevation data and electrode station locations, southeastern Manitoba. Anomalies at depth are outlined with black dashed lines. Areas where anomalies trend toward the surface are outlined in white dashed lines. Cooler colours indicate areas with lower resistivity, warmer colours indicate areas with higher resistivity. See Figure GS2024-27-1 for locations of lines. Abbreviations: Ω•m, ohm-metre; L, line; m asl, metres above sea level.*

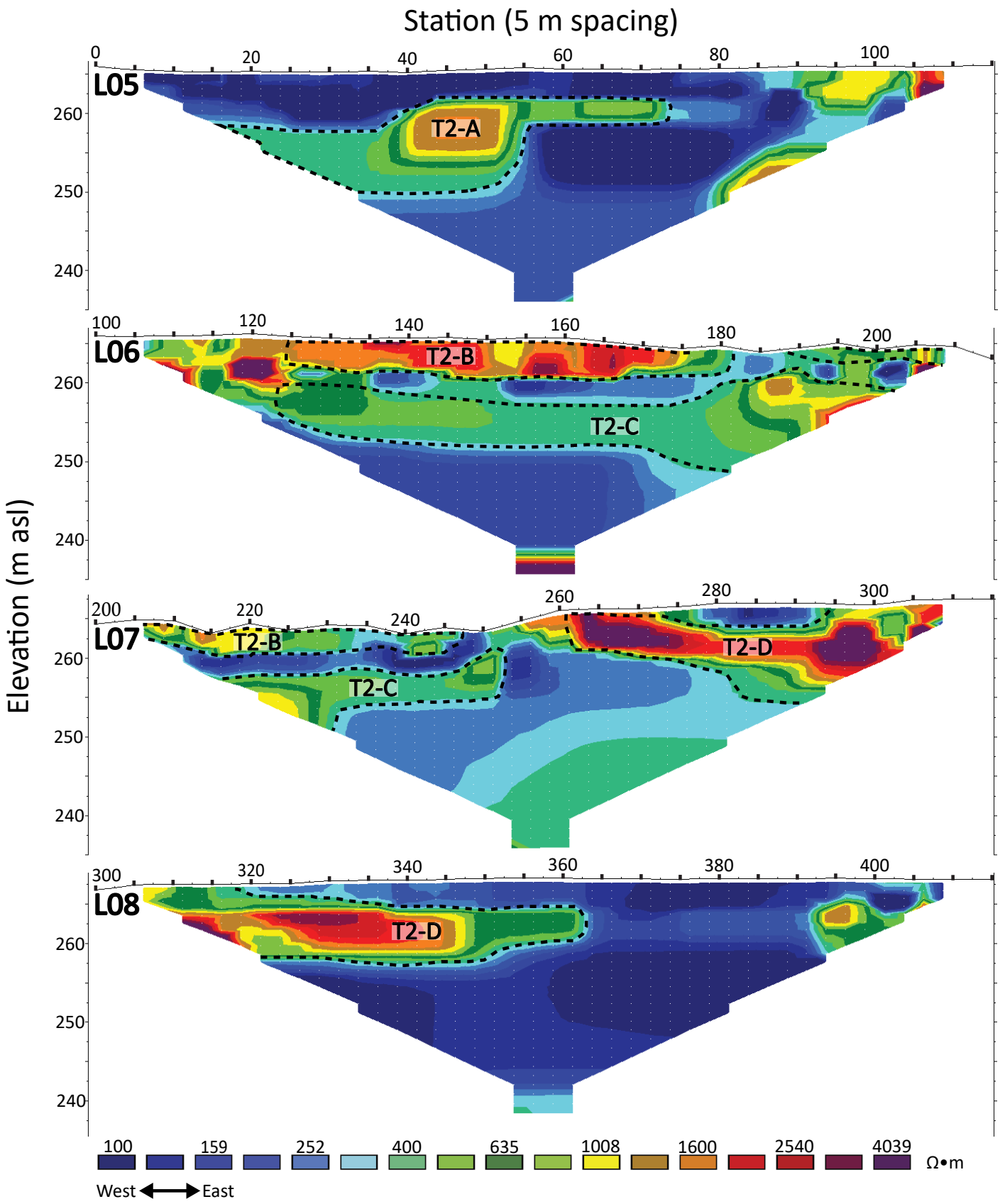


Figure GS2024-27-3: *Inversion results for transect 2 showing a resistivity cross-section with elevation data and electrode station locations. Anomalies at depth are outlined with black dashed lines. Cooler colours indicate areas with lower resistivity, warmer colours indicate areas with higher resistivity. See Figure GS2024-27-1 for locations of lines. Abbreviations: Ω•m, ohm-metre; L, line; m asl, metres above sea level.*

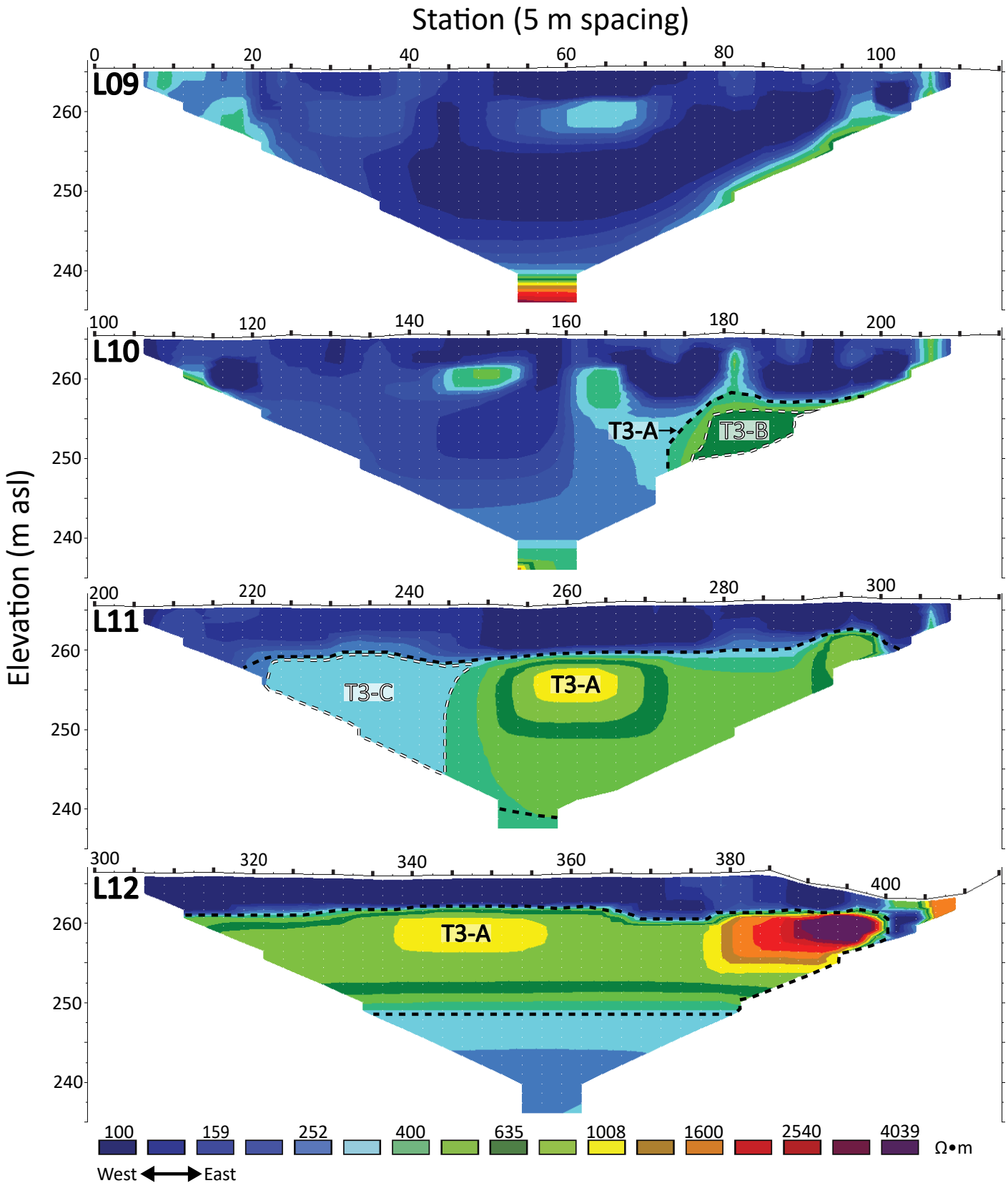


Figure GS2024-27-4: *Inversion results for transect 3 showing a resistivity cross-section with elevation data and electrode station locations. Anomalies at depth are outlined with black dashed lines. Areas showing discontinuity of resistivity intensity are outlined with white dashed lines. Cooler colours indicate areas with lower resistivity, warmer colours indicate areas with higher resistivity. See Figure GS2024-27-1 for locations of lines. Abbreviations: Ω•m, ohm-metre; L, line; m asl, metres above sea level.*

Table GS2024-27-1: Typical resistivity ranges of earth materials (from Palacky, 1988) and resistivity ranges of shallow-buried anomalies identified from the results of this multi-electrode resistivity study in southeastern Manitoba (see Figures GS2024-27-2 to -4 for details of anomalies).

Earth material	Resistivity (ohm-metre)
Fresh water	2–100
Clay	3–100
Till	50–1100
Sand and gravel	400–10000

Anomaly	Resistivity (ohm-metre)
T1-A	400–2540
T1-B	1008–4039
T1-E	252–800
T2-A	400–1600
T2-B	400–3200
T2-C	400–1300
T2-D	400–4039
T3-A	300–4039

their resistivity equipment and assistance throughout this study. A. Brandt, from the Rural Municipality of Taché, is thanked for co-ordinating access to the Monominto pit during the fieldwork.

References

ATLIS Geomatics Inc. 2016: Cooks Creek LiDAR DEM; Manitoba Infrastructure, URL <https://mli.gov.mb.ca/dems/index_external_lidar.html> [June 2023].

Esri® 2021: World imagery map, April 05, 2021; Esri, no scale given, URL <https://services.arcgisonline.com/ArcGIS/rest/services/World_Imagery/MapServer> [September 2024].

Matile, G.L.D. and Conley, G.G. 1979a: Quaternary geology and sand and gravel resources of the municipal surveys area; *in* Report of Field Activities 1979, Manitoba Department of Mines, Natural Resources and Environment, Mineral Resources Division, p. 86–87, URL <https://manitoba.ca/iem/geo/field/rfa1979.pdf> [September 2024].

Matile, G.L.D. and Conley, G.G. 1979b: Quaternary geology and sand and gravel resources of the Rural Municipality of Tache; Manitoba Department of Energy and Mines, Mineral Resources Division, Municipality Map AR80-2, scale 1:50 000, URL <https://manitoba.ca/iem/info/libmin/AR80-2.pdf> [September 2024].

Palacky, G.J. 1988: Resistivity of geologic targets; *in* Electromagnetic Methods in Applied Geophysics, Society of Exploration Geophysicists, v. 1, sec. 3, p. 53–129.

Rentz, J.W. 2023: Manitoba's aggregate program: past, present, future; *in* Report of Activities 2023, Manitoba Economic Development, Investment, Trade and Natural Resources, Manitoba Geological Survey, p. 124–130, URL <https://manitoba.ca/iem/geo/field/roa23pdfs/roa23_book.pdf> [September 2024].

Rentz, J.W., Marks, J., Frederiksen, A. and Guerard, R. 2024: Geophysical imaging of a buried gravel deposit in the Rural Municipality of Taché, southeastern Manitoba (part of NTS 62H15); *in* Report of Activities 2024, Manitoba Economic Development, Investment, Trade and Natural Resources, Manitoba Geological Survey, p. 219–225.

PUBLICATIONS

Data Repository Items

DRI2023007

Till-matrix geochemistry re-analyses data from far northeastern and far northwestern Manitoba (parts of NTS 54E, F, L, 64J, K, N, O)

by M.S. Gauthier and P.-M. Godbout

DRI2023015

Till geochemistry and heavy mineral analyses (gold, MMSIM®, visual KIM) of the western Fox River greenstone belt area, northeastern Manitoba (NTS 53M15, 16, parts of 53N13, 54C4, 54D1): year 2

by M.S. Gauthier and T.J. Hodder

DRI2023016

Compilation of Sm-Nd isotope results for archived samples from the Manitoba Geological Survey's Far North projects (parts of NTS 64I, K, M, N, P)

by Manitoba Geological Survey

DRI2024001

Till heavy mineral analysis (gold, MMSIM, visual KIM) from eight sections near the confluence of the Hayes and Gods rivers, northeastern Manitoba (parts of NTS 54C2, 7)

by M.S. Gauthier, L.N. Mesich and T.J. Hodder

DRI2024002

Till geochemistry from eight sections near the confluence of the Hayes and Gods rivers, northeastern Manitoba (parts of NTS 54C2, 7)

by L.N. Mesich, M.S. Gauthier and T.J. Hodder

DRI2024003

Till-matrix geochemistry data from the 2022–2023 field seasons in southeastern Manitoba (parts of NTS 52L, 62P, 63A)

by T.J. Hodder

DRI2024004

Gold and indicator-mineral data derived from glacial sediments (till) in southeastern Manitoba (parts of NTS 52L, 62P, 63A)

by T.J. Hodder

DRI2024005

Till-clast–lithology data, western Fox River greenstone belt area, northeastern Manitoba (NTS 53M15, 16, parts of 53N12, 13, 54C4, D1)

by M.S. Gauthier, M. Budge and M. Friesen

DRI2024006

Till-clast–lithology data, Gillam area, northeastern Manitoba (parts of NTS 54C, D, 64A)

by M.S. Gauthier

DRI2024007

2023 aggregate field visits: Quaternary site data, composition, and ice-flow indicators from gravel pits in southern Manitoba (parts of NTS 62H15, I13, P5)

by M.S. Gauthier and J. Rentz

DRI2024008

Rock Volatiles Stratigraphy data from drill cuttings from four oil wells in southwestern Manitoba (parts of NTS 62F2, K3)

by M.P.B. Nicolas, C.M. Smith and M.P. Smith

Microsoft® Excel® file supplements:

Nicolas, M.P.B., Smith, C.M. and Smith, M.P. 2024: Rock volatiles analysis of drill cuttings to evaluate the helium and hydrocarbon prospectivity of southwestern Manitoba (parts of NTS 62F2, K3); *in* Report of Activities 2024, Manitoba Economic Development, Investment, Trade and Natural Resources, Manitoba Geological Survey, p. 153–163.

DRI2024009

Salvaged diamond-drillcore at the Thompson Facility and Compound, east-central Manitoba (parts of NTS 54C, 63P, 64A): updated

by C.G. Couëslan

Microsoft® Excel® file supplements:

Couëslan, C.G. 2024: Thompson Facility and Compound core recovery project, east-central Manitoba (parts of NTS 64A1, 8): year two; *in* Report of Activities 2024, Manitoba Economic Development, Investment, Trade and Natural Resources, Manitoba Geological Survey, p. 127–128.

DRI2024010

Field-based ice-flow–indicator data collected during the 2023 and 2024 field seasons in southeastern Manitoba (parts of NTS 52L, M, 62P)

by T.J. Hodder

Microsoft® Excel® file supplements:

Hodder, T.J. and Lian, O.B. 2024: Reconnaissance-scale Quaternary geology investigations to support lithium exploration in southeastern Manitoba (parts of NTS 52L, M, 62P, 63A); *in* Report of Activities 2024, Manitoba Economic Development, Investment, Trade and Natural Resources, Manitoba Geological Survey, p. 200–208.

DRI2024011

Geochemical data of bulk-rock samples collected in the 2022 and 2023 field seasons from the Lynn Lake greenstone belt, northwestern Manitoba (parts of NTS 64C10–12, 14–16)

by X.M. Yang

Microsoft® Excel® file supplements:

Yang, X.M. 2024: New uranium-lead zircon dates from the Lynn Lake greenstone belt, northwestern Manitoba (part of NTS 64C14): implications for diverse granitoid magmatism and gold mineralization; *in* Report of Activities 2024, Manitoba Economic Development, Investment, Trade and Natural Resources, Manitoba Geological Survey, p. 129–144.

DRI2024012

Compilation of gas compositions from oil and gas wells in southwestern Manitoba (NTS 62G12, 62K3, parts of 62F)

by M.P.B. Nicolas

Microsoft® Excel® file supplements:

Nicolas, M.P.B. 2024: Geologic hydrogen in the Williston and Hudson Bay basins, southwestern and northeastern Manitoba (parts of NTS 53, 54, 62, 63); *in* Report of Activities 2024, Manitoba Economic Development, Investment, Trade and Natural Resources, Manitoba Geological Survey, p. 164–171.

DRI2024013

Whole-rock geochemistry and interactive GIS map file from the Cross Lake pegmatite field (parts of NTS 63I3–6, 11–14, 63J1–3, 6–11, 14–16)

by T. Martins, J. Janssens, P. Lenton, T. Corkery and A. Anderson

Microsoft® Excel® file supplements:

Martins, T., Janssens, J. and Lenton, P. 2024: Spodumene-bearing pegmatites from the Cross Lake pegmatite field, east-central Manitoba: mineralogy and petrography descriptions (parts of NTS 63I12, 63J9); *in* Report of Activities 2024, Manitoba Economic Development, Investment, Trade and Natural Resources, Manitoba Geological Survey, p. 77–84.

GeoFiles

GeoFile 2-2023

Manitoba till-matrix geochemistry compilation: silt plus clay (<63 µm) size-fraction by inductively coupled plasma–mass spectrometry after an aqua-regia or modified aqua-regia digestion

by M.S. Gauthier

GeoFile 5-2023

Updates to the Manitoba Mineral Deposits Database

by M.L. Rinne

GeoFile 7-2023

Manitoba till-matrix geochemistry compilation: total carbonate of the silt plus clay (<63 µm) size-fraction

by M.S. Gauthier

GeoFile 8-2023

Manitoba till-matrix geochemistry compilation: visible gold grains in the heavy mineral (<2 mm) size-fraction

by M.S. Gauthier

GeoFile 2-2024

Manitoba till-matrix geochemistry compilation: silt plus clay (<63 µm) size fraction by inductively coupled plasma–mass spectrometry after an aqua-regia or modified aqua-regia digestion

by M.S. Gauthier

GeoFile 5-2024

Updates to the Manitoba Mineral Deposits Database

by M.L. Rinne

Open Files

OF2024-1

Quaternary site, till composition and ice-flow indicator datasets in the Kaskattama highland area, northeastern Manitoba (parts of NTS 53N, O, 54B, C)

by T.J. Hodder, M.S. Gauthier, S.E. Kelley and M. Ross

OF2024-4
Bedrock geology of Manitoba
by Manitoba Geological Survey (scale 1:1 000 000)

Preliminary Map

PMAP2024-1
Bedrock geology of the northwestern Burntwood Lake area, west-central Manitoba (part of NTS 63N7)
by C.G. Couëslan (scale 1:10 000)

Amor, S.D., Couëslan, C.G., Gauthier, M.S., Martins, T., McCurdy, M.W., Day, S.J.A. and Adcock, S.W. 2024: Regional lake-sediment geochemical data from northern Manitoba (NTS 064-G): reanalysis data and QA/QC evaluation; Geological Survey of Canada, Open File 9197, 27 p.

Amor, S.D., Couëslan, C.G., Gauthier, M.S., Martins, T., McCurdy, M.W., Day, S.J.A. and Adcock, S.W. 2024: Regional lake-sediment geochemical data from northern Manitoba (NTS 064-J and 064-K): reanalysis data and QA/QC evaluation; Geological Survey of Canada, Open File 9187, 28 p.

Annesley, I.R., Cardenas-Vera, A., Santos, A.C., Martins, T. and Partin, C.A. 2024: Tapping the rare earth elements (REE) potential of northern Saskatchewan, Canada: new critical minerals initiative, research approach, and potential implications [abstract]; AGU2024, December 9–13, 2024, Washington, D.C., United States.

Breasley, C.M., Barker, I.R., Linnen, R.L, Martins, T. and Groat, L.A. in press: The use of X-ray micro-computed tomography to visualize and quantify lithium-bearing silicate minerals in pegmatites: examples from the Tanco pegmatite, Manitoba, Canada; American Mineralogist.

Breasley, C.M., Groat, L.A., Martins, T., Linnen, R.L. and Larson, K. in press: Petrology and mineralogy of the petalite-type Prof pegmatite, Revelstoke, British Columbia, Canada; Mineralogical Magazine.

Breasley, C.M., Groat, L.A., Martins, T., Linnen, R.L., Larson, K. and Henry, R.E. 2024: Mineralogy and petrology of the petalite-subtype prof pegmatite, Revelstoke, British Columbia, Canada; Geological Association of Canada–Mineralogical Association of Canada and the 10th International Symposium on granitic pegmatites, Joint Annual Meeting, May 19–22, 2024, Brandon, Manitoba, Program with Abstracts, v. 47, oral presentation.

Brennan, C.J., Student, J.J., Hill, T., Martins, T. and Sirbescu M.-L.C. 2024: Trace element concentrations and chemical zoning of spodumene from magmatic and hydrothermal origins; Ore Geology Reviews, v. 169, art. 106089, URL <https://doi.org/10.1016/j.oregeorev.2024.106089>.

Brewer, V., Hodder, T., Gauthier, M., Schaarschmidt, M. and Lian, O.B. 2024: Optical dating of proglacial lake sediments, Roseau River, Manitoba, Canada; Canadian Quaternary Association and Canadian Geomorphology Research Group Biennial Meeting, August 18–21, 2024, Regina, Saskatchewan, poster presentation.

Chen, Y., Li, L. and Yang, X.M. 2024: Nitrogen isotopic insight into the genesis of Archean continental crust [abstract]; Geological Association of Canada–Mineralogical Association of Canada and the 10th International Symposium on granitic pegmatites, Joint Annual Meeting, May 19–22, 2024, Brandon, Manitoba, Program with Abstracts, v. 47, oral presentation; Geoscience Canada, v. 51, p. 127, URL <https://doi.org/10.12789/geocanj.2024.51.211>.

Chinaglia, S., Miles, A., Martins, T., Goodenough, K. and Groat, L. 2024: The petrogenesis of pegmatites from Shatford Lake and Cat Lake, Manitoba, Canada; Geological Association of Canada–Mineralogical Association of Canada and the 10th International Symposium on granitic pegmatites, Joint Annual Meeting, May 19–22, 2024, Brandon, Manitoba, Program with Abstracts, v. 47, poster presentation.

Couëslan, C.G. 2023: GAC-MAC: field guide summary; Geoscience Canada, v. 50, p. 313–315.

Couëslan, C.G. 2023: Stratigraphy and implications for magmatic Ni-Cu deposits in the Halfway Lake area, Thompson nickel belt, Manitoba; Central Canada Mineral Exploration Convention, November 6–7, 2023, Winnipeg, Manitoba, abstract and oral presentation.

Couëslan, C.G. 2024: The Tower VMS deposit, a juvenile arc-hosted system within the Superior Boundary Zone [abstract]; Geological Association of Canada–Mineralogical Association of Canada and the 10th International Symposium on granitic pegmatites, Joint Annual Meeting, May 19–22, 2024, Brandon, Manitoba, Program with Abstracts, v. 47, p. 75.

Dias, F., Lima, A., Roda-Robles, E. and Martins, T. 2024: Lithium aluminosilicate textures and lithium distribution from the aplite-pegmatites of northern Portugal: outcrop and drill core comparisons; Geological Association of Canada–Mineralogical Association of Canada and the 10th International Symposium on granitic pegmatites, Joint Annual Meeting, May 19–22, 2024, Brandon, Manitoba, Program with Abstracts, v. 47, poster presentation.

Dias, F., Ribeiro, R., Lima, A., Gonçalves, F., Roda-Robles, E. and Martins, T. 2024: Impact of using a 3.5 µm film to analyze the chemical composition of crystal samples with a handheld x-ray fluorescence equipment; European Geosciences Union General Assembly 2024 (EGU24), April 14–19, 2024, Vienna, Austria, abstract and poster presentation.

Garate-Olave, I., Roda-Robles, E., Santos-Loyola, N., Martins, T., Lima, A. and Errandonea-Martin, J. 2024: Crystallization sequence of the spodumene-rich Alijó pegmatite (northern Portugal) and related metasomatism on its host rock; Minerals, v. 14, no. 7, art. 701, URL <https://doi.org/10.3390/min14070701>.

Gauthier, M.S., Hodder, T.J., Dalton, A.S., Brewer, V., Lian, O., Finkelstein, S.A., Schaarschmidt, M. and Mereghetti, A. 2024: MIS 3 Laurentide Ice Sheet retreat and advance in the Roseau River area of southern Manitoba, Canada; Canadian Quaternary Association and Canadian Geomorphology Research Group Biennial Meeting, August 18–21, 2024, Regina, Saskatchewan, oral presentation.

Gauthier, M.S., Hodder, T.J., Dalton, A.S., Brewer, V., Lian, O.B., Finkelstein, S.F., Schaarschmidt, M. and Mereghetti, A. in press: South-central Laurentide Ice Sheet dynamics and the formation of proglacial Lake Vita during MIS 3; Quaternary Research.

Gauthier, M.S., Hodder, T.J., Dalton, A.S., Lian, O.B., Schaarschmidt, M., Ross, M., Väliranta, M. and Finkelstein, S.A. 2024: Preservation of probable MIS 7 deglacial and nonglacial deposits near the edge of the Hudson Bay Lowland in Manitoba, Canada; Canadian Journal of Earth Sciences, e-First, URL <https://doi.org/10.1139/cjes-2024-0019>.

Hart, B., Hofmann, M., Flynn, J., Nicolas, M., Ko, T. and Longstaffe, F. 2024: Geochemistry- and petrophysics-based detection of breaks in the stratigraphic record of Cenomanian-Turonian deposit, eastern Cretaceous Western Interior Seaway: how complete is the stratigraphic record and why does it matter?; SEPM International Sedimentary Geosciences Congress 2024, May 5–8, 2024; Flagstaff, Arizona, United States, Program with Abstracts, oral presentation, URL <https://virtual.oxfordabstracts.com/#/event/public/4532/submission/78> [May 2024].

Hnatiuk, T., MacDonald, J.A., Chakhmouradian, A.R., Couëslan, C.G. and Martins, T. 2023: Determining the origins of Precambrian-hosted carbonates by petrographic observation and trace element investigation, northern Manitoba, Canada; Central Canada Mineral Exploration Convention, November 6–7, 2023, Winnipeg, Manitoba, poster presentation.

Hodder, T.J. and Martins, T. 2024: Effective drift prospecting for Li-bearing pegmatites in Manitoba, Canada; Geological Association of Canada–Mineralogical Association of Canada and the 10th International Symposium on granitic pegmatites, Joint Annual Meeting, May 19–22, 2024, Brandon, Manitoba, abstract and oral presentation.

Hodder, T.J., Gauthier, M.S., Ross, M., Kelley, S.E., Lian, O.B., Dalton, A.S. and Finkelstein, S.A. 2024: Unravelling the fragmented sediment–landform assemblage in an area of thick Quaternary sediment, western Hudson Bay Lowland, Canada; Canadian Journal of Earth Sciences, e-First, URL <https://doi.org/10.1139/cjes-2024-0018>.

Hodder, T.J., Gauthier, M.S., Ross, M., Lian, O.B., Schaarschmidt, M., Dalton, A.S., Finkelstein, S.A. and Gowan E. 2024: Stratigraphic evidence for early ice advances and predominance of Quebec-Labrador Dome glacial dynamics across the western Hudson Bay Lowland; Canadian Quaternary Association and Canadian Geomorphology Research Group Biennial Meeting, August 18–21, 2024, Regina, Saskatchewan, oral presentation.

MacRae, B., Partin, C., McDonald, B., Pastula, C., Hodder, T. and Martins, T. 2024: The Kipalu Formation of the Belcher group, Nunavut, as a possible source of jasper clasts in Manitoba till; Geological Association of Canada–Mineralogical Association of Canada and the 10th International Symposium on granitic pegmatites, Joint Annual Meeting, May 19–22, 2024, Brandon, Manitoba, abstract and poster presentation.

Martins, T. 2023: Lithium in Manitoba: production and exploration potential; Central Canada Mineral Exploration Convention, November 6–7, 2023, Winnipeg, Manitoba, oral presentation.

Martins, T. 2024: Cs enrichment in white mica from Manitoba Li pegmatites; Lunch and Learn talk series, Department of Earth Sciences, University of New Brunswick, Fredericton, New Brunswick.

Martins, T. 2024: Li mineralization styles in LCT pegmatites: compare and contrast; 50th AGS Colloquium and Annual Meeting, February 2–3, 2024, Moncton, New Brunswick, oral presentation.

Martins, T. 2024: Lithium: a key element for decarbonization; Geological Association of Canada–Mineralogical Association of Canada and the 10th International Symposium on granitic pegmatites, Joint Annual Meeting, May 19–22, 2024, Brandon, Manitoba, oral presentation.

Martins, T. 2024: Lithium-cesium-tantalum pegmatites: concepts and exploration techniques; 50th AGS Colloquium and Annual Meeting, February 2–3, 2024, Moncton, New Brunswick, abstract and oral presentation.

Martins, T. 2024: The legacy of Petr Černý in the study of granitic pegmatites [abstract]; 37th International Geological Congress 2024, August 25–31, 2024, Busan, Republic of Korea.

Martins, T., Deveau, C. and Falck, H. 2024: Classifying the production of lithium, caesium and tantalum from the Tanco Mine, Manitoba, Canada, according to the United Nations Framework Classification for Resources – a case study; ECE/ENERGY/GE.3/2024/12, UNECE Resource Management Week 2024, April 22–26, 2024, Geneva, Switzerland, URL <https://unece.org/sites/default/files/2024-04/Tanco Lithium CS_ECE-ENERGY-GE3-2024-12.pdf> [October 2024].

Martins, T., Deveau, C. and Falck, H. 2024: Classifying the production of lithium, cesium and tantalum from the Tanco mine, Manitoba, Canada, according to UNFC – a case study; UNECE Resource Management Week 2024, April 22–26, 2024, Geneva, Switzerland, oral presentation.

Martins, T., McFarlane, C. and Yang, P. 2024: Complex zoning in white mica from spodumene pegmatites at Cross Lake, Manitoba, Canada [abstract]; AGU2024, December 9–13, 2024, Washington, D.C., United States.

Martins, T., Breasley, C., Groat, L., Linnen, R., Deveau, C. and Rankmore, S. 2024: The Tanco pegmatite: geological setting, internal zonation, mineralogy, and mining of a world-class rare element pegmatite deposit; Field trip guidebook, Geological Association of Canada–Mineralogical Association of Canada and the 10th International Symposium on granitic pegmatites, Joint Annual Meeting, May 19–22, 2024, Brandon, Manitoba, 39 p.

Maxeiner, R.O., Boseman, S.A., Card, C.D., Marsh, A., Morelli, R.M., Couëslan, C.G., Martins, T., Reid, R., Easton, R.M., Knox, B., Mihalynuk, M.G., Ootes, L., Cui, Y., Grobe, M., Guemache, M.A., Lawley, C.J.M., Böhm, C. and Ashton, K. 2024: Classifying intrusive and strongly metamorphosed rock units: CLASS – a cooperative lithodemic and stratigraphic system; Canadian Journal of Earth Sciences, v. 61, p. 1014–1042.

Menzies, J., Paulen, R.C., Reitner, J.M., Gao, C., Hodder, T. and Ross, M. 2023: Subglacial tills: a process model based on microsedimentological clues; Journal of Sedimentary Research, v. 93, no. 110, p. 705–728, URL <https://doi.org/10.2110/jsr.2022.017>.

Mesich, N., Ross, M., Gauthier, M., Hodder, T.J. and Hathaway, J. 2024: Unravelling the complex Quaternary history and till provenance along the Gods and Yakaw rivers, northeastern Manitoba; Canadian Quaternary Association and Canadian Geomorphology Research Group Biennial Meeting, August 18–21, 2024, Regina, Saskatchewan, poster presentation.

Nicolas, M.P.B., Smith, C.M. and Smith M.P. 2024: Volatiles analysis of drill cuttings to evaluate helium prospectivity in Manitoba; Canadian Energy Geoscience Association–Canadian Society of Exploration Geophysicists Annual Convention (GeoConvention 2024), June 17–19, 2024, Calgary, Alberta, URL <https://geoconvention.com/wp-content/uploads/abstracts/2024/103996-volatiles-analysis-of-drill-cuttings-to-evaluate-h.pdf> [September 2024].

Pastula, C., Partin, P., McDonald, B., Hodder, T. and Martins, T. 2024: Testing the provenance of omar glacial erratics in Manitoba glacial till: preliminary results and insights from the Omarolluk Formation in the Belcher Islands, Nunavut; Geological Association of Canada–Mineralogical Association of Canada and the 10th International Symposium on granitic pegmatites, Joint Annual Meeting, May 19–22, 2024, Brandon, Manitoba, abstract and poster presentation.

Roush, J., Martins, T., McFarlane, C.R.M., Rinne, M.L. and Groat, L. 2024: Preliminary results from the Tappy, Eagle and F.D. no.5 pegmatites, Cat Lake-Winnipeg River pegmatite field, southeastern Manitoba; 50th AGS Colloquium and Annual Meeting, February 2–3, 2024, Moncton, New Brunswick, abstract and oral presentation.

Roush, J., Martins, T., McFarlane, C.R.M., Rinne, M.L. and Groat, L. 2024: The Eagle, F.D. no. 5 and Tappy pegmatites from the Cat Lake-Winnipeg River pegmatite field, southeastern Manitoba; Geological Association of Canada–Mineralogical Association of Canada and the 10th International Symposium on granitic pegmatites, Joint Annual Meeting, May 19–22, 2024, Brandon, Manitoba, abstract and poster presentation.

Silva, D., Martins, T., Groat, L. and Linnen, R. 2024: Host rock lithogeochemical perspectives of Li-enriched pegmatite, Wekusko Lake pegmatite field, Manitoba; Geological Association of Canada–Mineralogical Association of Canada and the 10th International Symposium on granitic pegmatites, Joint Annual Meeting, May 19–22, 2024, Brandon, Manitoba, abstract and poster presentation.

Sotiriou, P., Polat, A., Kusky, T., Windley, B.F., Frei, R. and Yang, X.M. 2024: Geochemistry of Archean anorthosite-bearing layered intrusions; Earth-Science Reviews, v. 249, art. 104654, URL <https://doi.org/10.1016/j.earscirev.2023.104654>.

Wang, X., Yin, C., Lin, S., Couëslan, C.G., Böhm, C.O. and Qian, J. 2024: Ultrahigh temperature metamorphism recorded in mafic granulites from the Pikwitonei Granulite Domain of the northwestern Superior Province; Geological Association of Canada–Mineralogical Association of Canada and the 10th International Symposium on granitic pegmatites, Joint Annual Meeting, May 19–22, 2024, Brandon, Manitoba, Program with Abstracts, v. 47, p. 124.

Yang, X.M. 2023: Updating the study of granitoids in Manitoba: metallogenic and petrogenetic implications [abstract]; Central Canada Mineral Exploration Convention, November 6–7, 2023, Winnipeg, Manitoba, Program with Abstracts, oral presentation, URL <https://ccme-convention.ca/eric-yang-2/> [November 2023].

Yang, X.M. and Lawley, C.J.M. 2024: Adakite-like granitoid intrusions in the Paleoproterozoic Lynn Lake greenstone belt, northwestern Manitoba, Canada: implications for geodynamic setting and gold mineralization [abstract]; Geological Association of Canada–Mineralogical Association of Canada and the 10th International Symposium on granitic pegmatites, Joint Annual Meeting, May 19–22, 2024, Brandon, Manitoba, Program with Abstracts; Geoscience Canada, v. 51, p. 127, URL <https://doi.org/10.12789/geocanj.2024.51.211>.

Yang, X.M. and Lawley, C.J.M. 2024: Rapid switch in geodynamic setting revealed by episodic granitoid magmatism in the Lynn Lake greenstone belt of Paleoproterozoic Trans-Hudson Orogen, Manitoba, Canada; Lithos, v. 470–471, art. 107534, URL <https://doi.org/10.1016/j.lithos.2024.107534>.